

DISSERTATION

TOWARDS THE TOTAL SYNTHESIS OF 14-ACETOXYGELSENICINE AND
SYNTHESSES OF LARGAZOLE ANALOGS

Submitted by

Tenaya L. Newkirk

Department of Chemistry

In partial fulfillment of the requirements

for the degree Doctor of Philosophy

Colorado State University

Fort Collins, CO

Summer, 2009

COLORADO STATE UNIVERSITY

June 22nd, 2009

WE HEREBY RECOMMEND THAT THE DISSERTATION PREPARED UNDER OUR SUPERVISION BY TENAYA L. NEWKIRK ENTITLED "TOWARDS THE TOTAL SYNTHESIS OF 14-ACETOXYGELSENICINE AND SYNTHESSES OF LARGAZOLE ANALOGS" BE ACCEPTED AS FULFILLING IN PART REQUIREMENTS FOR THE DEGREE DOCTOR OF PHILOSOPHY.

Committee on Graduate Work

Professor Frank R. Stermitz

Professor Eric M. Ferreira

Professor Dawn Rickey

Professor Douglas H. Thamm

Advisor: Professor Robert M. Williams

Department Head: Professor Anthony K. Rappe

ABSTRACT OF DISSERTATION
TOWARDS THE TOTAL SYNTHESIS OF 14-ACETOXYGELSENICINE AND
SYNTHESES OF LARGAZOLE ANALOGS

Herein are documented our efforts in two projects, beginning with studies towards the total synthesis of 14-acetoxygelsenicine. We have developed different strategies towards this complex natural product, wherein we have developed routes towards an appropriate substrate for a novel, intramolecular hetero Diels-Alder cyclization. The developed route would also lead to related members of this family of alkaloids, and helps set the stage for future efforts.

In the second project discussed, we have successfully pursued the synthesis of numerous, biologically active analogs of the natural product (+)-largazole. Synthetic efforts have led to the design of inhibitors with unprecedented biological activity, as well as providing information regarding the structure-activity relationship of these molecules.

Tenaya L. Newkirk
Department of Chemistry
Colorado State University
Fort Collins, CO
Summer, 2009

ACKNOWLEDGEMENTS

I would like to give my heartfelt thanks to my advisor, Professor Robert M. Williams, for giving me this opportunity. You have given me the freedom to pursue my own ideas, while always stepping in to offer advice when I ran into trouble. You provided an atmosphere of communication and cooperation in which I have been able to take the first steps towards a career that I love, as well as giving me the opportunity to pursue my passion and teach while I have been here. I don't know how to find the words to thank you enough for giving me the chance to change my life - I am forever grateful.

I would also like to thank Professors Tarek Sammakia and Andy Phillips from the University of Colorado for helping me to start down this path, and Professors Nancy Levinger, Ellen Fisher and Debbie Crans for helping me so much while I have been here at Colorado State University.

My gratitude as well to all of the members of the Williams group, both past and present, for all of their help, advice and encouragement. In particular, I would like to thank Meriah Niessel-Valente and Brandon English for teaching me everything I needed to know when I started in the lab, and especial thanks to Dr. Albert Bowers, Dr. Tom Greshock, Dr. Dan Gubler, Dr. Kenny Miller, and Annie Troutman-Youngman for so many helpful discussions. I would also like to thank those with whom I have shared my home away from home, B317. To Ryan Rafferty, Michelle Sanchez, Tim Welch and Timmy McAfoos, thank you for putting up with me and listening to rather more Iron

Maiden than you probably pictured as being part of your graduate experience. Finally, my thanks to Jenni Finefield, who has always shared with me her seemingly endless reservoir of personal strength when I ran short. Without your friendship, support and constant encouragement I would never have survived graduate school (or enjoyed it so much).

I would like to thank my parents, Hal and Patty Gabow, for their unflagging support in whatever path I wanted to take, and their always helpful advice in how to get there. To my brother, Aaron Gabow, whose whole-hearted pursuit of his own goals and passion for life have been an inspiration to me, and whose careful eye ensures that any grammatical errors are solely of my own making, I extend my utmost gratitude. I would also like to thank my mom away from mom, Catherine Latessa, as well as my grandparents, Jack and Lisa Gabow, and Teresa and Dick Helmintoller for their love and support (and frequent pep-talks).

To Jennifer Parker, Bonnita Carlson, Jeremy Shaver and David Claypool, thank you for twenty years of friendship and fun. In good times and bad, you have all shaped who I am today, and I am so lucky to have a group of friends with such talent, intelligence and kindness.

Finally, to my husband, Scott Newkirk, I extend gratitude beyond words. Your unending love, support, and super-human powers of encouragement and understanding have brought me to this point, and it is thanks to you that I had the courage to begin this journey. I am truly fortunate to have shared my life with you, and I look forward to the next stage of our life together ... up the irons!

<u>TABLE OF CONTENTS</u>	<u>PAGE</u>
Chapter 1: Introduction and Overview	
1.1 Introduction.....	1
1.1.1 14-Acetoxygelsenicine.....	1
1.1.2 Overview of Results.....	3
1.2 Largazole.....	4
1.2.1 Overview of Results.....	5
Chapter 2: The Gelsemium Alkaloids	
2.1 Introduction	
2.1.1 Background.....	7
2.1.2 Biological Activity.....	8
2.1.3 Isolation.....	9
2.2 Proposed Biosynthesis	
2.2.1 Biosynthesis of Strictosidine.....	10
2.2.2 Biosynthesis of the Gelsemium Alkaloids.....	11
2.3 Biomimetic Syntheses of Gelsedine	
2.3.1 Attempts at Biomimetic Synthesis.....	13
2.3.2 Biomimetic Synthesis of Gelsedine.....	14
2.4 Prior Syntheses of Selected Gelsemium Alkaloids	
2.4.1 Syntheses of Gelsemine.....	16

2.4.2 Hiemstra's Total Synthesis of <i>ent</i> -Gelsedine.....	22
2.5 Related Natural Products	
2.5.1 Recent Additions to the Gelsedine Sub-family.....	23
Chapter 3: Towards the Total Synthesis of 14-Acetoxygelsenicine	
3.1 Challenges and Synthetic Strategy	
3.1.1 Synthetic Strategy.....	26
3.1.2 Retrosynthetic Analysis.....	26
3.1.3 Synthesis of the Spirooxindole.....	27
3.2 Second Generation Approach	
3.2.1 New Synthetic Design.....	29
3.2.2 Synthesis of the Tryptophan Derivative.....	32
3.2.3 Synthesis of the Butenoic Acid Derivative.....	34
3.3 Attempted Formation of the Diels-Alder Substrate	
3.3.1 First Generation Approach to Diels-Alder Substrate.....	34
3.3.2 Efforts Towards Protection of the Primary Amine.....	36
3.3.3 Revised Approach to the Diels-Alder Substrate.....	37
3.3.4 Attempted Diels-Alder Cyclization.....	40
3.3.5 Revised Protecting Group Strategy.....	41
3.3.6 Attempted Synthesis of Key Intermediate.....	42
3.3.7 Attempted Amide Enolate Strategy.....	43
3.3.8 Attempted Acid Chloride Addition.....	44
3.4 New Ideas and Concluding Remarks	
3.4.1 Possible Future Directions.....	45

3.4.2 Summary of Progress.....	47
3.4.3 Concluding Remarks.....	49
Chapter 4: Histone Deacetylase Inhibitors	
4.1 Introduction	
4.1.1 Overview of Histone Deacetylase Enzymes.....	50
4.2 Acyclic Histone Deacetylase Inhibitors	
4.2.1 Background.....	52
4.2.2 Acyclic Histone Deacetylase Inhibitors.....	53
4.3 Macrocyclic Peptide Histone Deacetylase Inhibitors	
4.3.1 Background.....	57
4.3.2 HC Toxin.....	58
4.3.3 Trapoxin.....	58
4.3.4 Apicidin.....	61
4.3.5 Microsporins.....	62
4.3.6 Azumamides.....	63
4.3.7 FR235222.....	66
4.4 Sulfur-Containing Histone Deacetylase Inhibitors	
4.4.1 Background.....	68
4.4.2 Spiruchostatins.....	69
4.4.3 FR901375.....	70
4.4.4 FK228 (Romidepsin).....	71
4.4.5 Biosynthesis of FK228.....	78

4.5 Largazole

4.5.1 Background and Isolation.....	79
4.5.2 Previous Syntheses.....	80

Chapter 5: Syntheses of Largazole Analogs

5.1 Synthetic Goals and Collaborations

5.1.1 Synthetic Goals.....	86
5.1.2 Biological Assays.....	87
5.1.3 Computational Modeling.....	88

5.2 Previous Work in the Williams Group

5.2.1 Retrosynthetic Analysis.....	89
5.2.2 Synthesis of (+)-Largazole.....	90

5.2 Synthesis of (-)-Largazole

5.2.1 Synthetic Goals.....	91
5.2.2 Synthesis of the Thiazoline-Thiazole.....	92
5.2.3 Synthesis of β -Hydroxy Acid.....	94
5.2.4 Completion of (-)-Largazole.....	96

5.3 Amide Isostere Analogs

5.3.1 Synthetic Goals.....	97
5.3.2 β -Amino Acid Synthesis.....	98
5.3.3 Completion of the Amide Isostere Core.....	100

5.4 Analogs of the Side Chain and Zinc-Binding Motif

5.4.1 Synthetic Goals.....	102
5.4.2 Accessing the Depsipeptide Core.....	103

5.4.3 Completion of Analogs.....	104
5.5 Further Linker Region Analogs	
5.5.1 Synthetic Goals.....	107
5.5.2 First Generation Attempts.....	108
5.5.3 Second Generation Approach.....	110
5.6 Cap Region Analogs	
5.6.1 Synthetic Goals.....	113
5.6.2 Towards the <i>Des</i> -Methyl Thiazoline-Pyridine Analog.....	116
5.6.3 Towards a New Thiazoline-Pyridine Analog.....	117
5.7 Summary and Concluding Remarks	
5.7.1 Summary of Progress.....	119
5.7.2 Concluding Remarks.....	120
References.....	122
Chapter 6: Experimental Section	
Table of Spectra and Procedures.....	129
6.1 General Considerations.....	130
6.2 Experimental Procedures.....	131
Appendix 1: Publications.....	325
Appendix 2: Research Proposal.....	360

LIST OF ABBREVIATIONS

Ac ₂ O	Acetic anhydride
AcCl	Acetyl chloride
AcOH	Acetic acid
AIBN	Azobisisobutyronitrile
Bn	Benzyl
BnBr	Benzyl bromide
Boc	<i>tert</i> -Butoxycarbonyl
Boc ₂ O	di- <i>tert</i> -Butyldicarbonate
BOMCl	Benzyloxymethyl chloride
BOP	(Benzotriazol-1-yloxy)tris(dimethylamino) phosphonium hexafluorophosphate
BuLi	Butyllithium
DABCO	1,4-Diazabicyclo[2.2.2]octane
DBU	1,8-Diazabicyclo[5.4.0]undec-7-ene
DCC	<i>N,N'</i> -Dicyclohexylcarbodiimide
DCM	Dichloromethane
Dess-Martin Periodinane	Triacetoxy <i>o</i> -iodoxybenzoic acid
DIAD	Diisopropyl azodicarboxylate

DIBAL-H	Diisobutylaluminum hydride
DIPA	Diisopropylamine
DIPEA	Diisopropylethylamine
DMAP	4-(Dimethylamino)pyridine
DME	Dimethoxyethane
DMF	Dimethylformamide
DMPU	1,3-Dimethyl-3,4,5,6-tetrahydro-2(1 <i>H</i>)- pyrimidinone
DMS	Dimethylsulfide
DMSO	Dimethylsulfoxide
DTNP	2,2'-Dithiobis(5-nitropyridine)
EDCI (or EDC)	<i>N</i> -(3-dimethylaminopropyl)- <i>N'</i> -ethylcarbodiimide
EtOAc	Ethyl acetate
Et ₂ O	Diethyl ether
Fmoc	Fluorenylmethoxycarbonyl
FmocOSu	9-Fluorenylmethyl <i>N</i> -succinimidyl carbonate, <i>N</i> -(9- Fluorenylmethoxycarbonyloxy)succinimide
HATU	<i>O</i> -(7-Azabenzotriazol-1-yl)- <i>N,N,N',N'</i> - tetramethyluronium hexafluorophosphate
HMDA	1,6-Diaminohexane
HOAt	1-Hydroxy-7-azabenzotriazole
HOBt	1-Hydroxybenzotriazole
imid.	Imidazole

KHMDS	Sodium (bis)trimethylsilyl amide
LDA	Lithium <i>N,N</i> -diisopropylamide)
LHMDS (or LiHMDS)	Lithium (bis)trimethylsilyl amide
<i>m</i> CPBA	<i>m</i> -Chloroperbenzoic acid
MeI	Iodomethane
MeOH	Methanol
MsCl	Methanesulfonyl chloride
Mukaiyama reagent	2-Chloro-1-methylpyridinium iodide
NHMDS (or NaHMDS)	Sodium (bis)trimethylsilyl amide
NMM	<i>N</i> -methylmorpholine
NMO	4-Methylmorpholine <i>N</i> -oxide
P(OEt) ₃	Triethyl phosphite
P(<i>o</i> -tol) ₃	tri <i>o</i> -Tolylpalladium
PCC	Pyridinium chlorochromate
Pd(OAc) ₂	Palladium (II) acetate
Pd ₂ (dba) ₃	Tris(dibenzylideneacetone)dipalladium
PFP	Pentafluorophenyl
PhI(OAc) ₂	Iodobenzene diacetate
PivCl	Trimethylacetyl chloride
PMB	<i>p</i> -Methoxybenzyl
PMBBBr	<i>p</i> -Methoxybenzyl chloride
PNB	<i>p</i> -Nitrobenzyl
PNBCl	<i>p</i> -Nitrobenzyl chloride

PPTS	Pyridinium-toluenesulfonate
<i>p</i> TSA	<i>p</i> -Toluenesulfonic acid
Py. or Pyr.	Pyridine
PyAOP	(7-Azabenzotriazol-1-yloxy) tripyrrolidinophosphonium hexafluorophosphate
PyBOP	Benzotriazol-1-yl- oxytripyrrolidinophosphonium hexafluorophosphate
Red-Al	Sodium bis(2-methoxyethoxy)aluminum hydride
SEMCI	2-(Triethylsilyl)ethoxymethyl chloride
TBAF	Tetrabutylammonium fluoride
TBAHS	Tetrabutylammonium hydrogen sulfate
TBAI	Tetrabutylammonium iodide
TBDPS	<i>tert</i> -Butyldiphenylsilyl
TBSCI	<i>tert</i> -Butyldimethylsilyl chloride
TBSOTf	<i>tert</i> -Butyldimethylsilyl trifluoromethanesulfonate
<i>t</i> -BuOK	Potassium <i>tert</i> -butoxide
Tce	Trichloroethane
TEMPO	2,2,6,6-Tetramethyl-1-piperidinyloxy, free radical
TESOTf	Triethylsilyl trifluoromethanesulfonate
TFA	Trifluoroacetic acid
TFAA	Trifluoroacetic anhydride
THF	Tetrahydrofuran
TMAD	<i>N,N,N',N'</i> -Tetramethylazodicarboxamide

TMEDA	<i>N,N,N',N'</i> -Tetramethylethylenediamine
TMS	Trimethylsilyl
TMSCl	Trimethylsilyl chloride
TPAP	Tetrapropylammonium perruthenate
TrocCl	Trichloroethyl chloroformate
TrSH (or TrtSH)	Triphenylmethanethiol
TrtCl (or TrCl)	(Chloromethanetriyl)tribenzene
Ts ₂ O	<i>p</i> -Toluenesulfonic anhydride
TsCl	<i>p</i> -Toluenesulfonyl chloride
TSE	2-Trimethylsilyl ethyl
TsOH	<i>p</i> -Toluenesulfonic acid

Chapter 1: Introduction and Overview

1.1 Introduction

Herein are discussed two different projects in the area of natural product synthesis: studies towards the total synthesis of 14-acetoxygelsenicine and syntheses of largazole analogs. In general, our studies in natural product synthesis are geared towards molecules displaying structural complexity and/or biological utility, and each of these projects highlights a different facet of our interests. 14-Acetoxygelsenicine is a structurally attractive target that presents opportunities for the development of a novel synthetic approach, although its biological activity is quite modest. Largazole, in contrast, possesses biological activity unprecedented at the time of its isolation. Its comparatively simpler structure make it an ideal candidate for the synthesis of analogs.

1.1.1 14-Acetoxygelsenicine

As mentioned above, our interest in this product lies in the structure of the molecule (Figure 1). The rather strained tricyclic core of the molecule represents an interesting synthetic challenge, as does the installation of the quaternary center of the spirooxindole. In addition to 14-acetoxygelsenicine, the Gelsemium family of alkaloids includes over fifty natural products isolated from both *Gelsemium elegans* Benthham and *Gelsemium sempervirens*¹. These other members of the family have also garnered considerable synthetic attention on the basis of their complex molecular architecture. Perhaps the best known of these alkaloids is gelsemine, which has been the target of

synthetic approaches by numerous laboratories. A summary of approaches to gelsemine are included in Chapter 2 of this work, as these prior efforts have influenced our synthetic design.

Of further note are the synthetic studies of a related natural product, gelsedine. This member of the Gelsemium family has been studied as part of an exploration of the possible biosynthesis of these alkaloids. The current proposal for the biosynthesis of the Gelsemium alkaloids is presented herein, alongside a biomimetic synthesis of gelsedine published by Sakai et al². A purely synthetic approach to gelsedine as published by Hiemstra and coworkers is also presented herein³. The similarity between gelsedine and 14-acetoxygelsenicine has allowed us to draw upon these reports as well in our work towards 14-acetoxygelsenicine.

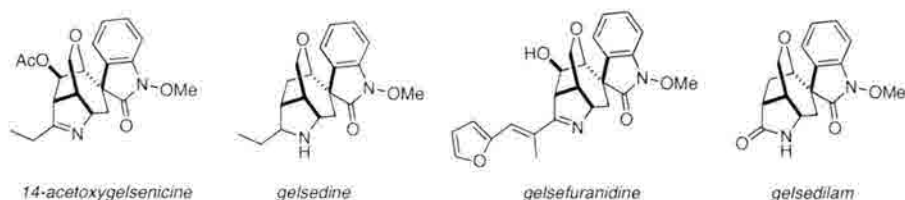


Figure 1: 14-Acetoxygelsenicine and related alkaloids.

Our synthetic efforts are discussed in detail in Chapter 3. We have developed two approaches towards this complex molecule. The first generation approach was designed to capitalize on an intramolecular Heck reaction to access the spirooxindole present in the natural product, a strategy which has proven successful in syntheses of related molecules. We met with early success using this route, in that we were able to access the product of the Heck reaction. However, concerns regarding the efficiency of this route, specifically the necessity of numerous repeated redox operations, caused us to abandon this route in favor of a more highly efficient strategy.

In the second generation approach, we proposed a novel intramolecular hetero Diels-Alder reaction as the key step to access the core of 14-acetoxygelsenicine. This route would provide access to gelsedilam as well as gelsefuranidine, two recently isolated alkaloids related to 14-acetoxygelsenicine. The novelty of the proposed key step, as well as possible routes to other Gelsemium alkaloids make this strategy both unique and versatile. In Chapter 3 of this work, our attempts towards the synthesis of the Diels-Alder substrate are presented, as well as the roadblocks we encountered in accessing the desired target.

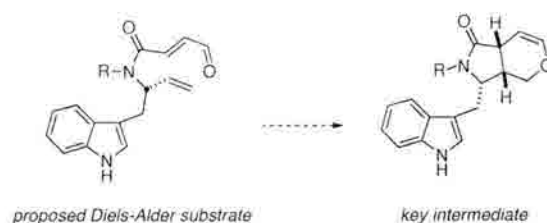


Figure 2: Proposed key step.

1.1.2 Overview of Results

Following the retrosynthetic approach to 14-acetoxygelsenicine mentioned above, we developed several different strategies towards the synthesis of the Diels-Alder adduct. Difficulties were encountered in accessing an appropriately substituted tryptophan derivative for use in the cyclization. Specifically, attempts to cyclize a substrate without further substitution at the amide nitrogen ($R=H$, Figure 2) were unsuccessful. However, attempts to couple the desired diene to a secondary amine did not provide product; likewise, attempts to protect the nitrogen with the diene already in place were unsuccessful. A summary of the substrates that were successfully synthesized, as well as the problems encountered in continuing forward with these compounds, is delineated in further detail in Chapter 3.

As we were unable to access the desired Diels-Alder substrate, we chose to cease our efforts towards the total synthesis of 14-acetoxygelsenicine. However, this retrosynthetic approach still seems a promising one, and to this end, possible future directions are discussed, wherein we believe that the difficulties mentioned above might be avoided.

1.2 Largazole

As we were deciding to leave our studies of 14-acetoxygelsenicine, the structure of a naturally occurring histone deacetylase inhibitor (HDACi), largazole, was disclosed. Histone deacetylase enzymes play an important role in the regulation of gene expression, and dysfunction in these enzymes has been linked with a variety of human diseases, including cancer⁴. An overview of the function of HDAC enzymes, as well as synthetic efforts towards other known HDACi (as excerpted from our review on the subject) is presented in Chapter 4⁵.

HDACi are emerging targets for use as possible cancer treatments; however, clinical trials have resulted in cardiac complications. It is possible that the reason for these deleterious effects lies in the lack of specificity of these compounds for different classes or isoforms of the HDAC enzymes. Largazole however, displays inherent selectivity for both class and isoform, properties which prompted our interest in the natural product, as a more specific inhibitor might not lead to these side effects. Furthermore, we felt that largazole was a promising target for possible use as a drug as we believe that the natural product exists as a prodrug - the octanoyl side chain (Figure 3) increases the hydrophobic nature of the molecule, allowing it to pass into cells. Once

inside the cell, enzymatic cleavage of the octanoyl tail would unmask a free thiol, which could bind to a zinc cation within the active site of the HDAC enzyme.

These desirable characteristics led us to use largazole itself as a starting point for the development of a series of analogs, through which we have begun to seek out a novel HDACi with greater biological activity and specificity than the natural product. To this end, our group participates in a collaboration with three others, two of which perform biological assays (*in vivo* or *in vitro*) and one of which uses computational studies to rationalize and predict biological activity. The data provided by these laboratories is discussed in Chapter 5, along with our synthetic efforts.

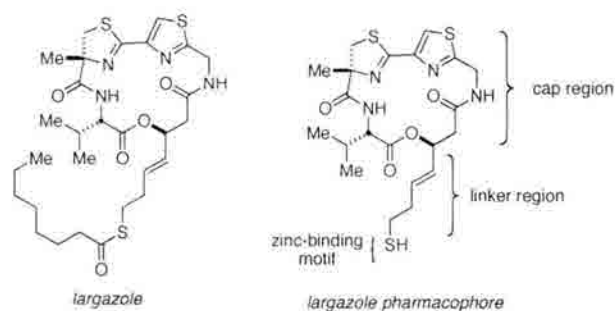


Figure 3: Largazole and its pharmacophore.

1.2.1 Overview of Results

We have developed a library of largazole analogs with variations in all points of the pharmacophore (shown in Figure 3). The HDACi pharmacophore is composed of three regions: the cap region (macrocyclic), a functional group capable of binding the zinc cation in the HDAC active site, and a linker region connecting the two. Through our synthetic efforts, we have explored the effect of variations in the stereochemistry of the cap region, variations in the heteroatoms and ring sizes contained therein, and a series of analogs with changes in the zinc-binding moiety and linker region. As a result of these studies, we have successfully developed three analogs possessing activity and specificity

equal to or greater than largazole itself. Syntheses of the aforementioned library of analogs, as well as biological data, are presented in Chapter 5.

From these results, we have identified a new series of targets for total synthesis. We have begun work on two of these analogs, and our early efforts in this direction are also discussed. A summary of the analogs that we have successfully synthesized to date is included in Chapter 5.

Chapter 2: The Gelsemium Alkaloids

Introduction 2.1

Background 2.1.1

The Gelsemium family of alkaloids has been the subject of extensive research dating back over 100 years⁶. This large family includes over 50 natural products to date, isolated from both *Gelsemium elegans* Benthham and *Gelsemium sempervirens*^{1,7}. *Gelsemium elegans* has been used in traditional Chinese and Native American medicine for over 1200 years in the treatment of skin disorders, and is still in use today in the United States as a homeopathic remedy for both influenza and anxiety^{8,9}.

The Gelsemium family is divided into six subsets, representatives of which are shown in Figure 4.

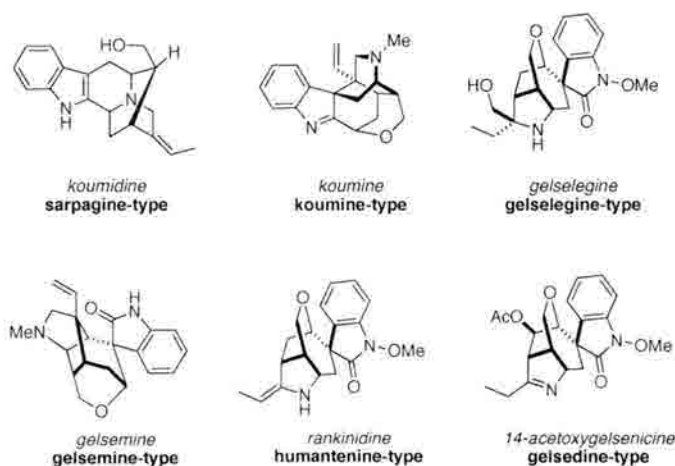


Figure 4: Representative members of the Gelsemium alkaloid family.

These classifications are made on the basis of the carbon skeleton arrangement, with the majority of these alkaloids known to date belonging to the humantenine- and gelsedine-type sub-families¹⁰. The principle alkaloid produced by *Gelsemium sempervirens*, gelsemine, was isolated in 1870 by Wormley, and its structure was solved by X-ray crystallography by Orgell in 1963^{11,12}. Since this time, many other related natural products have been isolated from the same plants, and have become targets for total synthesis in their own right on the basis of their complex molecular architecture.

Perhaps the most famous of this family of alkaloids is the aforementioned gelsemine, a member of the gelsemine subfamily. 14-Acetoxygelsenicine, the molecule which attracted our attention as a synthetic target, belongs to the gelsedine group of which gelsedine itself is the best known member. The structural complexity of these alkaloids has made them the target of many synthetic efforts, although 14-acetoxygelsenicine has yet to be successfully synthesized.

2.1.2 Biological Activity

Biological studies on specific members of the family are rare; the majority of research in this area appears to focus on the biological activity of the total alkaloidal extract from the plant¹³. These studies have shown that the alkaloidal fraction is highly toxic (in mice, oral doses of 25 mg/kg lead to 100% mortality, and interperitoneal injections of 7 mg/kg are also completely lethal), with death resulting from respiratory arrest^{13,14}. At lower doses, the plant acts as both an analgesic and a possible chemotherapeutic, being particularly effective against ovarian and breast cancer cell lines^{13,14}. However, the precise mechanism of action of either individual family members

or the alkaloidal extract as a whole remains unknown, although the biological activity of 14-acetoxygelsenicine was explored somewhat during the course of its isolation.

2.1.3 Isolation

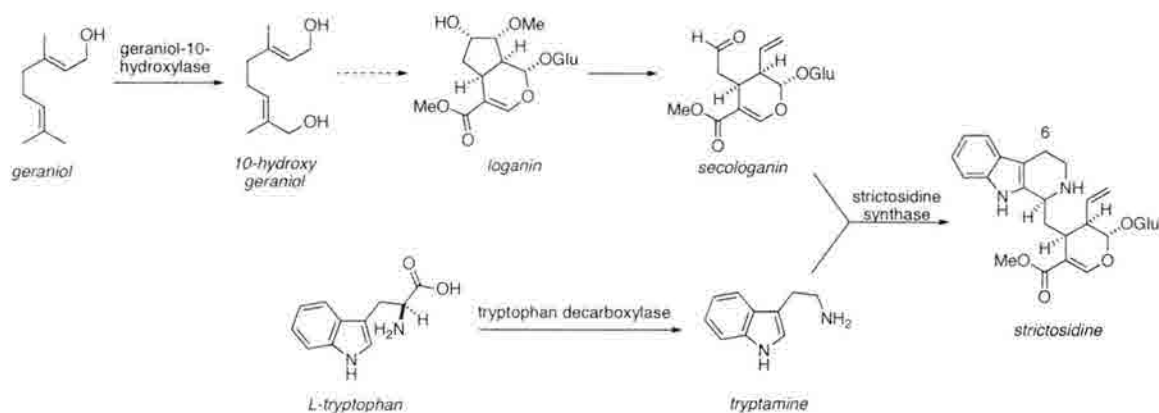
14-Acetoxygelsenicine was isolated in 2006 by Takayama and coworkers as a minor component of a mixture of 15 alkaloids extracted from the leaves of *Gelsemium elegans* Benth⁷. On the basis of UV absorption in conjunction with detailed NMR studies (¹H, ¹³C, HMBC and ¹H-¹H COSY), the structure shown in Figure 4 was assigned⁷. The isolated alkaloids were tested for biological activity, and it was reported that 14-acetoxygelsenicine displayed cytotoxic activity comparable to cisplatin against the A431 carcinoma cell line (EC₅₀ = 250 nM)⁷. However, it was later disclosed that the activity mentioned actually relates to another compound isolated from the same mixture - 14,15-diacetoxygelsenicine - while the activity of 14-acetoxygelsenicine was a much more modest 36 nM¹⁵. Although we are generally focused upon the synthesis of natural products with a higher degree of biological utility, we chose to continue with our efforts towards this molecule on the basis of its structure alone (discussed in more detail in the following chapter).

Given the somewhat scant reports on biological activity of these alkaloids, it is unsurprising that their mechanism of action remains largely unexplored. Overall, the attraction to these alkaloids is based upon their structures rather than any inherent biological use; according to Danishefsky, "[t]he degree of attention which has been lavished by many laboratories on total syntheses of gelsemine surely did not arise from any documented information suggesting that this alkaloid might have valuable properties."¹⁶

2.2 Proposed Biosynthesis

2.2.1 Biosynthesis of Strictosidine

The biosynthesis of the gelsemium alkaloids has been studied in somewhat more depth, leading to proposals of biosynthetic pathways. To the best of our knowledge, these remain unproven, although Sakai's proposal regarding the biosynthesis of gelsedine was upheld by his biomimetic synthesis following the same route². In large part, the proposed biosynthetic pathways are based upon a feeding experiment conducted in 1979 by Zenk and coworkers, which showed that 6-¹⁴C labeled strictosidine was incorporated into gelsemine in *Gelsemium sempervirens*¹⁷. This information has led to proposed biosynthetic pathways that rely upon strictosidine as a precursor. The biosynthesis of strictosidine has been extensively studied, and is shown below in Scheme 1^{18,19}.

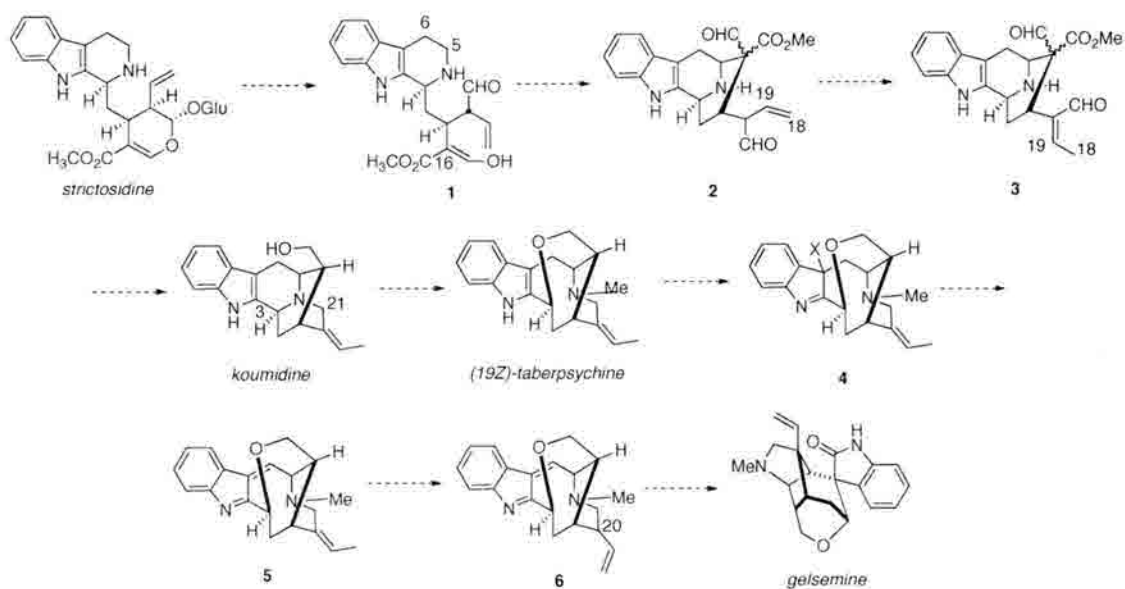


Scheme 1: Biosynthesis of strictosidine.

Following the synthesis of geraniol, enzyme mediated oxidation occurs to give 10-hydroxygeraniol. This compound is ultimately converted to secologanin which, through the action of strictosidine synthase, is combined with tryptamine to give strictosidine. The possible continuation of this pathway towards the Gelsemium alkaloids is discussed below.

2.2.2 Biosynthesis of the Gelsemium alkaloids

Knowing that strictosidine had successfully been incorporated into gelsemine, Ponglux et al. proposed a series of possible biosynthetic pathway for the gelsemium alkaloids²⁰. As seen below in Scheme 2, the pathway leading to the gelsemine subfamily is reasonably well supported by virtue of including previously isolated natural products as proposed intermediates. In this work, a total of three different pathways were proposed to account for the formation of all of the Gelsemium alkaloids known at the time (from the sarpagine, humantenine, gelsemine and gelsedine subfamilies), with each pathway branching from common intermediate **2**²⁰.

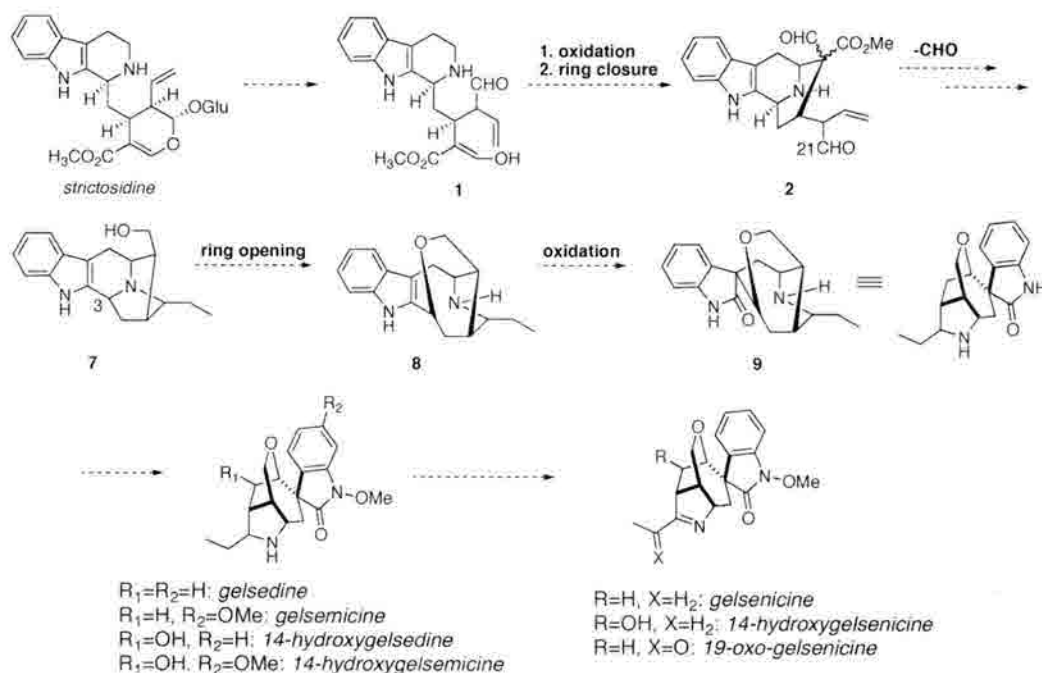


Scheme 2: Proposed biosynthesis of gelsemine.

Formation of the C5-C16 bond would give rise to **2**, and subsequent isomerization of the C18 double bond gives **3**. From this point, formation of the nitrogen-C21 bond gives the natural product *koumidine*, and N-C3 bond breakage with concomitant O-C3 bond formation would give *(19Z)-taberpsychine*. A proposed halogenation/elimination sequence would then set the stage for the final C6-C20 bond formation to give *gelsemine*.

While many synthetic studies of gelsemine have been undertaken, to the best of our knowledge, no biomimetic synthesis of this molecule has yet been accomplished. Currently, this particular proposal stands as the most reasonable pathway for the biosynthesis of gelsemine itself.

In the same work, Ponglux and co-workers also proposed a biosynthetic pathway for the gelsedine sub-family. While the route shown in Scheme 2 seems to have reasonable support for the gelsemine-type alkaloids, the proposal leading to the gelsedine sub-family lacks the benefit of known natural products serving as intermediates. In the proposal shown in Scheme 3, intermediate **2** would undergo the loss of the C21 aldehyde in addition to the formation of a nitrogen-C20 bond to ultimately give rise to **7**. Breakage of the N-C3 bond with formation of the O-C3 bond gives **8**, which would be oxidized to the oxindole to form the precursor to the gelsedine alkaloids.



Scheme 3: Proposed biosynthesis of gelsedine alkaloids.

While the Gelsemium alkaloids, including those of the gelsedine sub-family, have been the subject of many synthetic explorations, only one group has examined their biosynthesis in detail. Neither Ponglux's work nor Sakai's proposal (discussed below) included 14-acetoxygelsenicine as it had yet to be isolated; however, its similarity to gelsedine (which was included) suggests that perhaps they arise from a shared biosynthetic pathway. Gelsedine differs from 14-acetoxygelsenicine in its oxidation state at both C20 and C14. In 14-acetoxygelsenicine, C20 is oxidized to the imine and C14 bears the acetoxy substituent, while gelsedine contains an amine at C20 and is unsubstituted at C14 (Figure 5).

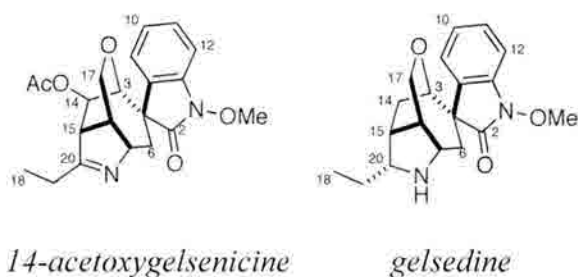
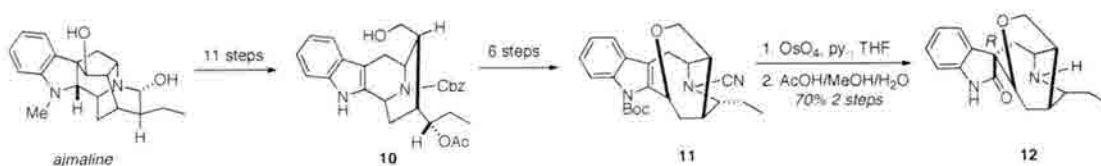


Figure 5: 14-Acetoxygelsenicine and gelsedine.

2.3 Biomimetic Syntheses of Gelsedine

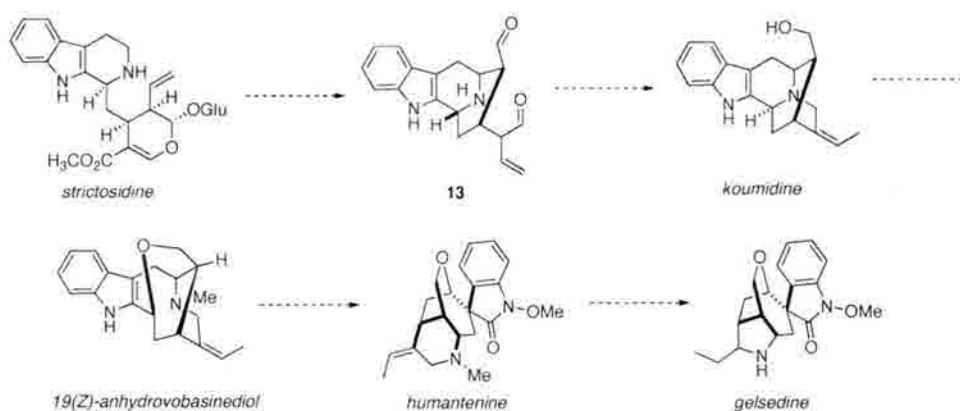
2.3.1 Attempts at Biomimetic Synthesis

Given the lack of supporting evidence for the biosynthetic proposal of the gelsedine-type alkaloids, Sakai and coworkers attempted a biomimetic synthesis of gelsedine in order to test this hypothesis. Following a preliminary study wherein they prepared several of the proposed intermediates, it was observed that this route gave the incorrect (*R*) stereochemistry at the quaternary center of the spirooxindole (Scheme 4)².



Scheme 4: Sakai's first generation approach to spirooxindole.

The oxindole shown with the incorrect (*R*) configuration (**12**) was the sole product of this sequence, isolated in 70 percent yield². In light of this finding, Sakai and coworkers devised a different biosynthetic proposal, as shown in Scheme 5.



Scheme 5: Sakai's revised biosynthetic proposal.

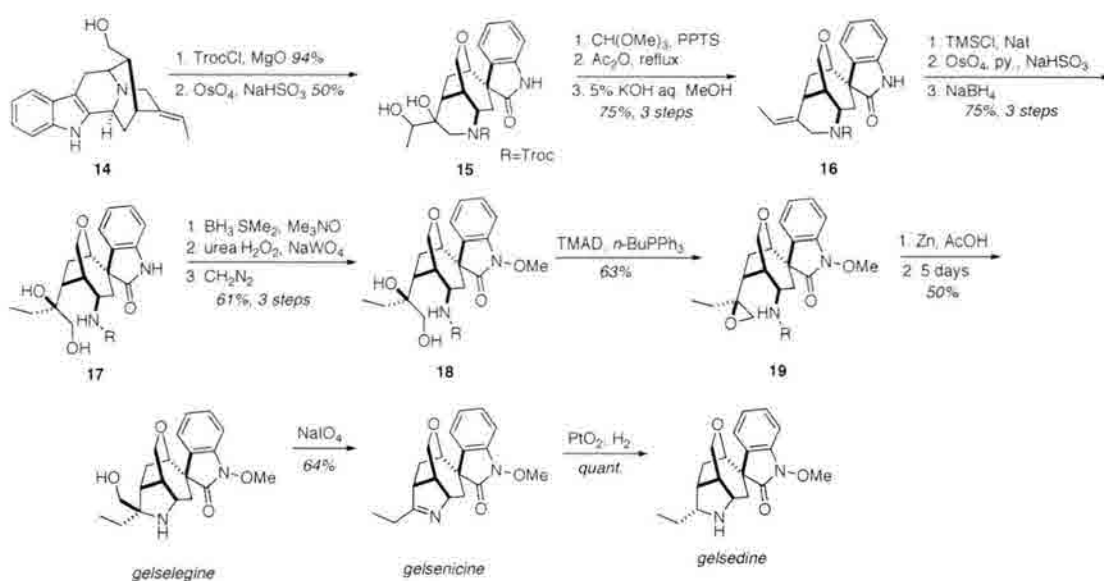
This sequence has the advantage over the previous proposal in that nearly all of the proposed intermediates are known in their own right, with only **13** remaining unknown²¹.

2.3.2 Biomimetic Synthesis of Gelsedine

With this new proposal in hand, Sakai et al. chose to pursue a total synthesis of gelsedine following the outline shown in Scheme 5. This approach proved to be successful, giving gelsedine in 22 steps from gardnerine, a commercially available indole alkaloid which can be converted to (*19E*)-koumidine (**14**) in seven steps (Scheme 6)²¹.

Following protection of amine **14**, treatment with osmium tetroxide gives the spirooxindole in 52 percent yield, with the correct (*S*) stereochemistry. The diol formed

in this reaction was removed to restore the olefin in a three step process. The alkene was then internalized to form the enamine with trimethylsilyl chloride in the presence of sodium iodide. Treatment with osmium tetroxide produces the diol, facilitating cleavage of the six-membered ring in **16**. Reduction of the resultant aldehyde with sodium borohydride gave **17** in 75 percent yield, and reduction of the oxindole to the indoline was accomplished with borane dimethylsulfide in 77 percent yield. Oxidation of the indole nitrogen and restoration of the oxindole was accomplished with a tungstate complex in the presence of peroxides, and methylation with diazomethane gave **18**. This substrate was then converted to gelselegine in two steps^{22,23}.



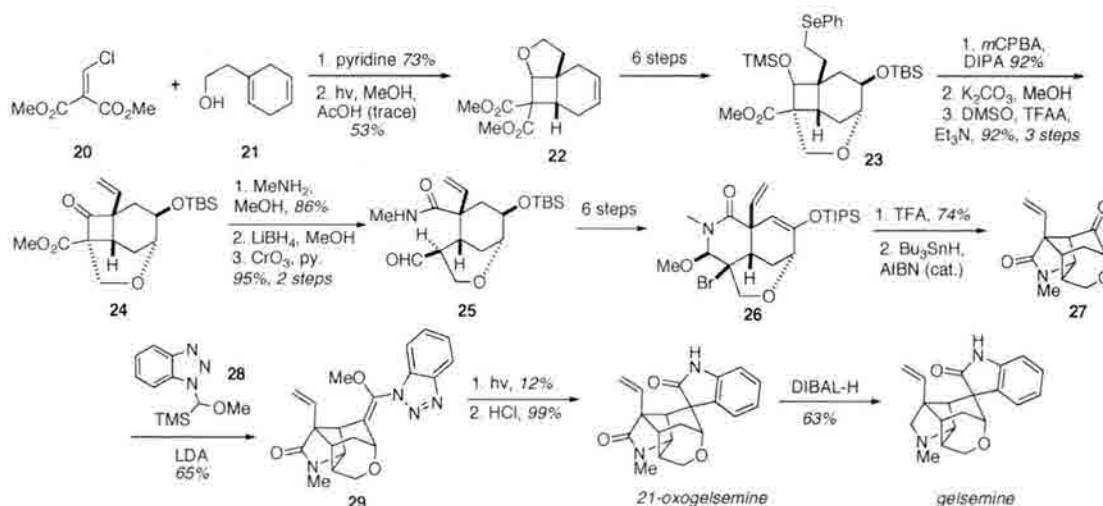
Scheme 6: Sakai's biomimetic synthesis of gelsedine.

In the course of pursuing this synthesis, Sakai et al. successfully accessed three different members of the gelsedine sub-family: gelselegine, gelsenicine and gelsedine, as shown above. This, in conjunction with the correct stereochemistry at the spirooxindole, appears to lend credence to their biosynthetic proposal.

2.4 Prior Syntheses of Selected Gelsemium Alkaloids

2.4.1 Syntheses of Gelsemine

As mentioned above, 14-acetoxygelsenicine has yet to be synthesized. However, other members of this family of alkaloids have been subjects of considerable synthetic attention, and the approaches used in these studies could, in principle, be applied to 14-acetoxygelsenicine as well. In particular, gelsemine has been the subject of numerous synthetic studies as well as several total syntheses. The complex three dimensional structure of this molecule has sponsored an enviable array of approaches, which are notable for the differing strategies used to access the carbon skeleton of the molecule¹⁶. Additionally, installation of the spirooxindole moiety has sponsored many creative and elegant approaches. Selected syntheses of gelsemine are shown below in Schemes 7-14.

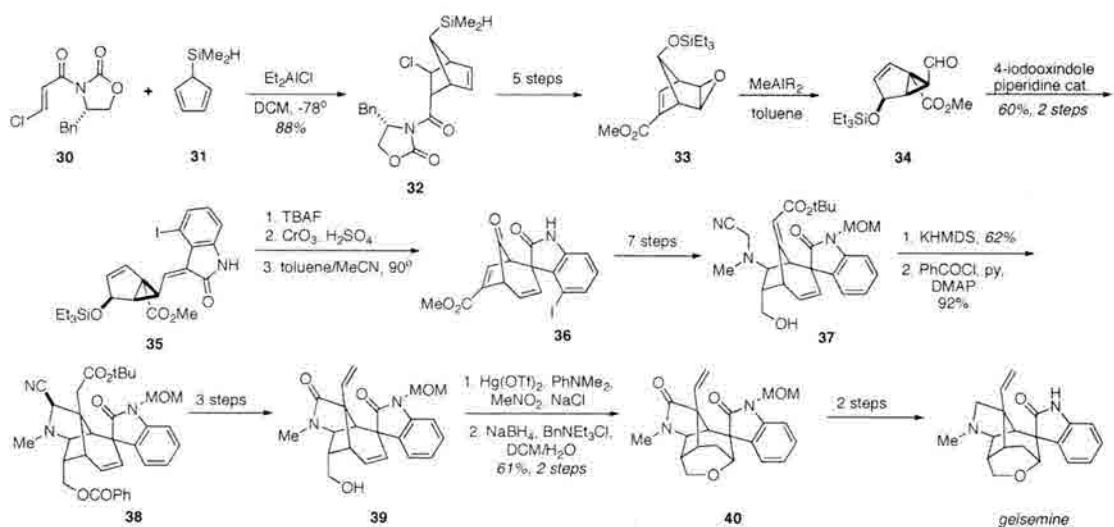


Scheme 7: Johnson's synthesis of gelsemine.

One of the first total syntheses of gelsemine was reported by Johnson and co-workers in 1994²⁴. Following a photoinduced cyclization to give tricycle **22**, reduction and tetrahydrofuran formation gave **23**. Installation of the requisite vinyl group and synthesis of amido ester **26** set the stage for a free-radical cyclization to give the

gelsemine core. A radical cyclization of benzotriazole **29** led to 21-oxogelsemine after hydrolysis, and reduction of the lactam gave gelsemine in 26 steps (Scheme 7).

Nearly six years later, Fukuyama and co-workers published their synthesis of gelsemine. This synthesis is particularly noteworthy, being to date the sole asymmetric synthesis of the natural product²⁵. Following a chiral auxiliary controlled Diels-Alder reaction, epoxide **33** was accessed in 5 steps. Treatment with methylaluminum bis(2,6-di-*tert*-butyl)-4-methylphenoxide gave cyclopropane **34**. Installation of the iodooxindole followed by deprotection, oxidation, and heating permitted the vinyl cyclopropane rearrangement, giving access the bicyclic core of gelsemine.

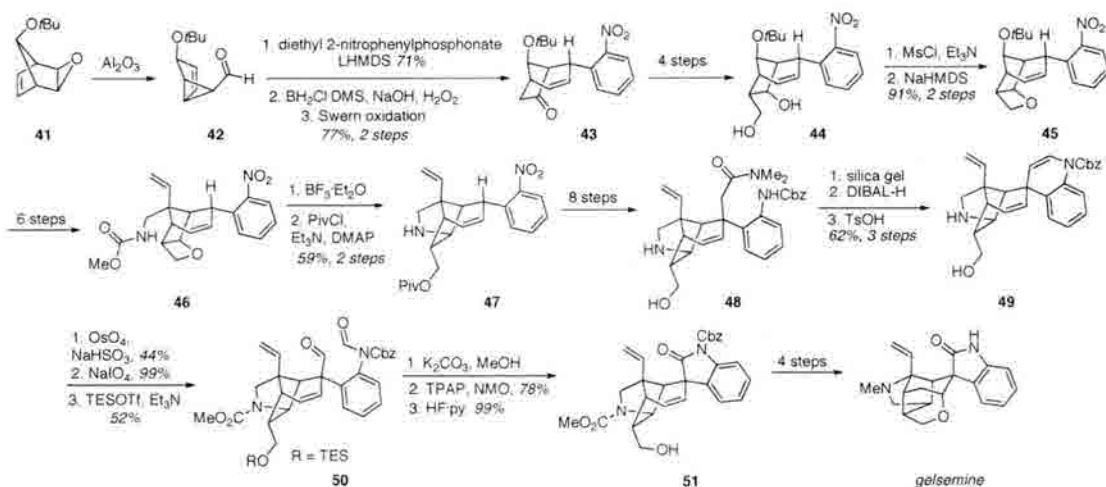


Scheme 8: Fukuyama's asymmetric synthesis of gelsemine.

Further manipulation of this compound led to **37**, which underwent a Michael addition to form the pyrrolidine ring. Oxymercuration followed by reductive demercuration gave the final ring, and deprotection followed by reduction of the *N*-methylactam gave gelsemine in 27 steps (Scheme 8)²⁵.

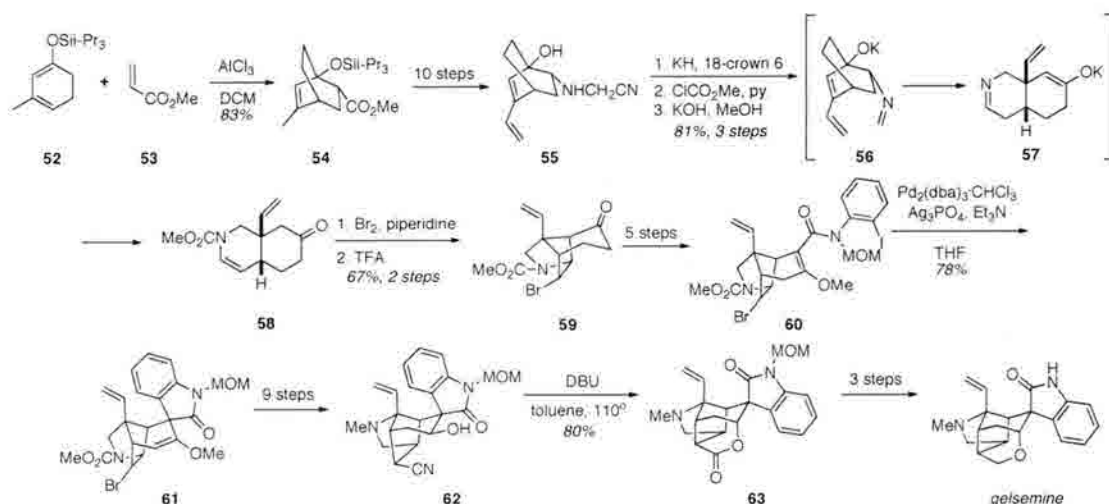
Two years later, a total synthesis of (+)-gelsemine was published by Danishefsky and co-workers (Scheme 9)²⁶. Following a similar rearrangement to that used by

Fukuyama, an oxetane ring was introduced to facilitate the installation of the pyrrolidine ring using Lewis acid catalysis.



Scheme 9: Danishefsky's synthesis of (+)-gelsemine.

In the original plans for this synthesis, the spirooxindole was to be directly accessed; however, due to severe steric strain, the five-membered ring was never observed. Installing the spirooxindole earlier in the synthesis via a Heck reaction was, in fact, successful. Unfortunately, it was found that the desired oxetane ring did not form in the presence of this completed portion of the molecule. In light of these findings, the six-membered ring (**49**) was manipulated by dihydroxylation followed by oxidative cleavage using sodium periodate to give dialdehyde **50**. Treatment with potassium carbonate in methanol effected deformylation of the aniline nitrogen with concomitant formation of the lactol, which was then oxidized to give the desired spirooxindole (**51**). Deprotection and formation of the final ring system using the same oxymercuration/demercuration sequence as shown above led to (+)-gelsemine in 39 steps.

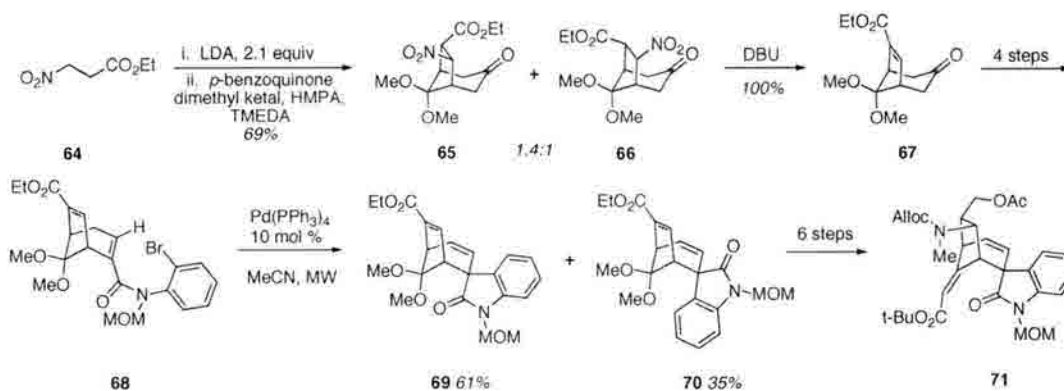


Scheme 10: Overman's synthesis of (+)-gelsemine.

A total synthesis of racemic gelsemine was published by Overman et al. in 2005 (Scheme 10). Of particular note in this work is the strategy used to install the spirooxindole through the use of an intramolecular Heck reaction²⁷. Additionally, an interesting approach to the core of the molecule was taken using an aza-Cope-Mannich strategy. Following the formation of bicycle **58**, bromination followed by acid catalyzed enol formation gave the tricyclic core of gelsemine²⁸.

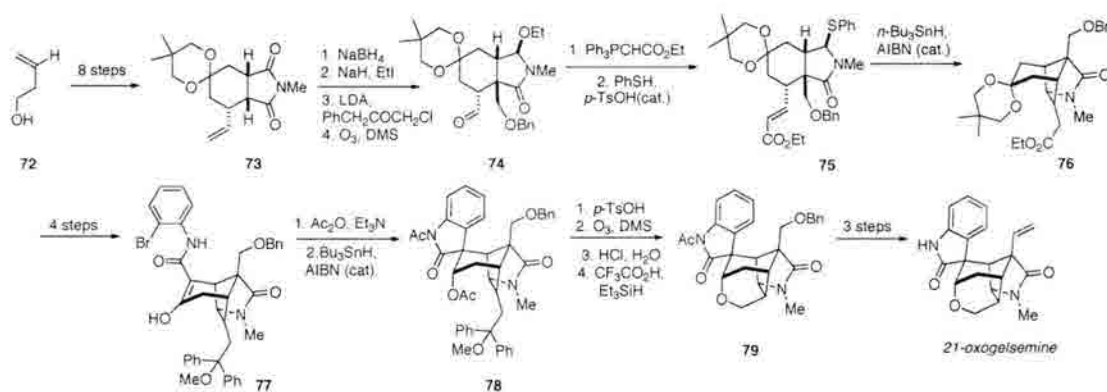
With the tricyclic core in hand, attempts were made towards the installation of the spirooxindole, which, while accessible in good yields, provided the incorrect stereochemistry at the quaternary center. While this was problematic, earlier studies by Hart and co-workers showed that this center could be epimerized by a retro-aldol/aldol process. Using this approach allowed for the synthesis of (+)-gelsemine to be completed in 35 steps.

In addition to the total syntheses discussed above, there have been numerous formal syntheses as well as various approaches to the gelsemine core. Recently, Aubé and coworkers disclosed their formal synthesis of gelsemine (Scheme 11).



Scheme 11: Aubé's formal synthesis of gelsemine.

Formation of the dianion from **64** permits a double conjugate addition to a quinone ketal to give **65** and **66** as an inconsequential mixture of diastereomers. Following base-mediated expulsion of the nitro group, four further steps were necessary to give the substrate for a Heck reaction (**68**) to provide oxindoles **69** and **70**. From this mixture of diastereomers, the major product (**69**) was carried on to **71**, constituting a formal synthesis of gelsemine in that earlier studies by Fukuyama and coworkers had shown that **71** could be converted into (+)-gelsemine in 13 further steps^{29,30}.

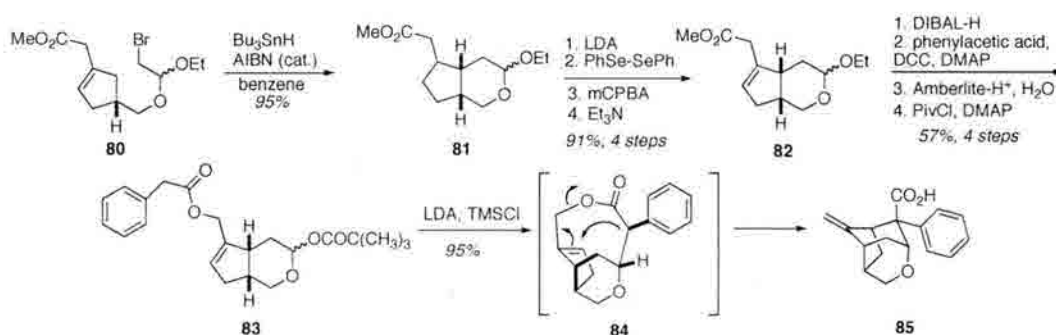


Scheme 12: Hart's formal synthesis of gelsemine.

Hart et al. also completed a formal synthesis of gelsemine utilizing a free radical cyclization approach³². Following a Diels-Alder reaction to access **73**, further manipulations gave thiol **75**. Previous studies by this group had shown that such a thiol,

when treated with AIBN and tributyltin hydride, would selectively form the α -acylamino radical³¹. Here, an intramolecular radical cyclization provided **76** in 87 percent yield³¹. The installation of the spirooxindole was also accomplished through a radical cyclization procedure to give 46 percent of the desired product. To complete the synthesis, installation of the final ring was accomplished through the formation of a hemiacetal, which was reduced to tetrahydropyran **79**. Installation of a vinyl group and removal of the acetate protecting group gave 21-oxogelsemine, which had previously been transformed into gelsemine (as seen above in work by both Johnson and Fukuyama)³².

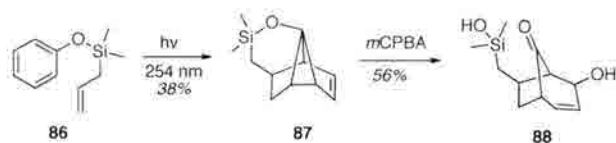
In one of the first approaches to gelsemine, Stork and co-workers chose an approach dependent upon a transannular Claisen rearrangement (Scheme 13)³³. Following a radical reaction to set the stereochemistry of the bicyclic system in **81**, a phenylacetic acid substituent was installed. Formation of the ester enolate led to the aforementioned Claisen rearrangement, giving the gelsemine core which could, in principle, be elaborated to gelsemine by taking advantage of the functional handles present in **85**.



Scheme 13: Stork's approach to gelsemine.

Finally, an interesting approach to the core of gelsemine involves the *meta* cycloaddition used by Penkett and co-workers (Scheme 14). It has been noted that

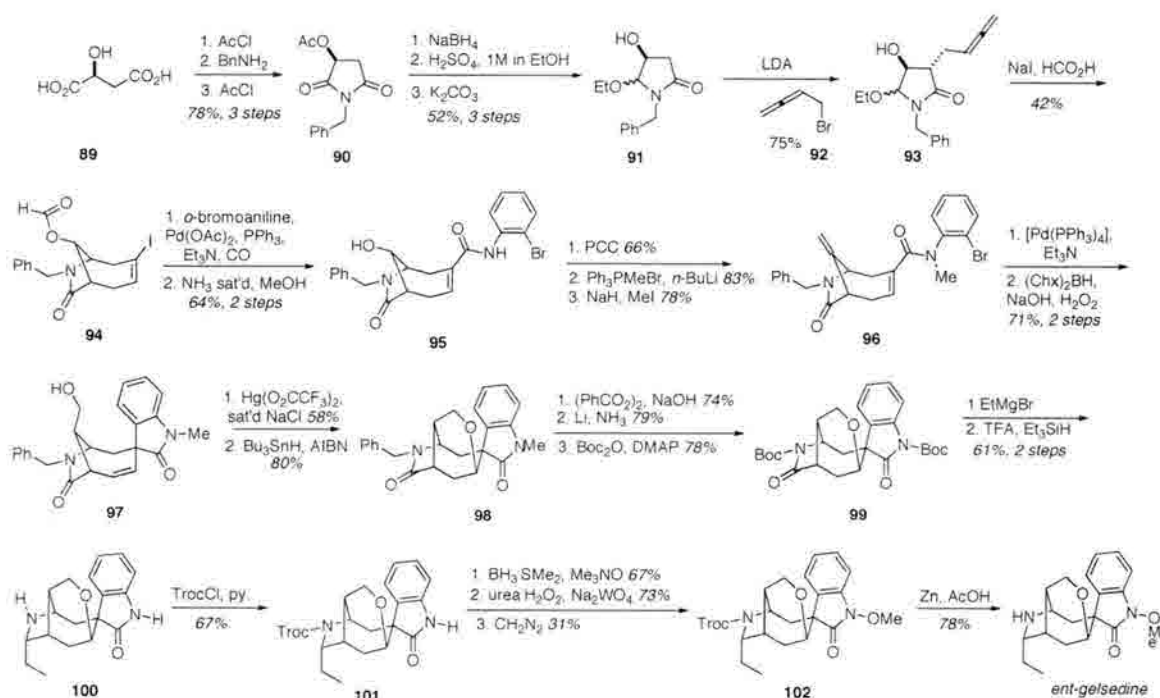
electron-donating groups lead to the regiochemical outcome shown in Scheme 14; therefore, an electron donating silicon tether was used in order to access the molecule shown³⁴. Although this compound was not taken on to form the natural product, it was thought that this substrate could be further elaborated to give gelsemine, in part, by using the secondary alcohol as a functional handle to introduce the requisite spirooxindole³⁵.



Scheme 14: Penkett's approach to the gelsemine core.

2.4.2 Hiemstra's Total Synthesis of *ent*-Gelsedine

In 1999, Hiemstra and coworkers completed an elegant total synthesis of *ent*-gelsedine, relying upon an iodide-promoted *N*-acylimminium ion cyclization as their key step (Scheme 15)³⁷.



Scheme 15: Total synthesis of *ent*-gelsedine.

Following the synthesis of allene **93**, treatment with sodium iodide in the presence of formic acid gave bicycle **94**, which underwent a palladium-catalyzed amino carbonylation to give **95**³. In the hopes that an sp²-hybridized carbon at the bridging position would be less sterically demanding, thereby permitting access to the desired spirooxindole stereochemistry, oxidation followed by Wittig olefination helped set the stage for the intramolecular Heck reaction. Following the successful synthesis of the spirooxindole, hydroboration/oxidation then gave **97**, and a mercury-mediated closure of the final six-membered ring using an approach similar to those discussed above gave the completed core of gelsedine. The exclusive formation of the six-membered ring (as opposed to the five-membered ring) was studied in somewhat more detail by this group. Molecular modeling suggested that the six-membered ring was considerably less sterically strained (41.85 kcal/mol) than the five-membered system (45.48 kcal/mol)³⁶. Following the introduction of the final ring system, several protecting group manipulations were accomplished, after which the *N*-methoxy group on the spirooxindole was installed. A final deprotection step gave *ent*-gelsedine in 27 steps^{36,37}.

2.5 Related Natural Products

2.5.1 Recent Additions to the Gelsedine Sub-Family

Newly isolated members of this group of the gelsemium alkaloids are of interest to us in the hopes of identifying related molecules that may also be accessible via our synthetic routes. Recently, three novel members of the gelsedine sub-family were isolated by Takayama and co-workers: gelsedilam, 14-acetoxygelsedilam and gelsefuranidine (Figure 6)³⁸.

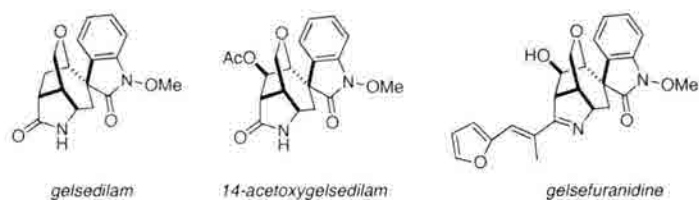
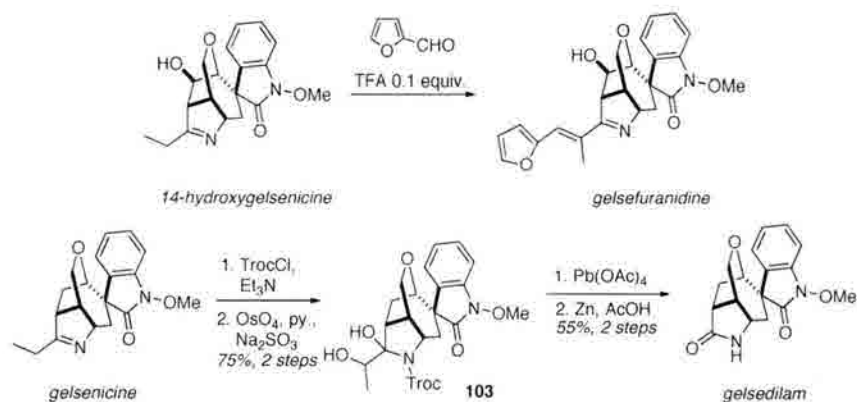


Figure 6: Recently isolated gelsedine-type alkaloids.

Interestingly, this group noted that gelsenicine could be converted to gelsedilam, and 14-hydroxygelsenicine to gelsefuranidine³⁸. These transformations suggest that perhaps 14-acetoxygelsedilam would also be available from 14-acetoxygelsenicine following the same route. In addition to our interest in 14-acetoxygelsenicine as a synthetic target in its own right, the possibility of designing a synthesis wherein we would be able to access related members of the family was attractive to us. The transformations shown below in Scheme 16 were therefore of great interest.



Scheme 16: Formation of gelsedilam and gelsefuranidine.

This varied and ever-growing family of alkaloids presents great opportunities for synthetic study. The complex molecular architecture of these compounds make them desirable synthetic targets; indeed, it was the three-dimensional structure of 14-acetoxygelsenicine which attracted our attention at the time of its isolation in 2006. The chemistry developed in the syntheses discussed above has broad applications, particularly

in the formation of strained cyclic systems and approaches to spirooxindole synthesis. Herein, we have discussed a sampling of the creative approaches towards these molecules and will now turn our attention to the efforts made in our laboratories.

Chapter 3: Towards the Total Synthesis of 14-Acetoxygelsenicine

3.1 Challenges and Synthetic Strategy

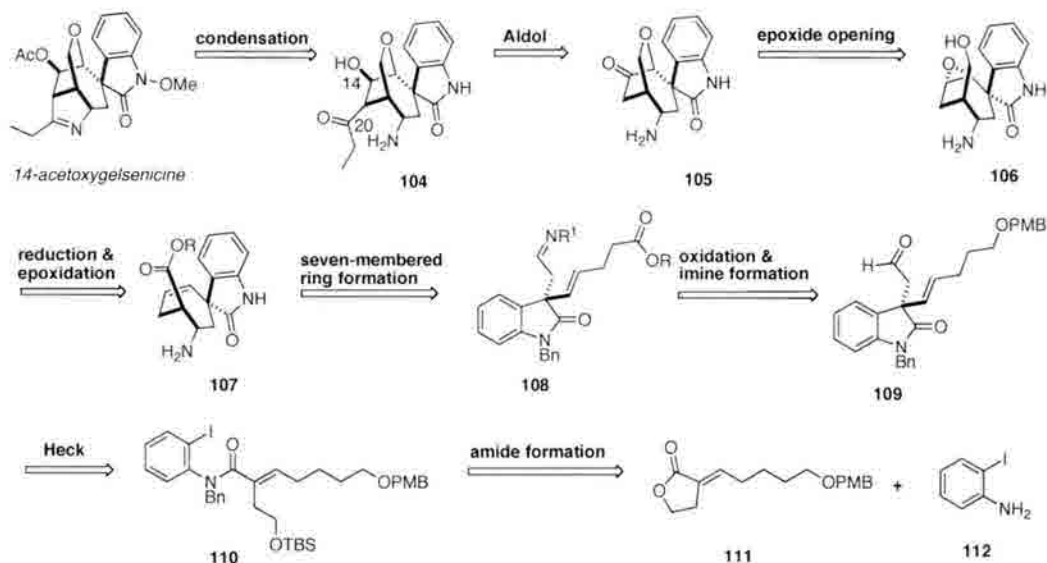
3.1.1 Synthetic Strategy

In designing the original approach, we wanted to achieve an asymmetric synthesis of 14-acetoxygelsenicine in which we could rely upon some of the methods discussed in the previous chapter, particularly with respect to the formation of the spirooxindole system. We foresaw several notable synthetic questions in accessing this molecule - specifically, the stereochemistry of the quaternary center on the spirooxindole would need to be addressed, installation of the methoxy group on the indole nitrogen would need to be explored, and formation of the seven-membered ring with appropriate functionality was seen as a significant challenge.

3.1.2 Retrosynthetic Analysis

In surveying the available literature on the subject, it appeared that the stereochemistry of the oxindole could be accessed via a Heck reaction using a chiral catalyst. The methoxy group on the indole nitrogen could be installed using the same strategy employed by Sakai and Hiemstra as previously discussed^{21,36}. Finally, we hoped to attempt an aldol-type reaction to close the seven-membered ring. The original retrosynthetic approach encapsulating these ideas is shown below in Scheme 17.

Following this route, the quaternary center of the spirooxindole would be installed through a Heck reaction early in the synthesis. The seven-membered ring would arise from the reaction of an ester enolate with an imine to give **107**, and the six membered ring would be formed by opening epoxide **106**.



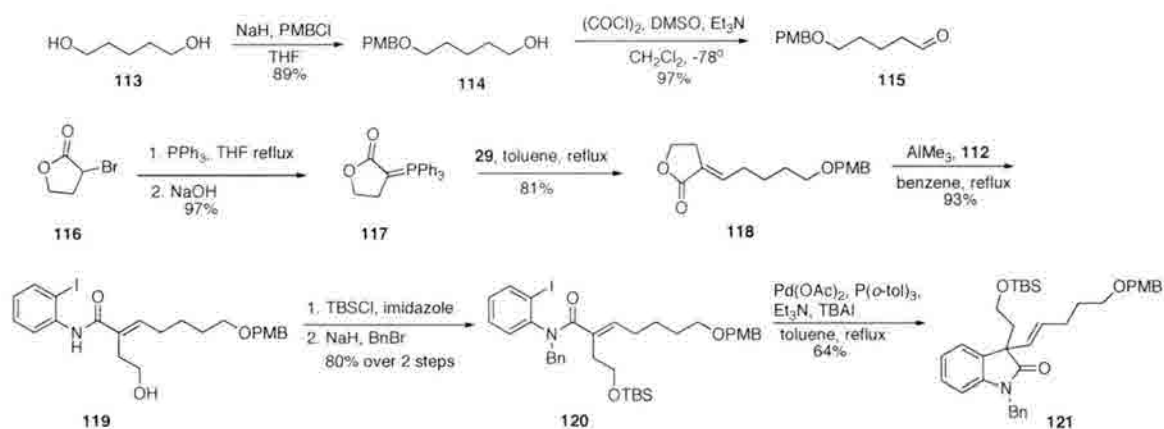
Scheme 17: First generation retrosynthesis.

The final steps of the synthesis would be fairly straightforward, with a condensation reaction to close the remaining five-membered ring, followed by the aforementioned known procedure for oxidation and methylation to give the methoxy group on the oxindole nitrogen³⁹.

3.1.3 Synthesis of the Spirooxindole

In the forward direction, the synthesis proceeded smoothly, as shown in Scheme 18. Monoprotection of pentane diol as the PMB ether followed by Swern oxidation gives aldehyde **115** in excellent yield. The subsequent Wittig reaction with easily accessible ylide **117** gives substituted lactone **118**, which is opened with iodoaniline using Weinreb's conditions⁴⁰. It has been shown that substrates that are unsubstituted at the

amide nitrogen do not cyclize in the Heck reaction; therefore, this nitrogen was protected using benzyl bromide⁴¹. This step, in addition to protection of the free alcohol as the silyl ether, gives the precursor to the Heck reaction, which itself proceeds in 64 percent yield to give substituted oxindole **121**. For the purposes of these early attempts, the synthesis was conducted in a racemic fashion, with the thought that a chiral catalyst could be employed during the Heck reaction at a later date in order to set the stereochemistry at the quaternary center.

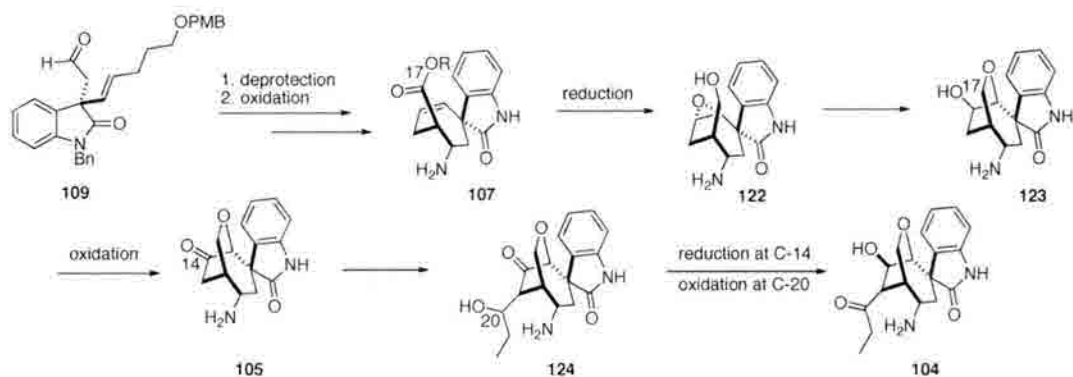


Scheme 18: Synthesis of the spirooxindole.

The Heck reaction did appear to give the desired product; however, an inseparable by-product was present. While we felt that optimization of chromatographic conditions would obviate this concern, more worrisome was the fact that the reaction appeared to give the *trans*-olefin, from which it would not be possible to create the proposed seven-membered ring. These issues caused us to re-evaluate our proposed synthetic route: in looking forward from this point, it became clear that the retrosynthesis shown in Scheme 17 (above) was perhaps not the most efficient approach towards this molecule.

The inefficiencies of this synthesis are particularly clear with regard to carbons 14, 17 and 20 (shown in Scheme 19, below). The oxygen atom at carbon 17 is introduced

as the protected alcohol, which must be deprotected and oxidized in order to close the seven membered ring.



Scheme 19: Problems with first generation approach.

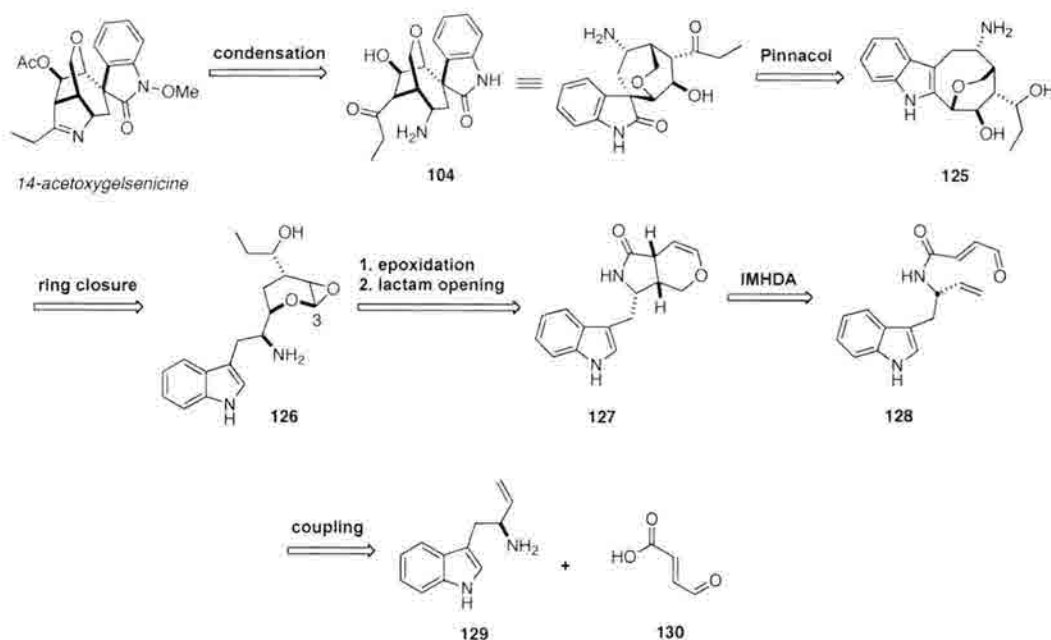
Following these reactions, the ester present in **107** must be reduced to the alcohol to close the six membered ring present in **122**. Of greater concern are the oxygen atoms at carbons 14 and 20. The C14 oxygen is introduced via epoxide **122** to give alcohol **123**, which must then be oxidized to ketone **105** in order to facilitate aldol addition of propanal. Finally, the same C14 oxygen must be reduced back to the alcohol in order to give **104**. Furthermore, the oxygen atom at C20 would be installed from propanal to give the alcohol, which must be re-oxidized following aldol addition to give the necessary ketone shown in **104**. The repeated oxidation and reduction sequences were deemed sufficient reason to seek a new, more efficient approach.

3.2 Second Generation Approach

3.2.1 New Synthetic Design

In order to avoid the problems discussed above, a new retrosynthetic approach to 14-acetoxygelsenicine was devised, as shown in Scheme 20. While the final steps of the synthesis remain the same, it was envisioned that the oxindole would be installed via a

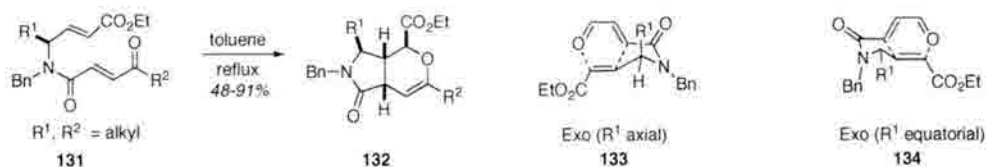
Pinacol rearrangement of **125**. The eight-membered ring would be formed by nucleophilic attack of the indole C2 position onto the epoxide at C3 (gelsedine numbering, shown below). The substrate for this epoxidation could arise from an intramolecular hetero-Diels Alder reaction to form the fused rings shown in **127**. The substrate for the Diels-Alder reaction would in turn arise from a peptide coupling between tryptophan derivative **129** and carboxylic acid **130**. In addition to involving fewer redox operations, this route would be five planned steps shorter (20 steps overall, with the longest linear sequence being 16). This route would bring a unique approach to the synthesis of this type of alkaloid in addition to providing access to other natural products in the family (discussed in more detail below).



Scheme 20: Revised retrosynthetic approach.

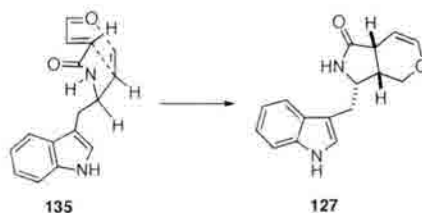
Searching the literature revealed little precedent for the proposed intramolecular hetero Diels-Alder reaction, although the few existing examples seemed promising. In

particular, studies by Murray and co-workers on a similar system are shown below in Scheme 21⁴².



Scheme 21: Diels-Alder cyclization models.

This work showed that, while the *trans* ring juncture is accessible, the *cis* ring juncture appears to be preferred under thermodynamic conditions. In all cases, only the *exo* cyclization product was observed, with the *cis*-fused product (as determined by NOE studies) being the sole product of the reaction⁴³. In our specific case, we were unsure about the stereochemical outcome of the reaction with regard to the position of the indole moiety (R^1). We hoped that the indole would be located *trans* to the hydrogens at the ring juncture, as opposed to the *cis* relative stereochemistry observed by Murray. Modeling experiments (PC model) suggested very little difference between the two outcomes (0.33 kcal/mol difference, favoring the undesired diastereomer). The stereochemistry, therefore, remained an open question, although we felt that cyclization according to the model shown below was possible.



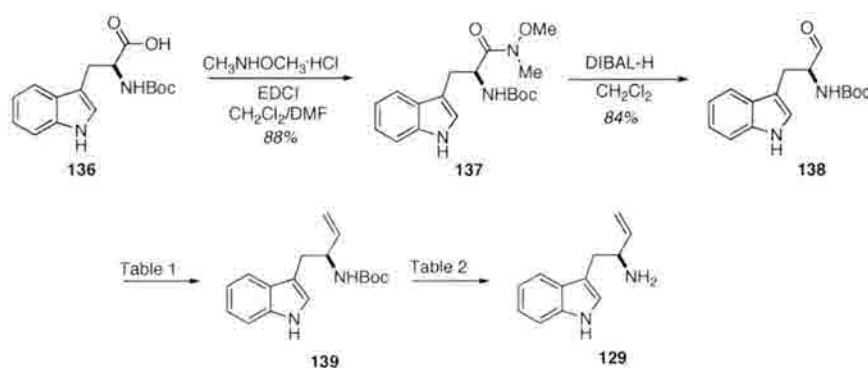
Scheme 22: Model for proposed Diels-Alder.

In our retrosynthetic design, we also hoped to make the synthesis as versatile as possible so as to allow synthetic access to different members of the gelsedine family in

addition to 14-acetoxygelsenicine. Using the route shown, we should be able to access 14-acetoxygelsedilam and gelsefuranidine through the syntheses discussed in Chapter 1.

3.2.2 Synthesis of the Tryptophan Derivative

Work on this approach began with the synthesis of tryptophan derivative **129**, which was accessed in four steps from *N*-Boc-L-tryptophan as shown below (Scheme 23).



Scheme 23: Synthesis of Tryptophan Derivative **129**.

Conversion of **138** to **139** proved to be somewhat problematic (Table 1). Initial attempts following literature precedent resulted in very low yield⁴⁴. Eventually, conditions were found (final line, Table 1) which worked satisfactorily on a small scale⁴⁵.

Table 1: Wittig olefination.

Wittig salt	Base	Solvent	Conditions	Result
H ₃ CPh ₃ PBr 1.2 equiv	<i>n</i> -BuLi 1.2 equiv	THF	15 hrs, R.T.	trace
H ₃ CPh ₃ PBr 4 equiv	<i>t</i> -BuOK 3 equiv	THF	15 hrs, R.T.	trace
H ₃ CPh ₃ PBr 4 equiv	<i>t</i> -BuOK 3 equiv	THF	3 hrs, R.T.	20%
H ₃ CPh ₃ PI 1.2 equiv	<i>t</i> -BuOK 1.2 equiv	THF	3 hrs, R.T.	trace
H ₃ CPh ₃ PBr 4 equiv	<i>t</i> -BuOK 3 equiv	THF	1 hr, R.T.	35%
H ₃ CPh ₃ PBr 4 equiv	<i>t</i> -BuOK 3 equiv	DME	1 hr, R.T.	33%
H ₃ CPh ₃ PBr 5 equiv	<i>t</i> -BuOK 4 equiv	THF	1 hr, R.T.	33%
H ₃ CPh ₃ PBr 3.5 equiv	KHMDS 3.67 equiv	THF	13 min, -78 ^o	30-79%
H ₃ CPh ₃ PBr 3.5 equiv	LiHMDS 3.67 equiv	THF	13 min, -78 ^o	trace
H ₃ CPh ₃ PBr 3.5 equiv	NaHMDS 3.67 equiv	THF	13 min, -78 ^o	92%

Although successful on a ~100 mg scale, when scale-up of this reaction was attempted, yields dropped precipitously. It may be that the presence of toluene (KHMDS is available in toluene in 0.5 M concentration) in the reaction causes this problem; if the starting material were only sparingly soluble in toluene, it stands to reason that with increased volume of toluene in the reaction mixture, yields would suffer. With this in mind, bases available in THF were tried. While LiHMDS did not prove fruitful, NaHMDS in THF gave product in excellent yield.

Deprotection of **139** also presented difficulties (Table 2). Initial attempts using standard conditions (TFA in dichloromethane or thermal deprotection) failed. Deprotection was ultimately effected with Ohfuné's conditions (TBSOTf followed by KF), as shown in the last line of Table 2, in a reaction that was successful on gram scale⁴⁶.

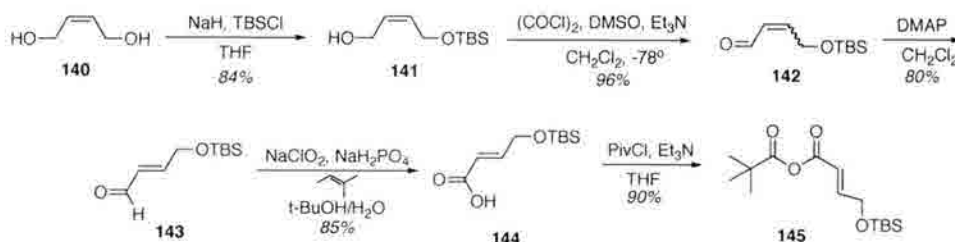
Table 2: Boc deprotection of **139**.

Reagent	Conditions	Result
TFA 2 equiv	CH ₂ Cl ₂ , 2 hrs, R.T.	N.R.
TFA 6.5 equiv	CH ₂ Cl ₂ , 2 hrs, R.T.	N.R.
TFA 130 equiv	CH ₂ Cl ₂ , 2 hrs, R.T.	N.R.
TFA neat	2 hrs, R.T.	N.R.
-----	MeCN, 10 min, 180 ^o (μ-wave)	N.R.
-----	MeCN, 30 min, 180 ^o (μ-wave)	N.R.
TBSOTf 1.1 equiv	CH ₂ Cl ₂ , 3 hrs, -78 ^o to R.T.	51%
TBSOTf 2.1 equiv	CH ₂ Cl ₂ , 3 hrs, -78 ^o to R.T.	98%

The route illustrated above provides access to the desired tryptophan derivative in four steps and 67 percent overall yield, in reactions that are successful on gram scale. With a route to this tryptophan derivative, attention could then be given to the butenoic acid component of the molecule to access both of the proposed coupling partners.

3.2.3 Synthesis of the Butenoic Acid Derivative

This synthesis proceeds smoothly, with the desired butenoic acid derivative being accessed in 5 steps from *cis*-butenediol. The diol is monoprotected to give **141**, which is oxidized using a Swern oxidation to give aldehyde **142** as a mixture of the *cis*- and *trans*-isomers. This mixture was then isomerized to **143** by stirring for 24 hours with DMAP, and then oxidized to the acid via a Pinnick oxidation to give **144** (Scheme 24).



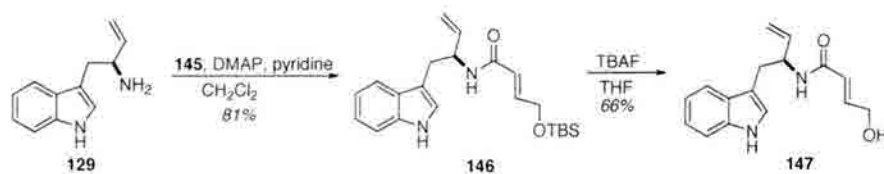
Scheme 24: Synthesis of butenoic acid component.

This route gave access to the desired unsaturated carboxylic acid (**144**) in 55 percent overall yield. For reasons discussed below, it was transformed into mixed anhydride **145** to complete this portion of the synthesis.

3.3 Attempted Formation of the Diels-Alder Substrate

3.3.1 First Generation Approach to Diels-Alder Substrate

To complete the synthesis of the Diels-Alder substrate, fragments **144** and **129** would be coupled; however, attempts using standard peptide coupling conditions were unsuccessful. Given this result, **144** was further elaborated to the more reactive mixed anhydride **145** using pivaloyl chloride. Treatment of anhydride **145** and tryptophan derivative **129** with DMAP and pyridine gave coupled product **146**, which was then deprotected to give the free alcohol (Scheme 25).



Scheme 25: Synthesis of the Diels-Alder substrate.

Although the deprotection proceeds in fairly modest yield, these conditions were selected as other attempts to deprotect using different conditions failed, and we chose to test the remaining synthetic steps prior to extensive optimization.

With alcohol **147** in hand, only one step remained in order to access the desired Diels-Alder substrate, and we turned our attention to the oxidation of this primary alcohol. These attempts met only with limited success: Swern conditions led to complex mixtures of products, TEMPO oxidation using TCC as the stoichiometric oxidant resulted in an intractable mixture of products of which one may have been the undesired chlorination of the indole. Dess-Martin periodinane provided material in extremely small amounts as part of a mixture of numerous, unidentified by-products. Furthermore, we were concerned about the feasibility of the proposed Diels-Alder reaction on this particular substrate. As discussed above, the systems tested by Murray and coworkers involved an amide nitrogen with more substitution; presumably the tertiary amine assists in forcing the existence of the necessary rotamer for cyclization.

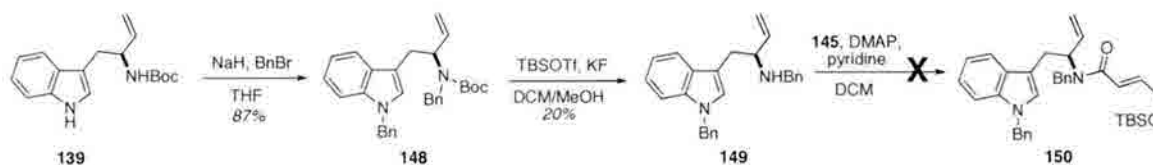
In light of these concerns, attention was turned to the selection of an appropriate protecting group. Specifically, protection of the amide nitrogen with an alkyl protecting group was desirable, as this type of substrate has been shown to undergo successful cyclization^{42,43}. In order to use as few protecting group manipulations as possible in the course of the synthesis, at this point we decided against protection of the indole nitrogen.

3.3.2 Efforts Towards Protection of the Primary Amine

In this first approach, protection of the primary amine via reductive amination was attempted. Treatment with anisaldehyde in conjunction with either sodium cyanoborohydride or sodium borohydride to provide the PMB-protected nitrogen did not provide product. While following the reaction by ^1H NMR to investigate whether the imine was present (an aliquot was removed from the reaction following treatment with anisaldehyde but prior to introduction of sodium borohydride), results showed that the imine had not formed. Care was taken during these studies to ensure that water was excluded from the NMR sample; the fact that the desired product was not formed also suggests that the imine did not form. The reason for this was unclear; sterically, the primary amine seems fairly unhindered, and the basic work-up following Boc deprotection suggests that the nitrogen should not be protonated and its nucleophilicity should be as expected.

Due to the difficulties experienced with the reductive amination approach, the next attempts were made to protect this nitrogen as a benzyl amine using benzyl bromide in conjunction with base. Here, deprotonation of the nitrogen would improve nucleophilicity at this site, if this were indeed the problem. This presented another issue in that the high pKa of the primary amine would dictate fairly basic harsh conditions. In light of this concern, it was decided that protection of carbamate **139** with benzyl followed by Boc deprotection would be preferable. However, the pKa of the carbamate (~24 in DMSO) is such that the indole nitrogen would most likely also be deprotonated (pKa ~21 in DMSO)^{47,48}. Nonetheless, given the apparent necessity for protection of the

amine, the strategy was pursued with the understanding that the *bis*-benzyl protected compound was the most likely outcome (Scheme 26).



Scheme 26: Further attempts at protection and coupling.

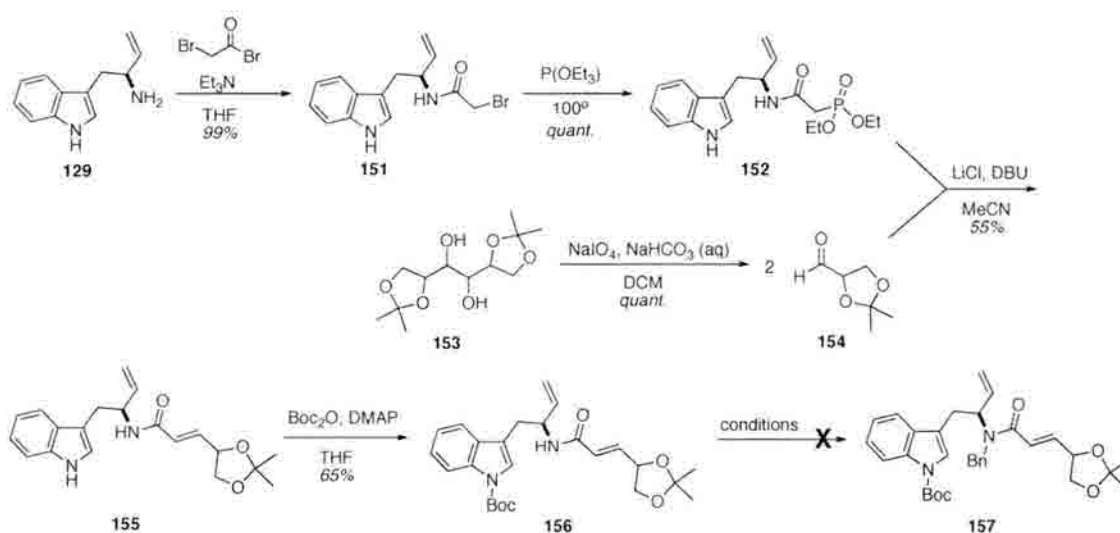
As shown above, the *bis*-benzyl protected substrate was accessed, although subsequent Boc deprotection using Ohfuné's conditions resulted in lower yields than those seen above. However, all attempts at deprotection using TFA or thermal conditions failed, and we therefore decided to continue with this mode of deprotection despite the low yield in order to test the remaining steps, starting with the addition of **145** to form the requisite amide bond. Unfortunately, attempts to add the mixed anhydride to the secondary amine failed, most likely due to steric encumbrance from the benzyl group.

3.3.3 Revised Approach to the Diels-Alder Substrate

At this point, we chose to re-evaluate this portion of the synthesis in order to address the following issues: 1) the oxidation of the primary alcohol had proven difficult in earlier attempts, and 2) it appeared that protection of the indole nitrogen might be unavoidable. We therefore chose to pursue a strategy wherein the indole nitrogen would be protected with an electron withdrawing group in the hopes of lessening the possibility of side reactions involving the C3 position of the indole ring. Given the difficulties discussed above in the formation of the amide bond with the benzyl-protected substrate, we decided that the amide bond would be formed prior to any attempt at protection. This strategy would also provide a route towards selective protection of the indole nitrogen

due to the lessened nucleophilic character of the amide nitrogen and its lower (~ 22 in DMSO) pKa, should deprotonation prove necessary⁴⁸.

Furthermore, as seen below in Scheme 27, a different strategy was adopted for the construction of the amide bond and access to the hetero Diels-Alder substrate. In this approach, a Horner-Wadsworth-Emmons reaction was used to install the double bond⁴⁹. The aldehyde for this conversion was generated from racemic bis-protected mannitol which was treated with sodium periodate⁵⁰. In addition to the advantages of this approach discussed above with respect to protecting group manipulations, the use of this protected diol would obviate the need for the problematic oxidation step discussed above.



Scheme 27: Revised approach to the Diels-Alder substrate.

Here, following removal of the acetal, treatment with sodium periodate would provide the requisite aldehyde. Prior to aldehyde formation however, the aforementioned protection steps were necessary. While treatment of **155** with acetic anhydride gave only starting material, treatment with Boc anhydride in the presence of DMAP gave **156** in 65% yield. We could then turn our attention to protection of the amide nitrogen; however, attempts to protect with benzyl failed under all attempted conditions (Table 3).

Table 3: Attempted benzyl protection.

Electrophile	Base	Additive	Solvent	Conditions
BnBr 1 equiv	NaH 1 equiv	-----	THF	0° to RT; 15 h
BnBr 1.2 equiv	NaHMDS 1 equiv	-----	THF	0° to RT; 15 h
BnBr 1.2 equiv	NaHMDS 3 equiv	-----	THF	0° to RT; 48 h
BnBr 1.2 equiv	NaHMDS 1 equiv	TBAI, 0.1 equiv	THF	0° to RT; 48 h
BnBr 1.2 equiv	KHMDS 1 equiv	-----	THF	0° to RT; 15 h
BnBr 1.2 equiv	NaH 3 equiv	TBAI, 0.1 equiv	DMF	0° to RT; 15 h

Original attempts with sodium hydride appeared not to effect deprotonation; therefore, NaHMDS was used. A strong color change suggested that deprotonation was occurring, but the desired product was not observed. We therefore attempted to form the more reactive benzyl iodide *in situ* by adding tetrabutylammonium iodide, although this did not change the outcome. The fact that a more reactive electrophile did not lead to introduction of the benzyl group caused us to think that the problem lay with the nitrogen. Specifically, perhaps the sodium counterion was forming a tight ion pair with the deprotonated nitrogen making the lone pair unavailable and thus preventing addition of the electrophile. To test this hypothesis, attempts were made using KHMDS, although this approach also proved unsuccessful. Finally, we changed solvents to DMF in the hopes of improving the nucleophilicity of the nitrogen; however, the outcome remained the same.

Given these results, we attempted protection with other electrophiles. A survey of the literature showed that *para*-methoxybenzyl, SEM and BOM had been used in somewhat similar systems^{51,52}. In the case of this specific substrate however, it did not appear to be possible to accomplish these transformations. When these trials proved to be unsuccessful, we investigated the feasibility of adding methyl iodide. While we did not wish to use methyl as a protecting group due to the anticipated difficulties with its

ultimate removal, we did wish to see whether it was possible to add a sterically non-demanding electrophile at this position, although in the event, the desired product was not observed (Table 4).

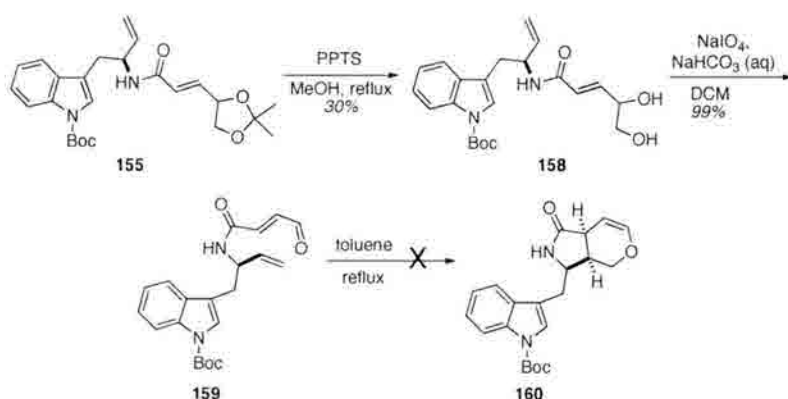
Table 4: Further protection attempts.

Electrophile	Base	Solvent	Conditions
PMBBr 1.2 equiv	NaH 1 equiv	DMF	0° to RT; 2 h
PMBBr 1.2 equiv	NaHMDS 1 equiv	DMF	0° to RT; 2 h
BOMCl 1.4 equiv	NaHMDS 1 equiv	DMF	0° to RT; 5 h
SEMCl 1.2 equiv	NaHMDS 1 equiv	DMF	0° to RT; 15 h
MeI 1.2 equiv	NaHMDS 1 equiv	DMF	0° to RT; 15 h

These results suggested that protection at this stage of the synthesis would not be possible. Color changes upon the addition of base and a noticeable exotherm suggested that deprotonation may have occurring; however, it was not possible to isolate identifiable products from the complex mixtures generated from these reactions. Although it was not clear where the problem lay in these reactions, it may be that the conjugated system in which the anionic nitrogen could participate precludes the addition of an electrophile.

3.3.4 Attempted Diels-Alder Cyclization

At this point, although we were uncertain of a successful outcome given the apparent necessity of further substitution at the amide nitrogen, we chose to attempt the Diels-Alder reaction in the hopes that protection might prove to be unnecessary. Deprotection of the acetonide proceeded in modest yield to give the desired diol, and the proposed oxidative cleavage gave the desired aldehyde in nearly quantitative yield in a very clean reaction. This represented a significant improvement from the previously used deprotection/oxidation sequence (Scheme 28).

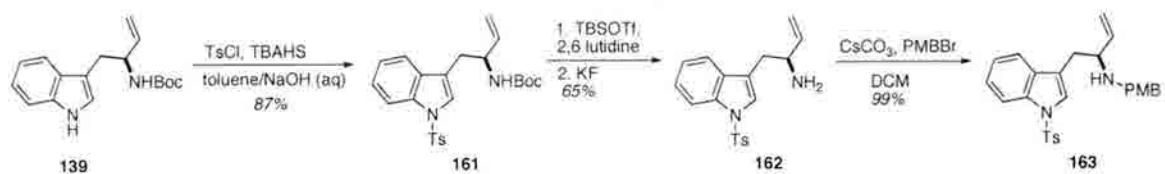


Scheme 28: Attempted Diels-Alder reaction.

Unfortunately however, as seen above, the attempted cyclization resulted in no reaction after sixteen hours, and continued stirring resulted in decomposition. This result supported our original hypothesis regarding the necessity of protection at this nitrogen. Given the difficulties encountered in the protection of amide **155**, this would require redesigning this portion of the synthesis.

3.3.5 Revised Protecting Group Strategy

In order to avoid protection of amide **155**, protection of this nitrogen would need to take place at an earlier stage of the synthesis. Although addition of a mixed anhydride to the protected amine was unsuccessful, we felt that the new Horner-Wadsworth-Emmons route might prove fruitful on such a substrate. We again chose **139** as the best point to effect the protection of this nitrogen, but this choice necessitated a change in protecting group strategy given that the indole nitrogen had also been protected using Boc. However, we felt that selective protection of the indole nitrogen would be possible given the aforementioned difference in pKa between the two nitrogens. In order to keep an electron-withdrawing group on the indole nitrogen, we therefore pursued the route shown in Scheme 29, using tosyl at this position.

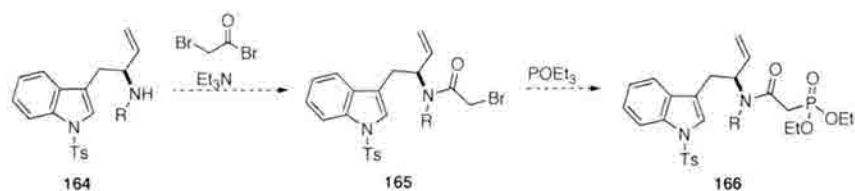


Scheme 29: Successful protecting group strategy.

Original attempts using somewhat less exotic conditions to install the tosyl group (sodium hydride in conjunction with either tosyl chloride or tosyl anhydride) resulted in low yields, although the conditions shown resulted in clean reactions with excellent yields⁵³. Following deprotection of the Boc group, the nitrogen was originally protected with *para*-methoxybenzyl; this change from our earlier work using benzyl was prompted by concerns over the eventual removal of the benzyl group from an amide nitrogen.

3.3.6 Attempted Synthesis of Key Intermediate

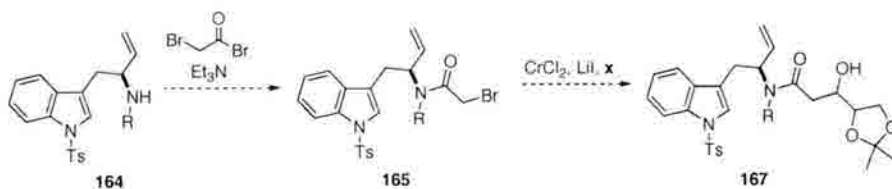
Our earlier attempts to add a mixed anhydride to a similar secondary amine had failed; however, it was hoped that the addition of bromoacetyl bromide, being less sterically demanding, might be successful. This particular electrophile was chosen for its possible use in two different strategies: the Horner-Wadsworth-Emmons route shown in Scheme 30, wherein following introduction of bromoacetyl bromide, treatment with triethylphosphite would give the desired Horner-Wadsworth-Emmons substrate.



Scheme 30: Proposed synthesis of HWE substrate.

Given our earlier success with a similar substrate following this route, we were hopeful that this would yield the desired product, although the attraction to this method was its possible application to a different strategy as well. Specifically, the Reformatsky-

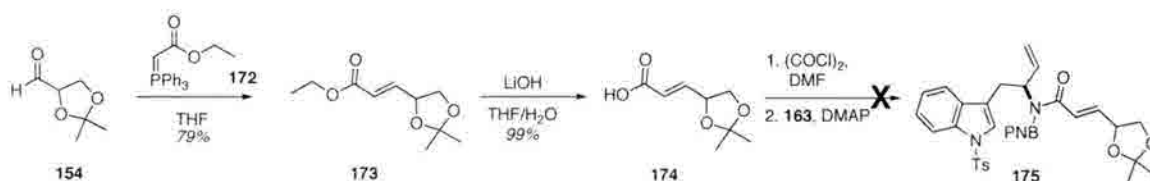
type reaction shown in Scheme 31 would also involve treatment of **164** with bromoacetyl bromide, following which exposure to chromium chloride could give the amide enolate to allow introduction of the desired masked aldehyde⁵⁴.



Scheme 31: Proposed Reformatsky reaction.

Several attempts to introduce bromoacetyl bromide to **164** were unsuccessful, resulting in recovery of the starting material. It may be that the added steric bulk of the secondary amine is sufficient to prevent the reaction from occurring; recovery of the starting material shows that the conditions do not cause decomposition pathways to arise. It also seemed possible to us that the electronics of the system might have changed with the introduction of the electron-rich protecting group, although an alkyl group was still preferable at this position. We were reluctant to introduce an electron withdrawing group at this position for fear that, due to the conjugated nature of the substrate, this would result in a less reactive diene for the Diels-Alder reaction which was already planned with a somewhat unreactive dienophile. However, we did want to change the electronics of the system to see whether a different group on the nitrogen would help. In an attempt to satisfy both of these requirements, as well as the expected ease of removal later in the synthesis, we selected *para*-nitrobenzyl. Unfortunately, this substrate gave the same result. In light of this outcome, we chose to again re-evaluate our strategy as discussed below.

strategy to capitalize on this success, as shown in Scheme 34.



Scheme 34: Attempted acid chloride addition.

Following olefination of aldehyde **154**, saponification gave **174**, which was treated with oxalyl chloride and dimethylformamide to give the corresponding acid chloride. Addition of this acid to *para*-nitrobenzyl protected amine **163** led to a complex mixture of products. Wondering whether the acidic conditions used to form the acid chloride might have resulted in deprotection of the isopropylidene acetal and contributed to this issue, we also synthesized the acid chloride from a more robust cyclohexyl protected diol, although the addition was again unsuccessful. While we had hoped that the additional steric demands of this particular substrate in comparison to acetyl chloride or bromoacetyl bromide would not be too great for the reaction to proceed, it appears that this was not the case.

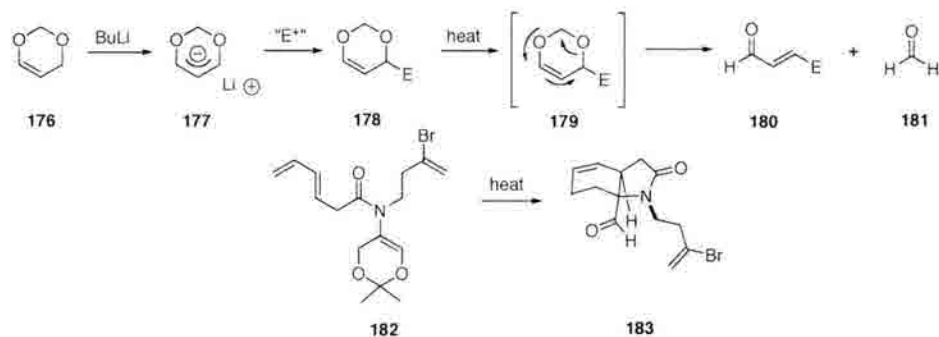
3.4 New Ideas and Concluding Remarks

3.4.1 Possible Future Directions

At this point, we decided to cease our efforts towards 14-acetoxygelsenicine and turn our attention to a different project (discussed in the following chapters), although there are clearly possibilities for future attempts on this molecule. The proposed Diels-Alder based approach remains an attractive one, as this would constitute a unique approach to the gelsemium alkaloids as well as being one of a handful of examples in the

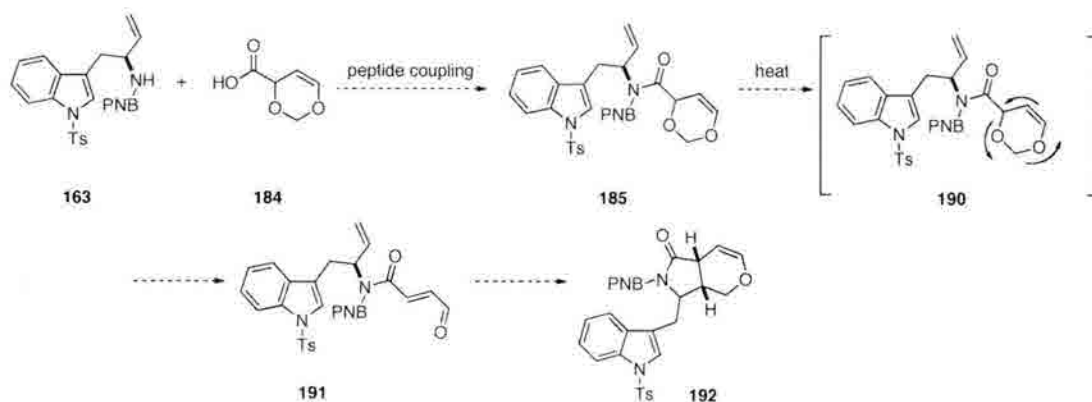
literature of this type of Diels-Alder reaction. However, it is clear that our current method would need further revision.

In this light, one possibility may be the type of retro-cycloaddition/cycloaddition reactions used to great effect by Funk and coworkers.



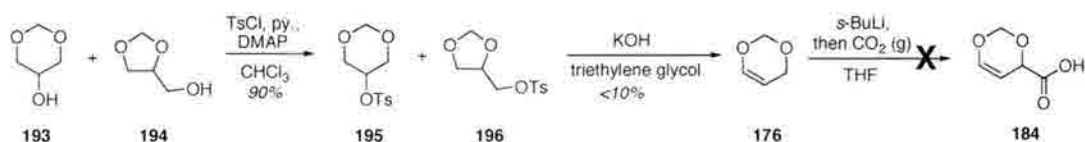
Scheme 35: Retro-cycloaddition/cycloaddition sequence.

As seen above, a 1,3 dioxin can be deprotonated to create the allylic anion, which in turn can be trapped by an electrophile⁵⁵. This substituted dioxin, when exposed to heat, unmask an α,β -unsaturated aldehyde with concomitant loss of formaldehyde. This sequence, along with a relevant example from the literature, are shown in Scheme 36⁵⁶. In the context of 14-acetoxygelsenicine, this proposed route would follow the sequence shown below (Scheme 36).



Scheme 36: Proposed retro-cycloaddition/cycloaddition route.

It seems that a simple peptide coupling reaction would be sufficient to join the two halves. If not, we felt that there was also reason to believe that the deprotonation of the amide followed by introduction of an appropriate electrophile would work in this particular case. We thought that we might achieve success here due to the fact that the amide is not in conjugation with the olefin contained in the masked diene; perhaps this change from our earlier efforts would lead to success. Preliminary work along this route is shown below in Scheme 34, ending with the attempted formation of acid **184**.



Scheme 37: Preliminary work towards proposed new route.

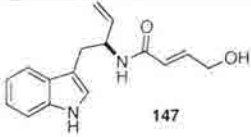
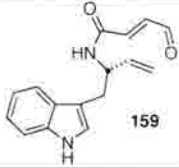
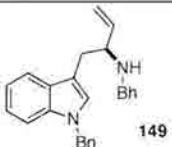
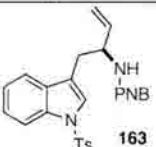
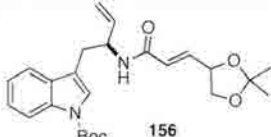
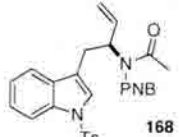
In this attempt, we followed a literature precedent for the elimination of the tosylate. However, yields were extremely low, hovering closer to ten percent than the reported 40 percent⁵⁷. We did attempt the carbonylation reaction as well, although this proved unsuccessful. A survey of the literature shows that deprotonation with *sec*-butyllithium is somewhat uncommon, with *tert*-butyllithium being the reagent of choice in most reports. It therefore seems reasonable that this change could lead to a successful outcome. Following installation of the acid, peptide coupling could join the two halves, and the route proposed in Scheme 36 could be attempted.

3.4.2 Summary of Progress

Despite our efforts, access to 14-acetoxygelsenicine has remained elusive. Our original synthetic design was replaced early on due to several severe flaws, notably repeated manipulations of oxidation states. Following the development of a second, more efficient approach, we found considerable difficulty in accessing an appropriately

substituted substrate for the proposed intramolecular hetero Diels-Alder reaction which we had hoped to use as the centerpiece of our synthetic approach. We have, however, been able to access a variety of compounds in the pursuit of this substrate. These molecules, along with the difficulties encountered in their further manipulation, are summarized below in Table 5.

Table 5: Summary of Diels-Alder precursors.

Substrate	Problem	Substrate	Problem
 147	Unable to oxidize	 159	Unable to cyclize
 149	Unable to add electrophile	 163	Unable to add electrophile
 156	Unable to protect	 168	Unable to form enolate

It would seem that the difficulty in further manipulations of these substrates does not lie with one single factor. In the case of secondary amide **159**, it is possible that the desired rotamer population was not accessed so as to allow cyclization to occur. In accessing substrates with further substitution however, we have met with numerous roadblocks. In the cases of **149** and **163**, it seems probable that the bulky protecting groups chosen interfered with the addition of an electrophile. We have attempted to change the reactivity and sterics of the electrophiles in question by using free acids, mixed anhydrides and acid halides. However, when we have met with success in these efforts (as in **147**, **156** or **168**), we have been unable to effect further substitution on the amide nitrogen. We believe that this may be an electronic problem in that this nitrogen

lone pair appears to be particularly unavailable. Specifically, it may be that the conjugated nature of this system is causing the problem. This, then, is why we feel that the ideas proposed in the previous section may have a better chance of success.

3.4.3 Concluding Remarks

Herein, we have described our studies towards the total synthesis of 14-acetoxygelsenicine. Although we elected not to pursue this synthesis further, the idea remains an attractive one as it would open avenues towards other members of the family, notably, 14-acetoxygelsedilam and gelsefuranidine in addition to 14-acetoxygelsenicine. We have developed a more efficient retrosynthesis towards this goal, and have experimented with a variety of approaches. Although these efforts have not been successful, perhaps the work presented here may provide a starting point for further efforts towards this molecule.

Chapter 4: Histone Deacetylase Inhibitors

4.1 Introduction

4.1.1 Overview of Histone Deacetylase Enzymes

Our group has also been interested in the synthesis of small molecules that act as histone deacetylase (HDAC) inhibitors. Here, an overview of synthetic efforts towards selected HDAC inhibitors is presented, including some of the previous work from our laboratories (excerpted from our review on this topic)⁵. Prior to a discussion of synthetic work, a brief overview of the role of HDAC enzymes in normal and diseased cells is presented below.

HDAC enzymes play an important role in chromatin remodeling and therefore in the regulation of gene expression^{58,59}. Dysfunction of HDAC enzymes has been linked with a variety of human diseases, including cancer, sickle cell anemia, rheumatoid arthritis and cardiac hypertrophy^{60,61,62}. With the discovery of molecules that act as HDAC inhibitors (HDACi), a substantial amount of insight into the function of these enzymes has been gained. Furthermore, particularly with respect to cancer, HDACi are extremely promising drug targets. Through the study of naturally occurring HDACi and their synthetically derived analogs, much progress has been made towards this goal.

In mammalian cells, DNA is packaged into chromatin, a highly condensed structure which limits access to the DNA by transcription factors⁵⁸. In the first step of this packaging, DNA is wound around a histone octamer^{59,63}. This interaction is made

favorable by virtue of positively charged lysine residues on the histone proteins, which attract the negatively charged DNA backbones⁶⁴. This strong electrostatic interaction renders the DNA inactive with respect to transcription, as cellular machinery responsible for transcription cannot access the DNA in this condensed, or closed, state^{65,66}. When transcription is required, the interaction must be lessened to permit access to the DNA. Histone acetyl transferase (HAT) installs an acetyl group onto the ϵ -nitrogen of lysine residues, neutralizing their positive charge and attenuating the interaction between the DNA and the histone^{64,67}. Once replication has been completed, HDAC enzymes remove the *N*-acetyl group from the lysine residue, restoring positive charge to the histone and returning the DNA to its inactive state^{67,68,69}.

There are currently eighteen known HDAC enzymes which are divided into four classes on the basis of their structural homology with yeast proteins^{70,71}. Class I enzymes (HDACs 1,2,3 and 8) are Zn^{2+} dependent, as are class II (HDACs 4,5,6,7, 9 and 10) and class IV (HDAC 11).^{65,69,72,73} In contrast, class III enzymes (SirT1-7, also known as Sirtuins) are NAD^+ dependent, and appear to be resistant to molecules capable of inhibiting class I and II enzymes; the class III enzymes will therefore not be mentioned further here^{63,65,74}. Class I and II isoforms differ with respect to both their size and catalytic domains, as well as their localization within the cell. Class I HDACs tend to be smaller (49-55 kDa) than the multidomain class II enzymes (80-131 kDa)⁶⁶. Class I isoforms share sequence homology in the catalytic domain located at the N-terminus, while the class II enzymes have a catalytic domain on the C-terminus, with an N-terminal adapter domain not seen in the class I HDACs^{58,75}. The two classes share a 390 amino acid region of homology within the deacetylase core⁷⁶. These differences suggest that the

classes possess distinct functions; notably, while class I HDACs are ubiquitously expressed and confined to the nucleus, class II enzymes display tissue-selective expression and shuttle between the nucleus and cytoplasm^{59,73,77}.

A further complication arises from the classification of each of these enzymes as *histone* deacetylases, which would tend to suggest that histone proteins are the only substrate for these enzymes. However, emerging research has shown that HDACs can act to deacetylate many non-histone proteins, including hormone receptors, chaperone proteins, transcription factors and cytoskeletal proteins^{68,77}. While the specific function of individual isoforms remains unclear, it has been noted that aberrant HDAC activity is associated with cancerous cells^{67,78,79,80}. HDAC 1, for example, appears to be upregulated in both prostate and gastric cancers, while HDAC 3 is overexpressed in lung cancers⁶⁷. In general, the class I enzymes appear to play a role in survival and proliferation of cancer cells, while class II, notably HDAC 8, may be responsible for tumorigenesis^{67,77,81,82}. This link between HDAC enzymes and cancer has led to a search for molecules that can function as HDAC inhibitors in the pursuit of possible cancer therapeutics.

4.2 Acyclic Histone Deacetylase Inhibitors

4.2.1 Background

Much of what is currently known with respect to the structure and function of HDAC enzymes has arisen from the study of molecules which act as HDAC inhibitors (HDACi); in fact, the first HDACs were originally isolated by affinity chromatography using a naturally occurring HDACi, trapoxin⁸³. HDACi have been shown to inhibit tumor progression, and are generally responsible for an antiproliferative effect⁷⁵.

Treatment with HDACi results in death of transformed cells through several different mechanisms: apoptosis via extrinsic or intrinsic pathways, mitotic catastrophe/cell death, autophagic cell death, senescence, and reactive oxygen species (ROS) facilitated cell death⁷³. Interestingly, normal cells appear to be resistant to the effects of HDACi, unlike their transformed counterparts.^{77,84,85} Many different naturally occurring HDACi are known; here, these molecules have been divided into two classes: acyclic small molecules and cyclic or bicyclic depsipeptides or peptides.

4.2.2 Acyclic Histone Deacetylase Inhibitors

The earliest known HDACi fall into the first category: acyclic small molecules. Of the naturally occurring HDACi in this class, perhaps the best known is trichostatin A (TSA, Figure 7). Furthermore, the sole FDA-approved HDACi, SAHA (marketed as Zolinza by Merck Pharmaceuticals) belongs to this class. SAHA is not a naturally occurring molecule, but rather was found through extensive surveys of small polar molecules capable of inhibiting HDAC enzymes⁷¹.

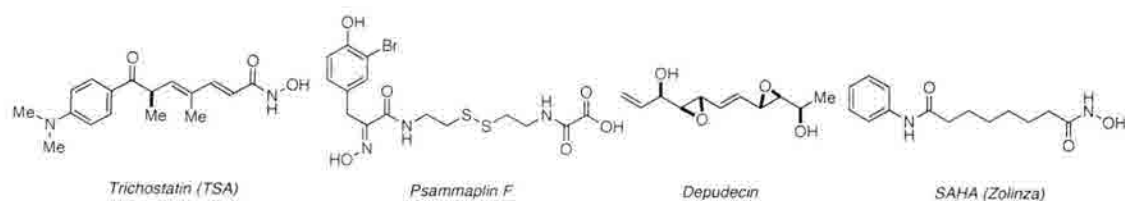


Figure 7: Selected acyclic HDACi.

TSA was isolated in 1976 from *Streptomyces hygroscopicus*, and identified as an HDAC inhibitor by Yoshida and colleagues in 1995^{86,87}. Research on this natural product has divulged many details with respect to the structure and function of HDAC enzymes. Notably, the crystal structure of HDLP (HDAC-like protein) was solved in 1999 by Finnin and coworkers⁷⁶. HDLP shares 35% sequence homology with human HDAC1;

importantly, identity is seen within the active site⁷⁶. These crystallographic studies showed a narrow channel $\sim 11\text{\AA}$ in depth, narrowing to a diameter of $\sim 7.5\text{\AA}$ at its narrowest point; at the bottom of this channel, a Zn^{2+} cation is coordinated to two aspartic acid residues, one histidine residue and a water molecule^{68,76}. In addition to providing information about the general structure of the enzyme, the crystal structure was also solved with bound TSA, giving rise to a model explaining the function of the enzyme (Figure 8)^{68,88}.

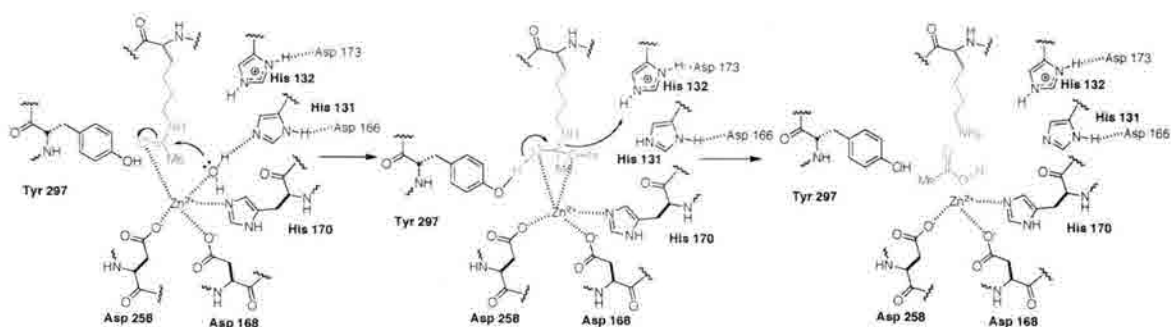


Figure 8: Proposed mechanism of action of Zn^{2+} -dependent HDACs.

It has been proposed that an acetylated lysine residue (shown in red) coordinates with the zinc cation in the active site. Formation of a tetrahedral intermediate by nucleophilic attack of the water molecule follows, after which the intermediate collapses to release a molecule of acetic acid and the free, deacetylated lysine residue.

The crystal structure containing a bound TSA molecule suggests that this HDACi acts as a substrate mimic, blocking access to the enzyme by the acetylated lysine residues on the histone tails⁷⁶. The cap region (Figure 9, blue) interacts with amino acid residues surrounding the rim of the channel to the active site, the linker region (Figure 9, black) lowers a zinc-binding arm through the hydrophobic channel, and the zinc-binding moiety (Figure 9, red) displaces the water molecule and coordinates to the cation.

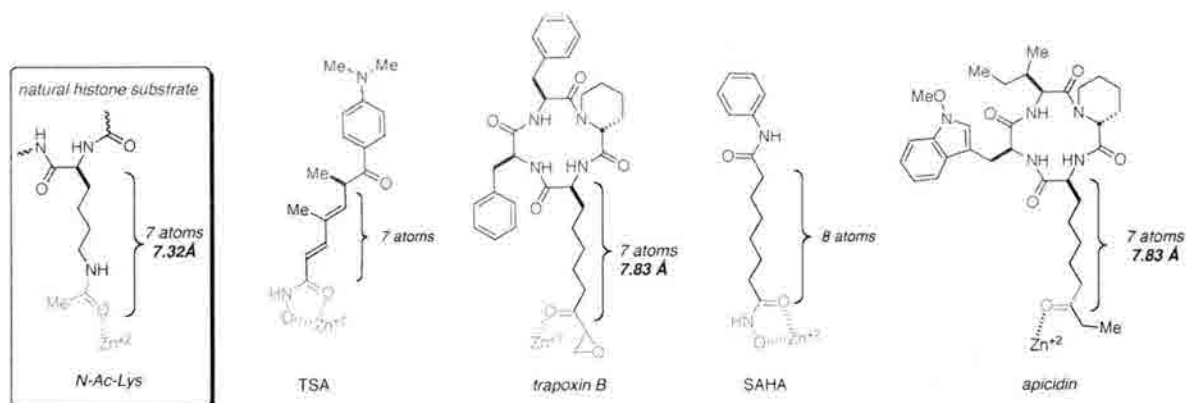
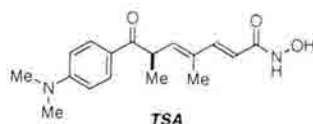


Figure 9: HDACi pharmacophore: cap region in blue; linker in black; zinc-binding moiety in red.

As is shown in Figure 9, this pharmacophore model of HDACi three regions is a general and useful classification in order to understand structure-activity relationships⁶⁸. Some of the earliest research in this area focused on derivatives of TSA, namely creating analogs with variance in both the zinc-binding and linker regions. Initial studies (prior to crystallographic data) focused on variance in linker length in an effort to determine the optimal distance between the cap and zinc binding regions (Table 6)^{89,90}.

These studies and others point to a 5-6 methylene unit as being the most effective with respect to HDAC inhibition^{64,68}. These data also suggest that bulkier cap regions may give rise to increased biological activity. With respect to the zinc-binding functionality, the hydroxamate moiety is quite common in naturally occurring HDACi; however, this functional group is considered unattractive for druggable compounds due to difficulties associated with its synthesis, as well as possible toxicity and low stability^{64,78}. For these reasons, other possibilities have been sought; in the studies mentioned above, numerous carboxylic acid compounds were tested, but all showed significantly attenuated biological activity (Table 6)⁸⁹.

Table 6: Biological data for TSA analogs and SAHA.

Cap region	Linker	Zn ²⁺ -binding arm	IC ₅₀ nM Maize HD-2	IC ₅₀ nM HDAC1
TSA	-----	NHOH	3	NT [†]
(4-Me ₂ N)PhC(O)NH	-(CH ₂) ₄ -	NHOH	2000	NT
(4-Me ₂ N)PhC(O)NH	-(CH ₂) ₅ -	NHOH	100	NT
(4-Me ₂ N)PhC(O)NH	-(CH ₂) ₆ -	NHOH	100	NT
(4-Me ₂ N)PhC(O)NH	-(CH ₂) ₇ -	NHOH	300	NT
(4-Me ₂ N)PhC(O)NH	-(CH ₂) ₆ -	OH	> 40,000	NT
C ₆ H ₅ C(O)	-(CH ₂) ₄ -	NHOH	NT [†]	1500
C ₆ H ₅ C(O)(CH ₂) ₂	-(CH ₂) ₄ -	NHOH	NT	65
C ₁₀ H ₇ C(O)(CH ₂) ₂	-(CH ₂) ₄ -	NHOH	NT	5
SAHA	-----	NHOH	1000	120

[†]NT: not tested

Considerable research has been done on analogs of TSA and other, synthetically derived, linear molecules, notably in testing variations on the linker region⁹¹. The conclusions of these studies point to a linker of approximately the same length as the natural substrate being the most effective, with hydrophobic linkers (to better interact with the hydrophobic channel of the enzyme) being the most promising.

The aforementioned acyclic HDACi have proven promising as cancer therapeutics. However, one disadvantage to this class of HDACi is their lack of specificity. These molecules tend to inhibit all isoforms in class I, and in some cases, show inhibitory effects on both class I and class II enzymes⁷⁵. Given that the function of individual isoforms remains poorly understood, this type of pan-HDAC inhibition may be less desirable in the clinic. Of the nine HDACi currently in clinical trials, all are pan-HDAC inhibitors, and it is proposed that cardiac complications (ranging from mild to severe) which have arisen in testing may be due to this lack of specificity^{92,93,94}.

4.3 Macrocyclic Peptide Histone Deacetylase Inhibitors

4.3.1 Background

For the reasons cited above, much of the current research in this area has focused on the isolation and synthesis of HDACi that display higher selectivity. A group of molecules displaying this desirable characteristic are the macrocyclic HDACi, although even these show varying degrees of selectivity across class and isoform. Furthermore, many macrocyclic HDACi possess more potent biological activity than what is seen in the acyclic molecules.

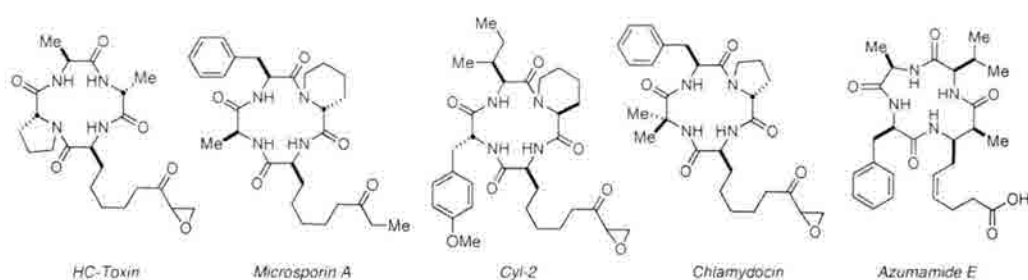


Figure 10: Selected macrocyclic peptide HDACi.

These differences between the two classes of HDACi most likely arise from both the greater variety in zinc-binding moieties and the greater functional complexity of the cap region, as seen above in Figure 10, and comparative biological data are shown below.

Table 7: Activity and selectivity of acyclic and macrocyclic HDACi.

Compound	IC ₅₀ nM HDAC1	IC ₅₀ nM HDAC4	IC ₅₀ nM HDAC6	HDAC6/HDAC1
TSA	6.0 nM	38 nM	8.6 nM	1.4
TPX A	0.82 nM	NT	524 nM	640
TPX B	0.11 nM	0.30 nM	360 nM	3,300
Chlamydocin	0.15 nM	NT	1,100	7,300
Cyl-2	0.70	NT	40,000 nM	57,000

While acyclic HDACi have smaller cap regions and therefore make contact only with highly conserved regions around the rim of the HDAC channels, the larger cap regions of

macrocyclic HDACi are able to interact with areas of higher variability which lie farther away⁷⁷. These more extensive contacts may explain the higher degree of specificity seen with some macrocyclic HDACi (Table 7)^{69,77}.

4.3.2 HC Toxin

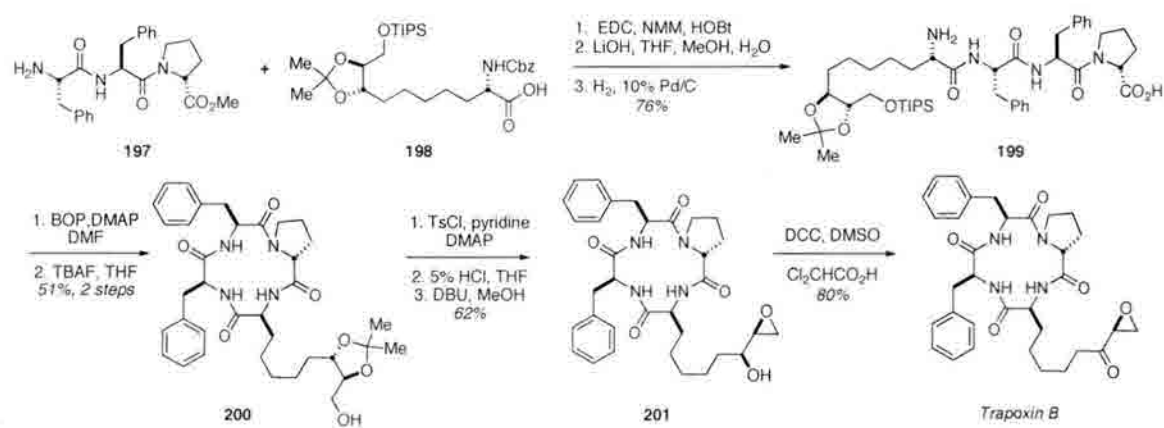
One of the first cyclic tetrapeptide HDACi to be isolated was HC-toxin, found in *Helminthosporium carbonum*, which contains an α -epoxy ketone as its zinc-binding functionality (Figure 7)⁹⁵. The side chain present in HC-toxin is a common motif among cyclic tetrapeptide HDACi, appearing in the chlamydocins, Cyl-1 and 2, WF-3161 and trapoxins A and B^{96,97,98}. This (*S*)-2-amino-8-oxo-9,10-epoxydecanoic acid (Aoe) side chain is essentially isosteric with an acetylated lysine residue, suggesting that these molecules also inhibit HDAC enzymes by acting as substrate mimics^{64,99}. HC-toxin displays modest biological activity in comparison with TSA (IC_{50} = 30 nM against HDACs from *E. tenella* vs. TSA's 3.8 nM)¹⁰⁰. However, a related natural product also containing the Aoe side chain, Cyl-2 (Figure 10), is a potent HDACi with an IC_{50} of 0.75 nM (HDAC I)^{101,102}. Perhaps more impressive is the selectivity displayed by Cyl-2: a 57,000 fold preference for HDAC 1 (class I) over HDAC 6 (class II) was noted in studies by Yoshida et al.⁶⁹

4.3.3 Trapoxin

Trapoxin (TPX) is arguably the best-known member of the group of macrocyclic HDACi containing the Aoe side chain. As mentioned above, isolation of HDAC1 by Schreiber and coworkers was made possible by affinity chromatography using an analog of trapoxin A⁸³. Part of the reason for this success lies in the particular manner in which trapoxin (and other α -epoxy ketone containing HDACi) inhibit HDAC enzymes. In

contrast to the hydroxamate zinc-binding functionalities discussed above, α -epoxy ketones bind to HDACs irreversibly, presumably through alkylation of the HDAC enzyme^{69,103}. The epoxide appears to be necessary for irreversible binding, as analogs containing the corresponding diol or methylene groups are biologically inactive⁶⁹.

Schreiber and coworkers published the total synthesis of trapoxin B in 1996, and the route is depicted in Scheme 38¹⁰⁴.



Scheme 38: Schreiber's synthesis of Trapoxin B.

Macrocyclizations of this type (**199** to **200**) have proven difficult; in fact, calculational studies have been undertaken in an attempt to predict the appropriate acyclic precursors¹⁰⁵. As this technology has yet to be perfected, Schreiber and coworkers instead looked to prior syntheses of chlamydocin, which had shown that successful cyclization appeared to dictate that macrocyclization occur between the piperolate C-terminus and the N-terminus of the Aoe residue^{104,106,107}.

Acid **198** was accessed in six steps from mono-protected (+)-2,3-*O*-isopropylidene-L-threitol, and coupled to free amine **197**. Following removal of the *N*-Cbz protecting group and saponification of the methyl ester, cyclization was effected by stirring for three days in DMF with BOP and DMAP. Following deprotection of the primary alcohol and

the acetonide, the requisite epoxide was installed by treatment with DBU in methanol. Oxidation under mild conditions furnished trapoxin B in fifteen linear steps.

Numerous analogs of trapoxins A and B have been explored, with variations in the stereochemistry of the amino acid residues and the zinc-binding region (Table 8)¹⁰¹.

Table 8: Biological data for TPX A, B and analogs.

Compound	Configuration	Sequence	B16/BL6 HDACs, IC ₅₀
<i>TPX B-type</i>			
CHAP1 [†]	LLLD	L-Asu(NHOH)-L-Phe-L-Phe-D-Pro*	6.03 nM
CHAP27	LDLD	L-Asu(NHOH)-D-Phe-L-Phe-D-Pro	3.44 nM
CHAP38	LDLL	L-Asu(NHOH)-D-Phe-L-Phe-L-Pro	5.32 nM
CHAP39	LLDL	L-Asu(NHOH)-L-Phe-D-Phe-L-Pro	226 nM
<i>TPX A-type</i>			
CHAP57	LDLD	L-Asu(NHOH)-D-Phe-L-Phe-D-Pro	2.91 nM
CHAP56	LLLD	L-Asu(NHOH)-L-Phe-L-Phe-D-Pro	4.78 nM
CHAP58	LDLL	L-Asu(NHOH)-D-Phe-L-Phe-L-Pro	4.18 nM

[†]CHAP = cyclic hydroxamic-acid-containing peptide; *Asu = α -aminosuberic acid

In compounds containing the hydroxamate prevalent in linear peptides, the biological activity was reduced by ~17 fold against HDAC1¹⁰¹. Interestingly, of the four stereochemical combinations tried (LDLD, LLLD, LDLL, LLDL: side chain-Phe-Phe-Pro), three showed no significant difference in HDAC inhibition, with only the LLDL isomer showing a large (2 orders of magnitude) decrease, standing somewhat in contrast to the proposal that unnatural amino acids are necessary in the cap region for tighter interaction with amino acid residues in the enzyme^{68,101}. This finding also highlights the differences between cyclic and linear HDACi, as the enantiomer of TSA has been shown to be biologically inactive¹⁰⁸.

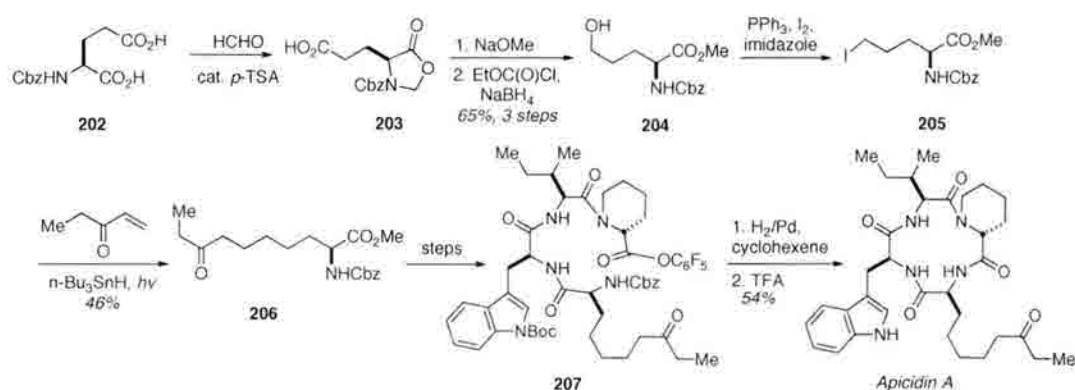
4.3.4 Apicidin

A similar HDACi, apicidin, was isolated in 1996, and was shown to have promising inhibitory activity^{109,110}. This is particularly noteworthy due to the side chain

present in the apicidins. Given that studies of *des*-epoxy trapoxin had shown it to be inactive, the Aoda (*S*)-2-amino-8-oxodecanoic acid) side chain present in the apicidins would be predicted to have insignificant biological activity⁶⁹. However, this natural product displays nanomolar potency (IC₅₀ 1-2 nM) against apicomplexan HDACs¹⁰⁹.

The structure of apicidin was determined by detailed ¹H and ¹³C NMR studies (COSY, TOCSY and HMQC), with the stereochemistry of the amino acids determined by degradation followed by derivatization and treatment with an amino-oxidase^{109,111}.

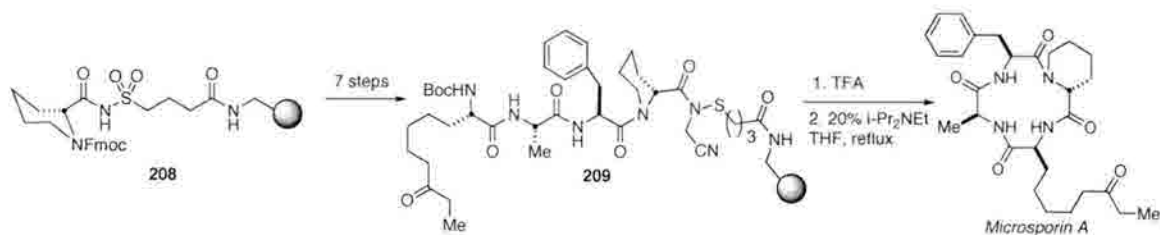
Following the isolation, two total syntheses were completed in 2001, and an interesting study using a metathesis reaction for macrocyclization was published in 2007, although this did not furnish the natural product^{112,113,114}.



Scheme 39: Singh's synthesis of apicidin A.

Of particular note is Singh and coworkers' approach to this molecule, shown below in Scheme 39. The major challenge in this synthesis was the formation of the Aoda side chain. Attempts to follow literature procedures for amino acid homology gave solely the dehydroamino acids. A radical reaction utilizing iodide **205** and ethyl vinyl ketone in the presence of tri-*n*-butyltin hydride gave the appropriately protected amino acid (**206**) in 46 percent yield.

Following the synthesis of the Aoda side chain used by Singh, a series of peptide couplings using resin-bound D-Pip gave the acyclic tetrapeptide, which was removed from the resin and cyclized, completing one of the few solid-phase syntheses of this class of HDACi^{113,118}.



Scheme 40: Silverman's synthesis of microsporin A.

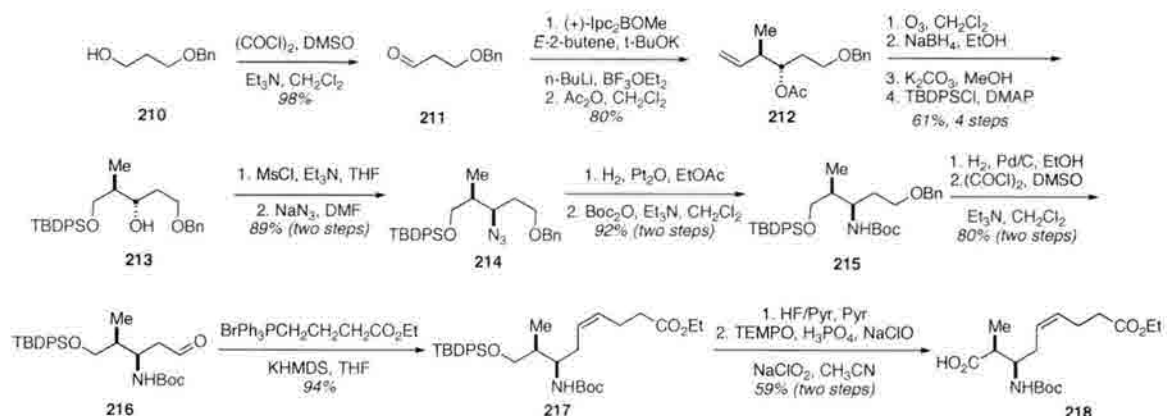
4.3.6 Azumamides

Another group of naturally occurring HDACi with unusual structures are the azumamides, which are cyclic tetrapeptides isolated from the marine sponge *Mycale izuensis*, although some have proposed that the actual source may be a sponge-associated fungus^{99,120}. The azumamides display an unusual stereochemical arrangement in comparison to chlamydocin, trapoxin, and apicidin, being composed exclusively of D-amino acids (D-Phe/D-Tyr, D-Ala, and D-Val)¹²⁰. The side chain of the azumamides, (*Z*,*2S*,*3R*)-3-amino-2-methyl-5-nonenedioic acid (Amnda) or (*Z*,*2S*,*3R*)-3-amino-2-methyl-5-nonenedioic acid 9-amide (Amnaa) possesses the opposite absolute configuration as those seen in the aforementioned compounds^{120,121}.

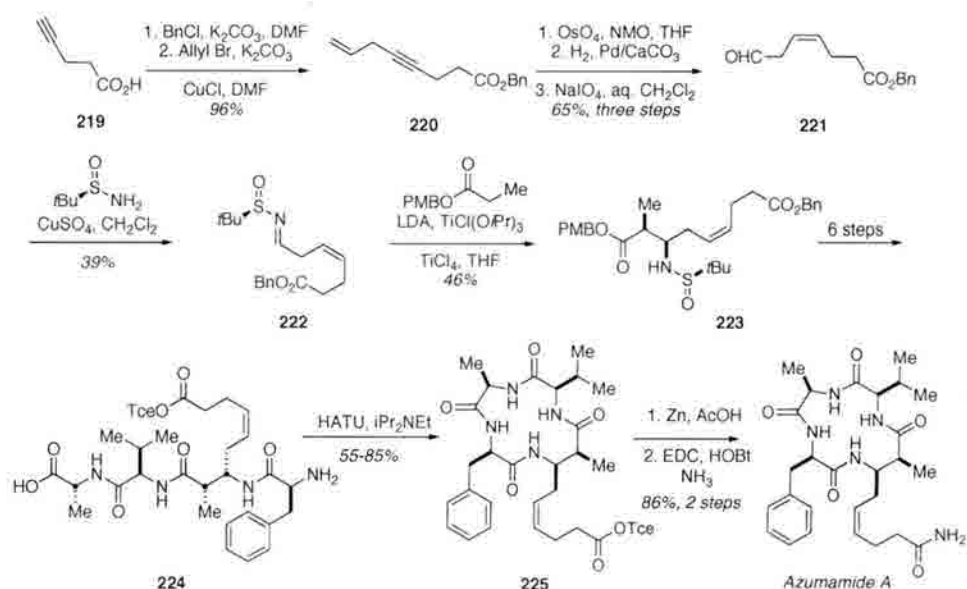
Furthermore, the azumamides display a high degree of potency as HDACi when tested against HDACs from human leukemia cells, with IC₅₀ values ranging from 45 nM (azumamide A) to 1.3 μM (azumamide D)¹²². This potency is notable for the fact that the azumamides present relatively weak zinc chelation motifs: azumamides A, B and D have carboxamides in this region, while C and E carry carboxylic acids.

Synthetic studies of the azumamides have provided some insight into this activity.

Routes to the key nonenediolic acid are shown in Schemes 41 and 42^{123,124}.



Scheme 41: De Riccardis' synthesis of Amnaa.



Scheme 42: Ganesan's synthesis of Amnaa and completion of azumamide A.

De Riccardis obtained asymmetric induction through the use of the Brown crotylboration methodology¹²⁵. Ganesan instead employed Ellman's auxiliary in a Mannich type reaction, as shown below in Scheme 42. In both cases, similar acyclic precursors were synthesized, with cyclization occurring between the N-terminus of the Amna side chain and the C-Phe terminus in De Riccardis' case, and between the N-Phe

terminus and C-Ala terminus in Ganesan's work^{123,124}. De Riccardis reported conformational analyses based on NMR ROESY correlations and calculational docking studies¹²¹. The solution NMR studies showed no defined secondary structure, and were used as a starting point for their docking calculations. These calculations show that the macrolactam sits within a shallow groove in the enzyme wherein it establishes Van der Waals interactions and hydrogen bonds with conserved amino acid residues. The phenylalanine side chain lies within a hydrophobic pocket; also a highly conserved region. Further calculations suggested that the enantiomer of azumamide E ((-)-azumamide E) would be capable of maintaining these interactions; indeed, the synthesis of (-)-azumamide E showed it to be biologically active, though with a significant loss in potency with respect to the natural (+)-azumamide E (Table 10).

Table 10: Biological data for the azumamides and analogs.

Compound	Zn ²⁺ -binding arm	HeLa HDAC IC ₅₀ μM	K562 HDAC IC ₅₀ μM	HDAC1 IC ₅₀ μM	HDAC4 IC ₅₀ μM	HDAC6 IC ₅₀ μM
Azumamide A	CONH ₂	5.8	0.045	>50	>50	>50
Azumamide B	CONH ₂	NT [†]	0.11	1.83	3.66	>50
Azumamide C	CO ₂ H	NT	0.11	1.17	3.16	>50
Azumamide D	CONH ₂	NT	1.3	>50	>50	>50
(+)-Azumamide E	CO ₂ H	0.033	0.064	1.22	2.28	>50
(-)-Azumamide E	CO ₂ H	26	NT	NT	NT	NT
Azumamide hydroxamate	CONHOH	0.007	NT	NT	NT	NT
TSA	CONHOH	NT	NT	0.037	0.063	0.083

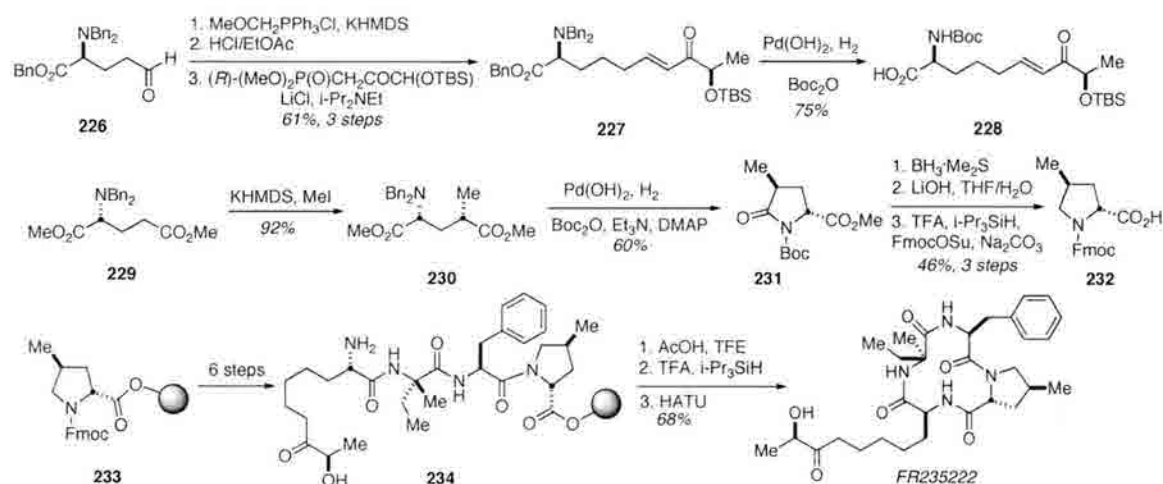
[†]NT: not tested

Another diastereomer, (2*R*,3*S*)-azumamide E, showed a complete loss of biological activity, presumably due to a loss of conformational rigidity¹²¹. Ganesan also examined possible improvements to the azumamides' biological activity, choosing to focus on the zinc-binding arm rather than the cap region. Conversion of the carboxamide side chain of azumamide A to a hydroxamate resulted in an analog with significantly

improved inhibitory potency in conjunction with the installation of this much stronger zinc-binding residue (Table 10)¹²⁴.

4.3.7 FR235222

Another naturally occurring HDACi in this class is FR235222, a fungal metabolite isolated in 2003 from the fermentation broth of *Acremonium* sp.¹²⁶ A potent (IC₅₀ 60 nM against HeLa HDACs) inhibitor of HDAC, this compound displays a variation on the α -keto epoxides seen in the trapoxins. Here, a (2*S*,9*R*)-2-amino-9-hydroxy-8-oxodecanoic acid (Ahoda) side chain is present (Figure 10), wherein the epoxide present in trapoxin A is replaced by a hydroxy group. This is notable in part as the di-hydroxy analog of trapoxin A is biologically inactive⁶⁹. As with other cyclic tetrapeptide HDACi, an unnatural amino acid is included in the macrocycle (D-4-MePro)¹²⁷. The first published synthesis of FR235222 was completed by Taddei and Gomez-Paloma in 2006, and is shown in Scheme 43¹²⁷.

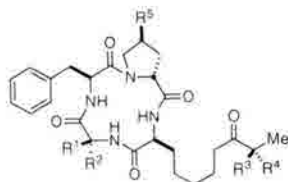


Scheme 43: Synthesis of FR235222.

Aldehyde **226** was prepared through a known procedure and converted to acid **228** in four steps¹²⁸. Following the construction of D-4-MePro (**231**), this substance was

attached to a polystyrene/2-chlorotrityl resin. Once synthesis of the acyclic precursor was completed, the tetrapeptide was removed from the resin and cyclized in 68% yield. Analogs of the natural product were synthesized by this group and others, as shown in Table 11^{129,130}.

Table 11: Inhibitory data for FR235222 and analogs.



Entry	R ¹	R ²	R ³	R ⁴	R ⁵	HeLa HDACs IC ₅₀ nM
1 (FR235222)	Et	Me	OH	H	Me	60
2	Et	Me	OH	H	H	50
3	Me	Me	OH	H	H	30
4	Ph	H	OH	H	H	280
5	Indole	H	OH	H	H	20
6	Me	Me	H	OH	H	330
7	Et	H	H	OH	H	1000

Bifulco and coworkers extended these studies by performing molecular modeling studies in order to identify further targets for synthesis¹³¹. Similar interactions to those mentioned above in De Riccardis' studies of the azumamides were noted between the macrocyclic cap and the HDAC enzyme. The proline ring was accommodated by a small hydrophobic cavity containing Tyr 91, Glu 92, and Gly 140. The Ahoda side chain made similar contacts with the pocket leading to the active site as those found by De Riccardis¹²¹. The stereochemistry at C9 was shown to be an important contributor to binding of the zinc cation, with the natural (*R*) configuration appearing to be more favorable; this is further supported by the inhibitory data shown below (Table 11)^{130,131}. The analog containing an indole ring, shown by HDAC inhibition assays to be more

potent than the natural product (Table 11), was shown to interact particularly well with the enzyme in docking studies. Hydrophobic pockets at the rim of the channel leading to the active sites made favorable contacts with the ring, suggesting that hydrophobic, bulky groups at this position are preferable¹³¹. Computational trends corresponding closely to experimental data suggest that this method of identifying target compounds is a valuable tool for predicting biological activity.

4.4 Sulfur-Containing Histone Deacetylase Inhibitors

4.4.1 Background

Recently, naturally occurring HDACi with a novel zinc-binding motif have been isolated. This group, which bears an unusual (3*S*,4*E*)-3-hydroxy-7-mercapto-4-heptenoic acid side chain, includes FK228, the spiruchostatins, FR901375 and largazole. The reduced form of spiruchostatin A has been shown to act as a potent and selective HDACi (IC₅₀ 0.62 nM against HDAC1; 360 nM against HDAC6)⁷⁷. While the total synthesis of FR901375 (an isolate from *Pseudomonas chloroaphis* No. 2522) has been completed, no inhibitory data has yet been reported for this molecule¹³².

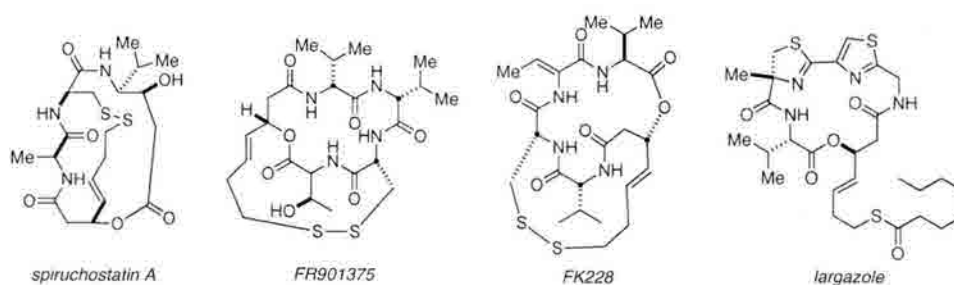


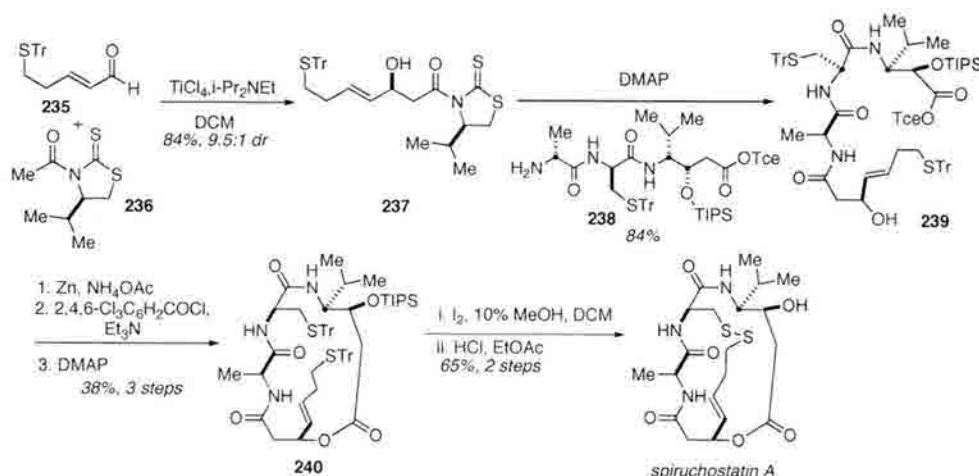
Figure 11: Sulfur-containing HDACi.

These compounds all contain the β -hydroxymercaptoheptenoic acid residue connected to a cysteine residue as the unsymmetrical disulfide. There are however, significant differences within the cap regions: in FK228, five sp^2 hybridized carbon

atoms are present within the macrocycle while the spiruchostatins and FR901375 contain only four. While FK228 features sixteen-membered and seventeen-membered rings about the cap group ring and disulfide ring respectively, the spiruchostatins contain a smaller, fifteen-membered ring in the cap group and a sixteen-membered ring about the depsipeptide linkage. FR901375 has a sixteen-membered ring depsipeptide ring, analogous to that of FK228, but the cysteine is shifted relative to the β -hydroxy acid, contracting the outer ring to fourteen atoms about the depsipeptide linkage.

4.4.2 Spiruchostatins

The spiruchostatins were isolated from a culture broth of a *Pseudomonas* sp. in 2001¹³³. There have been two total syntheses of spiruchostatin A and one of spiruchostatin B (the difference being either a C-4' valine or isoleucine)^{134,135,136}. Ganesan's synthesis of spiruchostatin A (below) is particularly of note¹³⁵.



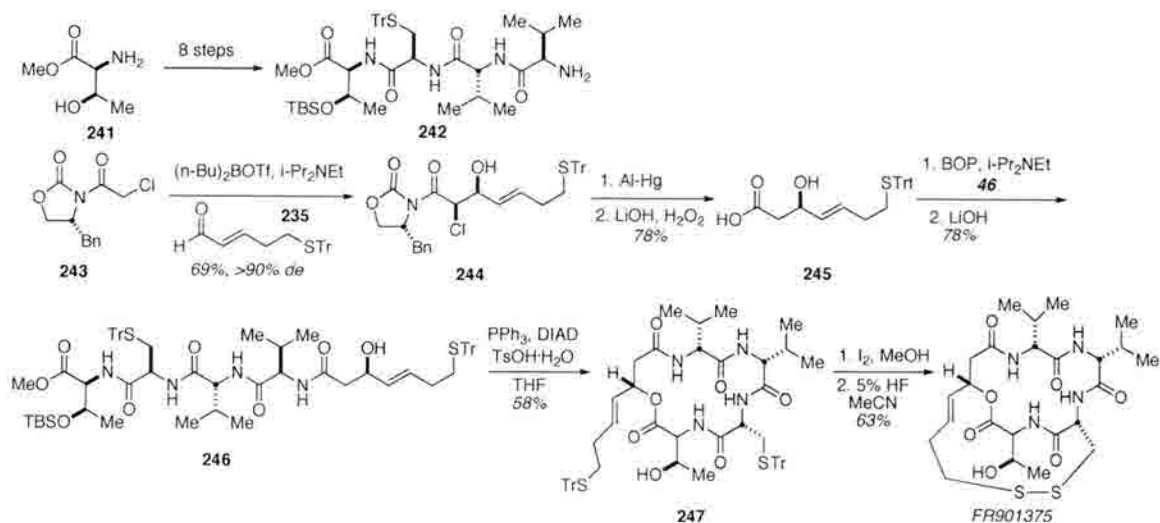
Scheme 44: Ganesan's synthesis of spiruchostatin A.

The β -hydroxy acid stereochemistry was introduced using the Nagao auxiliary in conjunction with Vilarrasa's TiCl_4 conditions^{137,138}. Acid derivative **237** was then coupled to an appropriately protected peptide (**238**) which was accessed in five steps from

commercially available materials. Following deprotection, Yamaguchi macrolactonization proceeded in good yield^{135,139}. Finally, deprotection of the thiols and concomitant formation of the disulfide bond, followed by TIPS deprotection gave spiruchostatin A. A small amount of *epi*-spiruchostatin A, with the *R*-stereochemistry at the β -hydroxy acid fragment was also synthesized, and shown to be biologically inactive at 10 μ M, suggesting that stereochemistry at this position is important for interactions with surface amino acid residues on the HDAC enzyme¹³⁵.

4.4.3 FR901375

FR901375 is a metabolite of *Pseudomonas chloroaphis* (No. 2522) and was reported by Fujisawa Pharmaceutical Company in 1991⁷⁵. Synthesis of FR901375 has been completed by Janda and co-workers (Scheme 45)¹³².



Scheme 45: Janda's synthesis of FR901375.

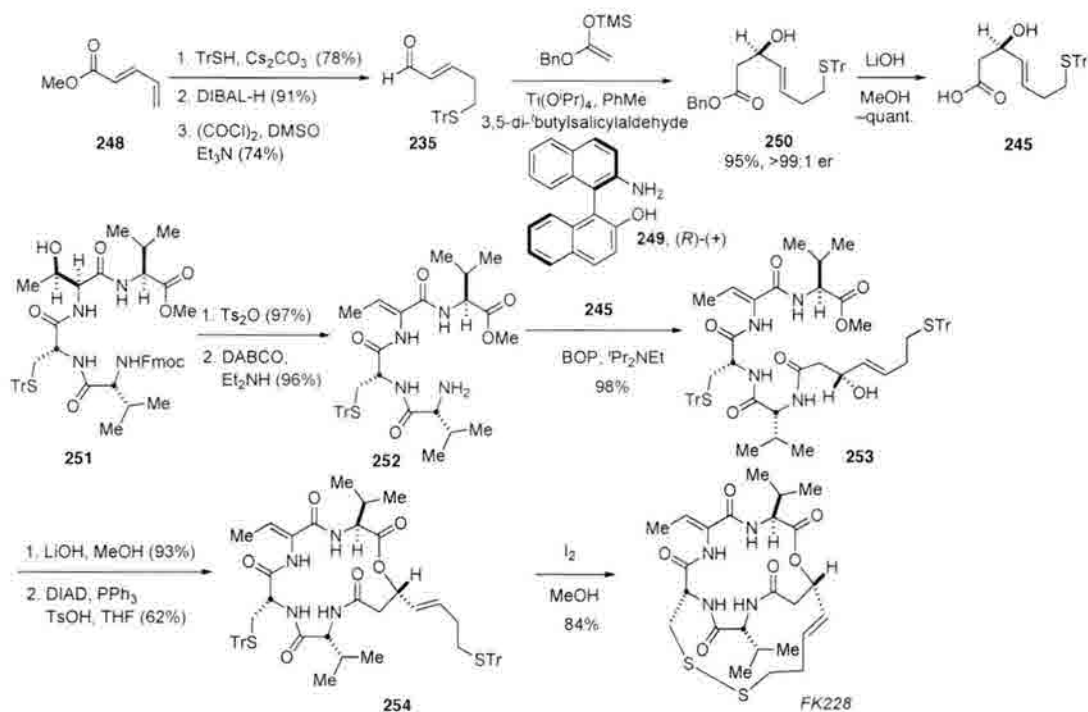
Original attempts to access the requisite β -hydroxy acid following Simon's protocol (see below, Scheme 45) were reported to result in poor yields and low diastereoselectivity. Therefore, a different approach was taken, utilizing Evans' auxiliary¹⁴⁰. This technique permitted access to the β -hydroxy acid (**48**) in greater than

95:5 diastereomeric ratio and 69 percent yield. Coupling to the tetrapeptide (**46**) and a Mitsunobu reaction furnished the cyclized product (**51**), and formation of the disulfide bond followed by alcohol deprotection gave FR901375.

4.4.4 FK228 (Romidepsin)

The first of the sulfur-containing HDACi to be discovered was FK228 (also referred to in the literature as FR901228 or depsipeptide, and registered as both NSC 630176 and Romidepsin)¹⁴¹. FK228 is currently in human clinical trials for peripheral and cutaneous T-cell lymphoma, and as such, has been extensively studied^{92,142}. Unlike other HDACi, studies have been conducted to identify the specific protein targets of FK228, showing that at least 27 proteins involved in a wide variety of cellular processes are affected by this inhibitor^{143,144}. Much of the current understanding of this class of HDACi has come from research on FK228.

The natural product was first isolated from the fermentation broth of *Chromobacterium violaceum* No. 968 in conjunction with a screening program for agents that reverse the malignant phenotypes^{145,146}. Structurally, FK228 is a bicyclic depsipeptide that features a 16-membered ring about the macrolactone and peptide backbone and a 17-membered ring about the ester and disulfide linkages¹⁴¹. In addition to the β -hydroxymercaptoheptenoic acid, the smaller ring contains the dehydrothreonine derivative, 2,3-dehydro-2-aminobutanoic acid (Dhb). The structure was determined by spectroscopic and X-ray analysis and confirmed by multiple total syntheses, the first of which, as completed by Simon et al., is shown below^{147,148}.

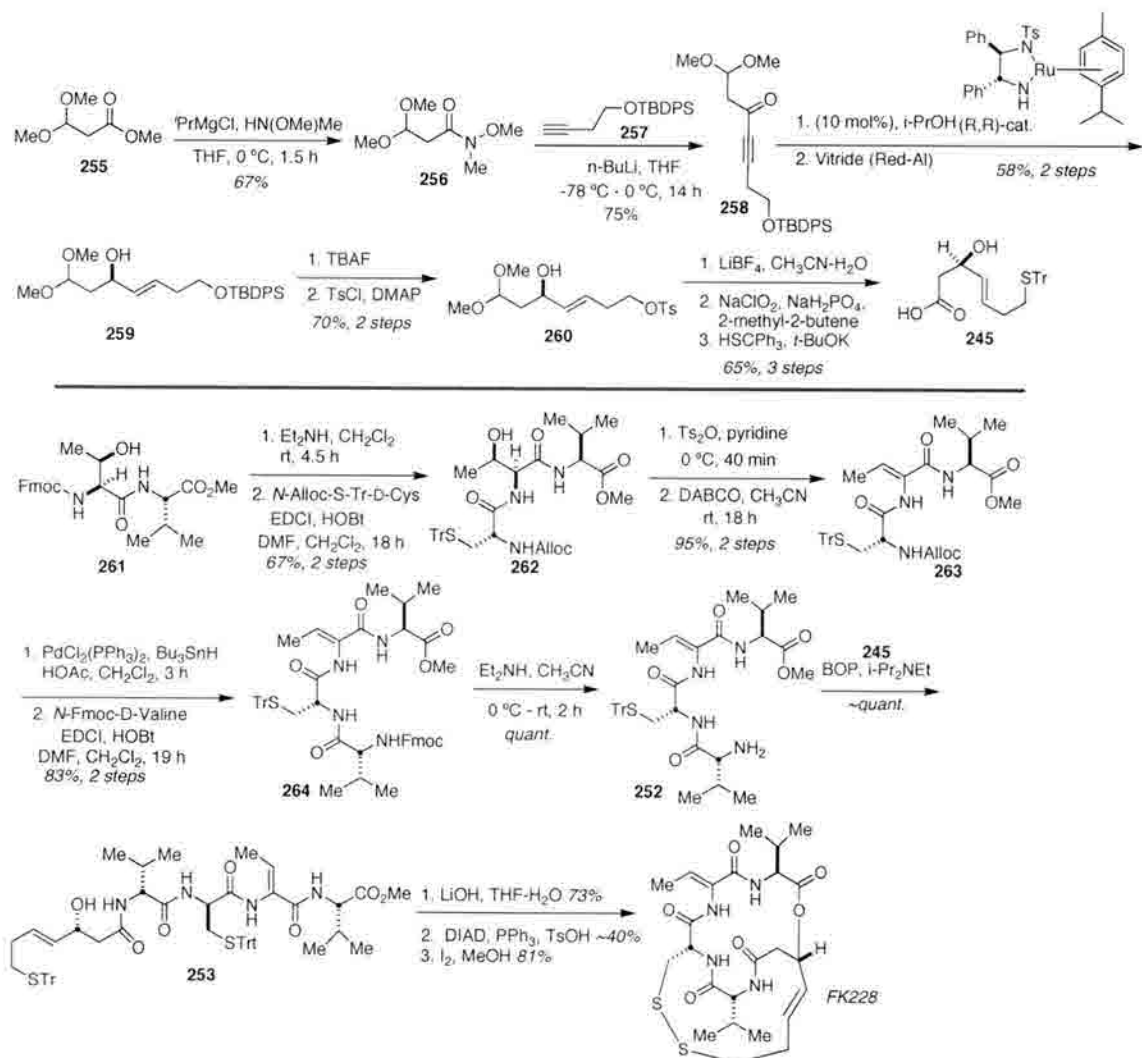


Scheme 46: Simon's synthesis of FK228.

Here, Simon made use of a titanium-mediated aldol reaction in conjunction with a ligand derived from (*S*)-(-)-binaphthyl amino alcohol (**249**) using conditions developed by Carreira to access the chiral β -hydroxy acid in 99:1 er^{148,149}. This acid was synthesized as the enantiomer of the natural stereoisomer such that macrocyclization could be effected under Mitsunobu conditions mandating inversion of stereochemistry. Following a nine-step sequence to access the acyclic precursor of FK228 (**253**), the Mitsunobu reaction gave the cyclized product (**254**) in a reported 62 percent yield with only trityl deprotection and disulfide bond formation remaining to give FK228 (Scheme 46)¹⁴⁸. Following publication of Simon's route to FK228, our group investigated a different synthesis which had its basis in Simon's work¹⁵².

As mentioned above, FK228 was in clinical trials; however, severe cardiac events were noted, resulting in a suspension of the trials (since then, clinical trials have begun

anew)^{92,150}. At the time, access to larger quantities of FK228 were needed for study such that a better understanding of the biochemistry of the natural product could be achieved prior to reintroduction to the clinic. As the natural product was not widely available, this demand necessitated a new, more scalable synthesis of FK228 as completed by Williams et al. is shown below in Scheme 47¹⁵².

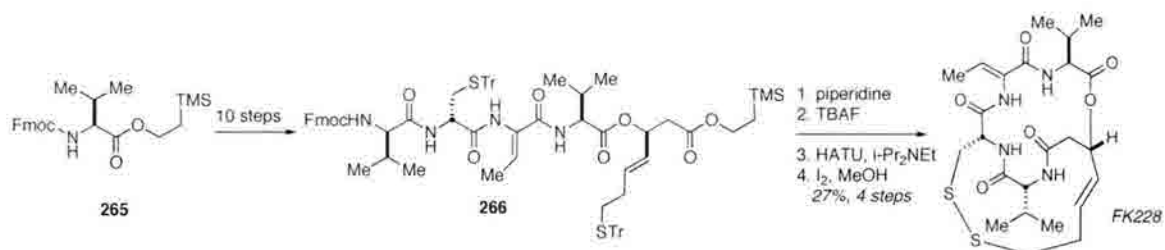


Scheme 47: Greshock and Williams' improved synthesis of FK228.

The synthesis of β -hydroxy acid **245** proved both reproducible and scalable, permitting access to this challenging portion of the molecule on a multigram scale¹⁵². Further changes were made in the formation of tetrapeptide **264**. The originally published

conditions required *N*-Fmoc-D-cysteine(STrT), which proved difficult to synthesize in good yield from D-cysteine; however, the synthesis of *N*-Alloc-D-cysteine(STrT) could be obtained in high yield following Kruse's method¹⁵¹. Finally, dehydration of the threonine residue early on in the synthesis improved the yield of the tripeptide (**263**) to 53 percent overall.

To conclude the synthesis, the final coupling of **252** with **245**, macrolactonization and disulfide formation from Simon's pioneering work was followed to give FK228. In the final macrocyclization step, both our group and Ganesan's have noted difficulties with respect to the reproducibility and yield of the Mitsunobu reaction^{152,153}. To obviate the need for this capricious reaction, an alternative macrolactamization route has recently been reported by Ganesan using both solution-phase and solid-phase chemistry. This approach appears to be more robust (despite the modest yield) than the Mitsunobu-based macrolactonization strategy (Scheme 48)^{153,154}.



Scheme 48: Ganesan's macrolactamization strategy to FK228.

Analogues of FK228 (Figure 12) have been prepared, with perhaps the most notable with respect to insight into structure-activity relationships being the reduced form of FK228 (redFK) and an FK228 amide isostere^{155,156,158}. RedFK was prepared by reducing the natural product with dithiothreitol in order to test the idea that FK228 may act as a produrg, with the disulfide bond allowing the molecule to be more readily incorporated through the cell wall¹⁵⁵. *In vivo* reduction by glutathione within the cell would then

reveal a free thiol, which strongly coordinates to the active-site Zn^{+2} cation^{155,157}. Biochemical testing indeed supports this hypothesis, where a 75-fold increase in inhibitory activity against HDAC1 for redFK228 vs FK228 was observed (Table 12).

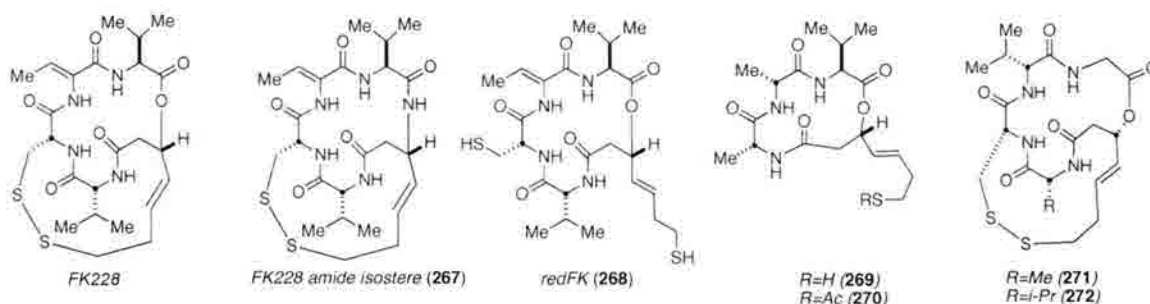


Figure 12: Analogs of FK228.

Some preliminary biochemical profiling of these analogs has been reported and comparative data are collected in Table 12. FK228 is a potent inhibitor of the Class I HDACs 1, 2 and 3, but is inactive against the Class IIB HDAC6¹⁵⁵.

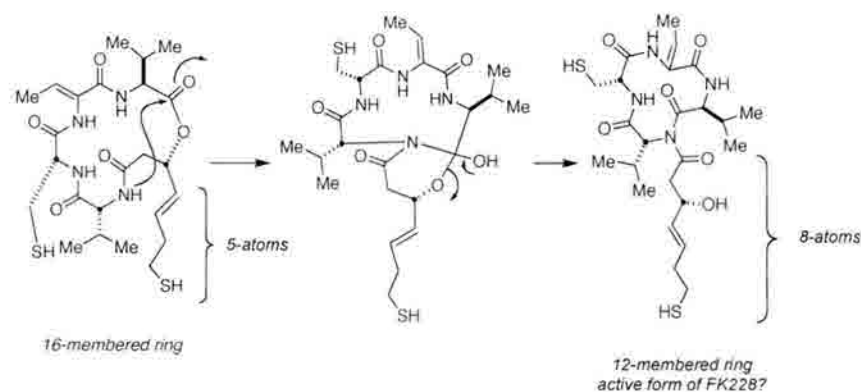
Table 12: Biological data for FK228 and selected analogs.

Compound	HeLa HDACs nM	HDAC1 nM	HDAC6 nM
FK228	NT [†]	30	14,000
redFK (268)	15	0.397	787
269	15	1.6	881
270	7.2	1.6	897
271	7	17.5	4900
272	242	>100	>10,000

[†]NT: not tested

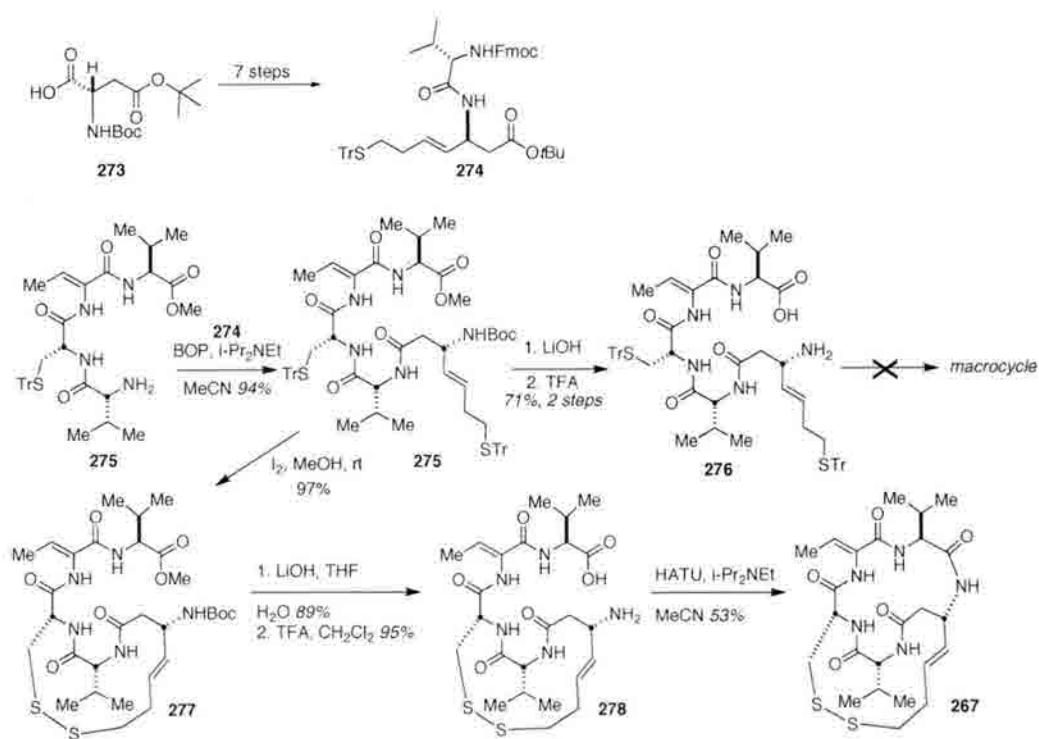
The biochemical activity of the simplified analogs **269** and **270** display a similar pattern of class selectivity with potency being maintained against HDAC1. The surprising drop in potency for the FK228 analogs **271** and **272** reveals that alteration of the conformation of the cap group, which is presumably a manifestation of the D-valine for dehydrothreonine residue substitution, is critical for high-affinity binding to the protein.

In order to investigate the importance of the depsipeptide linkage, Dr. Tom Greshock completed the synthesis of an FK228 peptide isostere (**267**), which showed that the more rigid amide isostere of FK228 demonstrates a 50-fold loss in potency against HDAC1 (Table 13)¹⁵⁸. This finding also allowed for insight into the possible mechanism of action of FK228, as shown below. Specifically, the size of the FK228 macrocycle is somewhat larger, and its 5-atom tether is shorter than those in other known cyclic HDACi. It was therefore proposed that a transannular ring closure (as shown in Scheme 49) could occur, giving rise to a seven atom tether such as those known in other molecules and a 12-membered ring in the cap group, again coinciding with other known inhibitors. The loss of biological activity (Table 13) of the amide isostere could serve as support for this proposal as this sequence of events would presumably not occur in that system.



Scheme 49: Possible transannular ring closure.

The synthesis of the FK228 amide isostere is shown below in Scheme 50, beginning with the synthesis of β -amino acid **273** (discussed in more detail in Chapter 4).



Scheme 50: Williams' synthesis of the FK228 amide isostere (**267**).

Acyclic precursor **276** was accessed following Simon's strategy with the intent to accomplish the macrolactamization prior to disulfide formation. However, unlike the syntheses of FK228 discussed above, all attempts at macrocycle formation failed. For this particular substrate, it was found that formation of the disulfide bond (**277**) prior to macrocyclization was necessary, giving the amide isostere of FK228 in 13 steps¹⁵⁸.

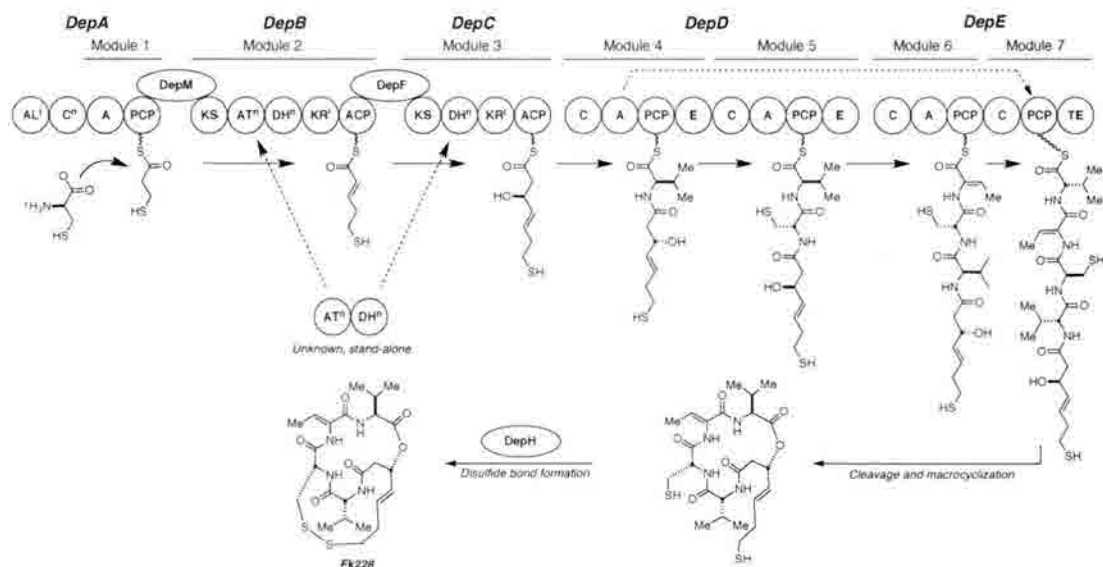
Table 13: Biological data for FK228, its amide isostere and a SAHA control.

Compound	HDAC1 IC ₅₀ nM	HDAC2 IC ₅₀ nM	HDAC3 IC ₅₀ nM	HDAC6 IC ₅₀ nM
FK228*	0.2	1	3	200
FK228 amide isostere* 267	10	80	70	>3000
SAHA	10	40	30	30

*assay performed in the presence of TCEP

3.4.5 Biosynthesis of FK228

Unlike other HDACi in this class, the biosynthesis of FK228 has recently been explored.



Scheme 51: Proposed biosynthesis of FK228.

Chang and co-workers have identified and partially characterized a gene cluster responsible for the biosynthesis of FK228. The gene cluster is predicted to encompass a fourteen-gene region of DNA, including six genes constituting a hybrid non-ribosomal synthetase-polyketide synthase (NRPS-PKS) assembly line. Their proposed biosynthetic model is shown in Scheme 51¹⁴¹. Activation of cysteine by the A domain in module 1 effects the formation of a cysteinyl-*S*-PCP intermediate. Following the formation of 4-mercaptobutanyl-*S*-PCP, PKS modules 2 and 3 extend the growing chain using C₂ units from malonyl CoA. Modules 4, 5 and 6 add activated D-Val, D-Cys and Dhb. Module 7 incorporates the final residue, as the A domain in module 4 aminoacylates the PCP domain. Finally, the terminal thioesterase domain on DepE catalyzes the macrolactonization, and an FAD-dependent pyridine nucleotide disulfide oxidoreductase closes the disulfide linkage. To date, Chang's work represents the only published proposal regarding the biosynthesis of the bicyclic disulfide-containing HDAC inhibitors.

4.5 Largazole

4.5.1 Background and Isolation

One of the most recent HDACi to be isolated is the marine natural product largazole, which was isolated by Luesch and co-workers from the Floridian marine cyanobacterium *Symploca* sp. and reported in early 2008¹⁵⁹. Largazole also demonstrates some structural similarity to FK228, in that largazole contains the same 3-hydroxy-7-mercaptohept-4-enoic acid moiety common to FK228, FR901375 and spiruchostatin¹⁵⁹. However, in the case of largazole, the thiol is capped as an octanoyl thiol ester as opposed to a disulfide linkage. This led to the proposal that largazole may in fact be a pro-drug. The more hydrophobic natural product would be capable of entering the cell; once inside, enzymatic removal of the octanoyl residue would reveal the zinc-binding portion of the molecule to give the hydrophilic, active form (Figure 13).

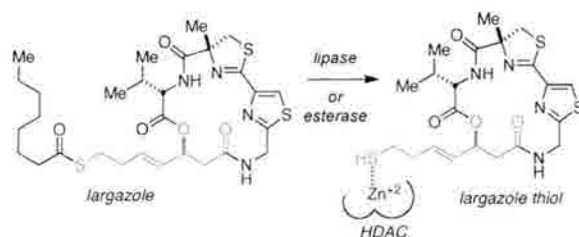
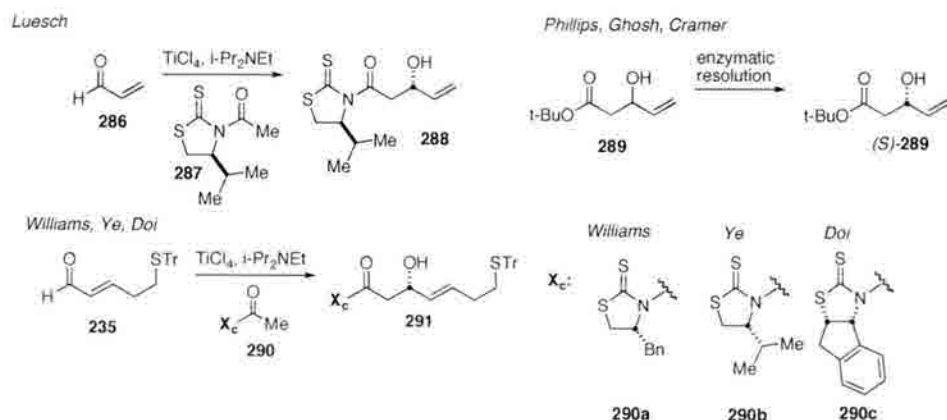


Figure 13: Enzymatic activation of pro-drug largazole.

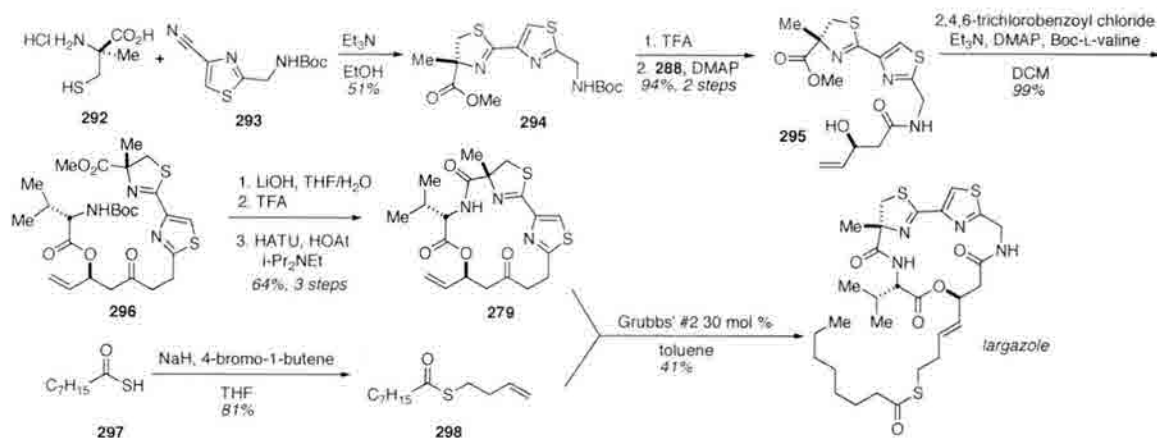
As with the reduced form of both FK228 and spiruchostatin, biological testing supports this theory with largazole itself being nearly inactive and the largazole thiol displaying unprecedented biological activity. The macrocycle itself is somewhat more rigid than that of FK228 by virtue of a thiazoline-thiazole moiety¹⁵⁸. This rigidity leads to a lowest energy solution conformation that matches the lowest energy bound conformation, as shown by calculations performed by our collaborator Olaf Wiest (discussed in further detail in the next chapter)¹⁵⁸. This may account for the increase in



Scheme 53: Approaches to the β -hydroxy acid moiety.

The opposite stereochemistry in the auxiliaries used by Luesch and Ye is explained by existing models, which suggest that the stereochemical outcome of these reactions are dependent upon the amount of base present^{163,164}.

Following synthesis of the β -hydroxy acid, each group's route proceeded in a similar manner, using a modular synthesis to combine the aforementioned β -hydroxy acid, L-valine and a thiazoline-thiazole moiety^{160,161,162}.



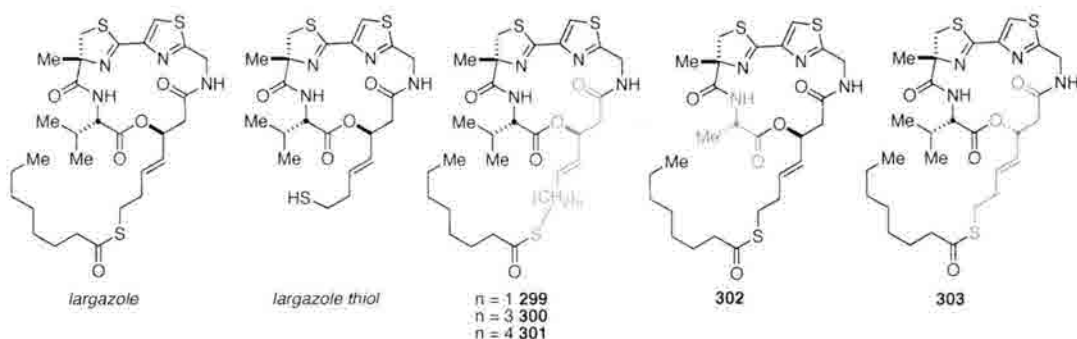
Scheme 54: Synthesis of largazole by Luesch and co-workers.

The first published synthesis of largazole was accomplished by Luesch and co-workers, and is of particular note due to the site of ring closure^{104a}. Of the seven published syntheses of the natural product, only Luesch chose to effect macrocyclization

between the valine amino group and the thiazoline carboxyl residue, while the remaining efforts use the less sterically hindered bond between the β -hydroxy acid and thiazole fragments.

The requisite nitrile (**293**) was accessed by Cramer in a four-step procedure in 40% overall yield, in a sequence that has proven to be quite scalable^{162c,165}. The α -methylcysteine piece (**292**) is accessible through a known four step procedure, and the condensation of the two proceeds in good yield^{162a,166}. Luesch and colleagues used this metathesis strategy to create both chain-shortened and lengthened analogs of the natural product¹⁶⁷. The attenuated biological activity of these analogs suggests that the chain length seen in the natural product is, in fact, the optimal length (Table 14). Furthermore, two variations in the cap group were explored - a valine to alanine substitution and an epimer (17*R*) of largazole¹⁶⁷.

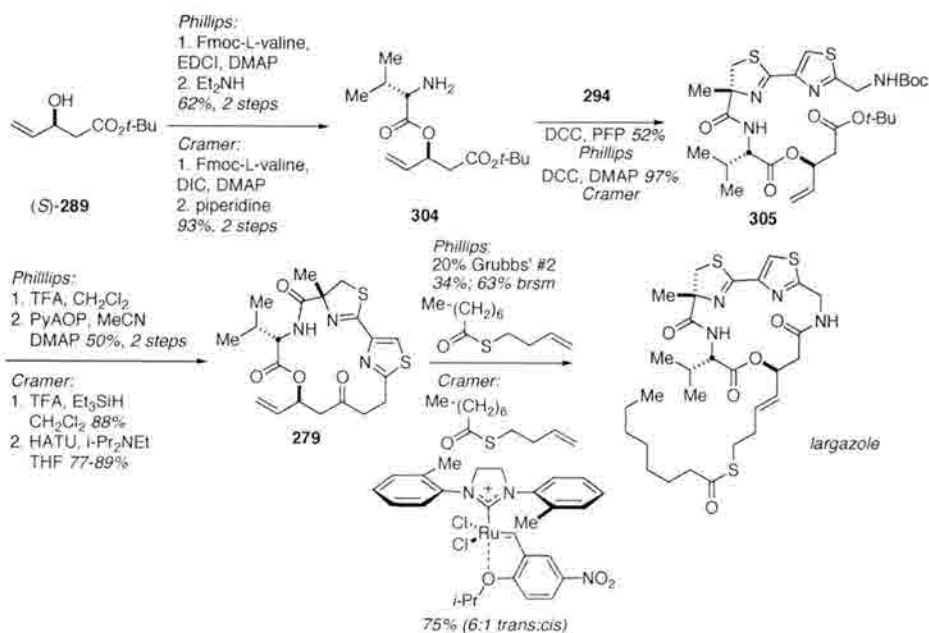
Table 14: Biological and biochemical activity of selected largazole analogs.



Compound	HeLa HDACs IC ₅₀ nM	HDAC1 IC ₅₀ nM	HDAC6 IC ₅₀ nM
Largazole	32	7.6	1800
Largazole thiol	NT [†]	0.77	570
Largazole <i>n</i> -1 side chain 299	>20000	NT	NT
Largazole <i>n</i> +1 side chain 300	7600	690	>10000
Largazole <i>n</i> +2 side chain 301	4100	1900	>10000
Alanine substitution 302	72	44	3300
(17 <i>R</i>) Largazole 303	3900	NT	NT

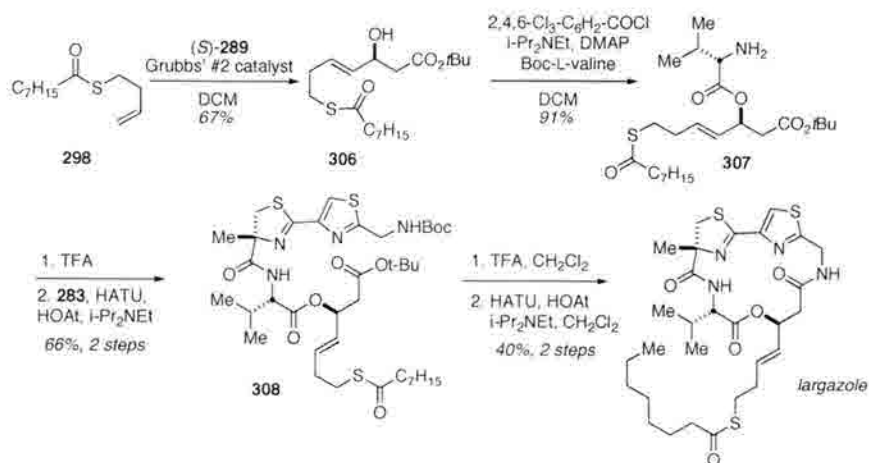
[†]NT: not tested

Phillips and Cramer converged on the same metathesis substrate (**279**) as that used by Luesch, and fashioned the acyclic precursor by nearly identical routes (Scheme 55).



Scheme 55: Synthesis of largazole by Phillips and Cramer.

The synthesis of largazole accomplished by Ghosh and Kulkarni is shown below (Scheme 56).

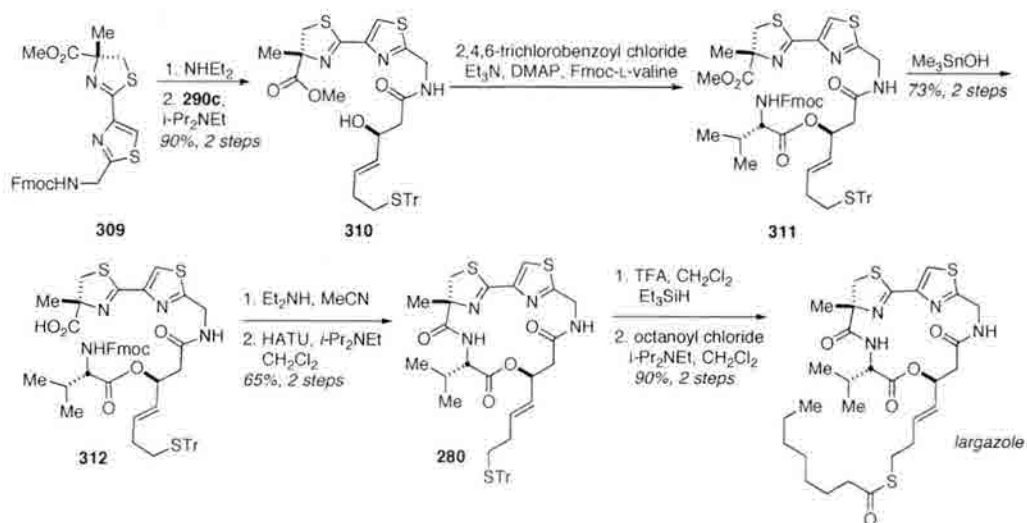


Scheme 56: Synthesis of largazole by Ghosh.

Here, a strategy was chosen wherein the zinc-binding arm would be installed in its entirety. A cross-metathesis reaction between **298** and **289** gave **306** in a reaction which

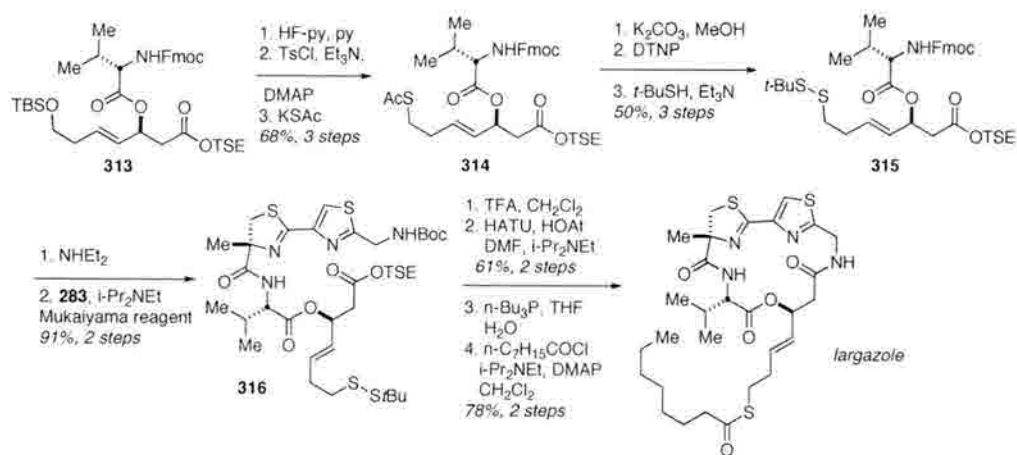
is still somewhat low yielding; however, starting material can be recovered and this choice regarding the sequence of events still prevents the loss of more advanced material. Following the metathesis, esterification using *N*-Boc-L-valine provided **307**. Condensation with acid **283** gave the acyclic precursor (**308**), which was converted to largazole by deprotection of both the *N*-Boc group and *t*-butyl ester, followed by macrolactamization to provide largazole.

The synthesis reported by Doi and co-workers (Scheme 57) effected macrolactamization using the same bond disconnection used by Luesch. Here, the *S*-trityl protected side chain was installed early in the synthesis, and a late-stage deprotection and acylation sequence provided both the largazole thiol and the natural product.



Scheme 57: Synthesis of largazole by Doi.

Finally, the approach to largazole taken by Ye and co-workers is shown in Scheme 58. This group made use of the unusual asymmetric *t*-butyl disulfide species (**315**) to mask the side chain thiol group. This substrate was converted to the largazole thiol by phosphine reduction, followed by acylation to provide largazole.



Scheme 58: Synthesis of largazole by Ye.

4.6 Summary of HDACi

While highly isoform-specific inhibitors have not yet been discovered, the selectivities observed for some families of inhibitors between classes, such as the class I-specific inhibitors FK228 and largazole, indicate that attaining such selectivity may be possible. This field of study has developed considerably since the isolation of TSA in the 1970's, and has exploded with the discovery and functional expression of the various isoforms of HDACs initiated by Schreiber and co-workers in 1996²⁶. The discovery of naturally occurring macrocyclic HDACi's have provided extremely potent mechanism-based inhibitors of the deacetylase enzymes whose myriad functions are still emerging from the work of numerous laboratories. Synthesis of these compounds as well as their analogs, along with computational studies, has begun to provide invaluable insight into the structure-activity relationships present in these molecules. As this field continues to evolve, these molecules present further opportunities for understanding the function of HDAC enzymes and the treatment of human disease.

Chapter 5: Syntheses of Largazole Analogs

5.1 Synthetic Goals and Collaborations

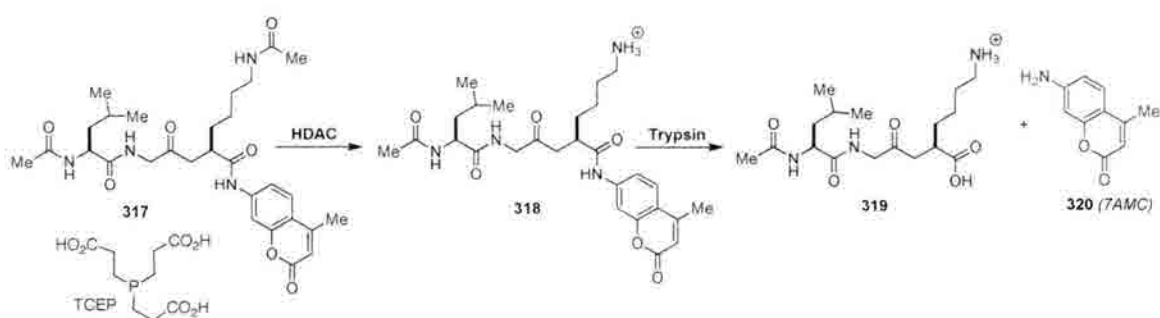
5.1.1 Synthetic Goals

As described earlier, the driving force behind our synthetic interest in largazole is its biological activity and selectivity for HDAC1. Although selectivity for any specific isoform is desirable in that a compound displaying such activity would contribute to the understanding of the function of the isoform, HDAC1 is a particularly desirable target. Knock-out experiments in mice have shown that the deletion of both HDAC1 alleles results in an embryonic lethal phenotype, illustrating its overall importance¹⁶⁸. Furthermore, knock-down experiments using siRNA have suggest that HDAC1 is essential for the proliferation and survival of cancerous cells⁶⁷. Given that most currently known HDACi lack specificity, we were interested in pursuing not only the synthesis of the natural product, but analogs as well. In so doing, we hoped to identify new compounds that would display improved activity and selectivity, with an eye towards the eventual goal of synthesizing an inhibitor with class- and eventually, isoform-specificity. To this end, we use a combination of synthetic work, biological assays and computational models in order to identify these molecules. In order to accomplish these goals, our group has joined others in a collaboration to study these newly created HDACi. The work of our collaborators is discussed below.

5.1.2 Biological Assays

Clearly, as we are guided in our synthetic work by biological data, we are greatly indebted to our collaborators in both Dr. Douglas Thamm's and Dr. James Bradner's groups. Dr. Thamm's work will focus on studies of the natural product and its analogs in mouse models. These studies are still underway, and will therefore not be discussed in further detail in this work. Dr. Bradner has developed an enzymatic assay to measure the activity of these compounds, as discussed below.

A coupled fluorogenic homogeneous assay was developed by this group, wherein purified HDACs are incubated with trypsin, serum albumin and a fluorogenic substrate (**317**, Scheme 59). Upon deacetylation of the lysine residue, 7AMC (7-amino-4-methylcoumarin, **320**) is rapidly released by trypsin cleavage and detected by a fluorimeter. The presence of albumin buffers the reaction mixture such that HDAC degradation is not observed. The assay is reproducible and sensitive, requiring limited amounts of enzyme (3 - 100 ng per well). To improve compatibility with studies of disulfide-containing compounds such as FK228, assay performance has been optimized under the reducing conditions required to observe potent inhibitory activity of these molecules.



Scheme 59: Coupled fluorogenic assay for HDAC inhibitors.

Interestingly, work in the Bradner group showed that the most commonly used reducing agents (dithiothreitol and β -mercaptoethanol) for this type of assay gave an unusual result: substantial enzyme inhibition was observed at concentrations of these agents required to reduce the FK228 disulfide bond. In contrast, tris(2-carboxyethyl)-phosphine hydrochloride (TCEP) demonstrated weak enzyme inhibition at concentrations markedly higher than that required to activate FK228. This suggests that both dithiothreitol and β -mercaptoethanol may, in their own right, attenuate the activity of the histone deacetylase enzyme. However, under reducing conditions with TCEP (200 mM), biochemical studies of individual isoforms reported accurately on the true inhibitory potency of this class of disulfide prodrug HDAC inhibitors. Thus, HDAC inhibitory activities previously reported for the disulfide-containing HDACi should be viewed with caution, as the presence of other thiols in the assay system may have interfered with the activity of the agent under analysis.

5.1.3 Computational Modeling

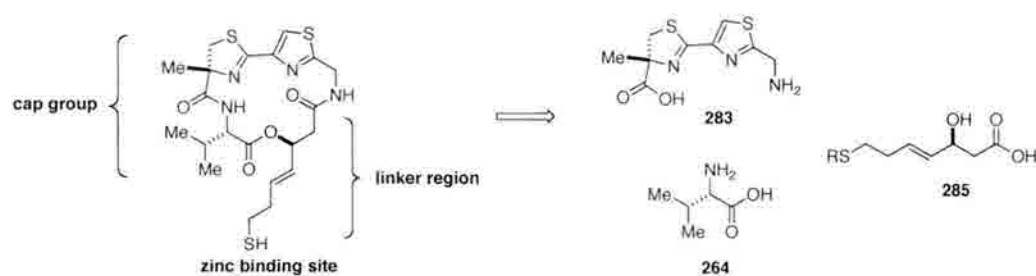
As mentioned in the previous chapter, much of the information with regard to the structure of the HDAC enzymes arose from the crystal structure of the HDAC-like protein (HDLP), a yeast homolog. To date, the crystal structure for human HDAC1 has not been solved, although a structure of HDAC8 was recently disclosed¹⁶⁹. The importance of these studies cannot be underestimated; however, given the lack of such direct information with regard to human HDAC1 specifically, other means of determining structure-activity relationships must be employed. To this end, we are indebted to our collaborators in the laboratories of Dr. Olaf Wiest for performing molecular modeling studies.

This group has developed models for HDACs 1,2,3 and 8, which can then be used to predict docking interactions between these enzymes and potential inhibitors^{169,170,171}. In fact, their model for HDAC8 was shown to be extremely accurate following the publication of the crystal structure. This powerful tool can be used, not only to rationalize interactions between the enzyme and substrate, but also to make predictions regarding promising synthetic targets. These computational models have aided us greatly in analyzing biological data and identifying new targets for synthesis (discussed in more detail below).

5.2 Previous Work in the Williams Group

5.2.1 Retrosynthetic Analysis

In keeping with the goal of developing analogs of the natural product, a modular synthesis was desirable so as to permit access to libraries of compounds as quickly as possible. As discussed in the previous chapter, the HDACi pharmacophore can be divided into the cap region (macrocycle), the zinc-binding region, and the tether connecting the two. The retrosynthetic approach shown below relies upon disconnections of those three regions to ease introduction of variation (Scheme 60).



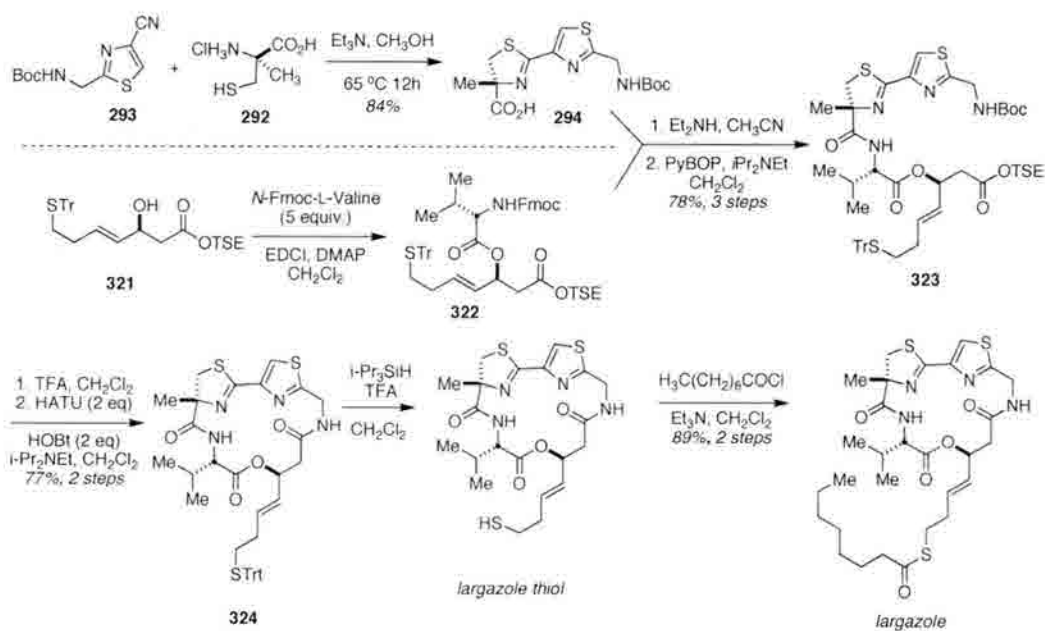
Scheme 60: Retrosynthetic approach.

As seen in the approaches taken by other groups, the molecule would arise from three separate pieces: a thiazoline-thiazole moiety, L-valine, and the β -hydroxy acid-

containing portion of the molecule, all of which could be replaced by differently modified pieces at a later date.

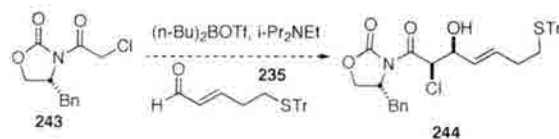
5.2.2 Synthesis of (+)-Largazole

The first important step in this project was the synthesis of largazole itself, which was completed by Dr. Albert Bowers as shown in Scheme 61. As discussed in the context of the syntheses of other macrocycles, the challenges in this route were the formation of the β -hydroxy acid piece and the macrocyclization.



Scheme 61: Synthesis of largazole.

In early attempts, we hoped to use a strategy similar to that used by Janda in the synthesis of FR901375; namely, the use of the Evans chiral auxiliary to access the β -hydroxy acid as shown in Scheme 62¹³².



Scheme 62: Original efforts towards the β -hydroxy acid.

The stereochemistry of the alcohol would be the opposite of that seen in the natural product, as the original attempts focused on the use of a Mitsunobu reaction to close the macrocycle at the depsipeptide bond in the interest of installing this somewhat labile functionality late in the synthesis.

However, in the event, these reactions provided complex mixtures of products. We were certain that this reaction could be optimized in order to reflect the reported yield and diastereoselectivity (69 percent and >90 percent, respectively); however, as we had a good supply of the requisite phenylalanol in hand, we chose to pursue a different strategy using the Nagao auxiliary (synthetic details supplied below and in the Experimental Section).

With access to the β -hydroxy acid, attention was turned to the completion of the synthesis; notably, the macrocyclization step. Unfortunately, the proposed Mitsunobu reaction proved to be unsuccessful, and a direct macrocyclization approach was then pursued, necessitating the synthesis of the opposite enantiomer of the alcohol, with the *S*-configuration seen in the natural product. Cyclization attempts utilizing Yamaguchi, Muykaiyama, Keck and Shiina protocols were also unsuccessful; other groups as well later reported difficulties with this particular bond formation. Therefore, in order to complete the synthesis, a different bond disconnection was chosen; namely, the least sterically hindered amide bond as shown above in Scheme 61¹⁶⁰.

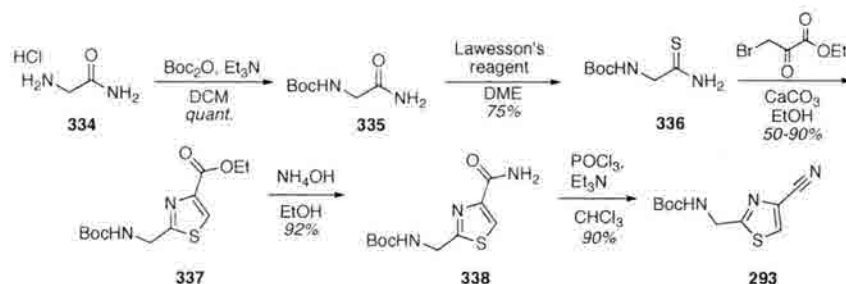
5.2 Synthesis of (-)-Largazole

5.2.1 Synthetic Goals

Following the completion of the total synthesis of (+)-largazole by Dr. Albert Bowers, we decided to attempt the total synthesis of its enantiomer. We chose to pursue

in methanol resulted in considerably longer reaction times (2 hours for thionyl chloride vs 2 days for sulfuric acid in methanol), the reaction was much cleaner, and this procedure was therefore chosen. Following formation of the methyl ester, treatment with pivalaldehyde and triethylamine in refluxing pentane with removal of water gave **330**, which was formylated and methylated to give **332**. Opening of the five-membered ring in refluxing 5N hydrochloric acid furnished the desired α -methylcysteine. This sequence proved to be both reliable and scalable up to at least 20 grams.

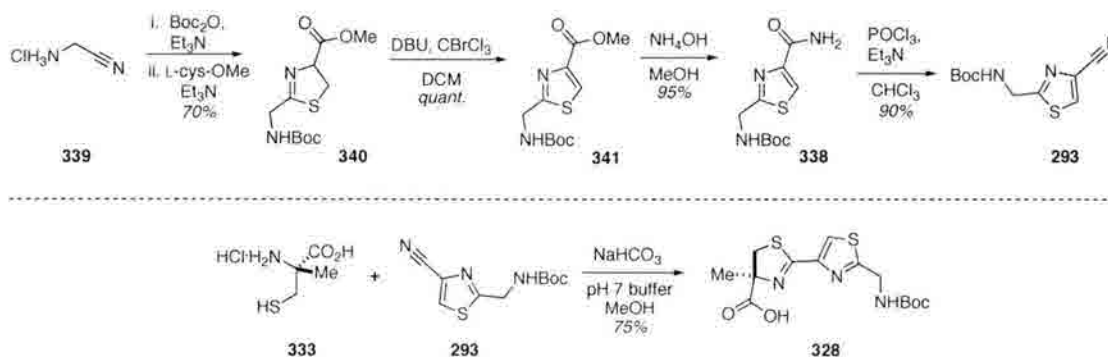
With access to the α -methylcysteine portion, we then turned our attention to the thiazole nitrile which was required to finish the construction of this section of the molecule. Originally, we followed the sequence shown below to synthesize the necessary nitrile (Scheme 65).



Scheme 65: Synthesis of thiazole nitrile.

Although this route did provide ample amounts of material, we decided to adopt a procedure published by Cramer instead^{162b}. Essentially, we were concerned about the highly variable yields in the formation of ethyl ester **337**. On a smaller scale, the reaction worked quite well; however, when scale-up for the synthesis was attempted, yields dropped rapidly. It seemed that the problem lay not in the reaction itself, but rather was associated with difficulties in purification. The product is highly crystalline, but attempts to recrystallize directly from the crude mixture gave unsatisfactory results.

Unfortunately, the product tends to crystallize on the column, leading to the lower yields observed. To avoid this problem, we then adopted Cramer's aforementioned route, as shown below (Scheme 66).

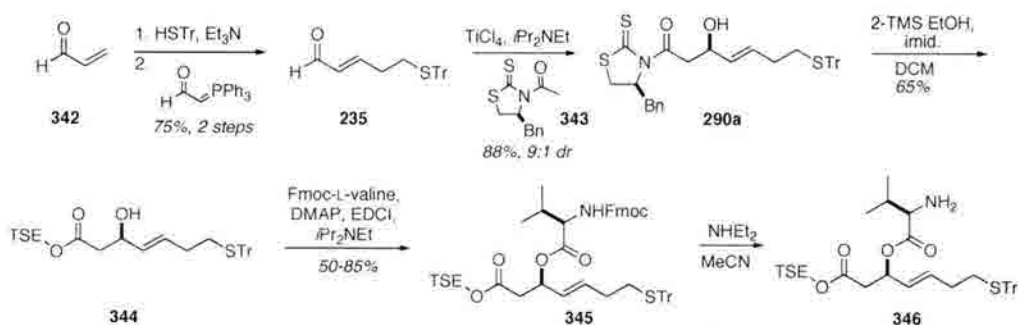


Scheme 66: Improved route to thiazole nitrile and completion of thiazoline-thiazole.

Although the number of steps remains the same, this route requires no chromatography step after formation of the ester, thereby avoiding the purification problems mentioned in the original route. With the nitrile in hand, it was then condensed with the α -methyl cysteine described above, as shown in Scheme 66.

5.2.3 Synthesis of β -Hydroxy Acid

We chose to use a strategy published by Ganesan to access aldehyde **235**, followed by an aldol reaction wherein a chiral auxiliary would control the stereochemical outcome¹³⁵.



Scheme 67: Synthesis of β -hydroxy acid piece.

We selected the Nagao auxiliary (**343**) shown in Scheme 67, which gave the appropriate stereochemistry for the alcohol in ~9:1 ratio of easily separable diastereomers. Removal of the chiral auxiliary followed by EDCI-mediated depsipeptide bond formation and Fmoc deprotection gave **346**, which was ready for coupling to thiazole-thiazoline portion of the molecule.

One lingering difficulty in this synthesis is the formation of the depsipeptide bond. This particular reaction is somewhat low yielding and rather inefficient, requiring five equivalents of valine and six equivalents of EDCI in conjunction with DMAP. Our originally published conditions called for the omission of an aqueous work-up in favor of immediate purification by column chromatography; however, the presence of such a large amount of sparingly soluble and insoluble material led to difficulties with this approach on a larger scale¹⁶⁰. An aqueous work-up improved the yield somewhat (from ~50-65% to ~70-80%). However, due to the presence of catalytic DMAP, Fmoc deprotection was also seen, which also presumably contributed to the low yield. In an attempt to improve this reaction, a small screening of different conditions was performed as shown in Table 15.

Table 15: Conditions for depsipeptide bond formation.

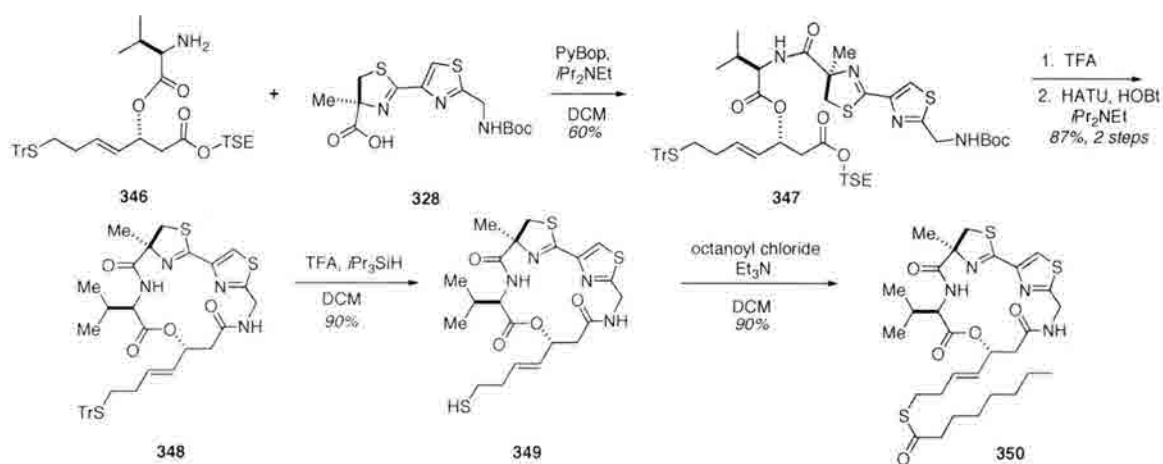
Fmoc-valine	Conditions	Yield
5 equiv	EDCI, 6 equiv; DMAP 0.1 equiv; DIPEA, 6 equiv; 15 h	50-80%
1.2 equiv	PyBop, 2 equiv; DIPEA, 3 equiv; 15 h	50%
1.2 equiv	HATU, 2 equiv; DIPEA, 3 equiv; 2 h	< 10%
1.2 equiv	HOBt, 2 equiv; HATU, 2 equiv; DIPEA, 3 equiv; 15 h	45%
3.4 equiv	DIAD, 2.98 equiv; PPh ₃ , 3.3 equiv; 2.5 h	15%
5 equiv	EDCI, 6 equiv; DMAP, 0.1 equiv; DIPEA, 6 equiv; 3 h	85%

It was hoped that more reactive peptide coupling reagents would permit less valine to be used in the course of the reaction, and perhaps limit the amount of Fmoc

deprotection. Unfortunately, we found extensive Fmoc deprotection in almost every case, and yields were not improved over the original conditions. In the case of the attempted Mitsunobu reaction, no Fmoc deprotection was seen; however, substantial elimination of the alcohol occurred. DCC-mediated coupling was also attempted by Dr. Kenneth Miller, but this reaction resulted in a complex mixture of products. Ultimately, we chose to return to a variation on the original conditions. Thinking that perhaps the longer reaction time was the major contributing factor to Fmoc deprotection (due to a longer exposure to DMAP), we attempted to run the reaction under somewhat more concentrated conditions for a shorter period of time. The yield is moderately improved under these circumstances, although this problem remains something of a bottleneck in the current synthesis.

5.2.4 Completion of (-)-Largazole

Although we continue to work towards more satisfactory conditions for the depsipeptide bond formation, we were able to use the route discussed above to synthesize the desired piece (**345**) in gram quantities. We therefore chose to move forward with the completion of the synthesis, as shown in Scheme 68.



Scheme 68: Completion of *ent*-largazole.

Following a PyBop-mediated coupling of acid **328** and amine **346**, deprotection of both the *N*-Boc group and trimethylsilylethyl ester was effected with TFA. Macrocyclization proceeded smoothly with HATU and HOBt to give the *S*-trityl protected macrocycle. Deprotection of the trityl group gave the enantiomer of the biologically active species, and acylation provided (-)-largazole in 90% yield. NMR spectra matched the published spectrum of the natural product, and the optical rotation was measured to be -20.5° ($c=1$ in methanol, literature value for the natural product = $+22^\circ$).

5.3 Amide Isostere Analogs

5.3.1 Synthetic Goals

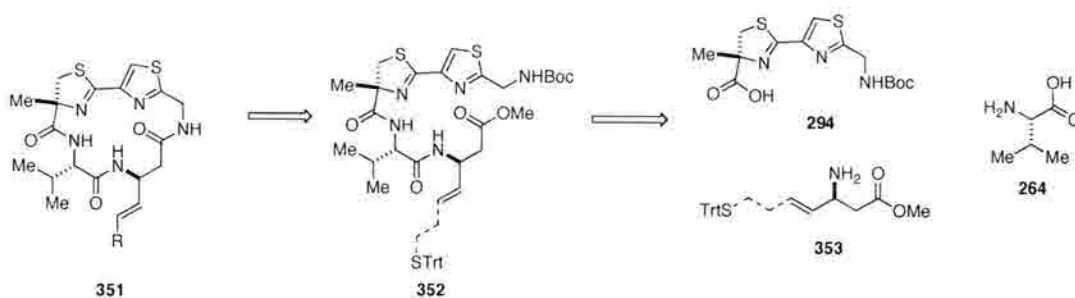
In addition to our desire to better understand the effect of stereochemistry on biological activity, we wished to explore variations on the depsipeptide bond. We therefore decided to target the amide isostere of largazole for three reasons: 1) as aforementioned, the depsipeptide bond is somewhat problematic to access synthetically; 2) we hoped that the more rigid amide bond might contribute to greater activity or specificity; and 3) with an eye towards possible druggable compounds, we wished to replace the labile depsipeptide bond with a more robust amide linkage.

With respect to the biological activity, we were hopeful that this change would not result in any loss of biological activity, as computational modeling studies performed by our collaborator Dr. Olaf Wiest suggested that the interactions between the cap region and the HDAC enzyme would remain the same. Specifically, in preliminary studies, it appeared that the thiol would extend towards the zinc ion at the bottom of the entrance channel with a Zn-S distance of ~ 2.5 Å, while the macrocycle would sit at the mouth of

the pocket in both cases. The hydrocarbon chain filled the hydrophobic channel lined by Phe 150 and Phe 205¹⁷⁰. Importantly, the orientation of the macrocycle was similar in the ester and the amide isostere, maximizing hydrophobic interactions between the cap region and the HDAC enzyme.

With the aforementioned goals in mind, we therefore began pursuing two synthetic projects in parallel. Dr. Albert Bowers synthesized the amide isostere of largazole itself. Concurrently, the amide isostere core was prepared with an eye towards further variation in the side chain via metathesis as had been successfully performed in prior syntheses of largazole using the depsipeptide core of the molecule.

In order to complete this synthesis, we again opted for the modular strategy discussed above, using the thiazoline-thiazole, L-valine, and an amino acid derivative to replace the β -hydroxy acid portion of the molecule.

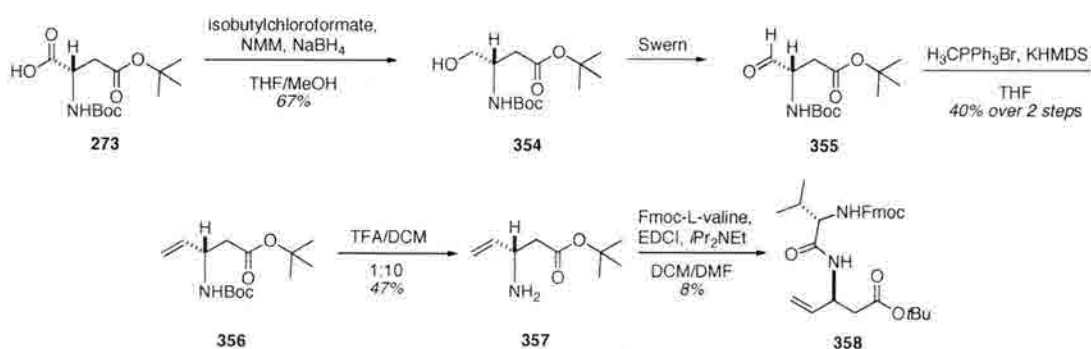


Scheme 69: Retrosynthetic analysis of amide isostere.

5.3.2 β -Amino Acid Synthesis

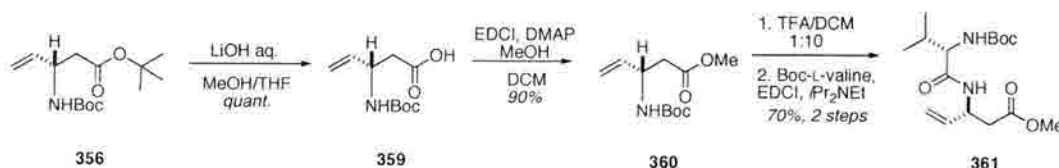
To begin our synthesis of the metathesis substrate of the amide isostere, we focused on the β -amino acid, using the route delineated below in Scheme 70. In a sequence similar to one used by Dr. Thomas Greshock in his synthesis of the FK228 amide isostere, reduction of *N*-Boc-Asp-*t*-butyl ester **273** to the corresponding alcohol, followed by Swern oxidation to the aldehyde gave **355**. This aldehyde had been shown to

be particularly prone to racemization; however, in his work, Dr. Greshock found a work-up procedure described by Zappia et al. which prevents this from occurring¹⁷². Still, we found that the aldehyde should be used immediately in the Wittig reaction that follows.



Scheme 70: First generation β -amino acid synthesis.

Once the terminal olefin was installed, Boc deprotection was effected, followed by introduction of Fmoc-L-valine. Unfortunately, this reaction proceeded in a disappointing eight percent yield. Furthermore, although we were originally pleased to see that the *tert*-butyl ester had survived the Boc deprotection conditions, looking ahead, we were somewhat concerned that we might need to employ harsher conditions in its eventual removal. For these reasons, we elected to instead pursue the route shown below.



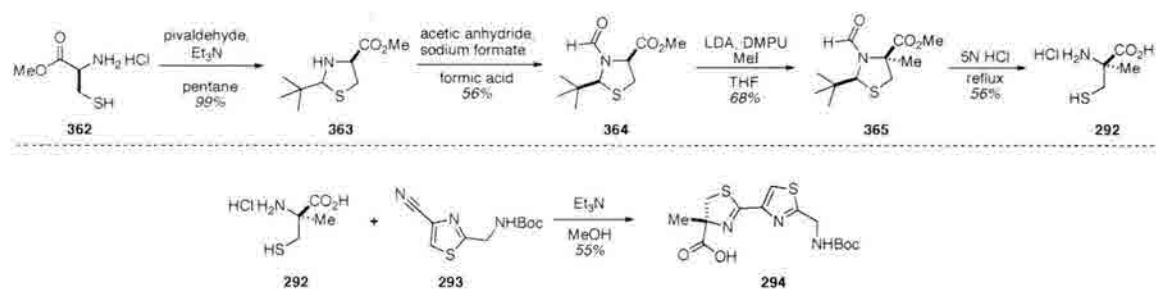
Scheme 71: Improved β -amino acid synthesis.

The *tert*-butyl ester was removed in order to be replaced with the methyl ester in a two-step procedure (Scheme 71). Deprotection of the *N*-Boc group, followed by coupling to *N*-Boc-L-valine was then attempted. In our original attempts, PyBop-mediated coupling seemed preferable due to overall shorter reaction times.

Unfortunately, these attempts furnished complex mixtures of products; however, EDCI-mediated coupling gave the desired product in 70 percent yield.

5.3.3 Completion of the Amide Isostere Core

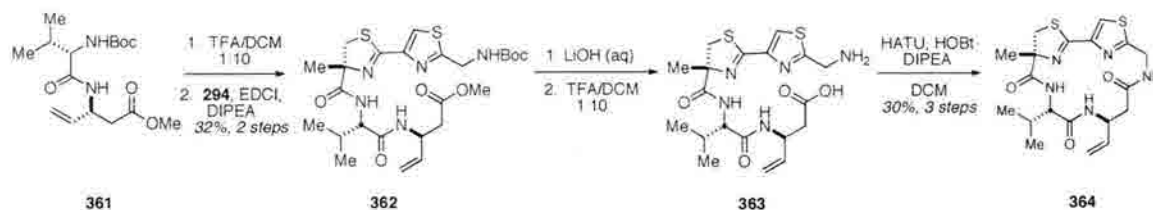
With a route secured to the β -amino acid, we were ready to complete the synthesis of the metathesis substrate. This required the synthesis of the opposite antipode of the thiazoline-thiazole subunit than previously shown, so as to possess the stereochemistry observed in the natural product (Scheme 72).



Scheme 72: Synthesis of thiazoline-thiazole.

Having accessed this portion of the molecule, we continued with the construction of the metathesis substrate as shown in Scheme 63. Following Boc deprotection, the free amine was coupled to **294**, albeit in poor yield. The reason for this presumably lies with problems during purification, in that an unidentified byproduct proved extremely difficult to remove under all conditions tried. However, with access to some quantity of the acyclic precursor, we continued the synthesis with deprotection of both the methyl ester and *N*-Boc groups. Cyclization was accomplished using a variation on the conditions reported in the synthesis of both largazole and its enantiomer. In the syntheses of those molecules, no significant amount of dimerization was seen; however, this proved not to be the case with the amide isostere analogs, regardless of the low (0.001 M)

concentration used. We therefore chose a slow addition of the acyclic precursor over ~12 hours; under these conditions, no noticeable dimerization occurred.



Scheme 73: Completion of the amide isostere core.

Although we were able to access the metathesis substrate (**364**), yields were poor. The most logical reason for this is, again, difficulties with purification. It did not prove possible to separate the macrocycle by column chromatography or preparatory thin layer chromatography under all conditions tried; specifically, regardless of eluent, the macrocycle appeared to co-elute with an unidentified by-product. However, separation by chromatotron proved possible, although this does somewhat limit the scale of the reaction.

At this point, as we prepared to begin the synthesis of analogs containing different side chains via metathesis reactions, biological data was received from our collaborators in Dr. James Bradner's research group. This showed that the amide isostere of largazole itself was significantly attenuated in its activity in comparison to largazole (Table 16).

Table 16: Biological data for largazole and its amide isostere.

Compound	HDAC1 IC ₅₀ nM	HDAC2 IC ₅₀ nM	HDAC3 IC ₅₀ nM	HDAC6 IC ₅₀ nM
largazole thiol	0.1	0.8	1	40
largazole isostere thiol 162	0.9	4	4	1500
largazole isostere 163	>3000	>3000	>3000	>3000
SAHA	10	40	30	30

The reason for this loss of biological activity was elucidated by computational studies performed by Dr. Olaf Wiest, as shown below in Figure 14.

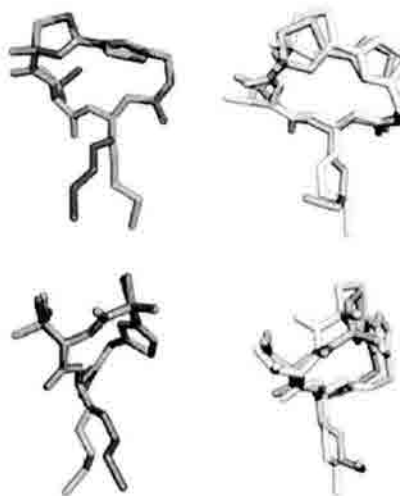


Figure 14: Top and side views of largazole and amide isostere conformations.

In orange, the lowest energy binding conformation of largazole is shown, superimposed by the average lowest energy conformation in blue. In yellow is shown the structure of the lowest energy binding conformation of the amide isostere, superimposed by its average lowest energy conformation in green. This shows the significant distortion that the amide isostere would need to undergo so as to bind the HDAC enzyme, and explains the decrease in biological activity. Given that our interest in this project is driven by the biological activity of the synthesized compounds, we did not further pursue analogs of the amide isostere.

5.4 Analogs of the Side Chain and Zinc-Binding Motif

5.4.1 Synthetic Goals

When studies of the amide isostere did not lead to compounds with improved biological activity, we decided to extend our work by examining the effects of variations in both the zinc binding moiety and the tether region. To this end, we elected to pursue a synthesis using the same depsipeptide core used to great effect by both Phillips and Luesch. In designing these analogs, we chose zinc binding motifs which were known in

other HDACi, as well as functional groups suggested by calculations⁸⁸. Using these criteria, we chose to use metathesis reactions to install the side chains shown below onto the depsipeptide core.

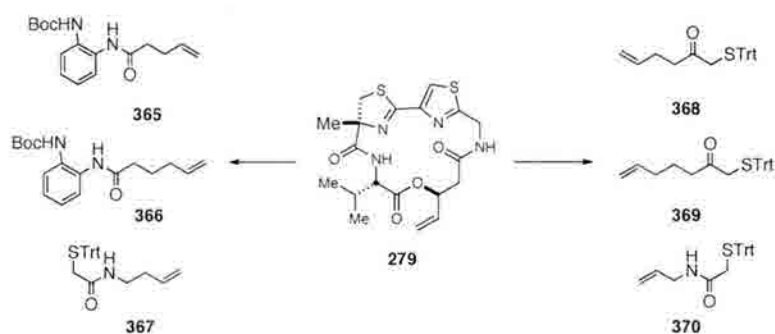


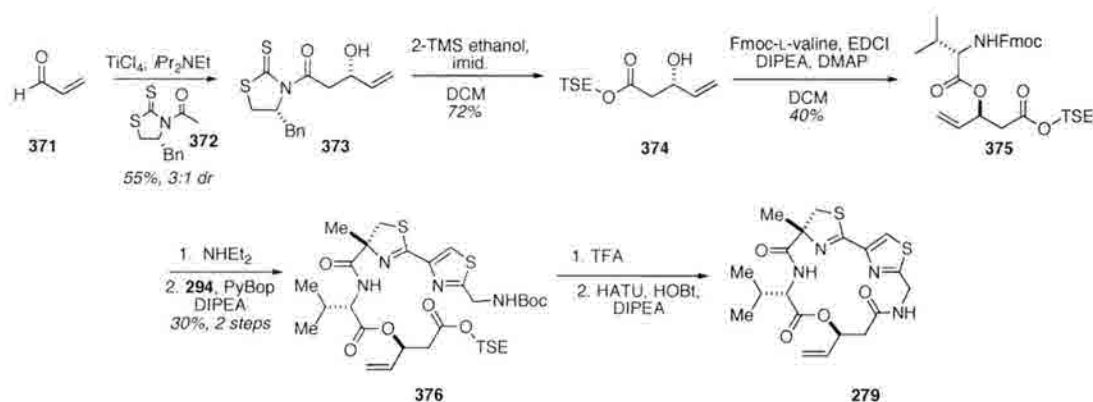
Figure 15: Proposed metathesis substrates.

Of these side chains, the benzamides were proposed so as to utilize the side chain contained in the known HDAC inhibitor MS-275. The remainder were suggested by calculations to be strong chelators of the zinc 2^+ cation⁸⁸. Although, as mentioned in the previous chapter, much research has been done on the appropriate length of the tether regions, we decided to synthesize each of these side chains in two different lengths. We made this decision on the basis of the fact that the macrocycle in largazole (a 16-membered ring) is somewhat larger than that seen in other cyclic HDACi (usually 12-13 membered rings), and we were therefore somewhat uncertain as to how side chains from other inhibitors would map onto largazole. Furthermore, although Cramer has shown that a distance of four atoms between the sulfur atom and the zinc-binding region is optimal, other work suggests a either a four or five methylene spacer^{162b}.

5.4.2 Accessing the Depsipeptide Core

To synthesize the depsipeptide core, we followed much the same route as we had in our earlier syntheses discussed above. Specifically, the major difference lies in the β -hydroxy acid portion of the molecule. Here, as opposed to the longer chain aldehyde

used in the synthesis of both largazole and its enantiomer, we used acrolein to provide the requisite pendant olefin (Scheme 74).

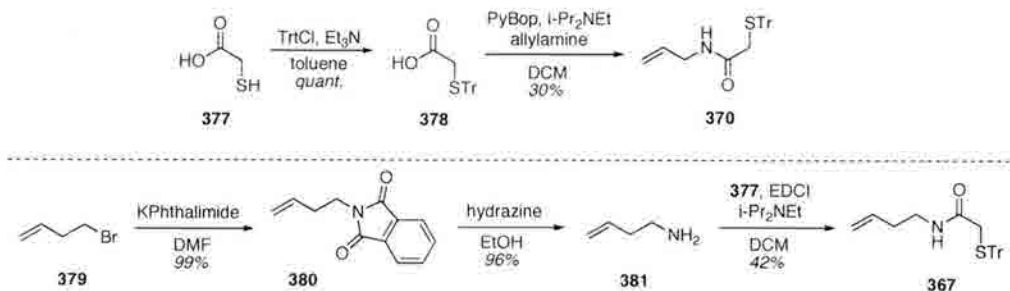


Scheme 74: Synthesis of the depsipeptide core.

The diastereoselectivity of the aldol reaction suffers somewhat, presumably due to the less sterically demanding nature of the aldehyde used in these reactions. The remainder of the synthesis however, proceeds with the use of similar conditions and gives similar yields to those previously discussed in the synthesis of the enantiomer.

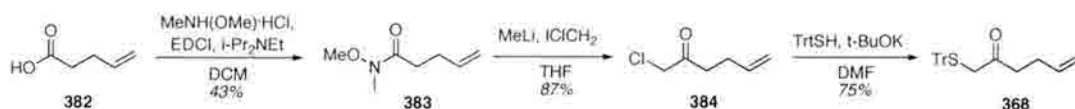
5.4.3 Completion of Analogs

Once the depsipeptide core was synthesized, we turned our attention to the synthesis of the side chains shown above. These were generally easily accessible through the routes shown in Schemes 75-77.



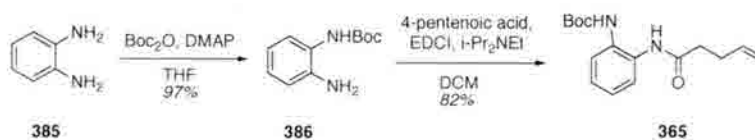
Scheme 75: Thioamide syntheses.

In each case, we relied upon *S*-trityl protected mercaptoacetic acid as the source of the thiol. The requisite amine for the coupling reaction was either commercially available (allylamine) or easily accessed from commercially available material (**381**). Although the yields in both coupling reactions are less than optimal, we were able to use these syntheses to access the ~1 g quantity needed for the metathesis reactions.



Scheme 76: Synthesis of α -thio ketone.

Next, we began the syntheses of the α -thio ketone and benzamide series. In the first case, formation of the Weinreb amide followed by treatment with methyllithium and chloriodomethane gave α -chloro ketone **384**. The chloride was then displaced with trityl thiolate to give the desired metathesis substrate (**368**). For the benzamide series, monoprotection of the diamine shown in Scheme 77 (**385**), followed by peptide coupling with pentenoic acid gave the desired compound (**365**) in good yield. The remaining two metathesis substrates were synthesized using the same approach by Dr. Albert Bowers, who also performed the metathesis reactions.



Scheme 77: Synthesis of benzamide.

Following cross-metathesis, the library of compounds shown below in Figure 16 was accessed, and each was sent for biological testing in the Bradner laboratories. The thiol-containing compounds were tested as the free thiol, and the benzamides as the free amine. The results for this testing are shown below in Table 17¹⁷³.

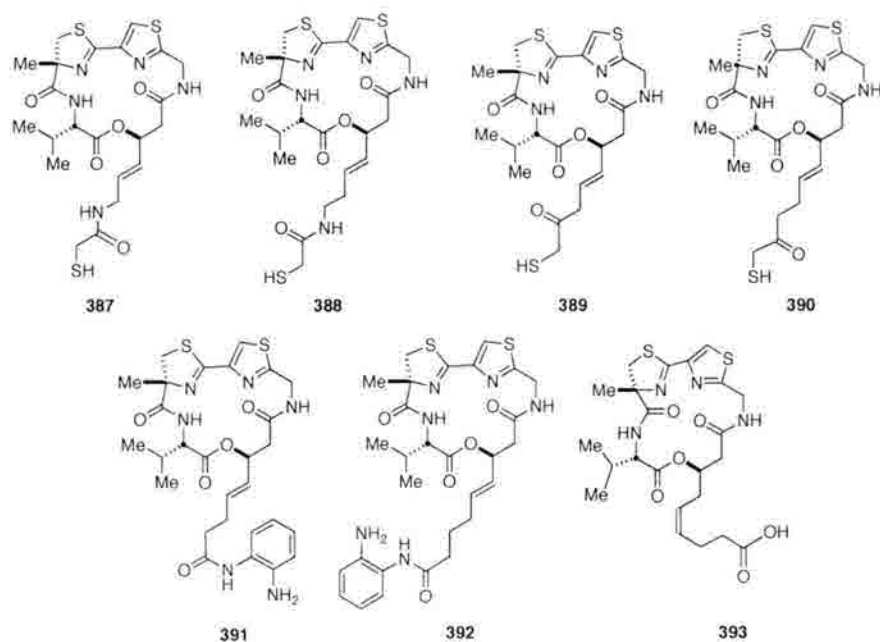


Figure 16: Side chain and zinc-binding region analogs.

Compound **393**, a larginolide-azumamide hybrid, was not accessed through the metathesis route due to the necessity of the *cis* olefin. Rather, this compound was synthesized by Ms. Annie Troutman-Youngman using a route similar to that taken to the enantiomer of larginolide wherein the aldehyde of the side chain as a whole was used as the substrate for the aldol reaction. Biological data for these compounds, as well as (-)-larginolide, are tabulated below in Table 17.

Table 17: Biological data for larginolide analogs.

Compound	HDAC1 IC ₅₀ nM	HDAC2 IC ₅₀ nM	HDAC3 IC ₅₀ nM	HDAC6 IC ₅₀ nM
(+)-larginolide thiol	1.2	3.5	3.4	49
(-)-larginolide thiol	1200	3100	1900	2200
larginolide-azumamide hybrid 393	>30000	>30000	>30000	>30000
benzamide 391	270	4100	4100	>30000
benzamide 392	23000	29000	14000	>30000
thioamide 387	670	1600	960	700
thioamide 388	1000	1900	1500	240
SAHA	10	26	17	13
MS-275	45	130	170	>30000

Interestingly, although clearly much less active than largazole itself, the activity of the enantiomer displays nearly the same pattern as the natural product. However, as can be seen above, none of the analogs of the zinc-binding region displays activity which was on par with largazole.

5.5 Further Linker Region Analogs

5.5.1 Synthetic Goals

Prior to receiving the rather disappointing results shown in Table 17, we had begun another set of studies on this region of the molecule. Although variation in linker length and the zinc-binding region had then been explored by our group and others, one possibility that remained largely unexamined was the position of the double bond. While the largazole-azumamide hybrid contains an olefin which is transposed by one carbon in its position in the side chain, we did not feel that this constituted a complete exploration into the effect of olefin migration on biological activity. In that particular compound (**393**), there were many other changes made to the molecule at the same time (*cis* olefin instead of *trans*, and a different zinc-binding moiety). In order to undertake a more detailed study of the possible effect of this variation, we decided to pursue a synthesis wherein we would change only the position of the double bond while testing similar lengths of the tether and the same zinc-binding regions as those discussed above. As such, we decided to pursue syntheses of the library of analogs shown below, wherein the double bond is transposed one carbon down on the side chain in relation to its location in the natural product (Figure 17).

It was hoped that these compounds could be accessed through the same type of metathesis reactions used in the creation of the library shown earlier in Figure 16;

however, the position of the double bond meant that the synthesis would need to be modified in two ways. First, in order to keep the length of the tether region consistent with the earlier library, each of the side chains would need to be truncated by one carbon. Additionally, a different depsipeptide core would need to be constructed containing a pendant allyl group as opposed to the pendant vinyl used in the first analogs.

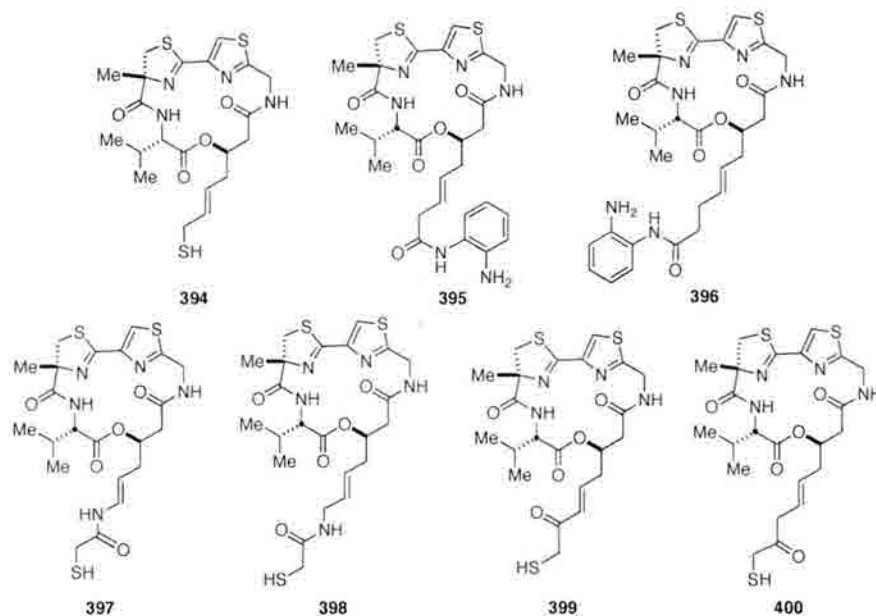
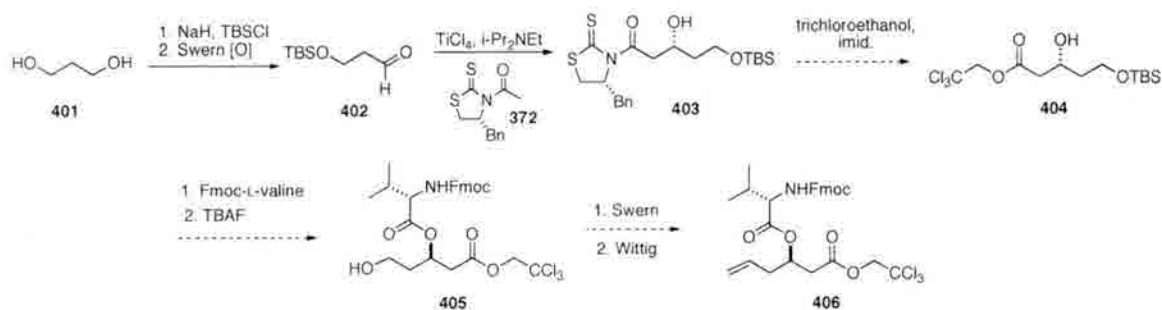


Figure 17: Proposed library of analogs.

5.5.2 First Generation Attempts

When designing the synthesis, we were somewhat concerned about possible migration of a β,γ unsaturated olefin in the presence of the aldehyde required for the aldol reaction. We therefore chose to pursue a route wherein the olefin would be installed somewhat later in the synthesis (Scheme 78). In order to avoid the β,γ unsaturated olefin, we hoped to carry protected alcohol **403** through the synthesis until after the introduction of L-valine. At this point, we could then deprotect and oxidize the alcohol, followed by introduction of a one-carbon unit through a Wittig reaction.



Scheme 78: Attempted synthesis of β -hydroxy acid.

This proposed sequence of events required the introduction of a different protecting group for the carboxylic acid. The trimethylsilyl ethyl ester which we had successfully used in prior syntheses is labile to a large variety of conditions; specifically, conditions for removal of the TBS group and conditions for the Wittig reaction. Although the use of TBS was certainly not our only choice (while we were slightly limited due to the presence of the Fmoc), the incompatibility of the TSE ester with olefination conditions was worrisome. We therefore selected the trichloroethyl ester instead, as it would be stable to these conditions and could be deprotected at the end of the synthesis under conditions that should not interfere with the remainder of the molecule as had been shown in syntheses of the azumamides¹²⁴.

Unfortunately however, in the event, we were unable to displace the chiral auxiliary under conditions similar to those we had used before. At this point, we chose to re-evaluate this route. Searching the literature revealed that our original concerns regarding the β,γ unsaturated aldehyde may have been unfounded. Examples of such compounds are known (although few in number), though these reports do show that isomerization is difficult to avoid. However, having found at least some precedent, we therefore chose to synthesize the β,γ unsaturated aldehyde, knowing that we would need to handle the compound carefully to prevent isomerization.

5.5.3 Second Generation Approach

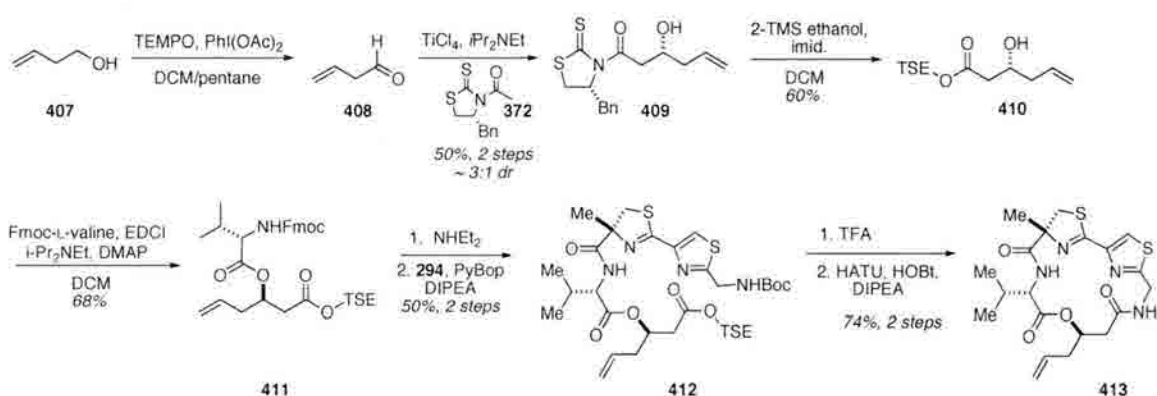
Having made the decision to attempt a direct oxidation of the appropriate alcohol, we tried several sets of conditions. The lingering difficulty with this particular route is the volatility of the desired aldehyde. Knowing that we would therefore most likely be unable to isolate the aldehyde (as proved to be the case), we sought conditions wherein purification would be as minimal as possible. We hoped to then add the aldehyde as a solution directly into the aldol reaction mixture. This requirement meant that, for example, Swern oxidation might be unrealistic. Although the alcohol we wished to oxidize was homoallylic instead of allylic, our first attempts focused on manganese dioxide-mediated oxidation, with the thought that a simple filtration of the reaction mixture would be the only purification necessary. Unfortunately, the homoallylic nature of the alcohol precluded success with this approach.

We then turned our attention to a promising report in the literature wherein the desired aldehyde was accessed through oxidation with Dess-Martin periodinane¹⁷⁴. This approach seemed quite promising: we found that starting material was completely consumed within two hours in a very clean reaction. However, the rather lengthy work-up procedure associated with this method meant that most of the aldehyde had evaporated, giving yields for the aldol reaction in only a trace amount. Furthermore, the use of a super-stoichiometric amount of Dess-Martin periodinane seemed to us rather inefficient.

This procedure being unsatisfactory, we then attempted oxidation with TEMPO using iodobenzene diacetate as the stoichiometric oxidant¹⁷⁴. This method also showed complete conversion of the alcohol to the aldehyde in two hours, and the somewhat

shorter work-up procedure allowed us to access somewhat more of the desired product. However, early attempts using only one equivalent of the alcohol (with respect to the chiral auxiliary and titanium tetrachloride in the aldol reaction) again were extremely low-yielding, giving less than 10 percent of the aldol product.

Finally, we chose to prepare the aldehyde in an apparent three-fold excess in the hopes that we would be able to carry on a full equivalent into the aldol reaction. This approach improves the yield greatly (to >50 percent), although the reaction clearly could be improved.



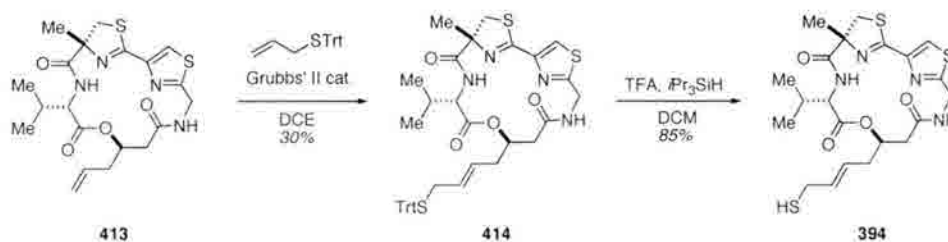
Scheme 79: Completion of allyl depsipeptide core.

The problem in the aldol reaction essentially lies in avoiding the introduction of water. While a greater excess of the aldehyde does improve the yield, the aqueous work-up following the reaction appears to be necessary in order to neutralize acetic acid. The idea of using the aldehyde as a solution also seems necessary, given that attempts to concentrate the product fail even at low temperatures. As a larger scale reaction to synthesize a larger excess of the aldehyde would clearly require more solvent, there is more opportunity to introduce water into the aldol reaction, leading to loss of the titanium tetrachloride. Furthermore, using more titanium tetrachloride in the reaction seems a poor idea as it is known that changing the ratio of titanium tetrachloride to Hünig's base

can affect the ultimate stereochemical outcome of the reaction¹⁷⁵. We therefore elected to pursue the route as shown in Scheme 79, as it does permit access to the desired product although yields remain low.

As with the previous depsipeptide core synthesis, the diastereoselectivity of the aldol reaction is somewhat lower than that seen using the more complete side chain. Furthermore, while the products of the aldol reactions in the other syntheses were known, this particular product was not. Luckily however, the corresponding acid is known in the literature^{176,177}. Removal of the chiral auxiliary with excess imidazole in the presence of water allowed us to access the acid. Optical rotation values were in agreement with the stereochemistry shown above ($\alpha_D +25.5^\circ$ $c = 1.0$ in CHCl_3 ; literature value for enantiomer: $\alpha_D -27.3^\circ$ $c = 1.0$ in CHCl_3)¹⁷⁷.

Having prepared the metathesis substrate, we completed the analog of the largazole thiol (Scheme 80).



Scheme 80: Completion of olefin-migration analog.

We were prepared to continue with the proposed library shown in Figure 17 using the same approach; however, at this point we received biological data from Dr. James Bradner's group from the previous library of side chain analogs (Table 17, above). Disappointingly, as shown earlier, all of these analogs showed significantly attenuated biological activity in comparison to largazole itself. These findings caused us to re-evaluate this portion of the project, given that none of the previously synthesized zinc-

binding regions improved the activity of the natural product to bring us closer to our goals. We therefore chose to turn our attention to different, hopefully more productive analogs, rather than continuing with the synthesis of this proposed library.

5.6 Cap Region Analogs

5.6.1 Synthetic Goals

Given the loss of biological activity observed in the side chain analogs, we chose to focus our attention on variation in the cap region instead. We had already explored the effects of stereochemistry through our synthesis of (-)-largazole, and Luesch had examined the effect of stereochemistry at the depsipeptide linkage (Table 14, Chapter 3). Our group and others had also examined the effects of substitution of the L-valine residue in favor of D-valine, L-alanine, and L- or D-proline. However, variations in the thiazoline-thiazole region of the molecule had not been attempted. This, therefore, was where we chose to engage our efforts. We began by performing some preliminary modeling studies in order to identify possible substitutions that would still map well onto the general structure of largazole itself (Figure 18).

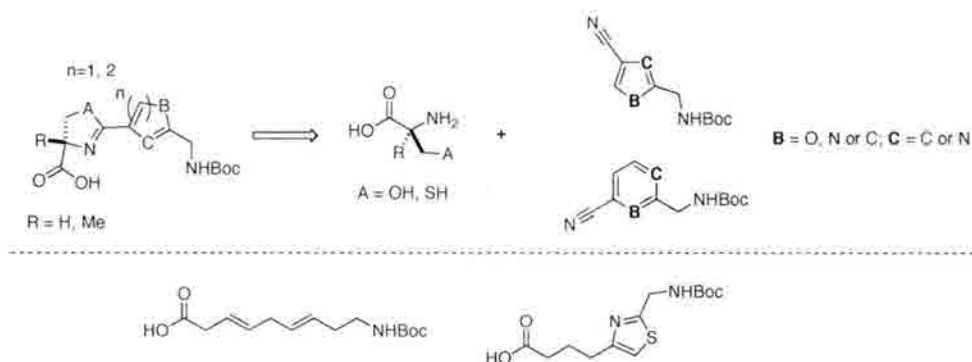


Figure 18: Possible analogs of the cap region.

Modeling studies using ChemDraw 3D, PC Model and physical models suggested that replacement of sulfur with oxygen would yield macrocycles which, although

somewhat smaller than largazole itself, would maintain the same general structure. Furthermore, it seemed that replacing the thiazole unit with a six-membered ring also maintained the desired scaffold. We also considered using completely saturated analogs of both ring systems, replacing the thiazoline with a hydrocarbon chain, or replacing the entire unit with an unsaturated all-carbon system as all of these were options wherein the general structure of the cap region was maintained.

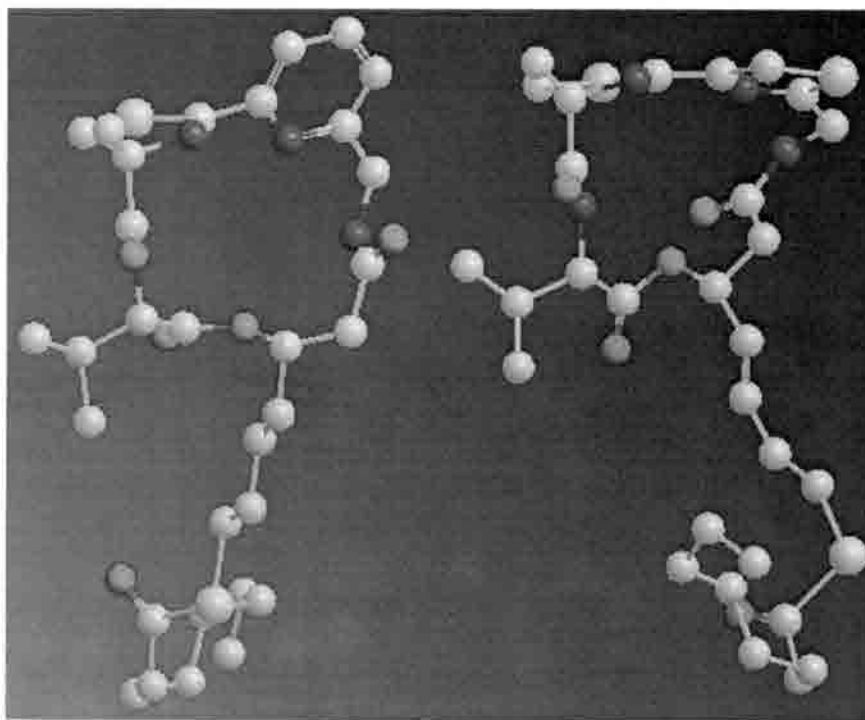
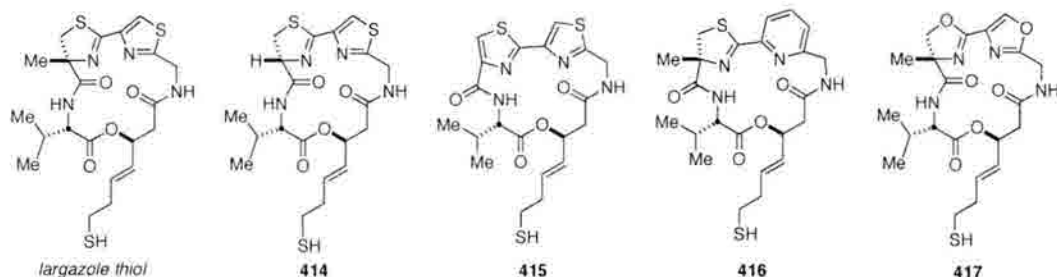


Figure 19: Thiazole to pyridine substitution (left) and largazole (right).

Ultimately, we chose to disqualify the fully saturated systems as targets for synthesis as we felt that the loss of rigidity in these systems would lead to a decrease in biological activity (as seen in the lesser biological activity displayed by the less rigid macrocycle of FK228 *vs* that of largazole). We also decided not to pursue the hydrocarbon replacements and benzene-type substitutions as we were concerned about the possible loss of hydrogen bonding interactions. However, the six-membered ring

system still appeared attractive as a target. Specifically, pyridine replacements for the thiazole appeared to be particularly promising (Figure 19). This analog, as well as several others shown below in Table 18 were later synthesized by Dr. Albert Bowers. Upon receipt of the biological data associated with these compounds, we were delighted by the results associated with three analogs (**414**, **416**, **417**). Compound **415** was a by-product from the synthesis of the α -methyl cysteine to cysteine substituted compound (**414**); air oxidation of such thiazolines is, unfortunately, a known problem¹⁷⁸. However, with access to an amount of **414** suitable for testing, we were interested to see that this compound displayed biological activity nearly equal to that of largazole itself. From a synthetic point of view, this finding might then permit us to cut the four steps and five days required for the synthesis of α -methyl cysteine from our route.

Table 18: Biological data for cap region analogs.



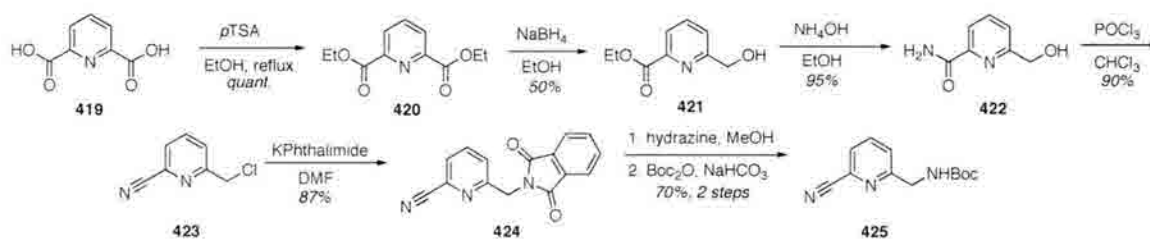
Compound	HDAC1 IC ₅₀ nM	HDAC2 IC ₅₀ nM	HDAC3 IC ₅₀ nM	HDAC6 IC ₅₀ nM
(+)-Largazole thiol	1.2	3.5	3.4	49
cysteine substitution 415	1.9	4.8	3.8	130
thiazole-thiazole 416	77	120	85	>30000
thiazoline-pyridine 417	0.32	0.86	1.1	29
oxazoline-oxazole 418	0.69	1.7	1.5	45
SAHA	10	26	17	13

More exciting still to us were the results pertaining to the oxazole-oxazoline (**418**) and thiazoline-pyridine (**417**). Both of these analogs are more active than the natural

product. Additionally, both showed a higher degree of selectivity for HDAC1 vs HDAC6 (~65-fold preference compared to largazole's 40-fold preference). Furthermore, we felt that these results gave us new possible targets to pursue in our synthetic efforts. Specifically, we wished to investigate the *des*-methyl thiazoline-pyridine analog, as the pyridine substitution has proven to have unprecedented biological activity.

5.6.2 Towards the *Des*-Methyl Thiazoline-Pyridine Analog

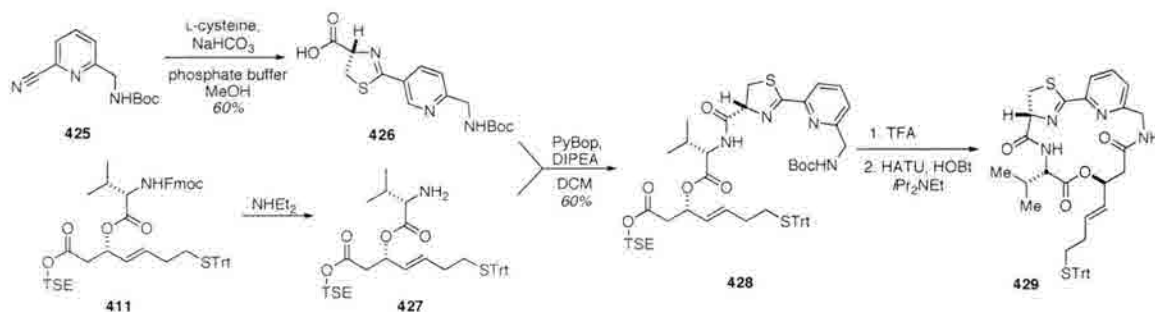
We first turned our attention to the synthesis of an appropriately substituted pyridine ring system (Scheme 81). Starting from 2,6-pyridinedicarboxylic acid, the diester was formed by treatment with excess *para*-toluenesulfonic acid in refluxing ethanol, after which reduction with sodium borohydride gave **421**. Formation of amide **422** by stirring overnight in ammonium hydroxide and ethanol, followed by dehydration and chlorination with phosphorous oxychloride gave nitrile **423** in a sequence of events similar to what we had used earlier to access the thiazole nitrile. From this point, installation of a nitrogen atom was required. This was accomplished by displacing the chloride with potassium phthalimide, followed by removal of the phthalimide and Boc protection to give **425**.



Scheme 81: Synthesis of pyridine nitrile.

From this point, we continued the synthesis in a manner similar to the syntheses discussed before. Our sole concern was possible oxidation of the thiazoline to the thiazole, as this had proven to be a problem in the synthesis of *des*-methyl analog **416**.

While yields in the coupling reaction between **425** and **427** were somewhat lower than what we had hoped for, we were able to isolate **428** in usable quantities. With access to the coupled substrate (**428**), we were able to complete the synthesis as shown below in Scheme 82.



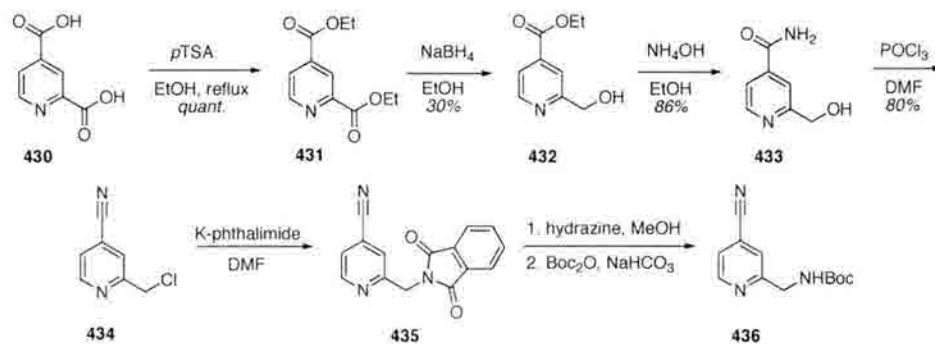
Scheme 82: *Des*-methyl pyridine analog.

¹H NMR of the crude mixture appeared to show formation of the macrocycle. In each macrocycle, the presence of two well-defined doublets at ~0.4 and ~0.7 ppm representing the valine protons is characteristic of a successful macrocyclization, and these signals were seen in the crude mixture. However, upon purification, the isolated (still somewhat impure) material displayed these doublets further downfield (1.44 and 1.52 ppm, respectively). Additionally, the appearance of a signal at 8.06 ppm was suggestive of a thiazole. Overall, this would seem to suggest that the sole isolated product was, in fact, a thiazole-pyridine containing macrocycle. As aforementioned, air oxidation of this type of compound is not unknown. The *des*-methyl analog (**415**) of largazole was isolable in ~30 percent yield; however, in this case, with a slightly less strained macrocycle, it may be that oxidation is unavoidable. We continue to search for appropriate purification conditions so as to avoid this issue, although at this time, the *des*-methyl pyridine analog remains a work in progress.

5.6.3 Towards a New Thiazoline-Pyridine Analog

As we began work on the substrate described above, we received information from our collaborator, Olaf Wiest. His calculations suggested that the pyridine analog series could be improved by moving the nitrogen contained in the pyridine ring to a different location. This suggestion was made on the basis of a hydrogen bonding interaction that would become available by virtue of changing the nitrogen atom to a position *para* to the thiazoline linkage. We decided to pursue this substrate, keeping the α -methylcysteine portion so as to avoid making too many changes to the molecule at once.

Our first step was again to focus on the synthesis of the pyridine nitrile, starting from 2,4-pyridinedicarboxylic acid, and following a sequence similar to the one shown in Scheme 80 for the previously discussed analog.



Scheme 83: Synthesis of nitrile **436**.

Of note is the low yielding nature of the reduction to form **432**. Originally, we had hoped that only the ester alpha to the nitrogen atom would be prone to reduction with sodium borohydride. However, some amount (~ten percent) of the undesired alcohol is seen. It is thought that the major issue with the yield in this reaction lies in difficulties with purification; we are currently seeking new conditions in order to improve upon this

step. Furthermore, the synthesis of **434** does not proceed as cleanly as that of the previously discussed pyridine analog. While we improve upon this synthesis, these reactions have been attempted only on very small scale, and yields are therefore not reported.

Once the desired nitrile can be accessed, we intend to pursue a route similar to that shown above for the *des*-methyl pyridine analog in order to complete the synthesis, whereupon this substrate can also be tested for its biological activity.

5.7 Summary and Concluding Remarks

5.7.1 Summary of Progress

Using the natural product (+)-largazole as a starting point, we have created numerous analogs in the pursuit of a highly active, highly specific histone deacetylase inhibitor. We have investigated the effects of changes in all three regions of the HDACi pharmacophore model - the cap, zinc binder, and tether (Figure 20).

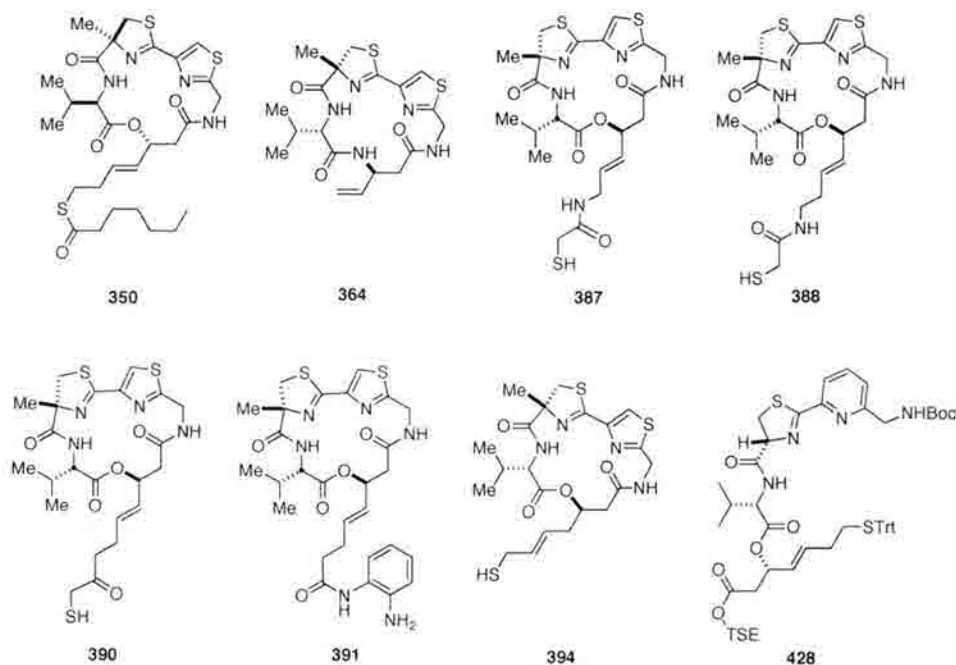


Figure 20: Summary of progress

Thus far, we have found that changes in the macrocycle - the cap region of the molecule - have been the most effective, although changes in stereochemistry (as shown by our synthesis of (-)-largazole, **350**) do not appear to be well tolerated. Furthermore, replacing the depsipeptide bond with an amide (as in **364**) resulted in the attenuation of biological activity. Likewise, changes in the length of the tether region and manipulation of the zinc-binding region (**387**, **388**, **390**, **391** - synthesized in a joint effort with Dr. Albert Bowers) result in a significant loss of biological activity; these findings led us to abandon our efforts towards metathesis reactions of the allyl-containing depsipeptide core (**413**), although the analog of the largazole thiol (**394**) was completed. Following the more promising biological data, we are currently pursuing the synthesis of two pyridine-containing analogs. In the first, we are working a *des*-methyl thiazole to pyridine substitution, with the farthest point reached thus far being **428**. In the second, the nitrogen in the pyridine ring is moved so as to take advantage of a possible favorable hydrogen bonding interaction. Work has begun on this project, and, as air oxidation is avoidable in this case, we anticipate success in this synthesis. It is hoped that results garnered from these molecules currently in progress will further guide us in our search for new histone deacetylase inhibitors.

5.7.2 Concluding Remarks

In the syntheses discussed above, we are guided in large part by both biological and calculational data from our collaborators, in addition to our own synthetic design. This has allowed us to create libraries of analogs in the hopes of improving on the biological activity and specificity of the natural product. Thanks to the rapid feedback that we receive, we are able to maintain a flexible approach to the targets selected for

total synthesis, focusing on those molecules that have the greatest probability for success in biological systems. In taking this approach, we have identified promising new candidates, and hope that our group's work will continue to contribute to this exciting field of research.

References

- ¹ Kitajima, M.; Nakamura, T.; Kogure, N.; Ogawa, M.; Mitsuno, Y.; Ono, K.; Yano, S.; Aimi, N.; Takayama, H. *J. Nat. Prod.* **2006**, *69*, 715-718.
- ² Takayama, H.; Horigome, M.; Aimi, N.; Sakai, S. *Tetrahedron Lett.* **1990**, *31*, 1287-1290.
- ³ Beyersbergen van Henegouwen, W.; Hiemstra, H. *J. Org. Chem.*, **1997**, *62*, 8862-8867.
- ⁴ Avila, A.; Burnett, B.; Tay, A.; Gabanella, F.; Knight, M.; Hartenstien, P.; Cizman, Z.; Di Prospero, N.; Pellizzoni, L.; Fishbeck, K.; Sumner, C. *J. Clin. Invest.* **2007**, *117*, 659-671.
- ⁵ Newkirk, T.; Bowers, A.; Williams, R. *Nat. Prod. Rep.*, **2009**, DOI 10.1039/b817886.
- ⁶ Sayre, L. *J. Am. Pharm. Assoc.*, **1919**, *8*, 708-711.
- ⁷ Schun, Y.; Cordell, G. *J. Nat. Prod.*, **1985**, *48*, 708-711.
- ⁸ Kitajima, M. *J. Nat. Med.* **2007**, *61*, 14-23.
- ⁹ Wahab, K.; Ahamd, F.; Din, L.; Hung, C.; Lian, M. *Tropical Biomed.* **2004**, *21*, 139-144.
- ¹⁰ Takayama, H.; Tominaga, Y.; Kitajima, M.; Aimi, N.; Sakai, S. *J. Org. Chem.* **1994**, *59*, 4381-4385.
- ¹¹ Wormley, T. *Am. J. Pharm.*, **1870**, *42*, 1-16.
- ¹² Orgell, W. *Lloydia*, **1963**, *11*, 36-43.
- ¹³ Rujjanawate, C.; Kanjanapothi, D.; Panthong, A. *J. Ethnopharmacol.*, **2003**, *89*, 91-95.
- ¹⁴ Wahab, K.; Ahmad, F.; Din, L.; Hung, C.; Lian, M. *Tropical Biomed.*, **2004**, *21*, 139-144.
- ¹⁵ Kitajima, M.; Nakamura, T.; Kogure, N.; Ogawa, M.; Mitsuno, Y.; Ono, K.; Yano, S.; Aimi, N.; Takayama, H. *J. Nat. Prod.* **2007**, *70*, 142.
- ¹⁶ Lin, H.; Danishefsky, S. *Angew. Chem. Int. Ed.*, **2003**, *42*, 36-51.
- ¹⁷ Nagakura, N.; Rüffer, M.; Zenk, M. *J. Chem. Soc. Perkin Trans.* **1979**, *9*, 2308-2312.
- ¹⁸ Kutchan, T. *Phytochem.*, **1993**, *32*, 493-506.
- ¹⁹ Dagnino, D.; Schripsema, J.; Verpoorte, R. *Phytochem.*, **1995**, *39*, 341-349.
- ²⁰ Ponglux, D.; Wongseripipatana, S.; Subhadhirasakul, S.; Takayama, H.; Yokota, M.; Ogata, K.; Phisalaphong, C.; Aimi, N.; Sakai, S. *Tetrahedron* **1988**, *44*, 5075-5090.
- ²¹ Takayama, H.; Odaka, H.; Aimi, N.; Sakai, S. *Tetrahedron Lett.* **1990**, *31*, 5483-5486.
- ²² Murahashi, S.; Oda, T.; Sugahara, T.; Masui, Y. *J. Org. Chem.*, **1990**, *55*, 1744-1749.
- ²³ Mitsui, H.; Zenk, S.; Shiota, T.; Murahashi, S. *J. Chem. Soc. Chem. Comm.*, **1984**, 874-875.
- ²⁴ a) Sheikh, Z.; Steel, R.; Tasker, A.; Johnson, A. *J. Chem. Soc. Chem. Comm.*, **1994**, 763-764. b) Dutton, J.; Steel, R.; Tasker, A.; Popsavin, V.; Johnson, A. *J. Chem. Soc. Chem. Comm.*, **1994**, 765-766.

- ²⁵ Yokoshima, S.; Tokuyama, H.; Fukuyama, T. *Angew. Chem. Int. Ed.*, **2000**, *39*, 4073-4075.
- ²⁶ Ng, F.; Lin, H.; Danishefsky, S. *J. Am. Chem. Soc.*, **2002**, *124*, 9812-9824.
- ²⁷ Early, W.; Jacobsen, J.; Madin, A.; Meier, P.; O'Donnell, C.; Oh, T.; Old, D.; Overman, L.; Sharp, M. *J. Am. Chem. Soc.*, **2005**, *127*, 18046-18053.
- ²⁸ Madin, A.; O'Donnell, C.; Oh, T.; Old, D.; Overman, L.; Sharp, M. *J. Am. Chem. Soc.*, **2005**, *127*, 18046-18053.
- ²⁹ Grecian, S.; Aubé, J. *Org. Lett.*, **2007**, *9*, 3153-3156.
- ³⁰ Fukuyama, T.; Liu, G. *J. Am. Chem. Soc.*, **1996**, *118*, 7426-7427.
- ³¹ Hart, D.; Tsai, Y.-M. *J. Am. Chem. Soc.*, **1982**, *104*, 1430-1432.
- ³² Atarashi, S.; Choi, J.-K.; Ha, D.-C.; Hart, D.; Kuzmich, D.; Lee, C.-S.; Ramesh, S.; Wu, S. *J. Am. Chem. Soc.*, **1997**, *119*, 6226-6241.
- ³³ Stork, G.; Krafft, M.; Biller, S. *Tetrahedron Lett.*, **1987**, *28*, 1035-1038.
- ³⁴ Penkett, C.; Byrne, P.; Teobald, B.; Rola, B.; Ozanne, A.; Hitchcock, P. *Tetrahedron*, **2004**, *60*, 2771-2784.
- ³⁵ Avent, A.; Byrne, P.; Penkett, C. *Org. Lett.*, **1999**, *1*, 2073-2075.
- ³⁶ Beyersbergen van Henegouwen, W.; Fieseler, R.; Rutjes, F.; Hiemstra, H. *J. Org. Chem.*, **2000**, *65*, 8317-8325.
- ³⁷ Beyersbergen van Henegouwen, W.; Fieseler, R.; Rutjes, F.; Hiemstra, H. *Angew. Chem. Int. Ed.*, **1999**, *38*, 2214-2217.
- ³⁸ Kogure, N.; Ishii, N.; Kitajima, M.; Wonscripipatana, S.; Takayama, H. *Org. Lett.*, **2006**, *8*, 3085-3088.
- ³⁹ Takayama, H.; Odaka, H.; Aimi, N.; Sakai, S. *Tetrahedron Lett.* **1990**, *31*, 5483-5486.
- ⁴⁰ Artman, G.; Weinreb, S. *Org. Lett.* **2003**, *5*, 1523-1526.
- ⁴¹ Abelman, M.; Oh, T.; Overman, L. *J. Org. Chem.* **1987**, *52*, 4130-4133.
- ⁴² Murray, W.; Mishra, P.; Sun, S.; Sengen, Maden, A. *Tetrahedron Lett.*, **2002**, *43*, 7389-7392.
- ⁴³ Murray, W.; Mishra, P.; Turchi, I.; Sawicka, D.; Maden, A.; Sun, S. *Tetrahedron*, **2003**, *59*, 8955-8961.
- ⁴⁴ White, J.; Xu, Q.; Lee, C.; Valeriote, F. *Org. Biomol. Chem.* **2004**, *2*, 2092-2102.
- ⁴⁵ Ragains, J.; Winkler, J. *Org. Lett.* **2006**, *8*, 4437-4440.
- ⁴⁶ Sakaitani, M.; Ohfuné, Y. *J. Org. Chem.*, **1990**, *55*, 870-876.
- ⁴⁷ Bordwell, F.; Drucker, G.; Fried, H. *J. Org. Chem.* **1981**, *46*, 632-635.
- ⁴⁸ Bordwell, F.; Fried, H. *J. Org. Chem.*, **1991**, *56*, 4218-4223.
- ⁴⁹ Pelly, S.; Govender, S.; Fernandes, M.; Schmalz, H.-G.; de Koning, C. *J. Org. Chem.*, **2007**, *72*, 2857.
- ⁵⁰ Ahrendt, K.; Williams, R. *Org. Lett.*, **2004**, *6*, 4539-4541.
- ⁵¹ Baran, P.; Hafensteiner, B.; Ambhaikar, N.; Guerrero, C.; Gallagher, J. *J. Am. Chem. Soc.*, **2006**, *128*, 8678-8693.
- ⁵² Dr. Tomas Greschock, personal communication.
- ⁵³ Berry, J.; Bradshaw, T.; Fichtner, I.; Ren, R.; Schwalbe, C.; Wells, G.; Chew, E.-H.; Stevens, M.; Westwell, A. *J. Med. Chem.*, **2005**, *48*, 639-644.
- ⁵⁴ Gabriel, T.; Wessjohann, L. *Tetrahedron Lett.*, **1997**, *38*, 1363-1366.
- ⁵⁵ Funk, R.; Bolton, G. *J. Am. Chem. Soc.*, **1988**, *110*, 1290-1292.
- ⁵⁶ He, Y.; Funk, R. *Org. Lett.*, **2006**, *8*, 3689-3692.

- ⁵⁷ Groth, U.; Schöllkopf, U.; Tiller, T. *Tetrahedron*, **1991**, *47*, 2835-2842.
- ⁵⁸ De Ruijter, A.; Van Gennip, A.; Caron, H.; Kemp, S.; Van Kuilenberg, A. *Biochem. J.*, **2003**, *370*, 737-749.
- ⁵⁹ Johnstone, R. *Nature Rev. Drug Disc.*, **2002**, *1*, 287-299.
- ⁶⁰ Avila, A.; Burnett, B.; Tay, A.; Gabanella, F.; Knight, M.; Hartenstien, P.; Cizman, Z.; Di Prospero, N.; Pellizzoni, L.; Fishbeck, K.; Sumner, C. *J. Clin. Invest.* **2007**, *117*, 659-671.
- ⁶¹ Lin, H.; Hu, C.; Chan, H.; Liew, Y.; Huang, H.; Lepescheux, L.; Bastianelli, E.; Baron, R.; Rawadi, G.; Clement-Lacroix, P. *British J. Pharmacol.*, **2007**, *150*, 862-872.
- ⁶² Dai, Y-S.; Xu, J.; Molkentin, J. *Mol. Cell Biol.*, **2005**, *25*, 9936-9948.
- ⁶³ Rodriguez, M.; Aquino, M.; Bruno, I.; De Martino, G.; Taddei, M.; Gomez-Paloma, L. *Curr. Med. Chem.*, **2006**, *13*, 1119-1139.
- ⁶⁴ Meinke, P.; Liberator, P. *Curr. Med. Chem.*, **2001**, *8*, 211-235.
- ⁶⁵ Glozak, M.; Seto, E. *Oncogene*, **2007**, *26*, 5420-5432.
- ⁶⁶ Grozinger, C.; Hassig, C.; Schreiber, S. *Proc. Natl. Acad. Sci. USA*, **1999**, *96*, 4868-4873.
- ⁶⁷ Khan, N.; Jeffers, M.; Kumar, S.; Hackett, C.; Boldog, F.; Khramtsov, N.; Qian, X.; Mills, E.; Berghs, S.; Carey, N.; Finn, P.; Collins, L.; Tumber, A.; Ritchie, J.; Jensen, P.; Lichenstein, H.; Sehested, M. *Biochem. J.*, **2008**, *409*, 581-589.
- ⁶⁸ Miller, T.; Witter, D.; Belvedere, S. *J. Med. Chem.*, **2003**, *46*, 5097-5116.
- ⁶⁹ Furumai, R.; Komatsu, Y.; Nishino, N.; Khochbin, S.; Yoshida, M.; Horinouchi, S. *Proc. Natl. Acad. Sci. USA*, **2001**, *98*, 87-92.
- ⁷⁰ Minucci, S.; Pelicci, P. *Nature Rev. Cancer*, **2006**, *6*, 38-51.
- ⁷¹ Marks, P.; Breslow, R. *Nature Biotech.*, **2007**, *25*, 84-90.
- ⁷² Gray, S.; Ekström, T. *Exp. Cell Res.*, **2001**, *262*, 75-83.
- ⁷³ Xu, W.; Parmigiani, R.; Marks, P. *Oncogene*, **2007**, *26*, 5541-5552.
- ⁷⁴ Imai, S-I.; Armstrong, C.; Kaeberlein, M.; Guarente, L. *Nature*, **2000**, *403*, 795-800.
- ⁷⁵ Gregoret, I.; Lee, Y-M.; Goodson, H. *J. Mol. Biol.*, **2004**, *338*, 17-31.
- ⁷⁶ Finnin, M.; Donigan, J.; Cohen, A.; Richon, V.; Rifkind, R.; Marks, P.; Breslow, R.; Pavletich, N. *Nature*, **1999**, *401*, 188-193.
- ⁷⁷ Crabb, S.; Howell, M.; Rogers, H.; Ishfaq, M.; Yurek-George, A.; Carey, K.; Pickering, B.; East, P.; Mitter, R.; Maeda, S.; Johnson, P.; Townsend, P.; Shin-ya, K.; Yoshida, M.; Ganesan, A.; Packham, G. *Biochem. Pharmacol.*, **2008**, 463-475.
- ⁷⁸ Jose, B.; Oniki, Y.; Kato, T.; Nishino, N.; Sumida, Y.; Yoshida, M. *Bioorg. Med. Chem. Lett.*, **2004**, *14*, 5343-5346.
- ⁷⁹ Wade, P. *Hum. Mol. Genet.*, **2001**, *10*, 693-698.
- ⁸⁰ Cress, W.; Seto, E. *J. Cell. Physiol.*, **2000**, *184*, 1-16.
- ⁸¹ Lagger, G.; O'Carroll, D.; Rembold, M.; Khier, H.; Tischler, J.; Weitzer, G.; Schuettengruber, B.; Hauser, C.; Brunmeir, R.; Jenuwein, T.; Seiser, C. *EMBO J.*, **2002**, *21*, 2672-2681.
- ⁸² Glaser, K.; Li, J.; Staver, M.; Wei, R.-Q.; Albert, D.; Davidsen, S. *Biochem. Biophys. Res. Comm.*, **2003**, *310*, 529-536.
- ⁸³ Taunton, J.; Hassig, C.; Schreiber, S. *Science*, **1996**, *272*, 408-411.
- ⁸⁴ Burgess, A.; Ruelfi, A.; Beamish, H.; Warrenner, R.; Saunders, N.; Johnstone, R.; Gabrielli, B. *Oncogene*, **2004**, *23*, 6693-6701.

- ⁸⁵ Kelly, W.; Marks, P. *Nature Prac. Clin. Oncol.*, **2005**, *2*, 150-157.
- ⁸⁶ Tsuji, N.; Kobayashi, N.; Nagashima, K.; Wakisaka, Y.; Koizumi, K. *J. Antibiot.*, **1976**, *29*, 1-6.
- ⁸⁷ Yoshida, M.; Horinouchi, S.; Beppu, T. *BioEssays*, **1995**, *17*, 423-430.
- ⁸⁸ Vanommeslaeghe, K.; De Proft, F.; Loverix, S.; Tourwé, D.; Geerlings, P. *Bioorg. Med. Chem.*, **2005**, *13*, 3987-3992.
- ⁸⁹ Jung, M.; Hoffmann, K.; Brosch, G.; Loidl, P. *Bioorg. Med. Chem. Lett.*, **1997**, *7*, 1655-1658.
- ⁹⁰ Remiszewski, S.; Sambucetti, L.; Atadja, P.; Bair, K.; Cornell, W.; Green, M.; Howell, K.; Jung, M.; Kwon, P.; Walker, H. *J. Med. Chem.*, **2002**, *45*, 753-757.
- ⁹¹ Sternson, S.; Wong, J.; Grozinger, C.; Schreiber, S. *Org. Lett.*, **2001**, *3*, 4239-4242.
- ⁹² Garber, K. *Nature Biotech.*, **2007**, *25*, 17-19.
- ⁹³ Piekarz, R.; Frye, A.; Wright, J.; Steinberg, S.; Liewehr, D.; Rosing, D.; Sachdev, V.; Fojo, T.; Bates, S. *Clin. Cancer Res.*, **2006**, *12*, 3762-3773.
- ⁹⁴ Remiszewski, S. *Curr. Med. Chem.*, **2003**, *10*, 2393-2402.
- ⁹⁵ Pringle, R. *Plant. Physiol.*, **1970**, *46*, 45-49.
- ⁹⁶ Closse, A.; Huguenin, R. *Helv. Chim. Acta*, **1974**, *57*, 533-545.
- ⁹⁷ Umehara, K.; Nakahara, K.; Kiyota, S.; Iwami, M.; Okamoto, M.; Tanake, H.; Kohsaka, M.; Oaki, H.; Imanaka, H. *J. Antibiot.*, **1983**, *36*, 478-483.
- ⁹⁸ Hirota, A.; Suzuki, A.; Suzuki, H.; Tamura, S. *Agric. Biol. Chem.*, **1973**, *37*, 643-647.
- ⁹⁹ Degenkolb, T.; Gams, W.; Brückner, H. *Chem. Biodiversity*, **2008**, *5*, 693-705.
- ¹⁰⁰ Shute, R.; Dunlap, B.; Rich, D. *J. Med. Chem.*, **1987**, *30*, 71-78.
- ¹⁰¹ Komatsu, Y.; Tomizaki, K-y.; Tsukamoto, M.; Kato, T.; Nishino, N.; Sato, S.; Yamori, T.; Tsuruo, T.; Furumai, R.; Yoshida, M.; Horinouchi, S.; Hayashi, H. *Cancer Res.*, **2001**, *61*, 4459-4466.
- ¹⁰² Nishino, N.; Yoshikawa, D.; Watanabe, L.; Kato, T.; Jose, B.; Komatsu, Y.; Sumida, Y.; Yoshida, M. *Bioorg. Med. Chem. Lett.*, **2004**, *14*, 2427-2431.
- ¹⁰³ Kijima, M.; Yoshida, M.; Sugita, K.; Horinouchi, S.; Beppu, T. *J. Biol. Chem.*, **1993**, *268*, 22429-22435.
- ¹⁰⁴ Taunton, J.; Collins, J.; Schreiber, S. *J. Am. Chem. Soc.*, **1996**, *118*, 10412-10422.
- ¹⁰⁵ Cavalier-Fortin, F.; Pepe, G.; Verducci, J.; Siri, D.; Jacquier, R. *J. Am. Chem. Soc.*, **1992**, *114*, 8885-8890.
- ¹⁰⁶ Baldwin, J.; Adlington, R.; Godfrey, C.; Patel, V. *Tetrahedron*, **1993**, *49*, 7837-56.
- ¹⁰⁷ Schmidt, U.; Lieberknecht, A.; Greisser, H.; Bartkowiak, F. *Angew. Chem. Int. Ed.*, **1984**, *23*, 318-320.
- ¹⁰⁸ Mori, K.; Koseki, K. *Tetrahedron*, **1988**, *44*, 6013-6020.
- ¹⁰⁹ Singh, S.; Zink, D.; Polishook, J.; Dombrowski, A.; Darkin-Rattray, S.; Schmatz, D.; Goetz, M. *Tetrahedron Lett.*, **1996**, *37*, 8077-8080.
- ¹¹⁰ Colletti, S.; Myers, R.; Darkin-Rattray, S.; Gurnett, A.; Dulski, P.; Galuska, S.; Allocco, J.; Ayer, M.; Li, C.; Lim, J.; Crumley, T.; Cannova, C.; Schmatz, D.; Wyvratt, M.; Fisher, M.; Meinke, P. *Bioorg. Med. Chem. Lett.*, **2001**, *11*, 113-117.
- ¹¹¹ Singh, S.; Zink, D.; Liesch, J.; Mosley, R.; Dombrowski, A.; Bills, G.; Darkin-Rattray, S.; Schmatz, S.; Goetz, M. *J. Org. Chem.*, **2002**, *67*, 815-825.
- ¹¹² Kuriyama, W.; Kitahara, T. *Heterocycles*, **2001**, *55*, 1-4.
- ¹¹³ Mou, L.; Singh, S. *Tetrahedron Lett.*, **2001**, *42*, 6603-6606.

- ¹¹⁴ Deshmukh, P.; Schulz-Fademrecht, C.; Procopiou, P.; Vigushin, D.; Coombes, R.; Barrett, A. *Adv. Synth. Catal.*, **2007**, *349*, 175-183.
- ¹¹⁵ Schmidt, U.; Schanbacher, U. *Angew. Chem. Int. Ed.*, **1981**, *20*, 1026-1027.
- ¹¹⁶ Schmidt, U.; Lierberknecht, A. *Synthesis*, **1986**, 361-366.
- ¹¹⁷ Meinke, P.; Colletti, S.; Ayer, M.; Darkin-Rattray, S.; Myers, R.; Schmatz, D.; Wyvratt, M.; Fisher, M. *Tetrahedron Lett.*, **2000**, *41*, 7831-7835.
- ¹¹⁸ Gu, W.; Cueto, M.; Jensen, P.; Fenical, W.; Silverman, R. *Tetrahedron*, **2007**, *63*, 6535-6541.
- ¹¹⁹ Marfey, P. *Carlsberg Res. Comm.*, **1984**, *49*, 591.
- ¹²⁰ Nakao, Y.; Yoshida, S.; Matsunaga, S.; Shindoh, N.; Terada, Y.; Nagai, K.; Yamashita, J.; Ganesan, A.; Van Soest, R.; Fusetani, N. *Angew. Chem. Int. Ed.*, **2006**, *45*, 7553-7557.
- ¹²¹ Maulucci, N.; Chini, M.; Di Micco, S.; Izzo, I.; Cafaro, E.; Russo, A.; Gallinari, P.; Paolini, C.; Nardi, M.; Casapullo, A.; Riccio, R.; Bifulco, G.; De Riccardis, F. *J. Am. Chem. Soc.*, **2007**, *129*, 3007-3012.
- ¹²² Nakao, Y.; Narazaki, G.; Hoshino, T.; Maeda, S.; Yoshida, M.; Maejima, H.; Yamashita, J. *Bioorg. Med. Chem. Lett.*, **2008**, *18*, 2982-2984.
- ¹²³ Izzo, I.; Maulucci, N.; Bifulco, G.; De Riccardis, F. *Angew. Chem. Int. Ed.*, **2006**, *45*, 7557-7560.
- ¹²⁴ Wen, S.; Carey, K.; Nakao, Y.; Fusetani, N.; Packham, G.; Ganesan, A. *Org. Lett.*, **2007**, *9*, 1105-1108.
- ¹²⁵ Brown, H.; Bhat, K. *J. Am. Chem. Soc.*, **1986**, *108*, 293-294.
- ¹²⁶ a) Mori, H.; Urano, Y.; Kinoshita, T.; Yoshimura, S.; Takase, S.; Hino, M. *J. Antibiot.*, **2003**, *56*, 181-185; b) Mori, H.; Abe, F.; Furukawa, S.; Sakai, M.; Hino, M.; Fuijii, T. *J. Antibiot.*, **2003**, *56*, 80-86. c) Mori, H.; Urano, Y.; Abe, F.; Furukawa, S.; Tsurumi, Y.; Sakamoto, K.; Hashimoto, M.; Takase, S.; Hino, M.; Fuijii, T. *J. Antibiot.*, **2003**, *56*, 72-79.
- ¹²⁷ Rodriguez, M.; Terracciano, S.; Cini, E.; Settembrini, G.; Bruno, I.; Bifulco, G.; Taddei, M.; Gomez-Paloma, L. *Angew. Chem. Int. Ed.*, **2006**, *45*, 423-427.
- ¹²⁸ Rodriguez, M.; Taddei, M. *Synthesis*, **2005**, *3*, 493-495.
- ¹²⁹ Singh, E.; Ravula, S.; Pan, C-M.; Pan, P-S.; Vasko, R.; Lapera, S.; Weerasinghe, S.; Pflum, M.; McAlpine, S. *Bioorg. Med. Chem. Lett.*, **2008**, *18*, 2549-2554.
- ¹³⁰ Gomez-Paloma, L.; Bruno, I.; Cini, E.; Khochbin, S.; Rodriguez, M.; Taddei, M.; Terracciano, S.; Sadoul, K. *ChemMedChem*, **2007**, *2*, 1511-1519.
- ¹³¹ Di Micco, S.; Terracciano, S.; Bruno, I.; Rodriguea, M.; Riccio, R.; Taddei, M.; Bifulco, G. *Bioorg. Med. Chem.*, **2008**, *16*, 8635-8642.
- ¹³² a) Chen, Y.; Gambs, C.; Abe, Y.; Wentworth, P.; Janda, K. *J. Org. Chem.*, **2003**, *68*, 8902-8905; b) Fujisawa Pharmaceutical Co., Ltd., Japan. Jpn. Kokai Tokkyo Koho JP, 03141296, **1991**.
- ¹³³ Masuoka, Y.; Nagai, A.; Shin-Ya, K.; Furihata, K.; Nagai, K.; Suzuki, K.; Hayakawa, Y.; Seto, H. *Tetrahedron Lett.*, **2001**, *42*, 41-44.
- ¹³⁴ Takizawa, T.; Watanabe, K.; Narita, K.; Kudo, K.; Oguchi, T.; Abe, H.; Katoh, T. *Heterocycles*, **2008**, *76*, 275-290.
- ¹³⁵ Yurek-George, A.; Habens, F.; Brimmell, M.; Packham, G.; Ganesan, A. *J. Am. Chem. Soc.*, **2004**, *126*, 1030-1031.

- ¹³⁶ Takizawa, T.; Watanabe, K.; Koichi, N.; Takamasa, O.; Hideki, A.; Tadashi, K. *Chem. Comm.*, **2008**, *14*, 1677-1679.
- ¹³⁷ Nagao, Y.; Hagiwara, Y.; Kumagai, T.; Ochiai, M.; Inoue, T.; Hashimoto, K.; Fujita, E. *J. Org. Chem.*, **1986**, *51*, 2391-2393.
- ¹³⁸ Aiguadé, J.; González, A.; Urpí, F.; Vilarrasa, J. *Tetrahedron Lett.*, **1996**, *37*, 8949-8952.
- ¹³⁹ Inanaga, J.; Hirata, K.; Saeki, H.; Katsuki, T.; Yamaguchi, M. *Bull. Chem. Soc. Jpn.*, **1979**, *52*, 1989-1993.
- ¹⁴⁰ Evans, D.; Sjorgen, E.; Weber, A.; Conn, R. *Tetrahedron Lett.*, **1987**, *28*, 39-42.
- ¹⁴¹ Chang, Y-Q.; Yang, M.; Matter, A. *Appl. Env. Microbiol.*, **2007**, *73*, 3460-3469.
- ¹⁴² Piekarz, R.; Robey, R.; Sandor, V.; Bakke, S.; Wilson, W.; Dahmouh, L.; Kingma, D.; Turner, M.; Altemus, R.; Bates, S. *Blood*, **2001**, *98*, 2865-2868.
- ¹⁴³ Chen, G.; Ailing, L.; Zhao, M.; Gao, Y.; Zhou, T.; Xu, Y.; Du, Z.; Zhang, X.; Yu, X. *J. Proteome Res.*, **2008**, *7*, 2733-2742.
- ¹⁴⁴ Yu, X.; Guo, Z.; Marcu, M.; Neckers, L.; Nguyen, D.; Chen, G.; Schrump, D. *J. Natl. Cancer Inst.*, **2002**, *94*, 504-513.
- ¹⁴⁵ Ueda, H.; Nakajima, H.; Hori, Y.; Fujita, T.; Nishimura, M.; Goto, T.; Okuhara, M. *J. Antibiot. (Tokyo)*, **1994**, *47*, 301-310.
- ¹⁴⁶ Ueda, H.; Nakajima, H.; Hori, Y.; Goto, T.; Okuhara, M. *Biosci. Biotechnol. Biochem.*, **1994**, *58*, 1579-1583.
- ¹⁴⁷ Shigematsu, N.; Ueda, H.; Takase, S.; Tanaka, H.; Yamamoto, K.; Tada, T. *J. Antibiot. (Tokyo)*, **1994**, *47*, 311-314.
- ¹⁴⁸ Khan, W.; Wu, J.; Sing, W.; Simon, J. *J. Am. Chem. Soc.*, **1996**, *118*, 7237-7238.
- ¹⁴⁹ Carreira, E.; Singer, R.; Lee, W. *J. Am. Chem. Soc.*, **1994**, *116*, 8837-8838.
- ¹⁵⁰ Shah, M.; Binklye, P.; Chan, K.; Xiao, J.; Arbogast, D.; Collamore, M.; Farra, Y.; Young, D.; Grever, M. *Clin. Cancer Res.*, **2006**, *12*, 3997-4003.
- ¹⁵¹ Kruse, C.; Holden, K. *J. Org. Chem.*, **1985**, *65*, 1192-1194.
- ¹⁵² Greshock, T.; Johns, D.; Noguchi, Y.; Williams, R. *Org. Lett.*, **2008**, *10*, 613-616.
- ¹⁵³ Wen, S.; Packham, G.; Ganesan, A. *J. Org. Chem.*, **2008**, *73*, 9353-9361.
- ¹⁵⁴ Di Maro, S.; Ping, R-C.; Hsieh, J-T.; Ahn, J-M. *J. Med. Chem.*, **2008**, *51*, 6639-6641.
- ¹⁵⁵ Furumai, R.; Matsuyama, A.; Kobashi, N.; Lee, K-H.; Nishiyama, M.; Nakajima, H.; Tanaka, A.; Komatsu, Y.; Nishino, N.; Yohsida, M.; Horinouchi, S. *Cancer Res.*, **2002**, *62*, 4916-4921.
- ¹⁵⁶ Yurek-George, A.; Cecil, A.; Mo, A.; Wen, S.; Rogers, H.; Habrens, F.; Maeda, S.; Yoshida, M.; Packham, G.; Ganesan, A. *J. Med. Chem.*, **2007**, *50*, 5720-5726.
- ¹⁵⁷ Nishino, N.; Jose, B.; Okamura, S.; Ebisusaki, S.; Kato, T.; Sumida, Y.; Yoshida, M. *Org. Lett.*, **2003**, *5*, 5079-5082.
- ¹⁵⁸ Bowers, A.; Greshock, T.; West, N.; Estiu, G.; Schreiber, S.; Wiest, O.; Williams, R.; Bradner, J. *J. Am. Chem. Soc.*, **2008**, *131*, 2900-2905.
- ¹⁵⁹ Taori, K.; Paul, V.; Luesch, H. *J. Am. Chem. Soc.*, **2008**, *130*, 1806-1807.
- ¹⁶⁰ Bowers, A.; West, N.; Taunton, J.; Schreiber, S.; Bradner, J.; Williams, R. *J. Am. Chem. Soc.*, **2008**, *130*, 11219-11222.
- ¹⁶¹ a) Ying, Y.; Taori, K.; Kim, H.; Hong, J.; Luesch, H. *J. Am. Chem. Soc.*, **2008**, *130*, 8455-8459; b) Ren, Q.; Dai, L.; Zhang, H.; Tan, W.; Xu, S.; Ye, T. *Synlett*, **2008**, *15*,

- 2379-2383; c) Numajiri, Y.; Takahashi, T.; Takagi, M.; Shin-ya, K.; Doi, T. *Synlett*, **2008**, *16*, 2483-2486.
- ¹⁶² a) Nasveschuk, C.; Ungermannova, D.; Liu, X.; Phillips, A. *Org. Lett.*, **2008**, *10*, 3595-3598; b) Seiser, T.; Kamena, F.; Cramer, N. *Angew. Chem. Int. Ed.*, **2008**, *47*, 6483-6485; c) Ghosh, A.; Kulkarni, S. *Org. Lett.*, **2008**, *10*, 3907-3909.
- ¹⁶³ Crimmins, M.; Shamszad, M. *Org. Lett.*, **2007**, *9*, 149-152.
- ¹⁶⁴ Hodge, M.; Olivo, H. *Tetrahedron*, **2004**, *60*, 9397-9403.
- ¹⁶⁵ Miller, K., unpublished.
- ¹⁶⁶ Mulqueen, G.; Pattenden, G.; Whiting, D. *Tetrahedron*, **1993**, *49*, 5359-5364.
- ¹⁶⁷ Ying, Y.; Liu, Y.; Byeon, S.; Kim, H.; Luesch, H.; Hong, J. *Org. Lett.*, **2008**, *10*, 4021-4024.
- ¹⁶⁸ Lager, G.; O'Carroll, D.; Rembold, M.; Khier, H.; Tischler, J.; Weitzer, G.; Schuettengruber, B.; Hauser, C.; Brunmeir, R.; Jenuwein, T.; Seiser, C. *EMBO Journal* **2002**, *21*, 2672-2681.
- ¹⁶⁹ Wang, D-F.; Helquist, P.; Wiech, N.; Wiest, O. *J. Med. Chem.*, **2005**, *48*, 6936-6947.
- ¹⁷⁰ Weerasinghe, S.; Estiu, G.; Wiest, O.; Pflum, M. *J. Med. Chem.*, **2008**, *51*, 5543-5551.
- ¹⁷¹ Estiu, G.; Greenberg, E.; Harrison, C.; Kwiatkowski, N.; Mazitschek, R.; Bradner, J.; Wiest, O. *J. Med. Chem.*, **2008**, *51*, 2898-2906.
- ¹⁷² Delle Monache, G.; Misiti, D.; Salvatore, P.; Zappia, G. *Chirality*, **2000**, *12*, 143-148.
- ¹⁷³ Bowers, A.; West, N.; Newkirk, T.; Troutman-Youngman, A.; Schreiber, S.; Wiest, O.; Bradner, J.; Williams, R. *Org. Lett.*, **2009**, *11*, 1301-1304.
- ¹⁷⁴ Vugts, D.; Veum, L.; al-Mafraji, K.; Lemmens, R.; Schmitz, R.; de Kanter, F.; Groen, M.; Hanefeld, U.; Orru, R. *Eur. J. Org. Chem.*, **2006**, *7*, 1672-1677.
- ¹⁷⁵ Dr. Aaron Smith, personal communication.
- ¹⁷⁶ Bennett, F.; Knight, D. *Tetrahedron Lett.*, **1988**, *29*, 4865-4868.
- ¹⁷⁷ Bennett, F.; Knight, D.; Fenton, G. *J. Chem. Soc. Perkin. Trans. 1*, **1991**, 133.
- ¹⁷⁸ Corbett, T.; Valeriote, F. *J. Am. Chem. Soc.*, **1990**, *112*, 8195-8197.

Chapter 6: Experimental Section

Table of Procedures and Spectra

14-Acetoxygelsenicine project (114 - 173).....	pp. 131-192
<i>ent</i> -Largazole (330-350).....	pp. 193-236
Amide isostere core (354-364).....	pp.237-261
Vinyl depsipeptide core and metathesis substrates (373-365).....	pp.262-286
Allyl depsipeptide core (401-414).....	pp. 287-303
<i>des</i> -Methyl pyridine analog (420-428).....	pp.304-318
Common intermediates:	
Thiazole nitrile 293.....	pp. 200-207
Aldehyde 235.....	p. 214
α -Methylcysteine hydrochloride 292.....	pp. 249-255
Thiazoline-thiazole 294.....	p. 256

6.1 General Considerations

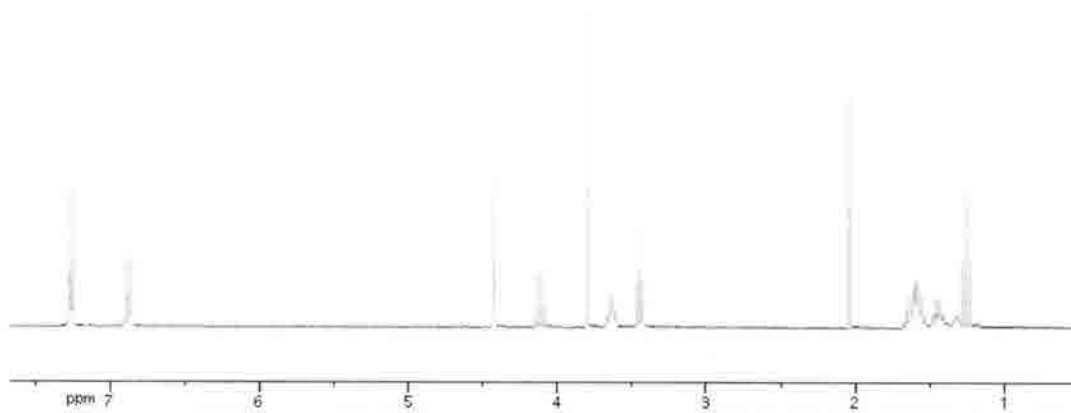
Unless otherwise noted, all reactions were run under an argon atmosphere in flame or oven dried glassware. Reactions were monitored by thin layer silica gel chromatography (TLC) using 0.25 mm silica gel 60F plates with fluorescent indicator (Merck). Plates were visualized by treatment with phosphomolybdic acid stain with gentle heating. Products were purified via column chromatography using the solvent system(s) indicated. Silica gel 60, 230-400 mesh, was purchased from Sorbent Technologies. Tetrahydrofuran (THF), dichloromethane (DCM), acetonitrile (CH₃CN), triethylamine (Et₃N), toluene, diethyl ether (Et₂O), and *N,N*-dimethylformamide (DMF) were passed through an alumina drying column (*Solv-Tek Inc.*) using argon pressure. All other reagents were purchased from Aldrich and used as received without additional purification. ¹H NMR and ¹³C NMR spectra were recorded on Varian 300, 400, or 500 MHz NMR spectrometers. Chemical shifts are reported in ppm relative to CHCl₃ at $\delta = 7.27$ (¹H NMR and $\delta = 77.23$ (¹³C NMR) or tetramethylsilane (TMS) $\delta = 0.00$, unless otherwise described. Mass spectra were obtained on Fisions VG Autospec. Optical rotations were collected at 589 nm on a Rudolph Research Automatic Polarimeter Autopol III.

6.2 Experimental Procedures

5-(4-Methoxybenzyloxy)pentan-1-ol (**114**)



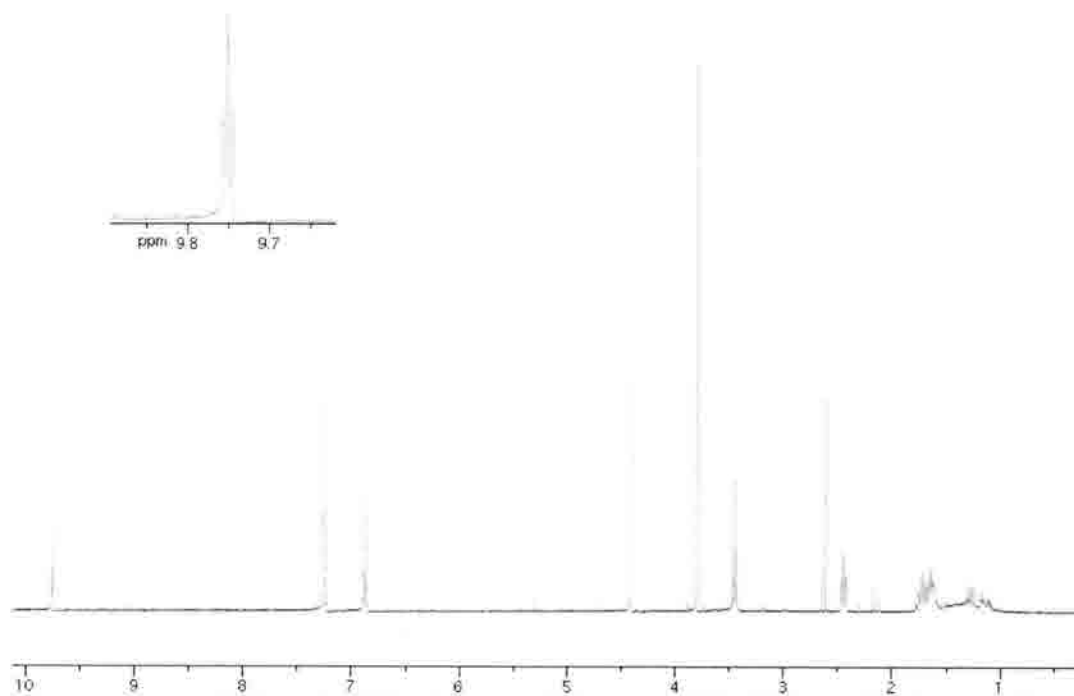
To a stirred solution of NaH (3.54 g of 60% NaH, 88.5 mmol) in THF (50 mL) at 0°C was slowly added 1,5-pentanediol (9.22 g, 88.5 mmol). The mixture was brought to room temperature and stirred for 15 minutes, at which point a solution of tetrabutylammonium iodide (1.0 g, 2.7 mmol) in 10 mL THF was added, followed by 4-methoxybenzyl chloride (5.78 g, 27.5 mmol). This mixture was stirred for 12 hours at room temperature. A saturated aqueous solution of NH₄Cl (20 mL) was added, and the resultant biphasic mixture stirred for 10 minutes and concentrated to roughly 20% of the original volume. The phases were separated, the aqueous layer extracted into EtOAc (3 x 25 mL) and the combined organic layers washed with brine (25 mL), dried over MgSO₄ and concentrated. The residue was purified by flash silica gel column chromatography (2:3 EtOAc/hexanes) to afford **114** (5.48 g, 89%) as a yellow oil. ¹H NMR (300 MHz) (CDCl₃) δ TMS: 1.40-1.49 (2H, m); 1.53-1.68 (4H, m); 3.45 (2H, t, *J* = 6.6); 3.65 (2H, q, *J* = 6.6); 3.80 (3H, s); 4.43 (2H, s); 6.89 (2H, d, *J* = 8.4); 7.27 (2H, d, *J* = 8.4). (TLNI-157_24-36)



5-(4-Methoxybenzyloxy)pentan-1-al (**115**)



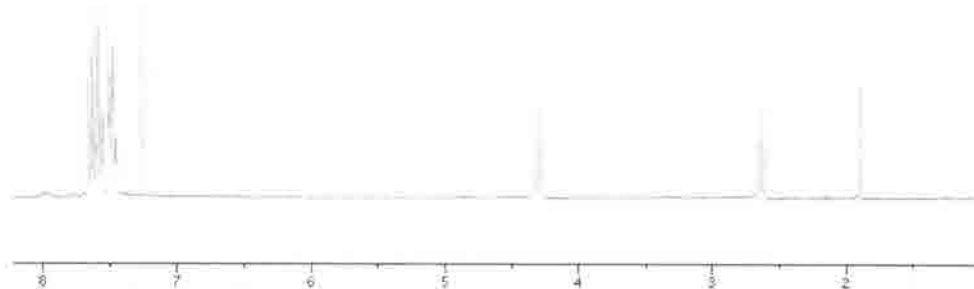
To a stirred solution of oxalyl chloride (4.65 g, 36.6 mmol) in 37 mL DCM at -78°C was slowly added DMSO (5.73 g, 73.3 mmol), and the resultant mixture stirred at this temperature for 30 minutes. A solution of alcohol **114** (5.48 g, 24.4 mmol) in 20 mL DCM was slowly added and stirred for 90 minutes, at which point the temperature was raised to -60°C , and diisopropylethylamine (12.6 g, 97.6 mmol) was added. The mixture was allowed to come to room temperature and stirred for 45 minutes. Water (50 mL) was added, and the resultant layers separated. The aqueous layer was extracted three times with DCM (3 x 50 mL), the combined organic layers washed with brine, dried over Na_2SO_4 and concentrated to afford **115** (5.25 g, 97%) as a yellow oil which did not require further purification. ^1H NMR (300 MHz) (CDCl_3) δ TMS: 1.58-1.78 (4H, m); 2.47 (2H, td, $J = 1.5, 6.9$); 3.45 (3H, t, $J = 6.3$); 3.79 (3H, s); 4.42 (2H, s); 6.89 (2H, dt, $J = 2.7, 9.3$); 7.23-7.26 (2H, m); 9.76 (1H, t, $J = 1.8$). (TLNI-158)



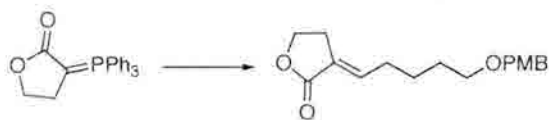
α -(Triphenylphosphoranylidene)- γ -butyrolactone (**117**)



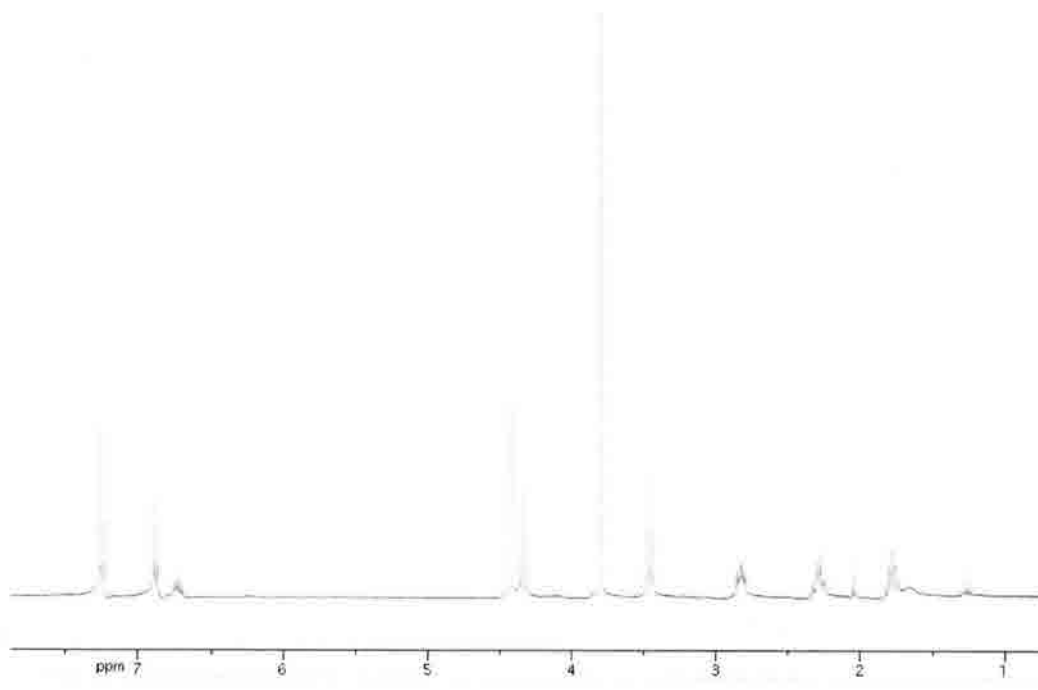
To a solution of triphenylphosphine (18.3 g, 70 mmol) in THF (35 mL) at room temperature was added α -bromo- γ -butyrolactone (11.5 g, 70 mmol). The mixture was brought to reflux and stirred for 22 hours, after which it was cooled to room temperature. The resulting light brown solid was washed with THF (500 mL), taken up in water (100 mL), and 300 mL of a 10% solution of NaOH was added dropwise over 20 minutes. The white solid was filtered and dried under high vacuum giving **117** in 97% yield without need of further purification. $^1\text{H NMR}$ (300 MHz) (CDCl_3) δ TMS: 2.64 (2H, t, $J=7.5$); 4.30 (2H, t, $J=7.5$); 7.45-7.51 (6 H, m); 7.55-7.66 (9H, m). (TLNI-101)



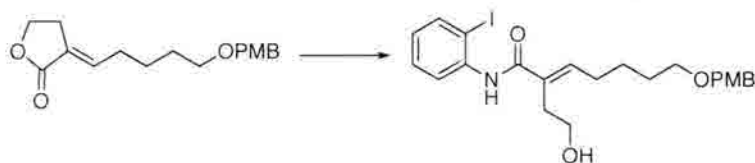
3-(5-(4-Methoxybenyloxy)pentylidene)dihydrofuran-2-one (**118**)



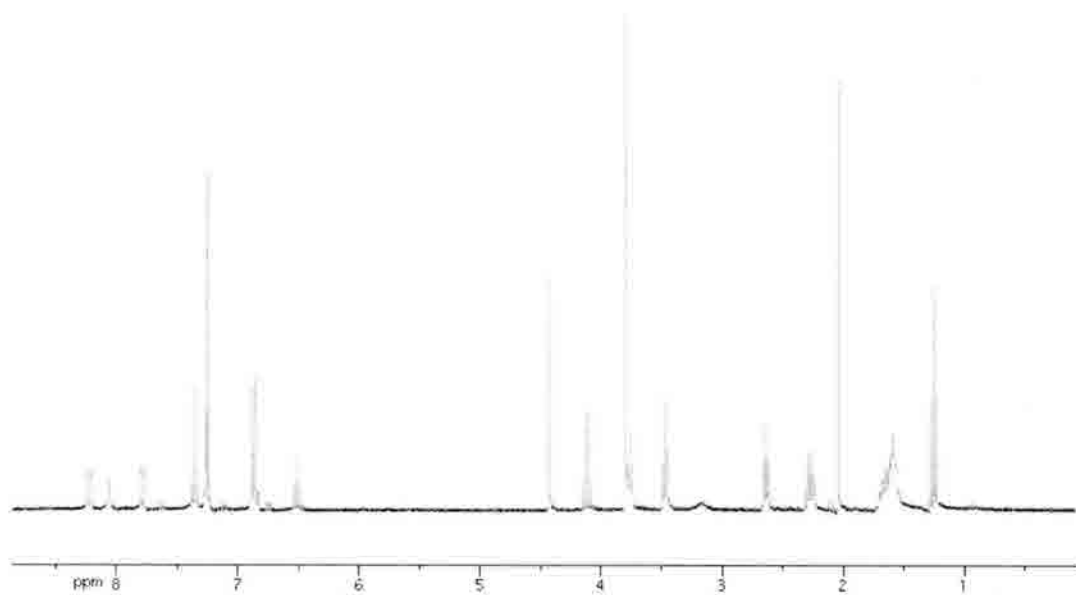
A solution of aldehyde **115** (0.93 g, 4.18 mmol) and ylide **117** (1.55 g, 4.48 mmol) in toluene (35 mL) was refluxed under Ar for 16 hours. The mixture was cooled to room temperature and the volatile organics removed under vacuum. The resultant black solid was taken up in EtOAc and purified via flash silica gel column chromatography (1:1 EtOAc/hexanes) to give **118** as a dark yellow oil (1.05 g, 81%). ^1H NMR (300 MHz) (CDCl_3) δ TMS: 1.74-1.83 (2H, m); 2.52-2.33 (2H, m); 2.79-2.85 (2H, m); 3.46 (2H, t, $J = 6.3$); 3.80 (3H, s); 4.34 (2H, t, $J = 7.2$); 4.42 (2H, s); 6.69-6.76 (1H, m); 6.89 (2H, d, $J = 8.7$); 7.26 (2H, d, $J = 8.7$) (TLNI-113pp)



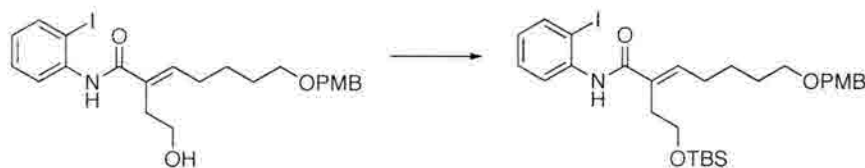
2-(2-Hydroxyethyl)-N-(2-iodophenyl)-7-(4-methoxybenzyloxy)hept-2-enamide (119)



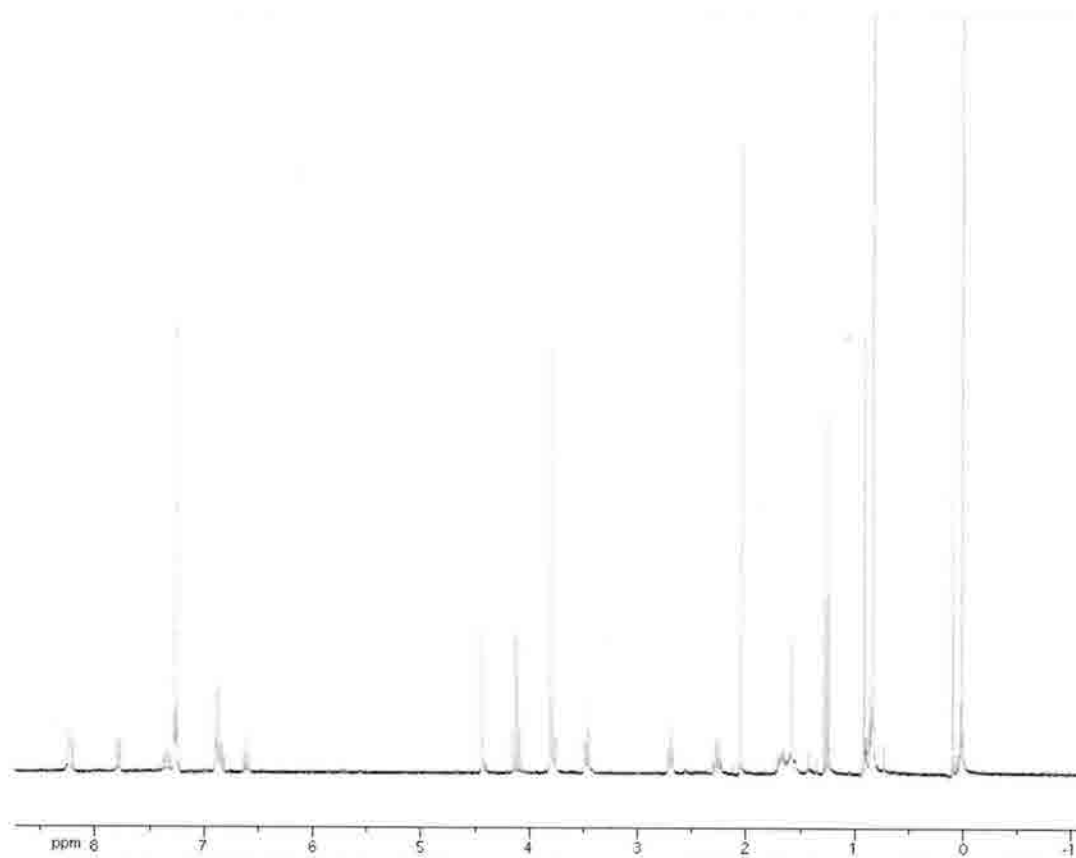
A 2-necked round bottom flask was flame dried, equipped with a condenser and flushed with Ar. Benzene (5 mL) was added, followed by trimethylaluminum (1 mL, 2.0 M in hexane, 2 mmol), and the mixture cooled to 0°C. A solution of iodoaniline **112** (0.44 g, 2 mmol) in benzene (2.5 mL) was added, followed by lactone **118** (0.53 g, 1.8 mmol) in benzene (2.5 mL). This mixture was stirred at 0°C for one hour, after which it was warmed to room temperature, then to reflux for 15 hours. The solution was then cooled to 0°C, and 5 mL 1 N HCl added slowly. After further stirring (30 minutes), the layers were separated. The aqueous layer was extracted three times with EtOAc (15 mL); the combined organics were washed with brine, dried over MgSO₄ and concentrated to give **119** as a yellow oil. Note: this compound appears to degrade over time, and should be taken on to the next step immediately. ¹H NMR (300 MHz) (CDCl₃) δ TMS: 1.57-1.70 (4H, m); 2.89 (2H, q, *J* = 7.5); 2.64 (2H, t, *J* = 5.7); 3.47 (2H, t, *J* = 6.3); 3.76 (2H, t, *J* = 5.7); 3.80 (3H, s); 4.34 (2H, s); 6.52 (1H, t, *J* = 7.5); 6.89 (2H, d, *J* = 8.4); 7.27 (2H, d, *J* = 8.4); 7.33-7.38 (1H, m); 7.78 (1H, d, *J* = 8.4); 8.06 (1H, s); 8.24 (1H, d, *J* = 8.4). (TLNI-169)



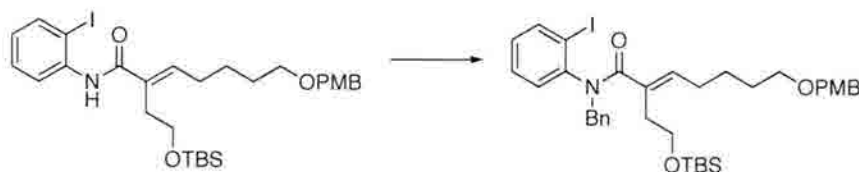
(E)-2-(2-(*tert*-butyldimethylsilyloxy)ethyl)-N-(2-iodophenyl)-7-(4-methoxybenzyloxy)hept-2-enamide (119a)



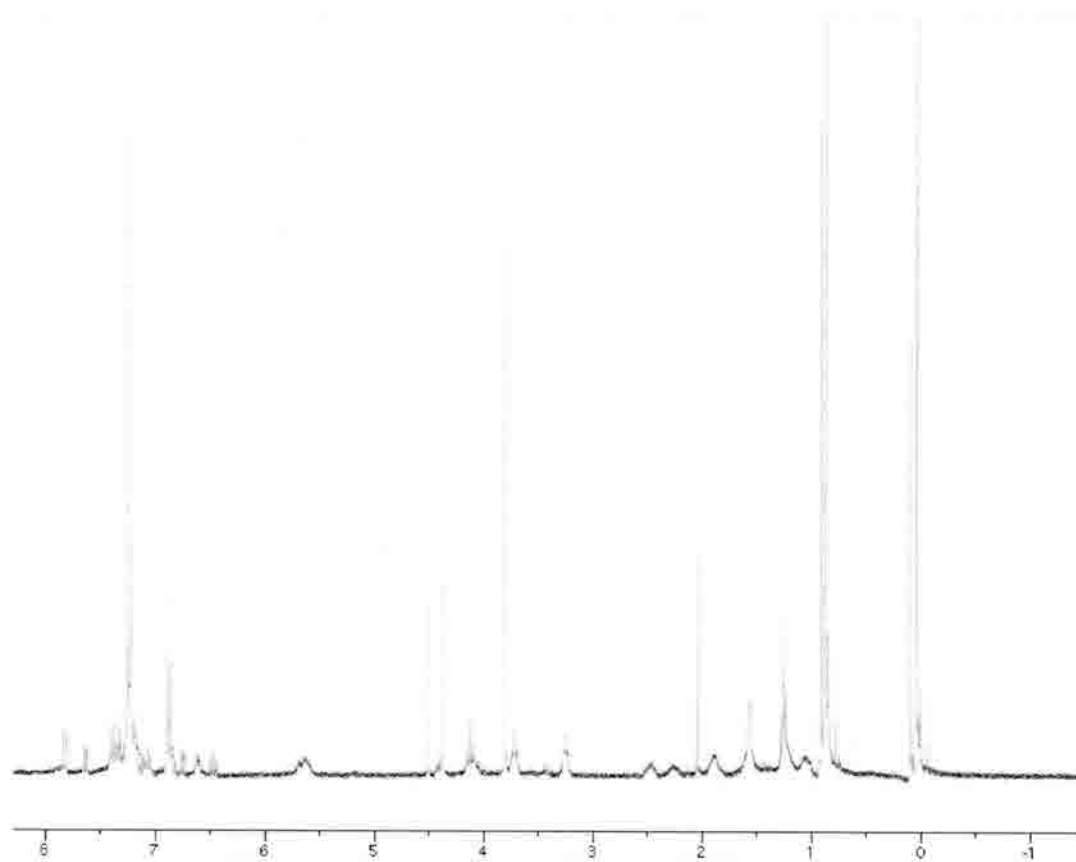
To a solution of **119** (0.59 g, 1.16 mmol) in DMF (7 mL) was added imidazole (0.18 g, 2.6 mmol), then TBSCl (0.21 g, 1.34 mmol); this mixture was stirred at room temperature under Ar for one hour, after which water (5 mL) was added. The layers were separated, and the aqueous layer was extracted three times with ether (15 mL). The combined organic layers were washed with brine, dried over Na₂SO₄, and concentrated. The residue was purified via flash silica gel column chromatography (1:1 EtOAc/hexanes), giving **119a** as a dark red oil (0.61 g, 79% over two steps). ¹H NMR (300 MHz) (CDCl₃) δ TMS: 0.01 (5H, s) (major rotamer); 0.1 (1H, s) (minor rotamer); 0.84 (7H, s) (major rotamer); 0.91 (2H, s, minor rotamer); 1.59-1.70 (2H, m); 2.28 (2H, q, *J* = 7.2); 2.69 (2H, t, *J* = 6.0); 3.47 (2H, t, *J* = 6.3); 3.77 (2H, t, *J* = 6.3); 3.80 (3H, s); 4.34 (2H, s); 6.61 (1H, t, *J* = 7.5); 6.81-6.89 (3H, m); 7.31-7.37 (2H, m); 7.79 (1H, dd, *J* = 1.5, 7.8); 8.23 (2H, dd, *J* = 1.8, 8.4). (TLNI-186)



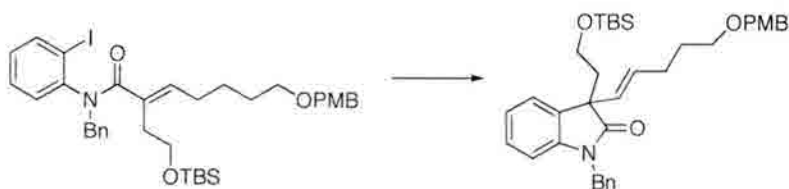
N-benzyl-2-(2-(tertbutyldimethylsilyloxy)ethyl)-N-(2-iodophenyl)-7-(4-methoxybenzyloxy)hept-2-enamide (120)



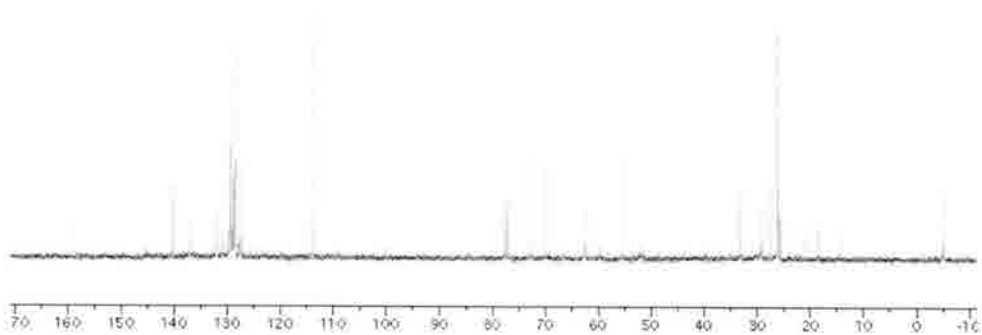
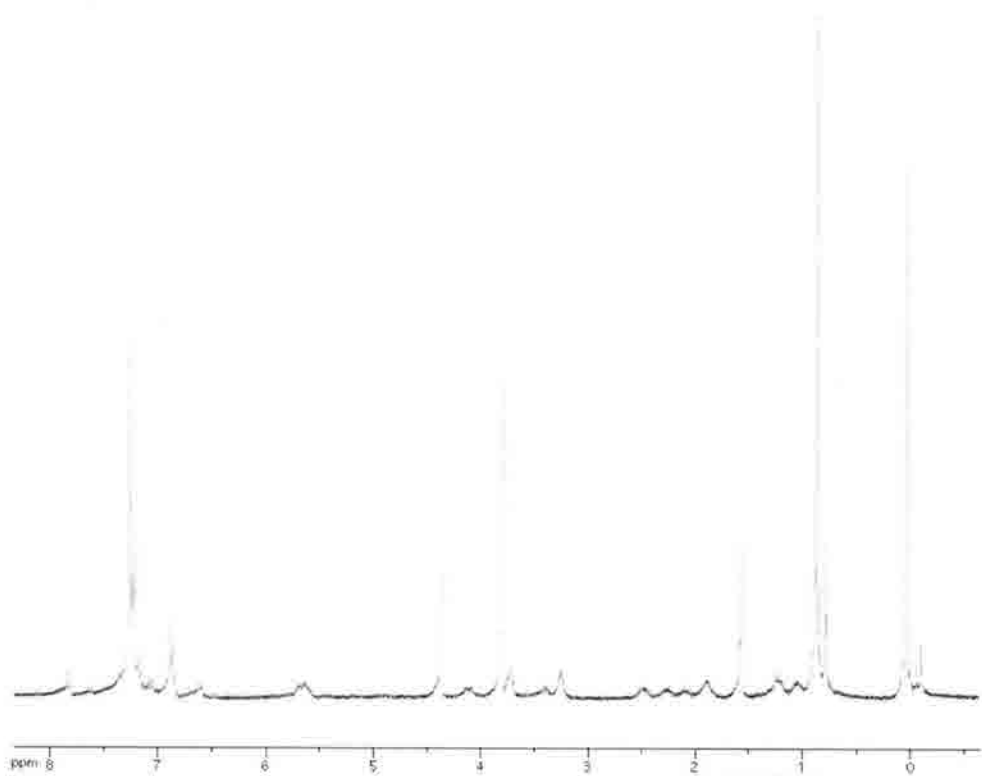
To a stirred solution of NaH (60% in mineral oil, 0.03 g, 0.77 mmol) in THF (2.5 mL) at 0°C under Ar was slowly added enamide **119a** (0.48 g, 0.77 mmol) in THF (5 mL). The mixture was warmed to room temperature and stirred for 15 minutes, after which benzylbromide (0.13 g, 0.77 mmol) was added. The mixture was stirred at room temperature for 15 hours, followed by addition of saturated aqueous ammonium chloride solution (1 mL). Most of the organic layer was evaporated under vacuum, followed by extraction of the aqueous layer with EtOAc (3 x 15 mL). The combined organics were washed with brine, dried over Na₂SO₄, and concentrated, giving **120** as a light brown oil without need of further purification. ¹H NMR (300 MHz) (CDCl₃) δ TMS: 0.05 (5H, s, minor rotamer) 0.10 (5H, s, major rotamer); 0.88 (7H, s) (major rotamer) 0.91 (2H, s) (minor rotamer); 2.25-2.59 (2H, m); 3.25 (2H, t, *J* = 5.7); 3.72 (2H, t, *J* = 7.2); 3.81 (3H, s); 4.37 (2H, s); 4.50 (2H, s); 5.55-5.72 (2H, m); 6.47 (1H, t, *J* = 7.2); 6.60-6.77 (1H, m); 6.82-6.89 (3H, m); 7.05-7.25 (5H, m); 7.29-7.42 (3H, m); 7.62 (1H, dd, *J* = 1.5, 8.1); 7.84 (1H, dd, *J* = 1.5, 7.8), (TLNI-166)



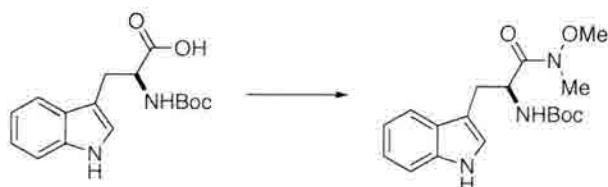
1-Benzyl-3-(2-(tertbutyldimethylsilyloxy)ethyl)-3-(5-(4-methoxybenzyloxy)pent-1-enyl)indolin-2-one (121)



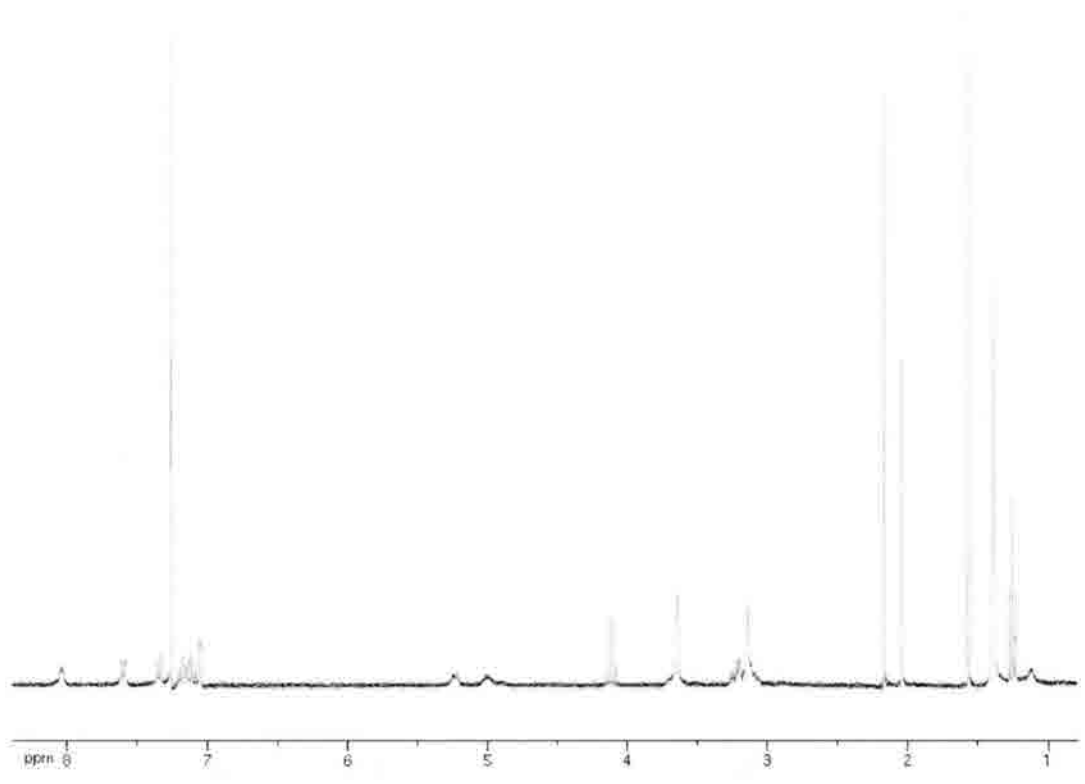
A solution of **120** (0.57 g, 0.8 mmol), Pd(OAc)₂ (0.009 g, 0.04 mmol), P(o-tol)₃ (0.04 g, 0.12 mmol), tetrabutylammonium iodide (0.30 g, 0.8 mmol) and triethylamine (0.32 g, 3.2 mmol) in toluene (11 mL) was heated to 75° and stirred under Argon for 15 hours. The mixture was cooled to room temperature, and a saturated aqueous solution of sodium bicarbonate (9.75 mL) was added. The aqueous layer was extracted with EtOAc (3 x 20 mL) and the combined organic layers were washed with brine, dried over MgSO₄ and concentrated. The residue was purified by silica gel chromatography (1:1 EtOAc/hexanes) to afford **121** (0.38 g, 64%). ¹³C NMR (CDCl₃) δ -5.0, 14.5, 18.5, 21, 25.5, 26, 26.2, 27.5, 30.92, 33, 55.4, 59.6, 60.6, 62.4, 62.8, 66.6, 70, 72.6, 77.2, 77.8, 113.8, 127.4, 127.6, 128.6, 128.8, 129, 129.2, 129.4, 129.6, 130.8, 132, 137.2, 140.4



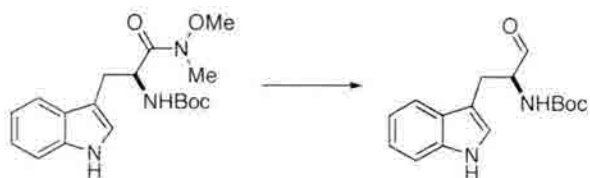
(S)-tert-butyl 3-(1H-indol-3-yl)-1-(methoxy(methyl)amino)-1-oxopropan-2-ylcarbamate (137)



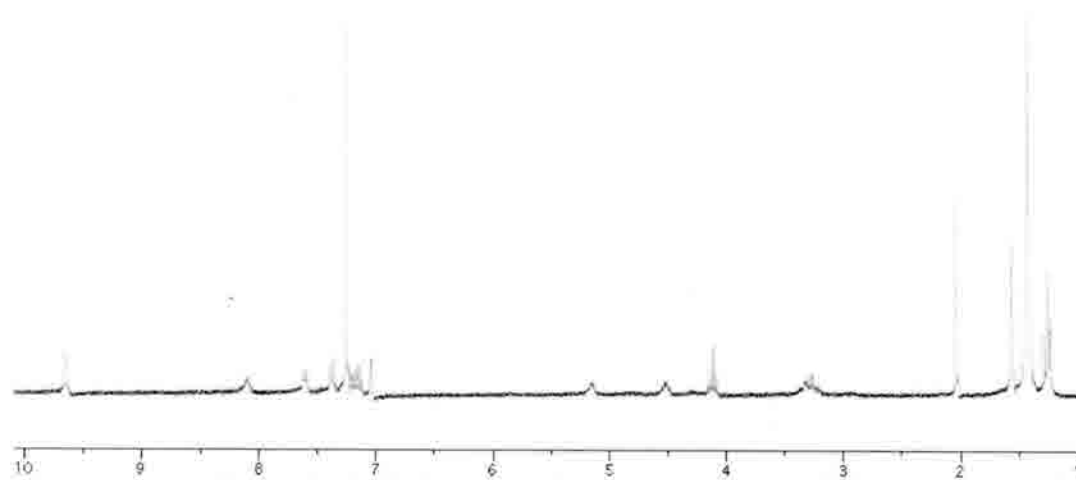
To a mixture of L-N-Boc-tryptophan (0.5g, 1.64 mmol) in DCM (34 mL) and DMF (6 mL) at 0° C was added EDCI (0.44 g, 2.3 mmol). The mixture was allowed to come to room temperature and stirred for a further ten minutes after which N,O-dimethylhydroxylamine hydrochloride (0.19 g, 1.97 mmol) was added, followed by diisopropylethylamine (0.31 mL, 1.8 mmol). The mixture was stirred for 18 hours at room temperature, after which the solvent was concentrated to roughly 10% of its original volume. Water (30 mL) and ethyl acetate (30 mL) was added, and the layers separated. The aqueous layer was extracted with ethyl acetate (3 x 30 mL), and the combined organics were washed with brine, dried over sodium sulfate and concentrated to give **137** (0.5 g, 88%) as white, needle-like crystals which were taken on without any further purification. HRMS (FAB): m/z calcd. for $C_{18}H_{25}N_3NaO_4$ ($M + Na$)⁺ 370.17, found 370.07. ¹H NMR (300 MHz) (CDCl₃) δ TMS: 1.40 (9 H, s); 3.15 (3 H, s); 3.20 (1H, d, $J = 6.0$); 3.26 (1H, d, $J = 6.0$); 3.65 (3H, s); 4.95-5.07 (1H, m); 5.21-5.27 (1H, m); 7.05-7.61 (5H, m); 8.03 (1H, s). (TLNI-198_3-12)



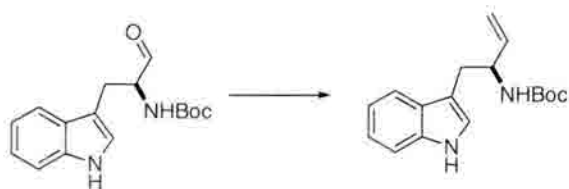
(S)-tert-butyl 1-(1H-indol-3-yl)-3-oxopropan-2-ylcarbamate (138)



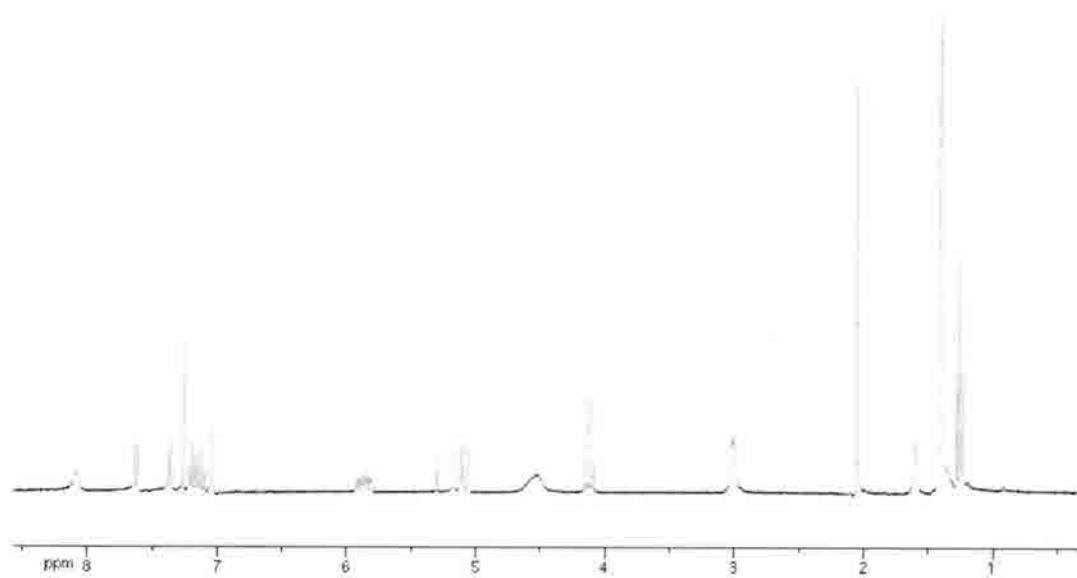
To a stirred solution of amide **137** (0.06g, 0.17 mmol) in dry DCM (3 mL) under argon atmosphere at -78° C was added DIBAL-H (1M in DCM, 0.68 mL, 0.68 mmol). The resultant mixture was stirred at -78° C for one hour, after which a saturated aqueous solution of sodium potassium tetrates (10 mL) was added. The mixture was allowed to come to room temperature and stirred vigorously for 3 h. The layers were separated and the aqueous layer extracted into DCM (3 x 10 mL). The combined organic layers were washed with brine, dried over sodium sulfate and concentrated. The residue was purified by flash column chromatography, using 1:1 hexanes/ethyl acetate as the eluant to give **138** as a light brown oil (0.04 g, 86%). HRMS (FAB): m/z calcd. for $C_{16}H_{21}N_2O_3$ ($M + H$)⁺ 289.15, found 289.15. 1H NMR (300 MHz) ($CDCl_3$) δ TMS: 1.44 (9H, s); 3.21-3.38 (2H, m); 4.47-4.56 (1H, m); 5.11-5.20 (1H, m); 7.04-7.62 (5H, m); 8.10 (1H, s); 9.64 (1H, s). (TLNI-201pp)



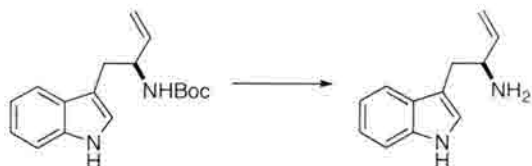
(S)-tert-butyl 1-(1H-indol-3-yl)but-3-en-2-ylcarbamate (139)



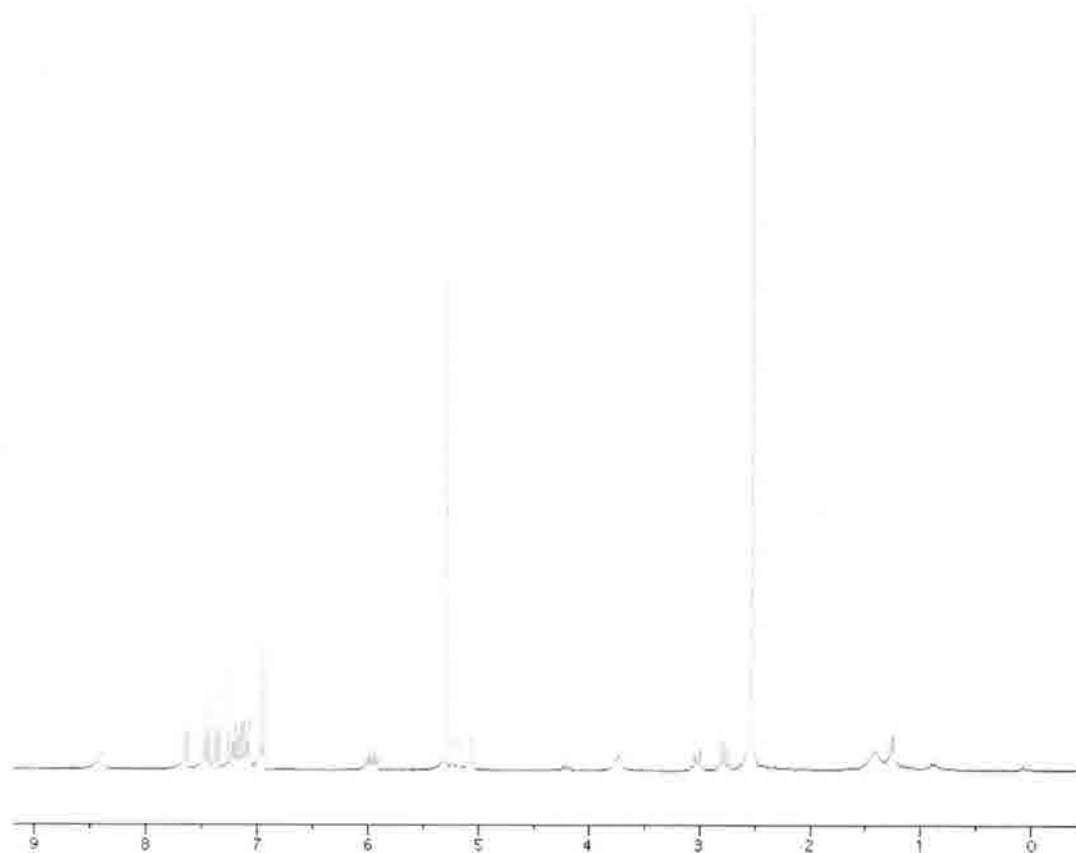
A stirred solution of methyltriphenylphosphonium bromide (4.85 g, 13.6 mmol) in THF (40 mL) was cooled to 0°, and NaHMDS (1M in THF, 14.3 mL, 14.3 mmol) was added dropwise. The mixture was stirred at room temperature for 30 min, then cooled to -78°. Aldehyde **138** (1.12 g, 3.88 mmol) in THF (10 mL) was added dropwise. The reaction was stirred for 15 min, then warmed to room temperature over 30 min. The mixture was poured onto water (50 mL), and the aqueous layer was extracted into EtOAc (3 x 25 mL). The combined organic layers were washed with brine, dried over sodium sulfate and concentrated. The residue was purified by column chromatography (5% Et₂O/DCM) to give **139** as a yellow oil (0.70g, 63%). HRMS (FAB): *m/z* calcd. for C₁₇H₂₃N₂O₂ (M + H)⁺ 289.15, found 286.17, found 286.20. $\alpha_D = +28$, *c* = 1 in DCM). ¹H NMR (300 MHz) (CDCl₃) δ TMS: 1.34 (9H, s); 2.99 (2H, d, *J*=12); 4.47-4.54 (1H, m); 4.56-4.68 (1H, m); 5.05 (1H, dd, *J* = 1.2, 18.9); 5.08 (1H, dd, *J* = 0.9, 25.7); 5.80 (1H, ddd, *J* = 4.5, 21.6, 27.6); 7.02-7.62 (5H, m); 8.25 (1H, s). (TLNI-217pp)



1-(1*H*-indol-3-yl)but-3-en-2-amine (**129**)



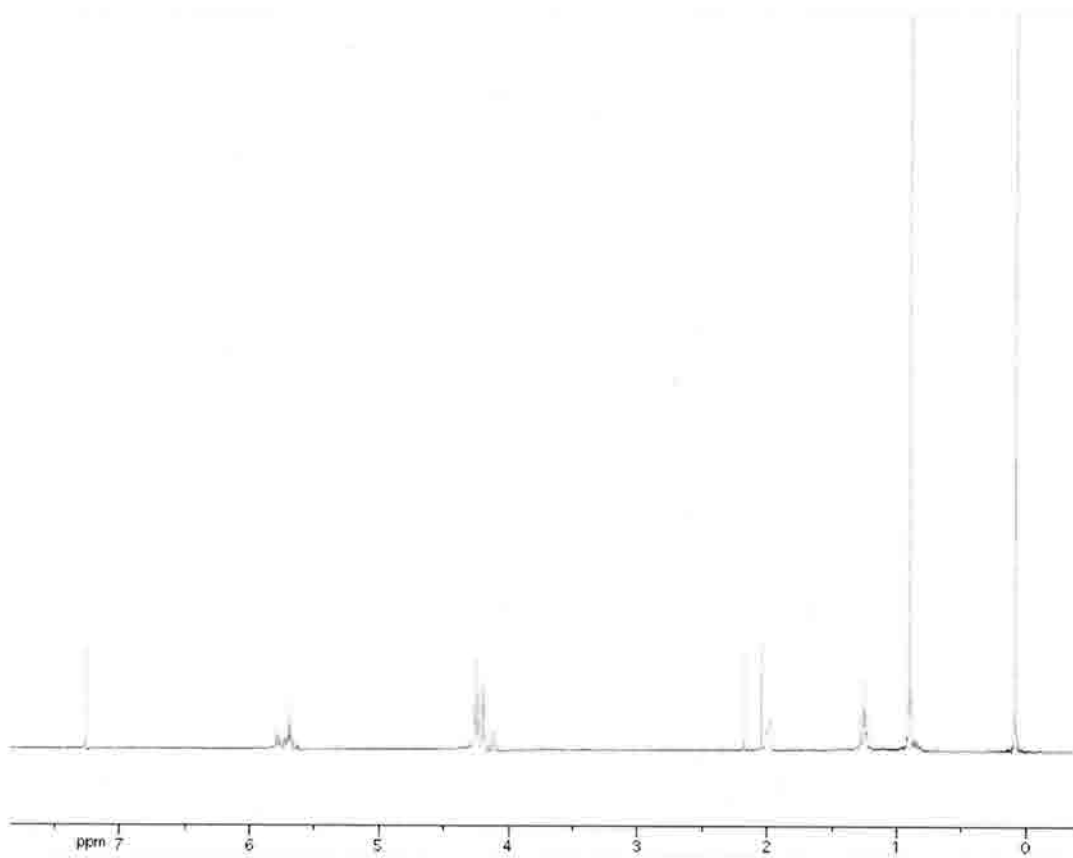
To a flame dried 50 mL round bottom flask under argon was added Boc-protected amine **139** (0.47g, 1.64 mmol) in DCM (25 mL). 2,6 Lutidine (0.46 mL, 3.93 mmol) was added, and the mixture cooled to -78° C, after which *t*-butyldimethylsilyl triflate (0.83 mL, 3.6 mmol) was added. The mixture was warmed to room temperature over 3.5 hours, and dry methanol (5 mL) was added. The reaction mixture was concentrated, then dissolved in methanol (25 mL) to which $\text{KF}\cdot 2\text{H}_2\text{O}$ (0.61g, 6.56 mmol) was added. After a further one hour of stirring, the mixture was diluted with brine and the layers separated. The aqueous layer was taken to pH 11 with 1N NaOH, after which it was extracted into DCM (3 x 20 mL). The combined organic layers were washed with brine, dried over sodium sulfate and concentrated to give **129** (0.29 g, 96%). $\alpha_{\text{D}} = +12$ ($c = 1$ in DCM). ^1H NMR (300 MHz) (CDCl_3) δ TMS: 1.34-1.49 (2H, s); 2.73-2.81 (1H, dd, $J=8.4, 14.1$); 2.98-3.05 (1H, dd, $J= 5.1, 14.4$); 5.04 (1H, dt, $J=1.2, 10.2$); 5.17 (1H, dt, $J= 1.5, 17.1$); 5.91 (1H, ddd, $J= 6.3, 10.2, 17.4$); 6.94-7.65 (5H, m); 8.40 (1H, s). (TLNI-239a)



(Z)-4-(*tert*-butyldimethylsilyloxy)but-2-en-1-ol (141)



To a flame-dried 50 mL round-bottom flask under argon atmosphere was added sodium hydride (60% in mineral oil, 0.48g, 12.1 mmol), followed by dry THF (20 mL). The stirred solution was cooled to 0° C, after which cis-butene diol (1.0 mL, 12.1 mmol) was added slowly via syringe. The mixture was allowed to come to room temperature and stirred for a further 60 minutes. TBSCl was added (0.60g, 4.0 mmol) and the mixture allowed to stir for 15 hours, after which a saturated aqueous solution of ammonium chloride (10 mL) was added. The organic layer was concentrated to roughly 10% of its original volume, after which the layers were separated. The aqueous layer was extracted with ethyl acetate (3 x 25 mL) and the combined organic layers were washed with brine and dried over sodium sulfate. The mixture was concentrated to give a light yellow oil (0.68g, 84%) and used without further purification. ¹H NMR (300 MHz) (CDCl₃) δ TMS: 0.08 (6H, s); 0.90 (9H, s); 4.19-4.26 (4H, m); 5.62-5.76 (2H, m). (TLNI-229pp)



4-(*tert*-butyldimethylsilyloxy)but-2-enal (**142**)



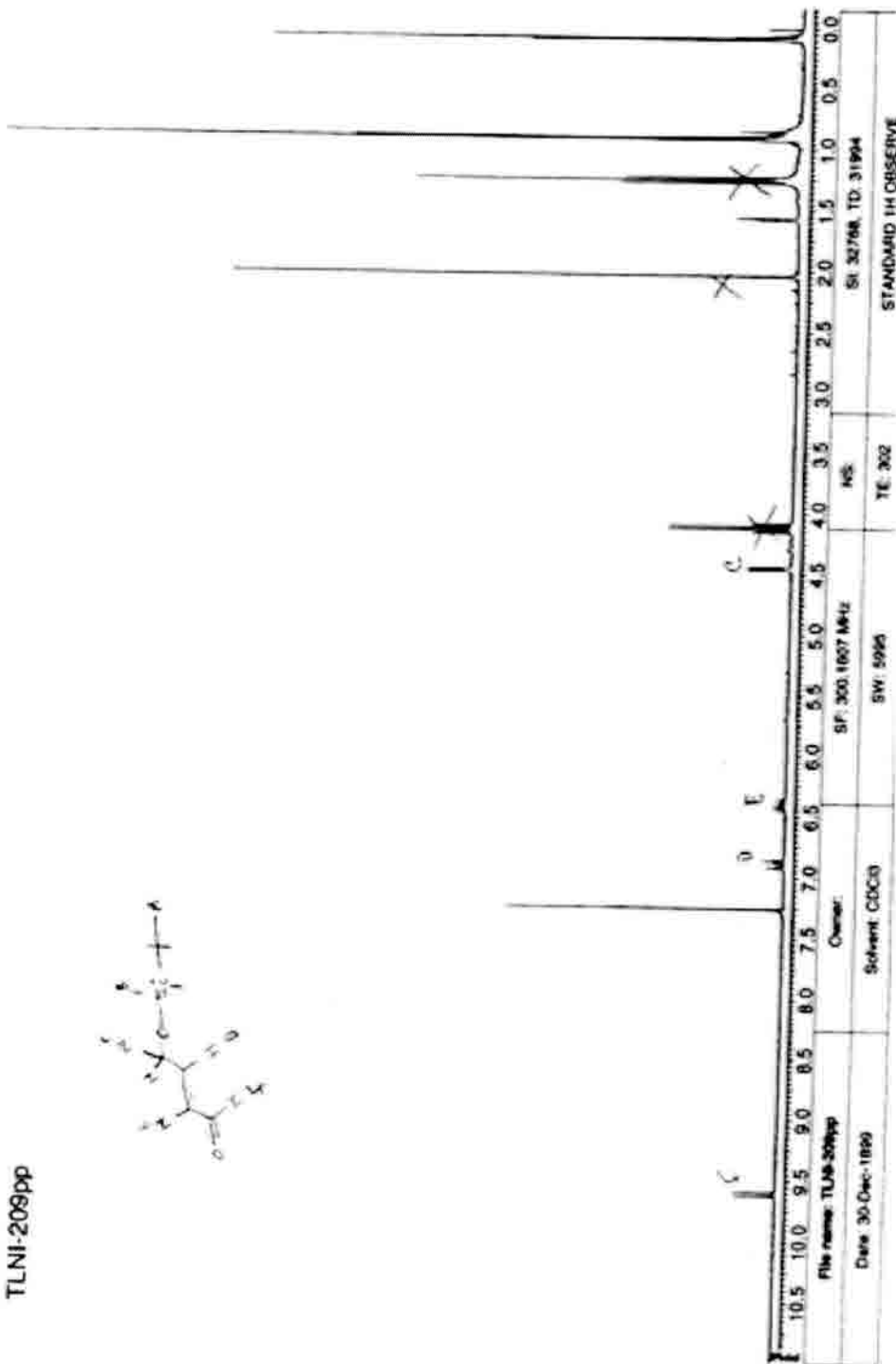
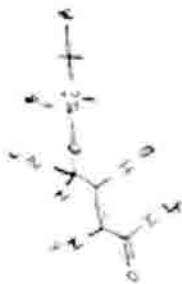
To a flame-dried 50 mL 2-neck round bottom flask under argon atmosphere was added dry dichloromethane (10 mL) followed by oxalyl chloride (0.56 mL, 5.0 mmol). The mixture was cooled to -78°C , after which a solution of dry DMSO (0.92 mL, 10 mmol) in DCM (3 mL) was slowly added via syringe. The mixture was stirred for 15 minutes, after which a solution of **141** in DCM (5 mL) was added. The mixture was stirred for a further 30 minutes, then removed from the ice bath, and dry triethylamine (1.86 mL, 13.4 mmol) was added. The mixture was allowed to warm to room temperature after which water (15 mL) was added. The layers were then separated, the aqueous extracted into DCM (3 x 20) and the combined organics were washed with brine, dried over sodium sulfate and concentrated.

(E)-4-(tert-butyldimethylsilyloxy)but-2-enal (143)



The mixture of E and Z isomers (**142**) was taken up in DCM (10 mL) and DMAP (0.04 g, 0.3 mmol) was added. The mixture was stirred for two days, after which it was washed with a saturated aqueous solution of ammonium chloride. The organic layer was dried over sodium sulfate and concentrated to afford **143** as a dark red oil (71% over 2 steps) which was carried on without further purification. ¹H NMR (300 MHz) (CDCl₃) δ TMS: 0.09 (6H, s); 0.91 (9H, s); 4.45 (2H, dd, *J* = 2.1, 3.3); 6.40 (1H, ddt *J* = 2.1, 7.8, 15.6); 6.89 (1H, dt, *J* = 3.3, 15.3); 9.62 (1H, d, *J* = 8.1). (TLNI-209pp)

TLNI-209ppp



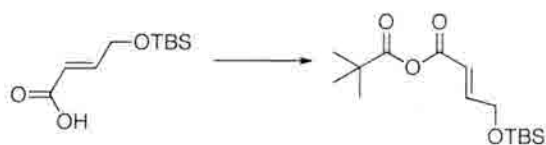
(E)-4-(*tert*-butyldimethylsilyloxy)but-2-enoic acid (144**)**



To a stirred mixture of aldehyde **143** (0.63g, 3.14 mmol) in *tert*-butanol (36 mL) was added 2-methyl-2-butene (6.7 mL, 62.9 mmol). A solution of sodium chlorite (2.55 g, 28.3 mmol) and monobasic phosphoric acid monohydrate (3.58g, 26.0 mmol) in water (37 mL) was added in four aliquots over 30 minutes. The mixture was stirred for 30 minutes, after which most of the solvent was evaporated. The remaining aqueous layer was extracted with DCM (3 x 20 mL), and the combined organics were washed with 1 N HCl (25 mL) in water (25 mL), dried over sodium sulfate and concentrated, giving **144** as a light yellow oil (0.48 g, 71%) which was taken on without further purification.

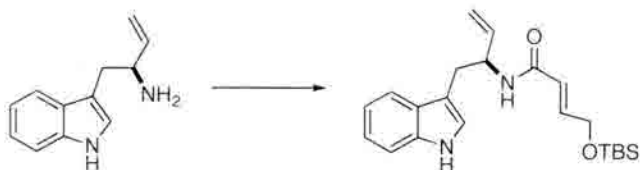
^1H NMR (300 MHz) (CDCl_3) δ TMS: 0.09 (6H, s); 0.92 (9H, s); 4.37 (2H, dd, $J = 2.1, 3.3$); 6.12 (1H, dt, $J = 2.4, 15.3$); 7.11 (1H, dt, $J = 3.3, 15.3$). (TLNI-211cr)

(E)-4-(tert-butyldimethylsilyloxy)but-2-enoic pivalic anhydride (145)

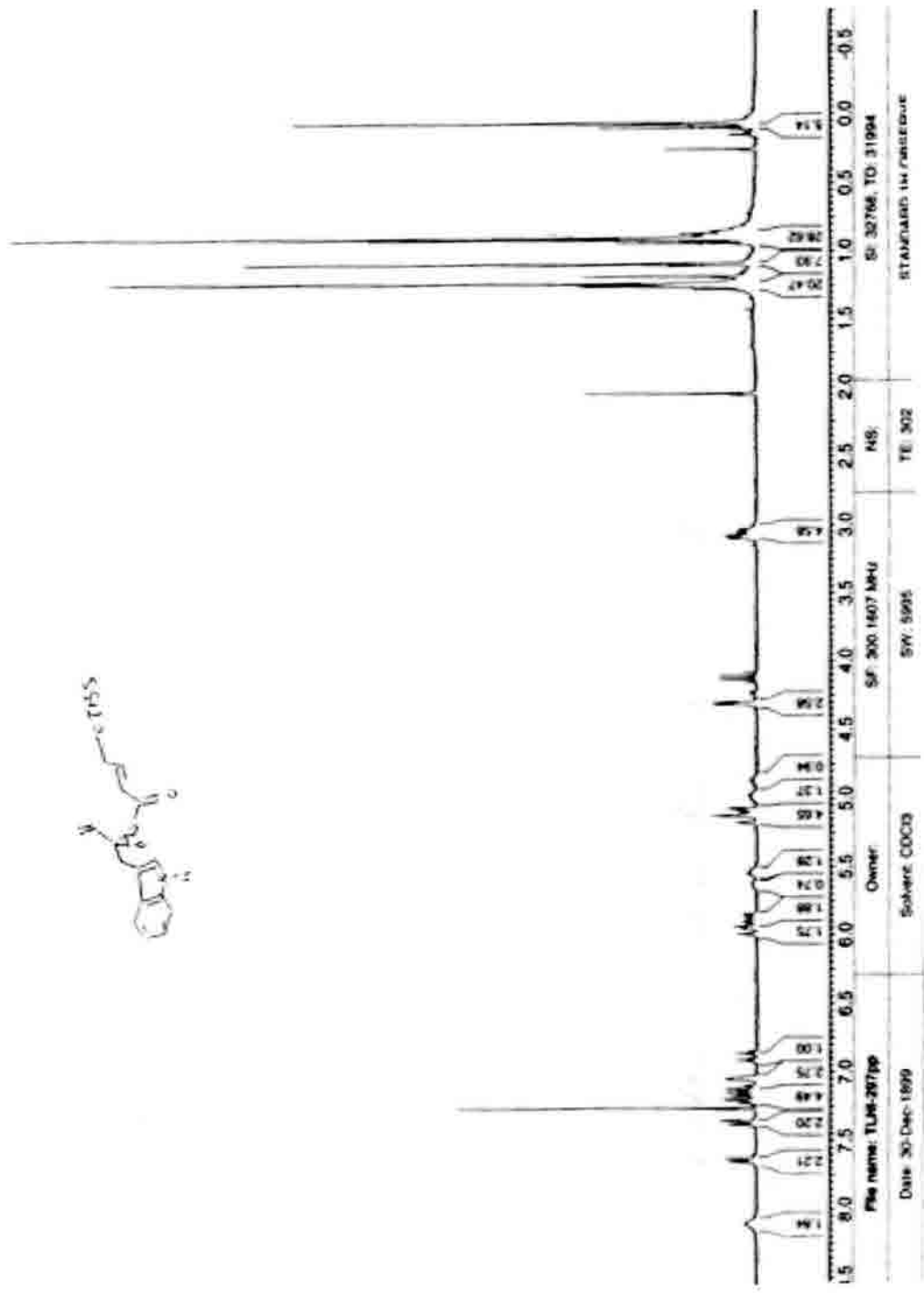


A stirred solution of **144** (0.13 g, 0.60 mmol) in THF (6 mL) was cooled to 0° under argon atmosphere. Triethylamine (0.12 mL, 0.90 mmol) was added dropwise, following which pivaloyl chloride (0.11 mL, 0.90 mmol) was also added dropwise. The mixture was warmed to room temperature and stirred for a further 1.5 hours. The reaction mixture was washed with brine (2 x 10 mL) and dried over sodium sulfate. The solvent was evaporated to give **145** as a yellow oil (0.17 g, 94%), which was used without further purification. HRMS (FAB): m/z calcd. for $C_{15}H_{28}NaO_4Si$ ($M + Na$)⁺ 323.17, found 323.164. ¹H NMR (300 MHz) (CDCl₃) δ TMS: 0.09 (6H, s); 0.92 (9H, s); 1.27 (9H, s); 4.37 (2H, dd, $J = 2.1, 3.3$); 6.12 (1H, dt, $J = 2.4, 15.3$); 7.11 (1H, dt, $J = 3.3, 15.3$).

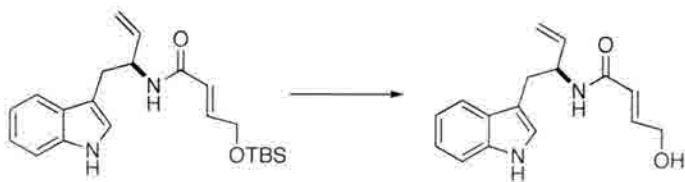
(*S,E*)-*N*-(1-(1*H*-indol-3-yl)but-3-en-2-yl)-4-(*tert*-butyldimethylsilyloxy)but-2-enamide
(146)



To a stirred solution of amine **129** (0.010 g, 0.054 mmol) in DCM (2 mL) was added pyridine (5 μ L, 0.06 mmol), DMAP (1 mg, 0.01 mmol) and mixed anhydride **145** (0.016 g, 0.054 mmol). The resultant mixture was stirred for 12 h, after which it was washed with a saturated aqueous solution of ammonium chloride and dried over sodium sulfate. The solvent was evaporated to give **146** as a light brown oil (0.014g, 69%). HRMS (FAB): m/z calcd. for $C_{22}H_{33}N_2O_2Si$ (M+H)⁺ 385.22, found 385.22. ¹H NMR (300 MHz) (CDCl₃) δ TMS: 0.05 (6H, s); 0.92 (9H, s); 3.01-3.11 (2H, m); 4.25-4.35 (2H, m); 4.77-4.90 (1H, m); 5.05-5.21 (2H, m); 5.80-6.05 (2H, m); 6.81 (1H, dt, $J = 2.4, 15.3$); 7.01-7.25 (3H, m); 7.35 (1H, d, $J = 10.5$); 7.62 (1H, d, $J = 10.5$); 8.10 (1H, bs).

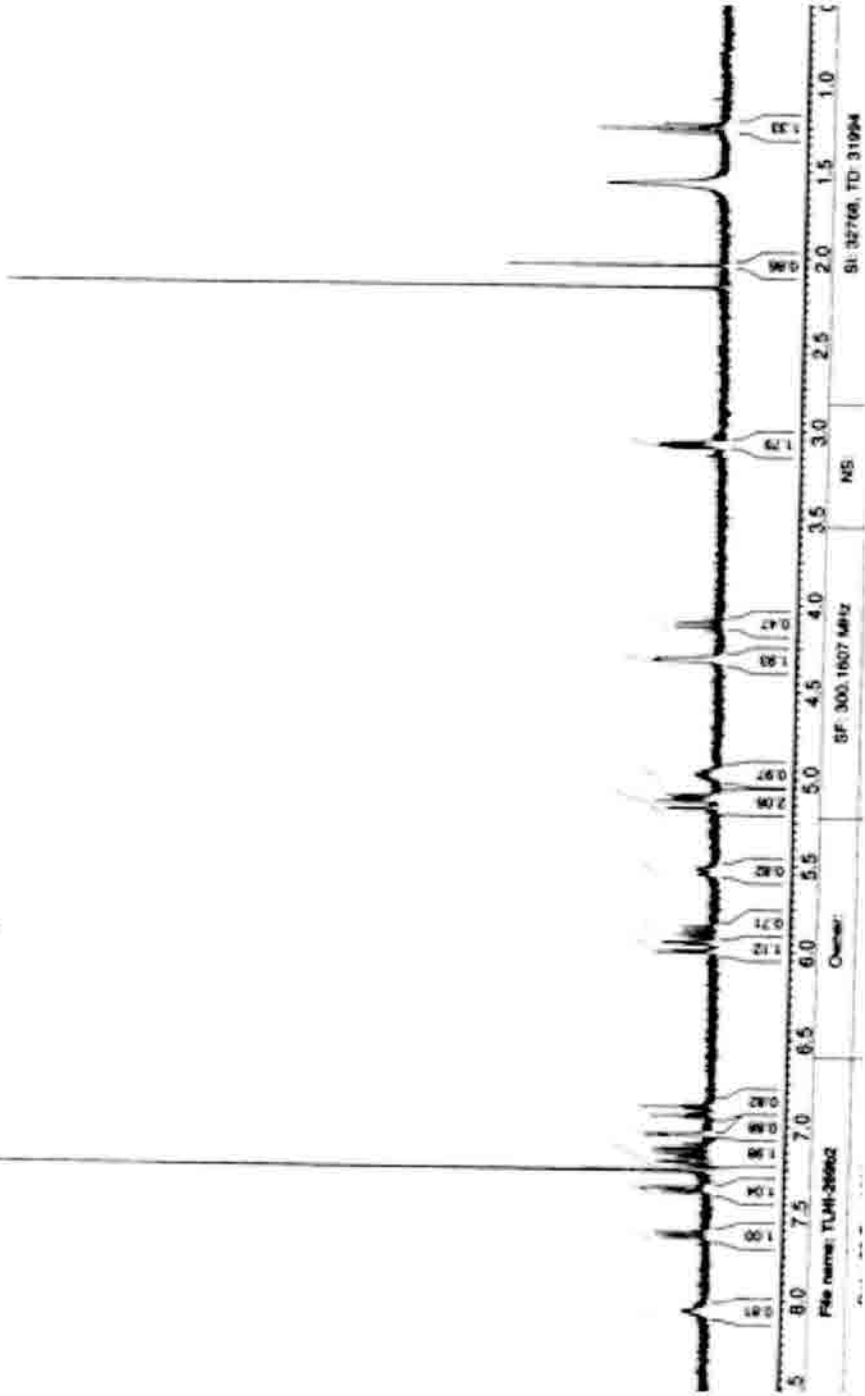
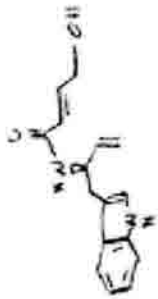


(*S,E*)-*N*-(1-(1*H*-indol-3-yl)but-3-en-2-yl)-4-hydroxybut-2-enamide (147**)**

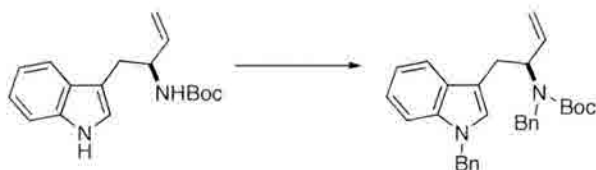


A stirred solution of amide **146** (0.15 g, 0.39 mmol) in THF (5 mL) was cooled to 0°. TBAF (1M in THF, 0.58 mL) was added dropwise. The reaction mixture was stirred at 0° for 1 h, after which a saturated aqueous solution of ammonium chloride (10 mL) was added. The aqueous layer was extracted into EtOAc (3 x 10 mL) and the combined organic layers were washed with brine and dried over sodium sulfate. The solvent was evaporated and the residue was purified by flash chromatography (EtOAc as eluent) to give **147** as a clear oil (0.07 g, 66%). HRMS (FAB): m/z calcd. for $C_{16}H_{19}N_2O_2$ ($M + H$)⁺ 271.14, found 271.144. ¹H NMR (300 MHz) (CDCl₃) δ TMS: 3.09-3.12 (2H, m); 4.25-4.35 (2H, m); 4.91-5.02 (1H, m); 5.08-5.17 (2H, m); 5.50-5.56 (1H, m); 5.81-6.05 (2H, m); 6.81 (1H, dt, $J = 2.4, 15.3$); 7.01-7.25 (3H, m); 7.35 (1H, d, $J = 10.5$); 7.62 (1H, d, $J = 10.5$); 8.10 (1H, bs).

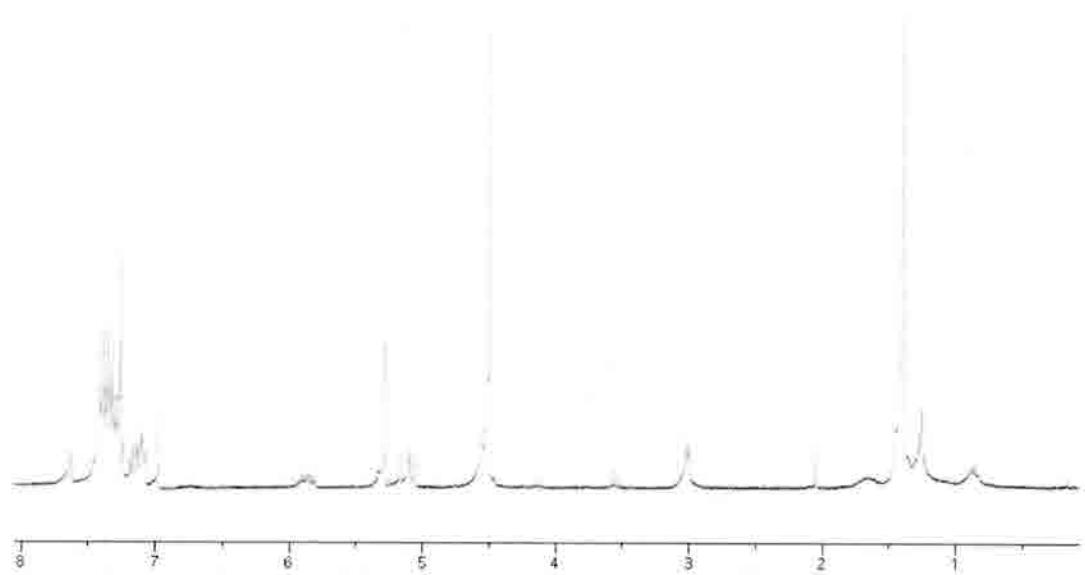
TLNI-269b2



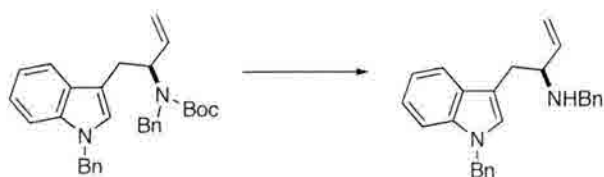
(S)-tert-butyl benzyl(1-(1-benzyl-1H-indol-3-yl)but-3-en-2-yl)carbamate (148)



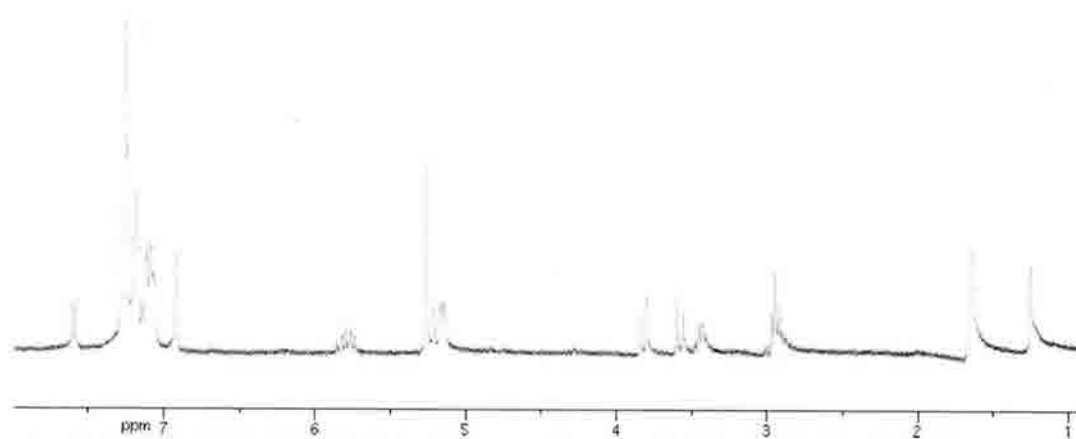
A suspension of NaH (0.09 g, 2.17 mmol) in THF (6 mL) was cooled to 0°, and **139** (0.31 g, 1.08 mmol) in THF (6 mL) was added dropwise. The reaction was allowed to come to room temperature and BnBr (0.26 mL, 2.19 mmol) was added. The mixture was stirred for 15 h, after which a saturated aqueous solution of ammonium chloride (15 mL) was added. The aqueous layer was extracted into EtOAc (3 x 20 mL) and the combined organic layers were washed with brine and dried over sodium sulfate. The solvent was evaporated and the residue purified by column chromatography (1:3 EtOAc/hexanes) to give **148** as a light brown solid (0.44 g, 87%). ¹H NMR (300 MHz) (CDCl₃) δ TMS: 1.4 (9H, s); 1.66 (1H, m); 3.01 (2H, d, *J* = 5.4); 4.51 (4H, s); 5.11 (2H, dd, *J* = 5.1, 17.1); 5.90 (1H, ddd, *J* = 5.1, 15.6, 22.2); 6.97 (1H, s); 7.08 - 7.42 (13 H, m); 7.65 (1H, d, *J* = 6.9). (TLNI-338)



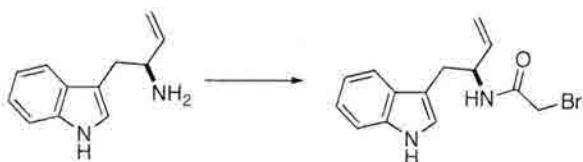
(S)-N-benzyl-1-(1-benzyl-1*H*-indol-3-yl)but-3-en-2-amine (149)



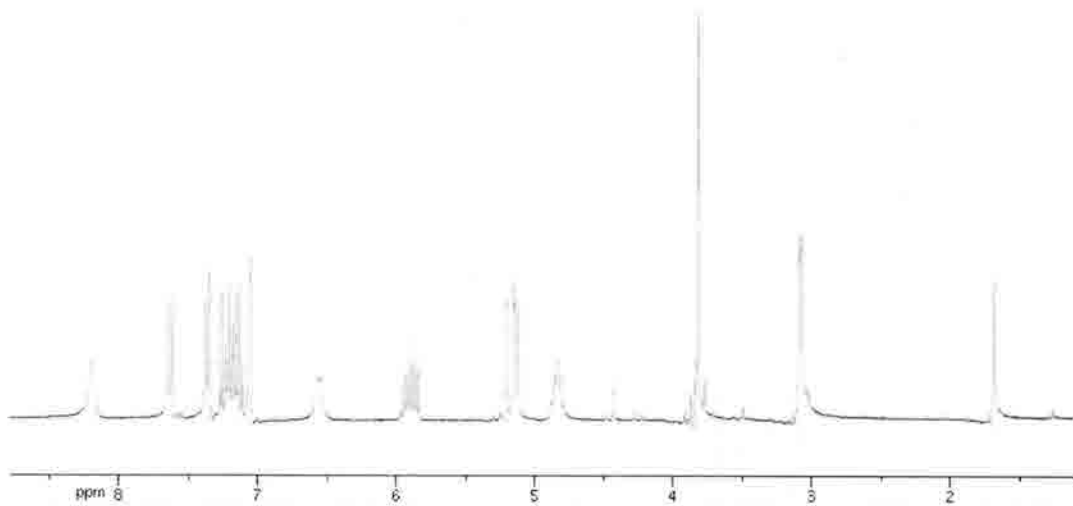
To a stirred solution of carbamate **148** (0.11 g, 0.24 mmol) in DCM (5 mL) was added 2,6-lutidine (0.06 mL, 2.2 mmol). The mixture was cooled to -78° , after which TBSOTf (0.11 mL, 0.48 mmol) was added dropwise. The mixture was warmed to room temperature over 3.5 hours, and the solvent was evaporated. The resultant residue was dissolved in MeOH (5 mL) and $\text{KF}\cdot\text{H}_2\text{O}$ (0.09 g, 0.96 mmol) was added. The mixture was stirred for 1 h, then concentrated remove the residual solvent. The residue was dissolved in DCM and a saturated aqueous solution of sodium bicarbonate (10 mL) was added. The aqueous layer was extracted into DCM (3 x 15 mL) and the combined organic layers were washed with brine and dried over sodium sulfate. The solvent was evaporated, and the residue was purified by column chromatography (2:5 EtOAc/hexanes) to give **149** (0.018g, 20%). HRMS (FAB): m/z calcd. for $\text{C}_{26}\text{H}_{27}\text{N}_2$ ($\text{M} + \text{H}$)⁺ 367.21, found 367.215. ¹H NMR (300 MHz) (CDCl_3) δ TMS: 2.97 (2H, t, $J = 5.4$); (3.41 - 3.48 (1H, m); 3.60 (1H, d, $J = 13.5$); 3.84 (1H, d, $J = 13.5$); 5.17 (2H, dd, $J = 12.3, 22.2$); 5.27 (2H, s); 5.80 (1H, ddd, $J = 7.8, 17.4, 25.2$); 6.92 (1H, s); 7.06-7.25 (13 H, m); 7.61 (1H, d, $J = 7.2$). (TLNI-345a)



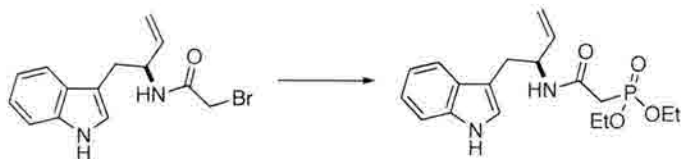
(S)-N-(1-(1*H*-indol-3-yl)but-3-en-2-yl)-2-bromoacetamide (151)



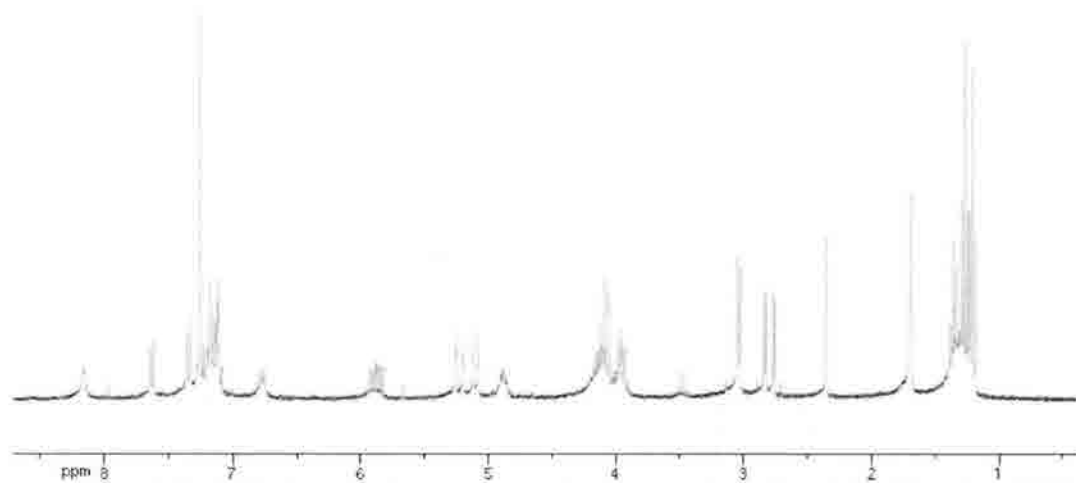
A stirred solution of amine **129** (0.1 g, 0.53 mmol) in THF (5 mL) was cooled to 0°. Triethylamine (0.11 mL, 0.80 mmol) was added dropwise. After ~5 minutes, bromoacetyl bromide (0.06 mL, 0.64 mmol) was added dropwise. The resultant suspension was stirred for a further 1.5 h at room temperature. The reaction mixture was washed with brine (3 x 10 mL), and the organic layer was dried over sodium sulfate. The solvent was evaporated to give **151** as a light brown oil in quantitative yield (0.16 g). ¹H NMR (300 MHz) (CDCl₃) δ TMS: 3.07 (2H, d, *J* = 4.8); 3.82 (2H, d, *J* = 2.1); 4.79-4.88 (1H, m); (2H, dd, *J* = 6, 12.8, 24.3); 5.89 (1H, ddd, *J* = 5.7, 16.2, 22.8); 6.56 (1H, d, *J* = 7.8); 7.06 (1H, s); 7.11-7.23 (2H, m); 7.38 (1H, d, *J* = 7.8); 7.64 (1H, d, *J* = 7.8); 8.19 (1H, s). (TLNI-377_8-10)



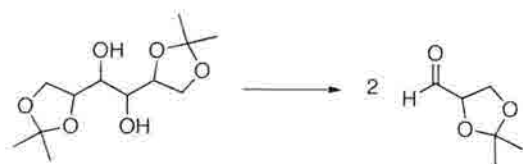
(S)-diethyl 2-(1-(1*H*-indol-3-yl)but-3-en-2-ylamino)-2-oxoethylphosphonate (152)



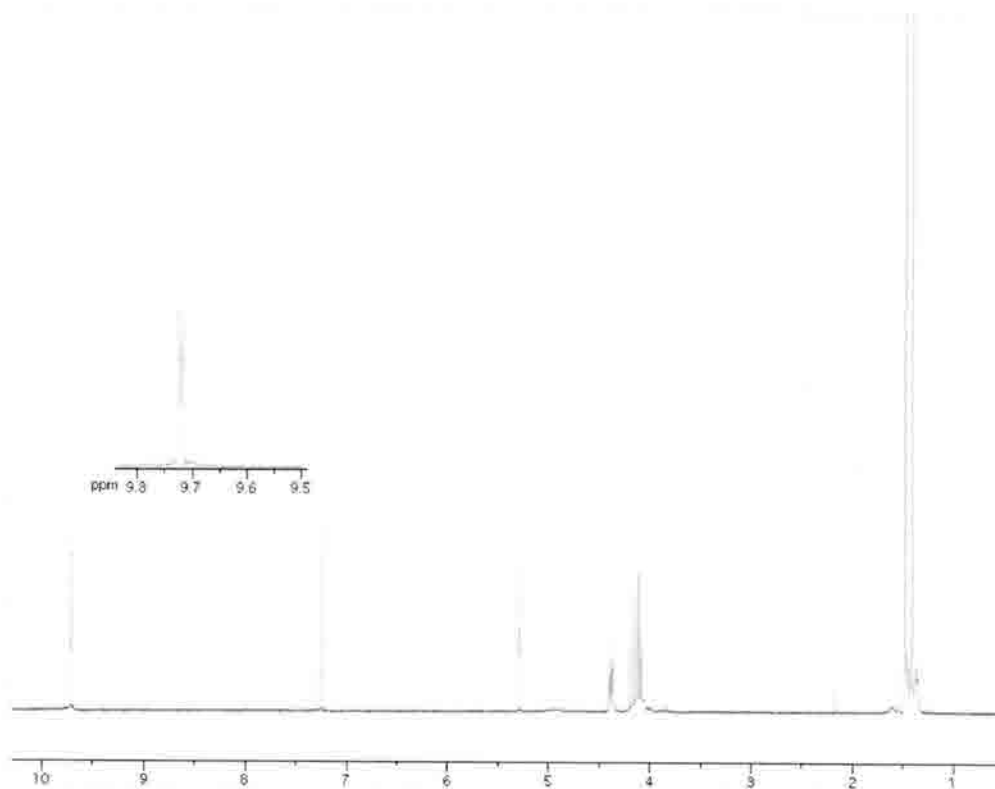
Amide **151** (0.063g, 0.205 mmol) was dissolved in triethylphosphite (0.11 mL, 0.62 mmol). This mixture was heated to 100° for 20 min, and then heated to 65° at reduced pressure for 45 minutes. The resulting residue was azeotroped with toluene (3 x 2 mL) and placed under high vacuum for 12 h to remove the remaining unreacted triethylphosphite, ultimately giving **152** in quantitative yield (0.074 g). ¹H NMR (300 MHz) (CDCl₃) δ TMS: 1.21 (3H, t, *J* = 7.2); 1.27 (3H, t, *J* = 6.9); 2.82 (2H, dd, *J* = 3.9, 20.7); 3.04 (2H, d, *J* = 6.3); 3.93-4.15 (4H, m); 4.84-4.92 (1H, m); 5.20 (2H, ddt, *J* = 1.2, 17.1, 19.8); 5.88 (1H, ddd, *J* = 5.4, 10.2, 17.1); 6.76 (1H, d, *J* = 6.9); 7.08-7.23 (3H, m); 7.36 (1H, d, *J* = 6.9); 7.64 (1H, d, *J* = 7.8); 8.16 (1H, s). (TLNI-380)



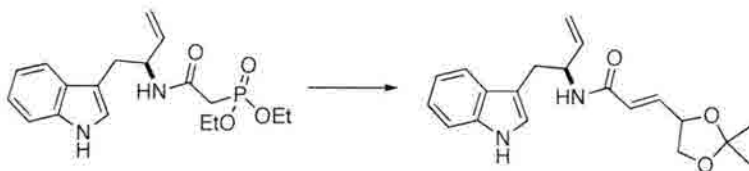
2,2-dimethyl-1,3-dioxolane-4-carbaldehyde (**154**)



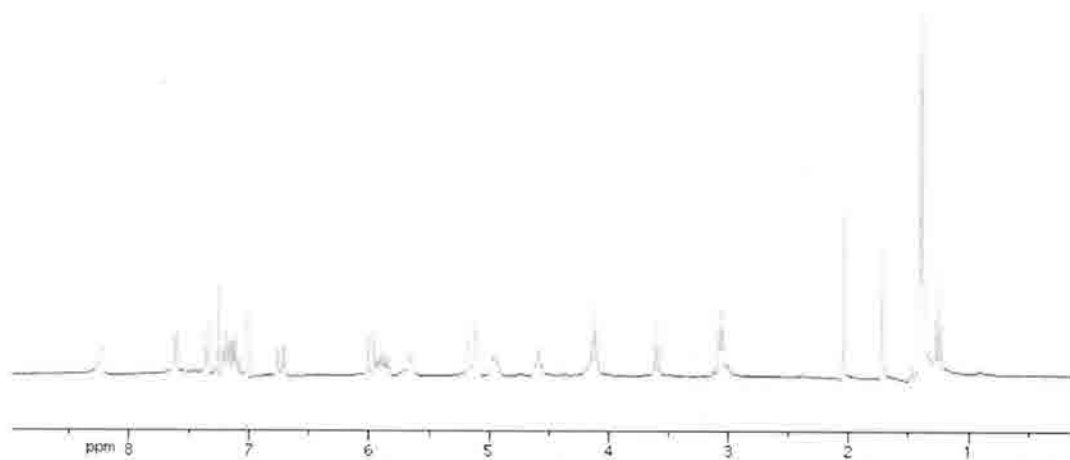
To a stirred solution of mannitol **153** (0.5 g, 1.9 mmol) in DCM (4.5 mL) was added a saturated aqueous solution of sodium bicarbonate (0.23 mL). Sodium periodate (0.61 g, 2.86 mmol) was slowly added. The mixture was stirred for 2 h, after which magnesium sulfate was added, followed by a further 10 minutes of stirring. The resulting suspension was filtered and the filtrate concentrated to give **154** as a clear oil (0.49 g, 100%). ^1H NMR (300 MHz) (CDCl_3) δ TMS: 1.49 (6H, d, $J = 20.4$); 4.15 (2H, ddd, $J = 9, 16.2, 23.4$); 4.39 (1H, ddd, $J = 1.8, 4.8, 6.8$), 9.72 (1H, d, $J = 1.8$). (TLNI-357)



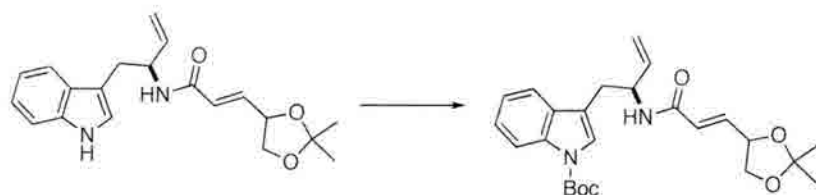
(E)-N-((S)-1-(1H-indol-3-yl)but-3-en-2-yl)-3-(2,2-dimethyl-1,3-dioxolan-4-yl)acrylamide (155)



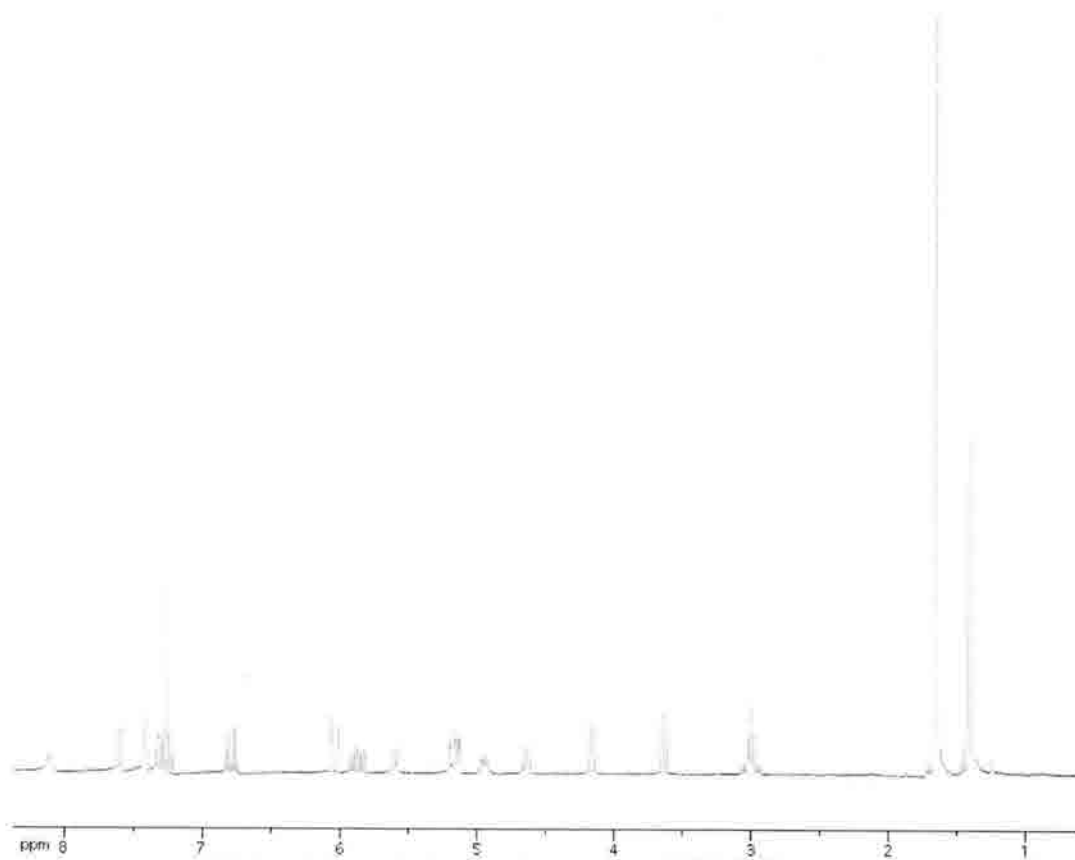
To a stirred solution of aldehyde **154** (0.029 g, 0.223 mmol) in MeCN (1.5 mL) was added phosphonate **154** (0.07g, 0.205 mmol) in MeCN (1.7 mL) followed by anhydrous lithium chloride (0.02g, 0.53 mmol). The reaction mixture was cooled to 0°, and DBU (0.03 mL, 0.20 mmol) was added dropwise. The resultant mixture was stirred for 1.5 h at room temperature, followed by addition of H₂O (15 mL) and EtOAc (15 mL). This biphasic mixture was stirred for 30 minutes, after which the aqueous layer was extracted into EtOAc (3 x 20 mL). The combined organic layers were washed with brine and dried over sodium sulfate. After evaporation of the remaining solvent, the residue was purified by column chromatography (EtOAc) to provide **155** as a light brown oil (0.04g, 55% over 2 steps). ¹H NMR (300 MHz) (CDCl₃) δ TMS: 1.41 (6H, d, *J* = 7.2); 3.07 (2H, t, *J* = 4.8); 3.60 (1H, t, *J* = 7.8); 4.08-4.15 (2H, m); 4.56-4.62 (1H, m); 4.95 (1H, s); 5.09-5.17 (2H, m); 5.67 (1H, d, *J* = 8.1); 5.89 (1H, ddd, *J* = 5.7, 10.8, 16.2); 6.01 (1H, dd, *J* = 1.2, 15.3); 6.75 (1H, dd, *J* = 5.7, 15.3); 7.02 (1H, s); 7.09-7.22 (2H, m); 7.37 (1H, d, *J* = 8.4); 7.63 (1H, d, *J* = 7.8); 8.23 (1H, s). (TLNI-381_6-13)



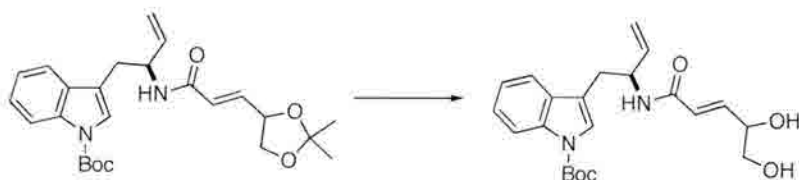
tert-butyl 3-((2*S*)-2-((*E*)-3-(2,2-dimethyl-1,3-dioxolan-4-yl)acrylamido)but-3-enyl)-1*H*-indole-1-carboxylate (**156**)



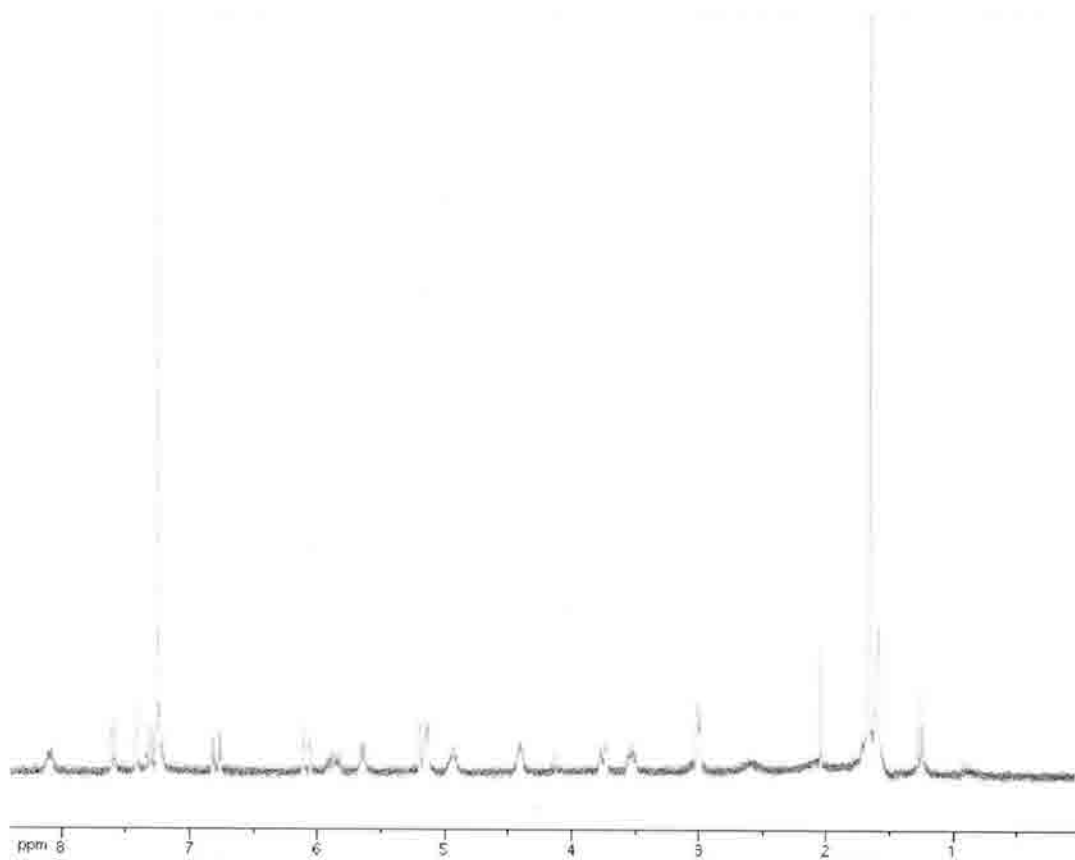
To a stirred solution of **155** (0.04g, 0.113 mmol) in THF (3 mL) was added Boc₂O (0.027g, 0.124 mmol) followed by DMAP (0.001g, 0.011 mmol). The mixture was stirred for 2 h prior to the addition of a saturated aqueous solution of ammonium chloride (5 mL). The aqueous layer was extracted into EtOAc (3 x 10 mL), and the combined organic layers were washed with brine, dried over sodium sulfate and concentrated. The residue was purified by column chromatography (1:1 EtOAc/hexanes) to give **156** (0.05g, 61%). ¹H NMR (300 MHz) (CDCl₃) δ TMS: 1.43 (6H, d, *J* = 8.7); 1.67 (9H, s); 3.00 (2H, t, *J* = 4.8); 3.64 (1H, dd, *J* = 7.5, 8.1); 4.16 (1H, dd, *J* = 6.6, 8.1); 4.63 (1H, q, *J* = 6.6); 4.90-4.99 (1H, m); 5.14 (2H, ddt, *J* = 1.2, 4.5, 11.4); 5.6 (1H, d, *J* = 8.4); 5.87 (1H, ddd, *J* = 5.4, 10.2, 15.9); 6.06 (1H, dd, *J* = 1.2, 15); 6.81 (1H, dd, *J* = 5.4, 15); 7.21-7.24 (*1H, m); 7.29-7.34 (1H, m); 7.41 (1H, s); 7.62 (1H, d, *J* = 7.5); 8.12 (1H, d, *J* = 7.5). (TLNI-389pp)



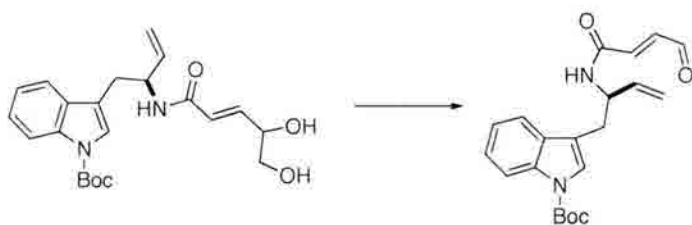
tert-butyl 3-((2*S*)-2-((*E*)-4,5-dihydroxypent-2-enamido)but-3-enyl)-1*H*-indole-1-carboxylate (**158**)



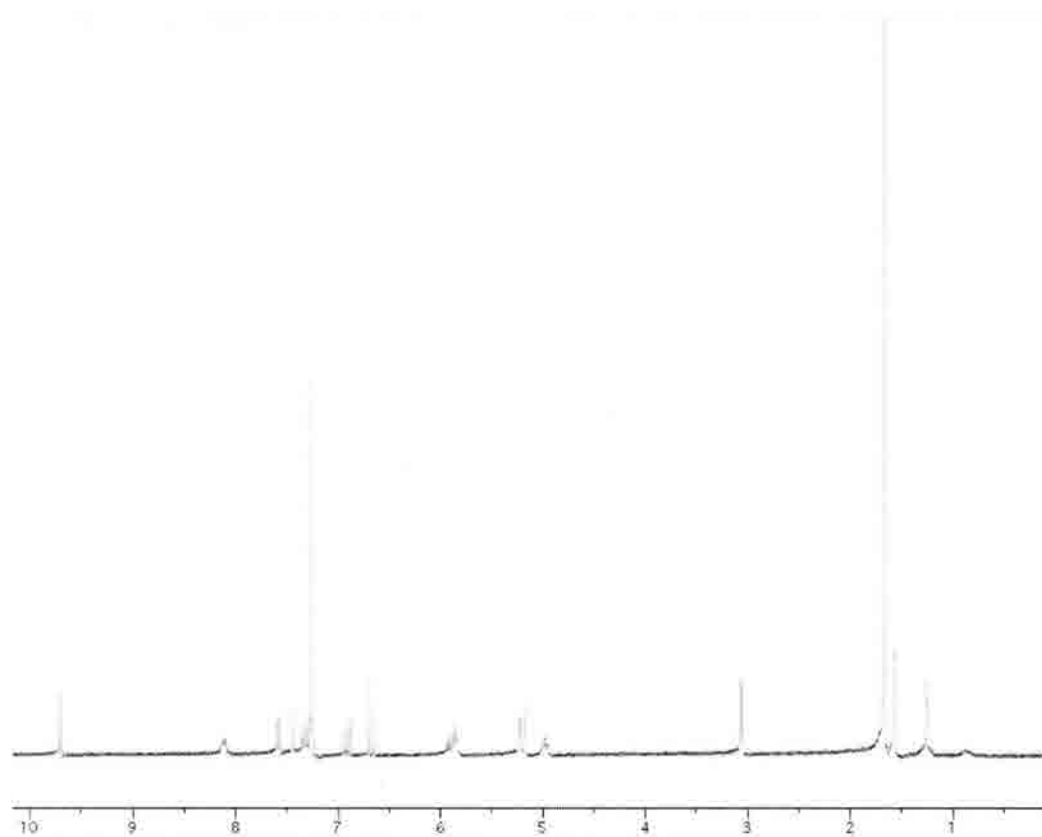
Acetal **155** (0.02g, 0.038 mmol) was dissolved in MeOH (2 mL) and PPTS (~ 1 mg, 0.004 mmol) was added. The mixture was heated to reflux for 15 h, after which the solvent was evaporated. Column chromatography (5% MeOH in EtOAc) gave diol **158** (0.004 g, 26%). $^1\text{H NMR}$ (300 MHz) (CDCl_3) δ TMS: 1.67 (9H, s); 3.01 (2H, d, $J = 6.3$); 3.56 (1H, m); 3.74, 1H, d, $J = 8.1$); 4.41 (1H, s); 4.92-4.98 (1H, m); 5.14 (2H, dd, $J = 3.6, 10.8$); 5.63 (1H, d, $J = 8.1$); 5.82-5.92 (1H); 7.42 (1H, s); 7.59 (1H, d, $J = 6.9$); 8.12 (1H, d, $J = 6.9$). (TLNI-410_11-37)



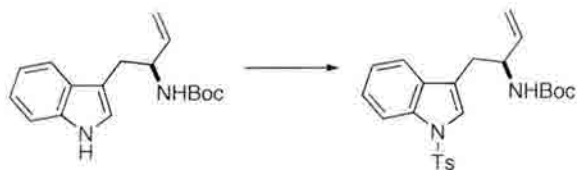
(*R,E*)-*tert*-butyl 3-(2-(4-oxobut-2-enamido)but-3-enyl)-1*H*-indole-1-carboxylate (159**)**



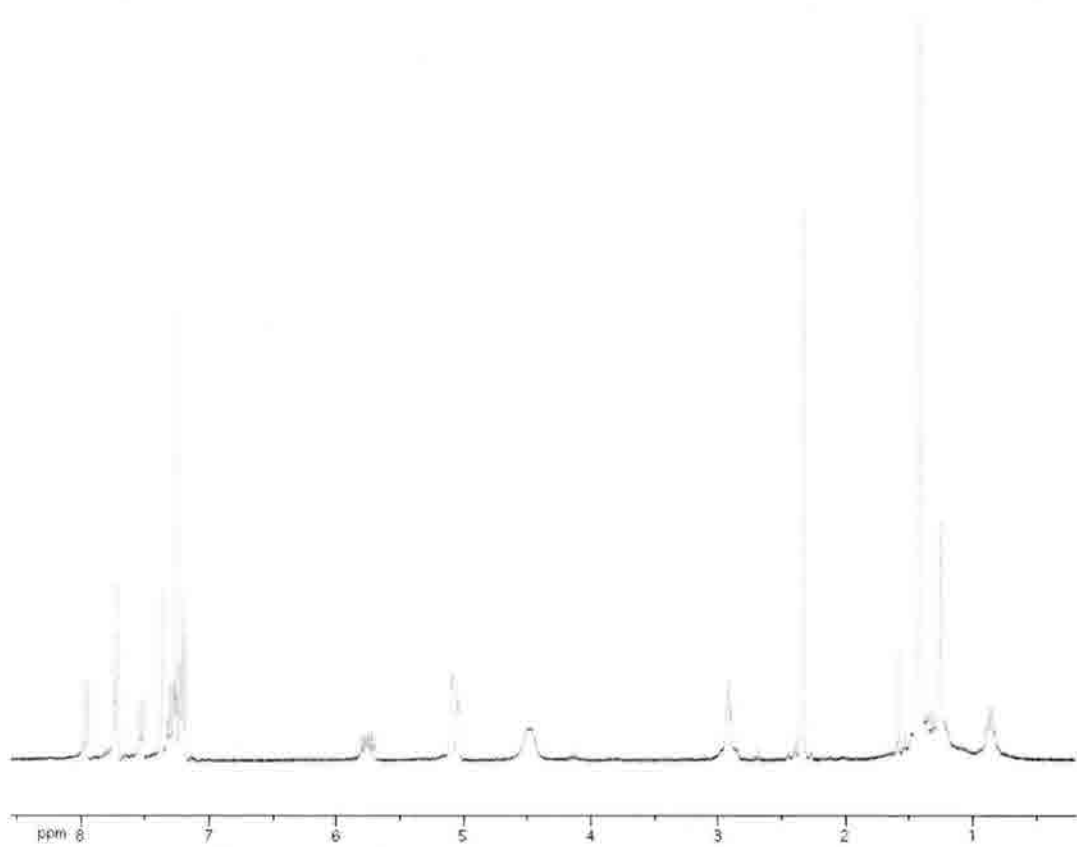
To a stirred solution of diol **158** (5 mg, 0.012 mmol) in DCM (2 mL) was added a saturated aqueous solution of sodium bicarbonate (10 μ L) followed by slow addition of sodium periodate (4 mg, 0.019 mmol). The resultant suspension was stirred for 2 h, after which TLC showed complete consumption of starting material. Magnesium sulfate was added, and the mixture stirred for 10 minutes further, followed by filtration. The filtrate was concentrated to give **159** (4 mg, 100%). ^1H NMR (300 MHz) (CDCl_3) δ TMS: 1.67 (9H, s); 3.07 (2H, d, $J = 6.6$); 4.96 (1H, m); 5.18-5.23 (2H, m); 5.83-5.95 (2H, m); 6.70 (1H, d, $J = 15.6$); 6.93 (1H, dd, $J = 7.5, 15.6$); 7.27-7.36 (2H, m); 7.44 (1H, s); 7.60 (1H, d, $J = 7.8$); 8.12 (1H, d, $J = 7.8$) (TLNI-414)



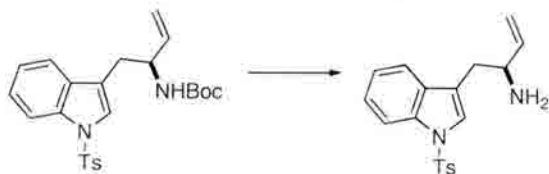
(S)-tert-butyl 1-(1-tosyl-1H-indol-3-yl)but-3-en-2-ylcarbamate (161)



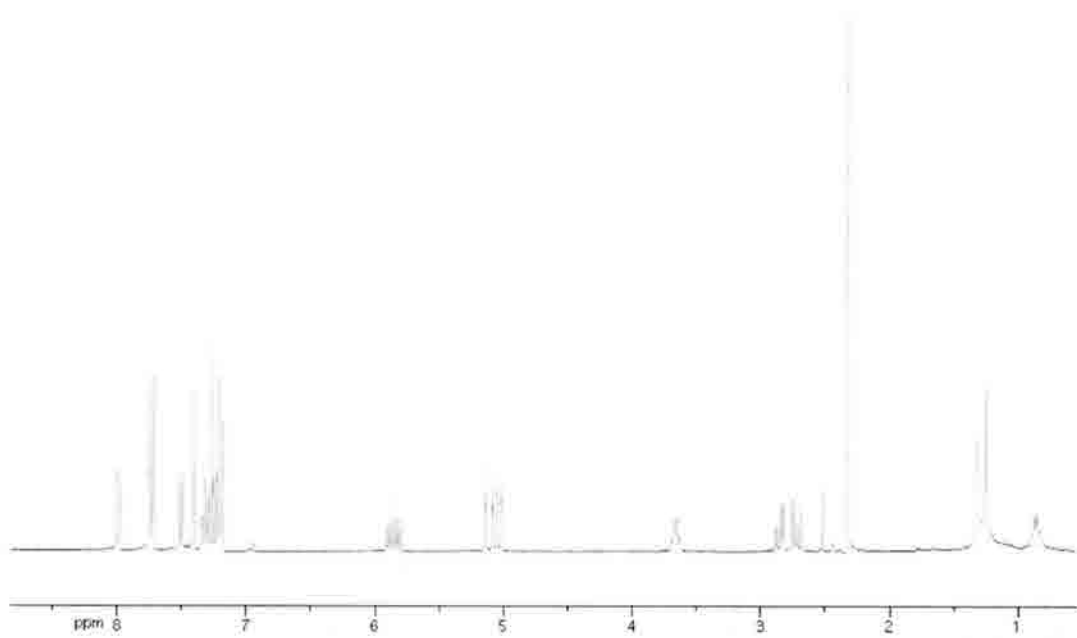
To a stirred solution of indole **139** (1.47g, 5.13 mmol) in toluene (15 mL) was added tosyl chloride (1.47g, 7.73 mmol) and tetrabutylammonium hydrogensulfate (0.26g, 0.77 mmol). The mixture was cooled to 0°, followed by the addition of a concentrated aqueous solution of sodium hydroxide (15 mL). The mixture was warmed to room temperature and stirred for a further 16 h. The organic layer was washed with 1N HCl (2 x 15 mL), then a saturated solution of sodium bicarbonate (2 x 15 mL), water (1 x 20 mL) and brine (1 x 20 mL). The organic layer was dried over sodium sulfate and concentrated to give **161** as a light yellow oil (1.96g, 87%). ¹H NMR (300 MHz) (CDCl₃) δ TMS: 1.42 (9H, s); 2.33 (3H, s); 2.92 (2H, m); 4.42-4.55 (2H, m); 5.09 (2H, dd, *J* = 2.4, 13.5); 5.75 (1H, ddd, *J* = 5.7, 10.5, 15.9); 7.18-7.23 (3H, m); 7.28-7.33 (1H, m); 7.37 (1H, s); 7.54 (1H, d, *J* = 7.5); 7.72 (2H, d, *J* = 8.4); 7.95 (1H, d, *J* = 7.5) (TLNI-465_3-7)



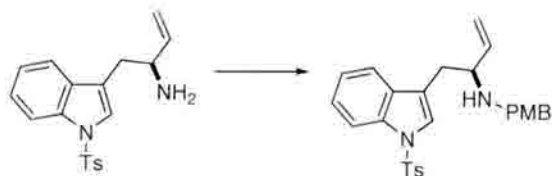
(S)-1-(1-tosyl-1*H*-indol-3-yl)but-3-en-2-amine (162)



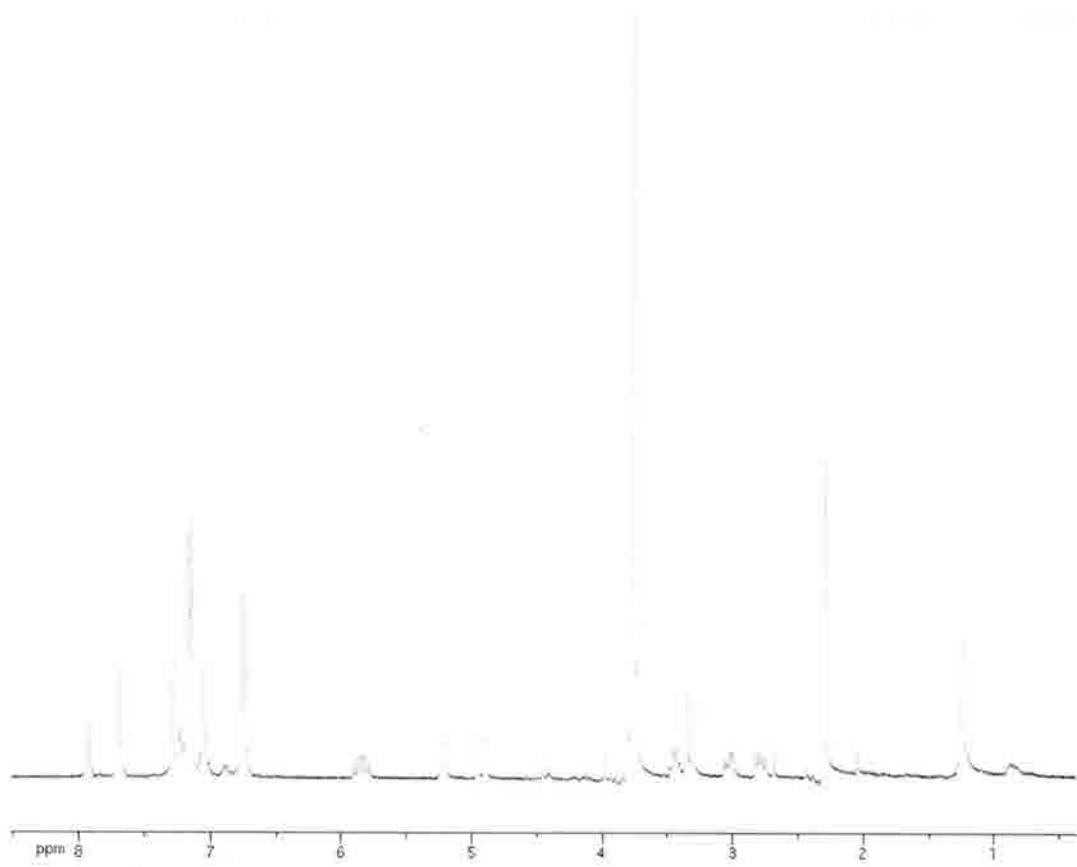
To a stirred solution of Boc carbamate **161** (0.045 g, 0.10 mmol) in DCM (2 mL) was added 2,6-lutidine (0.02 mL, 0.2 mmol). The mixture was cooled to -78° , and TBSOTf (0.05 mL, 0.2 mmol) was added dropwise. The reaction was warmed to room temperature over 3.5 h, followed by removal of the solvent under reduced pressure. The residue was dissolved in MeOH (2 mL) and $\text{KF}\cdot\text{H}_2\text{O}$ (0.04 g, 0.4 mmol) was added. After 1h of further stirring, the solvent was removed under reduced pressure and the residue dissolved in water (5 mL) and EtOAc (10 mL). A saturated aqueous solution of sodium bicarbonate was added until the pH reached ~ 8 . The aqueous layer was then extracted into EtOAc (3 x 20 mL). The combined organic layers were washed with brine, dried over sodium sulfate and concentrated to give **162** as a pale yellow oil (0.02g, 59%), with a small amount of residual t-butanol. ^1H NMR (300 MHz) (CDCl_3) δ TMS: 2.32 (3H, s); 2.73 (1H, dd, $J = 7.8, 14.4$); 2.87 (1H, dd, $J = 5.7, 14.4$); 3.67, 1H, q, $J = 6.6$); 5.08 (2H, ddt, $J = 1.2, 2.7, 10.2, 20.1$); 5.85 (1H, ddd, $J = 6.3, 10.2, 16.8$); 7.18-7.23 (3H, m); 7.29-7.34 (1H, m); 7.41 (1H, s); 7.75 (2H, d, $J = 8.4$); 7.98 (1H, d, $J = 8.4$) (TLNI-460)



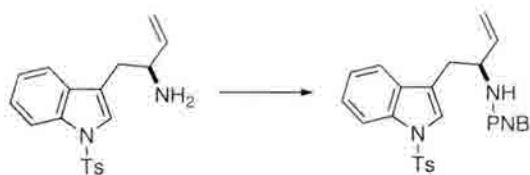
(S)-N-(4-methoxybenzyl)-1-(1-tosyl-1*H*-indol-3-yl)but-3-en-2-amine (163)



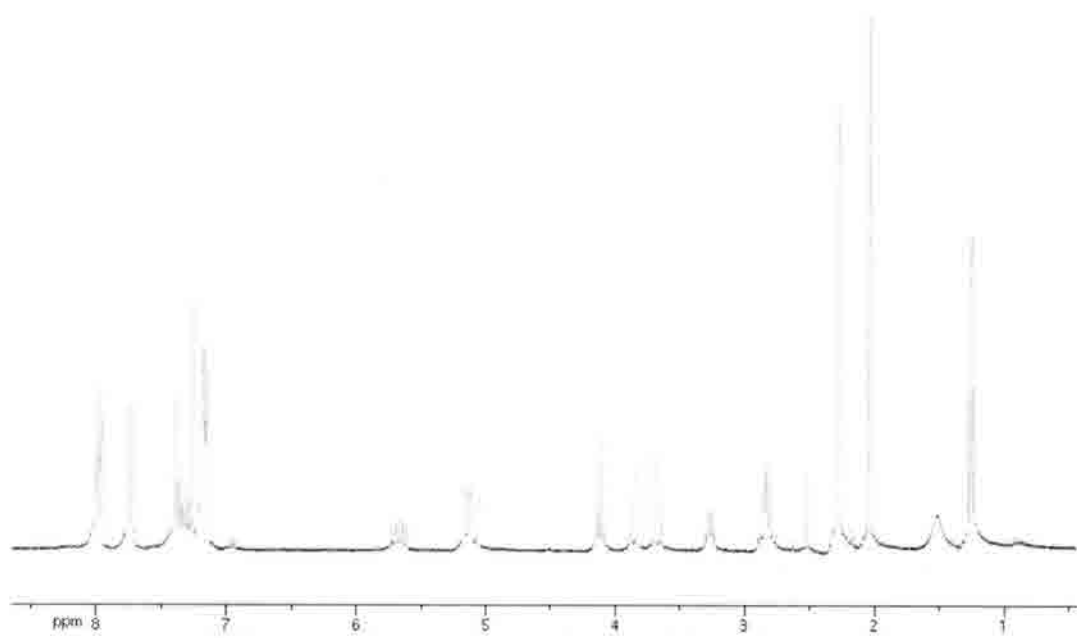
Amine **162** (0.02g, 0.06 mmol) was dissolved in DCM (1 mL) and cooled to 0°. Cesium carbonate (0.017g, 0.09 mmol) was added, followed by dropwise addition of freshly prepared PMBBBr (0.018g, 0.09 mmol) in DCM (1mL). The resultant suspension was stirred for 15 h, after which the solvent was evaporated under reduced pressure. The residue was dissolved in DCM (10 mL) and water (10 mL). The aqueous layer was extracted into DCM (3 x 5 mL), and the combined organic layers were washed with brine, dried over sodium sulfate and concentrated. The residue was purified by PTLC (9:1 hexanes/EtOAc) to give **163** as a light brown oil (0.012 g, 99%). ¹H NMR (300 MHz) (CDCl₃) δ TMS: 2.30 (3H, s); 2.80 (1H, dd, *J* = 7.5, 14.1); 3.04 (1H, dd, *J* = 6.9, 15.3); 3.35 (1H, d, *J* = 13.5); 3.42 (1H, q, *J* = 6.9); 3.77 (5H, s); 5.19 (2H, dd, *J* = 2.8, 17.1); 5.85 (ddd, *J* = 8.4, 10.2, 17.1); 6.76 (3H, d, *J* = 8.7); 7.04-7.06 (1H, m); 7.14-7.24 (5H, m); 7.30 (1H, s); 7.71 (2H, d, *J* = 8.4); 7.92 (1H, d, *J* = 8.7). (TLNI-462)



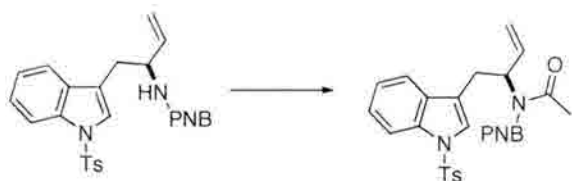
(S)-4-nitro-N-(1-(1-tosyl-1H-indol-3-yl)but-3-en-2-yl)benzamide (164)



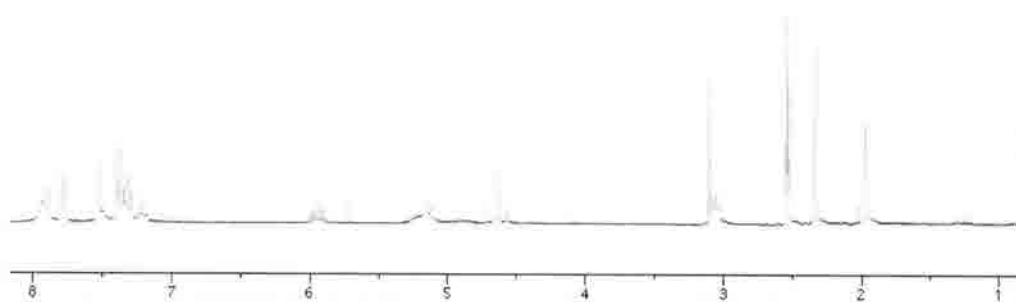
A stirred solution of amine **162** (0.04 g, 0.12 mmol) in DCM (2 mL) was cooled to 0°. Cesium carbonate (0.07 g, 0.21 mmol) was added. After ~5 minutes of stirring, PNBBBr (0.03 g, 0.14 mmol) was added. The mixture was slowly warmed to room temperature and stirred for 15 h. A saturated aqueous solution of ammonium chloride (5 mL) was then added, and the aqueous layer was extracted into DCM (3 x 10 mL). The combined organic layers were washed with brine, dried over sodium sulfate and concentrated. The residue was purified by column chromatography (7:3 hexanes/EtOAc) to give **164** as a brown oil (0.06 g, 65%). ¹H NMR (300 MHz) (CDCl₃) δ TMS: 2.28 (3H, s); 2.81-2.85 (2H, m); 3.28 (1H, q, *J* = 7.8); 3.70 (1H, d, *J* = 14.7); 3.88 (1H, d, *J* = 14.4); 5.16 (2H, dd, *J* = 1.8, 10.5); 5.67 (1H, ddd, *J* = 8.1, 10.2, 17.1); 7.15-7.18 (5H, m); 7.29-7.4 (3H, m); 7.72 (2H, d, *J* = 8.4); 7.96-8.00 (3H, m) (TLNII-33pp)



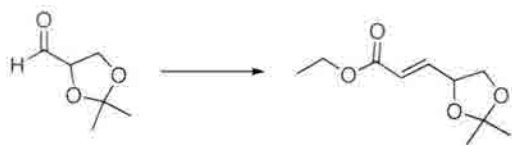
(S)-N-acetyl-4-nitro-N-(1-(1-tosyl-1H-indol-3-yl)but-3-en-2-yl)benzamide (168)



To a stirred solution of amine **164** (0.03 g, 0.06 mmol) in THF (2 mL) at 0° was added triethylamine (17 μ L, 0.12 mmol) followed by acetyl chloride (5 μ L, 0.072 mmol). The mixture was stirred for 2h, then washed with brine, dried over sodium sulfate and concentrated to give **168** as a yellow oil (0.02 g, 63%). ¹H NMR (300 MHz) (DMSO, 80°C) δ TMS: 1.97 (3H, s); 2.34 (3H, s); 3.08 (2H, m); 4.63 (2H, q, $J = 17.4$); 5.16 (1H, d, 10.2); 5.95 (1H, ddd, $J = 6.3, 10.2, 16.8$); 7.21 (1H, t, $J = 7.2$); 7.292-7.40 (6H, m); 7.53 (1H, s); 7.77 (2H, d, $J = 8.4$); 7.88-7.93 (3H, m). (TLNII-38.353K)



(E)-ethyl 3-(2,2-dimethyl-1,3-dioxolan-4-yl)acrylate (173)



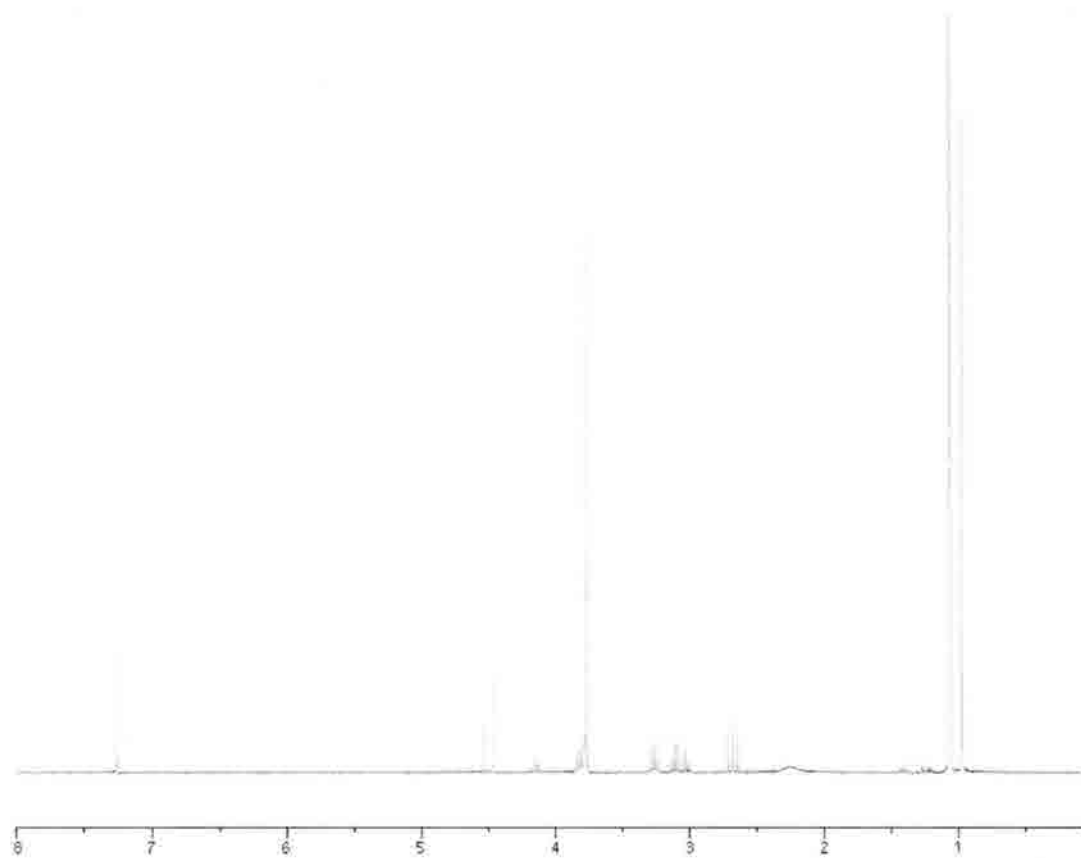
To a solution of ylide **172** (0.40g, 1.15 mmol) in THF (6 mL) was added aldehyde **154** (0.07g, 0.57 mmol). After 4h, TLC showed complete consumption of starting material. Water (10 mL) was added, and the aqueous layer was extracted into EtOAc (3 x 10 mL). The combined organic layers were washed with brine, dried over sodium sulfate and concentrated. The residue was purified by column chromatography (5% EtOAc in DCM) to give **173** as a clear oil (0.09 g, 79%).

(4*R*)-methyl 2-*tert*-butylthiazolidine-4-carboxylate (330)

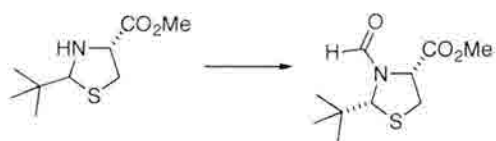


To a solution of D-cysteine (2.05 g, 13.0 mmol) in methanol (100 mL) was added sulfuric acid (10 drops). The mixture was heated to reflux for 16 h, after which the solvent was removed under reduced pressure to give the D-cysteine methyl ester.

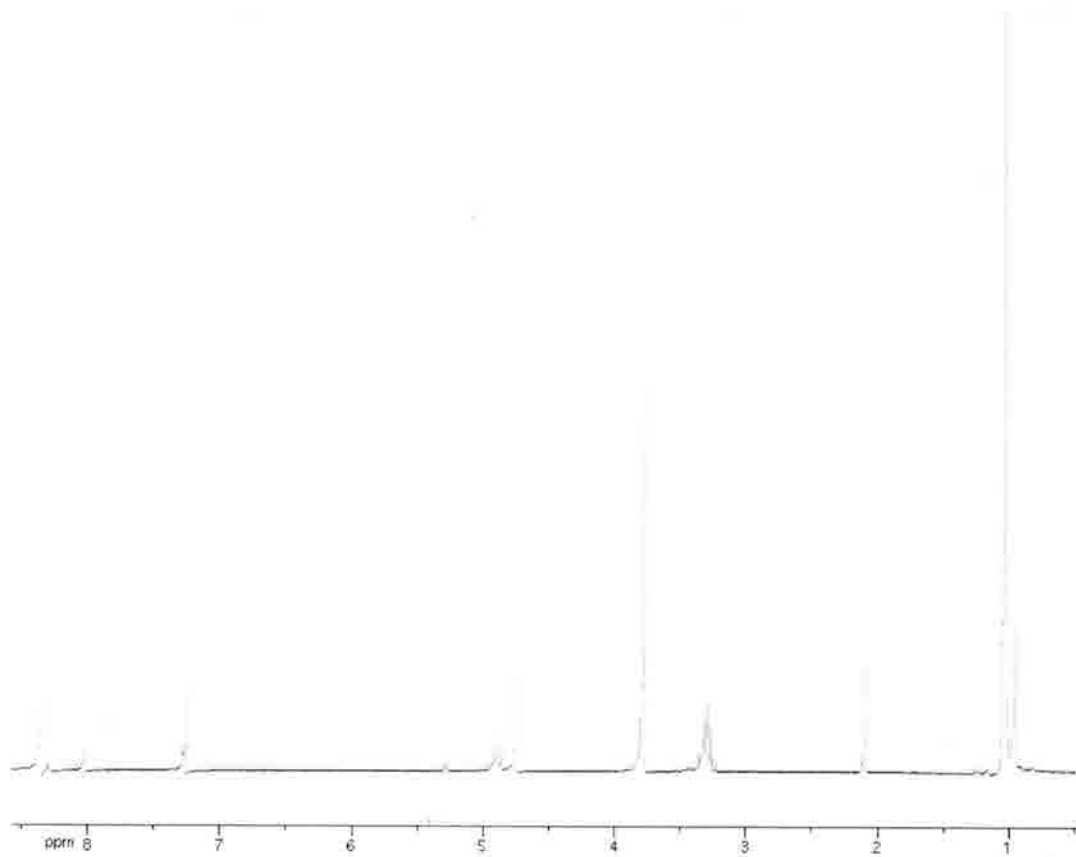
The methyl ester was then dissolved in pentane (140 mL). Pivaldehyde (1.7 mL, 15.4 mmol) was added, followed by the dropwise addition of triethylamine (2.13 mL, 15.4 mmol). The reaction flask was fitted with a Dean-Stark apparatus and a reflux condenser and heated to 60° for 24 h. The mixture was then cooled to room temperature and filtered through Celite. After washing with diethyl ether, the filtrate was concentrated to give 1.2 g (42%) of **330** as a mixture of diastereomers. ¹H NMR (300 MHz, CDCl₃) δ TMS: (major diastereomer) 1.07 (9H, s); 2.68 (1H, app. t, *J* = 9.9); 3.26 (1H, dd, *J* = 6.6, 10.2); 3.78 (3H, s); 3.82 (1H, dd, *J* = 6.9, 9.9); 4.47 (1H, s); (minor diastereomer) 0.98 (9H, s); 3.09 (2H, dq, *J* = 6.3, 10.5); 3.76 (3H, s); 4.15 (1H, t, *J* = 6.0); 4.53 (1H, s).



(2*R*,4*R*)-methyl 2-*tert*-butyl-3-formylthiazolidine-4-carboxylate (331)



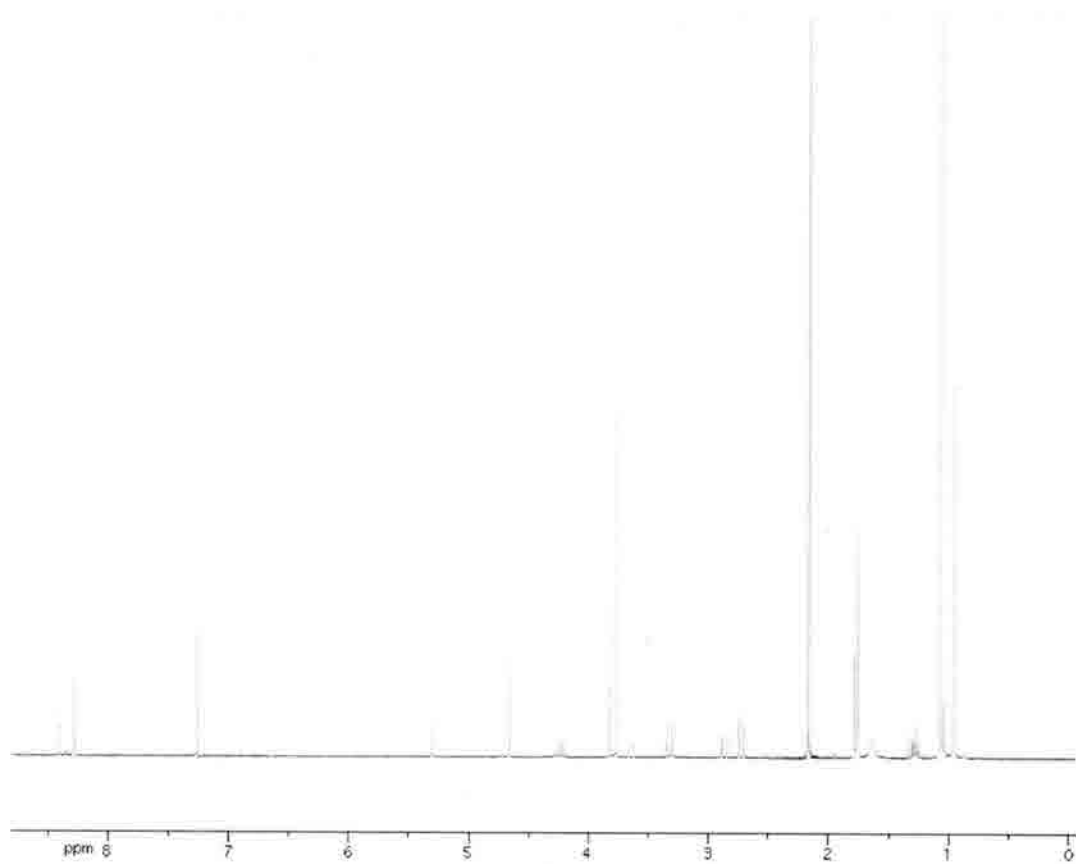
To a stirred solution of amine **330** (1.22 g, 6.00 mmol) in formic acid (9 mL) was added sodium formate (0.45 g, 6.6 mmol). This mixture was cooled to 0°, whereupon acetic anhydride (1.7 mL, 18 mmol) was added over 1 h *via* syringe pump. The mixture was allowed to come to room temperature over 15 h, after which the solvent was evaporated under reduced pressure. The residue was cooled to 0° and neutralized with a saturated aqueous solution of sodium bicarbonate. The resultant aqueous mixture was extracted into EtOAc (3 x 30 mL). The combined organic layers were washed with brine, dried over sodium sulfate and concentrated. The residue was further purified by recrystallization (EtOAc/hexanes) to give **331** as light purple crystals (1.09 g, 79%). ¹H NMR (300 MHz, CDCl₃) δ TMS: (major) 1.03 (9H, s); 3.23-3.36 (2H, m); 3.77 (3H, s); 4.74 (1H, s); 4.89 (1H, t, *J* = 8.7); 8.36 (1H, s).



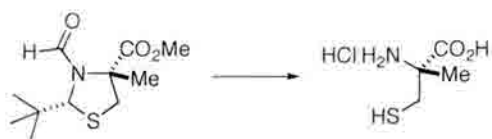
(2*R*,4*R*)-methyl 2-*tert*-butyl-3-formyl-4-methylthiazolidine-4-carboxylate (332**)**



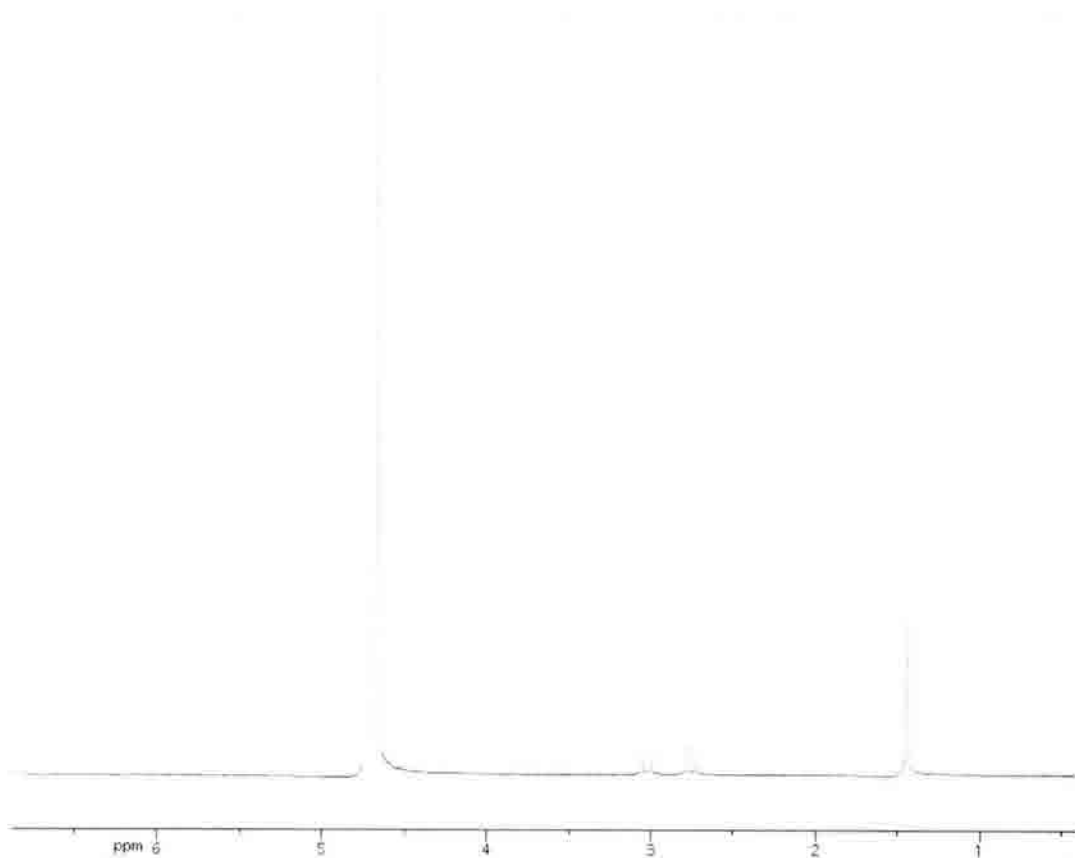
A stirred solution of diisopropylamine (0.99 mL, 7.07 mmol) in THF (20 mL) was cooled to -78° . Butyllithium (1.6 M in hexanes, 3.1 mL, 4.95 mmol) was then added dropwise. DMPU (3.2 mL, 26.4 mmol) was then added, and the resultant mixture was stirred at -78° for a further 1.5 h. The reaction was then cooled to -90° (liquid nitrogen/hexanes) and aldehyde **331** (1.09 g, 4.71 mmol) in THF (8 mL) was added dropwise over ~ 5 min. The mixture was stirred at -90° for 45 min, after which methyl iodide (0.35 mL, 5.65 mmol) was added dropwise. After a further 2 h, methanol (5 mL) was added, and the reaction was warmed to room temperature. Following removal of the solvent under reduced pressure, the residue was dissolved in a mixture of diethyl ether (30 mL) and brine (30 mL). The aqueous layer was extracted into ether (3 x 20 mL), and the combined organic layers were washed with brine, dried over sodium sulfate and concentrated. The resulting residue was further purified by column chromatography (10% EtOAc/hexanes) to give **332** as a light yellow oil (0.5 g, 46%). ^1H NMR (300 MHz, CDCl_3) δ TMS: (major) 1.06 (9H, s); 1.75 (3H, s); 2.70 (1H, d, $J = 11.7$); 3.30 (1H, d, $J = 11.7$); 3.77 (3H, s); 4.66 (1H, s); 8.28 (1H, s); (minor) 0.95 (9H, s); 1.78 (3H, s); 2.84 (1H, d, $J = 12.3$); 3.62 (1H, d, $J = 12.6$); 3.82 (3H, s); 5.30 (1H, s); 8.40 (1H, s).



(R)-2-amino-3-mercapto-2-methylpropanoic acid hydrochloride (333)



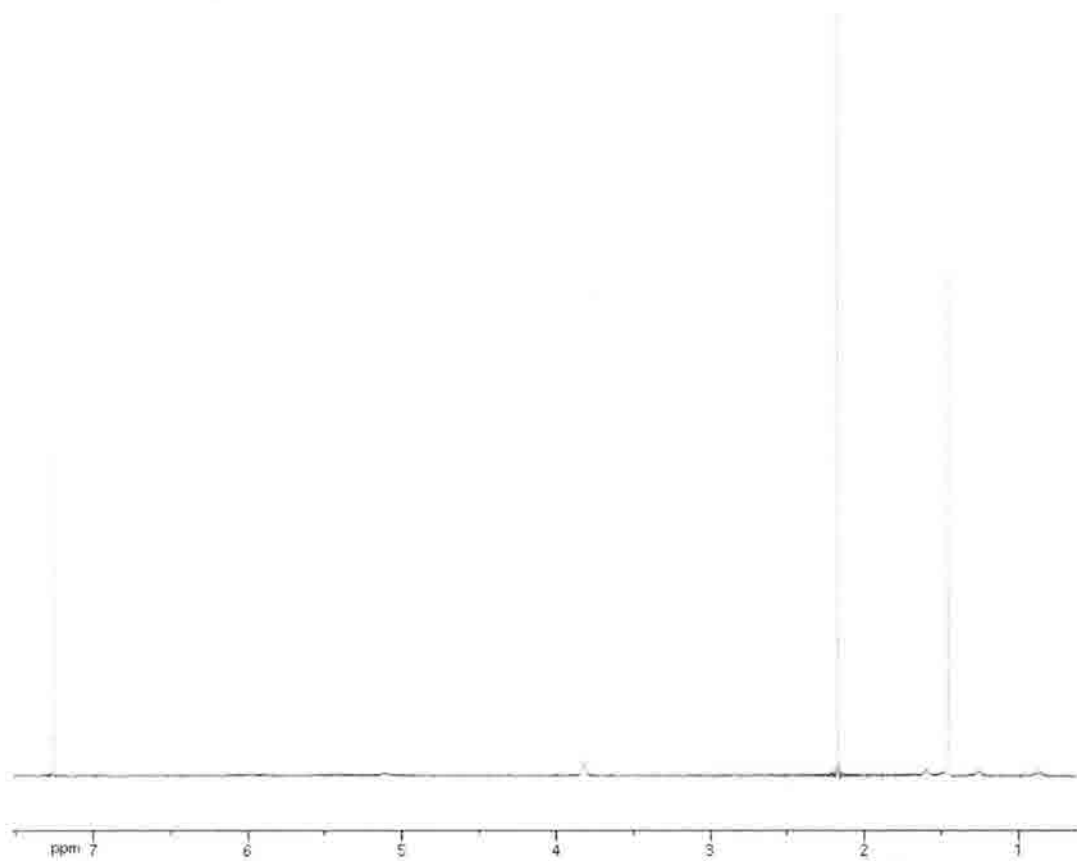
Aldehyde **332** (0.5 g, 2.16 mmol) was dissolved in 5N HCl (8 mL) and heated to reflux for a period of 20 h. The mixture was then cooled to room temperature and washed with EtOAc (3 x 5 mL). The aqueous layer was concentrated under reduced pressure to give **333** as a light brown, amorphous solid in quantitative yield (0.37 g). $\alpha_D = +8.4$ ($c = 1$ in H_2O). 1H NMR (300 MHz, D_2O) δ TMS: 1.44 (3H, s); 2.72 (1H, d, $J = 15$); 3.00 (1H, d, $J = 15$).



***tert*-butyl 2-amino-2-oxoethylcarbamate (335)**



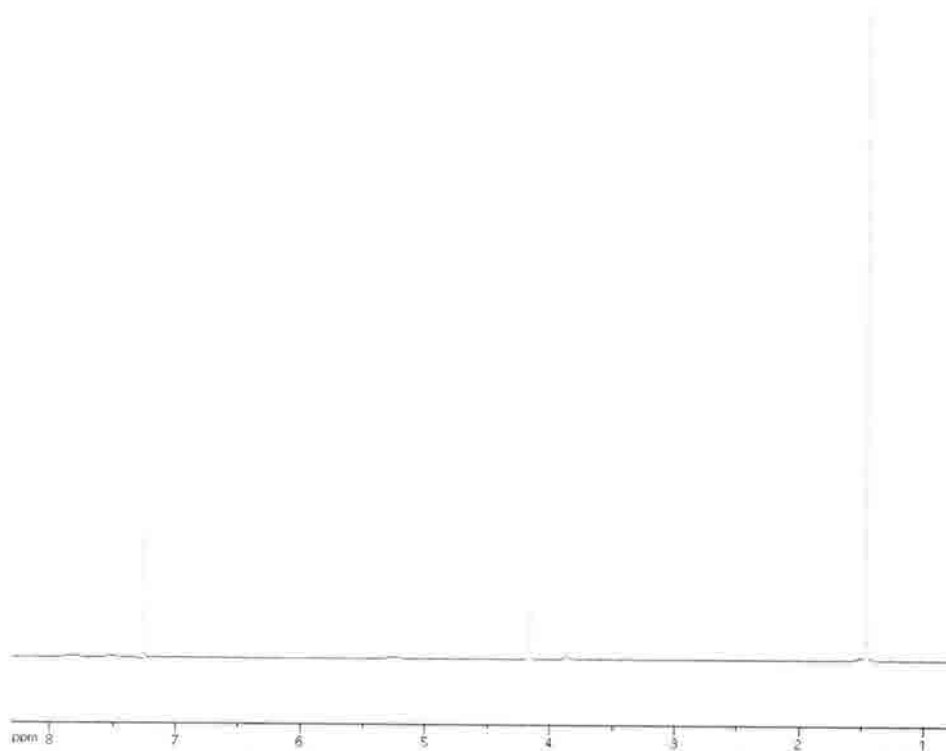
A stirred solution of glycine (20 g, 0.266 mol) in 1N NaOH (300 mL) was cooled to 0°. A solution of Boc₂O (69.8 g, 0.320 mol) in dioxane (200 mL) was added over ~1 h *via* addition funnel. The resulting mixture was stirred for a further 3.5 h and concentrated to ~1/2 the original volume. After cooling to 0°, KHSO₄ (1M) was added to pH 3. The aqueous layer was extracted into EtOAc, and the organic layers were dried over sodium sulfate and concentrated. The resulting *N*-Boc glycine (16.67 g, 0.222 mol) was then dissolved in THF (450 mL) and triethylamine (31 mL, 0.222 mol) was added. The mixture was cooled to -10°, and methylchloroformate (22 mL, 0.222 mol) was added dropwise over 30 min. The reaction was warmed to room temperature, and ammonium hydroxide (30% solution, 58 mL) was added. The mixture was stirred for 1 h more, after which the aqueous layer was extracted into EtOAc (2 x 100 mL). The combined organic layers were washed with brine, dried over sodium sulfate and concentrated to give **335** as a clear, viscous oil (34.4 g, 89%). ¹H NMR (300 MHz) (CDCl₃) δ TMS: 1.46 (9H, s); 3.81 (2H, d, *J* = 5.7) (TLNII-121a)



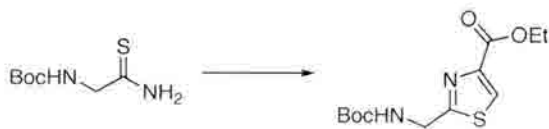
***tert*-butyl 2-amino-2-thioethylcarbamate (336)**



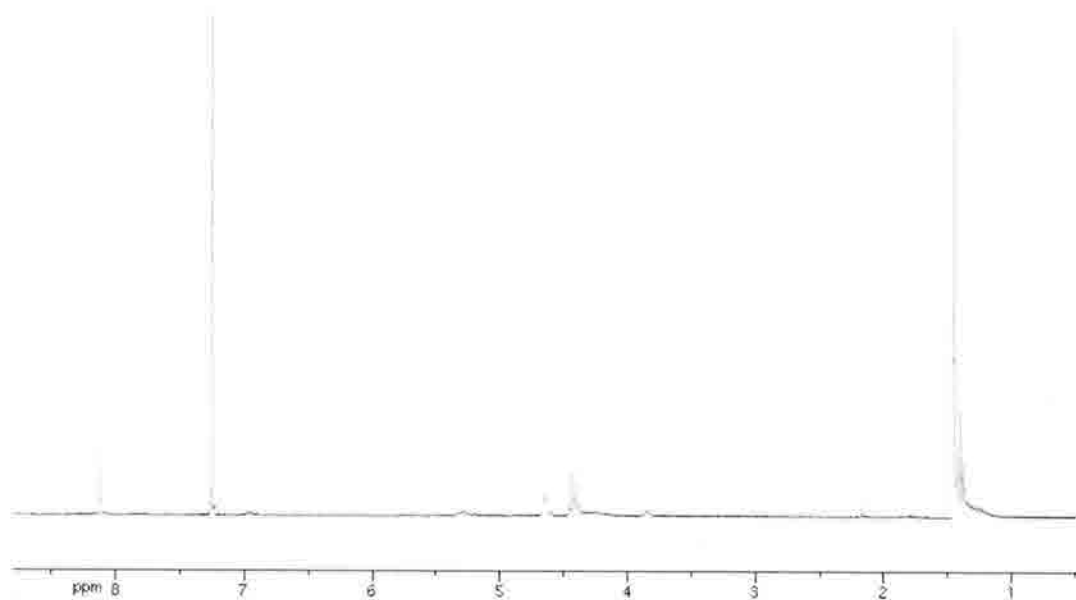
To a stirred solution of glycineamide **335** (6.67 g, 38.29 mmol) in DME (200 mL) was added Lawesson's reagent (7.74 g, 19.14 mmol). The mixture was stirred overnight, after which the solvent was removed under reduced pressure. The residue was dissolved in a mixture of 10% sodium bicarbonate (aq) and EtOAc. The aqueous layer was extracted into EtOAc (3 x 50 mL) and the combined organics were washed with brine, dried over sodium sulfate and concentrated to give **336** as a yellow, amorphous solid (5.7 g, 78%). ¹H NMR (300 MHz) (CDCl₃) δ TMS: 1.46 (9H, s); 4.16 (2H, s); 5.30 (1H, s). (TLNII-183)



ethyl 2-((*tert*-butoxycarbonylamino)methyl)thiazole-4-carboxylate (337)



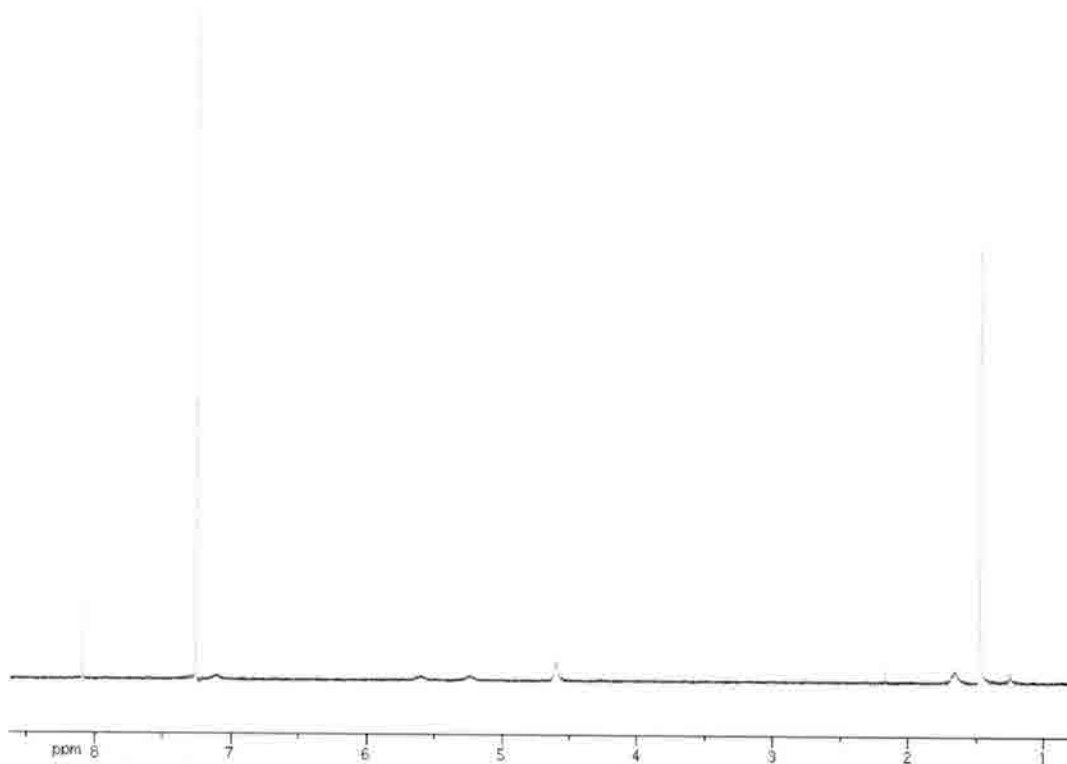
To a stirred solution of **336** (4.07 g, 21.39 mmol) in EtOH (61 mL) was added calcium carbonate (1.09 g, 10.91 mmol), followed by ethylbromopyruvate (2.96 mL, 23.53 mmol). The mixture was stirred overnight, then filtered through a pad of Celite, and concentrated. The resulting residue was dissolved in chloroform and washed first with a saturated aqueous solution of sodium bicarbonate (50 mL), then water (50 mL), then brine (50 mL), dried over magnesium sulfate and concentrated to give **337** (5.58 g, 91%).
¹H NMR (300 MHz) (CDCl₃) δ TMS: 1.40 (3H, t, *J* = 6.9); 1.46 (9H, s); 4.41 (2H, q, *J* = 6.9); 4.66 (2H, d, *J* = 5.7); 5.29 (1H, s); 8.12 (1H, s). (TLNII-185)



***tert*-butyl (4-carbamoylthiazol-2-yl)methylcarbamate (338)**



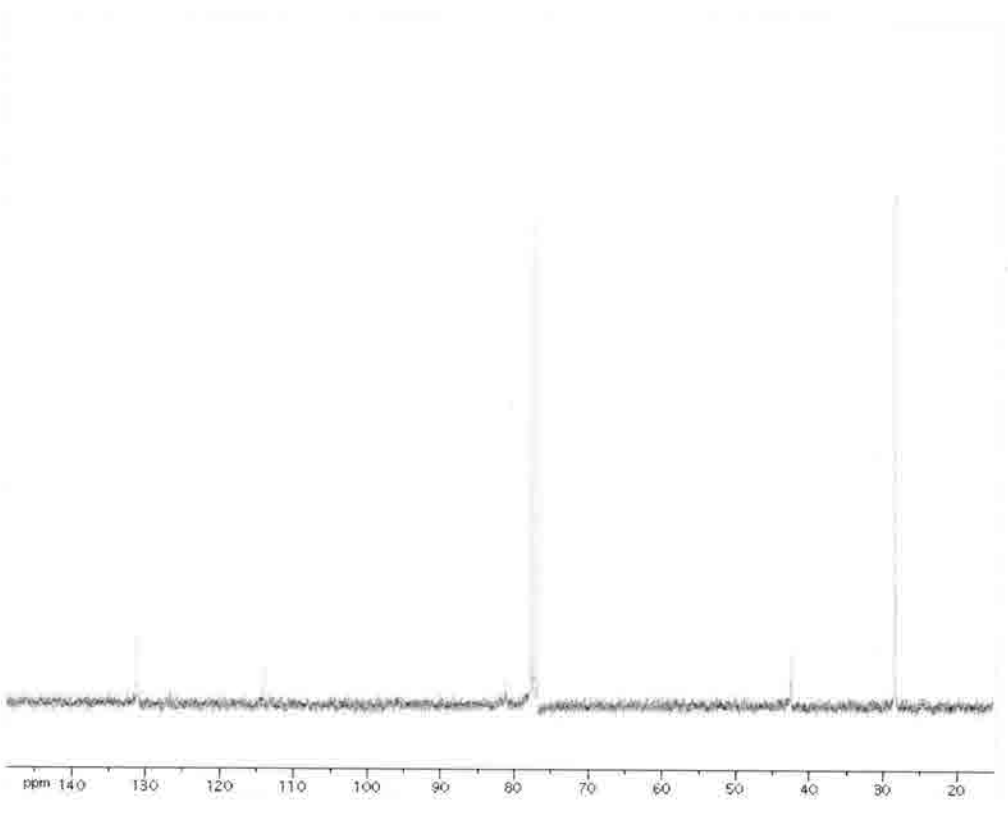
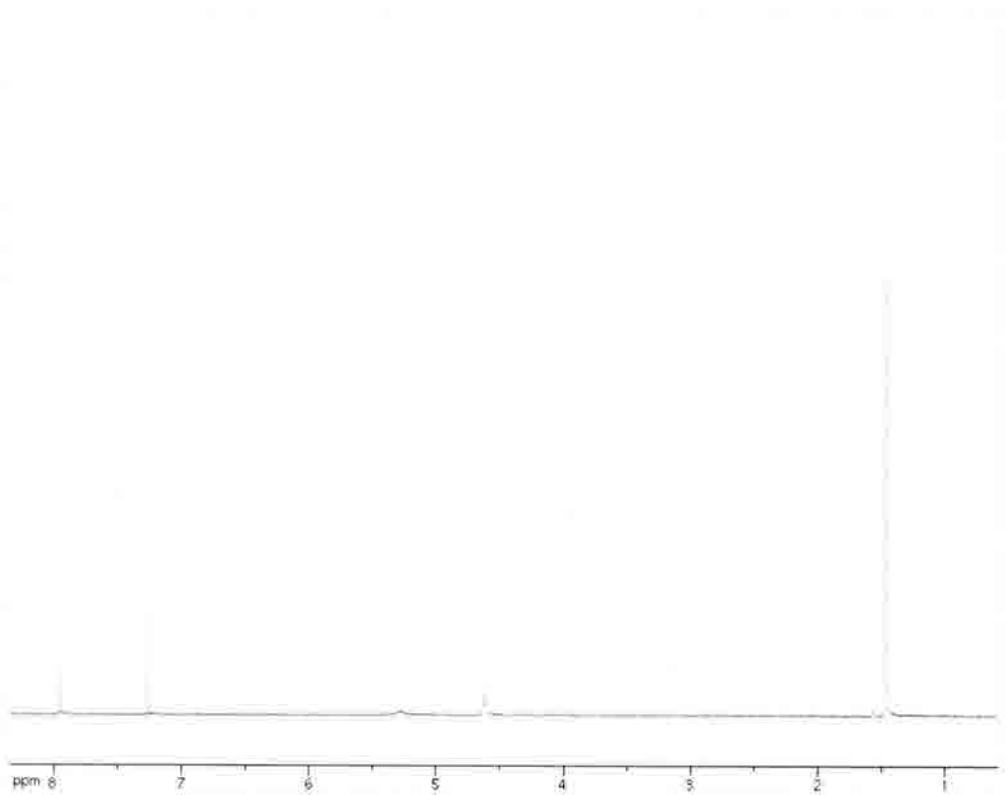
Ester **337** (5.58 g, 19.48 mmol) was stirred overnight in a mixture of 30% ammonium hydroxide (96 mL) and EtOH (70 mL). The solvent was evaporated to give **338** as a light brown powder (4.38 g, 87%). ^1H NMR (300 MHz) (CDCl_3) δ TMS: 1.47 (9H, s); 4.60 (2H, d, $J = 6.6$); 5.24 (1H, s); 5.60 (1H, s); 8.09 (1H, s). (TLNII-141pp)



***tert*-butyl (4-cyanothiazol-2-yl)methylcarbamate (293)**

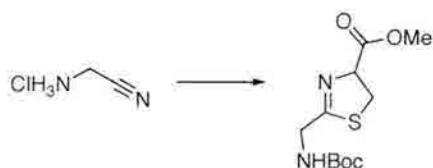


To a mixture of amide **338** (0.97 g, 3.77 mmol) in chloroform (30 mL) was added triethylamine (7.9 mL, 56.6 mmol). The reaction was cooled to -10° , after which phosphorous oxychloride (0.88 mL, 9.43 mmol) was added dropwise. The reaction was allowed to come to room temperature and stirred for a further 60 min. The solvent was removed under reduced pressure. The resulting residue was re-dissolved in DCM (20 mL) and washed with a saturated aqueous solution of sodium bicarbonate (30 mL), followed by brine (20 mL). The organic layer was dried over sodium sulfate and concentrated. The resultant black residue was further purified by column chromatography (2:1 hexanes/EtOAc) to give nitrile **293** as a white solid (0.81 g, 90%).
 ^1H NMR (300 MHz) (CDCl_3) δ TMS: 1.47 (9H, s); 4.61 (2H, d, $J = 6.0$); 5.29 (1H, s); 7.95 (1H, s).

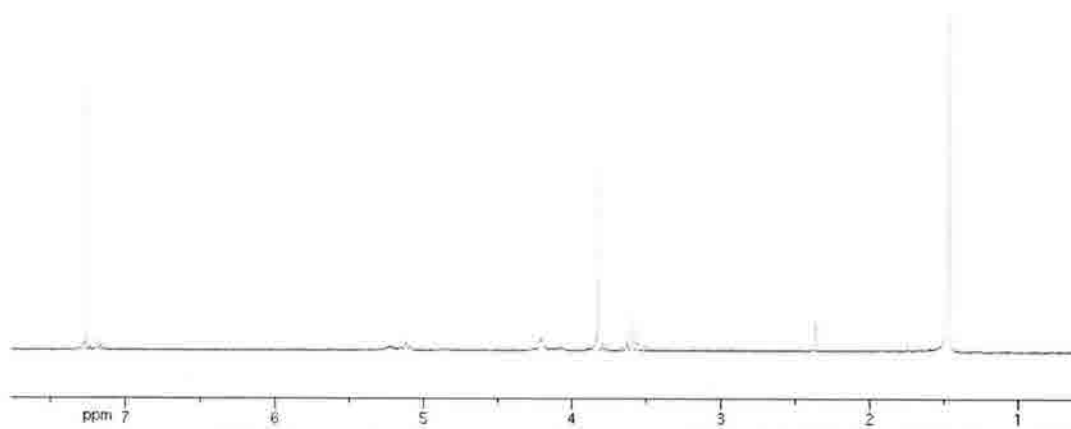


methyl 2-((*tert*-butoxycarbonylamino)methyl)-4,5-dihydrothiazole-4-carboxylate

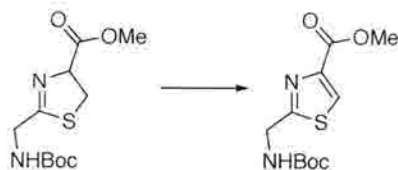
(340)



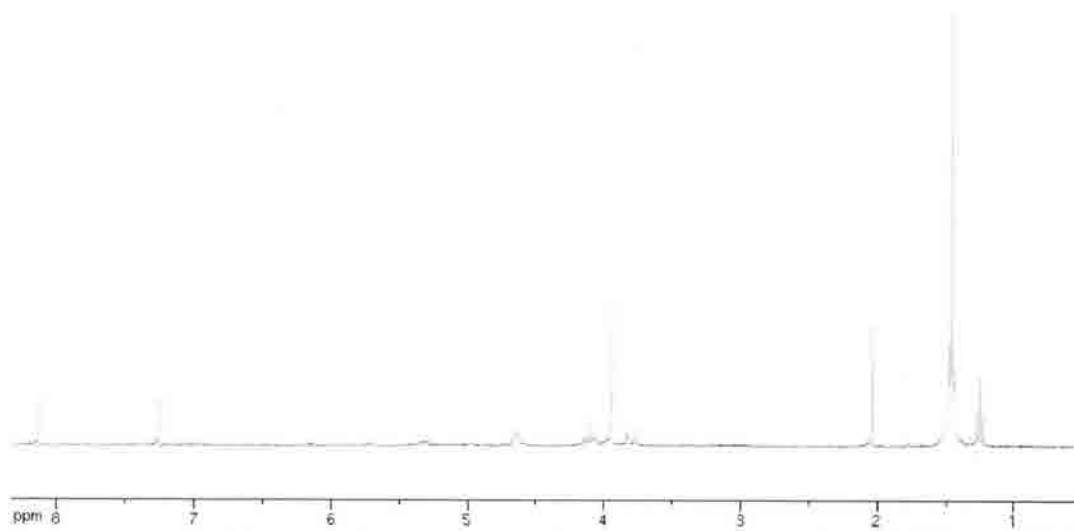
A solution of aminoacetonitrile (5g, 54.04 mmol) and Boc_2O (11.79 g, 54.04 mmol) in DCM (250 mL) was cooled to 0° . Triethylamine (15 mL, 108.1 mmol) was added dropwise. The mixture was allowed to come to room temperature and stirred for 15 h. The solvent was then removed under reduced pressure. The resulting residue was redissolved in diethyl ether (50 mL) and washed with water (2 x 50 mL), then brine. The ether layer was dried over sodium sulfate and concentrated to give 7.17 g of the *N*-Boc protected nitrile, 4.3 grams of which (27.53 mmol) was then dissolved in methanol (250 mL). L-Cysteine methyl ester hydrochloride (5.2 g, 30.29 mmol) was then added, followed by dropwise addition of triethylamine (4.9 mL, 35.79 mmol). The mixture was heated to 70° for 2.5 h, then cooled to room temperature. The solvent was concentrated to $\sim 1/2$ its original volume, and toluene (100 mL) was added. The organic layer was washed with water (2 x 100 mL), then brine, then dried over sodium sulfate and concentrated. The residue was left under high vacuum for 12 h to give **340** as a dark purple solid (4.03 g, 53%). ^1H NMR (300 MHz) (CDCl_3) δ TMS: 1.47 (9H, s); 3.60 (2H, app. t, $J = 9.0$); 3.83 (3H, s); 4.22 (2H, d, $J = 5.4$); 5.12 (1H, t, $J = 10.8$); 5.23 (1H, s). (TLNII-450)



methyl 2-((*tert*-butoxycarbonylamino)methyl)thiazole-4-carboxylate (341**)**



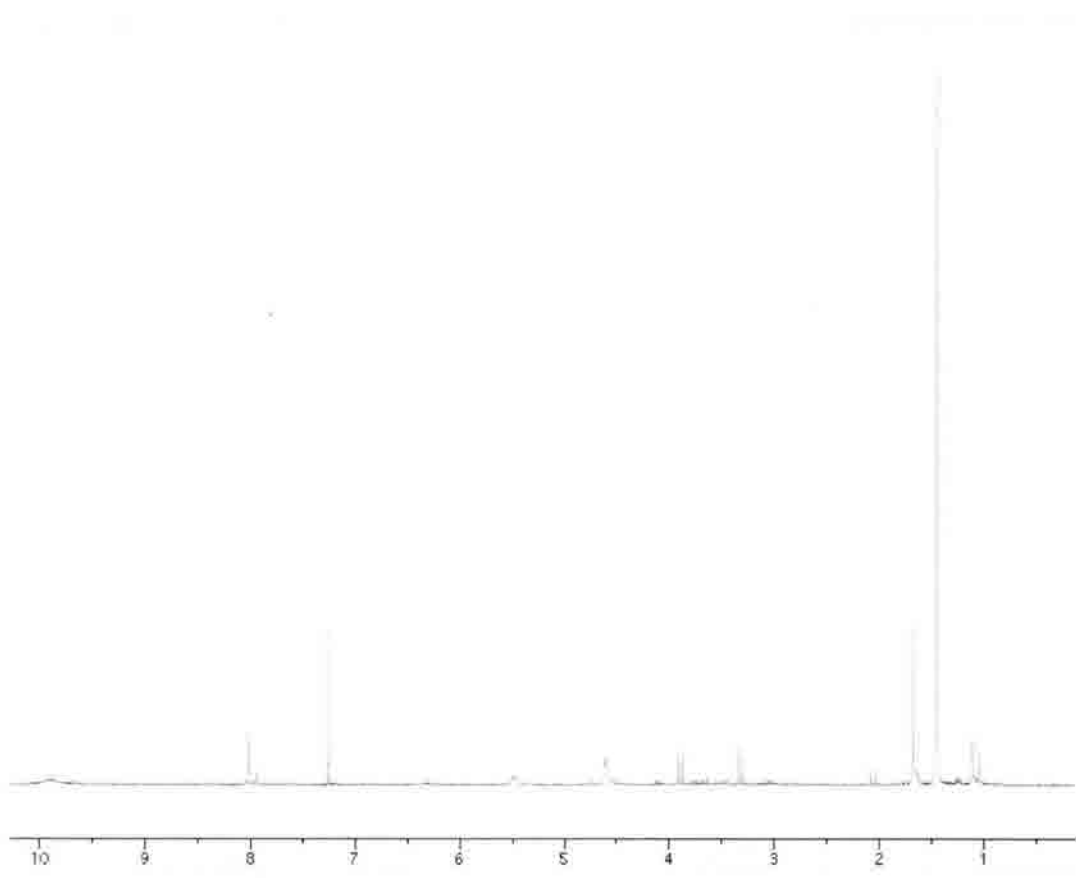
To a stirred solution of **340** (4.03 g, 14.69 mmol) in DCM (23 mL) was added DBU (2.2 mL, 14.69 mmol). The reaction was cooled to 0°, and bromotrichloromethane (1.4 mL, 14.69 mmol) was added dropwise. The mixture was stirred at 0° for 3 h, then warmed to room temperature and stirred for a further 15 h. 1N KHSO₄ (30 mL) was then added, and the aqueous layer extracted into EtOAc (3 x 50 mL). The combined organic layers were washed with brine, dried over sodium sulfate and concentrated to give **341**. ¹H NMR (300 MHz) (CDCl₃) δ TMS: 1.45 (9H, s); 3.94 (3H, s); 4.65 (2H, d, *J* = 6.3); 8.13 (1H, s). (TLNII-437)



(S)-2-(2-((tert-butoxycarbonylamino)methyl)thiazol-4-yl)-4-methyl-4,5-dihydrothiazole-4-carboxylic acid (328)



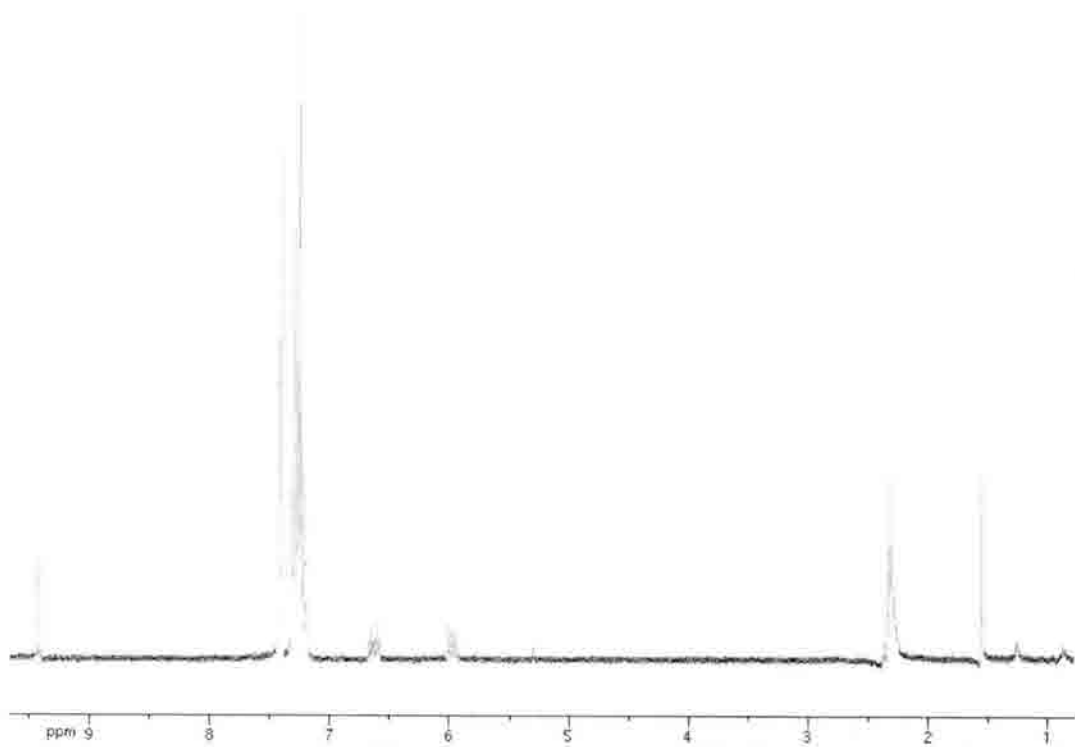
To a mixture of methanol (25 mL) and pH 7 phosphate buffer (21 mL) was added sodium bicarbonate (0.88 g, 10.52 mmol). α -methyl-D-cysteine hydrochloride (**333**) (1.05 g, 6.12 mmol) in methanol (3.5 mL) and nitrile **293** (1.26 g, 5.26 mmol) in methanol (3.5 mL) were added. The reaction was heated to 70° for 24 h, after which it was cooled to room temperature, and extracted into ether (3 x 30 mL). These organic layers were discarded, and the aqueous layer was acidified to pH 2 with dropwise addition of 3N HCl. The aqueous layer was then extracted into EtOAc. The combined organic layers were washed with brine, dried over sodium sulfate and concentrated to give **328** as a light brown oil (1.3 g, 70%) [α]_D = + 22, c = 1 in methanol. ¹H NMR (300 MHz) (CDCl₃) δ TMS: 1.45 (9H, s); 1.68 (3H, s); 3.30 (1H, d, J = 11.07); 3.90 (1H, d, J = 11.4); 4.62 (2H, d, J = 6.0); 4.89 (1H, s); 8.02 (1H, s); 9.91 (1H, s). (TLNII-146a)



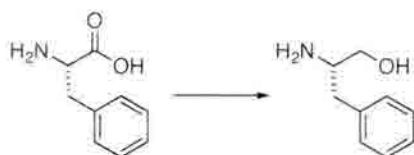
(E)-5-(tritylthio)pent-2-enal (235)



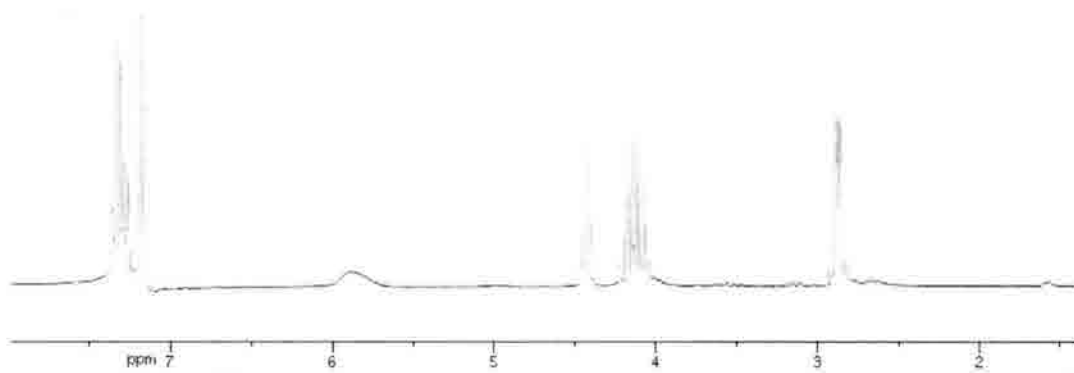
To a stirred solution of triphenylmethane thiol (4.0 g, 14.47 mmol) in DCM (120 mL) was added triethylamine (2.8 mL, 20.26 mmol) followed by acrolein (1.35 mL, 20.26 mmol). The solution was stirred for 1 h, after which the solvent was evaporated to give a white solid. To this solid was added benzene (120 mL) followed by (triphenylphosphoranylidene) acetaldehyde (5.28 g, 17.36 mmol). The mixture was heated to reflux for 20 h, after which the solvent was evaporated. The residue was purified by column chromatography (1:3 EtOAc/hexanes) to remove a highly polar byproduct. The less polar products were then adsorbed onto silica and purified again by column chromatography (10% Et₂O/hexanes) to give **235** as a light brown solid (3.6 g, 70%). ¹H NMR (300 MHz) (CDCl₃) δ TMS: 2.29-2.34 (4H, m); 5.99 (1H, dd, *J* = 8.1, 15.6); 6.64 (1H, dt, *J* = 6.3, 15.9); 7.20-7.25 (5H, m); 7.27-7.32 (5H, m); 7.42 (5H, d, *J* = 8.1); 9.44 (1H, d, *J* = 8.1). (TLNII-75bpp)



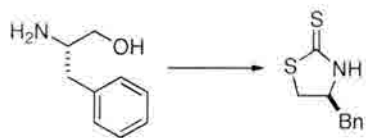
(S)-2-amino-3-phenylpropan-1-ol



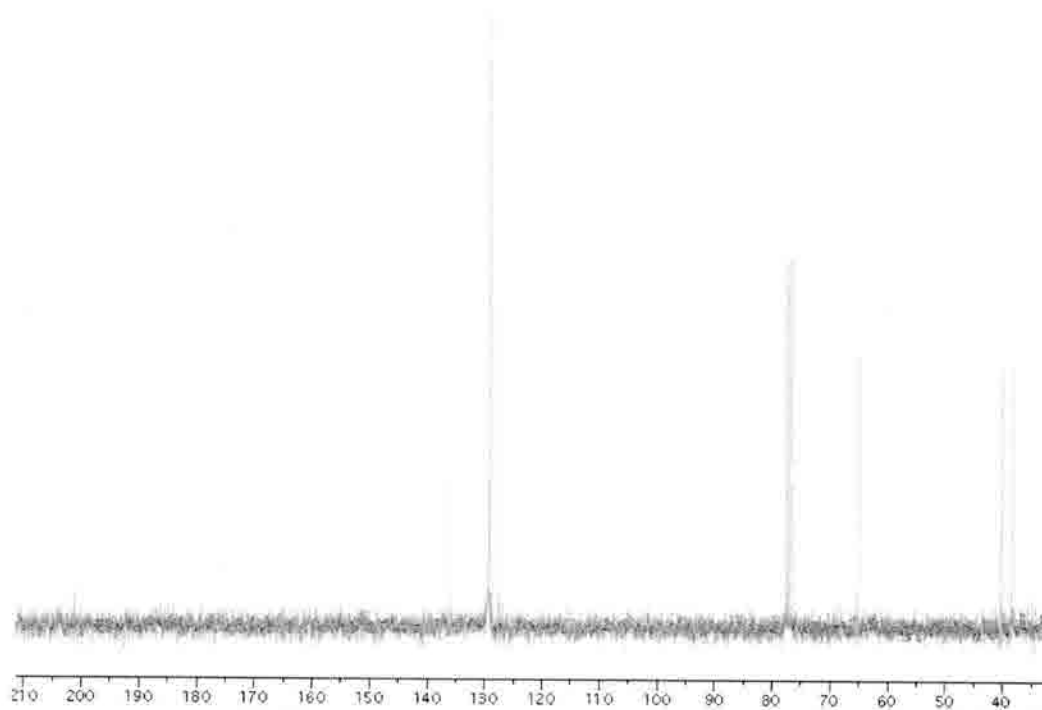
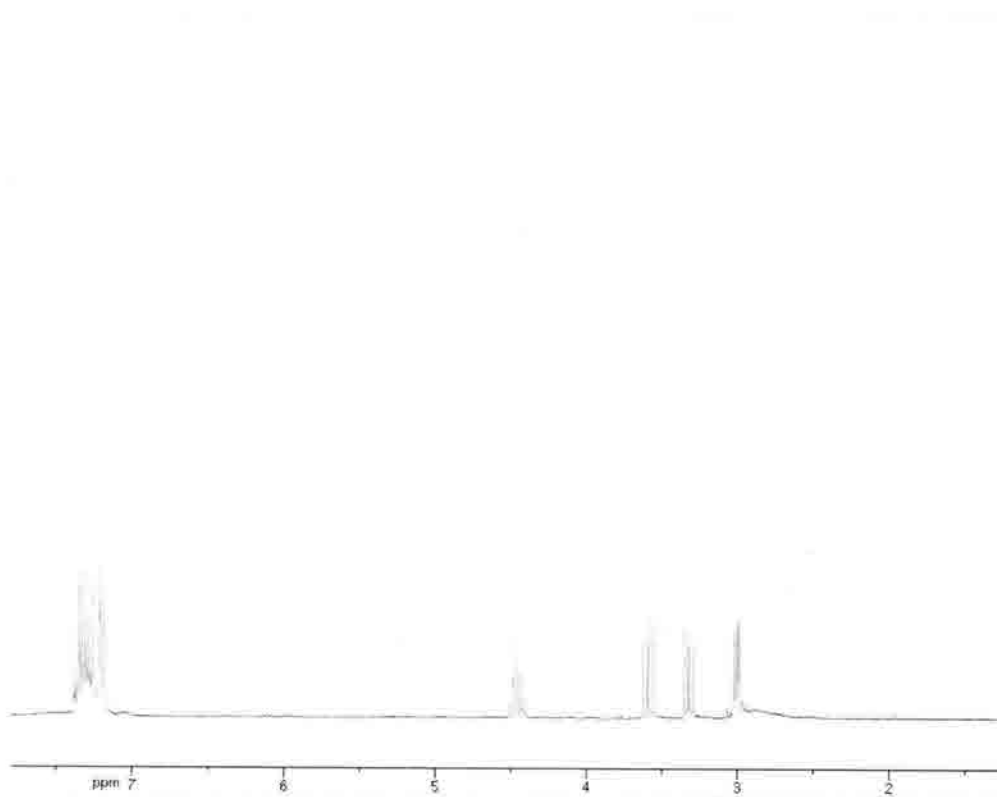
To a suspension of sodium borohydride (11.18 g, 0.296 mol) in THF (120 mL) was added L-phenylalanine (20 g, 0.118 mol). The mixture was cooled to 0° and a solution of concentrated sulfuric acid (7.8 mL) in diethyl ether (23 mL) was added dropwise *via* addition funnel over a period of 3 h, maintaining the internal temperature at less than 15°. Following addition of this solution, the reaction was stirred at room temperature overnight. Methanol (18 mL) was then slowly added, and the mixture stirred for 30 more minutes, after which the solvent was concentrated to ~1/2 its original volume. 5M NaOH (120 mL) was then added. The resultant mixture was heated, and everything which distilled at $\leq 60^\circ$ was discarded, after which the reaction was heated to reflux for 3 h. After cooling to room temperature, the mixture was filtered through a thick pad of Celite. The filtrate was extracted into EtOAc (3 x 100 mL). The combined organic layers were washed with brine, dried over sodium sulfate and concentrated to give L-phenylalanol as a white solid (14.88 g, 83%). $^1\text{H NMR}$ (300 MHz) (CDCl_3) δ TMS: 2.87 (2H, dd, $J = 3.0, 6.6$); 4.04-4.20 (2H, m); 4.23 (1H, t, $J = 7.8$); 5.88 (2H, s); 7.17 (2H, d, $J = 7.8$); 7.24-7.36 (3H, m). (TLNII-76).



(S)-4-benzylthiazolidine-2-thione



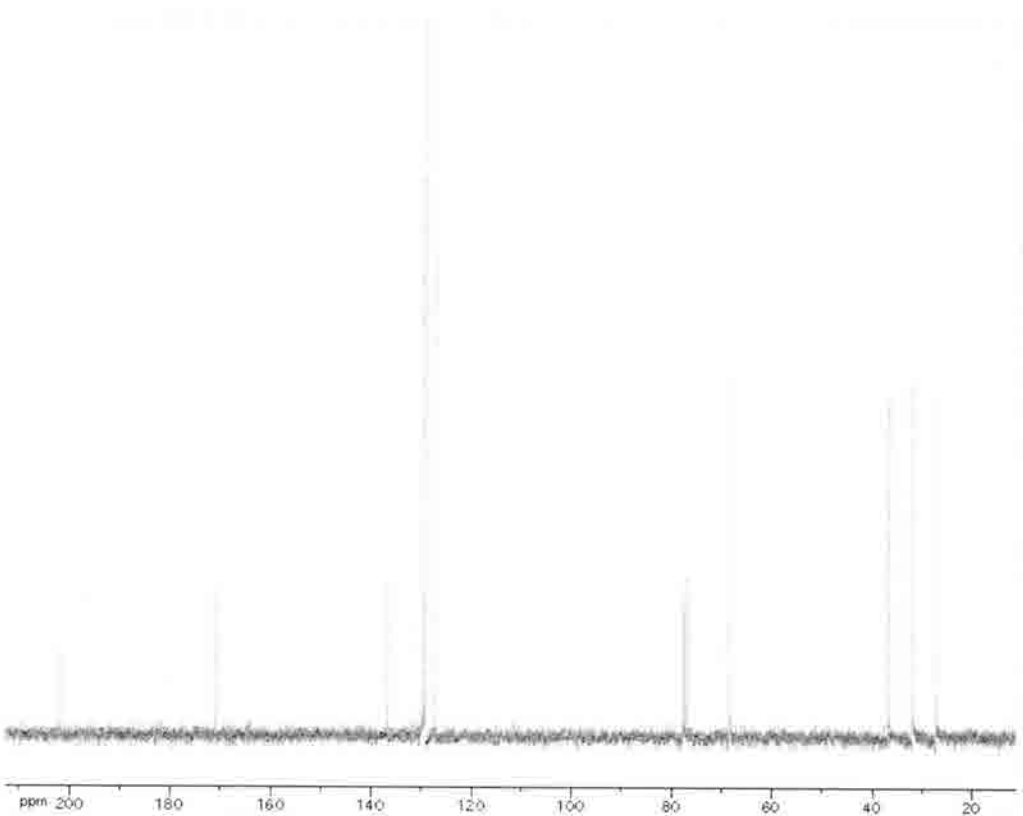
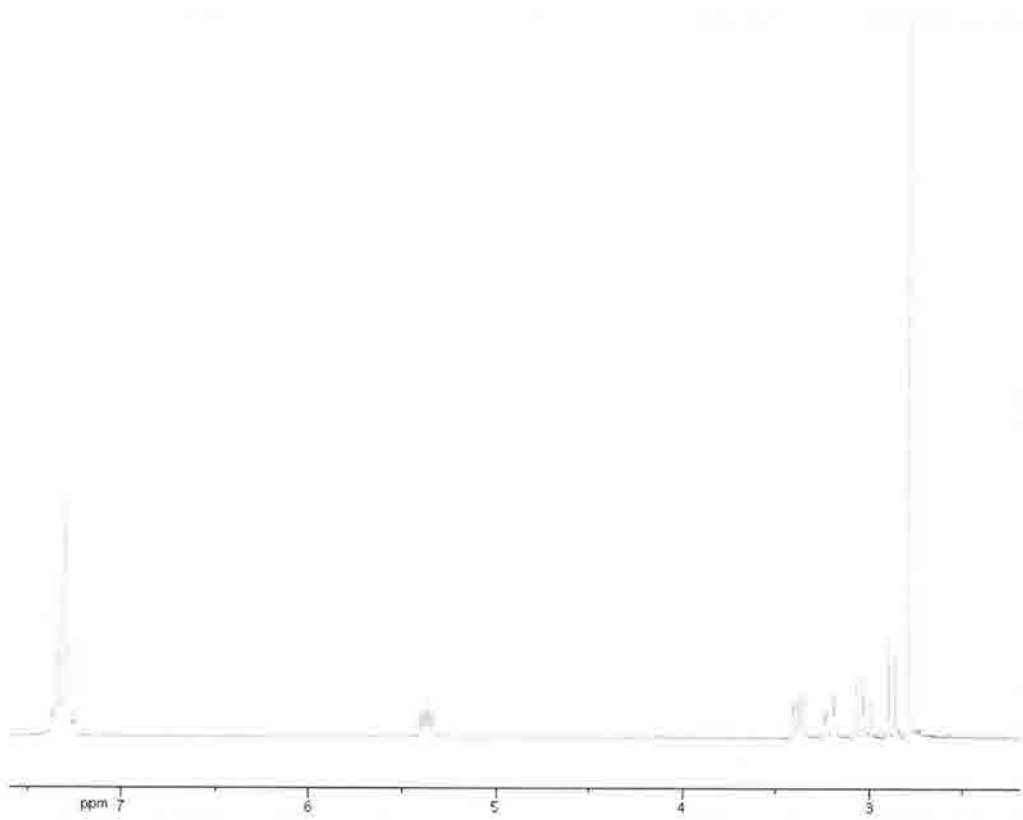
To a solution of L-phenylalaninol (7.2 g, 47.62 mmol) in 1M KOH (217 mL) was added carbon disulfide (14.4 mL, 238.1 mmol). The mixture was stirred for 1 h at room temperature, after which the flask was fitted with a reflux condenser and the reaction was heated to 110° for 15 h. After cooling to room temperature, the aqueous mixture was extracted into DCM (3 x 100 mL). The combined organic layers were washed with brine, dried over sodium sulfate and concentrated. The residue was purified by column chromatography (10% EtOAc/hexanes) to give the desired chiral auxiliary as a white solid (6.73g, 68%). ¹H NMR (300 MHz) (CDCl₃) δ TMS: 3.01 (2H, dd, *J* = 3.9, 10.8); 3.33 (1H, dd, *J* = 6.9, 11.4); 3.60 (1H, dd, *J* = 7.8, 11.4); 4.58 (1H, m); 7.19-7.22 (2H, m); 7.29-7.39 (3H, m). (TLNII-461). ¹³C NMR (170 MHz) (CDCl₃) δ TMS: 38.52, 40.34, 65.30, 127.75, 129.25, 129.44, 136.09, 201.25. (TLNII-461_c13)



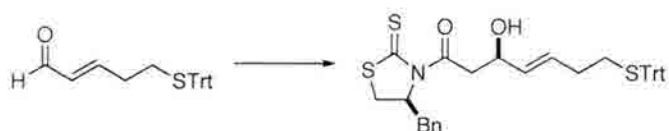
(S)-1-(4-benzyl-2-thioxothiazolidin-3-yl)ethanone (343)



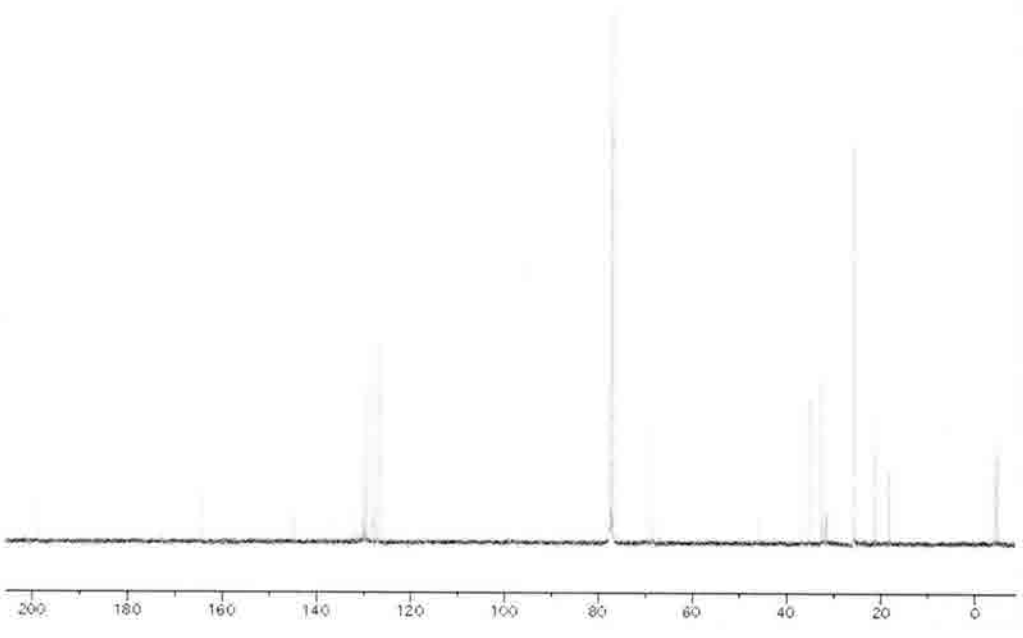
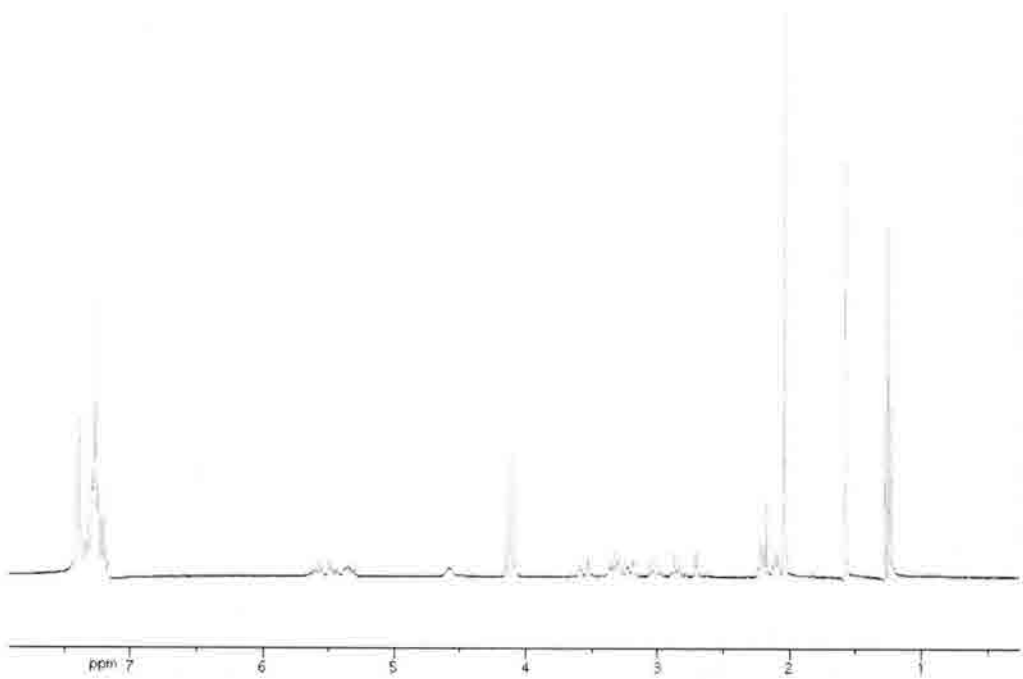
To a solution of thiazolidinone thione (above) (6.62 g, 31.62 mmol) in DCM (160 mL) was added pyridine (3.8 mL, 47.43 mmol). The reaction was cooled to 0°, after which acetyl chloride (2.7 mL, 37.95 mmol) was added dropwise. The mixture was stirred at room temperature for 2 h, after which it was washed with brine (100 mL), dried over sodium sulfate, and concentrated under reduced pressure. The residue was purified by column chromatography (10% EtOAc/hexanes) and recrystallized (EtOAc/hexanes) to give **343** as bright yellow crystals. (5.9 g, 75%). ¹H NMR (300 MHz) (CDCl₃) δ TMS: 2.79 (3H, s); 2.88 (1H, d, *J* = 11.7); 3.03 (1H, dd, *J* = 10.5, 12.9); 3.23 (1H, dd, *J* = 3.9, 13.2); 3.38 (1H, dd, *J* = 7.2, 11.7); 5.37 (1H, dddd, *J* = 3.9, 7.2, 10.8); 7.28-7.37 (5H, m). (TLNII-462). ¹³C NMR (170 MHz) (CDCl₃) δ TMS: 27.36, 32.07, 38.90, 68.46, 127.47, 129.16, 129.71, 136.74, 170.94, 201.80. (TLNII-462_c13)



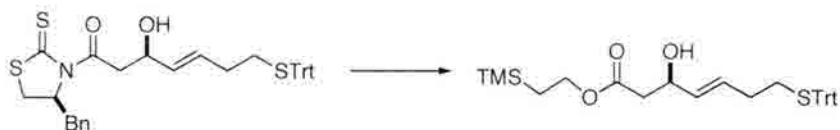
(*R,E*)-1-((*S*)-4-benzyl-2-thioxothiazolidin-3-yl)-3-hydroxy-7-(tritylthio)hept-4-en-1-one (*ent*-290a)



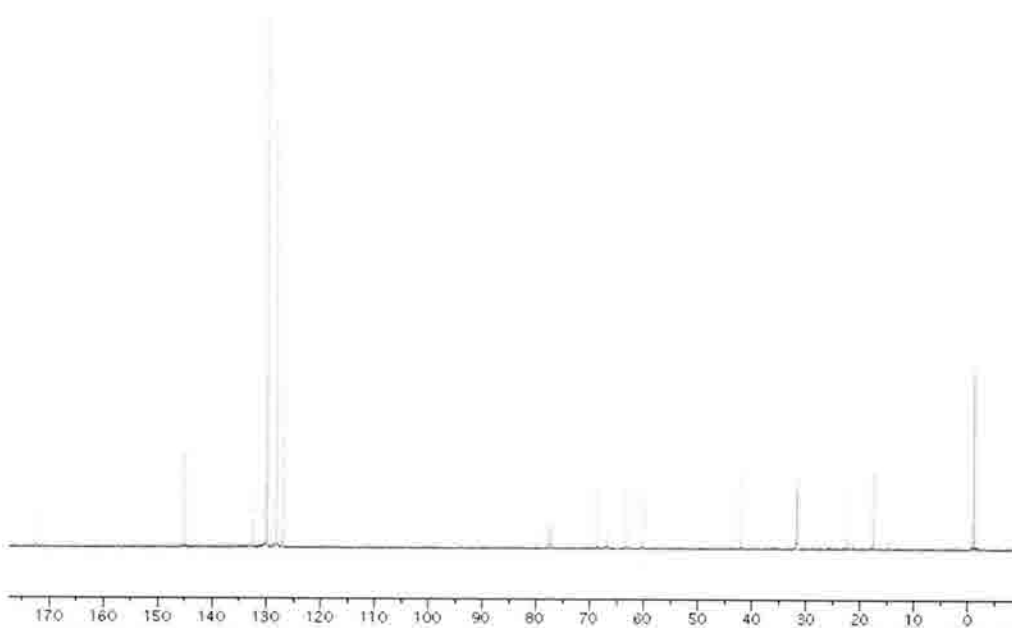
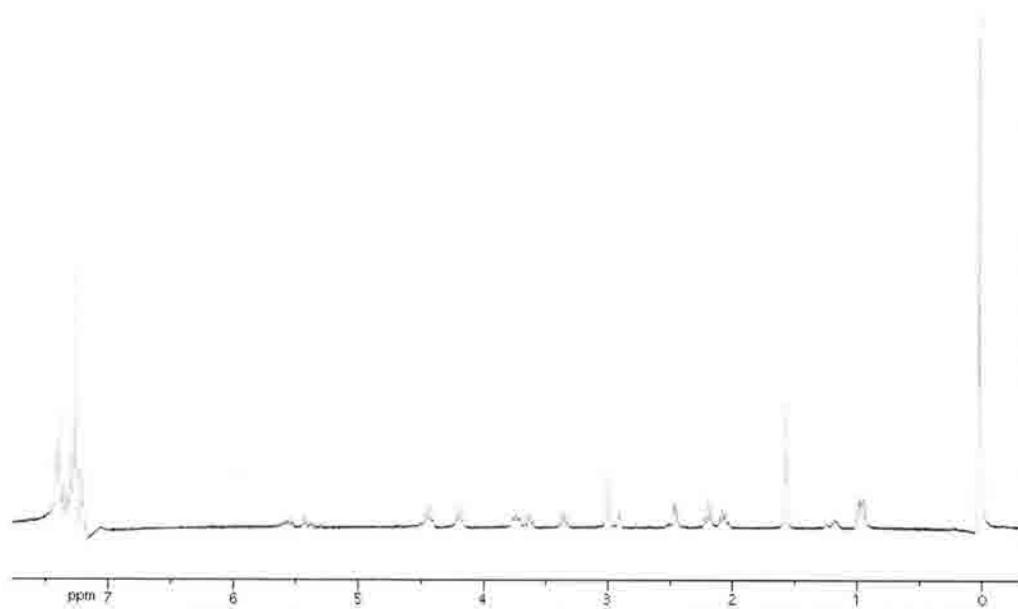
Thiazolium thione (0.5 g, 1.99 mmol) was dissolved in dichloromethane (15 mL) and cooled to 0°. Titanium tetrachloride (0.23 mL, 2.16 mmol) was added dropwise. After stirring for ~5 min, the mixture was cooled to -78°, and diisopropylethylamine (0.38 mL, 2.16 mmol) was added dropwise. After stirring for a further 2 h, (*E*)-5-(tritylthio)pent-2-enal¹ (0.59 g, 1.66 mmol) in dichloromethane (5 mL) was added dropwise, and the mixture was stirred for 1 h. A saturated aqueous solution of ammonium chloride (15 mL) was added, and the mixture warmed to room temperature. The biphasic mixture was extracted into dichloromethane (3 x 20 mL), washed with brine and dried over sodium sulfate. The solvent was evaporated and the residue purified by column chromatography (10:1 to 4:1 hexanes/ethyl acetate) to give ***ent*-290a** as a yellow oil (0.88 g, 87%). $[\alpha]_D^{24}$: +40.4, $c=5$ CHCl₃ ¹H NMR (300 MHz, CDCl₃) δ TM: 2.20 (4H, m); 2.7 (1H, d, $J=4.2$); 2.87 (1H, d, $J=10.7$); 3.03 (1H, t, $J=10.5$); 3.22 (1H, m); 3.33 (2H, m); 3.55 (1H, dd, $J=3, 17.7$); 4.58 (1H, bs); 5.35 (1H, dt, $J=6.2, 15.2$); 5.63-5.45 (2H, m); 7.24-7.17 (4H, m); 7.30-7.27 (10 H, m); 7.41-7.40 (6H, dd, $J=1, 8.8$). (TLNII-291pp) ¹³C NMR (75.5 MHz, CDCl₃) δ TMS: -4.1, 18.2, 21.3, 25.9, 31.5, 45.8, 68.6, 69.8, 126.8, 127.5, 128.1, 129.6, 129.8, 130.3, 132.1, 145.0, 172.8, 199.0.



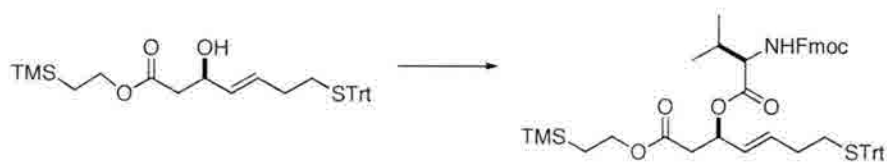
(*R,E*)-2-(trimethylsilyl)ethyl 3-hydroxy-7-(tritylthio)hept-4-enoate (344)



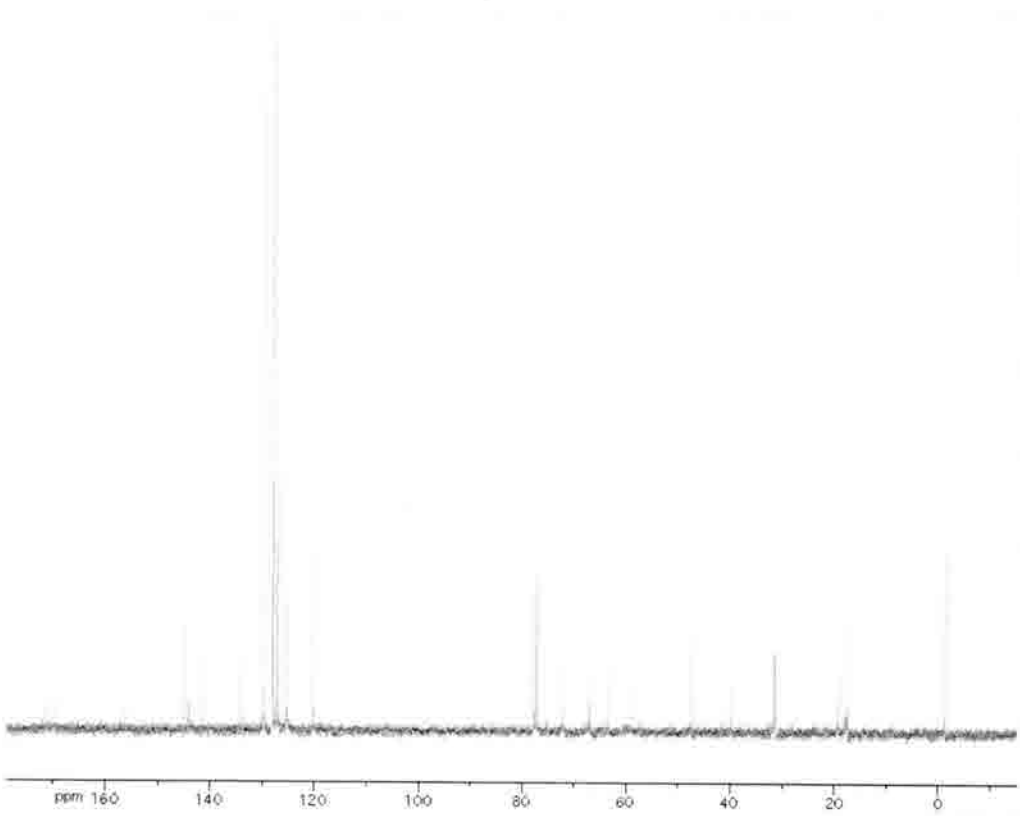
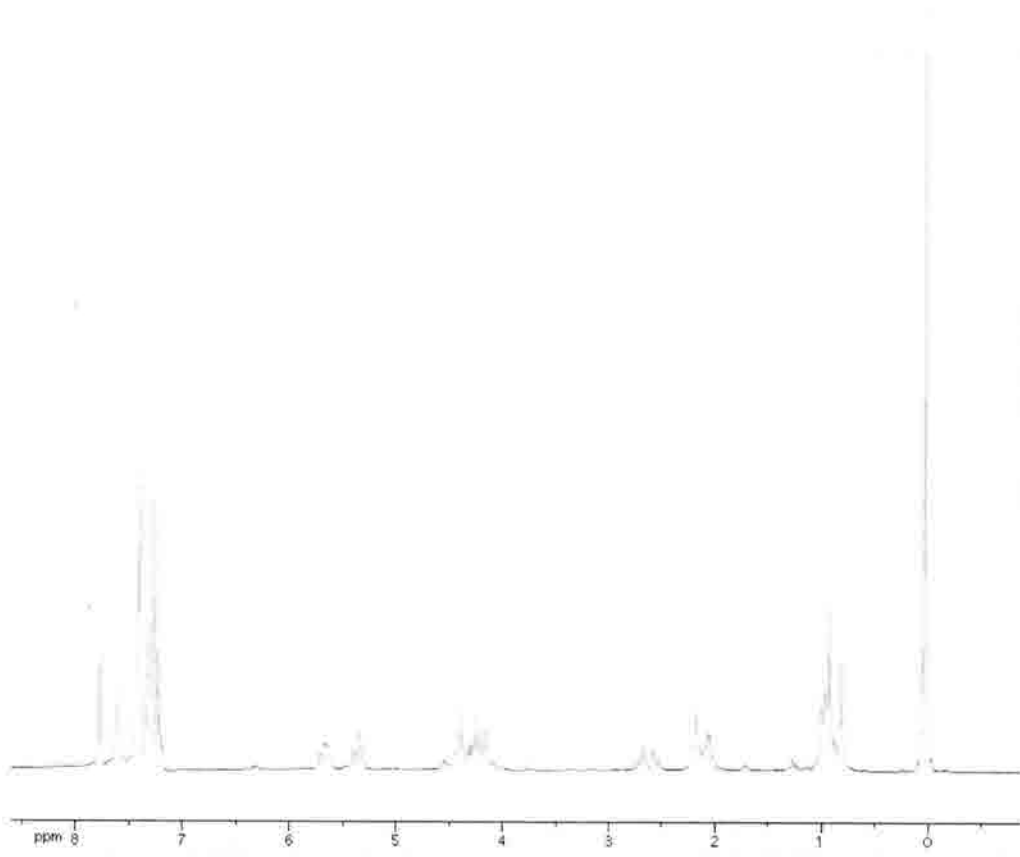
To a stirred solution of **ent-290a** (0.88 g, 1.44 mmol) in dichloromethane (14 mL) was added 2-TMS-ethanol (2 mL, 14.4 mmol) and imidazole (0.15 g, 2.16 mmol). The mixture was stirred overnight, after which the solvent was evaporated and the residue purified by column chromatography (10:1 to 4:1 hexanes/ethyl acetate) to give **344** as a clear oil (0.34 g, 45%). $[\alpha]_D^{24}$: +5, $c=2$ CHCl₃. ¹H NMR (300 MHz, CDCl₃) δ TMS: 0.02 (9H, s); 0.93-1.01 (2H, m); 1.58 (2H, m); 2.08 (1H, t, $J = 6.3$); 2.20 (1H, t, $J = 6.3$); 2.44-2.47 (1H, m); 2.99 (2H, d, $J = 7.2$); 3.40 (1H, dd, $J = 6.9, 11.1$); 3.60-3.77 (2H, m); 4.16-4.21 (1H, m); 4.45 (1H, q, $J = 6.9$); 5.30-5.62 (2H, m); 7.18-7.22 (5H, m); 7.27-7.42 (10H, m). (TLNII-325). ¹³C NMR (75.5 MHz, CDCl₃) δ TMS: -1.11, 17.53, 22.22, 31.60, 41.96, 60.09, 63.22, 66.80, 68.79, 126.83, 128.10, 129.81, 132.46, 145.11, 172.63. (TLNII-293_c13)



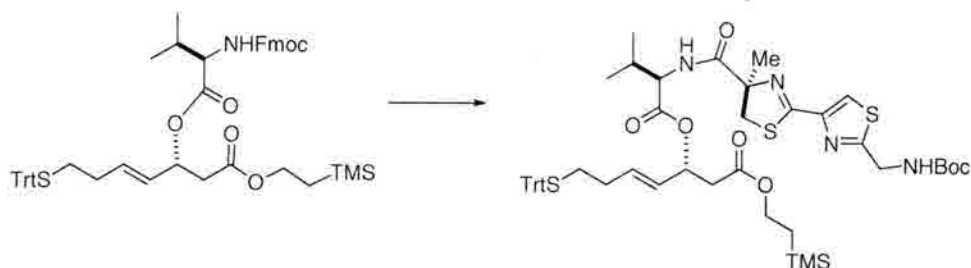
(*R,E*)-2-(trimethylsilyl)ethyl 3-((*R*)-2-(((9*H*-fluoren-9-yl)methoxy)carbonylamino)-3-methylbutanoyloxy)-7-(tritylthio)hept-4-enoate (345**)**



To a solution of alcohol **344** (0.35g, 0.67 mmol) and *N*-Fmoc-D-valine (1.14 g, 3.37 mmol) in DCM (14 mL) was added EDCI (0.77 g, 4.05 mmol) and DMAP (8 mg, 0.07 mmol). Diisopropylethylamine (0.71 mL, 4.05 mmol) was then added. The mixture was stirred for 14 h, and the solvent was evaporated. The residue was purified by column chromatography (1:4 EtOAc/hexanes) to give **345** as a light yellow oil (0.42 g, 75%). ¹H NMR (300 MHz, CDCl₃) δ TMS: 0.03 (9H, s); 0.81 (3H, d, *J* = 6.6); 0.92-1.00 (5H, m); 2.05-2.22 (4H, m); 2.66 (2H, dq; *J* = 7.8, 23.7); 4.14-4.57 (7H, m); 5.31-5.42 (2H, m); 5.62-5.75 (2H, m); 7.19-7.24 (2H, m); 7.27-7.35 (6H, m); 7.40 (5H, d, *J* = 7.2); 7.61 (2H, d, *J* = 6.9); 7.77 (2H, d, *J* = 7.5). ¹³C NMR (75.5 MHz, CDCl₃) δ TMS: -1.28, 17.51, 19.23, 31.31, 31.58, 31.63, 39.89, 47.42, 58.94, 63.39, 67.25, 72.09, 120.21, 125.35, 126.85, 127.31, 127.93, 128.10, 129.79, 134.31, 141.52, 144.01, 144.16, 145.03, 156.37, 169.88, 171.14.



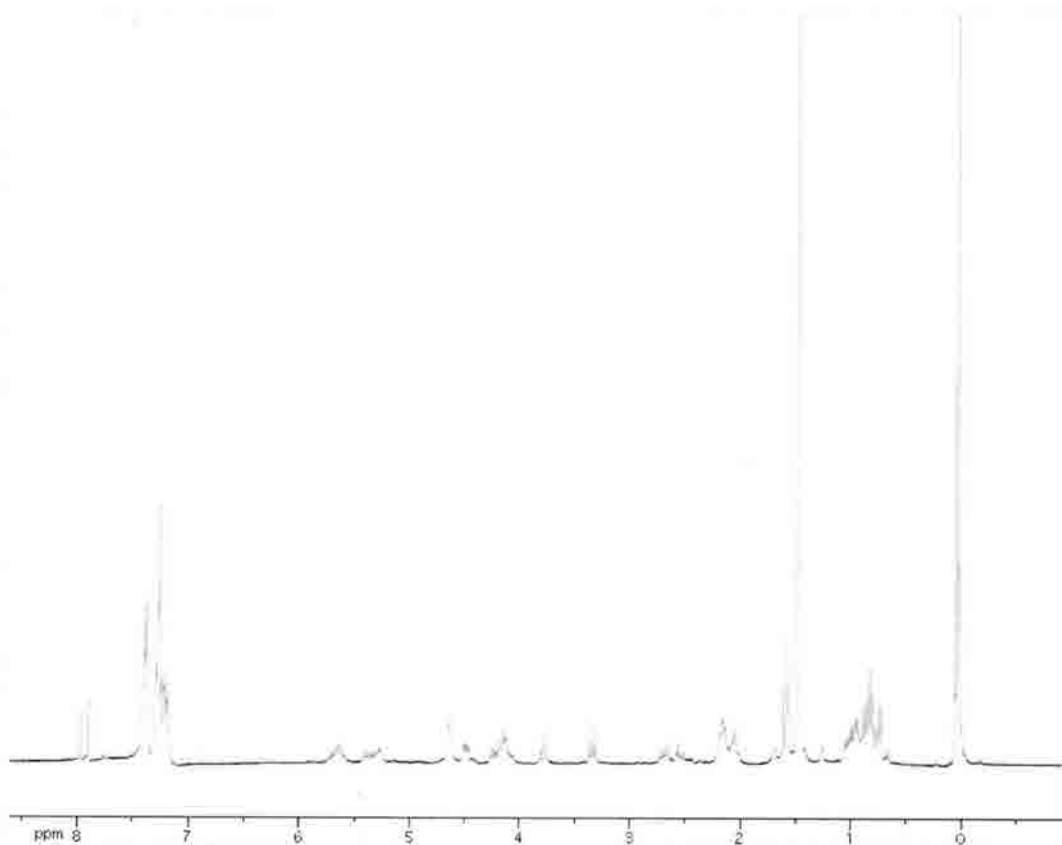
(*R,E*)-2-(trimethylsilyl)ethyl 3-((*R*)-2-((*R*)-2-(2-((*tert*-butoxycarbonylamino)methyl)thiazol-4-yl)-4-methyl-4,5-dihydrothiazole-4-carboxamido)-3-methylbutanoyloxy)-7-(tritylthio)hept-4-enoate (347**)**

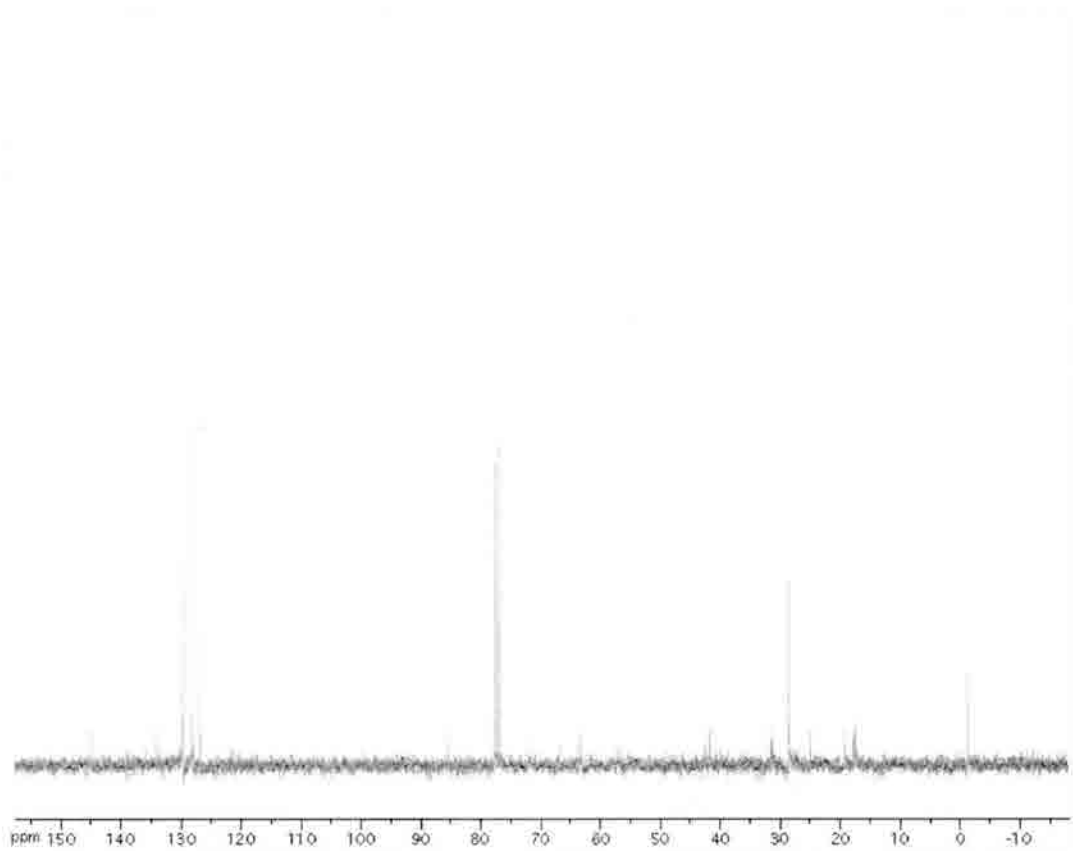


To a solution of Fmoc-protected amine **345** (0.39 g, 0.46 mmol) in MeCN (23 mL) was added diethylamine (2.3 mL). The resultant mixture was stirred for 2 h, after which the solvent was removed under reduced pressure. The residue was dissolved in EtOAc and concentrated again to give the free amine (**346**).

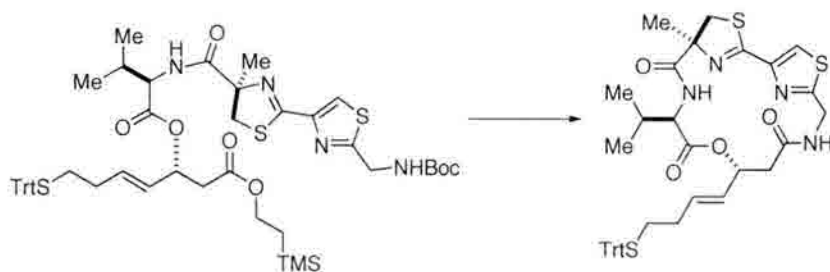
A solution of acid **328** (0.2 g, 0.46 mL) in DCM (9 mL) was cooled to 0° and PyBop (0.48 g, 0.92 mmol) was added, followed by dropwise addition of diisopropylethylamine (0.24 mL, 1.38 mmol). After ~5 min of stirring, amine **346** in MeCN (5.5 mL) was added dropwise. The resulting mixture was stirred for 3 h, followed by removal of the solvent under reduced pressure. The residue was purified by column chromatography (1:1 EtOAc/hexanes) to give **347** as a clear oil (0.34 g, 77%). $[\alpha]_D = +20$, $c=0.2$ in CHCl_3 . $^1\text{H NMR}$ (300 MHz, CDCl_3) δ TMS: 0.02 (9H, s); 0.73 (3H, d, $J = 6.9$); 0.78-1.06 (6H, m); 1.47 (9H, s); 2.00-2.18 (4H, m); 2.47-2.72 (2H, m); 3.34 (1H, dd, $J = 6.9, 11.7$); 3.77 (1H, dd, $J = 8.7, 11.7$); 4.06-4.26 (3H, m); 4.46-4.51 (1H, m); 4.63 (1H, bs); 5.25-5.40 (2H, m); 5.59-5.73 (1H, m); 7.19-7.26 (5H, m); 7.26-7.29 (5H, m); 7.37-7.39 (5H, m); 7.90 (1H, d, $J = 19.8$). (TLNII-469a) $^{13}\text{C NMR}$ (75.5 MHz, CDCl_3) δ TMS: -1.28,

17.48, 17.66, 17.92, 19.27, 24.96, 28.54, 31.27, 41.72, 63.35, 71.99, 85.37, 126.82,
128.08, 129.76, 134.14, 145.02, 174.65. (TLNII-469_c13)

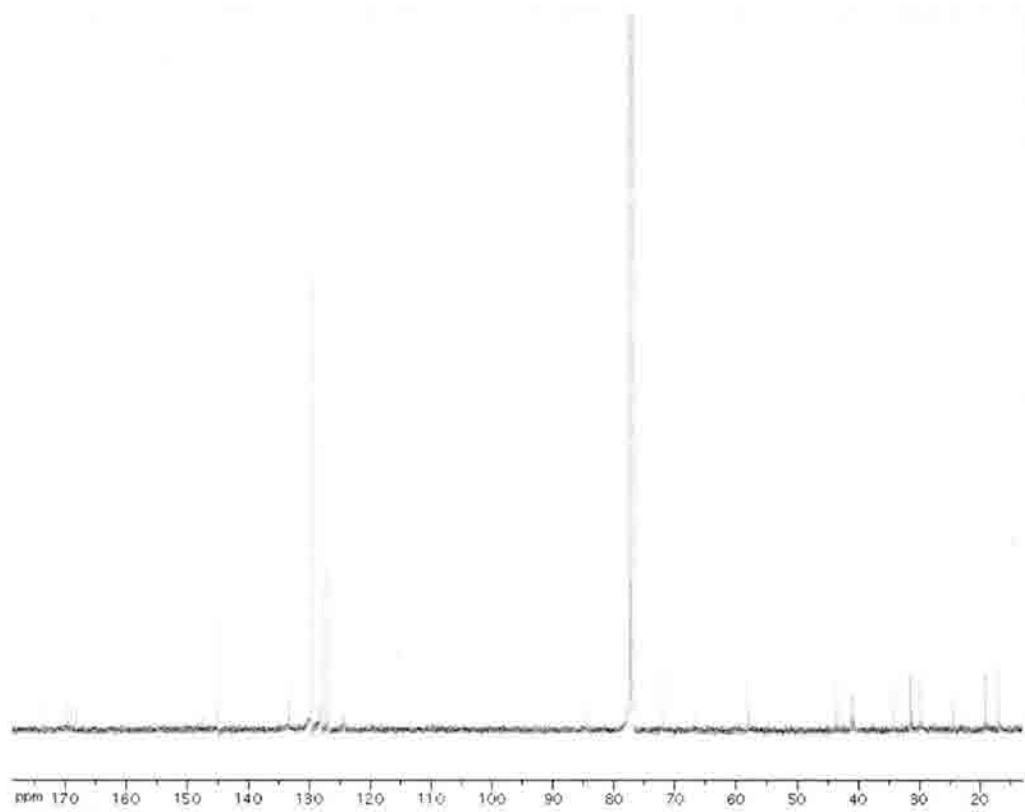
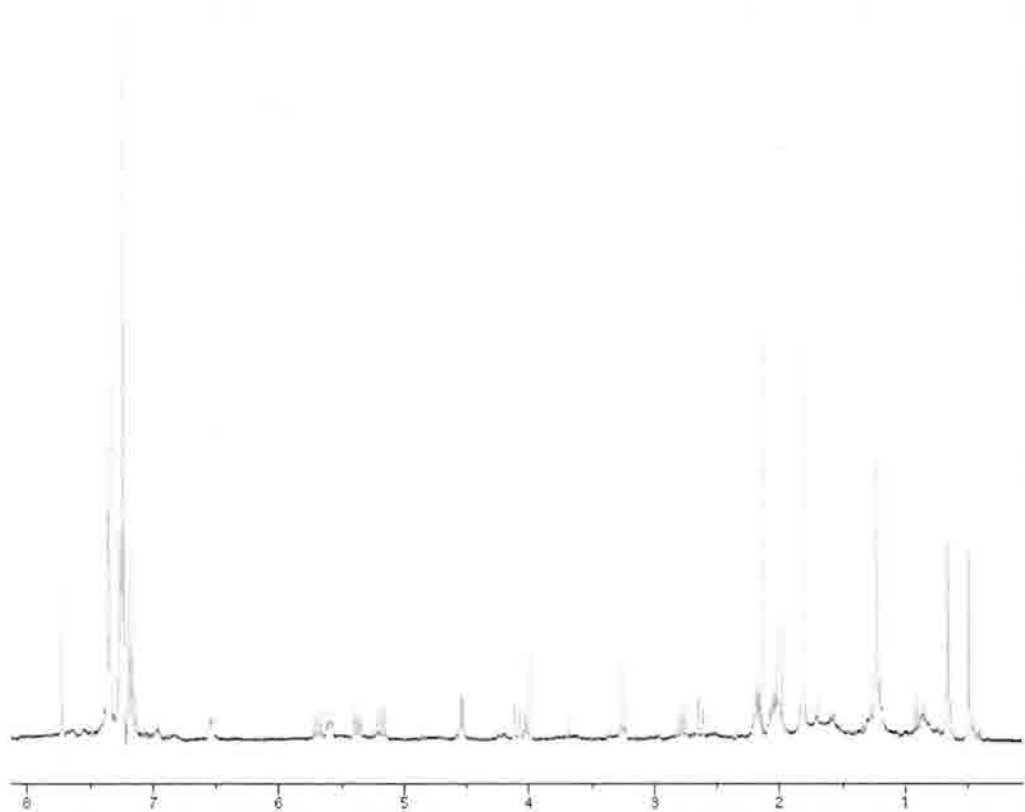




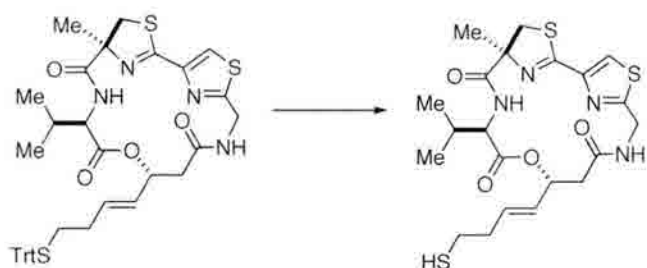
S-trityl protected macrocycle (348)



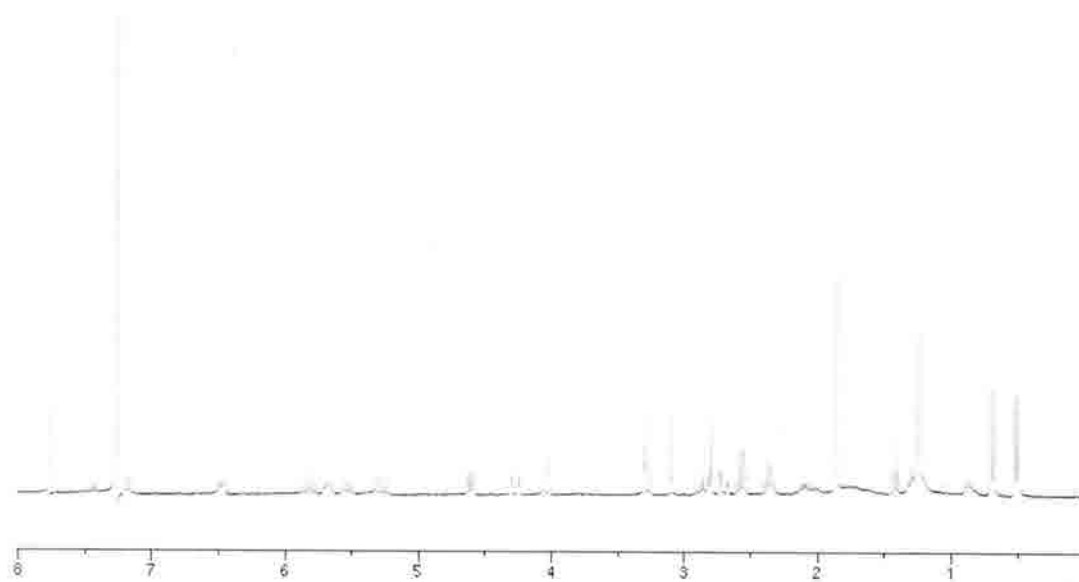
A solution of **347** (0.12 g, 0.125 mmol) in dichloromethane (6.7 mL) was cooled to 0° and TFA (1.1 mL) was added dropwise. The mixture was stirred overnight at room temperature. Solvent was then evaporated. The residue was redissolved in toluene and the solvent again evaporated. The residue was then taken up in dichloromethane (5 mL) and added dropwise to a solution of diisopropylethylamine (0.13 mL, 0.75 mmol) in acetonitrile (125 mL). After stirring for ~10 min, a solution of HATU (0.095 g, 0.25 mmol) and HOBt (0.034 g, 0.25 mmol) in acetonitrile (5 mL) was added dropwise. After a further 16 h, the solvent was evaporated and the residue purified by column chromatography (10:1 to 1:1 hexanes/ethyl acetate) to give macrocycle **348** as a clear oil (0.08 g, 87%). $[\alpha]_D = -6$, $c=0.0.1$ in methanol. ^1H NMR (400 MHz, CDCl_3) δ TMS: 0.49 (3H, d, $J = 6.8$); 0.66 (3H, d, $J = 6.8$); 1.82 (3H, s); 1.98-2.10 (3H, m); 2.15-2.22 (2H, m); 2.65 (1H, dd, $J = 3.2, 16.0$); 2.79 (1H, dd, $J = 9.6, 16.4$); 3.27 (1H, d, $J = 11.2$); 4.02 (1H, d, $J = 11.2$); 4.12 (1H, dd, $J = 3.2, 17.6$); 4.55 (1H, dd, $J = 3.6, 9.2$); 5.19 (1H, dd, $J = 9.2, 17.6$); 5.39 (1H, dd, $J = 6.8, 15.6$); 5.58-5.62 (1H, m); 5.68-5.73 (1H, m); 6.53 (1H, d, $J = 6.8$); 7.13-7.20 (3H, m); 7.23-7.29 (7H, m); 7.34-7.36 (5H, m) (TLNII-311_400) ^{13}C NMR (100.6 MHz, CDCl_3) δ TMS: 16.9, 19.1, 24.4, 29.9, 31.4, 31.6, 34.2, 40.8, 41.2, 43.5, 58.0, 66.8, 72.0, 84.5, 126.8, 128.1, 129.8, 133.3, 145.0, 147.0, 147.6, 168.2, 169.0, 169.5, 173.6 (TLNII-311_c13)



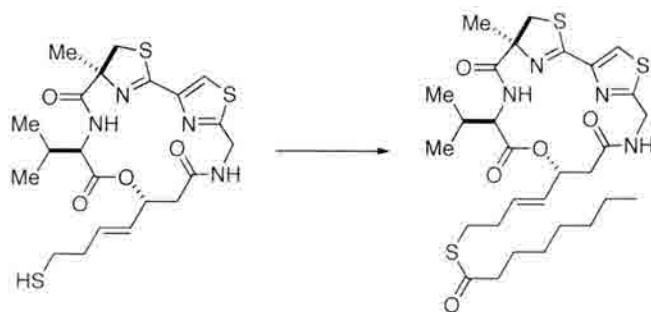
ent-largazole thiol (349)



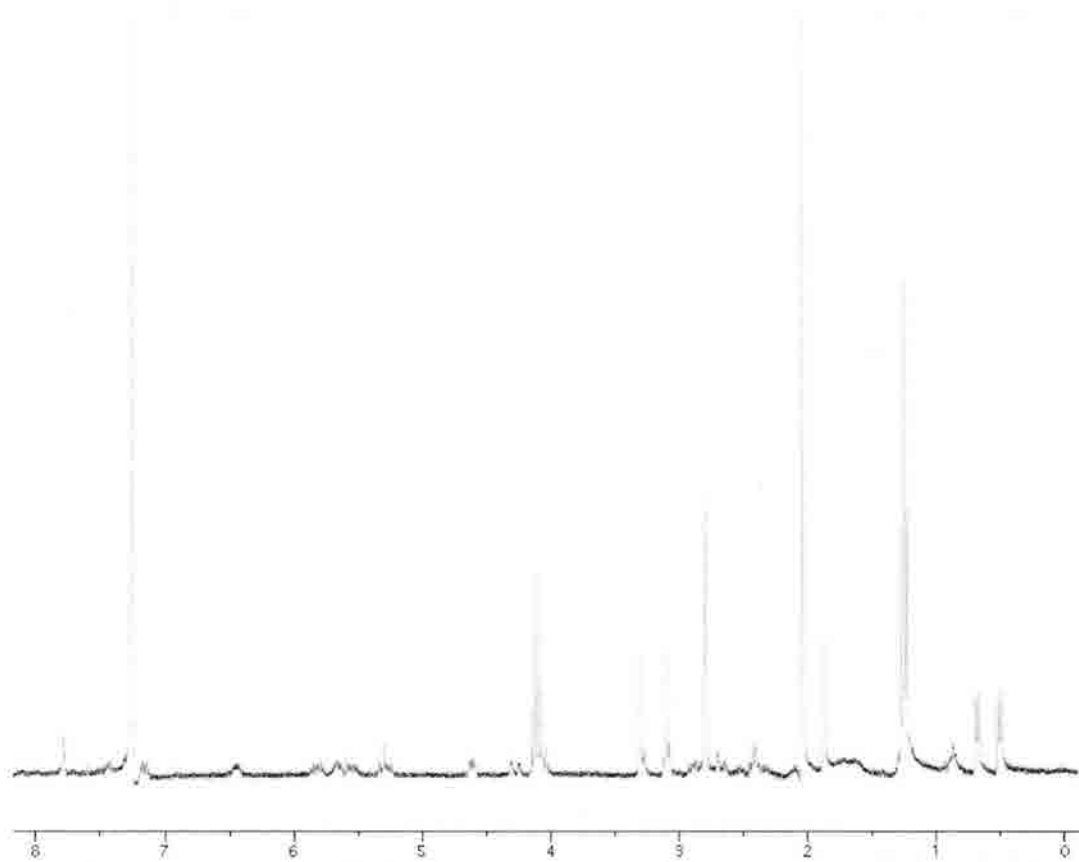
A solution of **348** (0.025 g, 0.034 mmol) in DCM (4.5 mL) was cooled to 0°. TFA (0.17 mL) was added dropwise, followed by triisopropylsilane (14 μ l, 0.068 mmol). The reaction was warmed to room temperature and stirred for 2 hours, after which the solvent was evaporated. The residue was purified by column chromatography (EtOAc) to give **349** (0.015 g, 90%) as a clear oil. $[\alpha]_D = -21$, $c=0.0.1$ in chloroform. $^1\text{H NMR}$ (300 MHz, CDCl_3) δ TMS: 0.50 (3H d, $J = 6.9$); 0.68 (3H, d, $J = 6.9$); 1.87 (3H, s); 1.43 (1H, t, $J = 7.8$); 2.07-2.13 (1H, m); 2.32-2.40 (2H, m); 2.56 (2H, q, $J = 7.2$); 2.68 (1H, dd, $J = 3.0, 16.2$); 2.88 (2H, dd, $J = 9.9, 16.2$); 3.26 (1H, d, $J = 8.7$); 4.02 (1H, d, $J = 11.5$); 4.30 (1H, dd, $J = 3.0, 17.4$); 4.62 (1H, dd, $J = 3.3, 9.3$); 5.29 (1H, dd, $J = 9.3, 17.7$); 5.46 (1H, dd, $J = 6.9, 15.6$); 5.65-5.72 (1H, m); 5.82 (1H, dt, $J = 7.2, 15.3$); 6.49 (1H, d, $J = 7.5$); 7.19 (1H, d, $J = 9.9$); 7.77 (1H, s) (TLNII-380)



(-)-largazole (350)



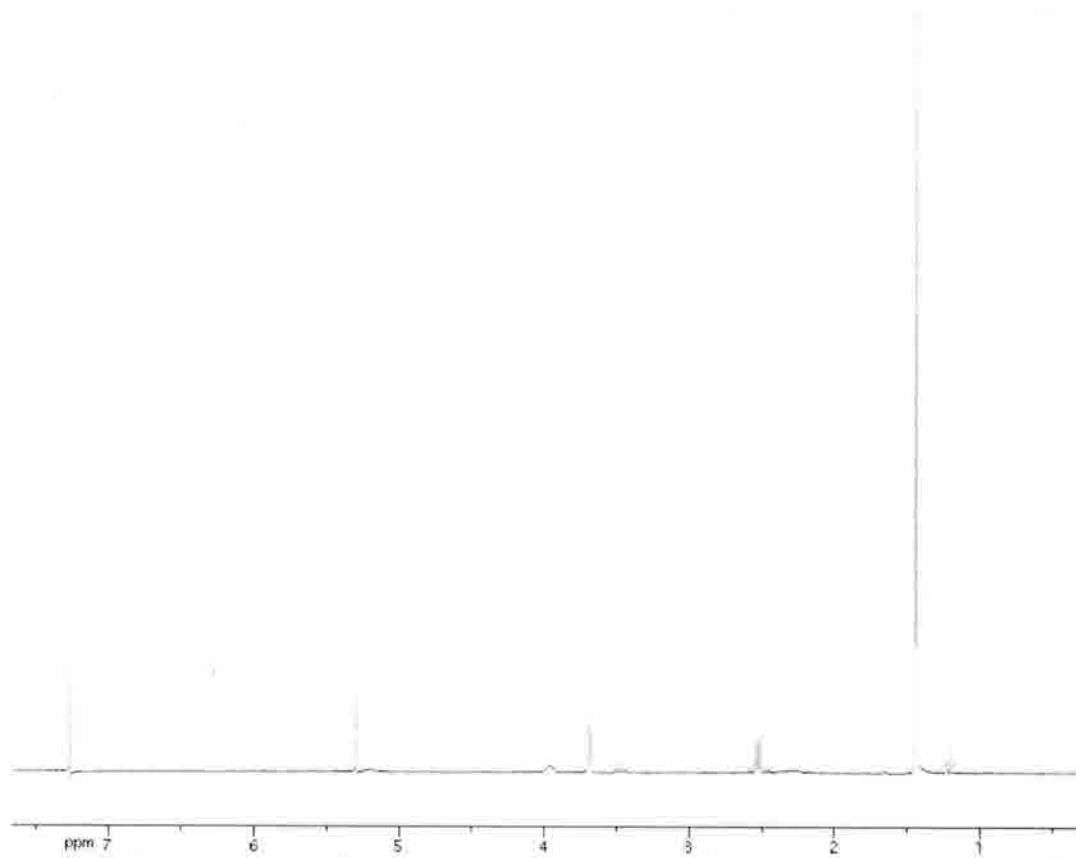
A solution of **349** (0.027 g, 0.054 mmol) in DCM (3 mL) was cooled to 0°. Triethylamine (15 μ l, 0.108 mmol) was added dropwise, followed by dropwise addition of octanoyl chloride (47 μ l, 0.272 mmol). The reaction was warmed to room temperature and stirred for 2 hours, then cooled to 0°. Methanol (10 mL) was added, and the solvent evaporated. The residue was purified by column chromatography (EtOAc) to give **350** as a clear oil (0.03 g, 90%). $[\alpha]_D = -20.5$, $c=1$ in methanol (lit value for (+)-largazole = +22).



(S)-tert-butyl 3-(tert-butoxycarbonylamino)-4-hydroxybutanoate (354)



A solution of amino acid **273** (5 g, 17.28 mmol) was cooled to -30° . *N*-methyl morpholine (1.9 mL, 17.63 mmol) was added dropwise, followed by dropwise addition of isobutylchloroformate (2.3 mL, 17.63 mmol). The mixture was warmed to -10° for 20 min, then cooled to -30° . Sodium borohydride (1.96 g, 51.84 mmol) was added, followed by the dropwise addition of methanol (18 mL). The reaction was stirred for 1 h, then quenched with a saturated aqueous solution of ammonium chloride, and stirred for a further 10 min. The aqueous layer was extracted into diethyl ether, and the combined organic layers were washed with brine, dried over sodium sulfate and concentrated. The residue was purified by column chromatography (1:4 Et₂O/DCM) to give **354** (3.18 g, 67%). ¹H NMR (300 MHz, CDCl₃) δ TMS: 1.44 (9H, s); 1.45 (9H, s); 2.52 (1H, dd, *J* = 4.8, 6.0); 3.77 (2H, d, *J* = 4.8); 3.95 (1H, bs); 5.19 (1H, bs). (TLNII-178)

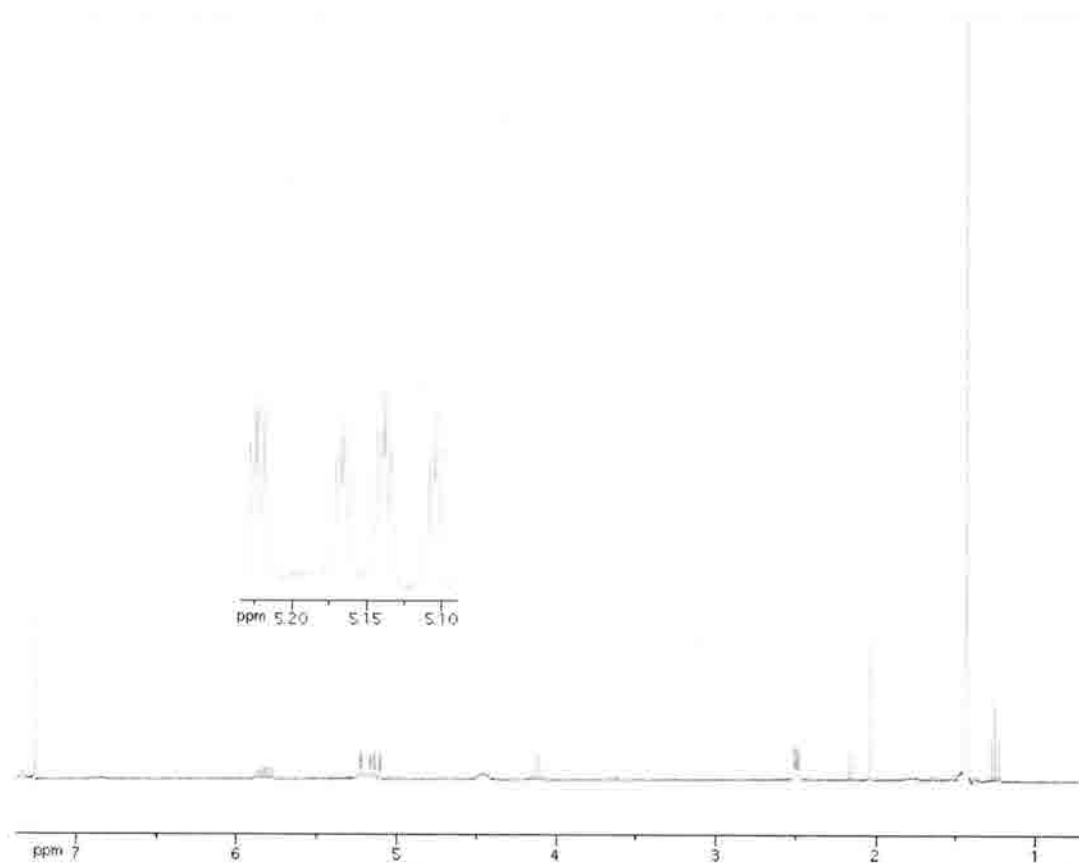


(S)-tert-butyl 3-(tert-butoxycarbonylamino)pent-4-enoate (356)



A solution of freshly distilled oxalyl chloride (4.5 mL, 40.5 mmol) in DCM (150 mL) was cooled to -78° . DMSO (5.75 mL, 81.0 mmol) in DCM (14 mL) was added dropwise, and the mixture was stirred to 15 min. Alcohol **354** (6.95 g, 27.0 mmol) in DCM (27 mL) was added dropwise. After a further 20 min, triethylamine (15.0 mL, 108.0 mmol) was added dropwise. The resulting suspension was warmed to -20° and stirred for a further 60 min, then poured onto diethyl ether (250 mL) and 1N KHSO_4 (100 mL). The aqueous layer was extracted into diethyl ether (3 x 100 mL). The combined organic layers were washed with brine, dried over sodium sulfate and concentrated. The resultant residue (**355**) was taken on immediately to the next reaction.

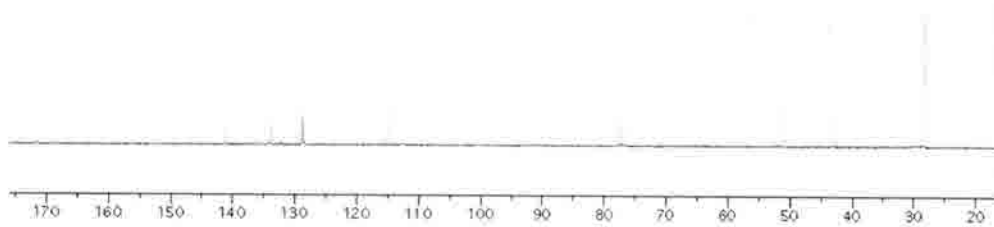
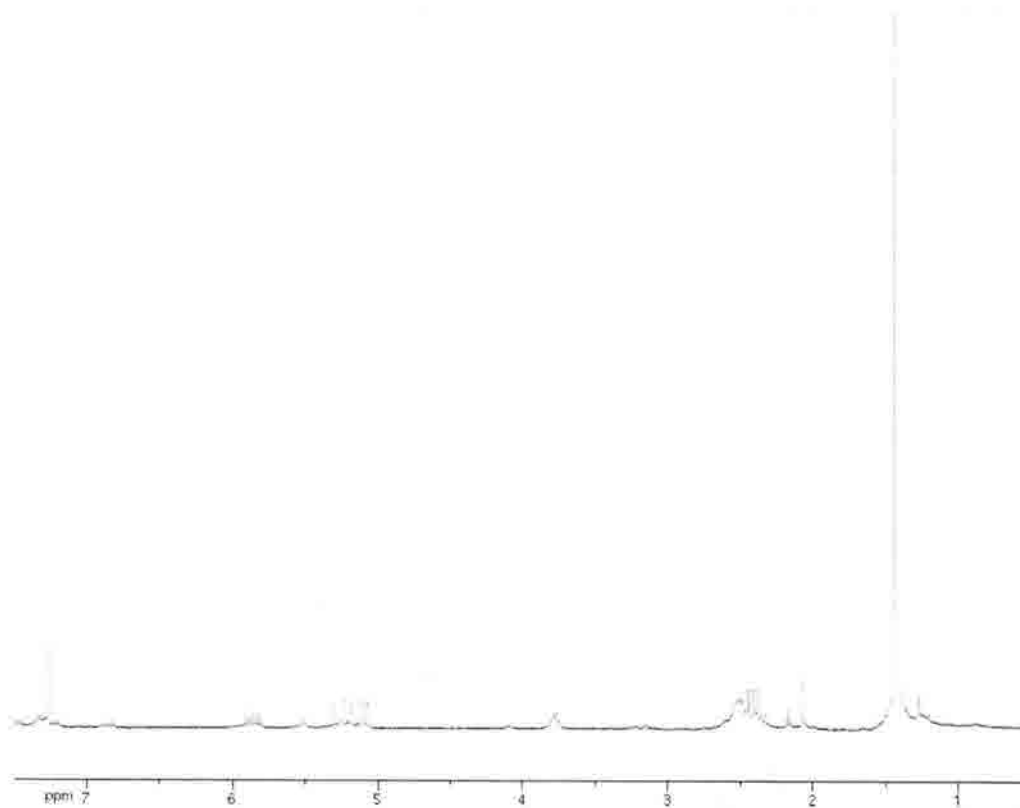
A solution of methyltriphenylphosphonium bromide (19.29 g, 54.0 mmol) in THF (240 mL) was cooled to 0° . Sodium HMDS (1M in THF, 50.8 mL, 50.8 mmol) was added dropwise *via* addition funnel. The mixture was warmed to room temperature and stirred for 1 h, after which it was cooled to -78° . Aldehyde **355** (27.0 mmol) in THF (30 mL) was added dropwise. The reaction was warmed to room temperature over 1 h, and stirred for a further 2 h. The mixture was then poured onto a saturated aqueous solution of ammonium chloride (200 mL), and the aqueous layer was extracted into diethyl ether (3 x 100 mL). The combined organic layers were washed with brine, dried over sodium sulfate and concentrated. The residue was further purified by column chromatography (1:4 EtOAc/hexanes) to give **356** (3.7 g, 50%). ^1H NMR (300 MHz, CDCl_3) δ TMS: 1.44 (18H, s); 2.50 (2H, dd, $J = 2.7, 5.7$); 4.46 (1H, bs); 5.16 (2H, dddd, $J = 1.2, 1.8, 2.7, 17.1$); 5.83 (1H, ddd, $J = 5.1, 15.6, 17.1$) (TLNII-202pp)



(S)-tert-butyl 3-aminopent-4-enoate (357)



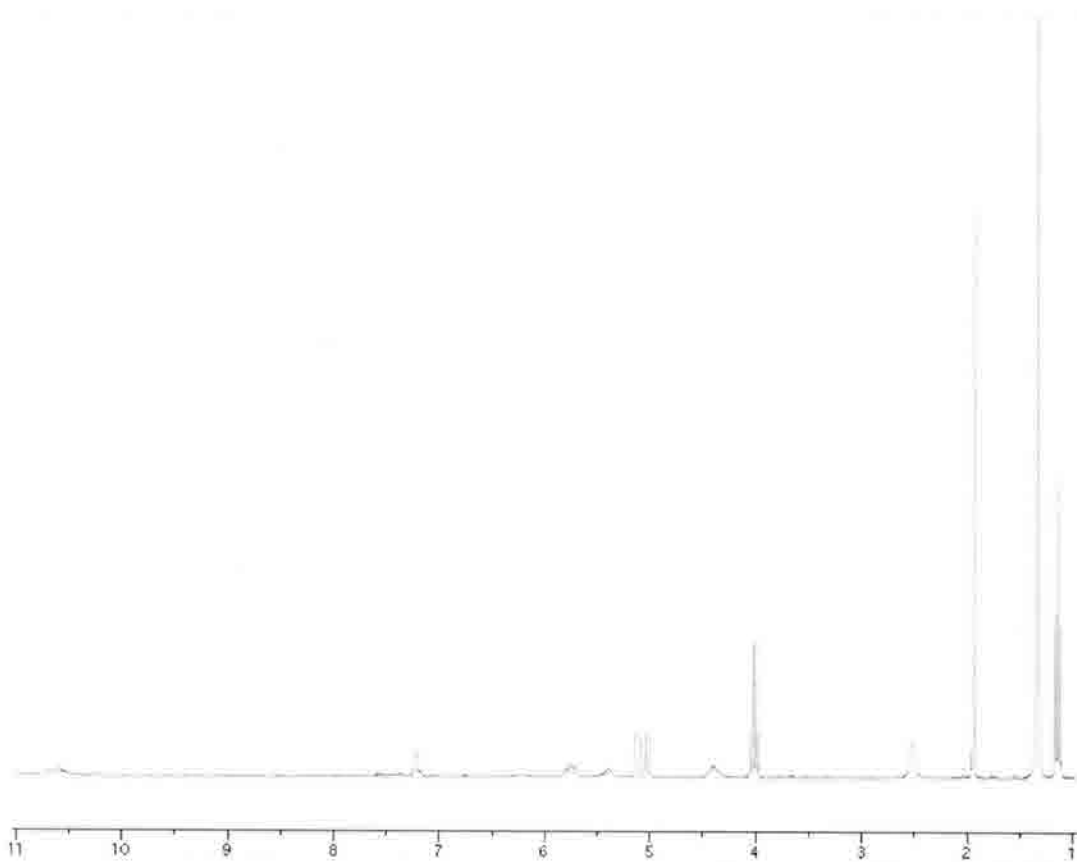
A stirred solution of alkene **356** (0.64 g, 2.36 mmol) in DCM (25 mL) was cooled to 0°, and TFA (2.5 mL) was added dropwise. The mixture was stirred at room temperature for 2 h, then poured onto an ice-cold saturated aqueous solution of sodium bicarbonate (25 mL). The organic layer was washed with sodium bicarbonate (25 mL), then brine; dried over sodium sulfate and concentrated to give free amine **357** as a clear oil (0.17 g, 42%).
¹H NMR (300 MHz, CDCl₃) δ TMS: 1.45 (9H, s); 2.32-2.50 (4H, m); 3.74 (1H, m); 5.07-5.30 (2H, m); 5.86 (1H, ddd, *J* = 6.6, 10.5, 16.8). (TLNII-166) ¹³C NMR (75.5 MHz, CDCl₃) δ TMS: 28.3, 43.2, 51.5, 81.1, 114.6, 171.4. (TLNII-182_c13)



(S)-3-(tert-butoxycarbonylamino)pent-4-enoic acid (359)



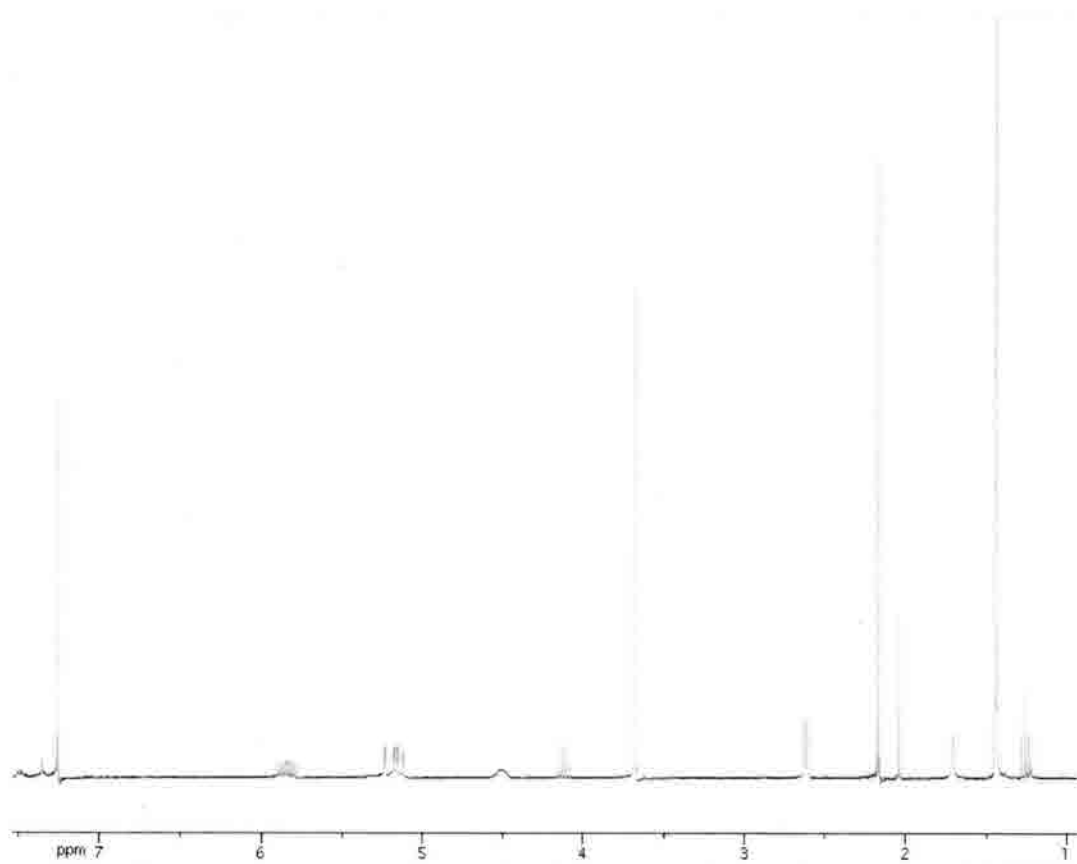
A solution of **356** (3.52 g, 12.97 mmol) in methanol (119 mL), THF (119 mL) and 1M LiOH (119 mL) was heated to 50° for 5 h. After cooling to room temperature, the majority of the solvent was removed under reduced pressure. The mixture was acidified to ~pH 4 with 1N HCl, and the aqueous layer was extracted into EtOAc (3 x 100 mL). The combined organic layers were washed with brine, dried over sodium sulfate and concentrated to give **359** as a clear oil in quantitative yield (2.79 g). ¹H NMR (300 MHz, CDCl₃) δ TMS: 1.34 (9H, s); 4.41 (1H, bs); 5.04 (2H, dd, *J* = 10.2, 17.1); 5.72 (1H, ddd, *J* = 5.1, 16.5, 17.1); 10.06 (1H, bs). (TLNII-206)



(S)-methyl 3-(tert-butoxycarbonylamino)pent-4-enoate (360)

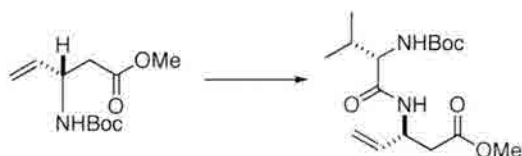


A solution of carboxylic acid **359** (1.40 g, 6.50 mmol) in DCM (65 mL) was cooled to 0°. EDCI (7.46 g, 38.91 mmol) was added, followed by DMAP (8 mg, 0.07 mmol). The reaction was warmed to room temperature, and diisopropylamine (6.8 mL, 38.91 mmol) was added, followed by methanol (3.0 mL, 65.0 mmol). The mixture was stirred for 8.5 h, when a saturated aqueous solution of ammonium chloride (50 mL) was added. The aqueous layer was extracted into DCM (3 x 20 mL), and the combined organic layers were washed with brine, dried over sodium sulfate and concentrated. The residue was purified by column chromatography (1:1 EtOAc/hexanes) to give **360** as a clear oil (1.33 g, 90%). ¹H NMR (300 MHz, CDCl₃) δ TMS: 1.44 (9H, s); 2.61 (2H, d, *J* = 5.7); 3.68 (3H, s); 4.51 (1H, bs); 5.17 (2H, dddd, *J* = 1.2, 1.8, 2.7, 17.4); 5.84 (1H, ddd, *J* = 5.4, 10.5, 17.4). (TLNII-214_2)



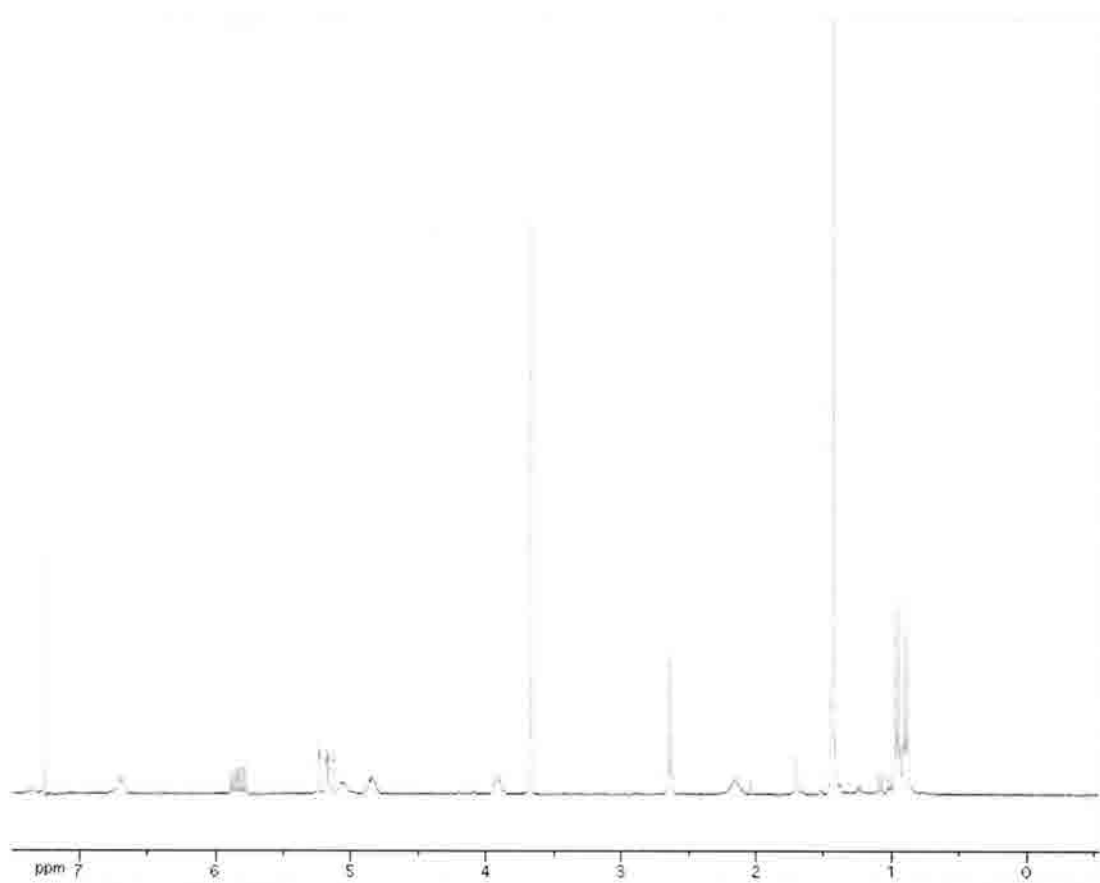
methyl 3-((*S*)-2-(*tert*-butoxycarbonylamino)-3-methylbutanamido)pent-4-enoate

(361)



A solution of **360** (0.05 g, 0.218 mmol) in DCM (7 mL) was cooled to 0°. TFA (0.7 mL) was added dropwise. The mixture was stirred at room temperature for 2 h, after which the solvent was evaporated. Toluene (10 mL) was added to the residue, and the solvent again removed under reduced pressure to give the free amine of **360**.

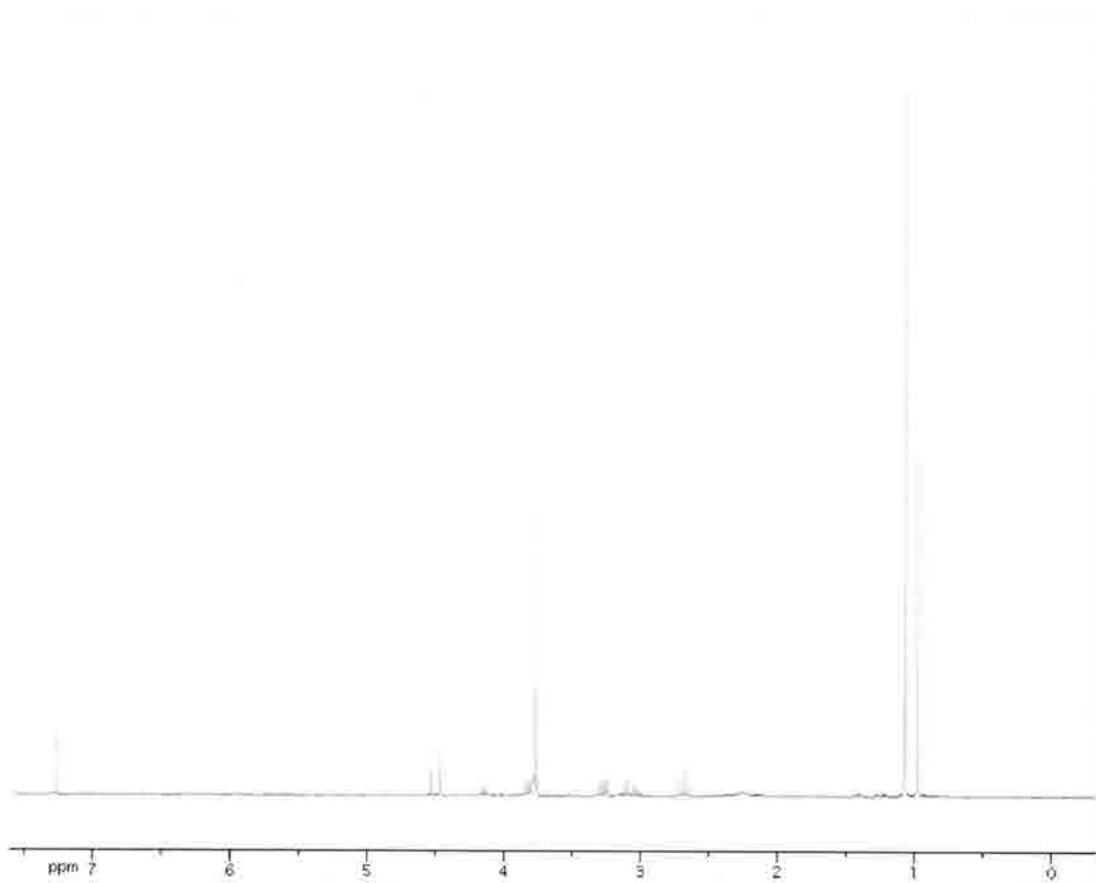
N-Boc-L-valine (0.095 g, 0.44 mmol) in DCM (1.5 mL) was cooled to 0°. EDCI (0.084 g, 0.44 mmol) was added, and the mixture was warmed to room temperature for 10 min. Diisopropylamine (0.11 mL, 0.65 mmol) was added, followed by the free amine in DCM (1.5 mL). The mixture was stirred for 14 h, then washed with a saturated aqueous solution of ammonium chloride (10 mL), then brine. The organic layer was dried over sodium sulfate and concentrated. The residue was purified by column chromatography (10:1 to 1:1 hexanes/EtOAc) to give **361** as a light yellow oil (0.05 g, 70%). HRMS (ESI): m/z calcd. for $C_{16}H_{28}N_2NaO_5$ ($M + Na$)⁺ 351.189, found 351.189. ¹H NMR (300 MHz, CDCl₃) δ TMS: 0.88 (3H, d, $J = 6.6$); 0.95 (3H, d, $J = 6.9$); 1.44 (9H, s); 2.10-2.12 (1H, m); 2.63 (2H, d, $J = 5.4$); 3.68 (3H, s); 3.90-3.94 (1H, m); 4.82-4.86 (1H, m); 5.06 (1H, bs); 5.16 (2H, dddd, $J = 0.9, 1.5, 10.5, 17.1$); 5.84 (1H, ddd, $J = 5.4, 10.5, 17.4$); 6.68 (1H, d, $J = 8.4$). (TLNII-217_4)



(4*S*)-methyl 2-*tert*-butylthiazolidine-4-carboxylate (363)



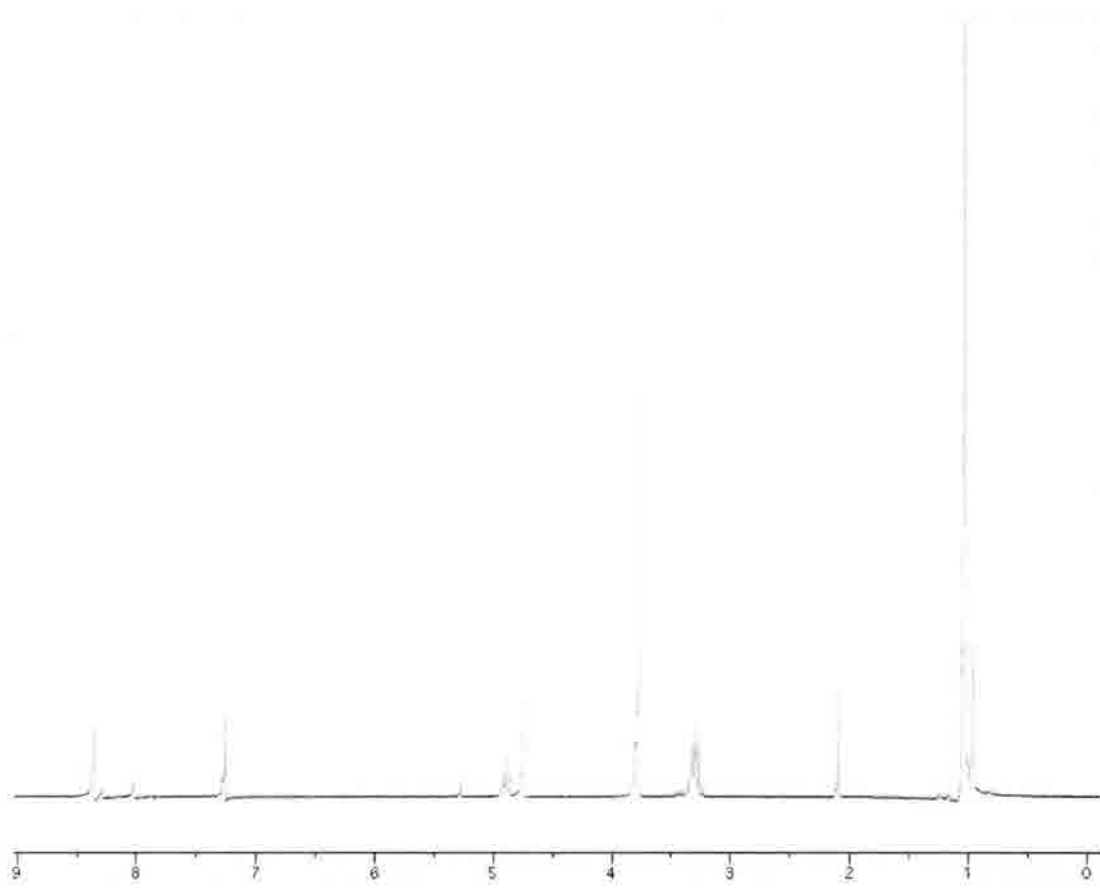
To a solution of L-cysteine methyl ester hydrochloride (10.8 g, 62.0 mmol) in pentane (120 mL) was added pivalaldehyde (7.5 mL, 68.2 mmol), followed by dropwise addition of triethylamine (9.5 mL, 68.2 mmol). The flask was fitted with a Dean-Stark apparatus and a reflux condenser and the mixture was heated to 60° for 48 h. After cooling to room temperature, the mixture was filtered through Celite and the solid washed with diethyl ether. The filtrate was concentrated under reduced pressure to give **363** as a clear oil (12.54 g, 99%). ¹H NMR (300 MHz, CDCl₃) δ TMS: (major diastereomer) 1.07 (9H, s); 2.68 (1H, app. t, *J* = 9.9); 3.26 (1H, dd, *J* = 6.6, 10.2); 3.78 (3H, s); 3.82 (1H, dd, *J* = 6.9, 9.9); 4.47 (1H, s); (minor diastereomer) 0.98 (9H, s); 3.09 (2H, dq, *J* = 6.3, 10.5); 3.76 (3H, s); 4.15 (1H, t, *J* = 6.0); 4.53 (1H, s).



(2*S*,4*S*)-methyl 2-*tert*-butyl-3-formylthiazolidine-4-carboxylate (364**)**



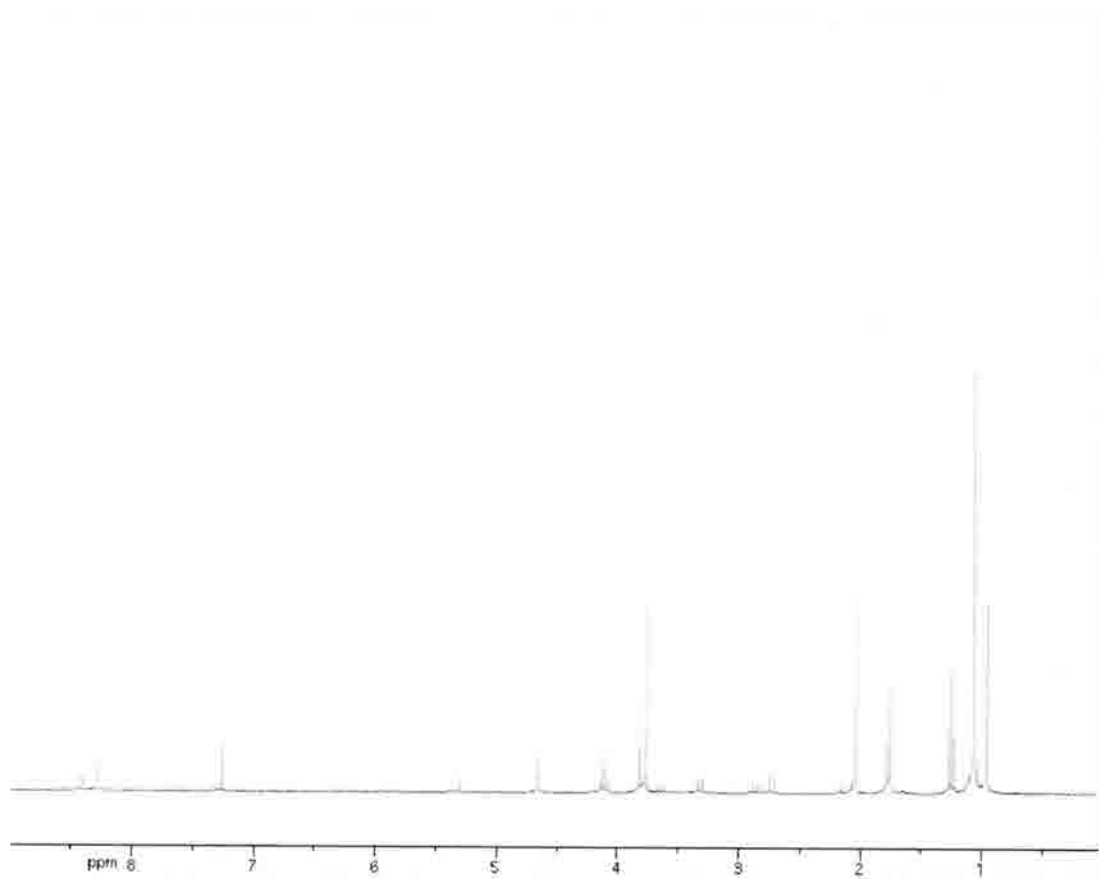
A mixture of **363** (5.5 g, 27.0 mmol) in formic acid (40 mL) was cooled to 0°. Sodium formate (2.0 g, 30.0 mmol) was added. Acetic anhydride (7.7 mL, 81.4 mmol) was added *via* syringe pump over 1 h, and the reaction was allowed to come to room temperature slowly and stirred for 15 h. Following evaporation of the solvent under reduced pressure, the residue was neutralized by addition of a saturated aqueous solution of sodium bicarbonate. The aqueous layer was extracted into EtOAc (3 x 50 mL), and the combined organic layers were washed with brine, dried over sodium sulfate and concentrated. The resulting solid was recrystallized (EtOAc/hexanes) to give **364** as off-white crystals (3.5 g, 56%). ¹H NMR (300 MHz, CDCl₃) δ TMS: (major) 1.03 (9H, s); 3.23-3.36 (2H, m); 3.77 (3H, s); 4.74 (1H, s); 4.89 (1H, t, *J* = 8.7); 8.36 (1H, s).



(2*S*,4*S*)-methyl 2-*tert*-butyl-3-formyl-4-methylthiazolidine-4-carboxylate (365)



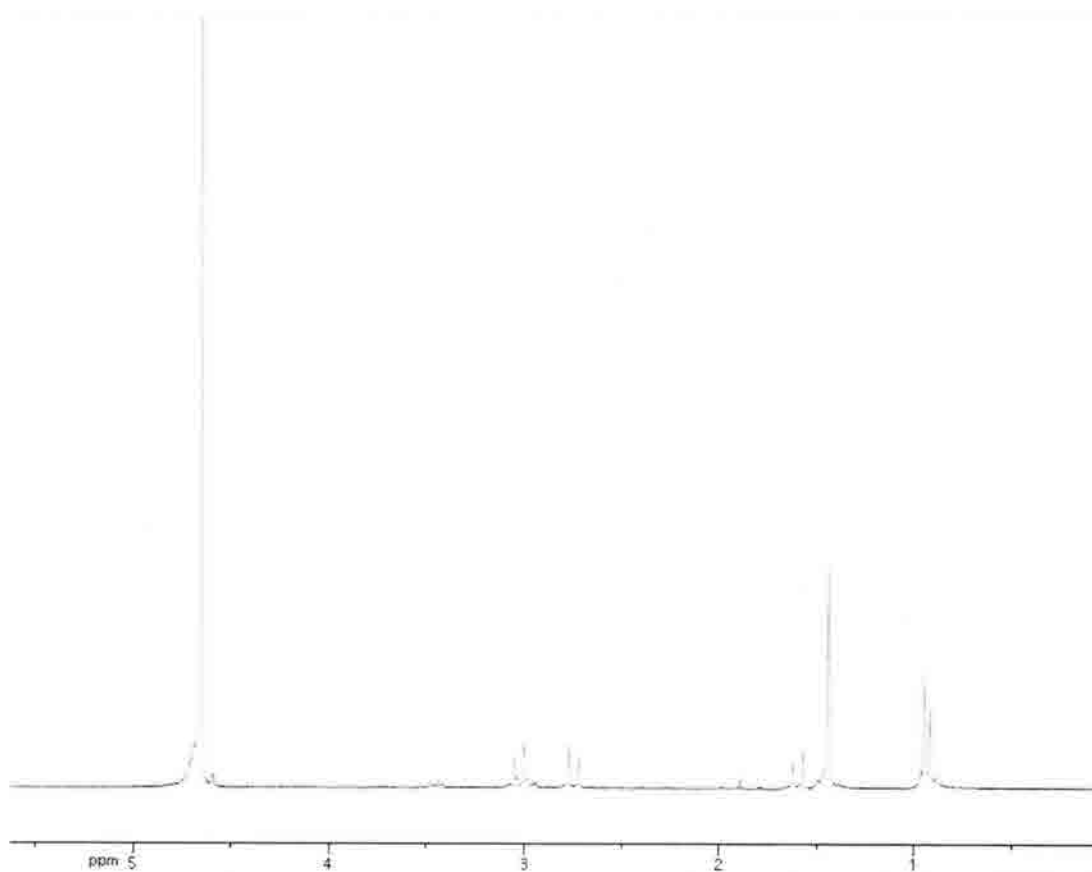
A solution of diisopropylamine (3.12 mL, 22.19 mmol) in THF (70 mL) was cooled to -78°. *n*-Butyllithium (1.6M in hexanes, 9.7 mL, 15.52 mmol) was added dropwise, followed by addition of DMPU (10.14 mL, 83.86 mmol). The mixture was stirred for 1 h, then cooled to -90°. **364** (3.42 g, 14.79 mmol) in THF (5 mL) was added dropwise, and the reaction was stirred at -90° for 45 min prior to the dropwise addition of iodomethane (1.1 mL, 17.75 mmol). After a further 2 h of stirring, methanol (10 mL) was added. The mixture was allowed to come to room temperature, and the solvent was removed under reduced pressure. The residue was dissolved in diethyl ether (50 mL) and brine (50 mL). The aqueous layer was extracted into diethyl ether (3 x 40 mL), and the combined organic layers were washed with brine, dried over sodium sulfate and concentrated. The residue was purified by column chromatography (10% EtOAc/hexanes) to give **365** as a light yellow oil (2.45 g, 68%). ¹H NMR (300 MHz, CDCl₃) δ TMS: (major) 1.06 (9H, s); 1.75 (3H, s); 2.70 (1H, d, *J* = 11.7); 3.30 (1H, d, *J* = 11.7); 3.77 (3H, s); 4.66 (1H, s); 8.28 (1H, s); (minor) 0.95 (9H, s); 1.78 (3H, s); 2.84 (1H, d, *J* = 12.3); 3.62 (1H, d, *J* = 12.6); 3.82 (3H, s); 5.30 (1H, s); 8.40 (1H, s).



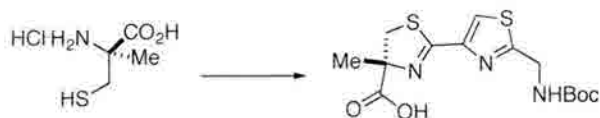
(S)-2-amino-3-mercapto-2-methylpropanoic acid hydrochloride (292)



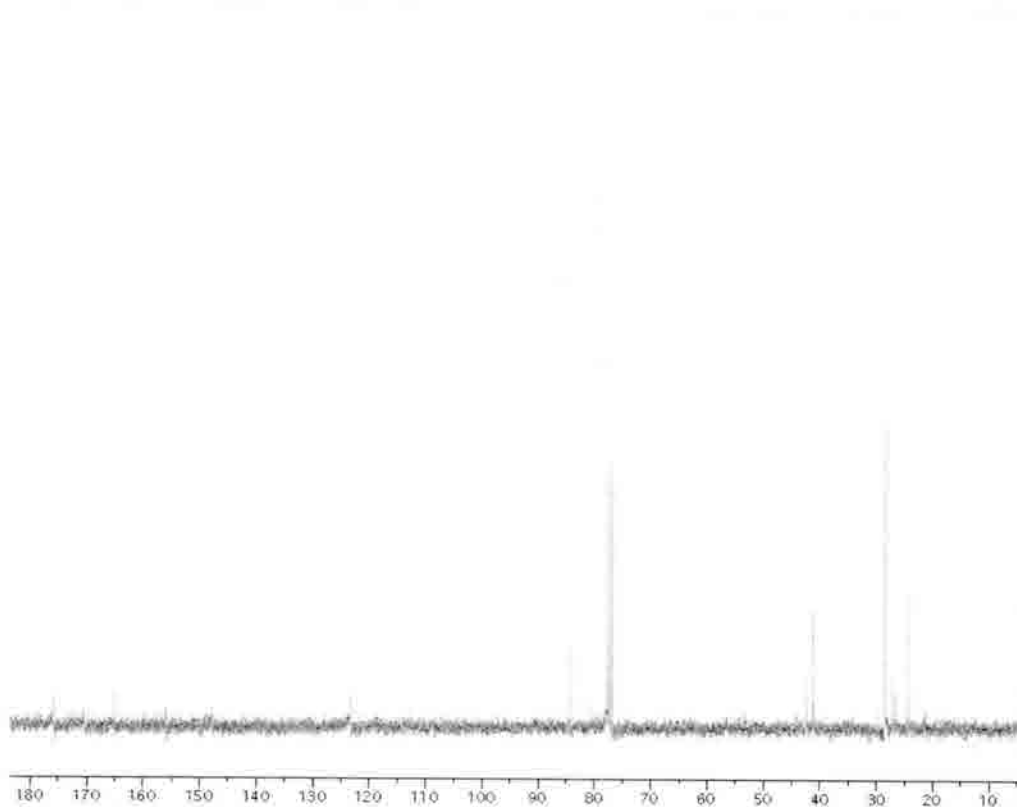
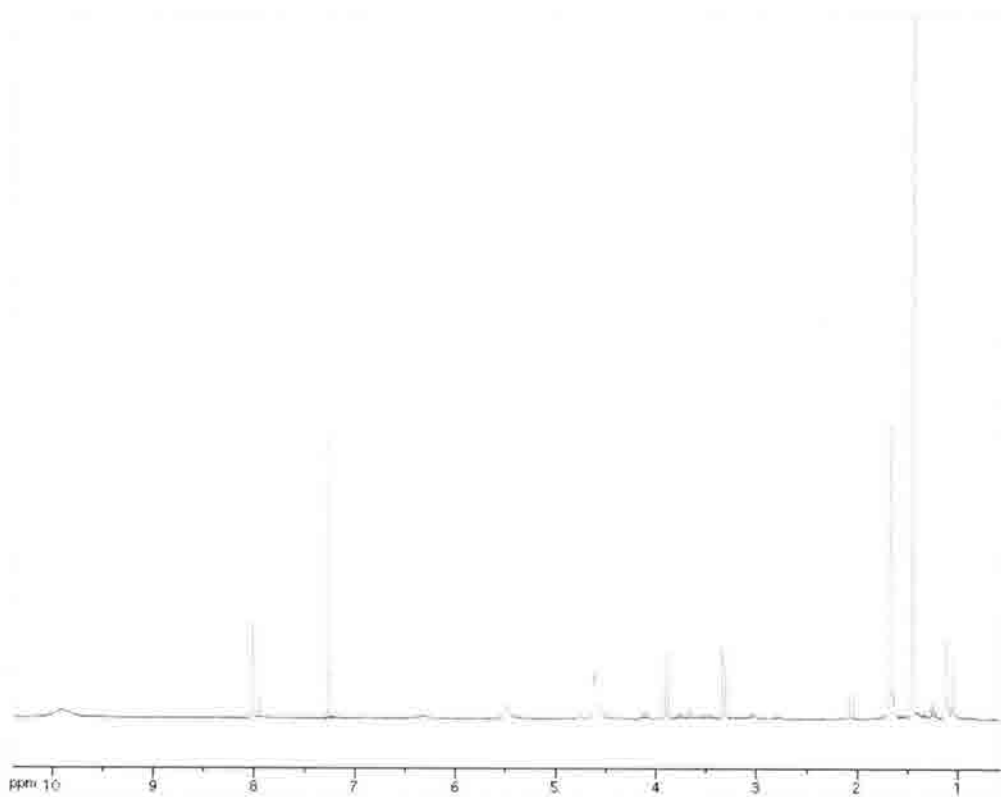
365 (2.45 g, 9.99 mmol) was dissolved in 5N HCl (38 mL) and heated to reflux for 36 h. The mixture was cooled to room temperature and washed with EtOAc (3 x 10 mL). The aqueous layer was concentrated under reduced pressure to give **292** as a light brown, amorphous solid (0.96 g, 56%). $\alpha_D = -8.2$ ($c = 1$ in H_2O). 1H NMR (300 MHz, D_2O) δ TMS: 1.44 (3H, s); 2.72 (1H, d, $J = 15$); 3.00 (1H, d, $J = 15$).



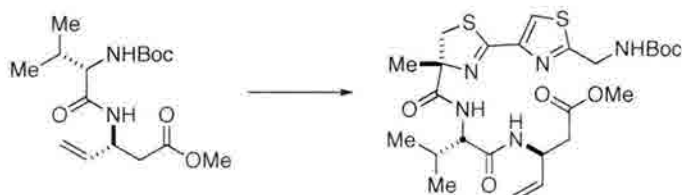
(R)-2-(2-((tert-butoxycarbonyl)amino)methyl)thiazol-4-yl)-4-methyl-4,5-dihydrothiazole-4-carboxylic acid (294)



To a solution of nitrile **293** (0.81 g, 3.39 mmol) and α -methyl cysteine **292** (0.70 g, 4.06 mmol) in methanol (34 mL) was added triethylamine (0.46 mL, 3.39 mmol). The mixture was heated to 66° for 24 h, then cooled to room temperature and the solvent was removed under reduced pressure. The residue was dissolved in diethyl ether (20 mL) and a saturated aqueous solution of sodium bicarbonate (20 mL). The aqueous layer was extracted into diethyl ether (3 x 15 mL); these organic layers were then discarded. The aqueous layer was acidified to pH 2 by dropwise addition of 3N HCl, then extracted into EtOAc (3 x 20 mL). The combined organic layers were washed with brine, dried over sodium sulfate and concentrated to give **294** as a light brown foam (0.61 g, 51%). (TLNII-169) $[\alpha]_D = -21$, $c = 1$ in methanol. $^1\text{H NMR}$ (300 MHz) (CDCl_3) δ TMS: 1.45 (9H, s); 1.68 (3H, s); 3.30 (1H, d, $J = 11.07$); 3.90 (1H, d, $J = 11.4$); 4.62 (2H, d, $J = 6.0$); 4.89 (1H, s); 8.02 (1H, s); 9.91 (1H, bs).

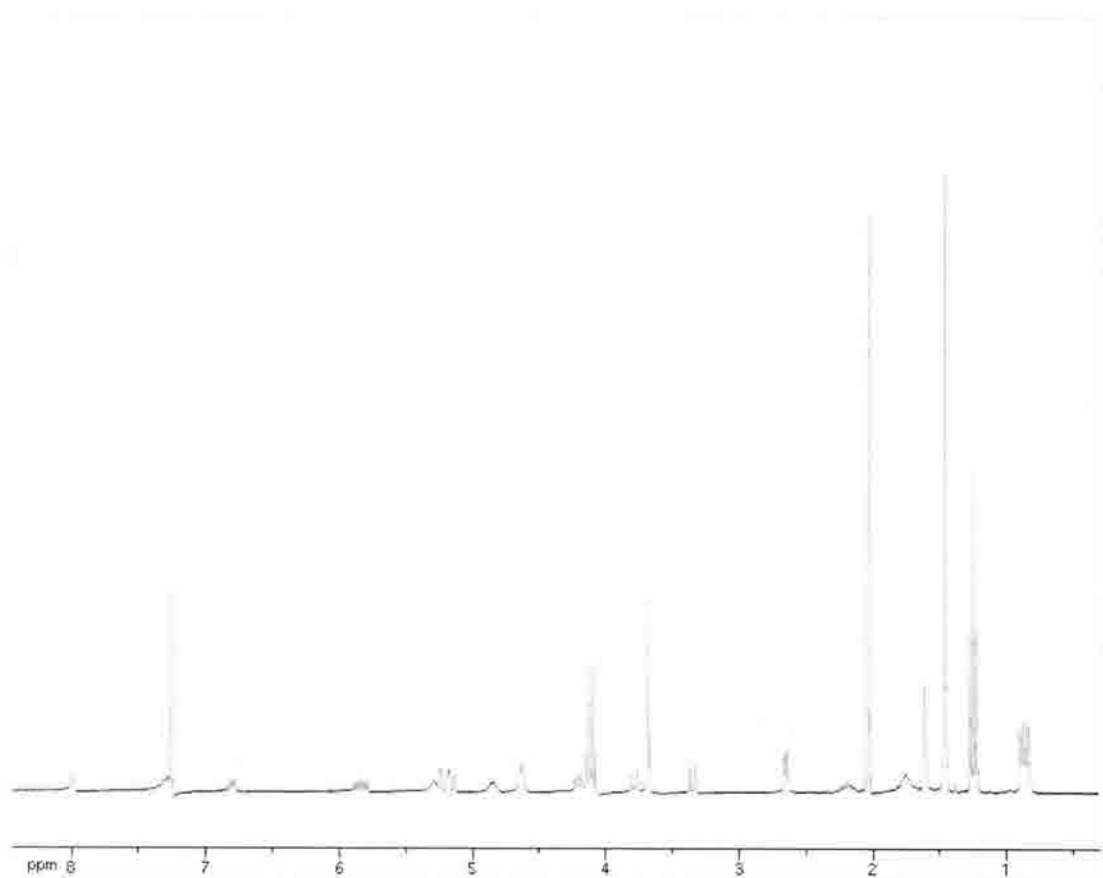


(S)-methyl 3-((S)-2-((R)-2-(2-((tert-butoxycarbonylamino)methyl)thiazol-4-yl)-4-methyl-4,5-dihydrothiazole-4-carboxamido)-3-methylbutanamido)pent-4-enoate
(362)

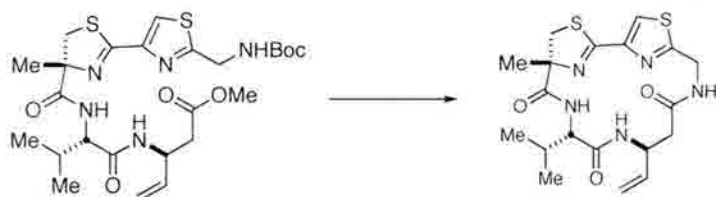


A solution of *N*-Boc amine **361** (0.18 g, 0.548 mmol) in DCM (18 mL) was cooled to 0°. TFA (1.8 mL) was added dropwise. The mixture was stirred at room temperature for 2 h, followed by evaporation of the solvent under reduced pressure. The residue was re-dissolved in toluene and re-concentrated.

To a solution of acid **294** (0.196 g, 0.548 mmol) in DCM (3 mL) was added EDCI (0.13 g, 0.66 mmol), followed by diisopropylethylamine (0.30 mL, 1.64 mmol). After 10 min, amine **x** (0.548 mmol) in DCM (3 mL) was added dropwise. The reaction was stirred for a further 15 h, and a saturated aqueous solution of ammonium chloride (10 mL) was added. The aqueous layer was extracted into DCM (3 x 6 mL). The combined organic layers were washed with brine, dried over sodium sulfate and concentrated. The residue was purified by column chromatography (1:1 to 2:1 EtOAc/hexanes) to give **362** as a light yellow foam (0.17 g, 55%). HRMS (ESI): *m/z* calcd. for C₂₅H₃₇N₅NaO₆S₂ (M + Na)⁺ 590.2077, found 590.207. ¹H NMR (300 MHz) (CDCl₃) δ TMS: 0.83 (3H, d, *J* = 6.9); 0.88 (3H, d, *J* = 6.9); 1.47 (9H, s); 2.65 (2H, d, *J* = 4.5); 3.34 (1H, d, *J* = 11.7); 3.69 (3H, s); 3.77 (1H, d, *J* = 11.7); 4.19-4.24 (2H, m); 4.63 (2H, d, *J* = 5.4); 4.85 (1H, bs); 5.14-5.30 (3H, m); 5.85 (H, ddd, *J* = 5.7, 10.5, 15.9); 6.81 (1H, d, *J* = 8.7); 7.99 (1H, s). (TLNII-228pp)



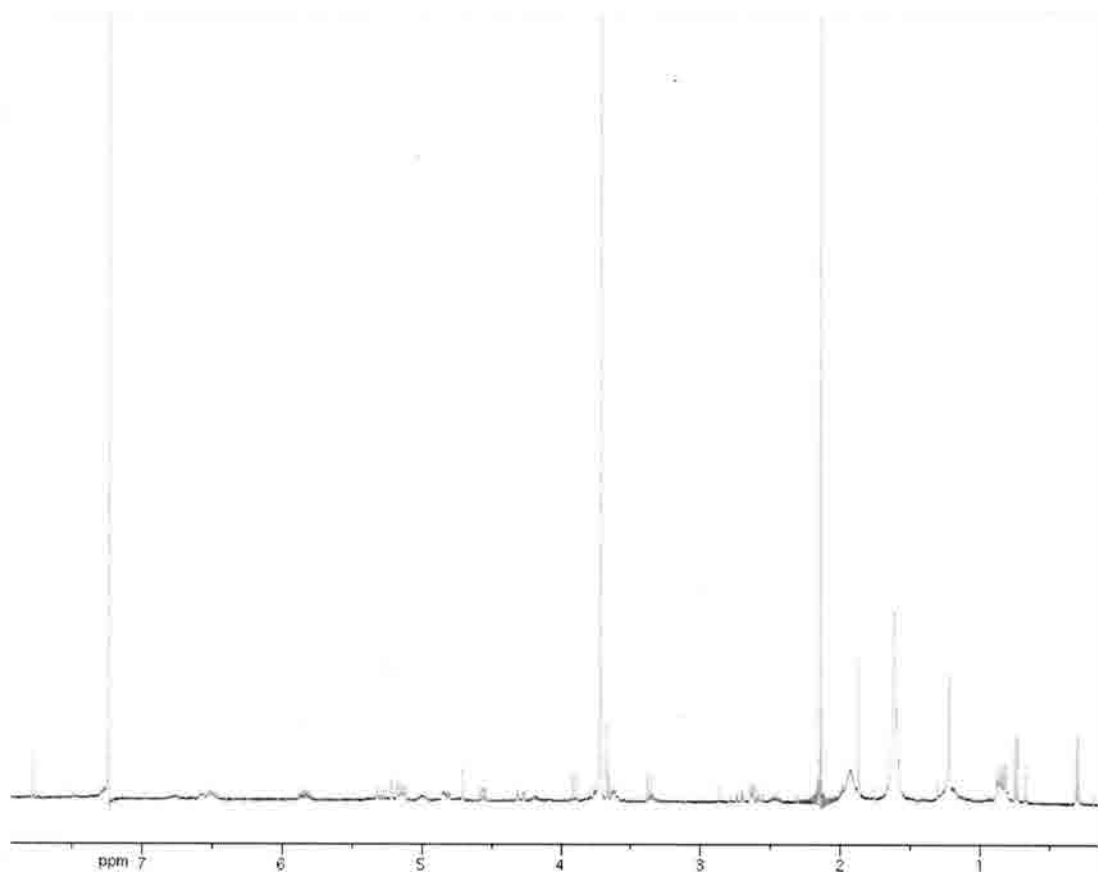
Amide isostere core (364)



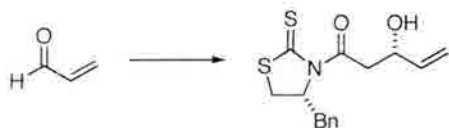
To a solution of methyl ester **362** (0.05 g, 0.088 mmol) in water (1 mL) and THF (2 mL) was added LiOH (0.06 g, 0.264 mmol). The mixture was stirred for 40 min, then quenched with 1N HCl. The aqueous layer was extracted into DCM (3 x 3 mL). The combined organics were washed with brine, dried over sodium sulfate and concentrated. The residue was dissolved in DCM (3 mL) and cooled to 0°. TFA (0.3 mL) was added dropwise, and the mixture was stirred at room temperature for 2 h. The solvent was removed under reduced pressure; toluene (3 mL) was added and the solvent again removed under reduced pressure.

The residue was dissolved in DCM (2.5 mL) and added slowly to a mixture of diisopropylethylamine (0.09 mL, 0.53 mmol) in MeCN (10 mL) at 0°. This mixture was added over 10 hours *via* syringe pump to a mixture of HOBt (0.024 g, 0.176 mmol), HATU (0.067 g, 0.176 mmol) and diisopropylethylamine (0.09 mL, 0.53 mmol) in MeCN (78 mL). Following addition, the reaction was stirred for a further 7 h. The solvent was evaporated under reduced pressure, and the residue purified on the chromatotron (DCM to 30:1 DCM/MeOH) to give **364** as a light brown foam (.040 g, 44%). HRMS (ESI): m/z calcd. for $C_{22}H_{21}N_5NaO_3S$ ($M + Na$)⁺ 458.1257, found 458.1259. ¹H NMR (400 MHz) (CDCl₃) δ TMS: 0.30 (3H, d, $J = 6.8$); 0.74 (3H, d, $J = 6.8$); 2.55-2.75 (3H, m); 3.35 (1H, d, $J = 11.6$); 3.72 (3H, s); 3.89 (1H, d, $J = 11.6$); 4.27 (1H, dd, $J = 3.2$,

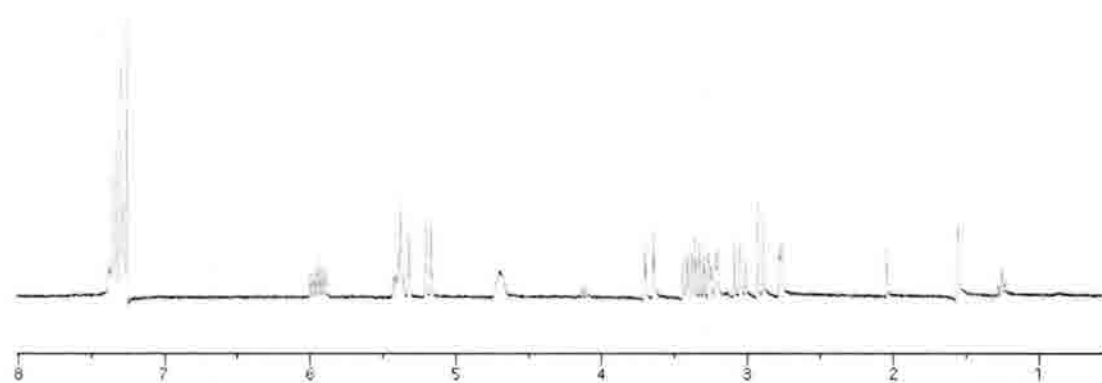
17.6); 4.55 (1H, dd, $J = 3.2, 10.8$); 4.80-4.86 (1H, m); 5.00 (1H, bs); 5.12-5.32 (3H, m);
5.85 (1H, dd, $J = 5.2, 15.6, 17.2$); 6.47-6.59 (3H, m); 6.73 (1H, m); 7.77 (1H, s). (TLNII-
236_400)



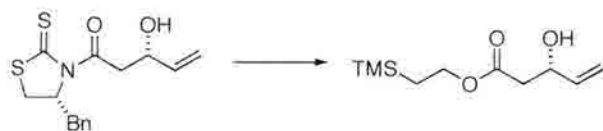
(S)-1-((R)-4-benzyl-2-thioxothiazolidin-3-yl)-3-hydroxypent-4-en-1-one (373)



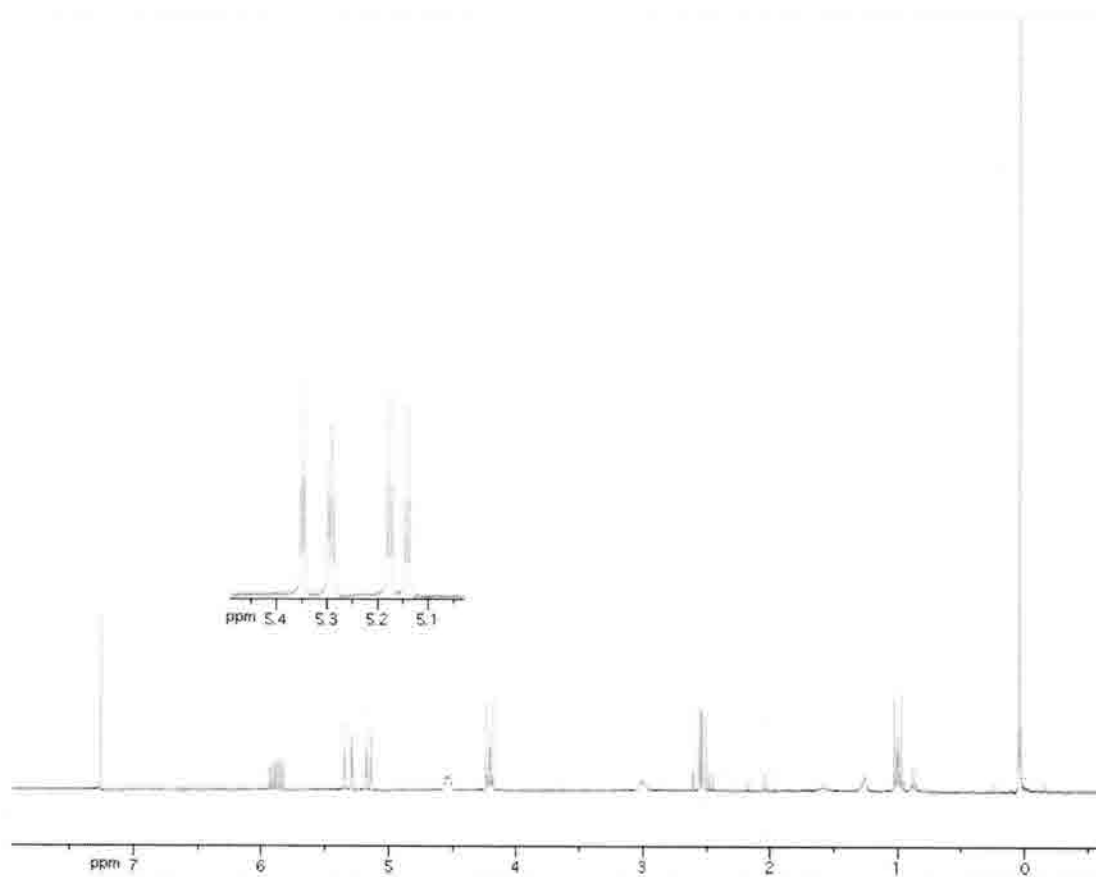
Thiazolidinone-thione **372** (1.0 g, 3.98 mmol) in DCM (25 mL) was cooled to 0°. Titanium tetrachloride (0.46 mL, 4.3 mmol) was added dropwise. After 5 min, the reaction was cooled to -78°, and diisopropylethylamine (0.75 mL, 4.3 mmol) was added dropwise. The mixture was stirred at -78° for 2 h, after which acrolein (0.25 mL, 3.31 mmol) in DCM (15 mL) was added dropwise. The mixture was stirred for 1 h; then a saturated aqueous solution of ammonium chloride (25 mL) was added. The reaction was warmed to room temperature, and the aqueous layer was extracted into DCM (3 x 20 mL). The combined organic layers were washed with brine, dried over sodium sulfate and concentrated. The residue was purified by column chromatography (10:1 to 4:1 hexanes/EtOAc) to give **373** as a yellow oil (0.58g, 57%). ¹H NMR (300 MHz) (CDCl₃) δ TMS: 2.77 (1H, d, *J* = 4.2); 2.89 (1H, d, *J* = 11.4); 3.05 (1H, m); 3.20-3.44 (3H, m); 3.65 (1H, dd, *J* = 3.0, 17.7); 4.69 (1H, m); 5.17-5.43 (3H, m); 5.95 (ddd, *J* = 5.4, 10.5, 17.4); 7.28-7.38 (5H, m). (TLNII-262a)



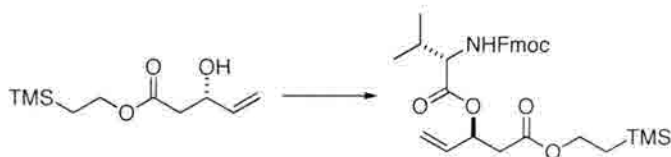
(S)-2-(trimethylsilyl)ethyl 3-hydroxypent-4-enoate (374)



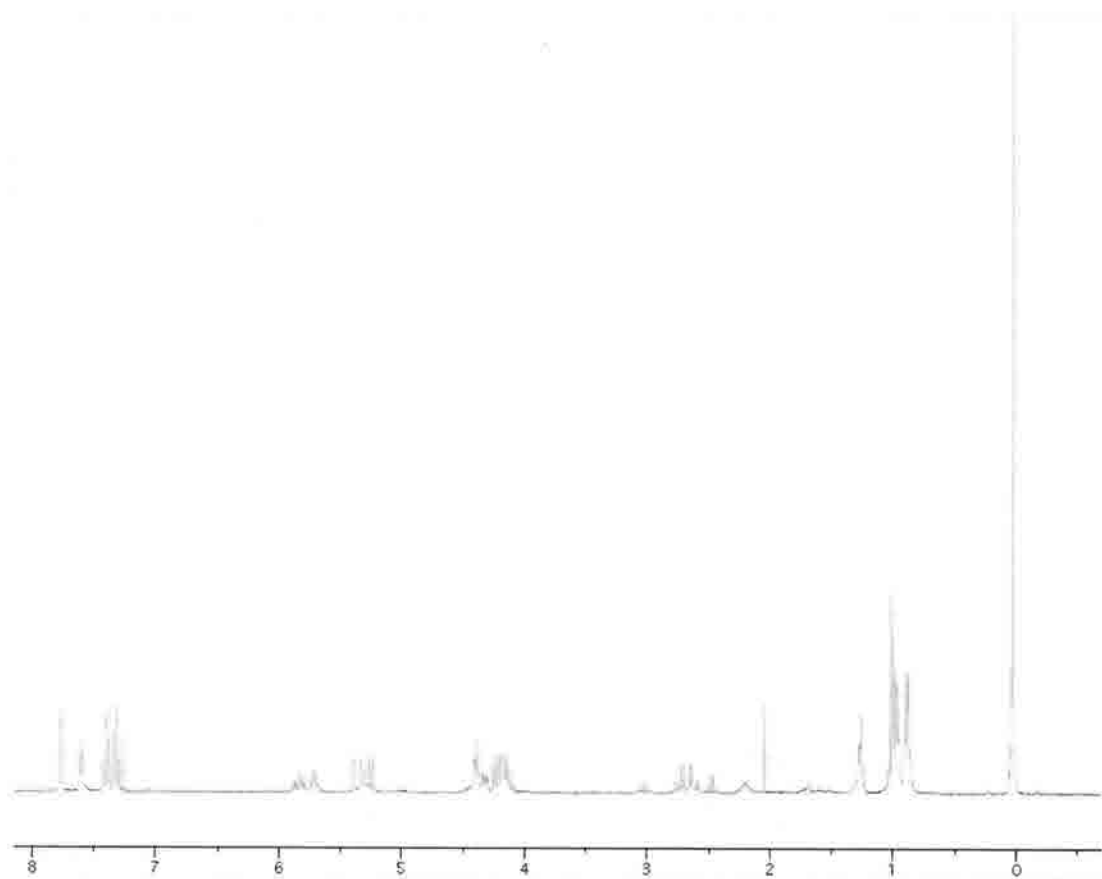
To a stirred solution of **373** (0.58 g, 1.89 mmol) in DCM (20 mL) was added 2-trimethylsilyl ethanol (2.7 mL, 18.87 mmol), followed by imidazole (0.19 g, 2.84 mmol). The mixture was stirred for 20 h, after which the solvent was removed under reduced pressure. The residue was purified by column chromatography (10:1 to 8:1 hexanes/EtOAc) to give **374** as a yellow oil (0.31 g, 72%). $^1\text{H NMR}$ (300 MHz) (CDCl_3) δ TMS: 0.44 (9H, s); 0.97-1.03 (2H, m); 2.53 (2H, dd, $J = 4.2, 7.2$); 4.18-4.24 (2H, m); 4.51-4.56 (1H, m); 5.29 (2H, ddt, $J = 1.5, 10.5, 17.1$); 5.88 (1H, ddd, $J = 5.4, 10.5, 17.1$). (TLNII-313pp)



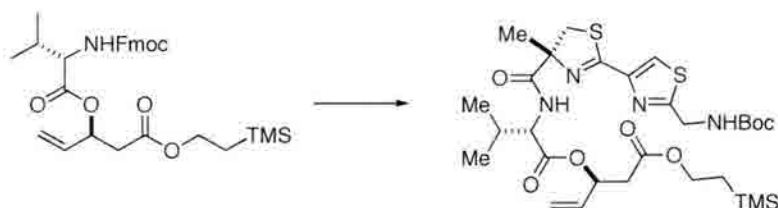
(S)-2-(trimethylsilyl)ethyl 3-((S)-2-(((9H-fluoren-9-yl)methoxy)carbonylamino)-3-methylbutanoyloxy)pent-4-enoate (375)



A solution of alcohol **374** (0.31 g, 1.35 mmol) and *N*-Fmoc-L-valine (2.28 g, 6.73 mmol) in DCM (20 mL) was cooled to 0°. EDCI (1.55 g, 8.1 mmol) and DMAP (0.015 g, 0.13 mmol) was added. The reaction was warmed to room temperature and diisopropylamine (1.4 mL, 8.1 mmol) was added. The reaction was stirred for 16 h, and the solvent removed under reduced pressure. The residue was purified by column chromatography (4:1 hexanes/EtOAc) to give **375** as a clear oil (0.29 g, 40%). (TLNII-267_end) ¹H NMR (300 MHz) (CDCl₃) δ TMS: 0.03 (9H, s); 0.88-1.03 (9H, m); 2.15-2.26 (1H, m); 2.70 (2H, dq, *J* = 7.8, 15.9); 4.11-4.41 (6H, m); 5.23-5.39 (2H, m); 5.72 (1H, q, *J* = 6.6); 5.84 (1H, ddd, *J* = 6.9, 10.5, 17.1); 7.32 (2H, t, *J* = 7.5); 7.40 (2H, t, *J* = 7.5); 7.62 (2H, d, *J* = 7.2); 7.78 (2H, d, *J* = 7.8). (TLNII-267_end)



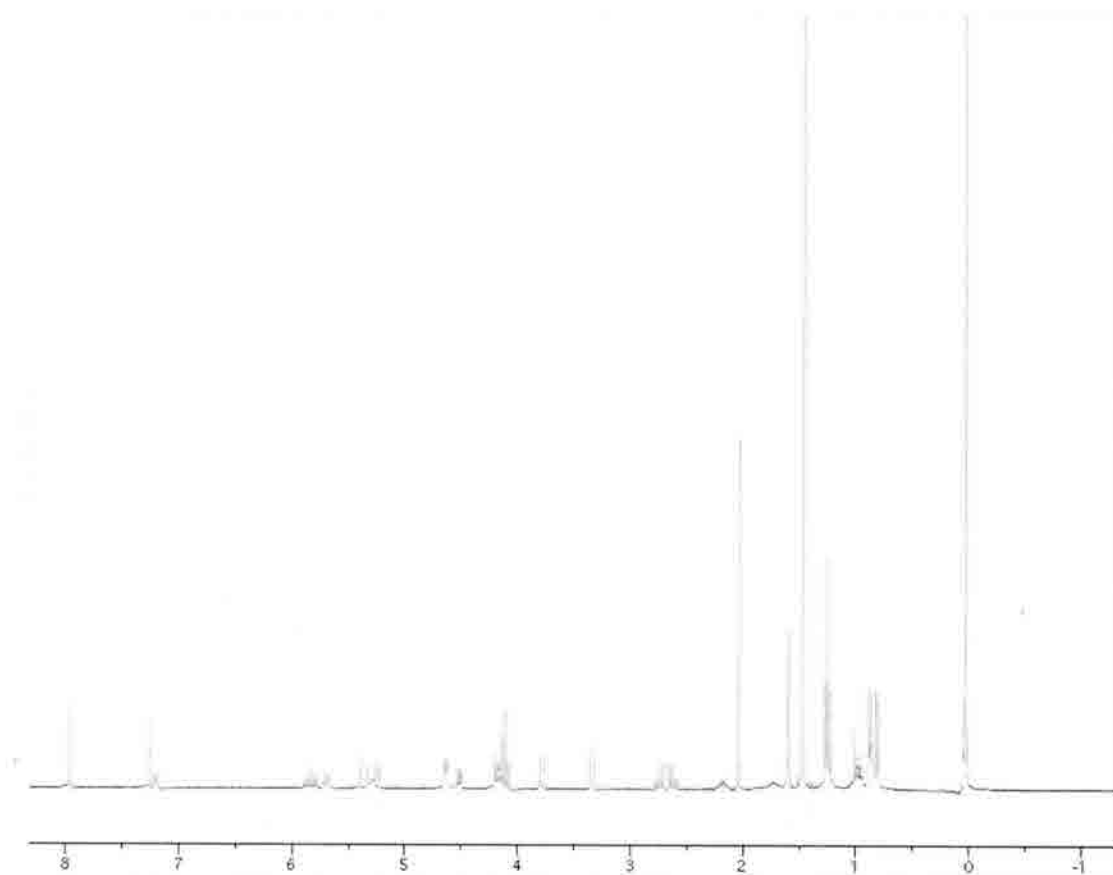
**(*S*)-2-(trimethylsilyl)ethyl 3-((*S*)-2-((*R*)-2-(2-((*tert*-
butoxycarbonylamino)methyl)thiazol-4-yl)-4-methyl-4,5-dihydrothiazole-4-
carboxamido)-3-methylbutanoyloxy)pent-4-enoate (**376**)**



N-Fmoc amine **375** (0.29 g, 0.54 mmol) was dissolved in MeCN (6 mL) and diethylamine (2.4 mL) was added. The mixture was stirred for 2.5 h, after which the solvent was removed under reduced pressure. The residue was re-dissolved in EtOAc and concentrated again to give the free amine of **375**.

Acid **294** (0.19 g, 0.54 mmol) was dissolved in DCM (9 mL). PyBop (0.56 g, 1.08 mmol) was added, followed by diisopropylamine (0.28 mL, 1.62 mmol). After 5 min, the amine in MeCN (4.5 mL) was added dropwise. The resulting mixture was stirred for 2 h, after which the solvent was removed under reduced pressure and the residue purified by column chromatography (1:1 hexanes/EtOAc) to give **376** as a clear oil (0.84 g, 77%).

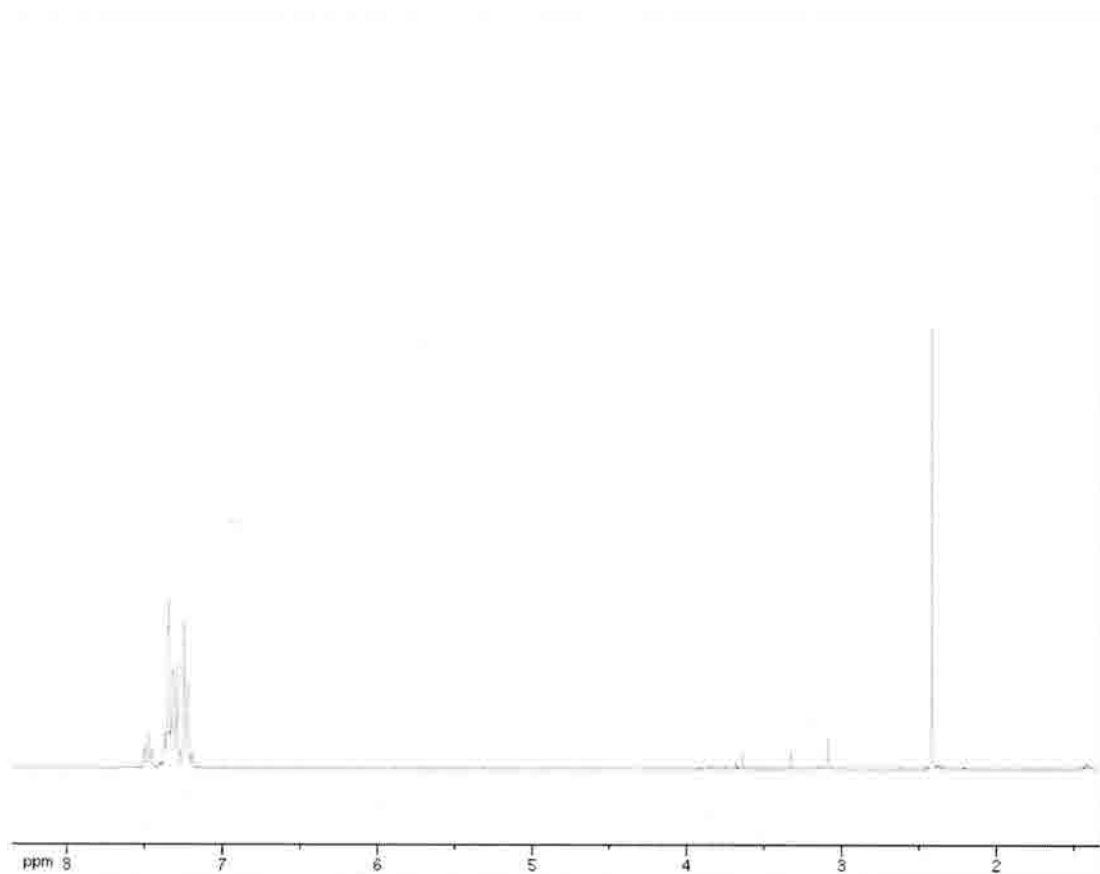
¹H NMR (300 MHz) (CDCl₃) δ TMS: 0.03 (9H, s); 0.80 (3H, d, *J* = 6.9); 0.86 (3H, d, *J* = 6.9); 0.95-1.01 (3H, m); 1.47 (9H, s); 1.60 (3H, s); 2.13-2.23 (1H, m); 2.65 (2H, dq, *J* = 7.5, 15.9); 3.31 (1H, d, *J* = 11.7); 3.76 (1H, d, *J* = 11.7); 4.15-4.20 (2H, m); 4.51 (1H, dd, *J* = 4.8, 9.0); 4.62 (2H, d, *J* = 6.3); 5.23-5.39 (3H, m); 5.68 (1H, q, *J* = 6.9); 5.84 (1H, ddd, *J* = 6.9, 10.5, 17.1); 7.19 (1H, d, *J* = 8.7); 7.97 (1H, s). (TLNII-273pp)



2-(tritylthio)acetic acid (378)



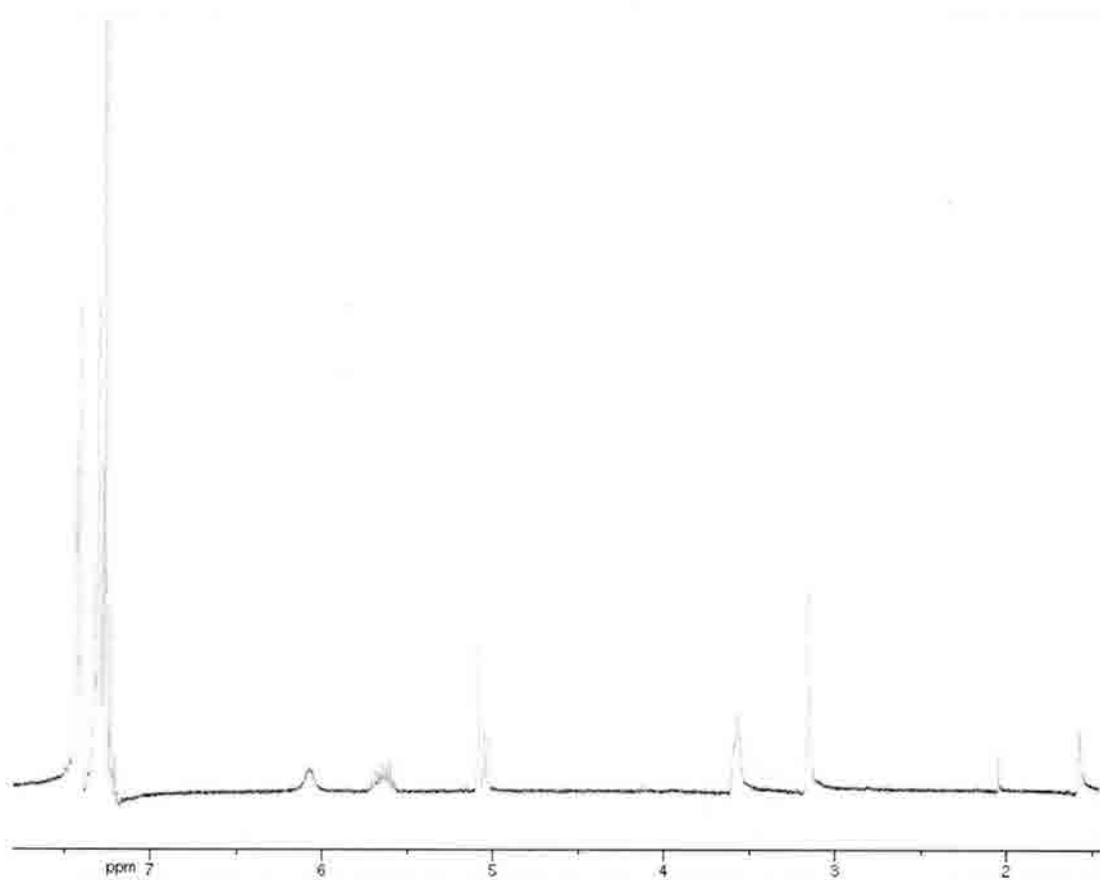
To a solution of trityl chloride (2.21 g, 7.94 mmol) in toluene (18 mL) was added triethylamine (1.1 mL, 7.94 mmol). Mercaptoacetic acid (0.5 mL, 7.22 mmol) was added dropwise, and the mixture stirred for 3 hours. The solvent was evaporated under reduced pressure. The residue was redissolved in dichloromethane, washed once with water, once with brine and dried over sodium sulfate. The solvent was evaporated and the resultant white solid recrystallized from toluene to give the trityl protected product in quantitative yield (2.40 g). ¹H NMR (300 MHz, CDCl₃) δ: 2.36 (2H, s); 7.17-7.24 (4H, m); 7.28-7.43 (11H, m). (TLNII-337)



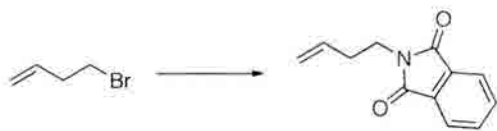
***N*-allyl-2-(tritylthio)acetamide (370)**



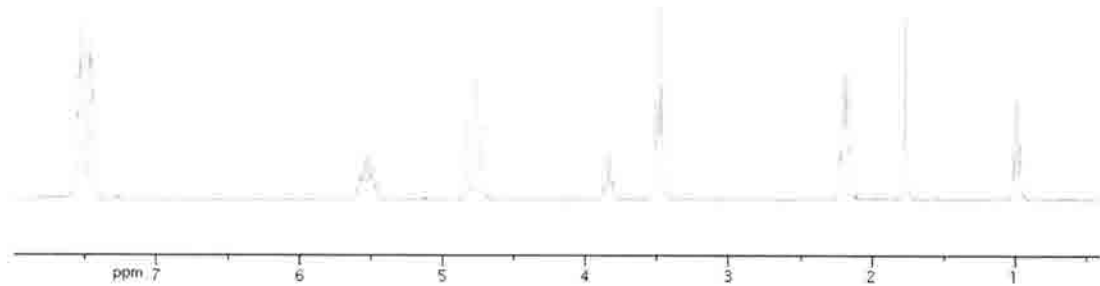
To a solution of *S*-trityl protected acid **378** (1.12 g, 3.35 mmol) in DCM (33 mL) was added PyBop (3.49 g, 6.7 mmol), followed by diisopropylethylamine (1.75 mL, 10.05 mmol). After 5 min, allylamine (0.3 mL, 4.02 mmol) was added dropwise. The mixture was stirred for 2 h, after which the solvent was evaporated and the residue purified by column chromatography (1:4 EtOAc/hexanes) to give **370** (0.38 g, 30%). HRMS (ESI): m/z calcd. for $C_{24}H_{23}NNaOS$ ($M + Na$)⁺ 396.1393, found 396.1383. ¹H NMR (300 MHz, CDCl₃) δ TMS: 3.16 (2H, s); 3.57 (2H, m); 5.05 (2H, dd, $J = 7.2, 10.5$); 5.64 (1H, ddd, $J = 5.7, 11.1, 27.3$); 6.08 (1H, bs); 7.21-7.23 (2H, m); 7.28-7.32 (7H, m); 7.40-7.43 (6H, m). (TLNII-417pp)



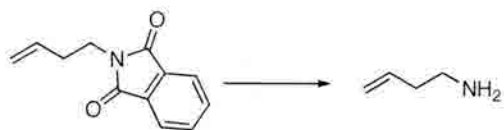
2-(but-3-enyl)isoindoline-1,3-dione (**380**)



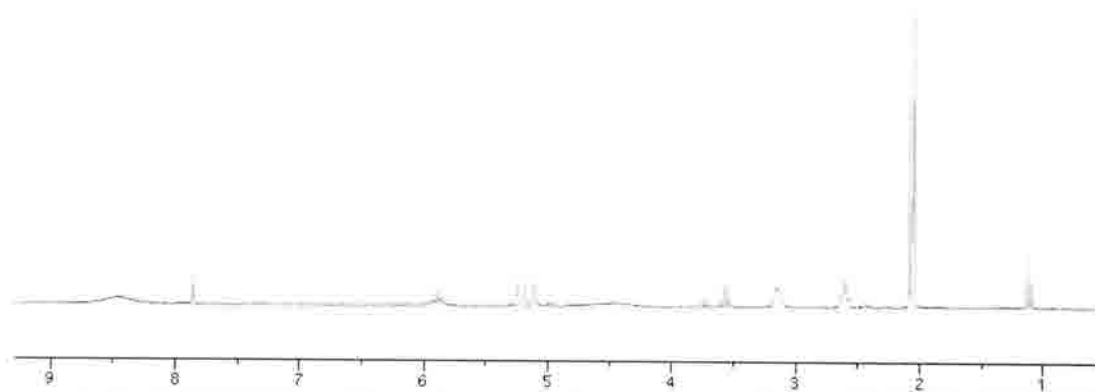
To a solution of 4-bromobutene (1.0 mL, 10.0 mmol) in DMF (40 mL) was added potassium phthalimide (2.78 g, 15.0 mmol). The mixture was heated to 110° for 12 h, after which a saturated aqueous solution of ammonium chloride (50 mL) and EtOAc (50 mL) was added. The organic layer was washed with a saturated aqueous solution of sodium bicarbonate (50 mL), followed by brine. The organic layer was dried over sodium sulfate and concentrated. The residue was purified by column chromatography (4:1 hexanes/EtOAc) to give **380** in quantitative yield (2.01 g). ¹H NMR (300 MHz, CDCl₃) δ TMS: 2.20 (2H, q, *J* = 6.9); 3.49 (2H, t, *J* = 7.2); 4.77 (2H, dd, *J* = 11.4, 18.0); 5.47-5.61 (1H, m); 7.53 (4H, d, *J* = 16.2). (TLNII-356_2-4)



but-3-en-1-amine (381)



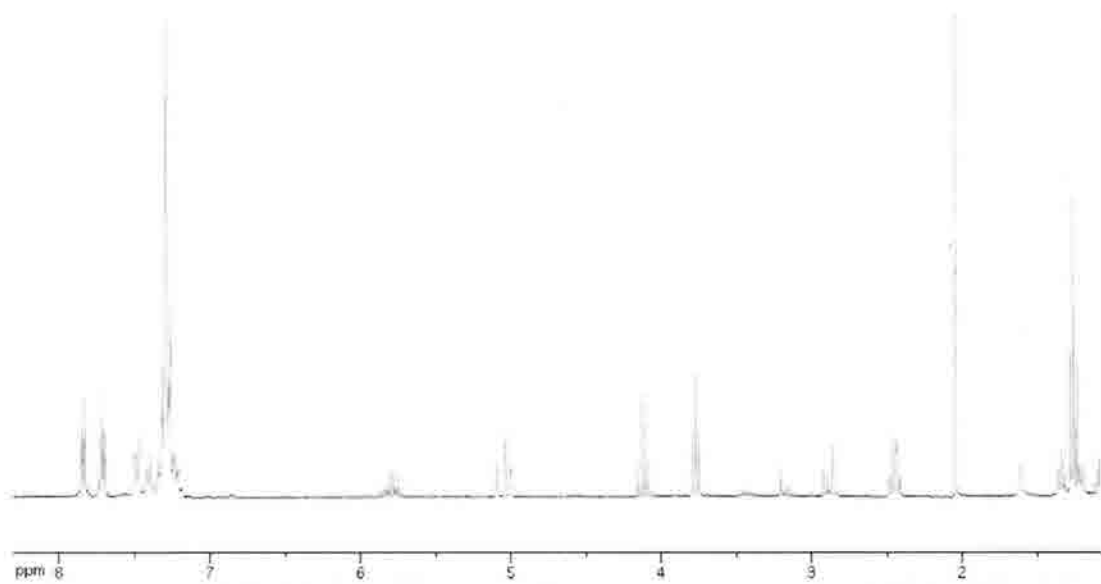
A solution of **380** (2.01 g, 9.99 mmol) in EtOH (50 mL) was heated to 50°. Hydrazine hydrate (0.62 mL, 20.0 mmol) was added. The mixture was stirred for 1 h, after which 3N HCl was added (to pH 1). The suspension was filtered through a thin pad of Celite, and the filtrate concentrated to give **381** (0.86 g, 96%). ¹H NMR (300 MHz, DMSO) δ TMS: 2.59 (2H, q, *J* = 6.9); 3.10-1.18 (2H, m); 5.18 (2H, dd, *J* = 10.2, 26.4); 5.83-5.96 (1H, m); 8.44 (2H, bs). (TLNII-359pp)



***N*-(but-3-enyl)-2-(tritylthio)acetamide (367)**



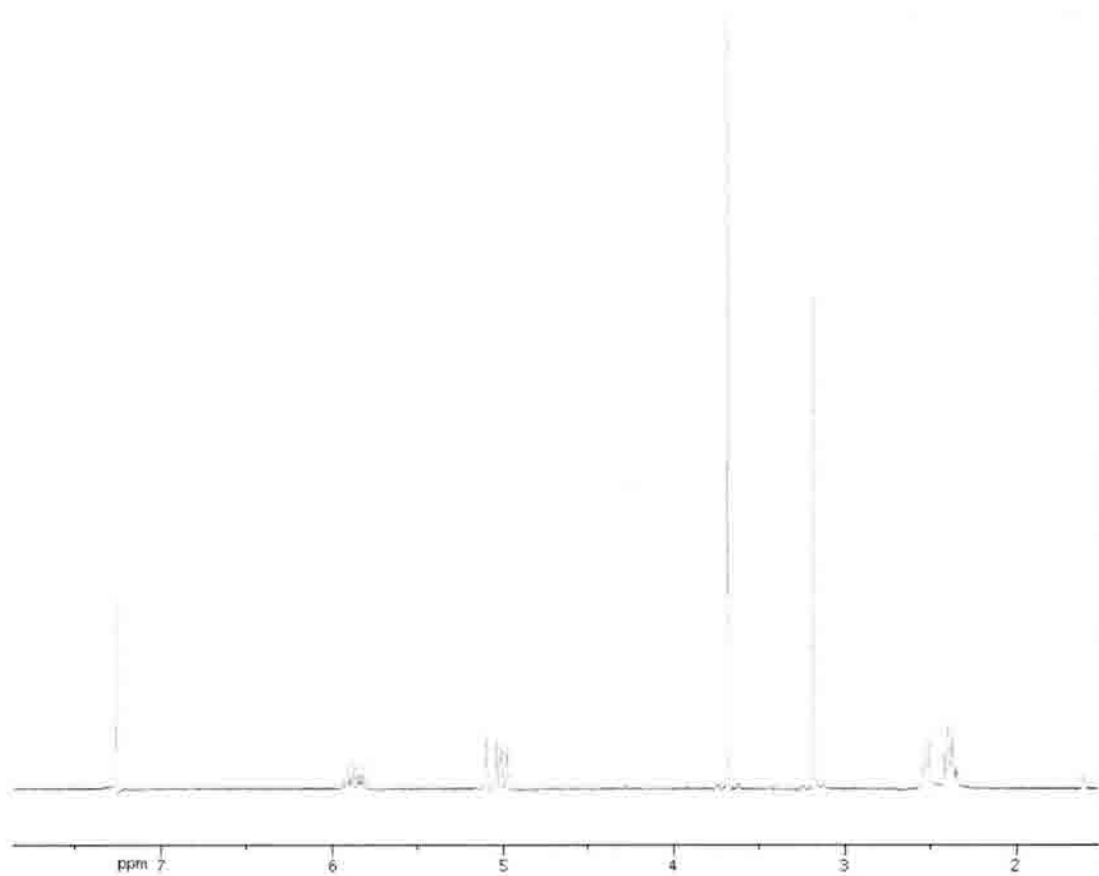
To a solution of *S*-trityl protected acid **377** (1.3 g, 4.02 mmol) in DCM (50 mL) was added EDCI (1.54 g, 8.04 mmol) followed by diisopropylethylamine (2.8 mL, 16.08 mmol). After 5 min, amine **381** (0.52 g, 4.83 mmol) was added. The mixture was stirred overnight, followed by removal of the solvent under reduced pressure. The residue was purified by column chromatography (4:1 hexanes/EtOAc) to give **381** as a brown oil (0.65 g, 42%). ¹H NMR (300 MHz, CDCl₃) δ TMS: 2.86-2.92 (2H, m); 2.44 (2H, q, *J* = 6.9); 3.77 (2H, t, *J* = 6.9); 5.00-5.10 (2H, m); 5.72-5.86 (1H, m); 7.19-7.25 (4H, m); 7.31-7.50 (7H, m); 7.70 (2H, dd, *J* = 3.0, 5.4); 7.83 (2H, dd, *J* = 3.3, 5.4). (TLNII-360pp)



***N*-methoxy-*N*-methylpent-4-enamide (383)**



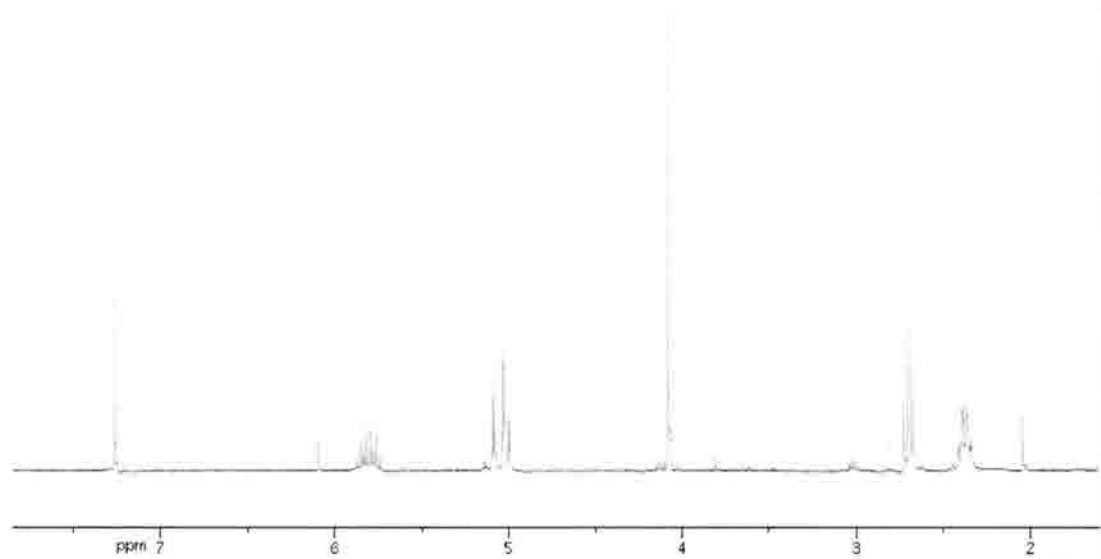
To a stirred solution of pentenoic acid (2.0 mL, 19.6 mmol) in DCM (100 mL) was added EDCI (6.25 g, 32.6 mmol), followed by diisopropylethylamine (8.5 mL, 48.9 mmol). After 5 min, *N,O*-dimethylhydroxylamine hydrochloride (1.59 g, 16.3 mmol) was added. The mixture was stirred for 15 h, after which a saturated aqueous solution of ammonium chloride (50 mL) was added. The aqueous layer was extracted into DCM (3 x 20 mL), and the combined organic layers were washed with brine, dried over sodium sulfate and concentrated. The residue was purified by column chromatography (1:1 EtOAc/hexanes) to give **383** as a light yellow oil (1.06 g, 45%). ¹H NMR (300 MHz, CDCl₃) δ TMS: 2.35-2.42 (2H, m); 2.50-2.55 (2H, m); 3.18 (3H, s); 3.68 (3H, s); 4.97-5.11 (2H, m); 5.80-5.93 (1H, m). (TLNII-419)



1-chlorohex-5-en-2-one (384)



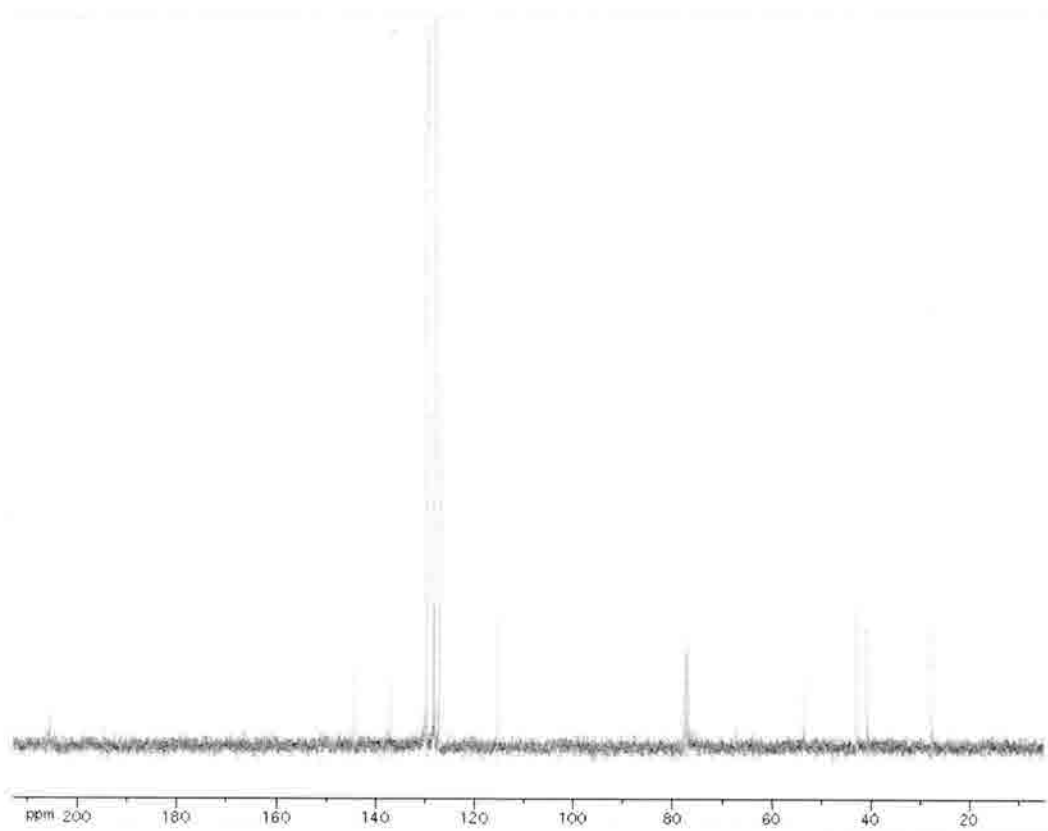
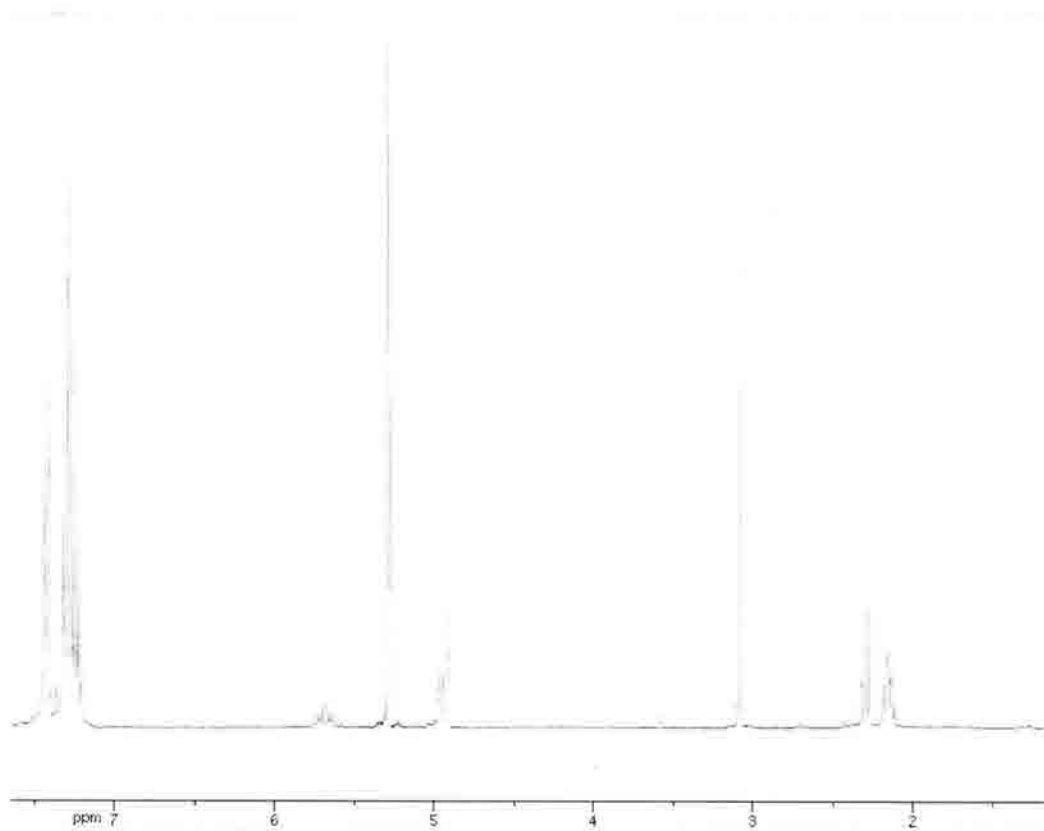
A solution of **383** (1.06 g, 7.4 mmol) and chloriodomethane (1.0 mL, 14.8 mmol) in THF (35 mL) was cooled to -78° . Methylolithium (1.6M in hexanes, 7 mL, 11.1 mmol) was added over 40 min *via* syringe pump. The reaction was stirred for a further 30 min, after which a saturated aqueous solution of ammonium chloride (30 mL) was added and the reaction was warmed to room temperature. The aqueous layer was extracted into diethyl ether (3 x 30 mL), and the combined organic layers were washed with brine, dried over sodium sulfate and concentrated. The residue was purified by column chromatography (10:1 to 4:1 hexanes/EtOAc) to give **384** as a dark red oil which was used immediately in the next step (0.53 g, 95%). $^1\text{H NMR}$ (300 MHz, CDCl_3) δ TMS: 2.34-2.41 (2H, m); 2.71 (2H, t, $J = 7.2$); 4.08 (2H, s); 4.99-5.10 (2H, m); 5.74-5.88 (1H, m). (TLNII-421)



1-(tritylthio)hex-5-en-2-one (368)



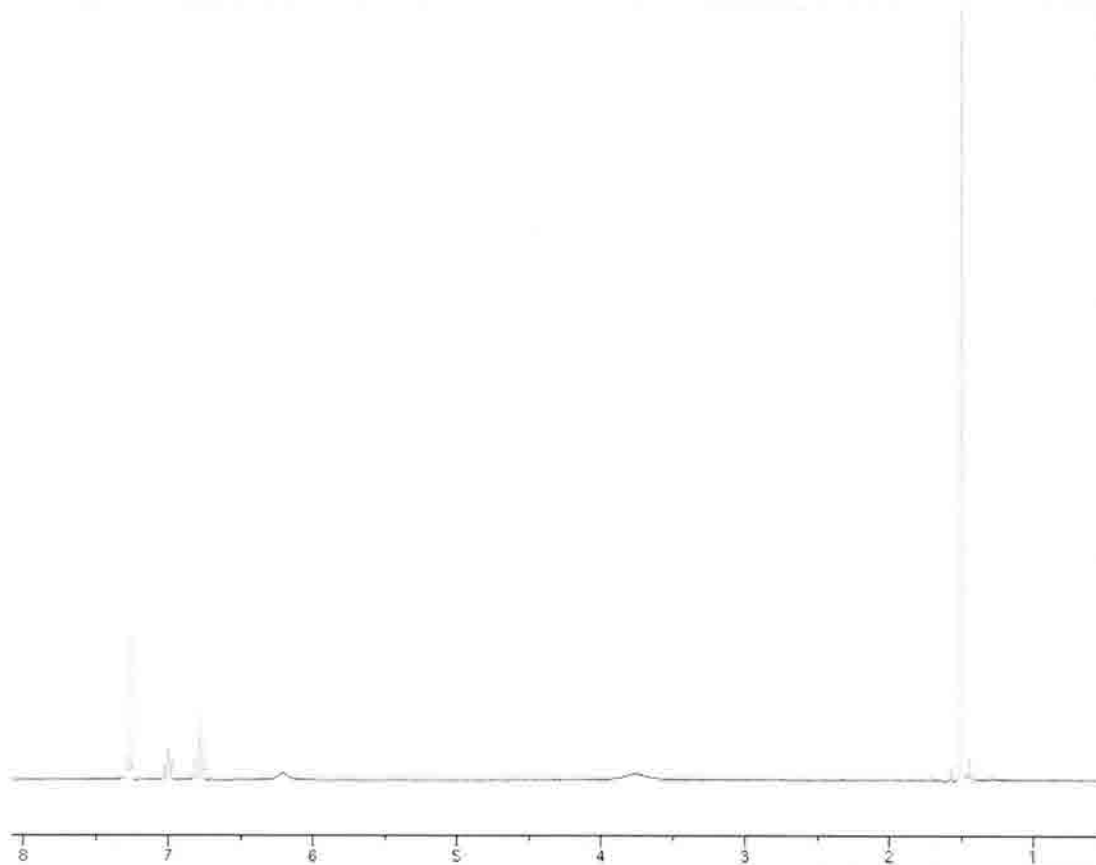
To a solution of triphenylmethanethiol (1.1 g, 4.0 mmol) in DMF (10 mL) was added potassium *t*-butoxide (0.45 g, 4.0 mmol). This mixture was then added dropwise to a solution of **384** (0.53 g, 4.0 mmol) in DMF (30 mL). The mixture was stirred for 3 h, then poured onto H₂O (50 mL). The aqueous layer was extracted into EtOAc (3 x 20 mL) and the combined organic layers were washed with brine, dried over sodium sulfate and concentrated. The residue was purified by column chromatography (1:4 EtOAc/hexanes) to give **368** as a light orange oil. ¹H NMR (300 MHz, CDCl₃) δ TMS: 2.11-2.18 (2H, m); 2.27-2.32 (2H, m); 3.08 (2H, s); 4.91-4.97 (2H, m); 5.62-5.75 (1H, m); 7.21-7.32 (10H, m); 7.42-7.44 (5H, m). (TLNII-420a) ¹³C NMR (75.5 MHz, CDCl₃) δ TMS: 27.9, 40.8, 42.9, 53.7, 115.5, 127.2, 128.3, 129.8, 136.9, 144.4, 205.5. (TLNII-420_c13)



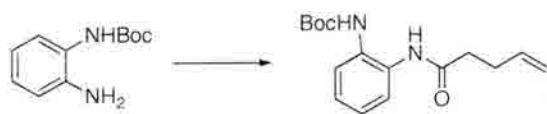
***tert*-butyl 2-aminophenylcarbamate (**386**)**



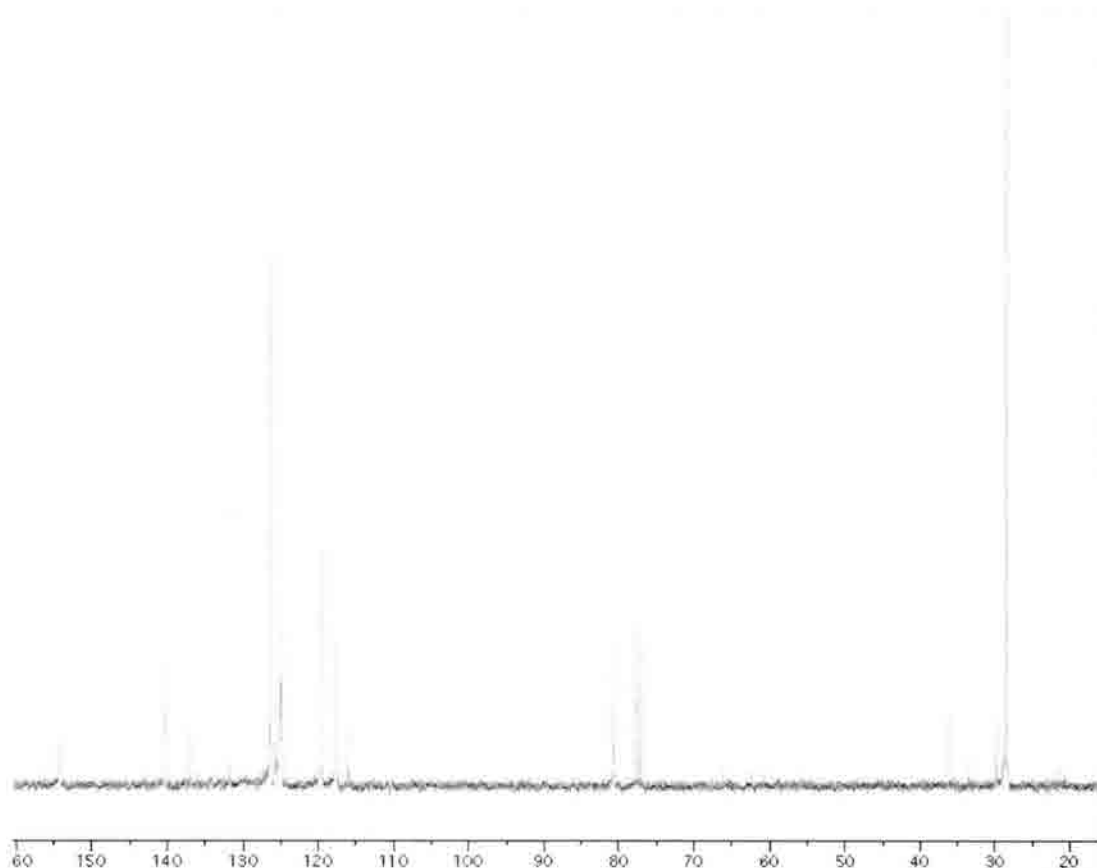
To a solution of benzene-1,2-diamine **385** (1.0 g, 9.24 mmol) in THF (92 mL) was added Boc_2O (2.02 g, 9.24 mmol) and DMAP (0.10 g, 0.90 mmol). The mixture was stirred overnight and washed with a saturated aqueous solution of ammonium chloride. The organic layer was dried over sodium sulfate and concentrated. The residue was recrystallized (EtOAc/hexanes) to give **386** as light pink crystals (1.1 g, 57%). ^1H NMR (300 MHz, CDCl_3) δ TMS: 1.51 (9H, s); 3.75 (2H, bs); 6.20 (1H, bs); 6.79 (2H, t, $J = 7.5$); 7.00 (1H, t, $J = 7.8$). (TLNII-418_recrys)



***tert*-butyl 2-pent-4-enamidophenylcarbamate (365)**



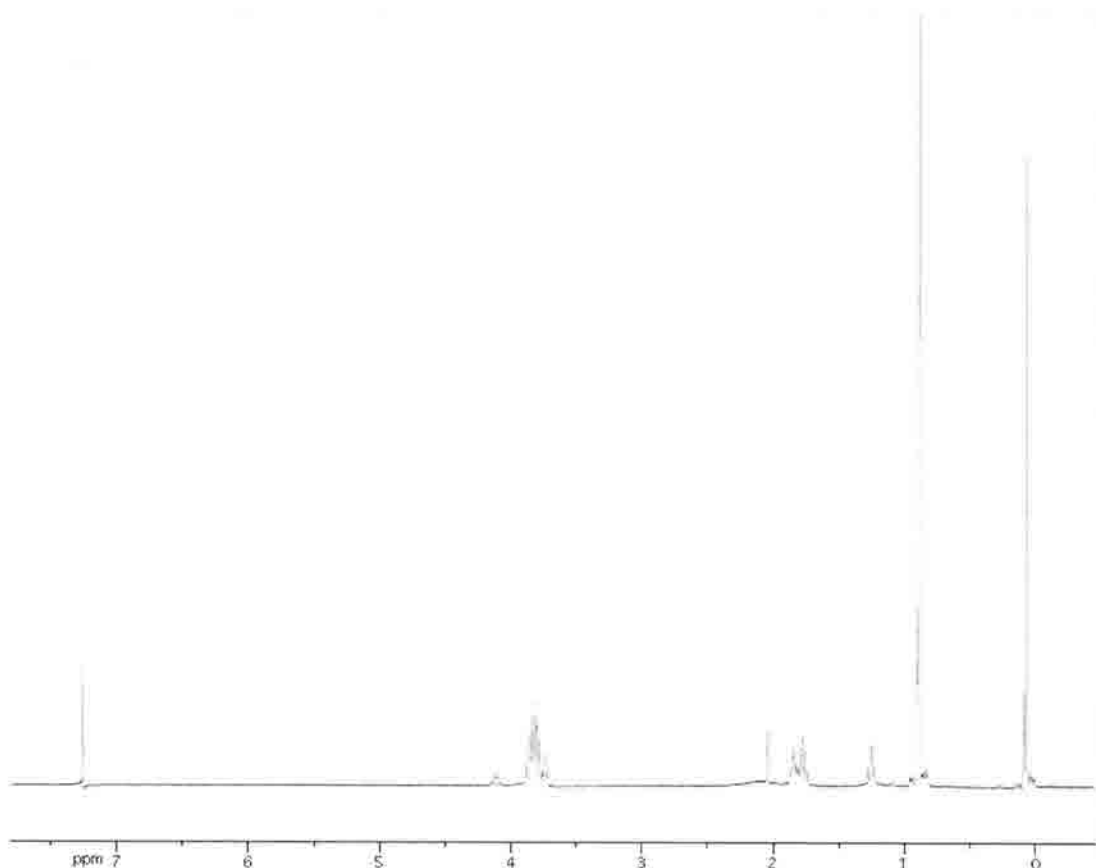
To a stirred solution of pentenoic acid (0.45 mL, 4.37 mmol) in DCM (50 mL) was added EDCI (1.84 g, 9.6 mmol), followed by diisopropylethylamine (2.3 mL, 13.1 mmol). After 5 min, amine **386** (1.0 g, 4.8 mmol) was added. The mixture was stirred for 12 h. Following removal of the solvent under reduced pressure, the residue was purified by column chromatography (1:1 EtOAc/hexanes) to give **365** as a white solid. ¹³C NMR (75.5 MHz, CDCl₃) δ TMS: 28.6, 36.2, 80.6, 117.7, 119.6, 124.9, 126.3, 137.0, 140.3, 154.3. (TLNII-426_c13)



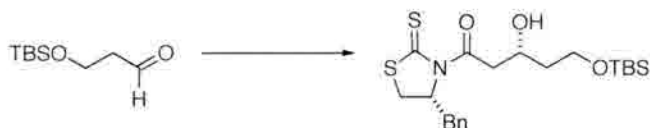
3-(*tert*-butyldimethylsilyloxy)propan-1-ol (401a)



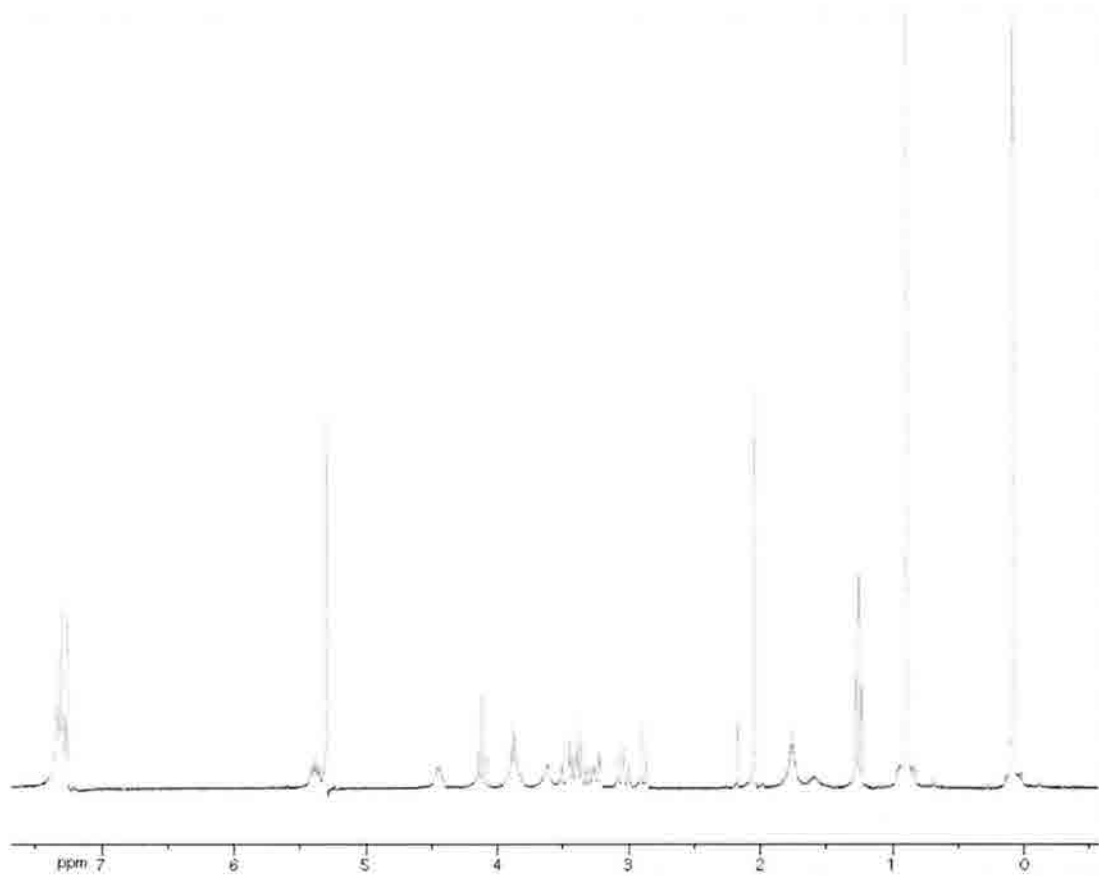
A suspension of NaH (0.53 g, 13.14 mmol) in THF (130 mL) was cooled to 0⁰. Propane diol (1.9 mL, 26.28 mmol) was added dropwise. After 10 minutes, TBSCl (1.98 g, 13.14 g) was added slowly. The mixture was stirred at room temperature for 3.5 h, after which a saturated aqueous solution of ammonium chloride (50 mL) was added. The aqueous layer was extracted into EtOAc (3 x 40 mL), and the combined organic layers were washed with brine, dried over sodium sulfate and concentrated to give **x** as a clear oil (2.3 g, 90%). ¹H NMR (300 MHz, CDCl₃) δ TMS: 0.07 (6H, s); 0.90 (9H, s); 1.78-1.85 (2H, m); 3.74-3.89 (4H, m). (TLNII-399)



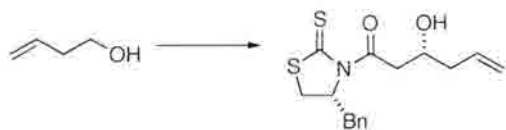
(*R*)-1-((*R*)-4-benzyl-2-thioxothiazolidin-3-yl)-5-(*tert*-butyldimethylsilyloxy)-3-hydroxypentan-1-one (403)



A solution of chiral auxiliary **372** (1.6 g, 6.37 mmol) in DCM (40 mL) was cooled to 0°. Titanium tetrachloride (0.73 mL, 6.9 mmol) was added dropwise. After 5 min, the reaction was cooled to -78°, and diisopropylethylamine (1.2 mL, 6.9 mmol) was added dropwise. The mixture was stirred for 2 h, after which the aldehyde (1.0 g, 5.31 mmol) in DCM (10 mL) was added dropwise. After stirring for 1 h, a saturated aqueous solution of ammonium chloride (40 mL) was added. The reaction was warmed to room temperature, and the aqueous layer was extracted into EtOAc (3 x 30 mL). The combined organic layers were washed with brine, dried over sodium sulfate and concentrated. The residue was purified by column chromatography (4:1 hexanes/EtOAc) to give **403** as a yellow oil (0.96 g, 42%). ¹H NMR (300 MHz, CDCl₃) δ TMS: 0.08 (6H, s); 0.89 (9H, s); 1.73-1.83 (2H, m); 2.87 (1H, d, *J* = 11.4); 3.00-3.08 (1H, m); 3.22-3.51 (4H, m); 3.81-3.94 (2H, m); 4.40-4.48 (1H, m); 5.40 (1H, ddd, *J* = 4.2, 7.2, 11.1); 7.27-7.37 (5H, m). (TLNII-402pp)



(R)-1-((R)-4-benzyl-2-thioxothiazolidin-3-yl)-3-hydroxyhex-5-en-1-one (409)

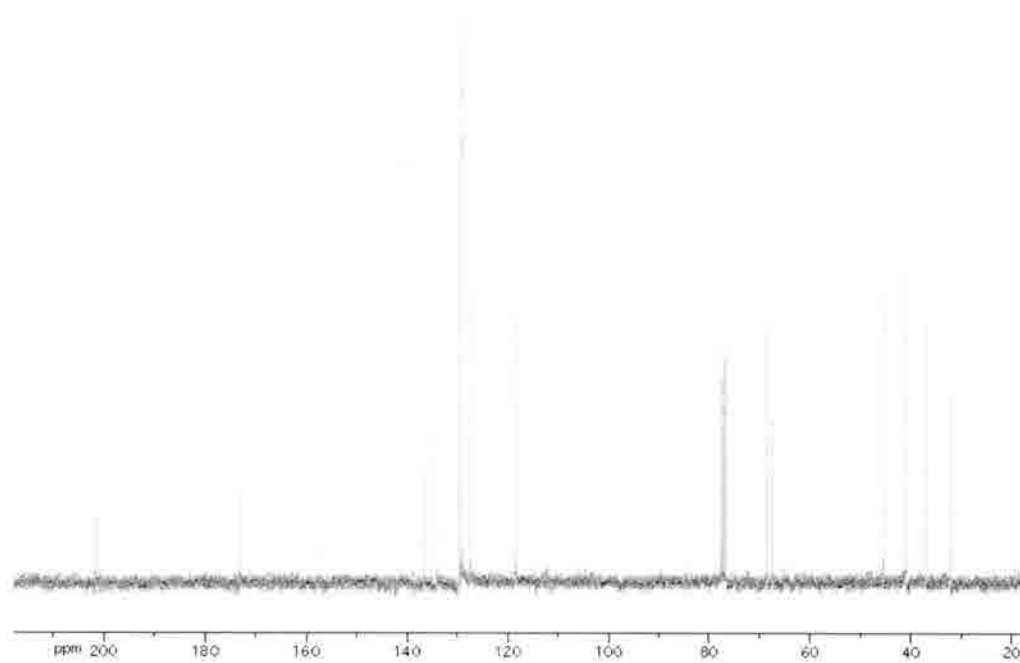
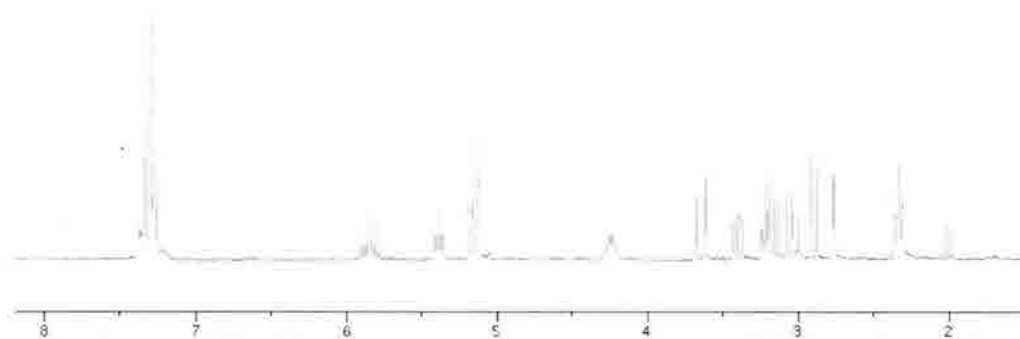


A solution of chiral auxiliary **372** (1.0 g, 3.98 mmol) in DCM (15 mL) was cooled to 0° and titanium tetrachloride (0.43 mL, 4.31 mmol) was added dropwise. After 5 min, the mixture was cooled to -78°, and diisopropylethylamine (0.75 mL, 4.31 mmol) was added dropwise. This mixture was stirred for 2 hrs.

Meanwhile, to a solution of 3-butenol (1.0 mL, 11.94 mmol) in DCM (2.4 mL) and pentane (21 mL) was added iodobenzene diacetate (4.23 g, 13.13 mmol) and TEMPO (0.19 g, 1.19 mmol). The mixture was stirred for 2.5 hours, then cooled to 0° and ice-cold saturated aqueous solution of sodium bicarbonate was added. The organic layer was washed with sodium bicarbonate solution (2 x 10 mL) and dried over magnesium sulfate for 1 min. This solution containing aldehyde **408** was used immediately.

This solution of aldehyde **408** was added dropwise to the above described mixture of chiral auxiliary, titanium tetrachloride and diisopropylethylamine. The reaction was stirred for 1 h, after which a saturated aqueous solution of ammonium chloride (30 mL) was added. The mixture was warmed to room temperature, and the aqueous layer was extracted into DCM (3 x 30 mL). The combined organic layers were washed with brine, dried over sodium sulfate and concentrated. The residue was purified by column chromatography (1:4 EtOAc/hexanes) to give **409** as a yellow oil (0.5 g, 47%). ¹H NMR (300 MHz, CDCl₃) δ TMS: 2.34 (2H, t, *J* = 6.9); 2.76 (1H, d, *J* = 3.9); 2.88 (1H, d, *J* = 11.4); 3.00-3.25 (3H, m); 3.40 (1H, dd, *J* = 7.2, 11.4); 3.62 (1H, dd, *J* = 2.4, 17.7); 4.20-4.29 (1H, m); 5.13-5.20 (2H, m); 5.39 (1H, ddd, *J* = 4.2, 7.2, 11.1); 5.78-5.92 (1H, m);

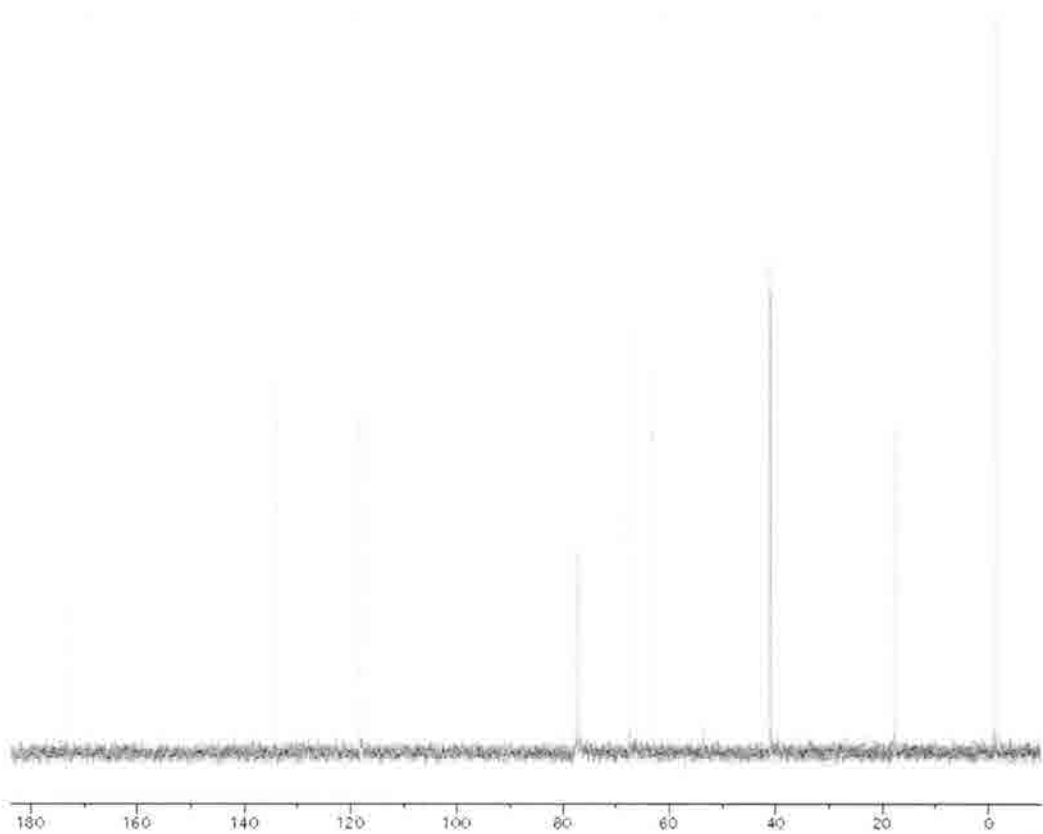
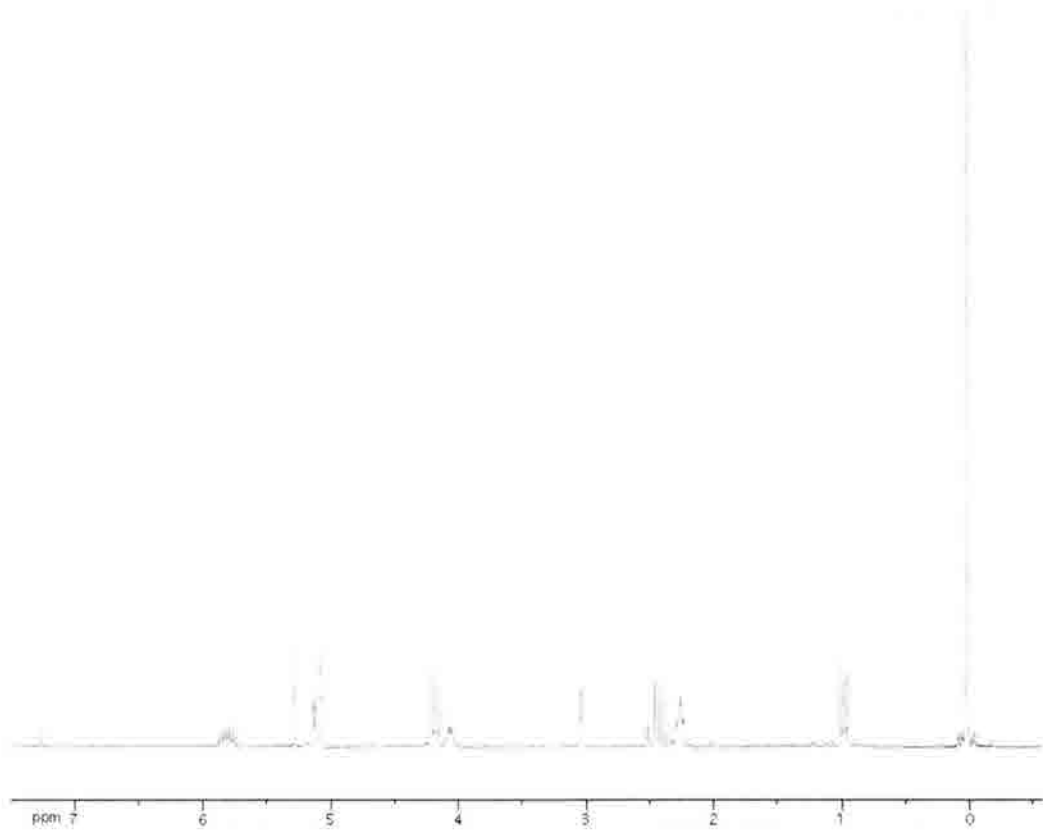
7.28-7.37 (5H, m). (TLNII-460_3) ^{13}C NMR (75.5 MHz, CDCl_3) δ TMS: 32.3, 37.0, 41.0, 45.5, 67.4, 68.6, 118.5, 127.5, 129.2, 129.7, 134.3, 136.6, 173.2, 201.6. (TLNII-460_c13)



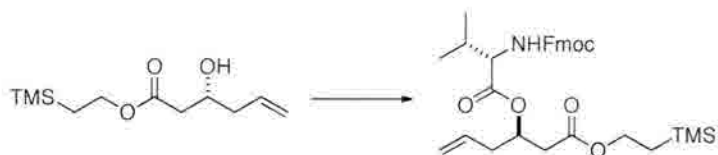
(R)-2-(trimethylsilyl)ethyl 3-hydroxyhex-5-enoate (410)



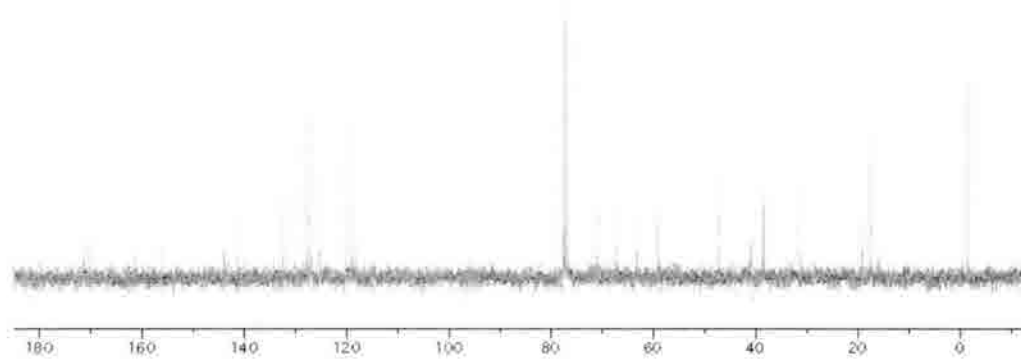
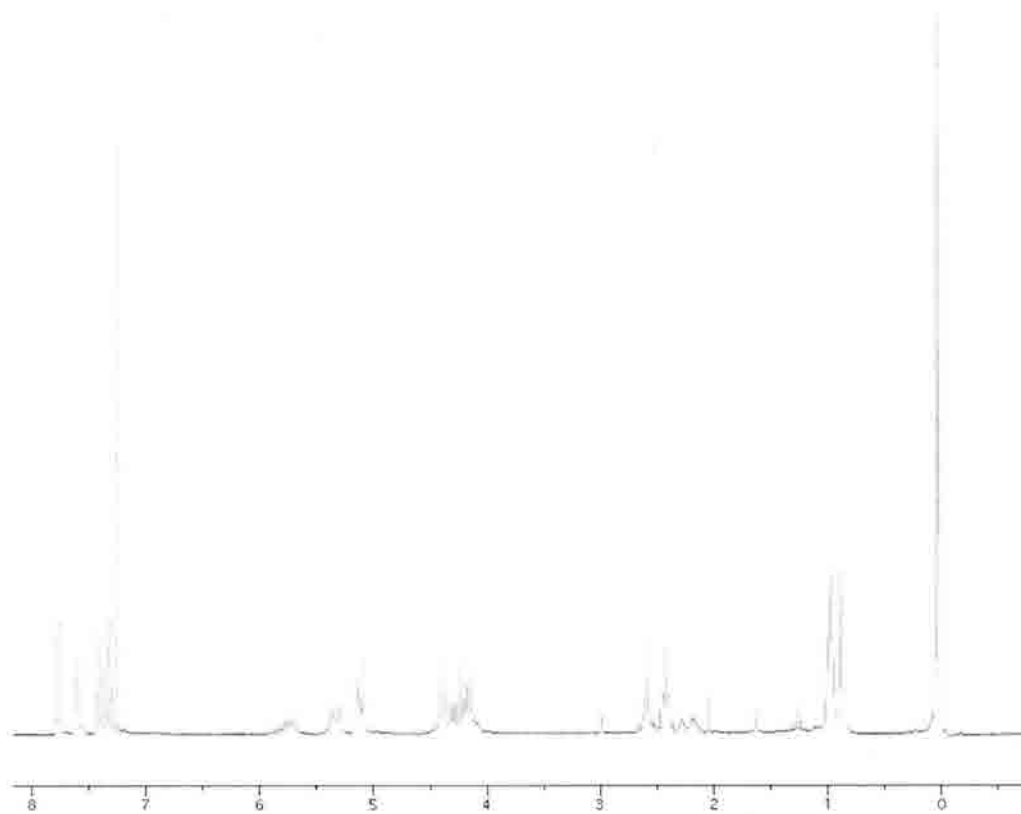
To a stirred solution of **409** (0.31 g, 0.96 mmol) in DCM (10 mL) was added 2-trimethylsilyl ethanol (1.38 mL, 9.6 mmol) and imidazole (0.16 g, 2.4 mmol). The mixture was stirred overnight, after which the solvent was removed under reduced pressure. The residue was purified by column chromatography (10:1 to 4:1 hexanes/EtOAc) to give **410** as a light yellow oil (0.13 g, 59%). $[\alpha]_D^{24}$: -7.0 (c=5 in CHCl_3). ^1H NMR (300 MHz, CDCl_3) δ TMS: 0.02 (9H, s); 0.95-1.01 (2H, m); 2.23-2.29 (2H, m); 2.37-2.52 (2H, m); 3.03 (1H, d, $J = 3.6$); 4.02-4.11 (1H, m); 4.15-4.21 (2H, m); 5.08-5.17 (2H, m); 5.74-5.88 (1H, m). (TLNII-464a). ^{13}C NMR (75.5 MHz, CDCl_3) δ TMS: -1.3, 17.5, 40.9, 41.1, 63.2, 67.5, 118.3, 134.2, 173.2. (TLNII-464a_c13)



(R)-2-(trimethylsilyl)ethyl 3-((S)-2-(((9H-fluoren-9-yl)methoxy)carbonylamino)-3-methylbutanoyloxy)hex-5-enoate (411)



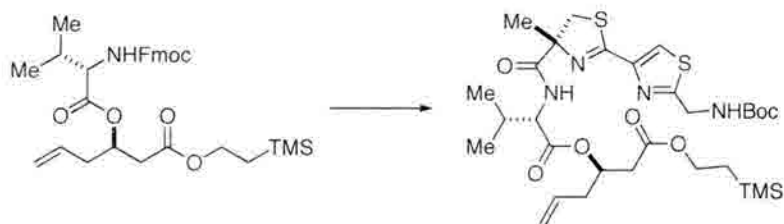
To a solution of alcohol **410** (0.13 g, 0.56 mmol) in DCM (13 mL) was added EDCI (0.64 g, 3.36 mmol) and DMAP (7 mg, 0.06 mmol), followed by diisopropylethylamine (0.59 mL, 3.36 mmol). After 5 min, *N*-Fmoc-*L*-valine (0.96 g, 2.82 mmol) was added. The mixture was stirred for 14 h, after which the solvent was removed under reduced pressure and the residue was purified by column chromatography (8:1 hexanes/EtOAc) to give **411** as a clear oil (0.21 g, 68%). HRMS (ESI): m/z calcd. for $C_{31}H_{41}NNaO_6Si$ ($M + Na$)⁺ 574.2595, found 574.2591. ¹H NMR (300 MHz, CDCl₃) δ TMS: 0.87 (3H, d, $J = 6.9$); 0.94-1.02 (4H, m); 2.25-2.31 (1H, m); 2.37-2.49 (2H, m); 2.60 (2H, t, $J = 7.2$); 4.03-4.44 (6H, m); 5.09-5.16 (2H, m); 5.29-5.39 (2H, m); 5.69-5.09 (1H, m); 7.32 (2H, t, $J = 7.2$); 7.40 (2H, t, $J = 7.5$); 7.59 (2H, d, $J = 7.2$); 7.75 (2H, d, $J = 7.2$). (TLNII-468rep) ¹³C NMR (75.5 MHz, CDCl₃) δ TMS: -1.3, 17.5, 19.3, 31.5, 38.4, 40.9, 47.4, 59.1, 63.3, 67.2, 71.1, 118.4, 119.3, 120.2, 125.3, 127.3, 127.9, 132.6, 134.2, 141.5, 144.0, 144.1, 156.4, 170.3, 170.4, 173.3. (TLNII-468a_c13)



(*R*)-2-(trimethylsilyl)ethyl

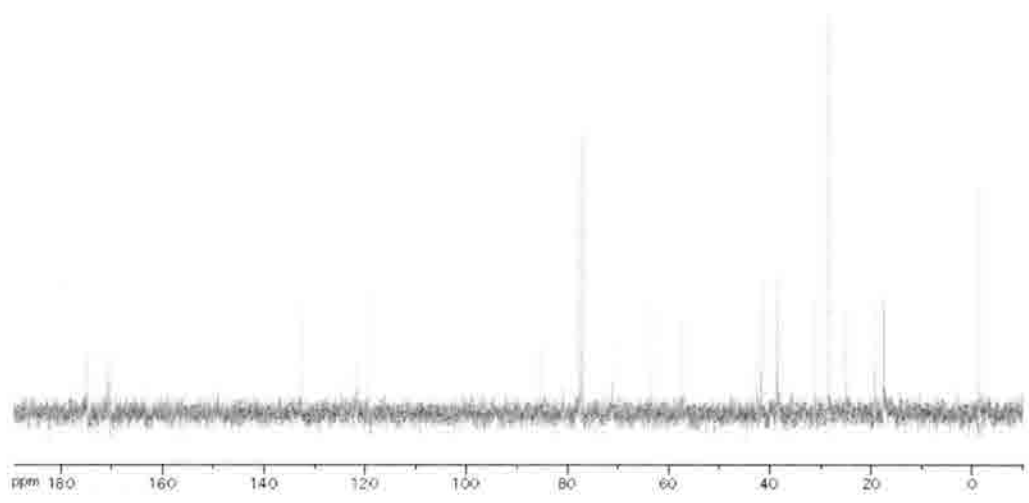
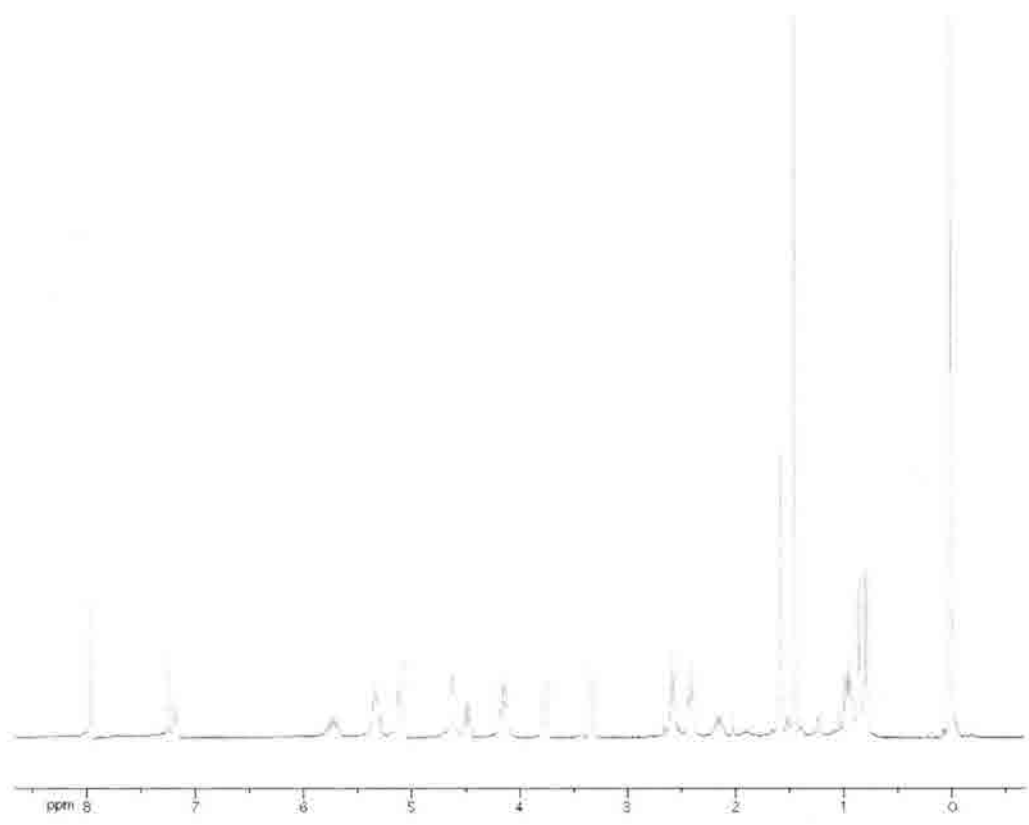
3-((*S*)-2-((*R*)-2-(2-((*tert*-

butoxycarbonylamino)methyl)thiazol-4-yl)-4-methyl-4,5-dihydrothiazole-4-carboxamido)-3-methylbutanoyloxy)hex-5-enoate (**412**)

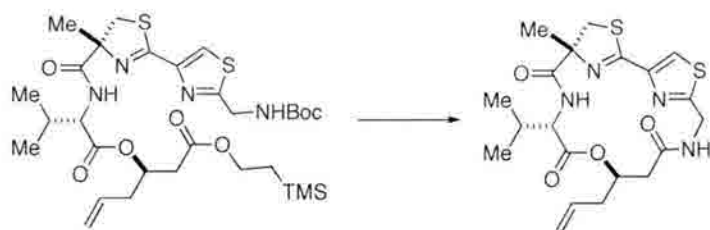


To a stirred solution of *N*-Fmoc amine **411** (0.21 g, 0.38 mmol) in MeCN (17 mL) was added diethylamine (1.7 mL). The mixture was stirred for 2 h, after which the solvent was removed under reduced pressure. The residue was dissolved in EtOAc and re-concentrated.

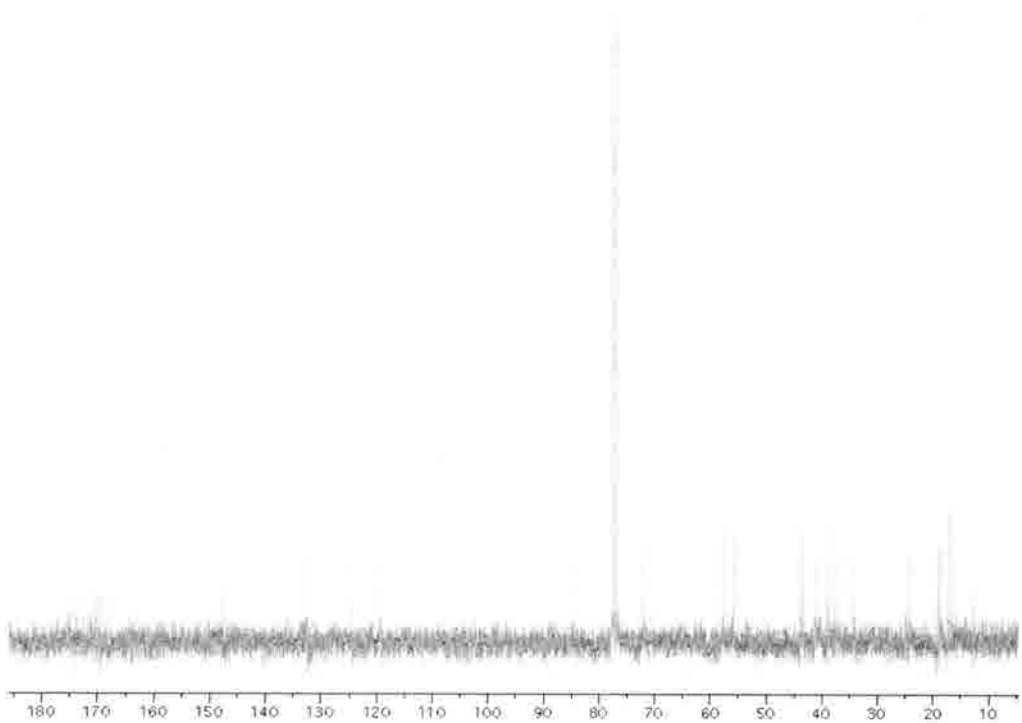
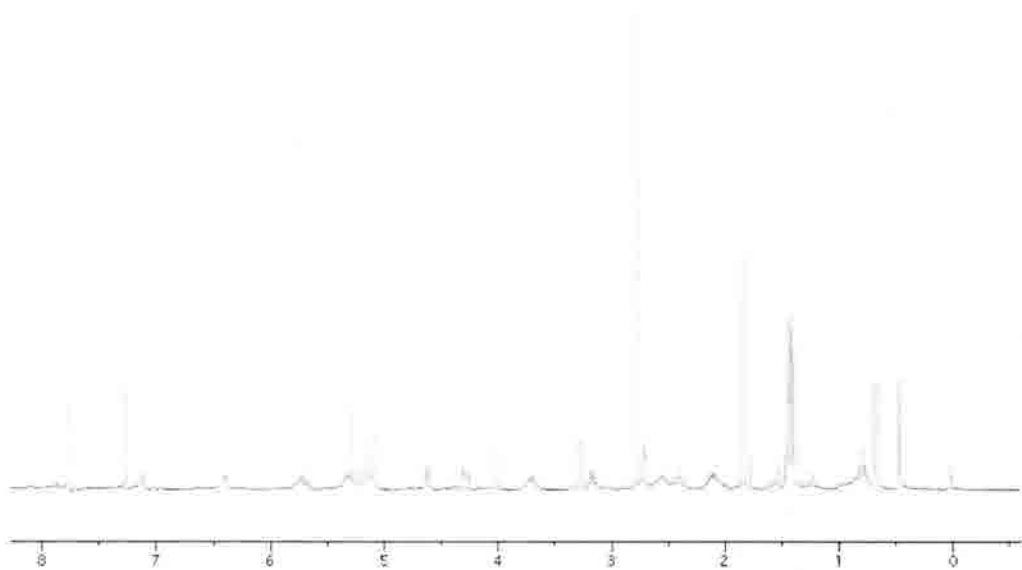
To a stirred solution of acid **294** (0.15 g, 0.42 mmol) in DCM (5 mL) was added PyBop (0.40 g, 0.76 mmol) followed by diisopropylethylamine (0.2 mL, 1.14 mmol). After 5 min, the free amine from the above reaction in MeCN (2 mL) was added dropwise. The mixture was stirred for 2 h, after which the solvent was removed under reduced pressure. The residue was purified by column chromatography (1:1 EtOAc/hexanes) to give **412** as a clear oil (0.08 g, 32%). HRMS (ESI): m/z calcd. for $C_{30}H_{48}N_4NaO_7S_2Si$ ($M + Na$)⁺ 691.2626, found 691.263. ¹H NMR (300 MHz, CDCl₃) δ TMS: 0.02 (9H, s); 0.79 (3H, d, $J = 6.6$); 0.85 (3H, d, $J = 6.9$); 0.94-1.00 (3H, m); 1.46 (9H, s); 1.59 (3H, s); 2.11-2.21 (1H, m); 2.41 (2H, t, $J = 6.9$); 2.52-2.67 (2H, m); 3.31 (1H, d, $J = 11.4$); 3.75 (1H, d, $J = 11.7$); 4.13-4.18 (2H, m); 4.48 (1H, dd, $J = 4.5$); 4.62 (2H, d, $J = 6.0$); 5.08-5.14 (2H, m); 5.29-5.38 (2H, m); 5.66-5.80 (1H, m); 7.17 (1H, d, $J = 9.0$); 7.97 (1H, s). (TLNII-473pp) ¹³C NMR (75.5 MHz, CDCl₃) δ TMS: -1.3, 17.5, 17.6, 19.4, 25.0, 28.5, 31.3, 38.4, 38.7, 41.7, 42.6, 57.2, 63.3, 71.0, 85.4, 119.2, 121.6, 132.7, 170.4, 170.8, 174.7. (TLNII-473_c13)



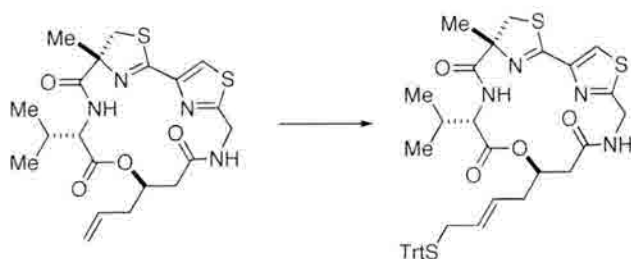
allyl depsipeptide core (413)



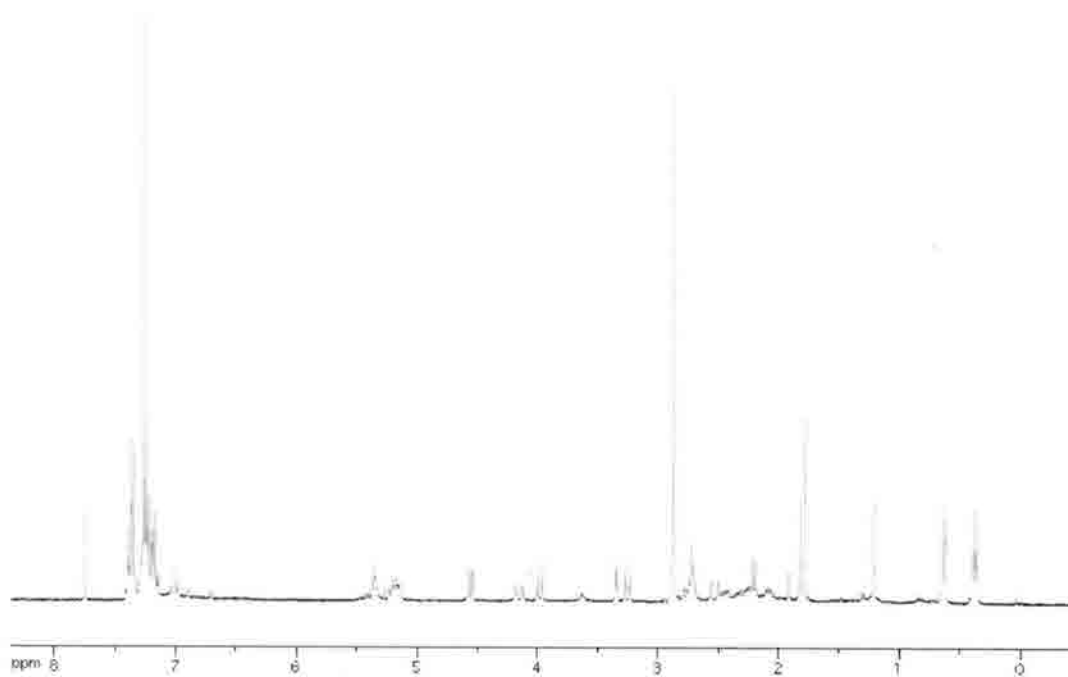
Acyclic precursor **412** (0.08 g, 0.12 mmol) was dissolved in DCM (4 mL) and cooled to 0°. TFA (0.8 mL) was added dropwise. The mixture was stirred for 15 h, after which the solvent was evaporated. Toluene (10 mL) was added, and the mixture was re-concentrated. The residue was dissolved in DCM (5 mL) and added dropwise to a mixture of HATU (0.09 g, 0.24 mmol), HOBt (0.03 g, 0.24 mmol) and diisopropylethylamine (0.06 mL, 0.36 mmol) in MeCN (120 mL). After 16 h of stirring, the solvent was removed under reduced pressure and the residue purified by column chromatography (1% methanol/DCM to 5% methanol/DCM). HRMS (ESI): m/z calcd. for $C_{20}H_{26}N_4NaO_4S_2$ ($M + Na$)⁺ 473.1288, found 473.1281. ¹H NMR (300 MHz, CDCl₃) δ TMS: 0.46 (3H, d, $J = 6.9$); 0.67 (3H, d, $J = 7.2$); 2.71-2.75 (2H, m); 2.79 (3H, s); 3.13-3.21 (1H, m); 3.25 (1H, d, $J = 11.4$); 3.64-3.76 (1H, m); 4.01 (1H, d, $J = 11.4$); 4.26 (1H, dd, $J = 3.3, 17.4$); 4.61 (1H, dd, $J = 3.3, 9.3$); 5.09-5.27 (4H, m); 5.31-5.36 (1H, m); 5.65-5.79 (1H, m); 6.39 (1H, dd, $J = 3.3, 9.3$); 7.10 (1H, d, $J = 9.6$); 7.76 (1H, s). (TLNII-485pp) ¹³C NMR (75.5 MHz, CDCl₃) δ TMS: 16.7, 18.8, 34.4, 37.8, 38.8, 41.3, 43.4, 55.9, 57.8, 72.0, 84.5, 119.3, 124.5, 132.5, 147.6, 168.2, 169.4, 169.6, 170.3, 173.9 (TLNII-485c13)



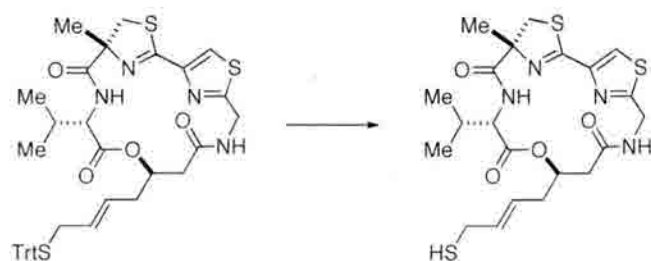
Trityl-protected macrocycle (414)



A solution of macrocycle **413** (0.027 g, 0.06 mmol) in dichloroethane (1.5 mL) was heated to reflux. 0.20 mL of a 0.06 M solution of Grubbs-Hoveyda 2 catalyst in dichloroethane (0.036 g in 0.80 mL) was added. 2.5 mL of a 0.048 M solution of allyl(trityl)sulfane in dichloroethane (0.15 g in 10 mL) was then added. These additions were repeated every hour for a further 3 hours for a total of four additions. Following the final addition, the mixture was refluxed for 1 h, then cooled to room temperature. Several drops of DMSO were added, and the mixture was stirred overnight. The solvent was removed under reduced pressure, and the residue was purified by column chromatography (0% to 100% hexanes in EtOAc) to give **414** as a white, amorphous solid (0.013 g, 30%). ¹H NMR (300 MHz, CDCl₃) δ TMS: 0.38 (3H, d, *J* = 6.9); 0.64 (3H, d, *J* = 7.2); 1.78 (3H, s); 2.23 (2H, d, *J* = 6.0); 2.44-2.45 (2H, m); 2.62-2.65 (1H, m); 2.74 (1H, d, *J* = 6.0); 3.25 (1H, dd, *J* = 3.0, 11.4); 3.68 (1H, m); 4.03 (1H, dd, *J* = 3.6, 11.4); 4.17-4.28 (2H, m); 4.61 (1H, dd, *J* = 3.3, 9.6); 5.20-5.27 (2H, m); 5.34-5.39 (2H, m); 6.27-6.29 (1H, m); 7.05 (1H, d, *J* = 9.3); 7.19-7.23 (3H, m); 7.27-7.33 (6H, m); 7.39-7.43 (6H, m); 7.75 (1H, s).



Olefin-migration analog (394)

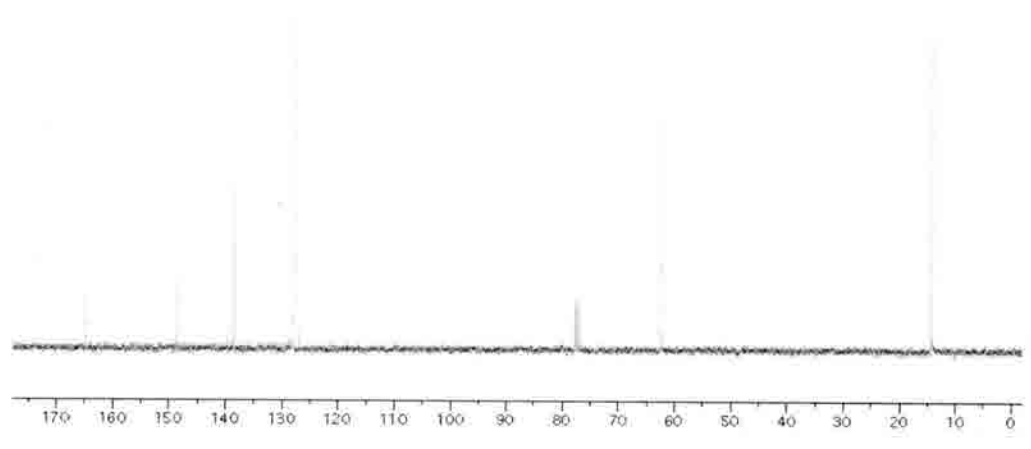
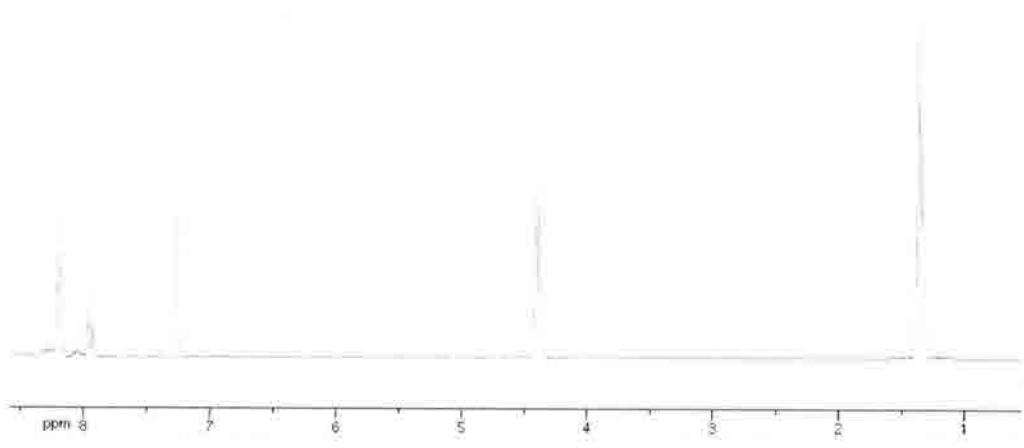


A solution of macrocycle **414** (7.4 mg, 0.01 mmol) in DCM (1.5 mL) was cooled to 0°. TFA (0.05 mL) and triisopropylsilane (4.0 μ L, 0.02 mmol) were added. The mixture was stirred at room temperature for 2 h, after which the solvent was removed under reduced pressure. The residue was purified by preparatory thin layer chromatography (EtOAc) to **394** as a clear oil (4.2 mg, 85%).

diethyl pyridine-2,6-dicarboxylate (**420**)



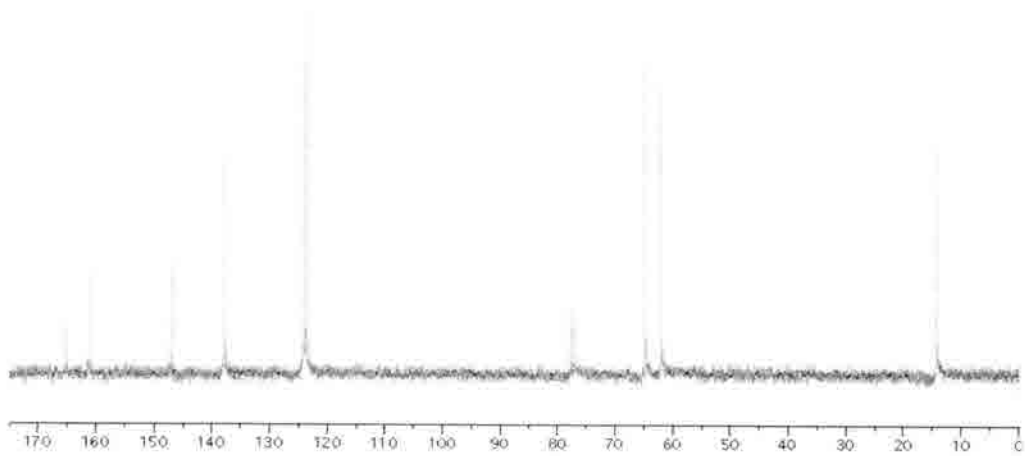
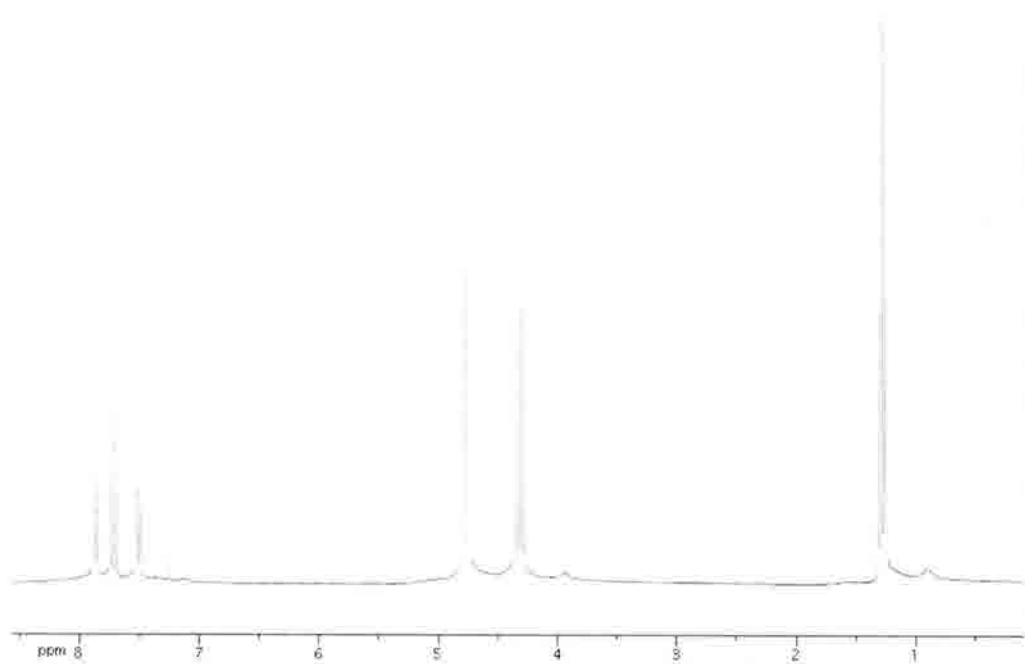
To a solution of 2,6-pyridine dicarboxylic acid (5.55 g, 33.21 mmol) in EtOH (250 mL) was added *para*-toluenesulfonic acid (13.3 g, 69.74 mmol). The mixture was heated to reflux for 24 h, after which the solvent was removed under reduced pressure. The residue was dissolved in chloroform (100 mL) and a saturated aqueous solution of sodium carbonate (100 mL) was added. The aqueous layer was extracted into chloroform (4 x 50 mL). The combined organic layers were washed with brine, dried over sodium sulfate and concentrated to give **420** as a light pink oil (7.4 g, 100%). ¹H NMR (300 MHz, CDCl₃) δ TMS: 1.36 (6H, t, *J* = 7.2); 4.41 (4H, q, *J* = 7.2); 7.95 (1H, t, *J* = 8.1); 8.22 (2H, d, *J* = 7.8). (TLNIII-18c) ¹³C NMR (75.5 MHz, CDCl₃) δ TMS: 14.4, 62.5, 128.0, 138.5, 148.7, 164.7. (TLNIII-18c_c13)



ethyl 6-(hydroxymethyl)picolinate (421)



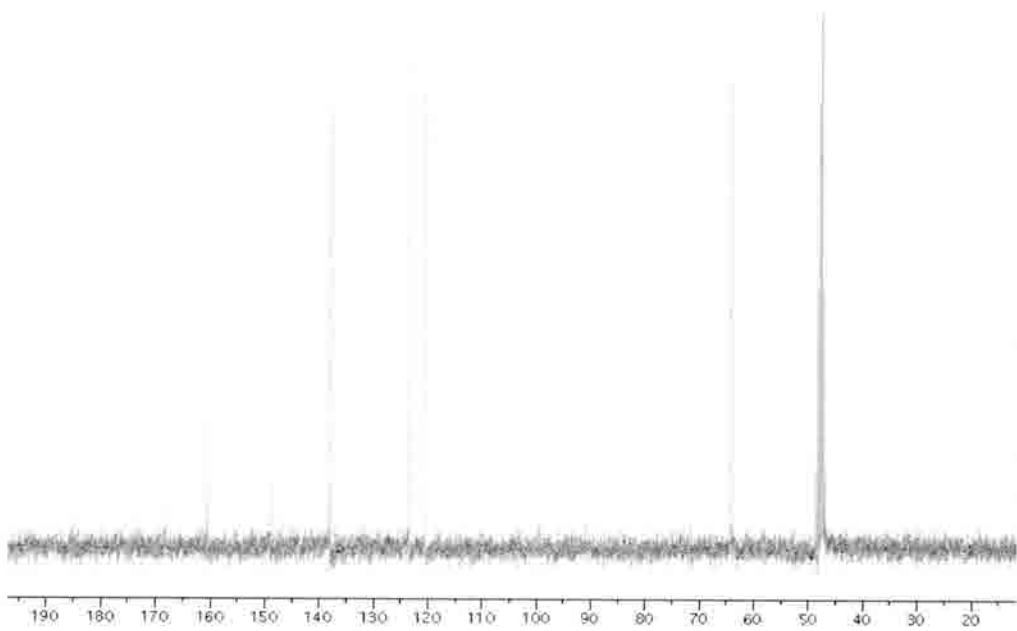
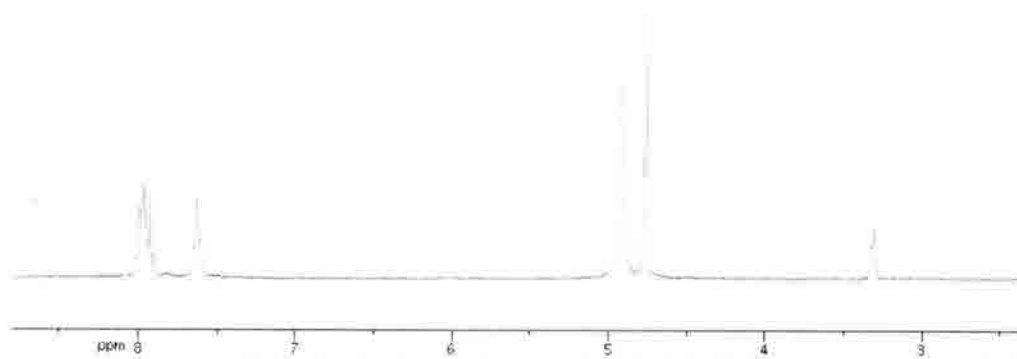
To a stirred solution of ester **420** (7.4 g, 33.2 mmol) in ethanol (250 mL) was added sodium borohydride (0.82 g, 21.59 mmol). The mixture was heated to reflux for 2 h, after which ~3/4 of the solvent was removed under reduced pressure. Water (150 mL) was then added, and the remainder of the ethanol removed under reduced pressure. The aqueous layer was extracted into chloroform (3 x 100 mL). The combined organic layers were washed with brine, dried over sodium sulfate and concentrated to give **421** as a clear oil (2.5 g, 42%). ¹H NMR (300 MHz, CDCl₃) δ TMS: 1.29 (3H, t, *J* = 6.9); 4.30 (2H, q, *J* = 6.9); 4.77 (2H, s); 7.49 (1H, d, *J* = 7.8); 7.71 (1H, t, *J* = 7.8); 7.85 (1H, d, *J* = 7.8). (TLNIII-23). ¹³C NMR (75.5 MHz, CDCl₃) δ TMS: 14.4, 62.1, 64.8, 123.7, 124.2, 137.8, 147.1, 161.2, 165.2. (TLNIII-23_c13)



6-(hydroxymethyl)picolinamide (**422**)



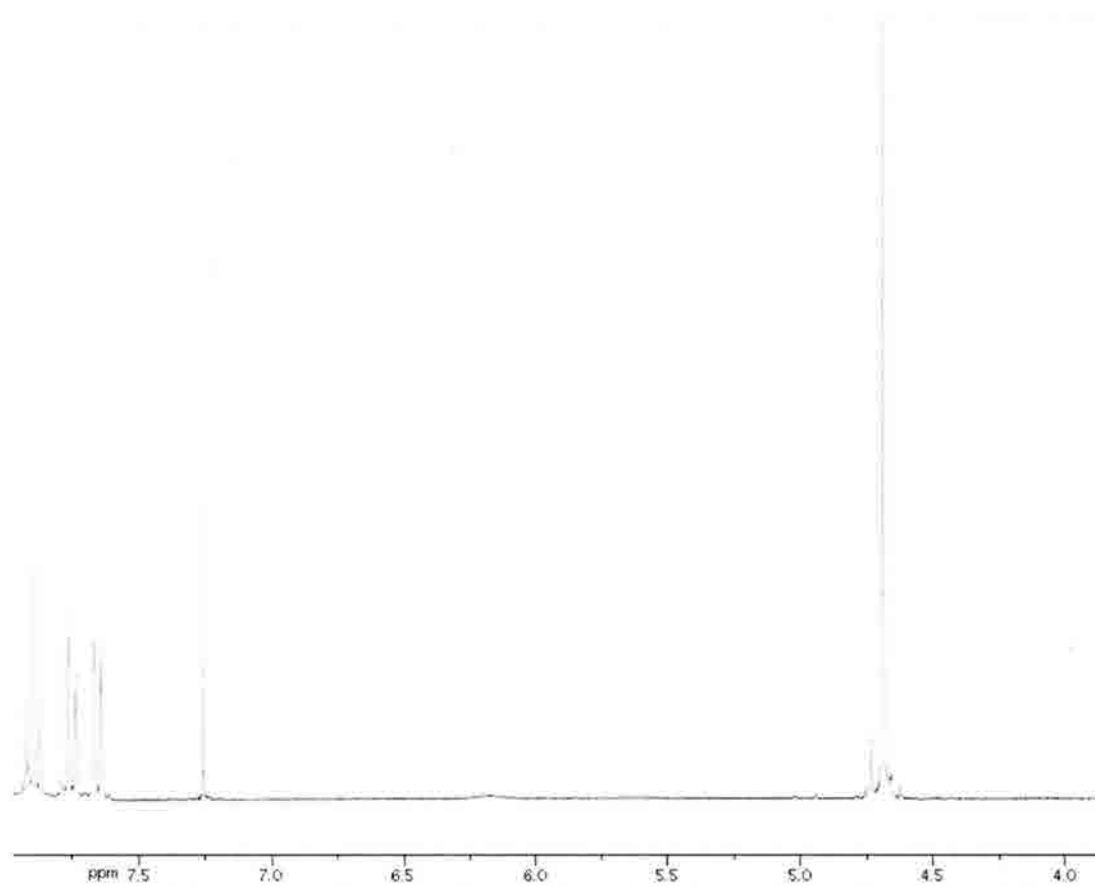
Alcohol **421** (2.5 g, 13.8 mmol) was dissolved in ethanol (48 mL), and concentrated ammonium hydroxide (71 mL) was added. The mixture was stirred for 15 h, after which the solvent was evaporated to give **422**. (2.0 g, 95%). ^1H NMR (300 MHz, CD_3OD) δ TMS: 4.75 (2H, s); 4.91 (2H, bs); 7.63 (1H, t, $J = 7.2$); 7.90-8.02 (2H, m). (TLNIII-24)
 ^{13}C NMR (75.5 MHz, CDCl_3) δ TMS: 64.4, 120.5, 123.4, 138.1, 149.0, 160.5, 168.2. (TLNIII-24_c13)



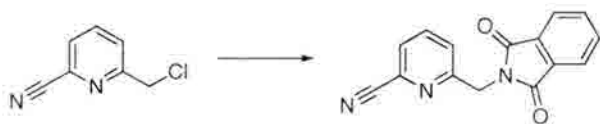
6-(chloromethyl)picolinonitrile (**423**)



A solution of amide **422** (1.91 g, 12.55 mmol) in DMF (120 mL) was cooled to 0°. Phosphorous oxychloride (3.5 mL, 37.66 mmol) was added dropwise. The mixture was stirred at 0° for 6 h, after which the solvent was evaporated. The resulting solid was cooled to 0° and water (40 mL) was added dropwise. The aqueous layer was extracted into EtOAc (3 x 30 mL). The combined organic layers were washed with brine, dried over sodium sulfate and concentrated to give **423** as a yellow oil (1.66 g, 87%) ¹H NMR (300 MHz, CDCl₃) δ TMS: 4.69 (2H, s); 7.64 (1H, d, *J* = 7.8); 7.74 (1H, d, *J* = 8.1); 7.90 (1H, t, *J* = 7.8). (TLNIII-27)



6-((1,3-dioxisoindolin-2-yl)methyl)picolinonitrile (424)



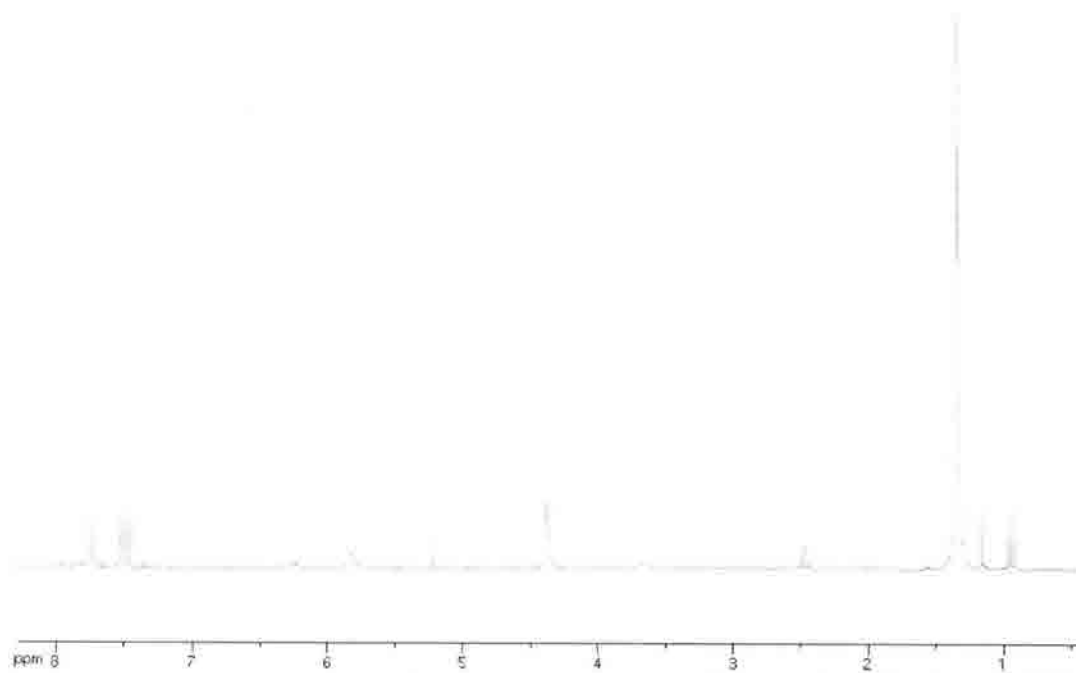
To a solution of chloride **423** (1.93 g, 12.65 mmol) in DMF (100 mL) was added potassium phthalimide (2.34 g, 12.65 mmol). The mixture was stirred for 5 h, after which the solvent was removed under reduced pressure. Water (100 mL) was added, and the resultant suspension was filtered through Celite to remove the precipitate. The water was then removed under reduced pressure to give **424** as an off-white solid. (2.7 g, 81%).

***tert*-butyl (6-cyanopyridin-2-yl)methylcarbamate (**425**)**

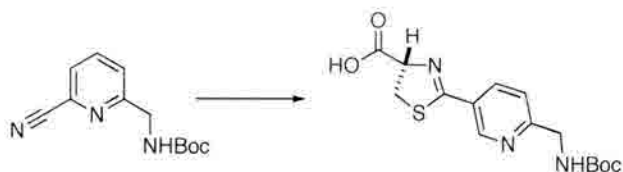


To a stirred solution of phthalimide **424** (1.0 g, 3.80 mmol) was in methanol (19 mL) and THF (19 mL) was added hydrazine monohydrate (0.2 mL, 4.18 mmol). The solution was stirred for 2 h, after which 1N HCl (4.2 mL) was added. This biphasic mixture was stirred for a further 3 h, the solvent was removed under reduced pressure. The residue was mixed with water (40 mL) and the solids were removed by filtration through a thin pad of Celite. The solvent was again removed to give the free amine of **424** as an off-white, amorphous solid (0.56g, 87%).

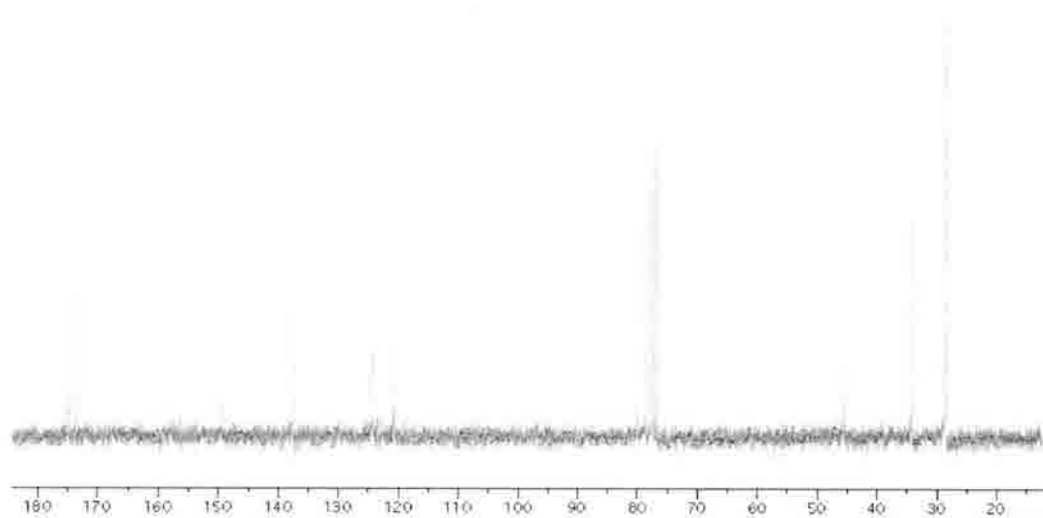
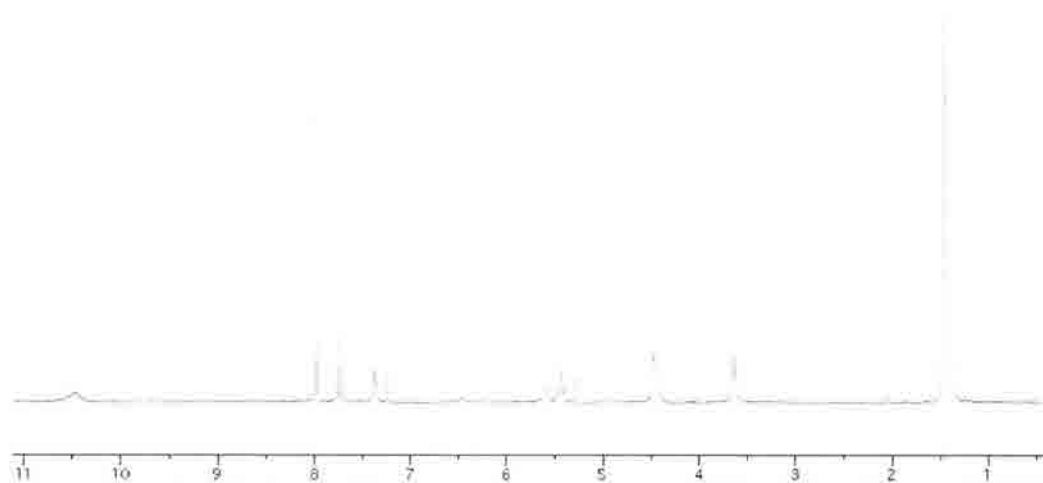
To a solution of the free amine of **424** (0.56 g, 3.30 mmol) in DCM (30 mL) was added triethylamine (1.4 mL, 9.90 mmol) followed by Boc anhydride (0.79 g, 3.63 mmol). The mixture was stirred for 12 h, then washed with a saturated aqueous solution of sodium bicarbonate. The organic layer was washed with brine, dried over sodium sulfate and concentrated to give **425**. ¹H NMR (300 MHz, CDCl₃) δ TMS: 1.36 (9H, s); 4.37 (2H, d, *J* = 5.7); 5.83 (1H, bs); 7.48 (1H, d, *J* = 8.1); 7.50 (1H, d, *J* = 7.8); 7.74 (1H, t, *J* = 7.8). (TLNIII-43)



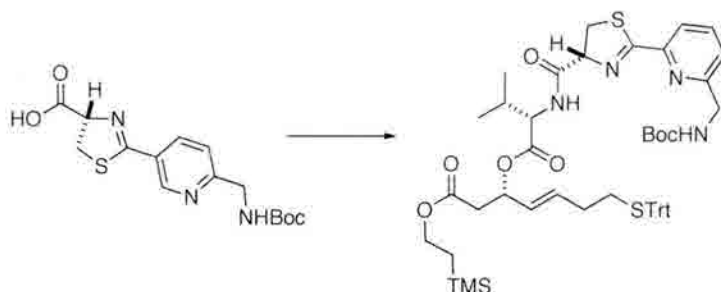
(S)-2-(6-((*tert*-butoxycarbonylamino)methyl)pyridin-3-yl)-4,5-dihydrothiazole-4-carboxylic acid (426**)**



To a stirred solution of sodium bicarbonate (0.35 g, 4.2 mmol) in methanol (12.6 mL) and pH 7 phosphate buffer (8.4 mL) was added nitrile **425** (0.49 g, 2.10 mmol) and α -methyl cysteine **333** (0.28 g, 2.31 mmol). The mixture was heated to 70° for 48 h, after which it was extracted into diethyl ether (3 x 15 mL). The organic layers were discarded, and the aqueous layer was acidified to pH 2 by dropwise addition of 1N HCl. The aqueous layer was extracted into EtOAc (3 x 20 mL), and the combined organic layers were washed with brine, dried over sodium sulfate, and concentrated to give **426** as a light yellow foam (0.48 g, 68%). $\alpha_D = -4.0$, $c=0.5$ in MeOH. ^1H NMR (300 MHz, CDCl_3) δ TMS: 1.46 (9H, s); 3.63 (2H, d, $J = 9.6$); 4.47 (2H, d, $J = 5.1$); 5.43 (1H, t, $J = 9.6$); 5.59 (1H, bs); 7.36 (1H, d, $J = 7.5$); 7.73 (1H, t, $J = 7.8$); 7.96 (1H, d, $J = 7.8$); 10.47 (1H, bs). (TLNII-438a). ^{13}C NMR (75.5 MHz, CDCl_3) δ TMS: 26.6, 34.3, 45.6, 80.1, 120.75, 124.4, 137.6, 149.6, 157.8, 173.8, 174.9. (TLNII-438c13)



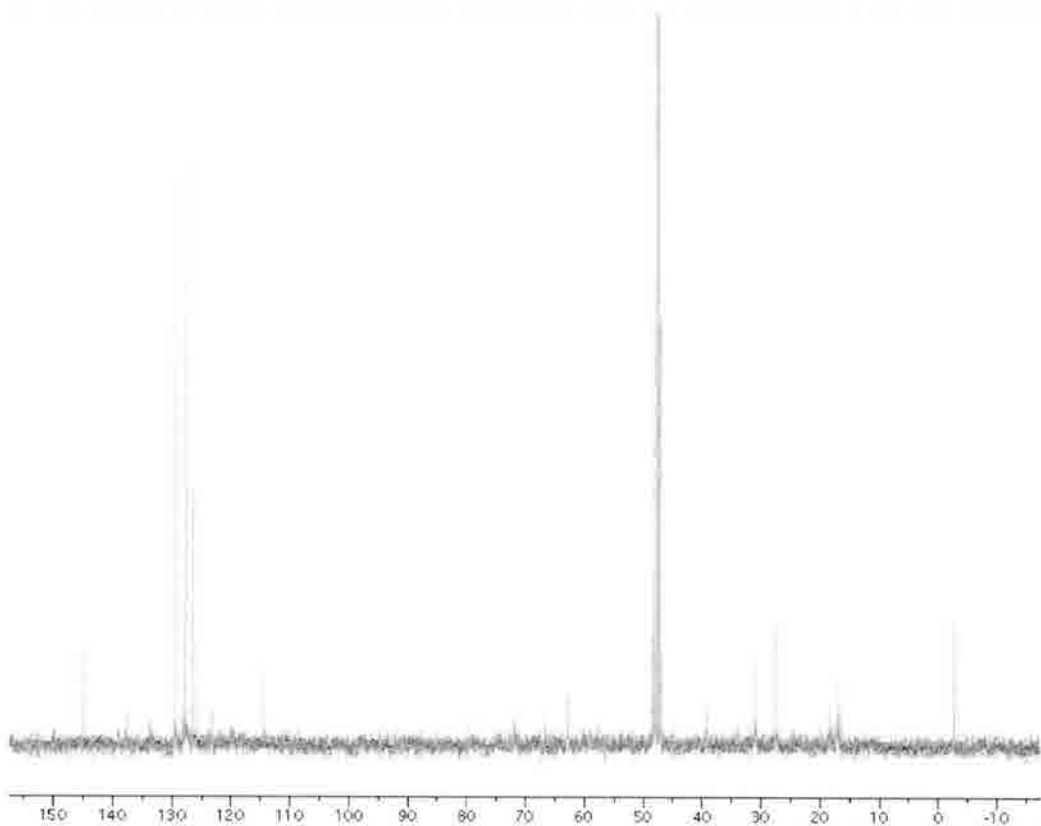
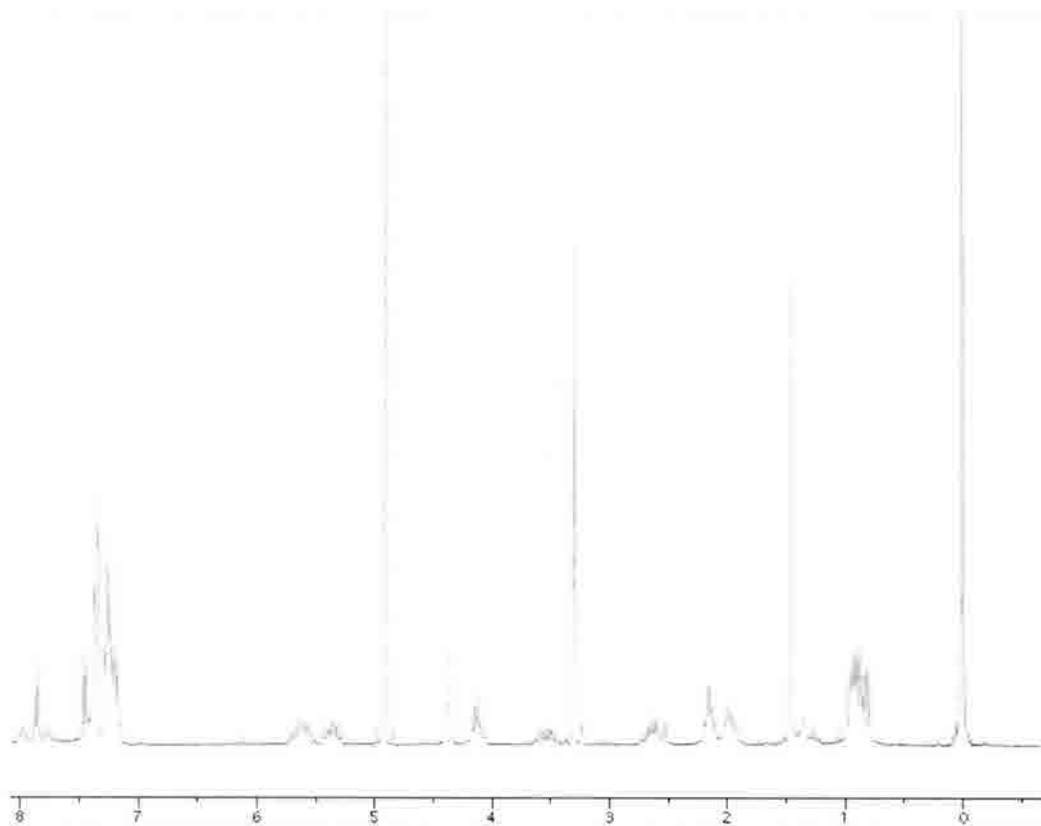
(*S,E*)-2-(trimethylsilyl)ethyl 3-((*S*)-2-((*R*)-2-(6-((*tert*-butoxycarbonylamino)methyl)pyridin-2-yl)-4,5-dihydrothiazole-4-carboxamido)-3-methylbutanoyloxy)-7-(tritylthio)hept-4-enoate (428**)**



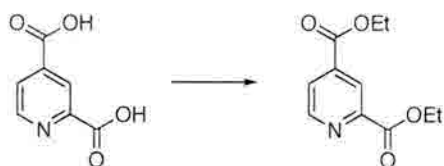
To a solution of Fmoc-protected amine **411** (0.42 g, 0.50 mmol) in acetonitrile (25 mL) was added diethylamine (2.5 mL). The mixture was stirred for 2 h, after which the solvent was evaporated under reduced pressure. The residue was dissolved in EtOAc, and the solvent again removed to give free amine **427**.

To a solution of acid **426** (0.17 g, 0.5 mmol) in DCM (10 mL) was added PyBop (0.26 g, 1.0 mmol), followed by diisopropylethylamine (0.26 mL, 1.5 mmol). After 10 min, **426** in acetonitrile (6 mL) was added dropwise. The mixture was stirred for 2 h, after which the solvent was removed under reduced pressure. The residue was purified by column chromatography (4:1 to 2:1 hexanes/EtOAc) to give **428** as a colorless oil (0.16 g, 34%).

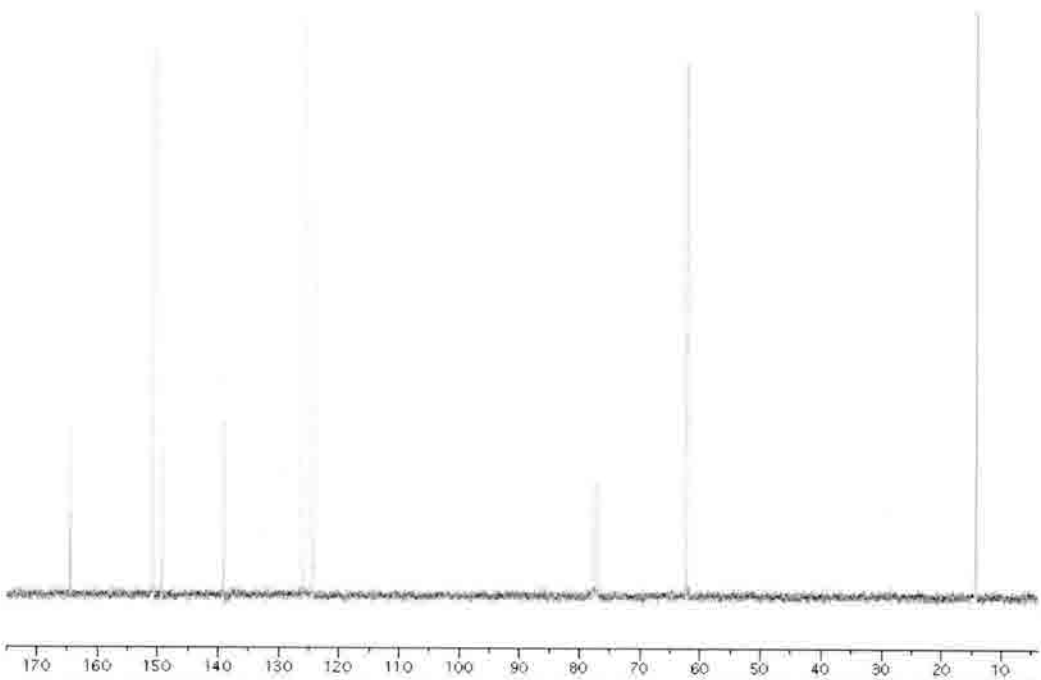
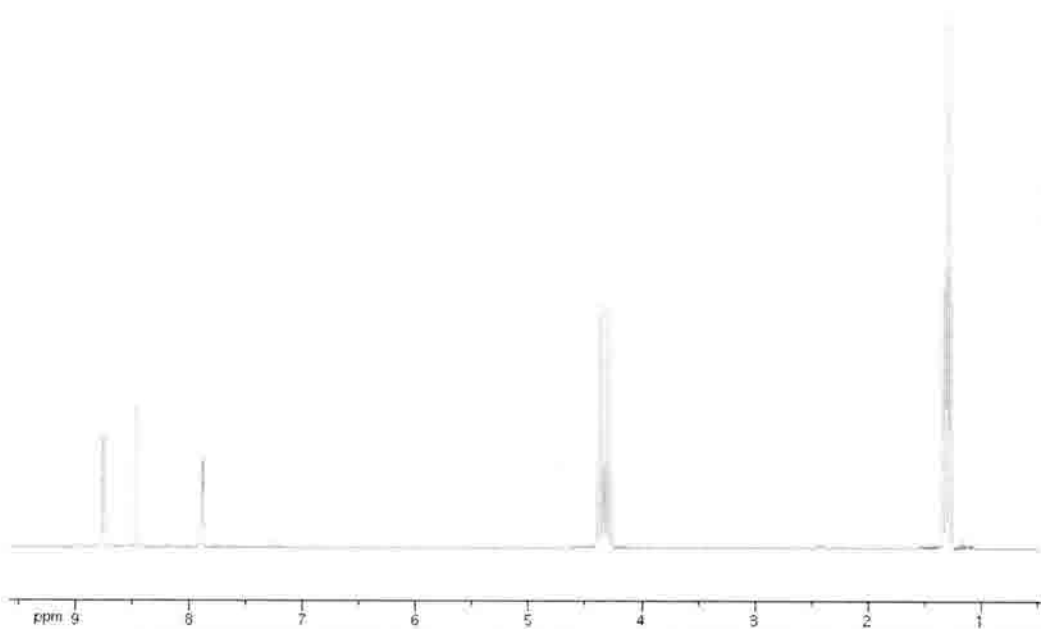
$^1\text{H NMR}$ (CD_3OD , 300 MHz) δ TMS: 0.025 (9H, s); 0.79-0.97 (9H, m); 1.46 (9H, s); 1.92-2.19 (6H, m); 2.52-2.74 (2H, m); 3.45-3.64 (1H, m); 4.06-4.18 (2H, m); 5.28-5.45 (2H, m); 5.51-5.74 (2H, m); 7.18-7.29 (9H, m); 7.45-7.38 (6H, m); 7.44-7.47 (2H, m); 7.84-7.88 (2H, m). (TLNII-476meoh) $^{13}\text{C NMR}$ (CD_3OD , 75.5 MHz) δ TMS: -2.6, 17.0, 27.6, 31.1, 39.3, 45.2, 62.8, 62.9, 66.6, 71.5, 71.9, 79.5, 79.6, 114.5, 125.8, 126.6, 127.7, 137.5, 145.1. (TLNII-476c13)



diethyl pyridine-2,4-dicarboxylate (**431**)



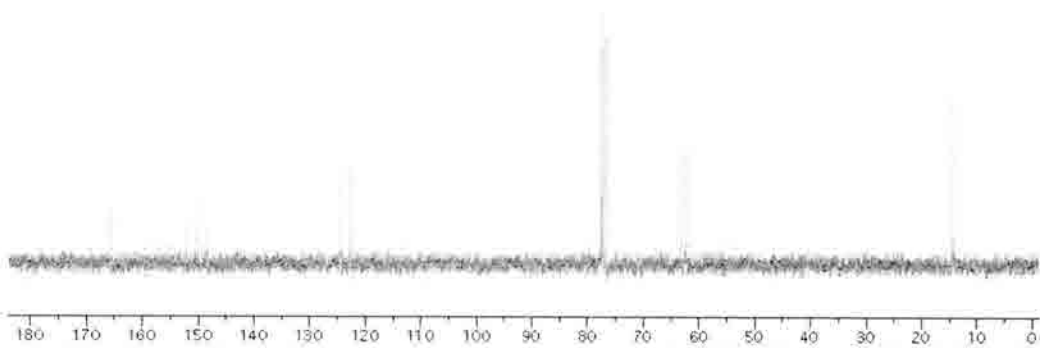
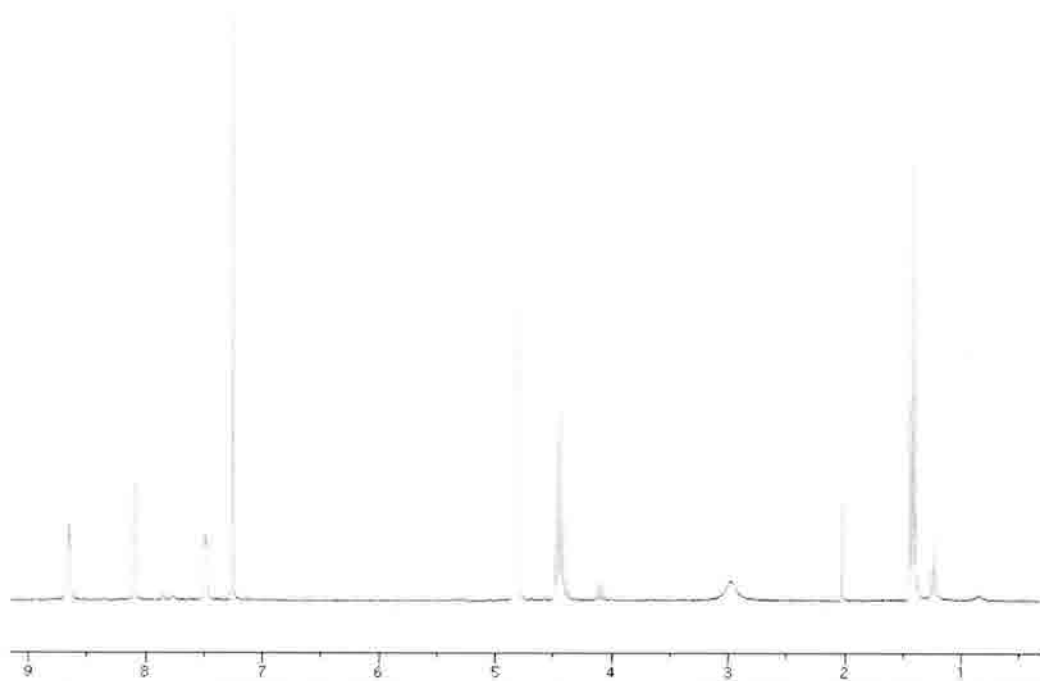
To a solution of 2,4-pyridinedicarboxylic acid monohydrate (2.0 g, 10.80 mmol) in EtOH (100 mL) was added *para*-toluenesulfonic acid monohydrate (4.3 g, 22.68 mmol). The mixture was heated at reflux for 24 h, then cooled to room temperature. The solvent was removed under reduced pressure, and the residue was dissolved in chloroform (50 mL). The organic layer was washed with a saturated aqueous solution of sodium bicarbonate (50 mL), and the resultant aqueous layer was extracted into chloroform (3 x 35 mL). The organic layers were washed with brine, dried over sodium sulfate and concentrated to give **431** as a light pink oil. (2.40 g, 100%). ¹H NMR (CDCl₃, 300 MHz) δ TMS: 1.28 (3H, t, *J* = 6.9); 1.31 (3H, t, *J* = 7.2); 4.29 (2H, q, *J* = 7.2); 4.35 (2H, q, *J* = 7.2); 7.88 (1H, dd, *J* = 1.5, 4.8); 8.48 (1H, m); 8.75 (1H, d, *J* = 4.8). (TLNIII-7a). ¹³C NMR (CDCl₃, 75.5 MHz) δ TMS: 14.4, 62.3, 124.3, 126.1, 139.1, 149.3, 150.8, 164.3, 164.6 (TLNIII-7c13)



4-(ethoxycarbonyl)picolinic acid (**432**)



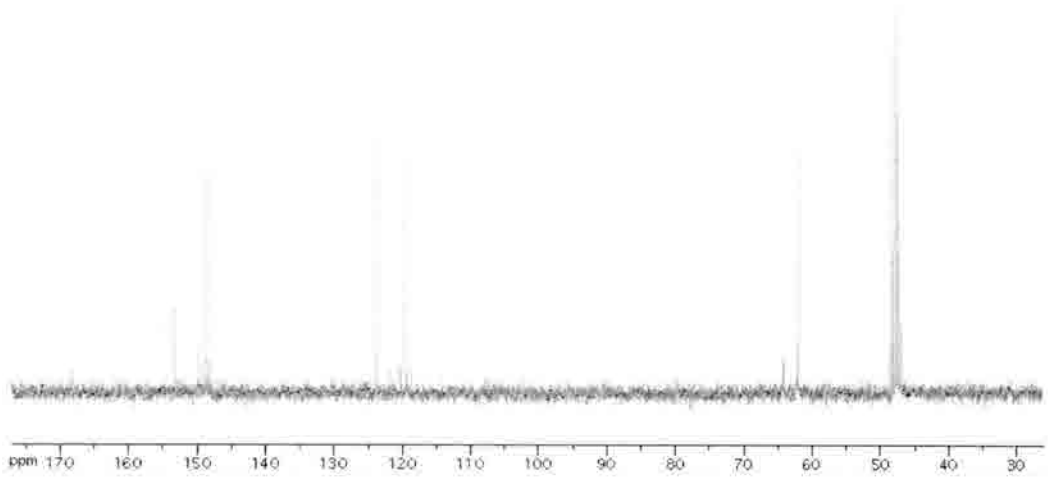
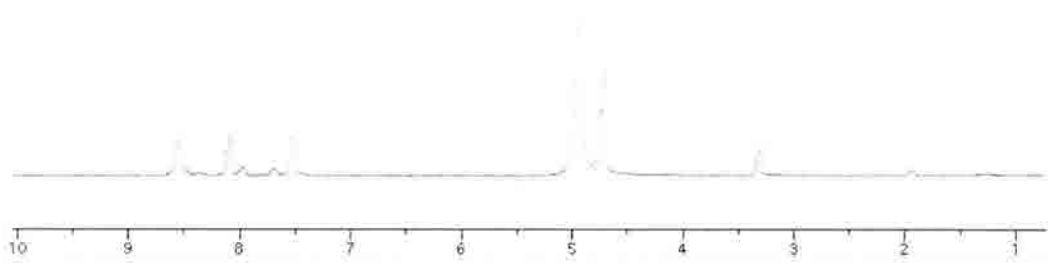
To a solution of diester **431** (0.85g, 3.80 mmol) in EtOH (38 mL) was added sodium borohydride (0.12 g, 3.24 mmol). The mixture was heated to reflux for 2 h, after which the solvent was concentrated to about 1/4 its original volume. Water (30 mL) was added, and the remainder of the ethanol was removed under reduced pressure. The aqueous layer was extracted into chloroform (3 x 40 mL), and the combined organic layers were washed with brine, dried over sodium sulfate and concentrated. The residue was purified by column chromatography (1:1 EtOAc/hexanes) to give **432** as a clear oil (0.24 g, 35%). ¹H NMR (CDCl₃, 300 MHz) δ TMS: 1.42 (3H, t, *J* = 7.2); 2.96 (1H, bs); 4.34 (2H, q, *J* = 7.2); 4.82 (2H, s); 7.48 (1H, d, *J* = 4.2); 8.09 (1H, s); 8.65 m(1H, d, *J* = 4.5). (TLNIII-11_4) ¹³C NMR (CDCl₃, 75.5 MHz) δ TMS: 14.5, 62.3, 63.3, 122.7, 124.4, 148.3, 150.0, 152.1, 165.4. (TLNIII-11_4c13).



2-(hydroxymethyl)isonicotinamide (**433**)



To a stirred solution of alcohol **432** (0.57 g, 3.15 mmol) in EtOH (11 mL) was added ammonium hydroxide (30% solution, 16.3 mmol). The mixture was stirred overnight, and the solvent was removed under reduced pressure to give **433** as a light yellow oil (0.41 g, 86%). ¹H NMR (CD₃OD, 300 MHz) δ TMS: 4.71 (2H, s); 4.94 (2H, s); 7.52 (1H, s); 8.09 (1H, s); 8.55 (1H, s). (TLNIII-31). ¹³C NMR (CD₃OD, 75.5 MHz) δ TMS: 61.2, 119.5, 123.9, 148.6, 149.8, 153.2, 168.3. (TLNIII-31c13).



The pharmacophore model for HDAC inhibition consists of three elements: (1) a surface recognition unit which interacts with the rim of the binding pocket, (2) a metal-binding domain which coordinates to the active site zinc ion, and (3) a linker that connects the surface recognition site to the zinc-binding domain.¹⁵ Numerous HDAC inhibitors (HDACi), both natural and synthetic, are known, and variations in all three features have variably contributed to potency and selectivity in new HDACi's.¹⁵

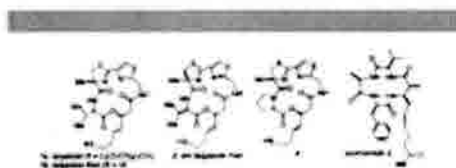


Figure 1. Selected lorgazolo analogs and azinomamide 9

To date, the most potent and selective HDACi known is lorgazolo (1a; Figure 1), a densely functionalized macrocyclic decapeptide isolated from the cyanobacterium *Symplaxia* sp. by Luesch and co-workers.⁸ We have recently disclosed a concise, modular, and scalable total synthesis of lorgazolo and demonstrated its picomolar activity against HDACs (1, 2, and 3, as well as low nanomolar cytotoxicity against a number of chemoresistant cancer cell lines.^{9–11} Additionally, we have disclosed a detailed conformation–activity relationship model for lorgazolo, FK228, and their corresponding

amide isosteres with insight into the key contacts and associated spatial determinants that provide this remarkable level of activity.¹² Hence, we describe our continuing efforts to modify the structural scaffold of lorgazolo with the goal of further defining and expanding structure–activity relationships within the family of macrocyclic HDACi's. Our overarching aim in this context is to perturb the class- and isoform-selectivity as initially observed in robust biochemical assays such that differences in specific enzymatic activity might later be correlated with phenotypic responses in cell-based assays.

Our reported route to lorgazolo proved highly reproducible, and we were able to rapidly adapt it to simple variants of the macrocyclic core.⁹ Thus we were able to easily access milligram quantities of the C-2 epimer (3) and the enantiomer (2) of lorgazolo. Additionally, we sought to perturb the conformation of the macrocycle by imparting greater rigidity; our initial foray in this capacity replaced the valine residue with proline (4). Compound 4 could be obtained in only slightly diminished overall yield via the same synthetic route we deployed in the total synthesis of lorgazolo (see Supporting Information).

Scheme 1. Synthesis of the Lorgazolo–Azinomamide Hybrid



Two methods were employed to alter side chain functionality and access a series of lorgazolo chimeras. For the lorgazolo–azinomamide hybrid (9), the *cis*-geometry of the alkene residue necessitated its early introduction. Thus, aldol condensation of aldehyde 5¹³ with thiazolidine-2-thione 6 provided the necessary β -hydroxy acid building block (7; Scheme 1 and Supporting Information). For other variants investigated, late-stage introduction of the zinc-binding side arm via cross metathesis proved expedient. Cross metathesis had previously been used by Luesch, Phillips, and Cramer to attach the natural side chain in their syntheses of lorgazolo itself and was investigated independently in our laboratories.^{9a–10}

Cramer et al. have demonstrated that, at least where lorgazolo is concerned, the four-atom linker length relative to the thiol is optimal for maximum HDAC inhibition.¹⁰ However, literature precedent has shown that a four- to five-atom chain is optimal in small molecules bearing alternative zinc-binding functionality.¹⁴ Therefore, in the series of analogs

(1) Karagiatou, T. C.; El-Osta, A. *Toxicology* **2007**, *21*, 61–5; and references therein.

(2) (a) Richon, V. M.; Erdlim, S.; Yoshii, E.; Webb, Y.; Bestou, R.; Kikind, R. A.; Marks, P. A. *Proc. Natl. Acad. Sci. U.S.A.* **1998**, *95*, 3033–7. (b) Yoshida, M.; Kojima, M.; Akita, M.; Bopp, T. *J. Biol. Chem.* **1990**, *265*, 17174–9. (c) Dinko-Karim, S. J.; Gorman, A. M.; Myers, K. W.; Dinko, P. M.; Cysowski, J. M.; Alibon, J. J.; Carriva, C.; Mitter, P. T.; Collins, S. L.; Bellizzi, M. A.; Nagel, S. B.; Goetz, M. A.; Dandroszko, A. W.; Polshak, J. D.; Schreier, D. M. *Proc. Natl. Acad. Sci. U.S.A.* **1996**, *93*, 13111–15. (d) Kojima, M.; Yoshida, M.; Sogita, K.; Horinouchi, S.; Bergo, T. *J. Biol. Chem.* **1993**, *268*, 22429–35. (e) Nakano, Y.; Yoshida, Y.; Mitsuoka, Y.; Shimada, N.; Terada, Y.; Nagai, K.; Yamashita, J. R.; Goto, A.; von Soczka-Gut, W.; Fineman, N.; Angew. Chem., *Int. Ed. Engl.* **2006**, *45*, 5553–7. (f) Iino, T.; Matsuura, N.; Hibino, G.; De Rubeis, F.; Strano, C. *Int. Ed. Engl.* **2006**, *45*, 7557–60. (g) Wen, S.; Carey, R. L.; Nakano, Y.; Fineman, N.; Packham, G.; Goto, A. *Org. Lett.* **2007**, *9*, 2105–8. (h) Oeda, H.; Nakajima, H.; Hori, Y.; Fujita, T.; Nishimura, M.; Goto, T.; Okikawa, M. *J. Antibiot. (Tokyo)* **1994**, *47*, 301–10. (i) Mitsuoka, S.; Oeda, H.; Takase, S.; Tanaka, H.; Yamamoto, K.; Tada, T. *J. Antibiot. (Tokyo)* **1994**, *47*, 311–4. (j) Oeda, H.; Manda, Y.; Matsumoto, S.; Mitsuoka, S.; Nishiyuki, F.; Kawamura, I.; Mitsuoka, K. *J. Antibiot. (Tokyo)* **1994**, *47*, 115–21. (k) York-Gould, A.; Hubert, P.; Boninelli, M.; Packham, G.; Goto, A. *J. Am. Chem. Soc.* **2004**, *126*, 1030–1.

(3) For seminal work on HDACi hybrids: (a) Frenkel, R.; Kozlov, Y.; Saitano, N.; Khechikyan, S.; Yoshida, M.; Horinouchi, S. *Proc. Natl. Acad. Sci. U.S.A.* **2003**, *100*, 82–87. (b) Nakano, Y.; Iino, B.; Okamura, S.; Kishimoto, S.; Kato, T.; Shimada, Y.; Yoshida, M. *Org. Lett.* **2003**, *5*, 9379–82.

(4) Tsui, K.; Paul, V. J.; Luesch, H. *J. Am. Chem. Soc.* **2005**, *127*, 1550.

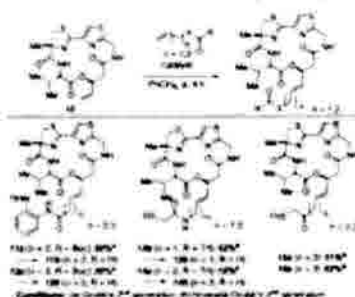
(5) Bennett, A. A.; Wen, S.; Fineman, T.; Schreiber, S. L.; Beutler, J. K.; Williams, B. M. *J. Am. Chem. Soc.* **2000**, *122*, 11219–22.

(6) For additional synthesis of lorgazolo, see: (a) Nishiyuki, J. G.; Igarashi, M.; Iino, Y.; Phillips, A. *J. Org. Chem.* **2000**, *65*, 1340–56. (b) Chou, X. K.; Nakajima, S. *Org. Lett.* **2003**, *5*, 2007–9. (c) Yang, Y.; Luo, K.; Kim, H.; Hong, J.; Luesch, H. *J. Am. Chem. Soc.* **2005**, *127*, 8155–59. (d) Nara, T.; Kikawa, T.; Cramer, N. *Angew. Chem., Int. Ed.* **2005**, *44*, 8485–88. (e) Ren, Q.; Han, J.; Zhang, H.; Liu, W.; Xu, J.; Yu, Y. *Angew. Chem., Int. Ed.* **2005**, *44*, 2574.

(7) Bennett, A. A.; Cardlock, J. J.; Wen, S.; Frenkel, R.; Schreiber, S. L.; Beutler, J. K.; Williams, B. M. *Beutler, J. E. J. Am. Chem. Soc.* **1998**, *120*, 14077–78.

(8) Wen, S.; Carey, R. L.; Nakano, Y.; Fineman, N.; Packham, G.; Goto, A. *Org. Lett.* **2007**, *9*, 1105–8.

Scheme 2. Metathesis Route to Lurzazole Hybrids



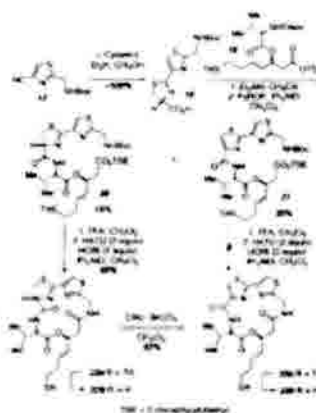
prepared via metathesis, both the four- and the five-atom lurzoles were synthesized.

Compounds **11** and **12** bear the well-known *o*-aminobenzamide group present in MS-275.¹¹ Meanwhile, compounds **13**, **14** and **15**, **16** contain α -thioamides and α -thioketones, respectively. These two motifs were identified as potential candidates in a computational study done by Vamounis et al. and have demonstrated promise in subsequent medicinal efforts.¹² Of note, our yields in the metathesis reaction conform to the results reported by Cramer.¹⁴ Our initial yields, employing Grubbs' second-generation ruthenium catalyst, were low with poor conversion (Scheme 2). The Hoveyda-Grubbs second-generation catalyst proved much more efficient. All Boc- and Tmsyl-protecting groups were removed prior to biological assay (see Supporting Information).

We also sought to probe the significance of the methyl substituent on the thiazoline ring. Condensation of nitrile **17** with *L*-cysteine proved remarkably facile, proceeding in near quantitative yield (Scheme 3). Initial efforts at coupling to enter **19** provided poor yields of the desired acyclic precursor **20**. The major product was thiazole (thiazole **21**, resulting from *in situ* oxidation). Optimization of conditions for this coupling eventually allowed for up to 62% yield of the desired product. Oxidation could be the cause of the somewhat diminished yields in the cyclization of **20**. Compound **23** could not be detected in NMR spectra of the crude reaction mixtures from cyclization of **20**. Moreover, **23** could not be prepared directly from its acyclic precursor **21**. Instead, oxidation of **22** under standard conditions provided **23**. This macrocycle clearly contains some added constraint as demonstrated by the presence of rotamers in the ¹H NMR spectrum in CDCl₃. Both substrates **22a** and **22b** could be deprotected in good yield using our standard conditions.

Replacement of the thiazole moiety with a pyridine residue in the heterocyclic backbone was readily amenable to our

Scheme 3. Synthesis of Oxazole and Thiazole-Thiazole Analogs



synthetic strategy (Scheme 4). Known *o*-thio nitrile **24** could be Boc-protected and then condensed with *m*-methyl cysteine to provide acid **27**. Subsequent deprotection, coupling, and cyclization provided analog **29**.

Scheme 4. Synthesis of Thiazole to Pyridine Substitution



We also sought to perform additional single atom replacements within the lurzazole macrocyclic scaffold to interrogate very small structural and attendant conformational changes manifest. Due to the inherent acid instability of oxazolines, additional protecting group manipulations were required for synthesis of oxazoline-oxazole substrate **30** (Scheme 5). Thus, oxazole **31** could be saponified and coupled to *m*-methyl serine.¹³ Switching the nitrogen-protecting group then allowed for cyclization and deprotection/cyclization with thiazolidine 2-thione **38** to obtain alcohol **36**. Coupling to Fmoc-L-valine then provided the acyclic precursor **38**.

Finally, deprotection under basic conditions and cyclization gave macrocycle **39a**. In this case, removal of the tmsyl group

(11) (a) Wang, D. F.; Benquet, P.; Wink, S. J.; West, O. J. *Med Chem* **2005**, *48*, 6936; (b) Ryan, G. C.; Heald, D.; Schrey, M.; Spambauer, A.; Prepel, J. B.; Ye, J.; Pigg, W. D.; Hwang, K.; Cheng, E. J.; Marjic, S.; Melillo, G.; Elwood, Y.; Monga, M.; Kabishevski, M.; Zbindel, J.; Swartz, Jr., K. J. *J Clin Oncol* **2005**, *23*, 5912-22; (c) Benichou, S.; Schlemm, O. *Curr Med Chem* **2003**, *10*, 2333-37.

(12) (a) Vamounis, D.; K. Liverton, S.; Gillingham, P.; Tsoukas, D. *Bioorg Med Chem* **2005**, *13*, 9734-42; (b) Vamounis, D.; K. Liverton, S.; Tsoukas, D.; Gillingham, P.; Gillingham, P. *Med Chem* **2005**, *13*, 3987-92.

(13) (a) Metathesis provided **24**; (b) Et_3N , HATU , HOBt , CH_2Cl_2 , 0°C , 4 h.

**Discovery, Biological Activity, Synthesis and Potential Therapeutic Utility of
Naturally Occurring Histone Deacetylase Inhibitors**

Tenaya L. Newkirk, Albert A. Bowels and Robert M. Williams*

*Department of Chemistry, Colorado State University, Fort Collins, CO 80523
University of Colorado Cancer Center, Aurora, Colorado 80045*

Abstract: A number of small molecule natural products have been shown to inhibit the activity of histone deacetylases (HDACs). These enzymes catalyze the hydrolysis of N-acetyl lysine residues of the histone proteins that package chromosomal DNA and thereby play a vital role in mediating gene expression. HDAC inhibitors (HDACi) are potent cytotoxic agents with significant potential as anticancer therapeutics and it is currently thought that their selective activity on members of specific subclasses of the eighteen known human HDAC isoforms is important to this activity and to moderation of their toxicity. Herein, we discuss both linear and cyclic HDACi, as well as selected synthetically derived analogs.

Covering: up to 2009

- 1 Introduction
- 2 Overview of Histone Deacetylase Enzymes
- 3 Acyclic Histone Deacetylase Inhibitors
- 4 Cyclic Tetrapeptidic Histone Deacetylase Inhibitors
- 5 Sulfur-Containing Histone Deacetylase Inhibitors
- 6 Conclusions
- 7 Acknowledgements
- 8 References

1 Introduction

Histone deacetylase (HDAC) enzymes play an important role in chromatin remodeling and therefore in the regulation of gene expression.^{1,2} Dysfunction of HDAC enzymatic has been linked with a variety of human diseases, including cancer, sickle cell anemia, rheumatoid arthritis and cardiac hypertrophy.³⁻¹¹ With the discovery of molecules that act as HDAC inhibitors (HDACi), a substantial amount of insight into the function of these enzymes has been gained. Furthermore, particularly with respect to cancer, HDACi are extremely promising drug targets. Through the study of naturally occurring HDACi's and their synthetically derived analogs, much progress has been made towards this goal.

2 Overview of Histone Deacetylase Enzymes

In mammalian cells, DNA is packaged into chromatin, a highly condensed structure which limits access to the DNA by transcription factors.¹ In the first step of this packaging, DNA is wound around a histone octamer.¹² This interaction is made favorable by virtue of positively charged lysine residues on the histone proteins, which attract the negatively charged DNA backbones.⁷ This strong electrostatic interaction renders the DNA inactive with respect to transcription, as cellular machinery responsible for transcription cannot access the DNA in this condensed, or closed, state.^{8,9} When transcription is required, the interaction must be lessened to permit access to the DNA. Histone acetyl transferase (HAT) installs an acetyl group onto the ϵ -nitrogen of lysine residues, neutralizing their positive charge and attenuating the interaction between the DNA and the histone.^{1,10} Once replication has been completed, HDAC enzymes remove the N-acetyl group from the lysine residue, restoring positive charge to the histone and returning the DNA to its inactive state.^{10,11,13}

There are currently eighteen known HDAC enzymes which are divided into four classes on the basis of their structural homology with yeast proteins.^{13,14} Class I enzymes (HDACs 1, 2, 3 and 8) are Zn²⁺ dependent, as are class II (HDACs 4, 5, 6, 7, 9 and 10) and class IV (HDAC 11).¹⁵⁻¹⁸ In contrast, class III enzymes (Sirt1-7, also known as Sirtuins) are NAD⁺ dependent, and appear to be resistant to molecules capable of inhibiting class I and II enzymes; the class III enzymes will therefore not be mentioned further.

here.^{6,8,17} Class I and II isoforms differ with respect to both their size and catalytic domains, as well as their localization within the cell. Class I HDACs tend to be smaller (49-55 kDa) than the multidomain class II enzymes (80-131 kDa).⁸ Class I isoforms share sequence homology in the catalytic domain located at the N-terminus, while the class II enzymes have a catalytic domain on the C-terminus, with an N-terminal adapter domain not seen in the class I HDACs.^{1,8} The two classes share a 390 amino acid region of homology within the deacetylase core.¹⁹ These differences suggest that the classes possess distinct functions; notably, while class I HDACs are ubiquitously expressed and confined to the nucleus, class II enzymes display tissue-selective expression and shuttle between the nucleus and cytoplasm.^{2,16,20}

A further complication arises from the classification of each of these enzymes as *histone* deacetylases, which would tend to suggest that histone proteins are the only substrate for these enzymes. However, emerging research has shown that HDACs can act to deacetylate many non-histone proteins, including hormone receptors, chaperone proteins, transcription factors and cytoskeletal proteins.^{11,20} While the specific function of individual isoforms remains unclear, it has been noted that aberrant HDAC activity is associated with cancerous cells.^{10,21,22,23} HDAC 1, for example, appears to be upregulated in both prostate and gastric cancers, while HDAC 3 is overexpressed in lung cancers.¹⁰ In general, the class I enzymes appear to play a role in survival and proliferation of cancer cells, while class II, notably HDAC 8, may be responsible for tumorigenesis.^{10,20,24,25} This link between HDAC enzymes and cancer has led to a search for molecules that can function as HDAC inhibitors in the pursuit of possible cancer therapeutics.

3 Acyclic Histone Deacetylase Inhibitors

Much of what is currently known with respect to the structure and function of HDAC enzymes has arisen from the study of molecules which act as HDAC inhibitors (HDACi); in fact, the first HDACs were originally isolated by affinity chromatography using a naturally occurring HDACi, trapoxin.²⁶ HDACi's have been shown to inhibit tumor progression, and are generally responsible for an antiproliferative effect.¹⁸ Treatment with HDACi's results in death of transformed cells through several different mechanisms: apoptosis via extrinsic or intrinsic pathways, mitotic catastrophe/cell death, autophagic cell death, senescence, and reactive oxygen species (ROS) facilitated cell death.¹⁸ Interestingly, normal cells appear to be resistant to the effects of HDACi's, unlike their transformed counterparts.^{20,27,28} Many different naturally occurring HDACi's are known; for the purposes of this review, these molecules have been divided into two classes: acyclic small molecules and cyclic or bicyclic depsipeptides or peptides.

The earliest known HDACi's fall into the first category: acyclic small molecules. Of the naturally occurring HDACi's in this class, perhaps the best known is trichostatin A (TSA, Figure 1). Furthermore, the sole FDA-approved HDACi, SAHA (marketed as Zolinza by Merck Pharmaceuticals) belongs to this class. SAHA is not a naturally occurring molecule, but rather was found through extensive surveys of small polar molecules capable of inhibiting HDAC enzymes.¹⁸

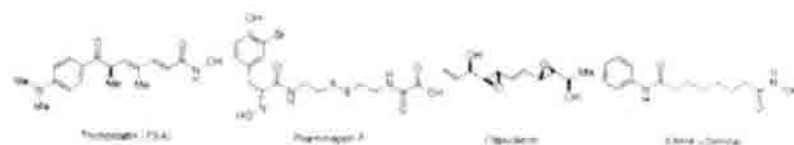


Figure 1: Selected acyclic HDACi's

TSA was isolated in 1976 from *Streptomyces hygroscopicus*, and identified as an HDAC inhibitor by Yoshida and colleagues in 1995.^{29,30} Research on this natural product has divulged many details with respect to the structure and function of HDAC enzymes. Notably, the crystal structure of HDLP (HDAC-like protein) was solved in 1999 by Finnin and coworkers.¹⁹ HDLP shares 35% sequence homology with human HDAC1; importantly, identity is seen within the active site.¹⁹ These crystallographic studies showed a narrow channel ~11Å in depth, narrowing to a diameter of ~7 Å at its narrowest point; at the bottom of this channel, a Zn²⁺ cation is coordinated to two aspartic acid residues, one histidine residue and a water molecule.^{11,18}

In addition to providing information about the general structure of the enzyme, the crystal structure was also solved with bound TSA, giving rise to a model explaining the function of the enzyme (Figure 2).^{11,21}

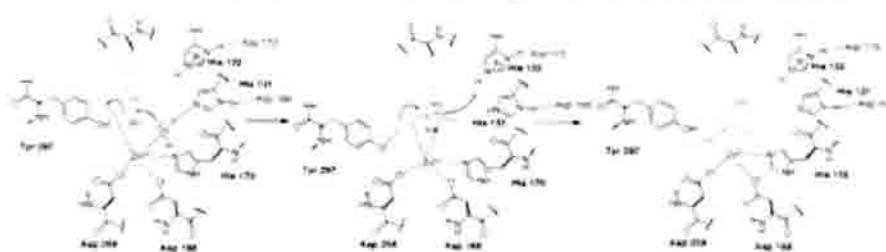


Figure 2: Proposed mechanism of action of Zn²⁺-dependent HDACs

It has been proposed that an acetylated lysine residue (shown in red) coordinates with the zinc cation in the active site. Formation of a tetrahedral intermediate by nucleophilic attack of the water molecule follows, after which the intermediate collapses to release a molecule of acetic acid and the free, deacetylated lysine residue.

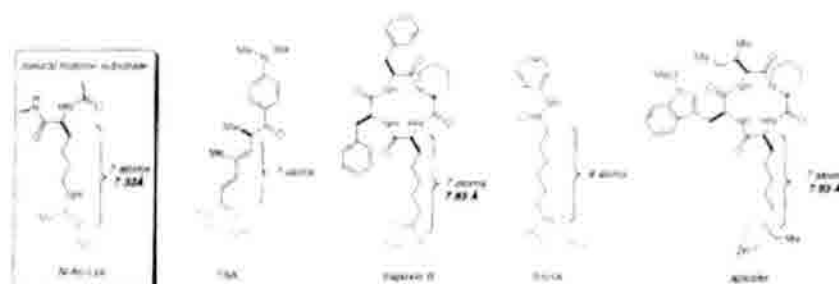


Figure 3: HDACi pharmacophore: cap region in blue; linker in black; zinc-binding moiety in red

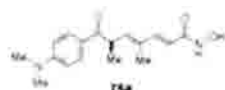
The crystal structure containing a bound TSA molecule suggests that this HDACi acts as a substrate mimic, blocking access to the enzyme by the acetylated lysine residues on the histone tails.¹⁹ The cap region (Figure 3, blue) interacts with amino acid residues surrounding the rim of the channel to the active site; the linker region (Figure 3, black) lowers a zinc-binding arm (through the hydrophobic channel), and the zinc-binding moiety (Figure 3, red) displaces the water molecule and coordinates to the cation.

As is shown in Figure 3, this pharmacophore model of HDACi's three regions is a general and useful classification in order to understand structure-activity relationships.¹¹ Some of the earliest research in this area focused on derivatives of TSA, namely creating analogs with variance in both the zinc-binding and linker regions. Initial studies (prior to crystallographic data) focused on variance in linker length in an effort to determine the optimal distance between the cap and zinc binding regions. In these studies, several variations were synthesized (data summarized in Table 1).^{12, 13}

These studies and others point to a 5-6 methylene unit as being the most effective with respect to HDAC inhibition.¹¹ These data also suggest that bulkier cap regions may give rise to increased biological activity. With respect to the zinc-binding functionality, the hydroxamate moiety is quite common in naturally occurring HDACi's, however, this functional group is considered unattractive for druggable compounds due to difficulties associated with its synthesis, as well as possible toxicity and low stability.²¹ For these reasons, other possibilities have been sought, in the studies mentioned above, numerous carboxylic acid compounds were tested, but all showed significantly attenuated biological activity.¹² Considerable research has been done on analogs of TSA and other, synthetically derived, linear molecules, notably in testing

variations on the linker region³⁴. The conclusions of these studies point to a linker of approximately the same length as the natural substrate being the most effective, with hydrophobic linkers (to better interact with the hydrophobic channel of the enzyme) being the most promising. While such synthetically derived compounds are not the focus of this review, the reader is referred to references 4 and 8 for excellent discussions of this subject.

Table 1: Biological data for TSA analogs and SAHA



Cap region	Linker	Zn ²⁺ -binding arm	IC ₅₀ nM Maize HD-2	IC ₅₀ nM HDAC1
TSA	-----	NHOH	3	NT ¹
(4-Me ₂ N)PhC(O)NH	-(CH ₂) ₄ -	NHOH	2000	NT
(4-Me ₂ N)PhC(O)NH	-(CH ₂) ₃ -	NHOH	100	NT
(4-Me ₂ N)PhC(O)NH	-(CH ₂) ₂ -	NHOH	100	NT
(4-Me ₂ N)PhC(O)NH	-(CH ₂) ₁ -	NHOH	300	NT
(4-Me ₂ N)PhC(O)NH	-(CH ₂) ₀ -	OH	> 40,000	NT
C ₆ H ₅ C(O)	-(CH ₂) ₄ -	NHOH	NT ¹	1500
C ₆ H ₅ C(O)(CH ₂) ₂	-(CH ₂) ₄ -	NHOH	NT	65
C ₆ H ₅ C(O)(CH ₂) ₂	-(CH ₂) ₃ -	NHOH	NT	5
SAHA	-----	NHOH	1000	120

¹NT: not tested

The aforementioned acyclic HDACi's have proven promising as cancer therapeutics. The sole FDA-approved HDACi, SAHA (marketed as Zolinza by Merck Pharmaceuticals), found through screening of numerous small molecules, belongs to this class³⁴. However, one disadvantage to this class of HDACi's is their lack of specificity. These molecules tend to inhibit all isoforms in class I, and in some cases, show inhibitory effects on both class I and class II enzymes.³⁵ Given that the function of individual isoforms remains poorly understood, this type of pan-HDAC inhibition may be less desirable in the clinic. Of the nine HDACi's currently in clinical trials, all are pan-HDAC inhibitors, and it is proposed that cardiac complications (ranging from mild to severe) which have arisen in testing may be due to this lack of specificity^{34,36,37}.

4 Macrocytic Peptide Histone Deacetylase Inhibitors

For the reasons cited above, much of the current research in this area has focused on the isolation and synthesis of HDACi's which display higher selectivity. A group of molecules displaying this desirable characteristic are the macrocyclic HDACi's, although even these show varying degrees of selectivity across class and isoform. Furthermore, many macrocyclic HDACi's possess more potent biological activity than what is seen in the acyclic molecules. These differences between the two classes of HDACi's most likely arise from both the greater variety in zinc-binding moieties and the greater functional complexity of the cap region (Figure 4).

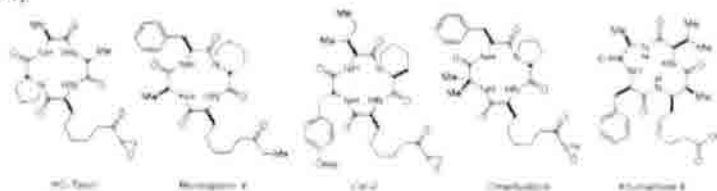


Figure 4: Selected macrocyclic peptide HDACi's

While acyclic HDACi's have smaller cap regions and therefore make contact only with highly conserved regions around the rim of the HDAC channels, the larger cap regions of macrocyclic HDACi's are able to

4

interact with areas of higher variability which lie farther away.²⁰ These more extensive contacts may explain the higher degree of specificity seen with some macrocyclic HDACi's (Table 2).^{12,20}

Table 2: Activity and selectivity of acyclic and macrocyclic HDACi

Compound	IC ₅₀ nM HDAC1	IC ₅₀ nM HDAC4	IC ₅₀ nM HDAC6	HDAC6/HDAC1
TSA	6.0 nM	38 nM	8.6 nM	1.4
TPX A	0.82 nM	NT	524 nM	640
TPX B	0.11 nM	0.30 nM	360 nM	3,300
Chlamydocin	0.15 nM	NT	1,100	7,300
Cyl-2	0.70	NT	40,000 nM	57,000

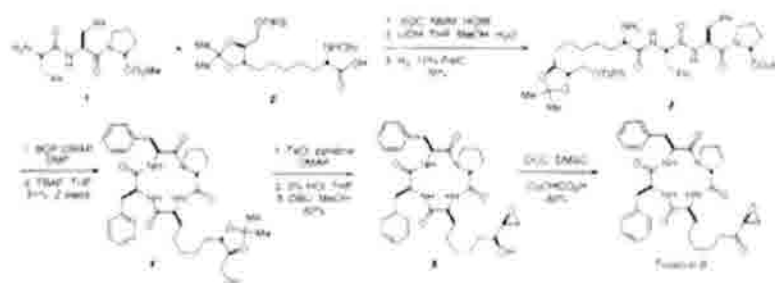
4.1 HC Toxin

One of the first cyclic tetrapeptide HDACi's to be isolated was HC-toxin, found in *Helminthosporium carbonum*, which contains an α -epoxy ketone as its zinc-binding functionality (Figure 4).³⁹ The side chain present in HC-toxin is a common motif among cyclic tetrapeptide HDACi, appearing in the chlamydocins, Cyl-1 and 2, WF-3161 and trapoxins A and B.^{20,40,41} This (S)-2-amino-8-oxo-9,10-epoxydecanoic acid (Aoe) side chain is essentially isosteric with an acetylated lysine residue, suggesting that these molecules also inhibit HDAC enzymes by acting as substrate mimics.^{7,42} HC-toxin displays modest biological activity in comparison with TSA (IC₅₀ = 30 nM against HDACs from *E. tenella* vs. TSA's 3.8 nM).⁴³ However, a related natural product also containing the Aoe side chain, Cyl-2 (Figure 4), is a potent HDACi with an IC₅₀ of 0.75 nM (HDAC 1).^{44,45} Perhaps more impressive is the selectivity displayed by Cyl-2: a 57,000 fold preference for HDAC 1 (class I) over HDAC 6 (class II) was noted in studies by Yoshida et. al.¹²

4.2 Trapoxin

Trapoxin (TPX) is arguably the best-known member of the group of macrocyclic HDACi containing the Aoe side chain. As mentioned above, isolation of HDAC1 by Schreiber and coworkers was made possible by affinity chromatography using an analog of trapoxin A.²⁰ Part of the reason for this success lies in the particular manner in which trapoxin (and other α -epoxy ketone containing HDACi) inhibit HDAC enzymes. In contrast to the hydroxamate zinc-binding functionalities discussed above, α -epoxy ketones bind to HDACs irreversibly, presumably through alkylation of the HDAC enzyme.^{12,46} The epoxide appears to be necessary for irreversible binding, as analogs containing the corresponding diol or methylene groups are biologically inactive.¹²

Schreiber and coworkers published the total synthesis of trapoxin B in 1996 and the route is depicted in Scheme 1.⁴⁷ Macrocyclizations of this type (3 to 4) have proven difficult; in fact, calculational studies have been undertaken in an attempt to predict the appropriate acyclic precursors.⁴⁸ As this technology has yet to be perfected, Schreiber and coworkers instead looked to prior syntheses of chlamydocin, which had shown that successful cyclization appeared to dictate that macrocyclization occur between the piperolate C-terminus and the N-terminus of the Aoe residue.^{47,49,50}

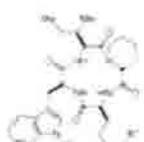


Scheme 1: Schreiber's synthesis of Trapoxin B

The major challenge in this synthesis was the formation of the Aoda side chain. Attempts to follow literature procedures for amino acid homologation gave solely the dehydroamino acids. A radical reaction utilizing iodide **9** and ethyl vinyl ketone in the presence of tri-*n*-butyllin hydride gave the appropriately protected amino acid (**10**) in 46% yield.

Having synthesized the Aoda side chain, a series of peptide couplings were carried out, using DCC/HOBt to give the acyclic precursor (**11**). Numerous peptide coupling reagents were used in attempts to access the macrocycle, ultimately, cyclization was effected using conditions developed by Schmidt, activating the acid as a pentafluorophenyl ester.^{54, 55, 56} A number of apicidin analogs were synthesized to test different zinc-binding motifs. Two such analogs showed activity which was increased with respect to the natural product (Table 4).⁵⁷

Table 4: Biological activity of apicidin A and analogs.

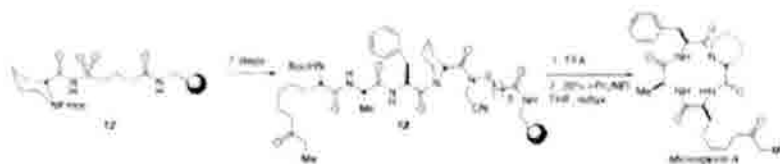


R ¹	R ²	IC ₅₀ , HeLa cell HDACs
C(O)CH ₂ CH ₃	OMe	1 nM
C(O)CH ₂ CH ₃	H	1 nM
CH ₂ SAc	OMe	3 nM
CH ₂ CO ₂ Me	OMe	0.40 nM
CH ₂ C(O)NHOH	OMe	0.24 nM

4.4 Microsporins

Microsporin A contains the same Aoda side chain as the apicidins. Microsporin A and the closely related Microsporin B are cyclic tetrapeptides isolated from a marine fungus, *Microsporium cf. gypseum*.⁵⁸ Detailed NMR studies in conjunction with degradation and derivitization with Marfey's reagent led to the structure shown in Figure 4, containing L-Ala, D-Pip and L-Phe.⁶² In biological testing, Microsporin A displayed activity and selectivity greater than SAHA, inhibiting class I HDACs (IC₅₀ 140 nM vs 300 nM for SAHA) four fold over HDAC8, a class II enzyme (550 nM vs 780 nM for SAHA).⁵¹ These observations led Silverman et al. to pursue a solid-phase synthesis of this natural product (Scheme 3).

Following the synthesis of the Aoda side chain used by Singh, a series of peptide couplings using resin-bound D-Pip gave the acyclic tetrapeptide, which was removed from the resin and cyclized, completing one of the few solid-phase syntheses of this class of HDAC's.^{56, 61}



Scheme 3 Silverman's synthesis of Microsporin A.

4.5 Azumamides

Another group of naturally occurring HDAC's with unusual structures are the azumamides, which are cyclic tetrapeptides isolated from the marine sponge *Mycale azuensis*, although some have proposed that the actual source may be a sponge-associated fungus.^{62, 63} The azumamides display a retro-enantiomeric arrangement with respect to chlamydocin, trapoxin, and apicidin, being composed exclusively of D-amino acids (D-Phe/D-Tyr, D-Ala, and D-Val).⁶⁷ The side chain of the azumamides, (Z,2S,3R)-3-amino-2-methyl-5-nonenedioic acid (Amnda) or (Z,2S,3R)-3-amino-2-methyl-5-nonenedioic acid 9-amide (Amnaa) possesses the opposite absolute configuration as those seen in the aforementioned compounds.^{63, 64}

Furthermore, the azumamides display a high degree of potency as HDAC's when tested against HDACs from human leukemia cells, with IC₅₀ values ranging from 45 nM (azumamide A) to 1.3 μM (azumamide D).⁶⁵ This potency is notable for the fact that the azumamides present relatively weak zinc chelation motifs. azumamides A, B and D have carboxamides in this region, while C and E carry carboxylic acids.

7

conjunction with the installation of this much stronger zinc-binding residue.⁶⁷ Data for these compounds, as compared to TSA, are summarized below (Table 5).

Table 5: Biological data for the azumamides and analogs

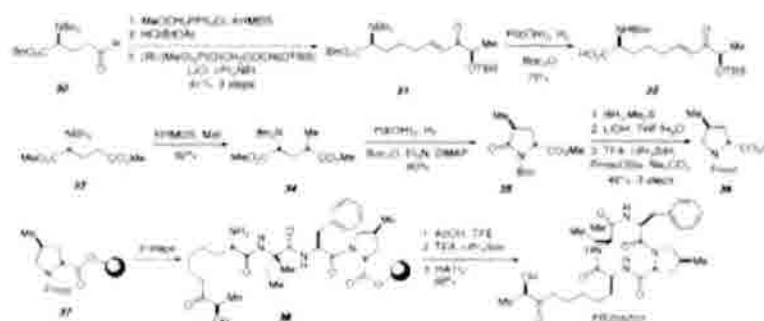
Compound	Zn ²⁺ -binding arm	HeLa HDAC IC ₅₀ μM	K562 HDAC IC ₅₀ μM	HDAC1 IC ₅₀ μM	HDAC4 IC ₅₀ μM	HDAC6 IC ₅₀ μM
Azumamide A	CONH ₂	5.8	0.045	>50	>50	>50
Azumamide B	CONH ₂	NT ^a	0.11	1.83	3.66	>50
Azumamide C	CO ₂ H	NT	0.11	1.17	3.16	>50
Azumamide D	CONH ₂	NT	1.3	>50	>50	>50
(+)-Azumamide E	CO ₂ H	0.033	0.064	1.22	2.28	>50
(-)-Azumamide E	CO ₂ H	26	NT	NT	NT	NT
Azumamide hydroxamate	CONHOH	0.007	NT	NT	NT	NT
TSA	CONHOH	NT	NT	0.037	0.063	0.083

^aNT: not tested

4.6 FR235222

Another naturally occurring HDACi in this class is FR235222, a fungal metabolite isolated in 2003 from the fermentation broth of *Acremonium* sp.⁶⁹ A potent (IC₅₀: 60 nM against HeLa HDACs) inhibitor of HDAC, this compound displays a variation on the α-keto epoxides seen in the trapoxins. Here, a (2*S*,9*R*)-2-amino-9-hydroxy-8-oxodecanoic acid (Ahoda) side chain is present (Figure 4), wherein the epoxide present in trapoxin A is replaced by a hydroxy group. This is notable in part as the di-hydroxy analog of trapoxin A is biologically inactive.¹² As with other cyclic tetrapeptide HDACi's, an unnatural amino acid is included in the macrocycle (D-4-MePro).⁷⁰ The first published synthesis of FR235222 was completed by Taddei and Gomez-Paloma in 2006, and is shown in Scheme 6.⁷⁰

Aldehyde **30** was prepared through a known procedure and converted to acid **32** in four steps.⁷¹ Following the construction of D-4-MePro (**36**), this substance was attached to a polystyrene/2-chlorotrityl resin. Once synthesis of the acyclic precursor was completed, the tetrapeptide was removed from the resin and cyclized in 68% yield. Analogs of the natural product were synthesized by this group and others, as shown in Table 6.^{72,73}



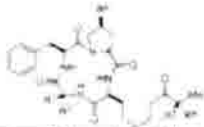
Scheme 6: Synthesis of FR235222

Bifulco and coworkers extended these studies by performing molecular modeling studies in order to identify further targets for synthesis.⁷⁴ Similar interactions to those mentioned above in De Riccardis' studies of the azumamides were noted between the macrocyclic cap and the HDAC enzyme. The proline ring was accommodated by a small hydrophobic cavity containing Tyr 91, Glu 92, and Gly 140, and the Ahoda side chain made similar contacts with the pocket leading to the active site as those found by De Riccardis.⁵⁴ The stereochemistry at C-9 was shown to be an important contributor to binding of the zinc cation, with the

9

natural (*R*) configuration appearing to be more favorable; this is further supported by the inhibitory data shown below (Table 6).^{73,74} The analog containing an indole ring, shown by HDAC inhibition assays to be more potent than the natural product (Table 6), was shown to interact particularly well with the enzyme in docking studies. Hydrophobic pockets at the rim of the channel leading to the active sites made favorable contacts with the ring, suggesting that hydrophobic, bulky groups at this position are preferable.⁷⁴ Computational trends corresponding closely to experimental data suggest that this method of identifying target compounds is a valuable tool for predicting biological activity.

Table 6: Inhibitory data for FR235222 and analogs



Entry	R ¹	R ²	R ³	R ⁴	R ⁵	HeLa HDACs IC ₅₀ nM
1 (FR235222)	Et	Me	OH	H	Me	60
2	Et	Me	OH	H	H	50
3	Me	Me	OH	H	H	30
4	Ph	H	OH	H	H	280
5	Indole	H	OH	H	H	20
6	Me	Me	H	OH	H	330
7	Et	H	H	OH	H	1000

5 Sulfur-Containing Histone Deacetylase Inhibitors

Recently, naturally occurring HDACi's with a novel zinc-binding motif have been isolated. This group, which bears an unusual (3*S*,4*E*)-3-hydroxy-7-mercapto-4-heptenoic acid side chain, includes FK228, the spiruchostatins, FR901375 and largazole. The reduced form of spiruchostatin A has been shown to act as a potent and selective HDACi (IC₅₀ 0.62 nM against HDAC1; 360 nM against HDAC6).²⁰ While the total synthesis of FR901375 (an isolate from *Pseudomonas chloroaphis* No. 2522) has been completed, no inhibitory data has yet been reported for this molecule.⁷⁵

These compounds all contain the β-hydroxy mercaptoheptenoic acid residue connected to a cysteine residue as the unsymmetrical disulfide. There are however, significant differences within the cap regions. In FK228, five sp² hybridized carbon atoms are present within the macrocycle while the spiruchostatins and FR901375 contain only four. While FK228 features sixteen-membered and seventeen-membered rings about the cap group ring and disulfide ring respectively, the spiruchostatins contain a smaller, fifteen-membered ring in the cap group and a sixteen-membered ring about the depsipeptide linkage. FR901375 has a sixteen-membered ring depsipeptide ring, analogous to that of FK228, but the cysteine is shifted relative to the β-hydroxy acid, contracting the outer ring to fourteen atoms about the depsipeptide linkage.

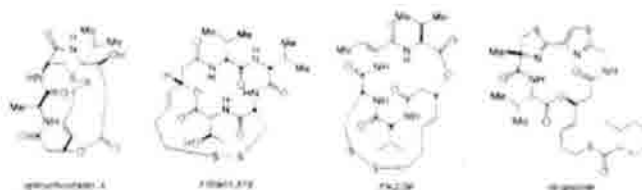
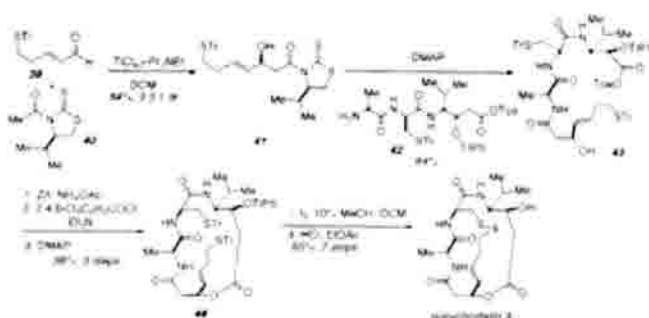


Figure 5: Sulfur-containing HDACi's

5.1 Spiruchostatins

The spiruchostatins were isolated from a culture broth of a *Pseudomonas* sp. in 2001.⁷⁶ There have been to date two total syntheses of spiruchostatin A and one of spiruchostatin B (the sole difference

between the two being the presence of either a C-4' valine or isoleucine)^{77,78,79} Ganesan's total synthesis of spiruchostatin A is particularly of note, and is shown below in Scheme 7.⁷⁸

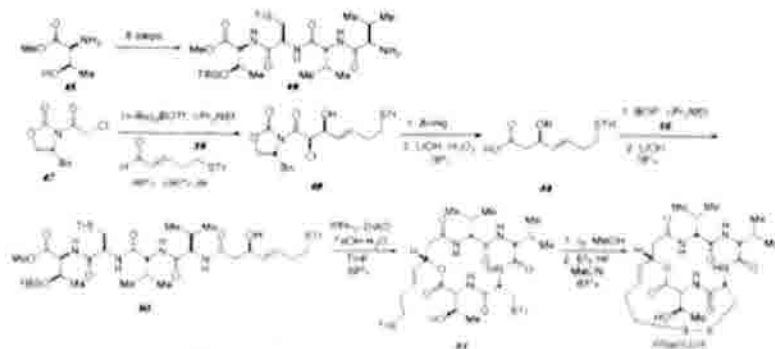


Scheme 7: Ganesan's synthesis of spiruchostatin A.

The β -hydroxy acid stereochemistry was introduced using the Nagao auxiliary in conjunction with Villarasa's TiCl_4 conditions.^{80,81} Acid derivative **41** was then coupled to an appropriately protected peptide (**42**) which was accessed in five steps from commercially available materials. Following deprotection, Yamaguchi macrolactonization proceeded in good yield.^{79,82} Finally, deprotection of the thiol and concomitant formation of the disulfide bond followed by TIPS deprotection gave spiruchostatin A. A small amount of *epi*-spiruchostatin A, with the *R*-stereochemistry at the β -hydroxy acid fragment was also synthesized, and shown to be biologically inactive at $10 \mu\text{M}$, suggesting that stereochemistry at this position is important for interactions with surface amino acid residues on the HDAC enzyme.⁷⁸

5.2 FR901375

FR901375 is a metabolite of *Pseudomonas chloroaphis* (No. 2522) and was reported by Fujisawa Pharmaceutical Company in 1991.⁷⁵ Synthesis of FR901375 has been completed by Janda and co-workers.⁷³ Original attempts to access the requisite β -hydroxy acid following Simon's protocol (see below, Scheme 9) were reported to result in poor yields and low diastereoselectivity. Therefore, a different approach was taken, utilizing Evans' auxiliary.⁸³ This technique permitted access to the β -hydroxy acid (**48**) in greater than 95:5 diastereomeric ratio and 69% yield. Coupling to the tetrapeptide (**46**) and a Mitsunobu reaction furnished the cyclized product (**51**), and formation of the disulfide bond followed by alcohol deprotection gave FR901375.

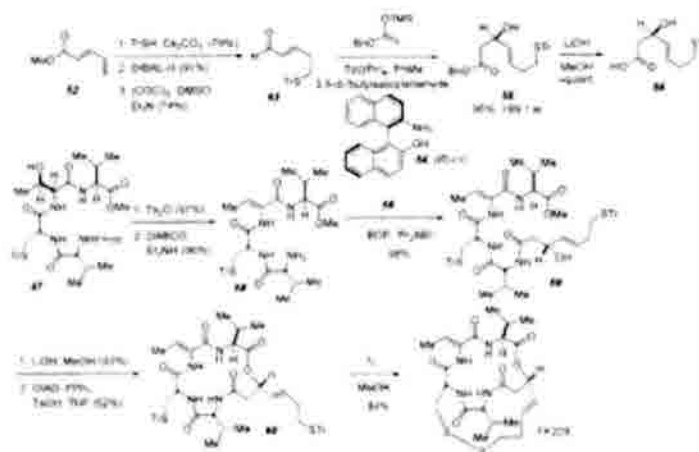


Scheme 8: Janda's synthesis of FR901375

5.3 FK228 (Romidepsin)

The first of the sulfur-containing HDACi's to be discovered was FK228 (also referred to in the literature as FR901228 or depsipeptide, and registered as both NSC 630176 and Romidepsin).⁸⁴ FK228 is currently in human clinical trials for peripheral and cutaneous T-cell lymphoma, and as such, has been extensively studied.⁸⁵⁻⁸⁷ Unlike other HDACi's, studies have been conducted to identify the specific protein targets of FK228, showing that at least 27 proteins involved in a wide variety of cellular processes are affected by this inhibitor.^{86,87} Much of the current understanding of this class of HDACi has come from research on FK228.

The natural product was first isolated from the fermentation broth of *Chromobacterium violaceum* No. 968 in conjunction with a screening program for agents that reverse the malignant phenotype of an Ha-ras oncogene transformed NIH 3T3 cell line.^{88,89} Structurally, FK228 is a bicyclic depsipeptide that features a 16-membered ring about the macrolactone and peptide backbone and a 17-membered ring about the ester and disulfide linkages.⁸⁴ In addition to the β -hydroxy mercaptoheptenoic acid, the smaller ring contains the dehydrothreonine derivative, 2,3-dehydro-2-aminobutanoic acid (Dhb). The structure was determined by spectroscopic and X-ray analysis and confirmed by multiple total syntheses.⁹⁰ The first synthesis reported by Simon made use of a titanium-mediated aldol reaction in conjunction with a ligand derived from (S)-(-)-binaphthyl amino alcohol (**54**) using conditions developed by Carreira to access the chiral β -hydroxy acid in 99:1 er.^{91,92} This acid was synthesized as the enantiomer of the natural stereoisomer such that macrocyclization could be effected under Mitsunobu conditions mandating inversion of stereochemistry. Following a nine-step sequence to access the acyclic precursor of FK228 (**59**), the Mitsunobu reaction gave the cyclized product (**60**) in a reported 62% yield with only trityl deprotection and disulfide bond formation remaining to give FK228 (Scheme 9).⁹¹

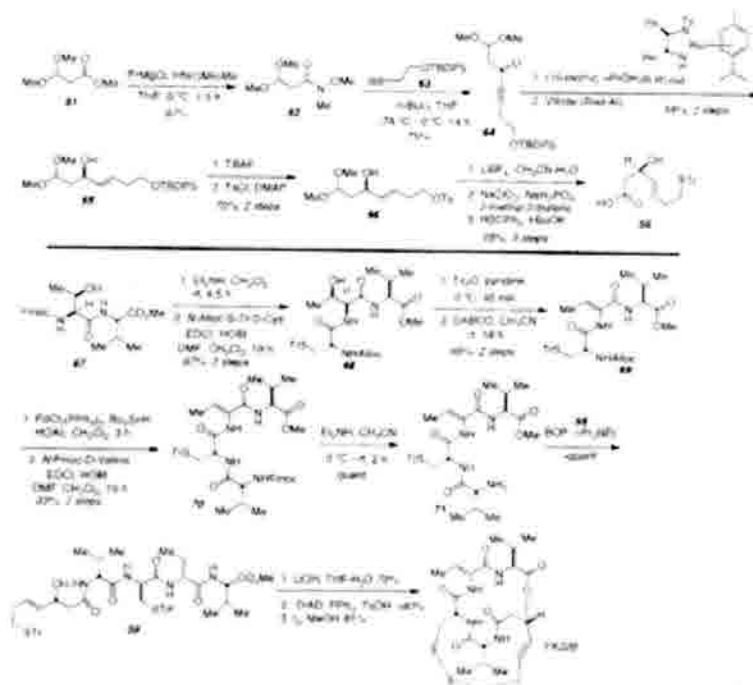


Scheme 9: Simon's synthesis of FK228.

Following publication of Simon's route to FK228, Williams and coworkers published an improved synthesis that was based on the synthetic strategy deployed by Simon.⁹⁵ As mentioned above, FK228 was in clinical trials; however, severe cardiac events were noted, resulting in a suspension of the trials (since then, clinical trials have begun anew).^{85,87} At the time, access to synthetic FK228 was needed such that a better understanding of the biochemistry of the natural product could be achieved prior to reintroduction to the clinic as the natural product was not widely available. This demand necessitated a new, more scalable synthesis of FK228. Williams' route is shown in Scheme 10.⁹⁵

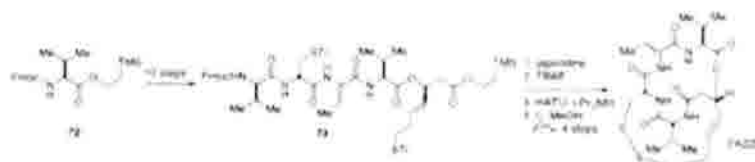
The synthesis of β -hydroxy acid **56** proved both reproducible and scalable, permitting access to this challenging portion of the molecule on a multigram scale.⁹⁵ Further changes were made in the formation of tetrapeptide **58**. The originally published conditions required *N*-Fmoc-D-cysteine(STrt), which proved difficult to synthesize in good yield from D-cysteine; however, the synthesis of *N*-Alloc-D-cysteine(STrt) could be

obtained in high yield following Kruse's method³⁴. Finally, dehydration of the threonine residue early on in the synthesis improved the yield of the tripeptide (69) to 53% overall. To conclude the synthesis, the final coupling of 71 with 56 macrolactonization and disulfide formation from Simon's pioneering work was followed to give FK228.



Scheme 10 Williams' improved synthesis of FK228

Both the Williams and Ganesan laboratories have noted difficulties with the respect to the reproducibility of the yield of the Mitsunobu reaction used in the critical macrocyclization step^{35,36}. To obviate this capricious reaction, an alternative macrolactamization route has recently been reported by Ganesan in both solution-phase and solid-phase formats, with reportedly more robust reproducibility (despite the modest yield) than the Mitsunobu-based macrolactonization strategy (Scheme 11)^{35,37}.



Scheme 11: Ganesan's macrolactamization strategy to FK228

Analogues of FK228 (Figure 6) have been prepared, with perhaps the most notable with respect to insight into structure-activity relationships being the reduced form of FK228 (redFK) and an FK228 amide isostere^{98-99,101}. RedFK was prepared by reducing the natural product with dithiothreitol in order to test the idea that FK228 may act as a prodrug, with the disulfide bond allowing the molecule to be more readily incorporated through the cell wall.⁹⁸ *In vivo* reduction by glutathione within the cell would then reveal a free thiol, which strongly coordinates to the active-site Zn²⁺.^{99,100} Biochemical testing indeed supports this hypothesis, where a 75-fold increase in inhibitory activity against HDAC1 for redFK228 versus FK228 was observed (Table 7).

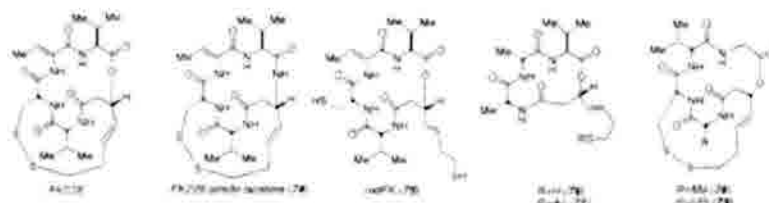


Figure 6: Analogs of FK228

Some preliminary biochemical profiling of these analogs has been reported and comparative data is collected in Table 7. FK228 is a potent inhibitor of the Class I HDACs 1, 2 and 3, but is inactive against the Class IIB HDAC6 (see below).⁹⁸ The biochemical activity of the simplified analogs 76 and 77 display a similar pattern of class selectivity with potency being maintained against HDAC1. The surprising drop in potency for the FK228 analogs 78 and 79 reveals that alteration of the conformation of the cap group, which is presumably a manifestation of the D-valine for dehydrothreonine residue substitution, is critical for high-affinity binding to the protein. These issues will be discussed in more detail below in the context of comparing the FK228 and largazole amide isosteres to their corresponding depsipeptide natural product congeners.

Table 7: Biological data for FK228 and selected analogs

Compound	HeLa HDACs nM	HDAC1 nM	HDAC6 nM
FK228	NT [†]	30	14,000
redFK (75)	15	0.397	787
76	15	1.6	881
77	7.2	1.6	897
78	7	17.5	4900
79	242	>100	>10,000

[†]NT not tested

Synthesis of an FK228 peptide isostere (74) by Williams and coworkers has provided insight into the importance of the depsipeptide linkage, as the more rigid amide isostere of FK228 demonstrates a 50-fold loss in potency against HDAC1.¹⁰² The β-amino acid (85) was synthesized in seven steps from a commercially available protected aspartic acid derivative (80). Acyclic precursor 87 was accessed following Simon's strategy with the intent to accomplish the macrolactamization prior to disulfide formation. However, unlike the syntheses of FK228 discussed above, all attempts at macrocycle formation failed. For this particular substrate, it was found that formation of the disulfide bond (88) prior to macrocyclization was necessary, giving the amide isostere of FK228 in 13 steps.¹⁰¹

Activation of cysteine by the A domain in module 1 effects the formation of a cysteinyl-S-PCP intermediate. Following the formation of 4-mercaptobutanoyl-S-PCP, PKS modules 2 and 3 extend the growing chain using C_2 units from malonyl CoA. Modules 4, 5 and 6 add activated D-Val, D-Cys and Dhb. Module 7 incorporates the final residue as the A domain in module 4 aminoacylates the PCP domain. Finally, the terminal thioesterase domain on DepE catalyzes the macrolactonization and an FAD-dependent pyridine nucleotide disulfide oxidoreductase, and DepH closes the disulfide linkage. To date, Chang's work represents the only published work on the biosynthesis of the bicyclic disulfide-containing HDAC inhibitors.

5.4 Largazole

One of the most recent HDACi's to be isolated is the marine natural product largazole, which was isolated by Luesch and co-workers from the Floridian marine cyanobacterium *Symploca* sp. and reported in early 2008.¹⁰² Largazole also demonstrates some structural similarity to FK228 in that largazole contains the same 3-hydroxy-7-mercaptohept-4-enoic acid moiety common to FK228, FR901375 and spiruchostatin.¹⁰² However, in the case of largazole, the thiol is capped as an octanoyl thiol ester instead of a disulfide linkage, and is therefore a pro-drug that must be activated by enzymatic removal of the octanoyl residue (Figure 7). The macrocycle itself is somewhat more rigid than that of FK228 by virtue of a thiazoline-thiazole moiety.¹⁰¹ This rigidity leads to a lowest energy solution conformation which matches the lowest energy bound conformation, as shown by calculations performed by Wiest and Williams (see below for a more complete discussion).¹⁰¹ This may account for the increase in biological activity of largazole with respect to FK228 (0.07 nM vs. 1.6 nM). Furthermore, the reduced form of largazole (largazole thiol) displays a pronounced (nearly 360-fold) preference for HDAC1 over HDAC6.¹⁰³

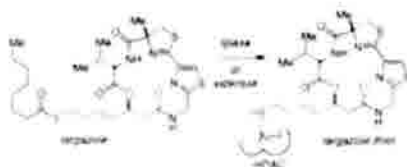
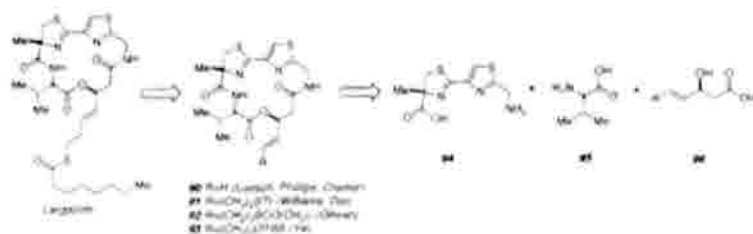


Figure 7: Enzymatic activation of pro-drug largazole.

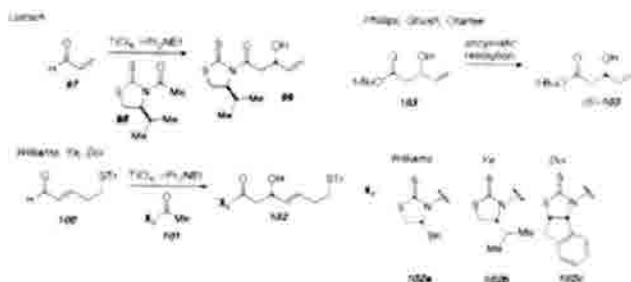
In light of both its unprecedented biological activity and promising selectivity, largazole has attracted a great deal of synthetic attention, with seven total syntheses being published in less than one year following the disclosure of the structure by Luesch and coworkers in early 2008.^{102, 101, 104, 105} A distinctive feature that was coincidentally deployed by several groups in their total syntheses of largazole involved a cross-metathesis reaction onto a pendant vinyl residue for installation of the thiol-containing zinc-binding arm (Scheme 14).



Scheme 14: Strategies employed towards largazole

The major challenges in these syntheses, as in those discussed with regard to other members of the class, are the formation of the β -hydroxy acid unit and the final macrocyclization step. Different approaches have been deployed for the formation of the β -hydroxy acid. Williams, Ye and Doi employed asymmetric

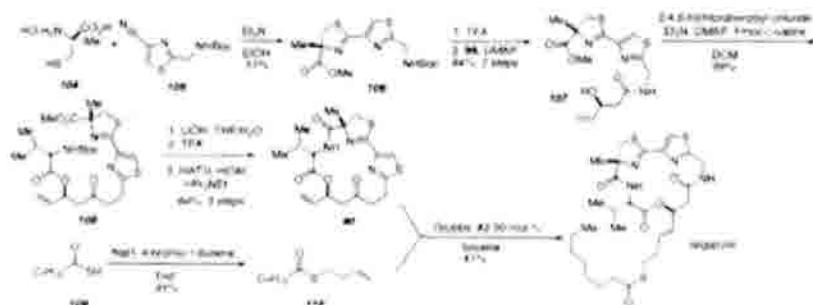
Crimmins-type acetate aldol reactions analogous to that used by Ganesan and colleagues in their synthesis of spiruchostatin A, but with a more complete version of the side chain in place.^{103, 104, 105} Luesch also utilized this method to access the β -hydroxy acid, while Phillips, Ghosh and Cramer employed an enzymatic resolution of achiral substrate **103** (Scheme 15).^{104a, 105}



Scheme 15: Approaches to the β -hydroxy acid moiety

The opposite stereochemistry in the auxiliaries used by Luesch and Ye is explained by existing models, which suggest that the stereochemical outcome of these reactions are dependent upon the amount of base present.^{106, 107}

Following synthesis of the β -hydroxy acid, each group's route proceeded in a similar manner, using a modular synthesis to combine the aforementioned β -hydroxy acid, L-valine and a thiazoline-thiazole moiety.^{103, 104, 105} The first published synthesis of largazole was accomplished by Luesch and co-workers.^{104a} This particular synthesis is notable in part due to the site of ring closure; of the seven published syntheses of the natural product, only Luesch and Ye chose to effect macrocyclization between the valine amino group and the thiazoline carboxyl residue, while the remaining efforts use the less sterically hindered bond between the β -hydroxy acid and thiazole fragments.

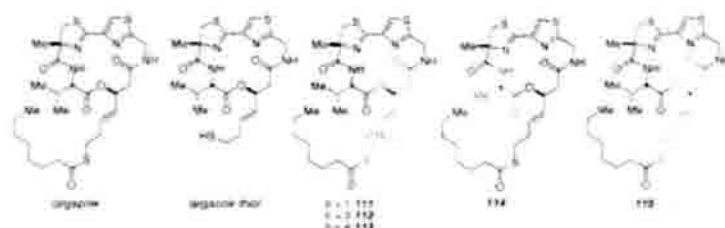


Scheme 16: Synthesis of largazole by Luesch and co-workers.

The requisite nitrile (**105**) was accessed by Cramer in a four-step procedure in 40% overall yield, in a sequence that has proven to be quite scalable.^{105c, 108} The α -methylcysteine piece (**104**) is accessible through a known four step procedure, and the condensation of the two proceeds in good yield.^{105a, 109} Luesch and colleagues used this metathesis strategy to create both chain-shortened and lengthened analogs of the natural product.¹¹⁰ The attenuated biological activity of these analogs suggest that the chain length seen in the natural product is, in fact, the optimal length (Table 8). Furthermore, two variations in the cap group were explored - a valine to alanine substitution and an epimer (**17R**) of largazole.¹¹¹

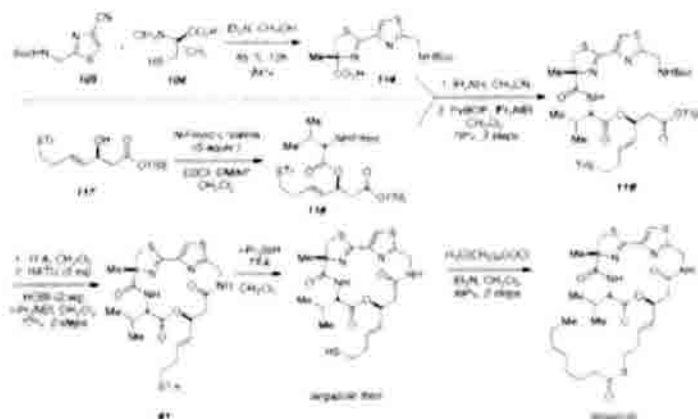
Williams and coworkers chose to install a more fully elaborated version of the β -hydroxy acid (117) at an early stage which obviated the relatively modest-yielding metathesis step utilized by other laboratories. Their synthesis of largazole thiol and largazole is shown in Scheme 17.¹⁰ This synthesis required eight linear steps and proceeded in 38% overall yield. This synthetic platform has been substantially harnessed by this laboratory to prepare numerous analogs of largazole to be discussed below.

Table 8: Biological and biochemical activity of selected largazole analogs



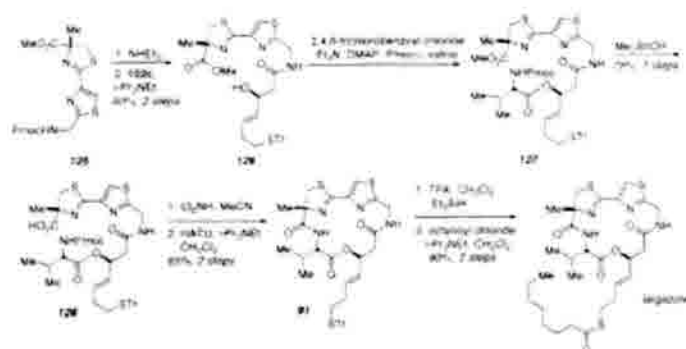
Compound	HeLa HDACs IC ₅₀ nM	HDAC1 IC ₅₀ nM	HDAC6 IC ₅₀ nM
Largazole	32	7.6	1800
Largazole thiol	NT ^a	0.77	570
Largazole n-1 side chain 111	>20000	NT	NT
Largazole n+1 side chain 112	7800	690	>10000
Largazole n+2 side chain 113	4100	1900	>10000
Alanine substitution 114	72	44	3300
(17R) Largazole 115	3900	NT	NT

^aNT not tested



Scheme 17: Synthesis of largazole by Williams and Bowers

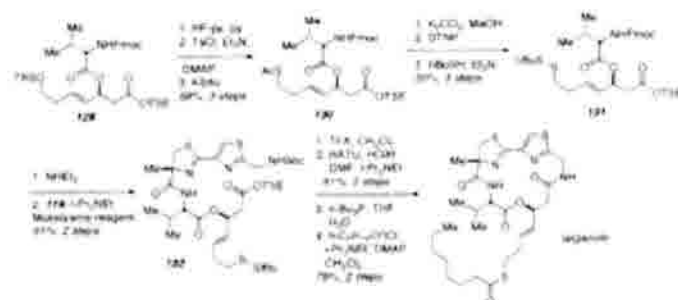
Philips and Cramer converged on the same metathesis substrate (90) as that used by Luesch and fashioned the acyclic precursor (121) by nearly identical routes as illustrated in Scheme 18. Cramer found that the nitro-substituted metathesis catalyst (shown) gave a better yield of 75% with a 6:1 *trans*:*cis* ratio for installation of the intact side chain.



Scheme 20: Synthesis of largazole by Doi

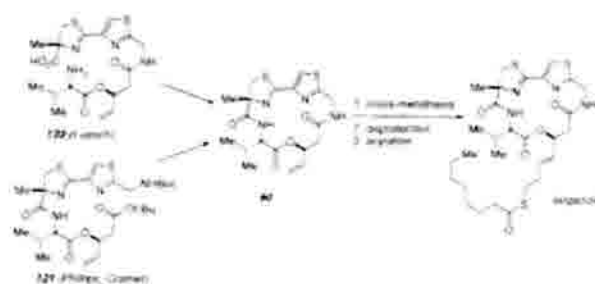
The synthesis of largazole reported by Ye and co-workers is shown in Scheme 21 and is very similar in strategy to that deployed by Williams. This group made use of the unusual unsymmetrical *t*-butyl disulfide species (**131**) to mask the side chain thiol group which was converted into the largazole thiol by phosphine reduction. Final acylation then gave largazole.

The striking similarity between the conceptual approaches to the largazole macrocycle which was independently arrived at by the seven laboratories discussed above reveals an underlying simplicity in the modular structural constitution of this natural product. Unlike FK228, which is a substantially more difficult macrocycle to assemble, the largazole framework appears ideally suited for additional synthetic modification for the identification of new analogs with improved activity.

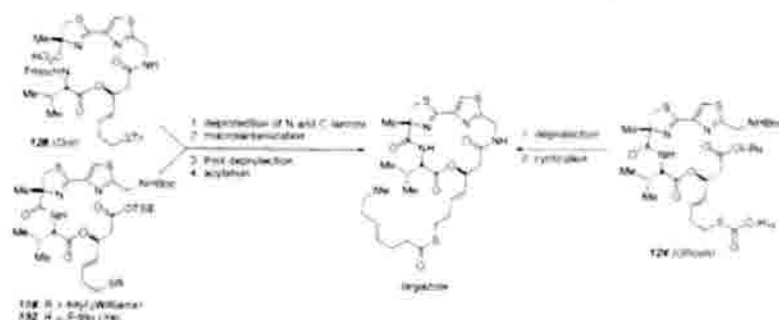


Scheme 21: Synthesis of largazole by Ye

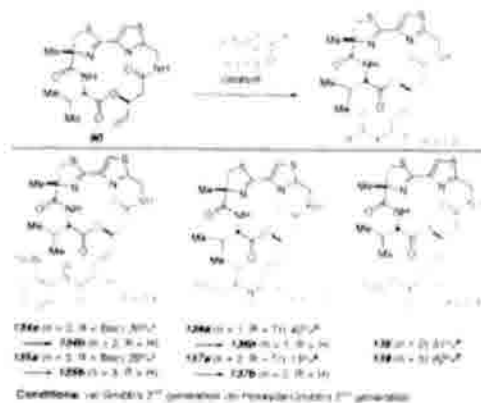
Several of the above syntheses converge upon similar or identical late-stage intermediates which are further manipulated by installation of the side chain by either metathesis or acylation following ring closure. We can thus summarize the above syntheses of largazole into two distinct strategic families: (1) convergence upon the identical macrocyclic metathesis substrate (**90**) that was deployed by the Luesch, Phillips and Cramer laboratories (Scheme 22); and (2) construction of acyclic precursors with sulfur-containing side chain derivatives in place prior to macrocycle formation (Scheme 23)



Scheme 22: Macrocyclic metathesis substrate to largazole



Scheme 23: Acyclic precursors with sulfur-containing side chain derivatives

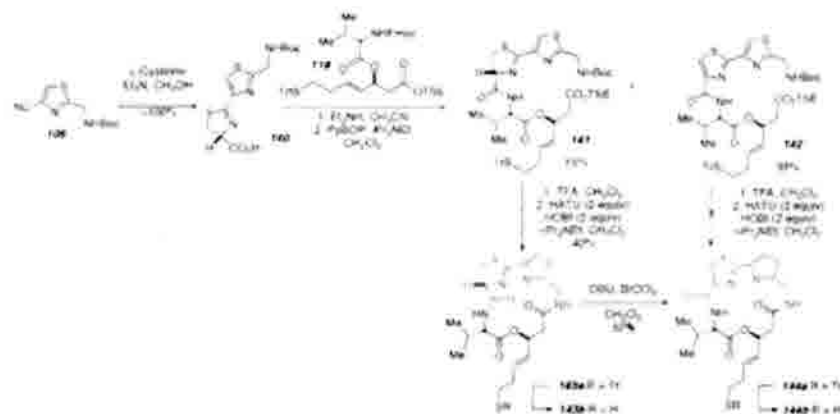


Scheme 24: Linker region and zinc-binding region analogs prepared by Williams

Williams et al. independently constructed the same metathesis substrate (90) used by Phillips, Cramer and Luesch to create a series of largazole analogs with variations of the zinc-binding arm. Most of these analogs, as seen with other linker region analogs described above, have proven to be considerably less potent HDACi's than largazole itself.¹¹¹ Table 9 summarizes the biological data for these compounds. Interestingly, as seen with the unnatural enantiomer of azumamide E, the enantiomer of largazole, first

reported by Williams, as well as epimers of the β -hydroxy acid and valine portions, still display biological activity although, as with (-)-azumamide E, this activity is significantly less than that displayed by the natural product (Table 9). Syntheses for a selection of these analogs are shown in Schemes 24-27.

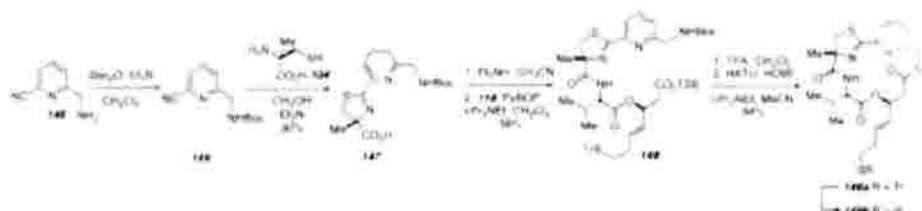
Williams and co-workers have prepared the des-methyl analog **143** based on the recognition that α -methyl cysteine is an expensive amino acid to obtain and is not available on industrial scale. An unexpected, yet interesting bis-thiazole autooxidation side-product (**142**) was obtained during the coupling of **140** and **118** (Scheme 25).



Scheme 25: Desmethyl and thiazoline to thiazole substitution (Williams)

The highly strained macrocycle **144** could not be obtained by attempted macrolactamization via **142** but was obtained by oxidation of the macrocycle **143a** by exposure to BrCCl_3 in the presence of DBU. Thiol **143b** retained potent class I HDAC inhibitory activity revealing that the thiazoline methyl group is not a critical functionality and renders the cysteine-based congeners a potentially simpler and less expensive series of analogs for further development.

The Williams laboratory also reported the synthesis of a largazole analog constituted with a more deep-seated structural change by replacing the thiazole with a pyridine nucleus as shown in Scheme 26. As seen in Table 9, thiol **149b** is the most potent HDACi reported in the literature to date.



Scheme 26: Thiazole to pyridine substitution (Williams).

Williams also reported the synthesis of the oxazoline-oxazole analog of largazole thiol (**157b**, Scheme 27), wherein replacement of the two heterocyclic ring sulfur atoms with oxygen atoms was accomplished. This species, tested as the disulfide homodimer (**157c**), also exhibited very potent biochemical activity as seen in Table 9.

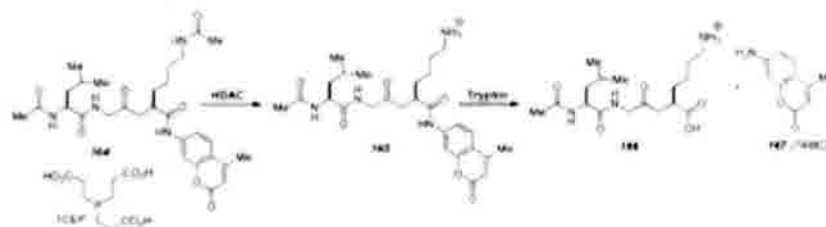
Table 10: Comparative biochemical activity of FK228, largazole and amide isosteres.

Compound	HDAC1 IC ₅₀ nM	HDAC2 IC ₅₀ nM	HDAC3 IC ₅₀ nM	HDAC6 IC ₅₀ nM
FK228*	0.2	1	3	200
FK228 amide isostere* 74	10	60	70	>3000
largazole thiol	0.1	0.8	1	40
largazole isostere thiol 162	0.9	4	4	1500
largazole isostere 163	>3000	>3000	>3000	>3000
SAHA	10	40	30	30

*assay performed in the presence of TCEP

The data in Table 10 reveals that the FK228 amide isostere (**74**) is ~50-80 times less potent than FK228. In the case of the largazole amide isostere thiol (**162**), this substance is ~4-9 times less potent than largazole thiol against the class I HDACs 1, 2 and 3. The essentially surgical, single-atom replacement of an oxygen atom with a nitrogen atom in these two amide isosteres was not expected, *a priori*, to result in a significant loss of biochemical potency. The marked differences in biochemical activity for the natural depsipeptides and their amide counterparts has been evaluated and rationalized computationally by West and is discussed below.

HDAC assay conditions. The measurement of histone deacetylase enzymatic activity in these studies, has been derived from a coupled fluorogenic homogeneous assay developed by Bradner, et al.^{101, 102} Purified HDACs are incubated with trypsin, serum albumin and a fluorogenic substrate (**164**, Scheme 29) comprised of a peptide or small molecule conjugated to acetylated lysine which connects through an amide bond to 7-amino-4-methylcoumarin (7AMC, **167**). Upon deacetylation of the lysine residue, 7AMC is rapidly released by trypsin cleavage and detected by a fluorimeter. The presence of albumin buffers the reaction mixture such that HDAC degradation is not observed. The assay is reproducible and sensitive, requiring limited amounts of enzyme (3 - 100 ng per well). Compatible substrates for HDACs 1-9 have been identified and the Km for each has been determined. The source of enzyme used in the reaction depends on the isoform being tested, and is derived from academic purification efforts or commercial vendors. To improve compatibility with studies of disulfide analogs of FK228, assay performance has been optimized under reducing conditions required to observe potent inhibitory activity of this structural series.



Scheme 29: Coupled fluorogenic assay for HDAC inhibitors.

Bradner, et al were surprised to observe confounding deacetylase inhibition by those reducing agents used most commonly in experimental biology (dithiothreitol and β -mercaptoethanol).^{101, 102} These workers observed that substantial enzyme inhibition was observed at concentrations of these agents required to reduce the FK228 disulfide bond (in contrast, tris(2-carboxyethyl)-phosphine hydrochloride (TCEP) demonstrated comparably weak enzyme inhibition at concentrations markedly higher than required to activate FK228. Under reducing conditions with TCEP (200 mM), biochemical studies of individual isoforms reported robustly on true inhibitory potency of this class of disulfide prodrug HDAC inhibitors. Thus, HDAC inhibitory activities previously reported for the disulfide-containing HDACi's should be viewed with caution, as the presence of other thiols in the assay system will have attenuated the native activity of the deacetylase enzyme.

Computational modeling Wiest and co-workers have developed homology models for several of the human HDACs and have initiated studies to gain high resolution insight into the interactions of various HDACi's at the entry point of the active sites. In an attempt to rationalize the differences in biochemical activities displayed by the natural depsipeptides FK228 and largazole and their more rigid amide counterparts (74 and 162, respectively), extensive computational studies have been performed on models of both largazole and FK228 by Wiest and co-workers. The homology and rigidity of the HDAC active site makes it an attractive target for the use of computational methods such as homology modeling, docking, molecular dynamics as well as ligand-based design. Homology models of human HDACs 1, 2, 3 and 8, as well as the C-terminal domain of HDAC6 based on its bacterial homolog, have been created and validated.^{112-115,114} Shortly after the first publication describing these models appeared, the prediction for the human HDAC8 structure was shown to be highly accurate by x-ray crystallography.¹¹⁵ A modified scoring function could rapidly predict the free energies of binding for a series of hydroxamic acids to a homology model of HDAC1 over a potency range of 10^5 with an $R=0.92$.¹¹⁶ Comparisons of docking scores for eight diverse HDACi's with five different HDACs gave good agreement between experiments and structures obtained from docking.^{117,118} The poses obtained from the docking calculations then served as the starting points for detailed MD simulations to rationalize the experimentally observed selectivities, as well as for potentially providing a tool for predicting new compounds with improved properties. Wiest and coworkers recently explained the structural origins of the experimentally observed HDAC IIb vs. class I selectivity of tubacin (Figure 8), which were traced to the differences in surface shape at the active site exit.^{114,119,120} The surface of HDAC6 is Y-shaped at this point, thus allowing tubacin to make contacts on both sides. However, HDAC1 shows two distinct populations with only one contact each. In addition to the well-known CH- π interactions, a novel sulfur-arene interaction between Met 184 and the aromatic rings of tubacin and NK308 as well as an interaction between Phe 182 and the sulfur linker of tubacin are maintained throughout the simulation.^{121,122,123} This protocol provides an explanation for the subtle effects within a given subclass, such as the observed pattern of low K_i for different inhibitors in HDAC8 compared to other isoforms of class I HDACs. It has been proposed that the origin of this phenomenon is the position of Trp 141, which makes the bottom of the binding pocket sterically more constrained.¹²⁴

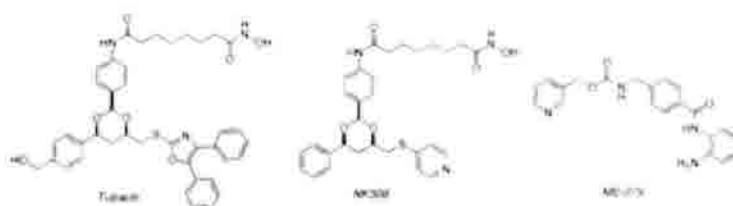


Figure 8: Tubacin, NK308 and MS-275

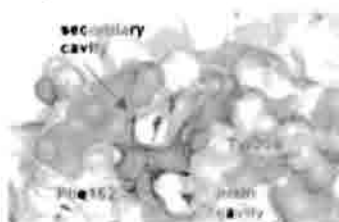


Figure 9: Snapshot from MD simulation of HDAC8.

While these investigations explain the low K_i of MS-275, it does not explain the fact that simple hydroxamic acids were also found to have low K_i 's. MD simulations showed that this is due to a reorientation of Phe 152 and Tyr 306 that combine the two experimentally observed binding pockets, shown

in red in Figure 9, into a large groove (yellow in Figure 9) that is much shallower than the deep binding pockets observed in other class I HDACs.¹¹⁶

Because of this substantial change in surface shape as well as differences in the sulfur-zinc interactions, neither MS-275 nor tubacin are good inhibitors of HDAC8. These results are in excellent agreement with the structures of the recently disclosed 'linkerless' HDAC8-selective inhibitors, which, after opening of the groove, can bind to both cavities.^{124,125} It is interesting to note that these effects are predominantly based on enzyme dynamics which cannot be deduced from X-ray structures alone, but which show subtle differences between the isoforms, even within the same class.

In a collaboration between the laboratories of Williams, Bradner and West, the findings from Table 10 were studied using computational methods. The conformational space of the free thiols of FK228, FK228 amide isostere, largazole and largazole isostere was determined by a Monte Carlo conformational search using the OPLS-AA force field in MacroModel.^{126,127} Subsequent structural clustering was performed according to the heavy atoms root-mean-squared (rms) value, and average structures for each cluster were docked to the homology model of HDAC1 using Glide XP.^{128,129,130}

The preferred coordination modes of the four aforementioned structures are shown in Figure 10. The thiol extends towards the zinc ion at the bottom of the entrance channel with a Zn-S distance of ~2.5 Å, while the macrocycle sits on the mouth of the pocket. The hydrocarbon chain fills the hydrophobic channel lined by Phe 150 and Phe 205.¹³³ The orientation of the macrocycle is similar in the ester and the amide isostere, maximizing lipophilic interactions with residues of the cap.



Figure 10: Coordination mode of FK228 (left) and largazole thiol (right) to HDAC1 active site. Depsipeptides are shown in orange and amide isosteres in yellow.

Analysis of the structures and energies of the conformational space of the four compounds reveals an interesting conformation-activity relationship. Figure 11 illustrates the top view of the superimposed binding conformations (orange for FK228 and largazole, yellow for amide isosteres) and the global minimum conformation (blue for depsipeptides and green for amide isosteres) as well as the relative energies (in kJ/mol) and rms values for higher energy conformations of the four compounds studied (Table 11).¹⁰¹ For FK228, the optimum binding geometry (cluster 6) is only 5 kJ/mol above the global minimum conformation, which is within an RMS of 1.8 Å and therefore structurally similar. In contrast, the amide isostere is much more rigid and the preferred geometry for binding (cluster 7) is not only much higher in energy (40 kJ/mol) than the lowest energy conformation, but with an RMS of 3.11 Å - also structurally very different. There are no conformations that are energetically accessible and that resemble the bound conformation. Binding of the amide isostere of FK228 will therefore involve a significant distortion of the protein surface and/or loss of binding interactions, leading to the experimentally observed loss of activity.

For the largazole thiol, the lowest energy conformation is also the preferred binding conformation. Although the optimal binding geometry for the largazole isostere (cluster 3) is 48 kJ/mol higher in energy than the most stable conformation, the geometries are within an RMS of 1.41 Å and thus very similar, as seen on the top right of Figure 11. As a result, the conformational change of the protein required to bind the low energy conformation of the macrocycle cap is relatively small, and much of the binding interaction will be maintained even if the low-energy conformation is bound. The effect of the isostere substitution in the largazole macrocycle is predicted to be smaller than in FK228, and in agreement with the experimental results.

These models serve to demonstrate the power of computational studies in identifying synthetic targets, particularly in those cases wherein crystal structures of the protein targets are unavailable.

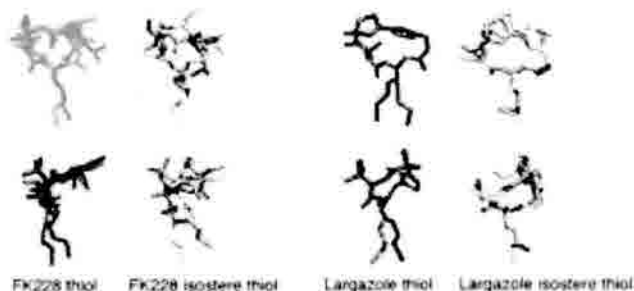


Figure 11 Top and side view of superimposed lowest energy binding conformations (orange for FK228 and largazole, yellow for peptide isosteres) and the average structure for the cluster of lowest energy (blue for depsipeptides and green for peptide isosteres)

Table 11: Energy differences of the average structures of the clusters grouped by heavy atom rms values, relative to the most stable cluster of each compound

Cluster	FK228	FK228 isostere	largazole	largazole isostere
1	0 (0)	0 (0)	0 (0)	0 (0)
2	28 (3.8)	13 (3.71)	30 (2.27)	39 (3.33)
3	35 (3.5)	31 (3.17)	35 (2.29)	48 (1.41)
4	35 (4.2)	30 (2.55)	49 (2.89)	22 (3.27)
5	37 (3.8)	41 (2.39)	35 (3.26)	43 (2.85)
6	5 (1.8)	45 (4.7)	49 (2.77)	28 (2.78)
7	39 (2.7)	40 (3.11)	27 (3.15)	33 (2.06)
8	36 (2.6)		32 (3.58)	
9	32 (3)		38 (3.18)	
10	21 (2.5)		37 (4.09)	
11	30 (2.5)			
12	32 (3.5)			

6 Conclusions

Naturally occurring as well as synthetic, non-natural histone deacetylase inhibitors hold great promise as cancer therapeutics as well as having potential applications in other therapeutic areas. In addition, highly isoform-specific inhibitors may provide this field with powerful new tools with which to study chromatin biology in cells. While highly isoform-specific inhibitors have not yet been discovered, the selectivities observed for some families of inhibitors between classes such as the class I-specific inhibitors FK228 and largazole, indicate that attaining such selectivity may be possible. This field has developed considerably since the isolation of TSA in the 1970's and has exploded with the discovery and functional expression of the various isoforms of HDACs initiated by Schreiber and co-workers in 1996.²⁶ The discovery of naturally occurring macrocyclic HDACi's have provided extremely potent mechanism-based inhibitors of the deacetylase enzymes whose myriad functions are still emerging from the work of numerous laboratories. Synthesis of these compounds as well as their analogs, along with computational studies has begun to provide invaluable insight into the structure-activity relationships present in these molecules. As this field continues to evolve, these molecules present further opportunities for understanding the function of HDAC enzymes and the treatment of human disease.

7 Acknowledgements

We are grateful to the Colorado State University Cancer Supercluster and the National Institutes of Health for financial support (in part) for our work on histone deacetylase inhibitors.

8 References

- ¹ De Ruijter, A.; Van Gennip, A.; Caron, H.; Kemp, S.; Van Kuilenberg, A. *Biochem J.* 2003, **370**, 737-749

- ² Johnstone, R. *Nature Rev. Drug Disc.*, 2002, **1**, 287-299.
- ³ Avila, A.; Burnett, B.; Tay, A.; Gabanella, F.; Knight, M.; Hartenstien, P.; Cizman, Z.; Di Prospero, N.; Pellizzoni, L.; Fishbeck, K.; Sumner, C. *J. Clin. Invest.*, 2007, **117**, 659-671.
- ⁴ Lin, H.; Hu, C.; Chan, H.; Liew, Y.; Huang, H.; Lepescheux, L.; Bastianelli, E.; Baron, R.; Rawadi, G.; Clement-Lacroix, P. *British J. Pharmacol.*, 2007, **150**, 862-872.
- ⁵ Dai, Y-S.; Xu, J.; Molkentin, J. *Mol. Cell Biol.*, 2005, **25**, 9936-9948.
- ⁶ Rodriguez, M.; Aquino, M.; Bruno, I.; De Martino, G.; Taddei, M.; Gomez-Paloma, L. *Curr. Med. Chem.*, 2006, **13**, 1119-1139.
- ⁷ Meinke, P.; Liberator, P. *Curr. Med. Chem.*, 2001, **8**, 211-235.
- ⁸ Gluzak, M.; Seto, E. *Oncogene*, 2007, **26**, 5420-5432.
- ⁹ Grozinger, C.; Hassig, C.; Schreiber, S. *Proc. Natl. Acad. Sci. USA*, 1999, **96**, 4868-4873.
- ¹⁰ Khan, N.; Jeffers, M.; Kumar, S.; Hackett, C.; Boldog, F.; Khramtsov, N.; Qian, X.; Millis, E.; Berghs, S.; Carey, N.; Finn, P.; Collins, L.; Tumber, A.; Ritchie, J.; Jensen, P.; Lichenstein, H.; Sehested, M. *Biochem. J.*, 2008, **409**, 581-589.
- ¹¹ Miller, T.; Witter, D.; Belvedere, S. *J. Med. Chem.*, 2003, **46**, 5097-5116.
- ¹² Furumai, R.; Komatsu, Y.; Nishino, N.; Khochbin, S.; Yoshida, M.; Horinouchi, S. *Proc. Natl. Acad. Sci. USA*, 2001, **98**, 87-92.
- ¹³ Minucci, S.; Pelicci, P. *Nature Rev. Cancer*, 2006, **6**, 38-51.
- ¹⁴ Marks, P.; Breslow, R. *Nature Biotech.*, 2007, **25**, 84-90.
- ¹⁵ Gray, S.; Ekström, T. *Exp. Cell Res.*, 2001, **262**, 75-83.
- ¹⁶ Xu, W.; Parmigiani, R.; Marks, P. *Oncogene*, 2007, **26**, 5541-5552.
- ¹⁷ Imai, S-I.; Armstrong, C.; Kaeberlein, M.; Guarente, L. *Nature*, 2000, **403**, 795-800.
- ¹⁸ Gregoret, I.; Lee, Y-M.; Goodson, H. *J. Mol. Biol.*, 2004, **338**, 17-31.
- ¹⁹ Finnin, M.; Donigan, J.; Cohen, A.; Richon, V.; Rifkind, R.; Marks, P.; Breslow, R.; Pavletich, N. *Nature*, 1999, **401**, 188-193.
- ²⁰ Crabb, S.; Howell, M.; Rogers, H.; Ishfaq, M.; Yurek-George, A.; Carey, K.; Pickering, B.; East, P.; Mitter, R.; Maeda, S.; Johnson, P.; Townsend, P.; Shin-ya, K.; Yoshida, M.; Ganesan, A.; Packham, G. *Biochem. Pharmacol.*, 2008, 463-475.
- ²¹ Jose, B.; Oniki, Y.; Kato, T.; Nishino, N.; Sumida, Y.; Yoshida, M. *Bioorg. Med. Chem. Lett.*, 2004, **14**, 5343-5346.
- ²² Wade, P. *Hum. Mol. Genet.*, 2001, **10**, 693-698.
- ²³ Cress, W.; Seto, E. *J. Cell. Physiol.*, 2000, **184**, 1-16.
- ²⁴ Lagger, G.; O'Carroll, D.; Rembold, M.; Khier, H.; Tischler, J.; Weitzer, G.; Schuettengruber, B.; Hauser, C.; Brunmeir, R.; Jenwein, T.; Seiser, C. *EMBO J.*, 2002, **21**, 2672-2681.
- ²⁵ Glaser, K.; Li, J.; Staver, M.; Wei, R.-Q.; Albert, D.; Davidsen, S. *Biochem. Biophys. Res. Comm.*, 2003, **310**, 529-536.
- ²⁶ Taunton, J.; Hassig, C.; Schreiber, S. *Science*, 1996, **272**, 408-411.
- ²⁷ Burgess, A.; Rueff, A.; Beamish, H.; Warren, R.; Saunders, N.; Johnstone, R.; Gabrielli, B. *Oncogene*, 2004, **23**, 6693-6701.
- ²⁸ Kelly, W.; Marks, P. *Nature Prac. Clin. Oncol.*, 2005, **2**, 150-157.
- ²⁹ Tsuji, N.; Kobayashi, N.; Nagashima, K.; Wakisaka, Y.; Koizumi, K. *J. Antibiot.*, 1976, **29**, 1-6.
- ³⁰ Yoshida, M.; Horinouchi, S.; Beppu, T. *BioEssays*, 1995, **17**, 423-430.
- ³¹ Vanommeslaeghe, K.; De Proft, F.; Loverix, S.; Tourwe, D.; Geerlings, P. *Bioorg. Med. Chem.*, 2005, **13**, 3987-3992.
- ³² Jung, M.; Hoffmann, K.; Brosch, G.; Loidl, P. *Bioorg. Med. Chem. Lett.*, 1997, **7**, 1655-1658.
- ³³ Remiszewski, S.; Sambucetti, L.; Atadja, P.; Bair, K.; Cornell, W.; Green, M.; Howell, K.; Jung, M.; Kwon, P.; Walker, H. *J. Med. Chem.*, 2002, **45**, 753-757.
- ³⁴ Stenson, S.; Wong, J.; Grozinger, C.; Schreiber, S. *Org. Lett.*, 2001, **3**, 4239-4242.
- ³⁵ Garber, K. *Nature Biotech.*, 2007, **25**, 17-19.
- ³⁶ Piekarz, R.; Frye, A.; Wright, J.; Steinberg, S.; Liewehr, D.; Rosing, D.; Sachdev, V.; Fojo, T.; Bates, S. *Clin. Cancer Res.*, 2006, **12**, 3762-3773.
- ³⁷ Remiszewski, S. *Curr. Med. Chem.*, 2003, **10**, 2393-2402.
- ³⁸ Pringle, R. *Plant Physiol.*, 1970, **46**, 45-49.
- ³⁹ Closse, A.; Huguenin, R. *Helv. Chim. Acta.*, 1974, **57**, 533-545.

- ⁴² Umehara, K.; Nakahara, K.; Kiyota, S.; Iwami, M.; Okamoto, M.; Tanaka, H.; Kohsaka, M.; Oaki, H.; Imanaka, H. *J. Antibiot.* 1983, **36**, 478-483.
- ⁴³ Hirota, A.; Suzuki, A.; Suzuki, H.; Tamura, S. *Agric. Biol. Chem.* 1973, **37**, 643-647.
- ⁴⁴ Degenkolb, T.; Gams, W.; Brückner, H. *Chem. Biodiversity* 2008, **5**, 693-705.
- ⁴⁵ Shute, R.; Dunlap, B.; Rich, D. *J. Med. Chem.* 1987, **30**, 71-78.
- ⁴⁶ Komatsu, Y.; Tomizaki, K.-y.; Tsukamoto, M.; Kato, T.; Nishino, N.; Sato, S.; Yamori, T.; Tsuruo, T.; Furumai, R.; Yoshida, M.; Horinouchi, S.; Hayashi, H. *Cancer Res.* 2001, **61**, 4459-4466.
- ⁴⁷ Nishino, N.; Yoshikawa, D.; Watanabe, L.; Kato, T.; Jose, B.; Komatsu, Y.; Sumida, Y.; Yoshida, M. *Bioorg. Med. Chem. Lett.* 2004, **14**, 2427-2431.
- ⁴⁸ Kijima, M.; Yoshida, M.; Sugita, K.; Horinouchi, S.; Beppu, T. *J. Biol. Chem.* 1993, **268**, 22429-22435.
- ⁴⁹ Taunton, J.; Collins, J.; Schreiber, S. *J. Am. Chem. Soc.* 1996, **118**, 10412-10422.
- ⁵⁰ Cavalier-Fortin, F.; Pepe, G.; Verducci, J.; Sin, D.; Jacquier, R. *J. Am. Chem. Soc.* 1992, **114**, 8885-8890.
- ⁵¹ Baldwin, J.; Adlington, R.; Godfrey, C.; Patel, V. *Tetrahedron*, 1993, **49**, 7837-56.
- ⁵² Schmidt, U.; Lieberknecht, A.; Greisser, H.; Bartkowiak, F. *Angew. Chem. Int. Ed.* 1984, **23**, 318-320.
- ⁵³ Mori, K.; Koseki, K. *Tetrahedron*, 1988, **44**, 6013-6020.
- ⁵⁴ Singh, S.; Zink, D.; Polishook, J.; Dombrowski, A.; Darkin-Rattray, S.; Schmatz, D.; Goetz, M. *Tetrahedron Lett.* 1996, **37**, 8077-8080.
- ⁵⁵ Colletti, S.; Myers, R.; Darkin-Rattray, S.; Gurnett, A.; Dulski, P.; Galuska, S.; Allocco, J.; Ayer, M.; Li, C.; Lim, J.; Crumley, T.; Cannova, C.; Schmatz, D.; Wyratt, M.; Fisher, M.; Meinke, P. *Bioorg. Med. Chem. Lett.* 2001, **11**, 113-117.
- ⁵⁶ Singh, S.; Zink, D.; Liesch, J.; Mosley, R.; Dombrowski, A.; Bills, G.; Darkin-Rattray, S.; Schmatz, S.; Goetz, M. *J. Org. Chem.* 2002, **67**, 815-825.
- ⁵⁷ Kuriyama, W.; Kitahara, T. *Heterocycles* 2001, **55**, 1-4.
- ⁵⁸ Mou, L.; Singh, S. *Tetrahedron Lett.* 2001, **42**, 6603-6606.
- ⁵⁹ Deshmukh, P.; Schulz-Fademrecht, C.; Procopiou, P.; Vigushin, D.; Coombes, R.; Barrett, A. *Adv. Synth. Catal.* 2007, **349**, 175-183.
- ⁶⁰ Schmidt, U.; Schanbacher, U. *Angew. Chem. Int. Ed.* 1981, **20**, 1026-1027.
- ⁶¹ Schmidt, U.; Lieberknecht, A. *Synthesis* 1986, 361-366.
- ⁶² Meinke, P.; Colletti, S.; Ayer, M.; Darkin-Rattray, S.; Myers, R.; Schmatz, D.; Wyratt, M.; Fisher, M. *Tetrahedron Lett.* 2000, **41**, 7831-7835.
- ⁶³ Gu, W.; Cueto, M.; Jensen, P.; Fenical, W.; Silverman, R. *Tetrahedron*, 2007, **63**, 6535-6541.
- ⁶⁴ Marley, P. *Carlsberg Res. Comm.* 1984, **49**, 591.
- ⁶⁵ Nakao, Y.; Yoshida, S.; Matsunaga, S.; Shindoh, N.; Terada, Y.; Nagai, K.; Yamashita, J.; Ganesan, A.; Van Soest, R.; Fusetani, N. *Angew. Chem. Int. Ed.* 2006, **45**, 7553-7557.
- ⁶⁶ Maulucci, N.; Chini, M.; Di Micco, S.; Izzo, I.; Cafaro, E.; Russo, A.; Gallinari, P.; Paolini, C.; Nardi, M.; Casapullo, A.; Riccio, R.; Bifulco, G.; De Riccardis, F. *J. Am. Chem. Soc.* 2007, **129**, 3007-3012.
- ⁶⁷ Nakao, Y.; Narazaki, G.; Hoshino, T.; Maeda, S.; Yoshida, M.; Maejima, H.; Yamashita, J. *Bioorg. Med. Chem. Lett.* 2008, **18**, 2982-2984.
- ⁶⁸ Izzo, I.; Maulucci, N.; Bifulco, G.; De Riccardis, F. *Angew. Chem. Int. Ed.* 2006, **45**, 7557-7560.
- ⁶⁹ Wen, S.; Carey, K.; Nakao, Y.; Fusetani, N.; Packham, G.; Ganesan, A. *Org. Lett.* 2007, **9**, 1105-1108.
- ⁷⁰ Brown, H.; Bhat, K. *J. Am. Chem. Soc.* 1986, **108**, 293-294.
- ⁷¹ a) Mori, H.; Urano, Y.; Kinoshita, T.; Yoshimura, S.; Takase, S.; Hino, M. *J. Antibiot.* 2003, **56**, 181-185; b) Mori, H.; Abe, F.; Furukawa, S.; Sakai, M.; Hino, M.; Fujii, T. *J. Antibiot.* 2003, **56**, 80-86; c) Mori, H.; Urano, Y.; Abe, F.; Furukawa, S.; Tsurumi, Y.; Sakamoto, K.; Hashimoto, M.; Takase, S.; Hino, M.; Fujii, T. *J. Antibiot.* 2003, **56**, 72-79.
- ⁷² Rodriguez, M.; Terracciano, S.; Cini, E.; Settembrini, G.; Bruno, I.; Bifulco, G.; Taddei, M.; Gomez-Paloma, L. *Angew. Chem. Int. Ed.* 2006, **45**, 423-427.
- ⁷³ Rodriguez, M.; Taddei, M. *Synthesis* 2005, **3**, 493-495.
- ⁷⁴ Singh, E.; Ravula, S.; Pan, C.-M.; Pan, P.-S.; Vasko, R.; Lapera, S.; Weerasinghe, S.; Pflum, M.; McAlpine, S. *Bioorg. Med. Chem. Lett.* 2008, **18**, 2549-2554.
- ⁷⁵ Gomez-Paloma, L.; Bruno, I.; Cini, E.; Khochbin, S.; Rodriguez, M.; Taddei, M.; Terracciano, S.; Sadoul, K. *ChemMedChem* 2007, **2**, 1511-1519.

- ⁷⁴ Di Micco, S.; Terracciano, S.; Bruno, I.; Rodriguea, M.; Riccio, R.; Taddei, M.; Bifulco, G. *Bioorg. Med. Chem.*, 2008, **16**, 8635-8642.
- ⁷⁵ a) Chen, Y.; Gamba, C.; Abe, Y.; Wentworth, P.; Janda, K. *J. Org. Chem.*, 2003, **68**, 8902-8905; b) Fujisawa Pharmaceutical Co., Ltd., Japan. Jpn. Kokai Tokkyo Koho JP, 03141296, 1991.
- ⁷⁶ Masuoka, Y.; Nagai, A.; Shin-Ya, K.; Furihata, K.; Nagai, K.; Suzuki, K.; Hayakawa, Y.; Seto, H. *Tetrahedron Lett.*, 2001, **42**, 41-44.
- ⁷⁷ Takizawa, T.; Watanabe, K.; Narita, K.; Kudo, K.; Oguchi, T.; Abe, H.; Katoh, T. *Heterocycles*, 2008, **76**, 275-290.
- ⁷⁸ Yurek-George, A.; Habens, F.; Brimmell, M.; Packham, G.; Ganesan, A. *J. Am. Chem. Soc.*, 2004, **126**, 1030-1031.
- ⁷⁹ Takizawa, T.; Watanabe, K.; Koichi, N.; Takamasa, O.; Hideki, A.; Tadashi, K. *Chem. Comm.*, 2008, **14**, 1677-1679.
- ⁸⁰ Nagao, Y.; Hagiwara, Y.; Kumagai, T.; Ochiai, M.; Inoue, T.; Hashimoto, K.; Fujita, E. *J. Org. Chem.*, 1986, **51**, 2391-2393.
- ⁸¹ Aiguadé, J.; González, A.; Urpi, F.; Vilarrasa, J. *Tetrahedron Lett.*, 1996, **37**, 8949-8952.
- ⁸² Inanaga, J.; Hirata, K.; Saeki, H.; Katsuki, T.; Yamaguchi, M. *Bull. Chem. Soc. Jpn.*, 1979, **52**, 1989-1993.
- ⁸³ Evans, D.; Sjørgen, E.; Weber, A.; Conn, R. *Tetrahedron Lett.*, 1987, **28**, 39-42.
- ⁸⁴ Chang, Y.-Q.; Yang, M.; Matter, A. *Appl. Env. Microbiol.*, 2007, **73**, 3460-3469.
- ⁸⁵ Plekarcz, R.; Robey, R.; Sandor, V.; Bakke, S.; Wilson, W.; Dahmouh, L.; Kingma, D.; Turner, M.; Altemus, R.; Bates, S. *Blood*, 2001, **98**, 2865-2868.
- ⁸⁶ Chen, G.; Ailing, L.; Zhao, M.; Gao, Y.; Zhou, T.; Xu, Y.; Du, Z.; Zhang, X.; Yu, X. *J. Proteome Res.*, 2008, **7**, 2733-2742.
- ⁸⁷ Yu, X.; Guo, Z.; Marcu, M.; Neckers, L.; Nguyen, D.; Chen, G.; Schrupp, D. *J. Natl. Cancer Inst.*, 2002, **94**, 504-513.
- ⁸⁸ Ueda, H.; Nakajima, H.; Hori, Y.; Fujita, T.; Nishimura, M.; Goto, T.; Okuhara, M. *J. Antibiot. (Tokyo)*, 1994, **47**, 301-310.
- ⁸⁹ Ueda, H.; Nakajima, H.; Hori, Y.; Goto, T.; Okuhara, M. *Biosci. Biotechnol. Biochem.*, 1994, **58**, 1579-1583.
- ⁹⁰ Shigematsu, N.; Ueda, H.; Takase, S.; Tanaka, H.; Yamamoto, K.; Tada, T. *J. Antibiot. (Tokyo)*, 1994, **47**, 311-314.
- ⁹¹ Khan, W.; Wu, J.; Sing, W.; Simon, J. *J. Am. Chem. Soc.*, 1996, **118**, 7237-7238.
- ⁹² Carreira, E.; Singer, R.; Lee, W. *J. Am. Chem. Soc.*, 1994, **116**, 8837-8838.
- ⁹³ Shah, M.; Binkiy, P.; Chan, K.; Xiao, J.; Arbogast, D.; Collamore, M.; Farra, Y.; Young, D.; Grever, M. *Clin. Cancer Res.*, 2006, **12**, 3997-4003.
- ⁹⁴ Kruse, C.; Holden, K. *J. Org. Chem.*, 1985, **65**, 1192-1194.
- ⁹⁵ Greshock, T.; Johns, D.; Noguchi, Y.; Williams, R. *Org. Lett.*, 2008, **10**, 613-616.
- ⁹⁶ Wen, S.; Packham, G.; Ganesan, A. *J. Org. Chem.*, 2008, **73**, 9353-9361.
- ⁹⁷ Di Maro, S.; Ping, R.-C.; Hsieh, J.-T.; Ahn, J.-M. *J. Med. Chem.*, 2008, **51**, 6639-6641.
- ⁹⁸ Furumai, R.; Matsuyama, A.; Kobashi, N.; Lee, K.-H.; Nishiyama, M.; Nakajima, H.; Tanaka, A.; Komatsu, Y.; Nishino, N.; Yoshida, M.; Horinouchi, S. *Cancer Res.*, 2002, **62**, 4916-4921.
- ⁹⁹ Yurek-George, A.; Cecil, A.; Mo, A.; Wen, S.; Rogers, H.; Habrens, F.; Maeda, S.; Yoshida, M.; Packham, G.; Ganesan, A. *J. Med. Chem.*, 2007, **50**, 5720-5726.
- ¹⁰⁰ Nishino, N.; Jose, B.; Okamura, S.; Ebisusaki, S.; Kato, T.; Sumida, Y.; Yoshida, M. *Org. Lett.*, 2003, **5**, 5079-5082.
- ¹⁰¹ Bowers, A.; Greshock, T.; West, N.; Estiu, G.; Schreiber, S.; West, O.; Williams, R.; Bradner, J. *J. Am. Chem. Soc.*, 2008, **131**, 2900-2905.
- ¹⁰² Taori, K.; Paul, V.; Luesch, H. *J. Am. Chem. Soc.*, 2008, **130**, 1806-1807.
- ¹⁰³ Bowers, A.; West, N.; Taunton, J.; Schreiber, S.; Bradner, J.; Williams, R. *J. Am. Chem. Soc.*, 2008, **130**, 11219-11222.
- ¹⁰⁴ a) Ying, Y.; Taori, K.; Kim, H.; Hong, J.; Luesch, H. *J. Am. Chem. Soc.*, 2008, **130**, 8455-8459; b) Ren, Q.; Dai, L.; Zhang, H.; Tan, W.; Xu, S.; Ye, T. *Synlett*, 2008, **15**, 2379-2383; c) Numajiri, Y.; Takahashi, T.; Takagi, M.; Shin-ya, K.; Doi, T. *Synlett*, 2008, **16**, 2483-2486.

- ¹⁰⁸ a) Nasveschuk, C.; Ungermannova, D.; Liu, X.; Phillips, A. *Org. Lett.*, 2008, **10**, 3595-3598; b) Seiser, T.; Kamena, F.; Cramer, N. *Angew. Chem. Int. Ed.*, 2008, **47**, 6483-6485; c) Ghosh, A.; Kulkarni, S. *Org. Lett.*, 2008, **10**, 3907-3909
- ¹⁰⁹ Crimmins, M.; Shamszad, M. *Org. Lett.*, 2007, **9**, 149-152
- ¹¹⁰ Hodge, M.; Olivo, H. *Tetrahedron*, 2004, **60**, 9397-9403
- ¹¹¹ Miller, K., unpublished
- ¹¹² Mulqueen, G.; Pattenden, G.; Whiting, D. *Tetrahedron*, 1993, **49**, 5359-5364
- ¹¹³ Ying, Y.; Liu, Y.; Byeon, S.; Kim, H.; Luesch, H.; Hong, J. *Org. Lett.*, 2008, **10**, 4021-4024
- ¹¹⁴ Bowers, A.; West, N.; Newkirk, T.; Troutman-Youngman, A.; Schreiber, S.; Wiest, O.; Bradner, J.; Williams, R. *Org. Lett.*, 2009, ASAP, DOI 10.1021/ol900078k
- ¹¹⁵ Wang, D-F.; Helquist, P.; Wiech, N.; Wiest, O. *J. Med. Chem.*, 2005, **48**, 6936-6947
- ¹¹⁶ Weerasinghe, S.; Estiu, G.; Wiest, O.; Plüm, M. *J. Med. Chem.*, 2008, **51**, 5543-5551
- ¹¹⁷ Estiu, G.; Greenberg, E.; Harrison, C.; Kwiatkowski, N.; Mazitschek, R.; Bradner, J.; Wiest, O. *J. Med. Chem.*, 2008, **51**, 2898-2906
- ¹¹⁸ Somoza, J.; Skene, R.; Katz, B.; Moi, C.; Ho, J.; Jennings, A.; Luong, C.; Arvaik, A.; Buggy, J.; Chi, E.; Tang, J.; Sang, B.; Verner, E.; Wynands, R.; Leahy, E.; Dougan, D.; Snell, G.; Navre, M.; Knuth, M.; Swanson, R.; McRee, D.; Tari, L. *Structure*, 2004, **12**, 1325-1334
- ¹¹⁹ Wang, D-F.; Wiest, O.; Helquist, P.; Lan-Hargest, H-Y.; Wiech, N. *J. Med. Chem.*, 2004, **47**, 3409-3417
- ¹²⁰ a) Ragno, R.; Simeoni, S.; Valente, S.; Massa, S. *J. Chem. Inf. Model.*, 2006, **46**, 1420-1430; b) Mukherjee, P.; Shah, F.; Tekwani, B.; Avery, M. *Bioorg. Med. Chem.*, 2008, **16**, 5254-5265; c) Chen, Y.; Jiang, Y-J.; Zhou, J-W.; Yu, Q-S.; You, Q-D. *J. Mol. Graph. Model.*, 2008, **26**, 1160-1168; d) Kim, H.; Kim, M.; Lee, E.; Kang, J.; Lee, K.; Park, S.; Han, J.; Lee, H.; Choi, Y.; Kwon, H.; Han, G. *Bioorg. Med. Chem. Lett.*, 2007, **17**, 6234-6238; e) Ragno, R.; Simeoni, S.; Rotili, D.; Caroli, A.; Botta, G.; Brosch, G.; Massa, S. *Eur. J. Med. Chem.*, 2007, **43**, 621-632
- ¹²¹ a) Lu, Q.; Wang, D.; Chen, C.; Hu, Y. *J. Med. Chem.*, 2005, **48**, 5530-5535; b) Mai, A.; Massa, S.; Ragno, R.; Cerbara, I.; Jesacher, F.; Loidl, P.; Brosch, G. *J. Med. Chem.*, 2004, **47**, 512-524; c) Mai, A.; Massa, S.; Cerbara, I.; Valente, S.; Ragno, R.; Bottoni, P.; Scatena, R.; Loidl, P.; Brosch, G. *J. Med. Chem.*, 2004, **47**, 1098-1109; d) Mai, A.; Massa, S.; Pezzi, R.; Simeoni, S.; Rotili, D.; Nebbioso, A.; Scognamiglio, A.; Altucci, L.; Loidl, P.; Brosch, G. *J. Med. Chem.*, 2005, **48**, 3344-3353; e) Ragno, R.; Mai, A.; Massa, S.; Cerbara, I.; Valente, S.; Bottoni, P.; Scatena, R.; Jesacher, F.; Loidl, P.; Brosch, G. *J. Med. Chem.*, 2004, **47**, 1351-1359; f) Methot, J.; Chakravarty, P.; Chenard, M.; Close, J.; Cruz, J.; Dahlberg, W.; Fleming, J.; Hamblett, C.; Hamill, J.; Harrington, P.; Harsch, A.; Heidebrecht, R.; Hughes, B.; Jung, J.; Kenific, C.; Kral, A.; Meinke, P.; Middleton, R.; Ozerova, N.; Sloman, D.; Stanton, M.; Szewczak, A.; Tyagarajan, S.; Witter, D.; Secrist, P.; Miller, T. *Bioorg. Med. Chem. Lett.*, 2008, **18**, 973-978
- ¹²² Hideshima, T.; Bradner, J.; Wong, J.; Chauhan, D.; Richardson, P.; Schreiber, S.; Anderson, K. *Proc. Natl. Acad. Sci. USA*, 2005, **102**, 8567-8572
- ¹²³ Haggarty, S.; Koeller, K.; Wong, J.; Grozinger, C.; Schreiber, S. *Proc. Natl. Acad. Sci. USA*, 2003, **100**, 4389-4394
- ¹²⁴ Chakrabarti, P.; Samanta, U. *J. Mol. Biol.*, 1995, **251**, 9-14
- ¹²⁵ Samanta, U.; Pal, D.; Chakrabarti, P. *Proteins*, 2000, **38**, 288-300
- ¹²⁶ Barnes, D.; Koehler, A.; Bradner, J.; Mazitschek, R.; Schreiber, S. *Patent* WO2008013569, 2008
- ¹²⁷ Krenn-Hrubec, K.; Marshall, B.; Hedglin, M.; Verdin, E.; Ulrich, S. *Bioorg. Med. Chem. Lett.*, 2007, **17**, 2874-2878
- ¹²⁸ Balasubramanian, S.; Ramos, J.; Luo, W.; Sirisawad, M.; Verner, E.; Buggy, J. *Leukemia*, 2008, **22**, 1026-1034
- ¹²⁹ Kaminski, G.; Friesner, R.; Tirado-Rives, J.; Jorgensen, W. *J. Phys. Chem. B*, 2001, **105**, 6474-6487
- ¹³⁰ Mohamadi, F.; Richards, N.; Guida, W.; Liskamp, R.; Lipton, M.; Caufiel, C.; Chang, G.; Hendrickson, T.; Still, W. *J. Comp. Chem.*, 1990, **11**, 440-467
- ¹³¹ Shenkin, P.; McDonald, D. *J. Comp. Chem.*, 1994, **15**, 889-916
- ¹³² Friesner, R.; Banks, J.; Murphy, R.; Repasky, M.; Frye, L.; Greenwood, J.; Halgren, R.; Sanschagrin, P.; Mainz, D. *J. Med. Chem.*, 2006, **49**, 6177-6196

Appendix 2: Research Proposal

Specific Aims:

The goal of this proposed research is to develop a library of analogs of (-)-stepholidine for biological testing, using methods accessible to undergraduate researchers. Current treatments for schizophrenia display major shortcomings with respect to side effects and concomitant patient non-compliance¹. Many of these unwanted side effects are caused by the mode of action of both traditional and atypical antipsychotic medications; current models for the underlying cause of schizophrenia suggest that optimal treatment for this disease would rely upon a combination of D2 receptor antagonism and D1 receptor agonism². However, antipsychotics currently in use function either exclusively as dopamine D2 receptor antagonists or effect many neurotransmitters³. (-)-Stepholidine is a natural product capable of acting as both a dopamine D2 receptor antagonist and a partial D1 receptor agonist, making it the first known natural product with this dual biological activity^{4,5,6}. We therefore aim to synthesize analogs of the natural product in order to improve its D1 agonist properties while maintaining its D2 antagonist activity in order to identify possible new treatments for schizophrenia. As cellular assays are available to measure these properties, a combination of chemical synthesis and biological testing will permit the study of these compounds in an environment where undergraduate students can be exposed to the synergy between biology and chemistry.

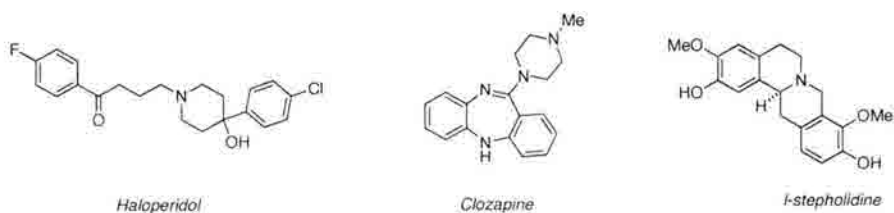
The Goals for this Proposal are as Follows:

1. Develop the first asymmetric synthesis of (-)-stepholidine.
2. Use this synthesis to create a small library of analogs.
3. Evaluate the activity of these analogs for D1 agonism and D2 antagonism through biological assays.
4. Use these preliminary data to further refine the D1 agonist/D2 antagonist pharmacophore.

Background and Significance:

Schizophrenia is a severe mental illness affecting 0.5-1.5% of the world population⁷. The symptoms of schizophrenia are grouped into positive or psychotic symptoms (hallucinations, delusion, severe thought disorganization) and negative symptoms (cognitive impairment, affect flattening, apathy and anhedonia)^{7,8,9}. Known antipsychotics such as haloperidol and clozapine (Figure 1) control psychotic symptoms but tend to leave untreated the more resistant negative symptoms of the disease¹⁰.

Figure 1: Known antipsychotics and *l*-stepholidine



Furthermore, patient noncompliance with current treatments due to disfiguring or undesirable side effects is extremely common; a recent study found >74% discontinuance of medications in less than 18 months of treatment¹¹. One of the most common side effects of antipsychotic medications is tardive dyskinesia; a disorder which causes involuntary movement (particularly of the face) and can lead to symptoms similar to those observed in Parkinson's disease. Oftentimes, tardive dyskinesia is severe enough to warrant the administration of medication for Parkinson's disease in conjunction with antipsychotic medications¹².

So-called traditional antipsychotic agents (e.g. haloperidol) act as powerful D2 antagonists, and are associated with worsening of negative symptoms. Although atypical agents such as clozapine are less powerful D2 antagonists, they too fail to control negative symptoms¹². Additionally, both traditional and atypical antipsychotic drugs have been associated with severe and fatal side effects, including sudden death from cardiac events and agranulocytosis^{13,14}. Improvements on the currently available treatments are therefore a necessity.

While the genetic predisposition towards schizophrenia remains incompletely understood, a methionine to valine polymorphism in the COMT (catechol-*O*-methyl transferase) protein is predictive of schizophrenia¹⁵. This enzyme inactivates dopamine *via* methylation; however, the valine allele has a four-fold greater capacity for dopamine methylation in comparison to the methionine allele^{9,16,17}. This leads to hypodopaminergia in the dorso-lateral prefrontal cortex (dlPFC), and is predictive of poor working memory and lowered central executive function, both of which are noted among the negative symptoms of schizophrenia⁸.

Numerous *in vivo* and post-mortem studies have found significant correlation between dopaminergic dysregulation and schizophrenia. However, the correlation is somewhat more complex than simple hypodopaminergia in the dlPFC. Specifically, it appears that different types of dopamine receptors play distinct roles in the progress of schizophrenia. Dopamine receptors are divided into two subfamilies: D1-type (including D₁ and D₅ receptors) and D2-type (including D₂, D₃ and D₄ receptors)¹². Post-mortem studies on the brains of schizophrenics display a higher than normal concentration of dopamine in the subcortical region in conjunction with increased D2 receptor binding; these findings have been supported by *in vivo* imaging studies^{9,18,19}. In contrast, lower than normal D1 binding has been noted in schizophrenic patients, and is correlated with poor working memory and other cognitive defects seen in conjunction with schizophrenia²⁰. Overall, the currently accepted dopaminergic model for schizophrenia suggests that lower D1 binding gives rise to the negative symptoms associated with the illness while overactivity in D2 receptors leads to the positive or psychotic symptoms²¹.

These findings suggest that better treatments for schizophrenia might rely upon a combination of D2 antagonism and D1 agonism; this hypothesis has been supported by supplemental treatment with D1 agonists for patients receiving antipsychotic medications (D2 antagonists)⁹. However, this solution does not address the side effects arising with currently used D2 antagonists. Furthermore, given the persistent problem of non-compliance among these patients, a more complicated medication regimen is not an ideal solution.

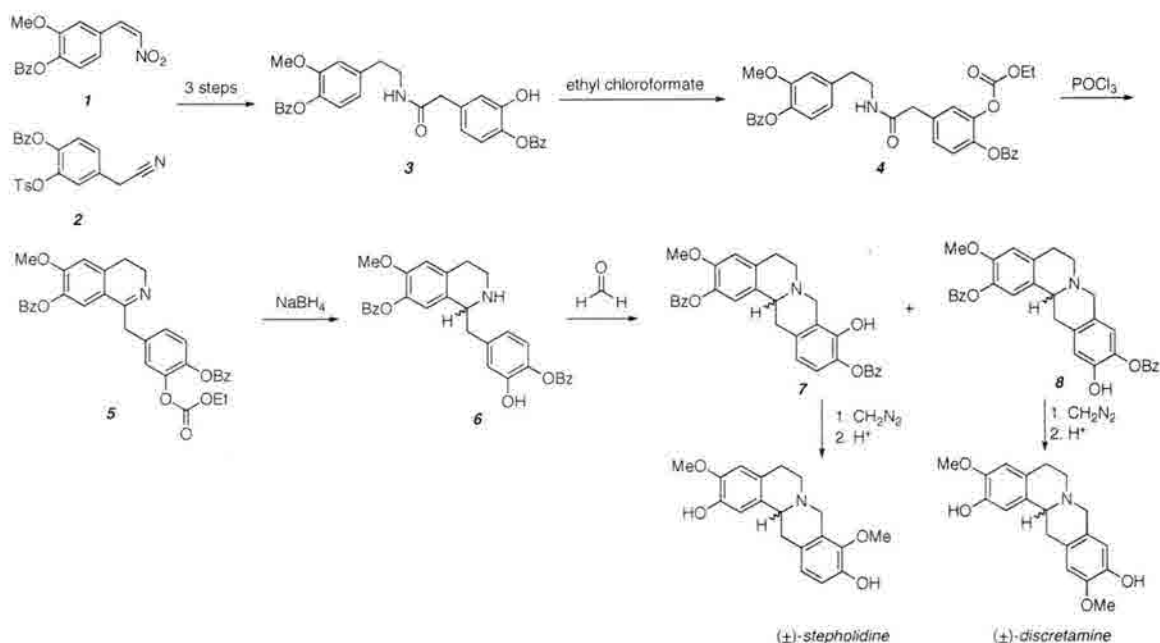
The finding that the natural product (-)-stepholidine acts as both a D2 antagonist and partial D1 agonist was therefore an extremely important advance in possible treatment for schizophrenia^{2,4}. (-)-Stepholidine belongs to the tetrahydroprotoberberine (THPB) class of alkaloids, and was isolated from *Stephania glabra* in 1968 by Weisbach²². Studies have shown that the levorotatory enantiomer is the active compound, and the structure of this natural product has twice been solved by X-ray crystallography, permitting the absolute stereochemistry to be assigned as *S*^{23,24,25}. While stepholidine and related natural products have been the targets of synthetic efforts, to the best of our knowledge, all of these efforts have culminated in racemic mixtures; this issue must therefore be addressed in the creation of possible druggable compounds.

With respect to the use of (-)-stepholidine or its analogs as possible treatments, another distinct advantage to this class of compounds is the lack of extrapyramidal side effects which are common with both traditional and atypical antipsychotic medications. (-)-Stepholidine was found in the Chinese herb *Corydalis yanhusuo* WT Wang, a treatment with a long history in traditional Chinese medicine, with no correlation to these deleterious effects²⁶. However, the partial agonistic effect seen with D1 receptors would need further tuning before this compound could become a realistic treatment. Substances that act solely as D2 antagonists tend to leave untreated or worsen negative symptoms of the disease; likewise, the improvement of negative symptoms appears to rely upon full D1 agonists²⁷.

Previous studies:

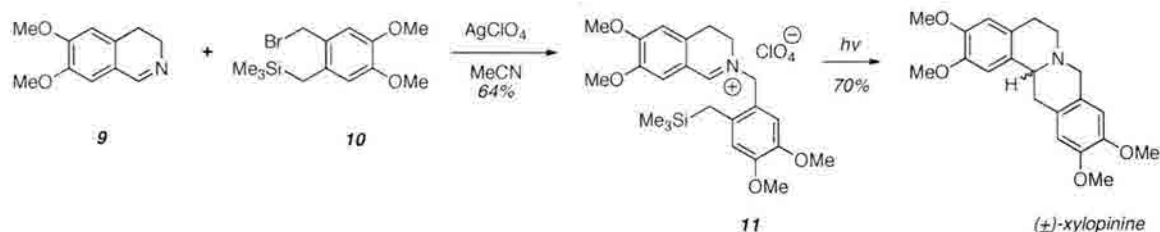
(±)-Stepholidine has been synthesized three times, utilizing the same approach (Scheme 1)^{28,29,30}. The requisite phenylethylamine was synthesized in one step from commercially available material (**1**), and the requisite phenylacetic acid was also easily accessed from the corresponding nitrile (**2**)³¹. These were then coupled to give amide **3**, which was further manipulated to give the substrate for a Bischler-Napieralski reaction. This reaction gives imine **5**, which was reduced with sodium borohydride. Introduction of formaldehyde permitted a Friedel-Crafts type reaction to occur, giving a mixture of two products, **7** and **8**, which were separable by either chromatography or crystallization. Following methylation and deprotection, both (±)-stepholidine and (±)-discretamine were accessed in nine steps for the longest linear sequence, although yields were not reported. Furthermore, the ratio of the two products from the Friedel-Crafts reaction is not discussed, although these workers were able to access usable quantities of both racemic products²⁸.

Scheme 1: Synthesis of (±)-stepholidine and (±)-discretamine



Another interesting approach to related tetrahydroprotoberberines relies upon a radical reaction as shown in Scheme 2; however, this approach also leads to racemic product³².

Scheme 2: Synthesis of (±)-xylopinine



In addition to the aforementioned synthetic efforts, biological testing has been performed on stepholidine and similar compounds. Due to the racemic nature of the syntheses to access these molecules, these studies of biological activity have depended upon isolation of existing natural products or separation of synthesized enantiomers³³. Of particular note are the differences in activity in relation to the substituents on the aromatic rings (Figure 2). A wide variety of tetrahydroprotoberberines are known which vary with respect to the substituents on the A and D rings and in the position of substituents on the D ring. In (-)-stepholidine, two hydroxyl groups are present; one at C-2 and the other at C-10, with C-3 and C-9 occupied by methoxy groups. A related natural product, *l*-scoulerine, contains the same functionality on the A ring, but the hydroxy and methoxy substituents are reversed in ring D (C-9 OH and C-10 OMe). Both of these natural products display similar biological profiles; interestingly, it appears that this class of dihydroxy tetrahydroprotoberberines share this profile³⁴. However, monohydroxy THPB's

display lower affinity for D2 receptors. Furthermore, those compounds wherein all four substituents are present as the methyl ether or the free alcohol display attenuated binding profiles³⁴. Table 1 shows the binding affinity for several of these compounds in comparison to dopamine itself^{34,35,36}.

Figure 2: Selected tetrahydroprotoberberines

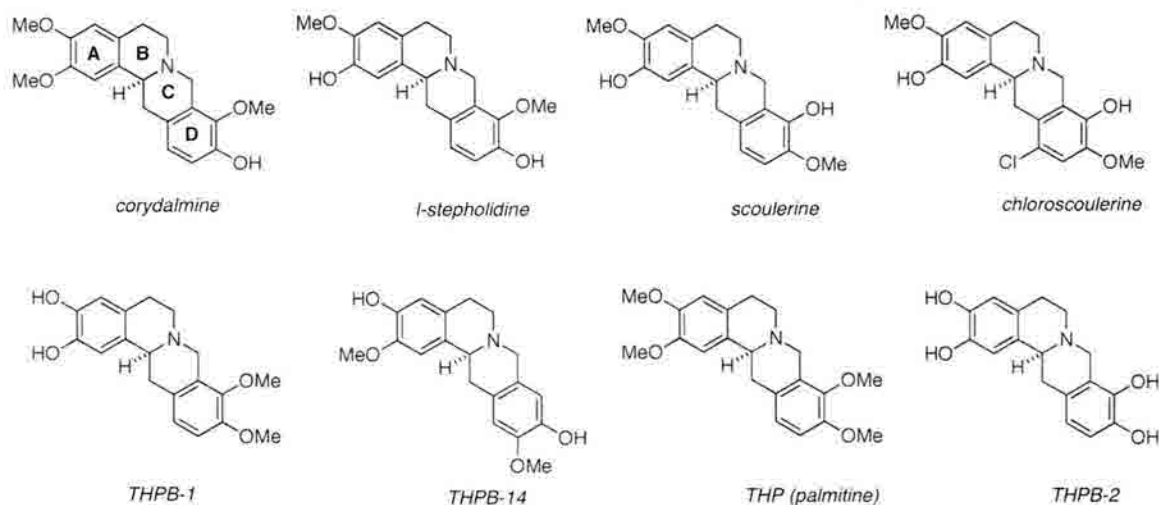


Table 1: Biological activity of selected tetrahydroprotoberberines*

Substituents	Compound	D1, K_i nM	D2, K_i nM
nonhydroxy THPB	<i>l</i> -THP	754	0.85
monohydroxy THPB	<i>l</i> -corydalmine	80	0.65
	<i>l</i> -xylopinine	NT**	7.5
dihydroxy THPB	<i>l</i> -stepholidine	280	0.08
	<i>l</i> -chloroscoulerine	5.7	0.0057
	<i>l</i> -scoulerine	42	0.18
	THPB-1	NT	18.5
	THPB-14	66	NT
	<i>l</i> -discretamine	NT	0.6
	tetrahydroxy THPB	THPB-2	NT

* Values for dopamine itself vary considerably with the assay in use; therefore, these data are not included.

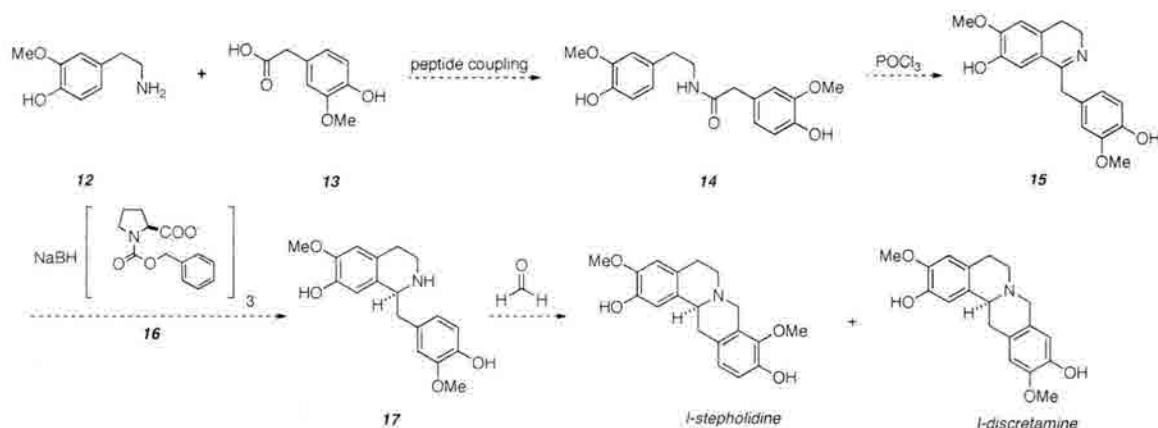
**NT: not tested

Research Design and Methods:

Given its unique biological activity and lack of side effects, (-)-stepholidine provides an excellent platform for the synthesis of analogs which could act as full D1 agonists while maintaining their D2 antagonistic activity. We propose to build a library of analogs, using chemistry accessible to undergraduate researchers. Extant assays for D1 and D2 binding will be used to identify promising compounds (see below for a more detailed explanation of the biological assays).

The proposed synthesis for (-)-stepholidine is shown below (Scheme 3), and closely follows work by Chiang²⁸. Given that undergraduate researchers will be performing the synthesis, we have chosen to rely upon known chemistry so as to ensure a higher probability of success. However, we have chosen to access **17** through the use of a chiral reducing agent to set the stereocenter. Given the importance of this stereocenter to the biological activity, an asymmetric synthesis is desired, and to the best of our knowledge, this would represent the first enantioselective synthesis of (-)-stepholidine.

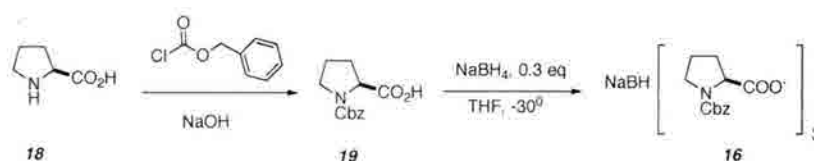
Scheme 3: Proposed synthesis of (-)-stepholidine



It is hoped that this synthesis could be carried out without relying on protecting groups, as there is some precedent for similar syntheses without protecting groups³⁷. Should protection of the hydroxyl groups prove necessary, benzyl has been used with success in prior syntheses.

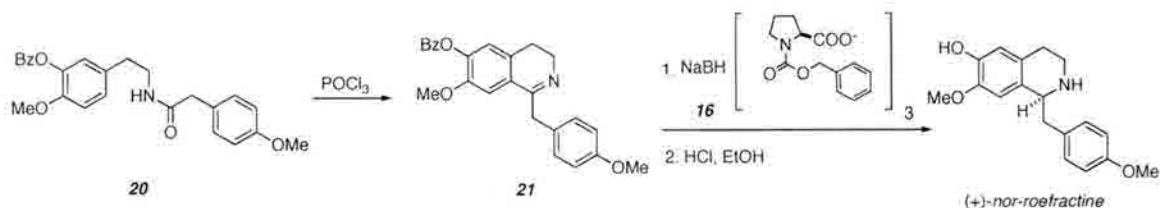
As seen above, it is anticipated that the ring closure to access (-)-stepholidine will give a mixture of products as has been observed in prior syntheses. However, other natural products corresponding to discretamine have been isolated, one of which (THPB-14) has higher affinity for D1 receptors than stepholidine itself, although it has not been tested with D2 receptors. This improved potency with respect to D1 receptors make this a desirable target in and of itself, provided that antagonistic potency for D2 receptors remains high. Given that the two products are separable, it is desirable to follow this route in order to have as many compounds available for testing as possible. The chiral borohydride reagent proposed in the above synthesis has been prepared by Iwakuma and coworkers as shown below^{38,39}.

Scheme 4: Synthesis of chiral reducing agent



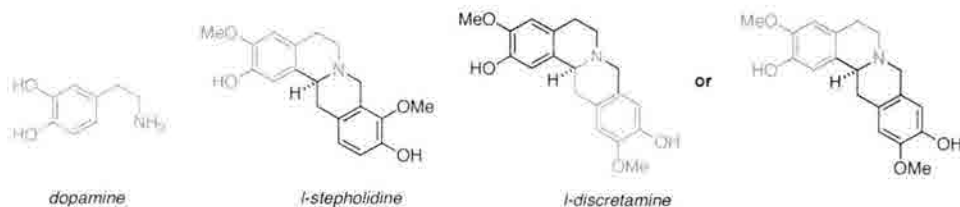
Furthermore, this reagent has been used in the preparation of a related alkaloid, (+)-*nor-roefractine* with success (Scheme 5)⁴⁰. Given their results, it is anticipated that the use of L-proline will give the desired stereochemistry.

Scheme 5: Synthesis of (+)-*nor-roefractine*



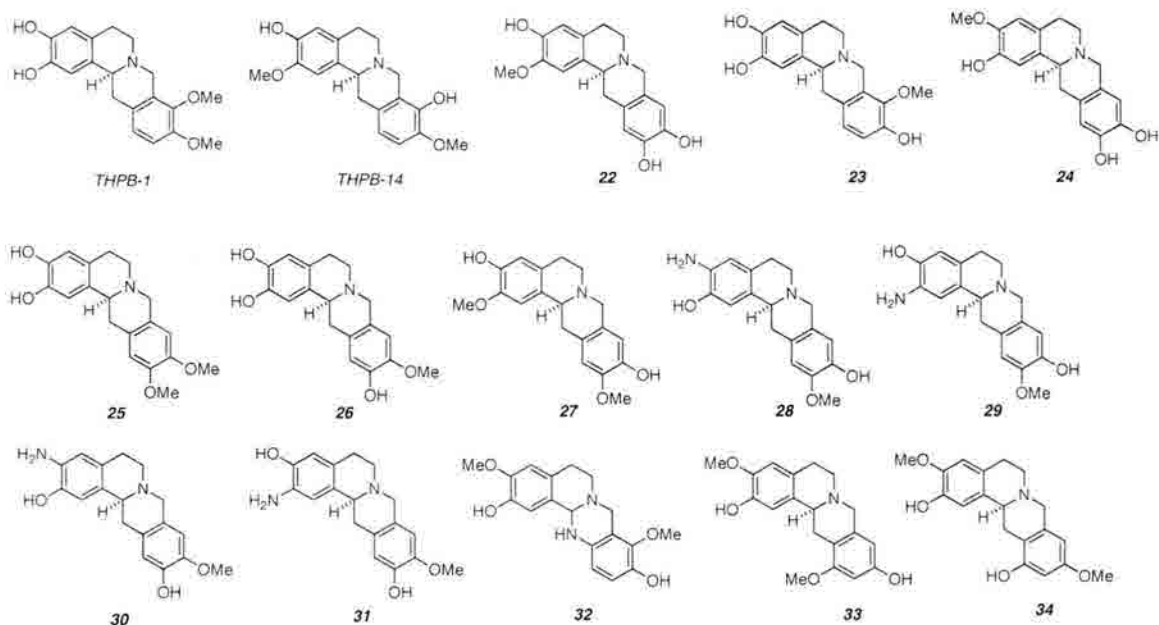
Much of the information regarding the pharmacophore model for (-)-stepholidine comes from mutagenesis experiments and molecular modeling^{21,41,42,43}. Through this work, certain key interactions are known, and this information can be applied to the proposed library of compounds to create rationally designed analogs. In modeling of stepholidine bound to D2 dopamine receptors, a very strong interaction between the A ring hydroxyl group and a protonated histidine residue (H-6.55) is seen. Due to a conformational difference wherein the dihedral angle between rings A and D (98° in D2 receptors; 150° in D1 receptors), this interaction is not present when stepholidine is bound to D1. However, the hydroxyl group on ring A does form a hydrogen bond with W-3.28 when bound to the D1 receptor; these data suggest that the A-ring hydroxyl group is necessary. Furthermore, when bound to the D1 receptor, the A ring participates in π -stacking interactions with three tryptophan residues, suggesting the necessity of an aromatic ring at this position for optimal D1 binding²¹. It has been proposed that two hydroxyl groups on the D ring may improve interactions with the D1 receptor, as this type of structure would more closely correspond to the dopamine pharmacophore (Figure 3).

Figure 3: Structural correlations between dopamine and tetrahydroprotoberberines



Finally, it has been shown that a protonated nitrogen may be necessary as *N*-alkylated products show lowered activity; the one exception to this is the *N*-propyl derivative which shows increased affinity for D2 receptors but a loss of potency for D1 binding⁴². With these data in mind, we propose the small library of analogs shown in Figure 4 as a first set of targets for biological testing.

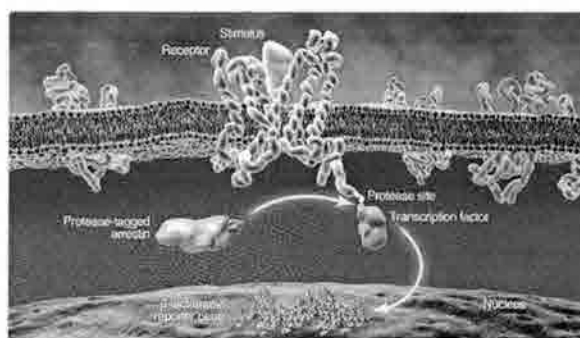
Figure 4: Proposed analogs



These compounds, with the exception of **32** (for which a synthetic route exists), are accessible through the synthesis shown in Scheme 3⁴⁴. All proposed compounds are shown with the same stereochemistry as studies on these and related alkaloids have shown this to be the active or naturally occurring configuration^{23,45,46,47,48,49}. The proposed library includes THPB's 1 and 14, as these compounds have shown biological activity (Table 1). However, as testing is incomplete and these have yet to be synthesized in enantiopure fashion, they are included in this first set of molecules.

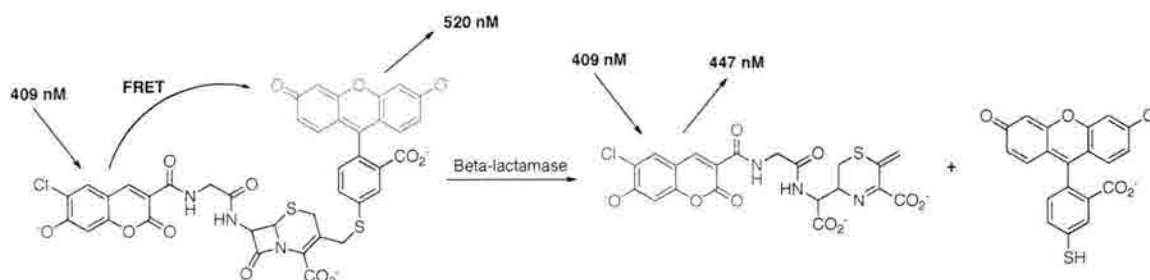
Following the synthesis of these analogs, assays for D1 and D2 binding will be performed. One option for this testing is a currently available assay which measures both antagonist and agonist effects by virtue of a fluorescent reporter gene⁵⁰. Upon binding to an agonist, the G-protein coupled receptor is activated and associates with a protein (arrestin) tagged with a protease. This protease releases a transcription factor bound to the C-terminus of the G-protein coupled receptor. Upon translocation into the nucleus, the transcription factor activates transcription of a β -lactamase.

Figure 5: Proposed biological assay



As shown in Scheme 6, the β -lactamase effects the cleavage of a fluorescent tag, causing a change in the color of fluorescence. This assay is available for G-protein coupled receptors and gives results for both antagonists and agonists. The ratio of blue to green fluorescence then provides information about the antagonist or agonist capabilities of the molecule.

Scheme 6: Mechanism of biological assay



The optimal compound will show D2 antagonist and D1 agonist properties; ultimately, a full D1 agonist (as determined by comparison with dopamine itself) while maintaining stepholidine's inherent D2 antagonist activity is the goal. It is expected that the first library will need further improvement; biological data from these assays will aid in tracking possible patterns for biological activity, giving information for further targets.

Potential Difficulties and Limitations with this Proposal:

As with any research, some difficulties are expected. Below are explained possible setbacks along with proposed solutions.

1. In the event that only one series of compounds (stepholidine-type or discretamine-type) proves biologically valuable, it will be necessary to alter the synthesis to access only one regioisomer in the Friedel-Crafts reaction. Blocking the undesired position with a bromine atom followed by de-bromination has been used successfully by Kametani and coworkers^{51,52}.
2. It is possible that none of the proposed analogs will display any increased activity over the natural product with respect to D1 receptors. Other ring systems (notably piperazines) have shown promising activity; making this substitution may improve D1 agonist properties⁴¹.
3. It is possible that the proposed chiral borohydride reduction will not provide good selectivity. There are many such known reagents which could be tried; however, to start these syntheses, the proposed proline derivative is preferable due to the inexpensive nature of the reagents.
4. It is possible that the free phenols may prove problematic in the synthesis of **14**. However, similar peptide couplings are precedented⁵³.
5. It is possible that the proposed biological assay may not work as planned. This is the preferred assay as it provides students with an opportunity to learn about the molecular basis for fluorescence as well as FRET. However, should it be necessary to use a different method, other assays are known; notably, there are commercially available assays using luciferase reporter genes which permit ranking of agonists and antagonists on the basis of relative light units⁵⁴.

Closing Remarks:

In conclusion, this proposal describes the synthesis of a library of analogs to be tested in biological assays for their possible utility as dopamine D1 receptor agonists and D2 receptor antagonists. Such molecules would represent a novel approach in the treatment of schizophrenia, a debilitating mental illness. Current medications, which act solely as D2 receptor antagonists, do not treat the serious negative symptoms of the disease, and their potentially harmful side effects lead to patient non-compliance. The synthesis of a compound which could regulate psychotic symptoms through D2 antagonism while improving negative symptoms through D1 agonism would therefore represent an important advance in the treatment of schizophrenia. In the course of this project, undergraduate researchers will be exposed to a variety of synthetic chemistry techniques as well as biological testing, giving them an opportunity to explore both of these sciences and the fusion between the two.

Literature Cited:

- ¹ Mamo, D.; Kapur, S.; Keshavan, M.; Laruelle, M.; Taylor, C.; Kothare, P.; Barsoum, P.; McDonnell, D. D2 receptor occupancy of olanzapine pamoate depot using positron emission tomography: An open-label study in patients with schizophrenia. *Neuropsychopharmacol.*, **2008**, *33*, 298-304.
- ² Mo, Y-Q.; Jin, S-J.; Chen, Y-T.; Jin, G-Z.; Shi, W-X. Effects of *l*-stepholidine on forebrain Fos expression: Comparison with clozapine and haloperidol. *Neuropsychopharmacol.*, **2005**, *30*, 261-267.
- ³ Auclair, A.; Kleven, M.; Besnard, J.; Depoortère, R.; Newman-Tancredi, A. Actions of novel antipsychotic agents on apomorphine-induced PPI disruption: Influence of combined serotonin 5-HT_{1A} receptor activation and dopamine D2 receptor blockade. *Neuropsychopharmacol.*, **2006**, *31*, 1900-1909.
- ⁴ Jin, G-Z.; Zhu, Z-T.; Fu, Y. (-)-Stepholidine: A potential novel antipsychotic drug with dual D1 receptor agonist and D2 receptor antagonist actions. *Trends Pharm. Sci.*, **2002**, *23*, 4-7.
- ⁵ Xu, S-X.; Yu, L-P.; Han, Y-R.; Chen, Y.; Jin, G-Z. Effects of tetrahydroprotoberberines on dopamine receptor subtypes in brain. *Acta Pharm. Sinica*, **1989**, *10*, 104-110.
- ⁶ Jin, G-Z.; Huang, K-X.; Sun, B-C. Dual actions of (-)-stepholidine on dopamine receptor subtypes after substantia nigra lesion. *Neurochem. Int.*, **1992**, *20S*, 175S-178S.
- ⁷ Laruelle, M.; Frankle, W.; Narendran, R.; Kegeles, L.; Abi-Dargham, A. Mechanism of action of antipsychotic drugs: From dopamine D2 receptor antagonism to glutamate NMDA facilitation. *Clin. Ther.* **2005**, *27*, Supplement A, S16-S24.
- ⁸ Sitskoorn, M.; Aleman, A.; Ebisch, S.; Appels, M.; Kahn, R. Cognitive defects in relatives of patients with schizophrenia: A meta-analysis. *Schizophrenia Res.* **2004**, *71*, 285-295.
- ⁹ Goldman-Rakic, P.; Castner, S.; Svensson, T.; Siever, L.; Williams, G. Targeting the dopamine D1 receptor in schizophrenia: Insights for cognitive dysfunction. *Psychopharmacol.* **2004**, *174*, 3-16.

- ¹⁰ Kapur, S.; Remington, G. Dopamine D2 receptors and their role in atypical antipsychotic action: Still necessary and may even be sufficient. *Biol. Psych.* **2001**, *50*, 873-883.
- ¹¹ Lieberman, J.; Stroup, T.; McEvoy, J.; Swartz, M.; Rosenheck, R.; Perkins, D.; Keefe, R.; Davis, S.; Davis, C.; Lebowitz, B.; Severe, J.; Hsaio, J. Effectiveness of antipsychotic drugs in patients with chronic schizophrenia. *New Engl. J. Med.* **2005**, *12*, 1209-1223.
- ¹² Leucht, S.; Pitschel-Walz, G.; Abraham, D.; Kissling, W. Efficacy and extrapyramidal side-effects of the new antipsychotics olanzapine, quetiapine, risperidone, and sertindole compared to conventional antipsychotics and placebo. A meta-analysis of randomized controlled trials. *Schizophrenia Res.* **1999**, *35*, 51-68.
- ¹³ Glassman, A.; Bigger, J. Antipsychotic drugs: Prolonged QTc interval, torsade de pointes, and sudden death. *Am. J. Psychiatry*, **2001**, *158*, 1774-1782.
- ¹⁴ Alvir, J.; Lieberman, J.; Safferman, A.; Schwimmer, J.; Schaaf, J. Clozapine-induced agranulocytosis - incidence and risk factors in the United States. *New Engl. J. Med.*, **1993**, *329*, 162-167.
- ¹⁵ O'Donovan, M.; Williams, N.; Owen, M. Recent advances in the genetics of schizophrenia. *Hum. Molec. Genet.*, **2003**, *12*, R125-R133.
- ¹⁶ Owen, M.; Craddock, N.; O'Donovan, M. Schizophrenia: Genes at last? *Trends Genet.*, **2005**, *21*, 518-525.
- ¹⁷ Harrison, P.; Owen, M. Genes for schizophrenia? Recent findings and their pathophysiological implications. *Lancet*, **2003**, *361*, 417-419.
- ¹⁸ Wong, D.; Wagner, H.; Tune, L.; Dannals, R.; Pearlson, G.; Links, J.; Tamminga, C.; Broussolle, E.; Ravert, H.; Snyder, S.; Kuhar, M.; Gjedde, A. Positron emission tomography reveals elevated D2 dopamine receptors in drug-naive schizophrenics. *Science*, **1986**, *234*, 1558-1563.
- ¹⁹ Laruelle, M.; Abi-Dargham, A.; Van Dyck, C.; Gil, R.; D'Souza, C.; Erdos, J.; McCance, E.; Rosenblatt, W.; Fingado, C.; Zoghbi, S.; Baldwin, R.; Seibyl, J.; Krystal, J.; Charney, D.; Innis, R. Single photon emission computerized tomography imaging of amphetamine-induced dopamine release in drug-free schizophrenic subjects. *Proc. Natl. Acad. Sci.*, **1996**, *93*, 9235-9240.
- ²⁰ Abi-Dargham, A.; Mawlawi, O.; Lombardo, I.; Gil, R.; Martinez, D.; Huang, Y.; Hwang, D-R.; Keilp, J.; Kochan, L.; Van heertum, R.; Gorman, J.; Laruelle, M. Prefrontal dopamine D1 receptors and working memory in schizophrenia. *J. Neurosci.*, **2002**, *22*, 3708-3719.
- ²¹ Fu, W.; Shen, J.; Luo, X.; Zhu, W.; Cheng, J.; Yu, K.; Briggs, J.; Jin, G.; Chen, K.; Jiang, H. Dopamine D1 receptor agonist and D2 receptor antagonist effects of the natural product (-)-stepholidine: Molecular modeling and dynamics simulations. *Biophys. J.*, **2007**, *93*, 1431-1441.
- ²² Cava, M.; Nomura, K.; Talapatra, S.; Mitchell, J.; Schlessinger, R.; Buck, K.; Beal, J.; Douglas, B.; Raffaui, R.; Weisbach, J. Alkaloids of *Stephania glabra*. Direct chemical correlation of the absolute configuration of some benzyltetrahydroisoquinoline, proaporphine, and aporphine alkaloids. New protoberberine alkaloid. *J. Org. Chem.*, **1968**, *33*, 2785-2790.

- ²³ Chen, L.-J.; Zhou, Q.-T.; Dong, Z.-J.; Yu, L.-P.; Jin, G.-Z. Comparison of 12-chloroscoulerine enantiomers on animal behavior to dopamine receptors. *Acta Pharmacol. Sinica*, **1999**, *20*, 884-888.
- ²⁴ Xuan, J.; Lin, G.; Jin, G.; Chen, Y. Relevance of stereo and quantum chemistry of four tetrahydroprotoberberines to their effects on dopamine receptors. *Acta Pharmacol. Sinica*, **1988**, *9*, 197-205.
- ²⁵ Wu, S.; Tinant, B.; Declercq, J.-P.; Van Meerssche, M. Structure of *l*-stepholidine monohydrate. *Acta Cryst.*, **1987**, *C43*, 2126-2128.
- ²⁶ Chu, H.; Jin, G.; Friedman, E.; Zhen, X. Recent development in studies of tetrahydroprotoberberines: Mechanism in antinociception and drug addiction. *Cell Mol. Neurobiol.*, **2008**, *28*, 491-499.
- ²⁷ Mu, Q.; Johnson, K.; Morgan, P.; Grenesko, E.; Molnar, C.; Anderson, B.; Nahas, Z.; Kozel, F.; Kose, S.; Knable, M.; Fernandes, P.; Nichols, D.; Mailman, R.; George, M. A single 20 mg dose of the full D1 dopamine agonist dihydrexidine (DAR-0100) increases prefrontal perfusion in schizophrenia. *Schiz. Res.*, **2007**, *94*, 332-341.
- ²⁸ Chiang, H.-C.; Brochmann-Hanssen, E. Total synthesis of (+)-discretamine and (+)-stepholidine. *J. Org. Chem.*, **1977**, *42*, 3190-3194.
- ²⁹ Liu, Y.; Xin, Z. Synthesis of ¹⁴C-labeled stepholidine. *J. Labelled Comp. & Radiopharm.*, **1988**, *5*, 569-572.
- ³⁰ Rajeswari, S.; Suguna, H.; Pai, B. Studies in protoberberine alkaloids. VIII. Synthesis of (+)-stepholidine. *Coll. Czech. Chem. Comm.*, **1977**, *42*, 2207-2216.
- ³¹ Hegedus, B. Syntheses of sulfuric acid esters of dopamine and related compounds. *Helv. Chim. Acta.*, **1963**, *46*, 2604-2612.
- ³² Dai-Ho, G.; Mariano, P. Exploratory, mechanistic, and synthetic aspects of silylarene-iminium salt SET photochemistry. Studies of diradical cyclization processes and applications to protoberberine alkaloid synthesis. *J. Org. Chem.*, **1998**, *53*, 5113-5127.
- ³³ Zhang, J.-G. (-)-Tetrahydropalmatine and its analogs as new dopamine receptor antagonists. *TIPS*, **1987**, *8*, 81-82.
- ³⁴ Mo, J.; Guo, Y.; Yang, Y.-S.; Shen, J.-S.; Jin, G.-Z.; Zhen, X. Recent developments in studies of *l*-stepholidine and its analogs: Chemistry, pharmacology and clinical implications. *Curr. Med. Chem.*, **2007**, *14*, 2996-3002.
- ³⁵ Hall, A.; Bryson, S.; Vaughan, P.; Ball, S.; Balmforth, A. Pharmacological characterization of the dopamine receptor coupled to cyclic AMP formation expressed by rat mesenteric artery smooth muscle cells in culture. *Brit. J. Pharmacol.*, **1993**, *110*, 681-686.
- ³⁶ Gerlach, M.; Double, K.; Arzberger, T.; Leblhuber, F.; Tatschner, T.; Riederer, P. Dopamine receptor agonists in current clinical use: Comparative dopamine receptor binding profiles defined in the human striatum. *J. Neural Transm.*, **2003**, *110*, 1119-1127.
- ³⁷ Cuny, G. Intramolecular *ortho*-arylation of phenols utilized in the synthesis of the aporphine alkaloids (+)-lirinidine and (+)-nuciferine. *Tetrahedron Lett.*, **2003**, *44*, 8149-8152.
- ³⁸ Yamada, K.; Takeda, M.; Iwakuma, T. A novel asymmetric reduction of imines with chiral sodium triacyloxyborohydrides. *Tetrahedron Lett.*, **1981**, *22*, 3869-3872.

- ³⁹ Yamada, K.; Takeda, M.; Iwakuma, T. Asymmetric reduction of cyclic imines with chiral sodium acyloxyborohydrides. *J. Chem. Soc. Perkin Trans. I*, **1983**, 265-270.
- ⁴⁰ Cabedo, N.; Protais, P.; Cassels, B.; Cortes, D. Synthesis and dopamine receptor selectivity of the benzyltetrahydroisoquinoline, (+)-*nor-roefractine*. *J. Nat. Prod.*, **1998**, *61*, 709-712.
- ⁴¹ Brown, D.; Kharkar, P.; Parrington, I.; Reith, M.; Dutta, A. Structurally constrained hybrid derivatives containing octahydrobenzo[*g* or *f*]quinoline moieties for dopamine D₂ and D₃ receptors: Binding characterization at D₂/D₃ receptors and elucidation of a pharmacophore model. *J. Med. Chem.*, **2008**, *51*, 7806-7819.
- ⁴² Mottola, D.; Laiter, S.; Watts, V.; Tropsha, A.; Wyrick, S.; Nichols, D.; Mailman, R. Conformational analysis of D1 dopamine receptor agonists: Pharmacophore assessment and receptor mapping. *J. Med. Chem.*, **1996**, *39*, 285-296.
- ⁴³ Javitch, J.; Fu, D.; Chen, J.; Karlin, A. Mapping the binding-site crevice of the dopamine D2 receptor by the substituted-cysteine accessibility method. *Neuron*, **1995**, *14*, 825-831.
- ⁴⁴ Zhang, C.; De, C.; Mal, R.; Seidel, D. α -Amination of nitrogen heterocycles: Ring fused amins. *J. Am. Chem. Soc.*, **2008**, *130*, 416-417.
- ⁴⁵ Jain, S.; Sinha, A.; Bhakuni, D. The biosynthesis of β -carboline and quinolizidine alkaloids of *Alangium lamarckii*. *Phytochemistry*, **2002**, *60*, 853-859.
- ⁴⁶ Chen, C-Y.; Chang, F-R.; Shih, Y-C.; Hsieh, T-J.; Chia, Y-C.; Tseng, H-Y.; Chen, H-C.; Chen, S-J.; Hsu, M-C.; Wu, Y-C. Cytotoxic constituents of *Polyalthia longifolia* var. *pendula*. *J. Nat. Prod.*, **2000**, *63*, 1475-1478.
- ⁴⁷ Abd El-Kawi, M.; Slatkin, D.; Schiff, P.; Dasgupta, S.; Chattopadhyay, S.; Ray, A. Additional alkaloids of *Pachygone ovata*. *J. Nat. Prod.*, **1984**, *47*, 459-464.
- ⁴⁸ Cava, M.; Nomura, K.; Talapatra, S.; Mitchell, M.; Schlessinger, R.; Buck, K.; Beal, J.; Douglas, B.; Raffauf, R.; Weisbach, J. Alkaloids of *Stephania glabra*. Direct chemical correlation of the absolute configuration for some benzyltetrahydroisoquinoline, proaporphine, and aporphine alkaloids. New protoberberine alkaloids. *J. Org. Chem.*, **1968**, *33*, 2785-2789.
- ⁴⁹ Bentley, K. β -Phenylethylamines and the isoquinoline alkaloids. *Nat. Prod. Rep.*, **2000**, *17*, 247-268.
- ⁵⁰ Tango GPCR assay, available from Invitrogen.
- ⁵¹ Kametani, T.; Ihara, M. Synthesis of heterocyclic compounds. CLXXII. An alternative total synthesis of (+)-scoulerine and (+)-tetrahydropalmatine. *J. Chem. Soc. C*, **1967**, *7*, 530-2.
- ⁵² Kametani, T.; Noguchi, I.; Saito, K.; Kaneda, S. Syntheses of heterocyclic compounds. CCCII. Alternative total syntheses of (+)-nandinine, (+)-canadine and berberine iodide. *J. Chem. Soc. C*, **1969**, *15*, 2036-2038.
- ⁵³ Ismail, N.; Salah El Dine, R.; Hattori, M.; Takahashi, K.; Ihara, M. Computer based design, synthesis and biological evaluation of novel indole derivatives as HCV NS3-4A serine protease inhibitors. *Bioorg. Med. Chem.*, **2008**, *16*, 7877-7877.
- ⁵⁴ Rapid Response Luciferase Assay, available from Promega.